Studies in Synthesis and Applications of Nitrogen and Oxygen containing Heterocycles for Anti-diabetic and Anti-cancer activity.

THESIS SUBMITTED TO
THE MAHARAJA SAYAJIRAO UNIVERSITY OF BARODA
FOR THE DEGREE OF

DOCTOR OF PHILOSOPHY

IN

CHEMISTRY

BY

RADHIKA D. BALONI

UNDER THE GUIDANCE OF

PROF. SHUBHANGI S SOMAN

DEPARTMENT OF CHEMISTRY
FACULTY OF SCIENCE
THE MAHARAJA SAYAJIRAO UNIVERSITY OF BARODA
VADODARA 390 002
INDIA

JUNE 2014

Department of Chemistry
Centre of Advanced Studies in Chemistry &
DST-FIST sponsored Department
Faculty of Science, Vadodara 390 002 India,
Tel: +91-265-2795552

The Maharaja Sayajirao University of Baroda

CHL/ Date :

CERTIFICATE

This is to certify that the work included in the thesis entitled **"Studies in Synthesis and Applications of Nitrogen and Oxygen containing Heterocycles for Anti-diabetic and Anti-cancer activity"** has been carried out by Ms. Radhika D. Baloni under my supervision and guidance at the Department of Chemistry, Faculty of Science, The M. S. University of Baroda, Vadodara and the same has not been submitted elsewhere for any degree.

(Prof. Shubhangi S. Soman)
Research Guide

(Prof. Neelima D. Kulkarni)
Head
Department of Chemistry

DEDICATED TO

MY BELOVED PARENTS

DECLARATION

I hereby declare that the matter embodied in this thesis is the result of investigations carried out by me at the Department of Chemistry, Faculty of Science, The M. S. University of Baroda, Vadodara, under the supervision of **Prof. Shubhangi S. Soman.** Keeping with the general practice of reporting scientific observations, due acknowledgements have been made where the work described is based on the findings of other investigators.

Radhika D. Baloni

ACKNOWLEDGEMENT

It gives me great pleasure that I have an opportunity to place on record, the contributions of several people, who have been instrumental in crystallizing this thesis. I have benefited from several people during the course of this work and I am also thankful to many others who have laid the foundations for this research post my graduation. I attempt to list them here, in no particular order and I fervently hope I have not missed anyone.

Firstly I thank my Ph.D. guide, Prof. Shubhangi S Soman, with whom my association dates back to my final year of undergraduate studies when I had the first opportunity to learn Organic Chemistry from her, theoretically as well as practically. She has been a constant source of encouragement, a major reason why I left industry to pursue Ph.D. under her able guidance. It is indeed due to her persistent efforts and encouragement even after facing a lot of failures during the course of research that this work has materialized.

I also thank Prof. Neelima Kulkarni, Head, Department of Chemistry and Prof. B. V. Kamath, former Head, Department of Chemistry, Faculty of Science, The M. S. University of Baroda for providing laboratory and analytical facilities at the department.

I specially thank Prof. Neelima Kulkarni for her help, advise and technical support during the course of research.

I am also thankful to my mentors, Dr. Pinkal Prajapati, Mr. Amit Giri Goswami, Dr. Rajendra Kharul who trained me to design, synthesize, analyse biological target from medicinal chemistry point of view.

I gratefully acknowledge the help extended by Dr. Mukul Jain, Sr. Vice President, Dr. Amit Jorhapurkar, Dr. Rajesh Bahekar, Dr. Harikishore Pingali, Dr. Saurin Raval and Dr. Preeti Raval for analytical or pharmacological analysis of the NCE's synthesized during the course of research.

Special thanks to Dr. Angshuman Pal, Dr. Harish Talale, Ms. Arti Bhadoria, Mr. Hemant Mande, Ms. Ishani Sahay, Mr. Aditya Khanvilkar, Mr. Nilesh Jain and all fellow research scholars, seniors Dr. Jagdish Patel, Dr. Tirth Thakker and fellow researchers in the lab: Mr. Jigar Soni, Mr.Nirav Shah, Ms. Namrata Sahasrabudhe, Ms. Abubhuti Samvatsare, Ms. Ruchita Thakore, Mr. Prashant Gautam, Mr. Kanu Kataria for their contributions to the fulfillment of this research.

I am also thankful to all the teaching and non-teaching staff for their continuous help and support.

I am grateful to my friends, Mr. Krunal Kothari, Mr. Jigar Patel, Mr. Nisarg Desai, Mr. Varun Mehta, Mr. Priye Ranjan, who helped me to the best of their ability.

My sincere gratitude to my best friends Ms. Stella Fency and Ms. Richa Garg and also Ms. Arpita Desai and Dr. Denni Mammen who have been instrumental in my perseverance for this study.

Having specialized in organic chemistry, I could not have been able to spread my work in the field of biology without the help from my sister, Priyanka Baloni, who helped me understand the biology and also improve the quality of my research by carrying out docking studies and my husband, Mr. Rajesh Kumar Sharma whose untiring efforts helped me realize my dreams, I am indeed indebted to them.

I am also grateful to my loving brother Mr. Harsh Baloni who inspired me and helped me face every difficulty with an affirmative and also my in-laws for their patience and support.

Last but not the least, I am thankful to my parent for their persistent help, support, encouragement and blessings which has helped me in the fulfillment of my goals in life.

ABBREVIATIONS

µg	micro gram
µL	micro liter
µM	micro molar
^{o}C	Degree Celsius
Ac_2O	Acetic anhydride
AcOH	Acetic acid
Br_2	Bromine
$CDCl_3$	Deutarated chloroform
CH_3COONa	Sodium acetate
DM	Diabetes Mellitus
DMAP	4-dimethylaminopyridine
DMF	N, N-dimethyl formamide
DMSO	Dimethylsulfoxide
DMSO-d_6	Deutarated Dimethylsulfoxide
EDCI	1-(3-dimethylaminopropyl)-3-ethylcarbodiimide hydrochloride
ESI-MS	Electron Spray Ionization Mass Spectrometry
EtOH	Ethyl alcohol, Ethanol
g	Gram
h	Hour
hz	Hertz

H_2SO_4	Sulphuric acid
HCl	Hydrochloric acid
HOBt	1-Hydroxybenzotriazole
I_2	Iodine
IC_{50}	50% Inhibitory Concentration
FTIR	Fourier Transform Infrared Spectrometry
KBr	Potassium bromide
kcal	kilo calorie
K_2CO_3	Potassium carbonate
KOH	Potassium hydroxide
LiOH	Lithium hydroxide
Lit.	Literature
MeOH	Methyl alcohol, Methanol
MHz	Mega Hertz
min	Minute
mL	Millilitre
mmol	Millimole
m.p.	melting point
MS	Mass Spectrometry
NaOH	Sodium hydroxide
NMR	Nuclear Magnetic Resonance

PDB ID	Protein Data Bank ID
T2D	Type 2 Diabetes
TEA	Triethylamine
TFA	Trifluoroacetic acid
TFAA	Trifluoroacetic anhydride
THF	Tetrahydrofuran
TLC	Thin Layer Chromatography

CONTENTS

CHAPTER 1

INTRODUCTION

Chemistry of heterocyclic compounds is the most extensively explored branch of organic chemistry. The cyclic organic compounds have been categorized into homocyclic and heterocyclic compounds, classification being based upon the atoms constituting the ring. A *homocyclic* compound comprising of a ring formed by carbon atoms is known as *carbocyclic* compound. But if one or more hetero atoms are present as a part of the carbocyclic ring system then it is known as *heterocyclic* compound. These heteroatoms are usually nitrogen, oxygen or sulfur, but there are reports of other heteroatoms being present in the ring. The size of the ring may vary depending on the charge and stereochemistry of the heteroatom [1, 2].

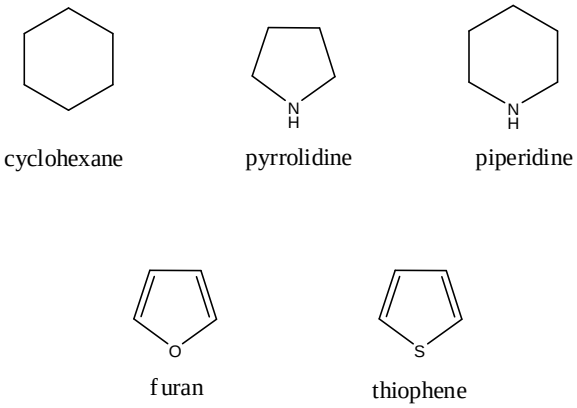

cyclohexane pyrrolidine piperidine

furan thiophene

Some variants of these heterocyclic compounds such as quinolones, coumarin, synthesized by fusion of benzene with the heterocyclic ring system gives rise to a new class of heterocyclic compounds known benzoderivaties.

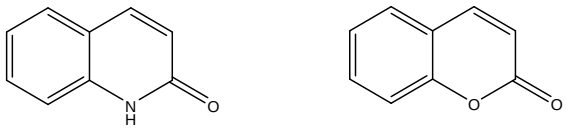

quinolin-2(1*H*)-one (quinolinone) 2*H*-chromen-2-one (coumarin)

These compounds are very useful in healthcare industry. Most of these heterocyclic compounds are either biosynthesized by plants or animals or are prepared synthetically. Three of the twenty amino acids, most of the essential vitamins are

examples of naturally occurring heterocyclic compounds. These compounds are also major components in nucleotides constituting DNA, RNA, chlorophyll, heme and others.

Heterocyclic compounds have major implications in various fields such as biochemistry, medicinal chemistry, material science and pharmaceuticals. Quinoxalines, triazoles, isooxazoles are regarded as important chemotherapeutic agents, and have clinical applications. Many pharmaceutical drugs as well as agrochemical products contain atleast one heterocyclic unit.

The field of heterocyclic chemistry has advanced substantially due the enormous research work done in this field. Heterocycles are known to be present in various biomolecules important for life, many vitamins, natural products, drugs and biologically active molecules such as antidiabetic compounds, antimalarial, antitumor, antifungal and others. Thus heterocyclic systems lay the foundation of new chemical entities with wide range of application due to their electronic, mechanical or biological properties.

Present research work is based on rationale of synthesis and applications of heterocyclic compounds, from medicinal chemistry point of view, as anti-diabetic and anti-cancer agents.

With the advances in industrialization, technology and improvement in health industry, although the quality of life and life expectancy of an individual has increased on one hand, it has resulted in amplification in the number of cases of "lifestyle diseases". Diabetes and cancer are two of the prominent lifestyle related health disorders and a major burden to global health care. Both, disorders have deleterious effect on human health worldwide and can often lead to medical complications. If left unattended or in advance stages, these diseases prove to be fatal to human life.

According to the definition given by American Diabetes Association, diabetes mellitus, also referred to as diabetes, is categorized as a group of metabolic diseases which have been symptomatically characterized by hyperglycemia or high blood sugar, caused due to lack of insulin secretion, insulin action or both [3]. Due to rampant increase in the number of cases of diabetes mellitus (DM), it has been reported that DM will reach epidemic proportions by the year 2025 [4, 5]. The National Diabetes Data Group (NDDG) had proposed the first classification of diabetes in 1979 [6]. After various revisions and modifications, the most recent classification has been published by WHO in 2006 [7]. The following is the classification for diabetes mellitus:

- Type 1 diabetes: also called as juvenile-onset diabetes (formerly called as Insulin-dependent diabetes mellitus) and although the mechanism is not entirely known, it is reported to be mostly caused by the auto-immune response against pancreatic β-cells. This form of diseases usually affects children or young adults.
- Type 2 diabetes: also termed as non-insulin dependent diabetes or adult-onset diabetes and is responsible for major cases of diabetes which are reported. The

patients generally exhibit insulin resistance and insulin deficiency and the diagnosis is possible at any age.

- Gestational diabetes (GDM): this form of diabetes is mostly prevalent during pregnancy. Such women exhibit high blood glucose and the symptoms generally disappear after pregnancy.
- Other types

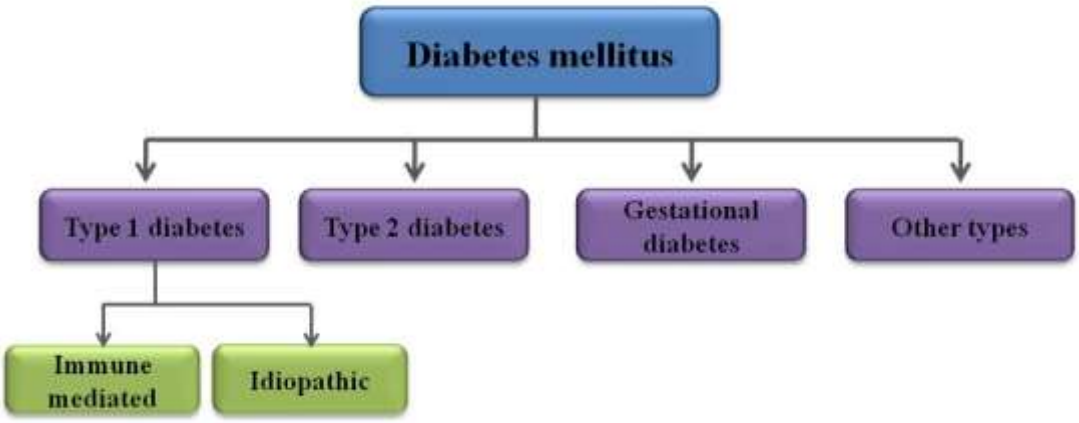

Figure 1.1: Classification of Diabetes mellitus [8]

The trends in most prevalent diseases in the human population were studied by experts in their respective fields and a comprehensive report was recently published in *The Lancet*. According to this report, there has been a significant increase in the number of deaths caused due to Diabetes in 2010 as compared to the data available in 1990 [9]. As can be seen in Figure 2, the rank of Diabetes soared from 15^{th} (in 1990) to 9^{th} (in 2010) in the category of diseases or risk factors responsible for largest number of deaths per year. Due to the alarming rate at which the percentage of deaths has increased because of Diabetes, it has become essential to take necessary measures in order to cure or prevent the disease.

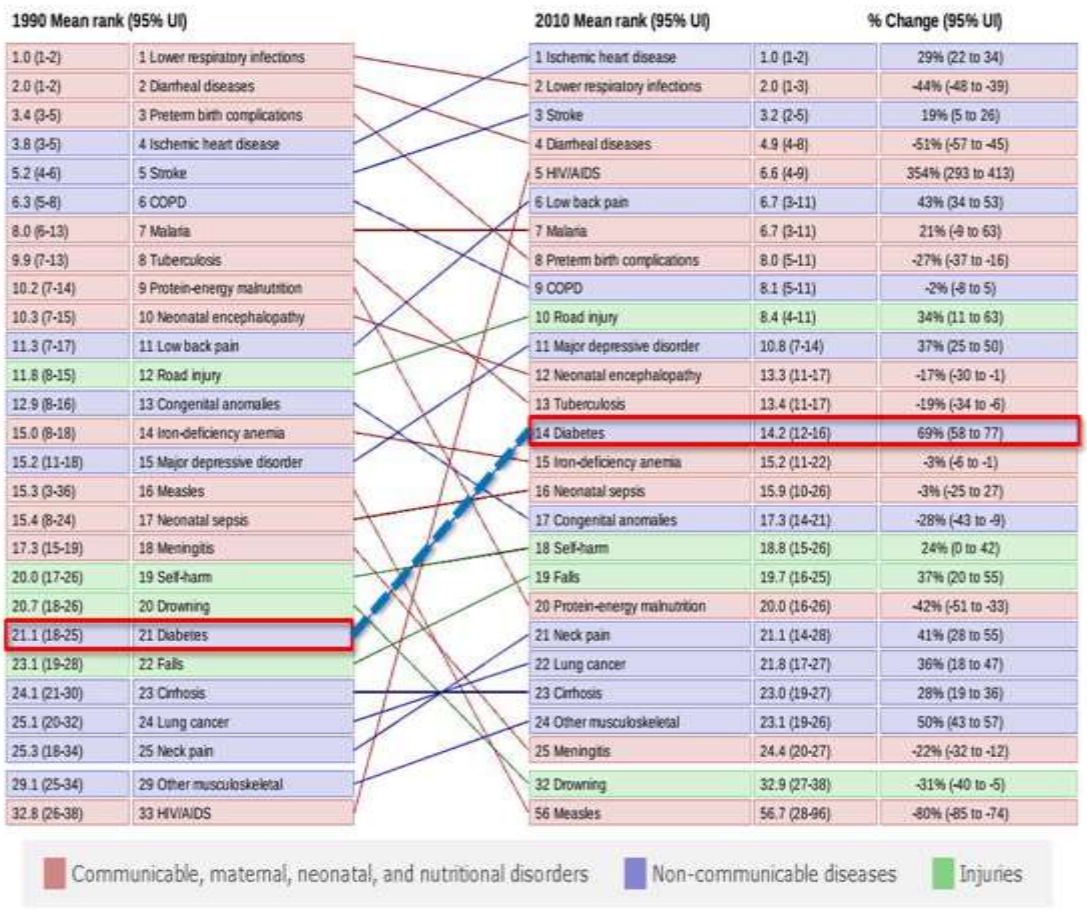

Figure 1.2: Arrow diagram depicting increase in the rank of Diabetes amongst other diseases and risk factors

Important factors responsible for (hallmarks of) type 2 diabetes are [10]:

(i) body-cell resistance to insulin (insulin resistance)

(ii) increased hepatic glucose production (e.g. from glycogen degradation)

(iii) lowered insulin mediated glucose transport into muscles and adipose tissues

(iv) impaired β-cell function leading to loss of early phase of insulin release in response to hyperglycemic stimuli (β-cell dysfunction) [11]

Insulin plays a major role in diabetes. It was first isolated in 1922 by Banting and Best and is known to regulate glucose homeostasis and other physiological functions [12]. Insulin is a polypeptide hormone secreted by the β-cells of Islet of Langerhans of pancreas. It is secreted as proinsulin (inactive form), which further processed by proteases in Golgi apparatus to form insulin. In biological systems uptake of insulin happens with the help of receptors present on fat or muscle cells of the body. This polypeptide hormone consists of 51 amino acid residues, having molecular weight of 5808Da, and the chains A and B are cross-linked to each other by disulphide bridges [13-15]. Insulin is able to undergo dimerization by forming hydrogen bonds between the ends of two B-chains [16]. Insulin is usually stored in the body in hexameric form, wherein three dimers come together in presence of zinc ions. Figure 3 illustrates the secondary structure of human insulin in dimeric and hexameric forms. The Physiological functions of insulin include glucose uptake into liver, muscles and fat cells. Thus insulin is an anabolic hormone promoting the synthesis of glycogen, triglycerides and proteins by promoting glucose uptake into cells of tissues, and hence essential to regulate the level of glucose in the body. Studies have been done to synthesize analogues of insulin and their potency has been as compared to the wild-type human insulin [14]. In order to modify the ADME (Absorption, Distribution, Metabolism and Excretion) properties of these analogues, chemical modifications are made at the side chains of C-terminus or N-terminus amino acids.

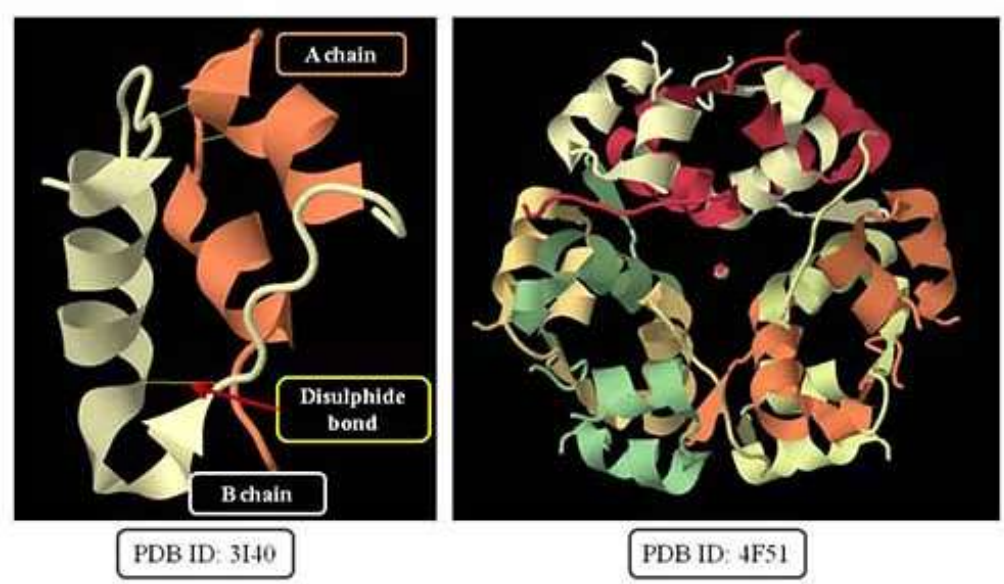

Figure 1.3: Crystal structure of a) monomeric form of human insulin and b) hexameric form of human insulin

Type 2 Diabetes Mellitus is usually caused due to the following defects: a) impaired insulin action in tissues such as skeletal muscles, liver and adipocytes b) defect in insulin secretion due to β-cell dysfunction and c) insulin resistance. Defects in insulin secretion i.e. either it is insufficiently produced or is ineffective on its target tissues, results in elevated blood glucose level or hyperglycemia [17]. The excess glucose in the blood subsequently spills over in urine, during diabetic condition (Greek: diabetes-siphon or running through; mellitus-sweet). Hence, there is "scarcity in plenty" as the body cells are starved of glucose despite its very high concentration in the blood. Deficiency of insulin thus results into chronic hyperglycemia, which in turn disrupts the carbohydrate, fat and protein metabolism. If the disease is left untreated, serious damage is caused to the heart, eyes, kidneys, blood vessels and nerves. Its symptoms include polyuria (frequent urination), polydipsia (increased thirst), polyphagia (constant hunger), weight loss and blurred vision [3]. Insulin resistance is

mainly due to impaired insulin-mediated glucose clearance into target tissues. Insulin resistance in non-diabetic as well as type 2 diabetics is associated with a cluster of metabolic abnormalities, which are collectively termed as the metabolic syndrome [11]. Metabolic syndrome is associated with a markedly increased incidence of coronary, cerebral and peripheral artery disease [18]

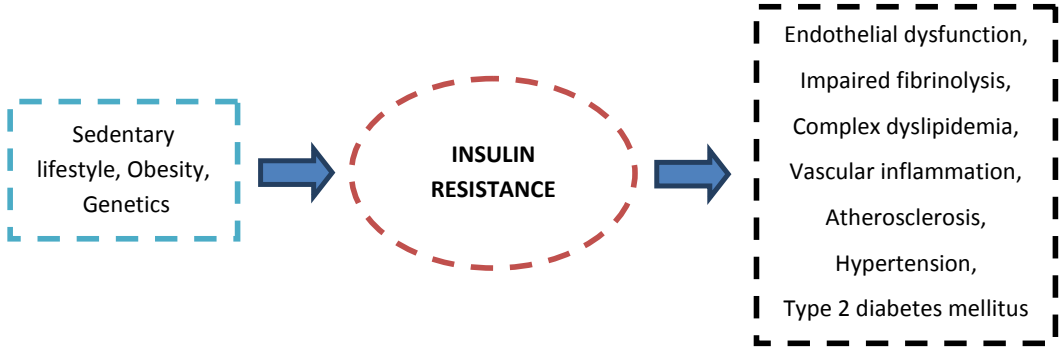

Figure 1.4: Insulin resistance and metabolic syndrome.

The World Health Organization recommends the oral glucose tolerance test (OGTT) while the fasting plasma glucose is the recommended method by the American Diabetes Association (ADA) for the diagnosis of diabetes [Definition and diagnosis of diabetes mellitus and intermediate hyperglycemia: Report of a WHO/IDF consultation **2006**]

Diagnostically, an individual is considered to be diabetic when

- Fasting plasma glucose level ≥ 7.0 mmol/l (126 mg/dl)
- Plasma glucose ≥ 11.1 mmol/l (200 mg/dL) two hours after a 75 g oral glucose load as in a glucose tolerance test
- Symptoms of hyperglycemia and casual plasma glucose ≥ 11.1 mmol/l (200 mg/dl)
- Glycated hemoglobin (Hb A1C) ≥ 6.5%

Hence, management of Type 2 Diabetes Mellitus can be achieved by controlling hyperglycemia thereby significantly reducing the risk of microvascular and macrovascular complications. At an early stage diet control and exercise helps to achieve normal body weight in turn reducing insulin resistance [19]. However, in most of the cases, dependence on exogenous insulin, drug intervention or both are required to control the blood glucose levels.

At present therapy for Type 2 Diabetes Mellitus involves various targets/approaches, which reduce hyperglycemia by enhancing insulin secretion by pancreatic β-cell. The first line therapy involves use of sulfonylurea insulin secretagogues [20-22], which acts on ATP dependent K^+ channels and sulfonylurea receptors. Sulfonylureas induce insulin secretion and suppress gluconeogenesis in the liver. The first generation sulfonylureas include tolbutamide, tolazamide, acetohexamide and chlorproamide. All have similar efficacy and require bulky hydrophores and acidic proton on sulphonylurea.

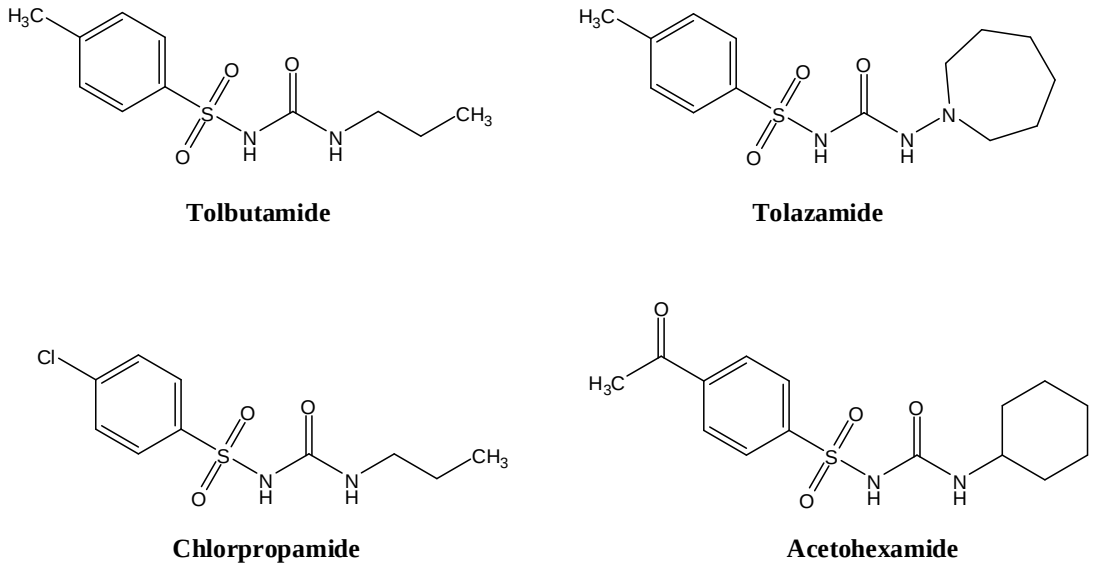

Figure 1.5: First generation Sulfonylureas.

Sulphonylureases operate by closing K^+ gate in absence of glucose, which in turn opens Ca^{+2} gate and allows Ca^{+2} influx thereby increases insulin secretion.

The second-generation agents have more rapid onset. Few examples of such drugs are glibenclamide (glyburide), glimepiride and glipizide. They act through different receptor but mechanism of action remains same. Among second generation sulphonylureases, Glimepiride acts longer for sustained insulin secretion. The major drawback of sulfonylureas is hypoglycemia and weight gain.

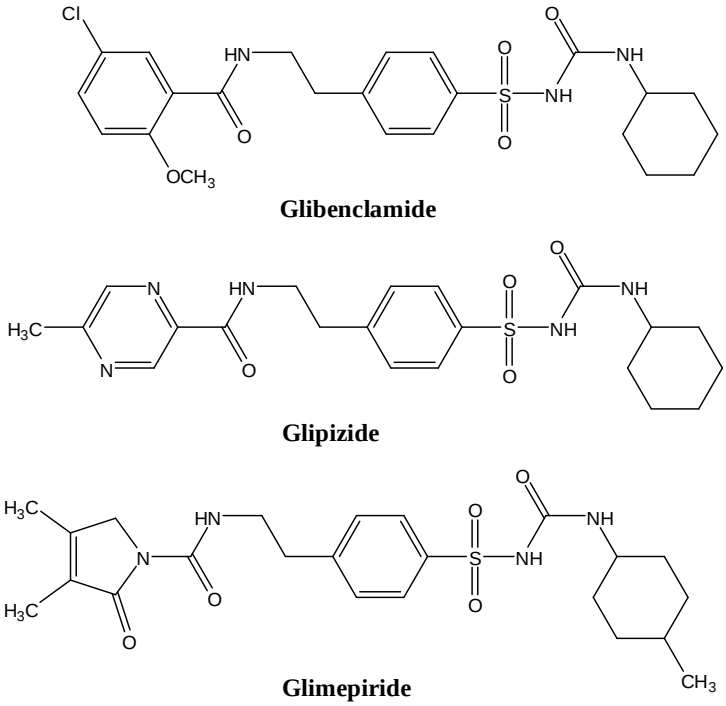

Figure 1.6: Second generation sulfonylureas

Biguanides induces their anti-hyperglycemic effect by inhibiting glucose synthesis in liver [21-23]. The exact mechanism of action for this class is still unknown. Some examples of biguanides are phenformin, buformin, metformin. Amongst these different biguanides, metformin is the most potent. Metformin helps the patients with NIDDM (non-insulin dependent diabetes mellitus) by decreasing basal hepatic glucose output, thus lowering fasting plasma glucose concentrations and in turn

improving insulin sensititvity [23]. If the metformin therapy is taken for prolonged duration it increases the blood lactate concentrations and reduction in plasma triglyceride concentrations.

Some of the advantages of biguanides is that they are not protein bound and hence are not metabolized. They are rapidly excreted from the kidney and are highly bioavailable. Usually, they are used in monotherapy or in conjunction with sulfonylureas [23].

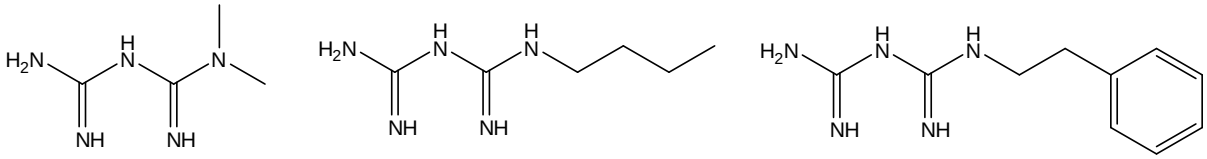

Figure 1.7: Anti-hyperglycemic biguanides.

Meglinitides analogues improve early-phase insulin secretion by binding to sulfonylurea receptor 1 on the pancreatic β-cell and closing the K^+ ATP channel but at a site different from that of sulfonylurea receptor e.g. nateglinide, repaglinide [21-24]. The advantage of meglinitides over other drugs available for diabetes is rapid stimulation of insulin secretion with low risk of hypoglycemia (since its action is confined to intermediate concentrations of glucose).

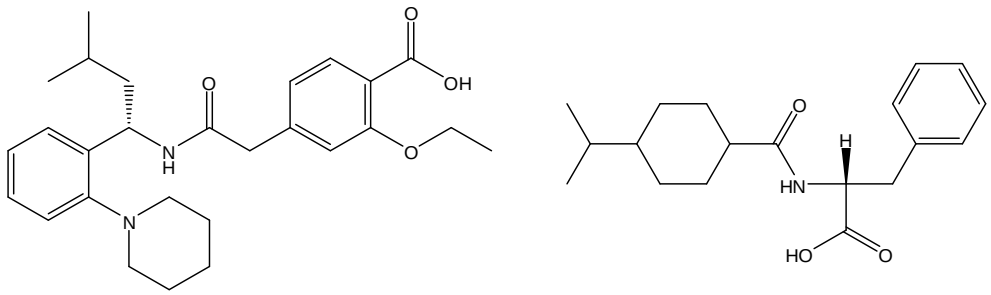

Nateglinide **Repaglinide**

Figure 1.8: Anti-diabetic meglinitides analogues.

α-glucosidase inhibitors inhibit absorption of complex sugars/glucose by interfering with the action of α-glucosidase present in the small intestinal brush border. Some examples of α-glucosidase are acarborse and miglitol. They are less potent than the sulfonylureas and exhibit side-effects which include abdominal bloating, diarrhea and flatulence [21-22]. These inhibitors significantly reduce postprandial glycemia and have excellent safety profile.

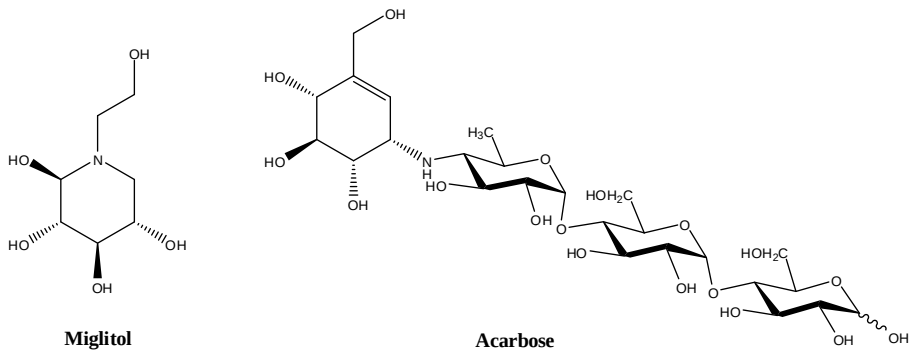

Miglitol **Acarbose**

Figure 1.9: Potent α-glucosidase inhibitors.

Thiazolidinedione act as peroxisome proliferator activated receptor-γ (PPAR-γ) agonist which increases gene expression for insulin release, fatty acid oxidation and insulin sensitivity while decreasing gene expression for lipid production [20, 25-27]. Troglitazone was withdrawn from the market due to serious hepatotoxicity while rosiglitazone is the most potent thiazolidinedione [27].

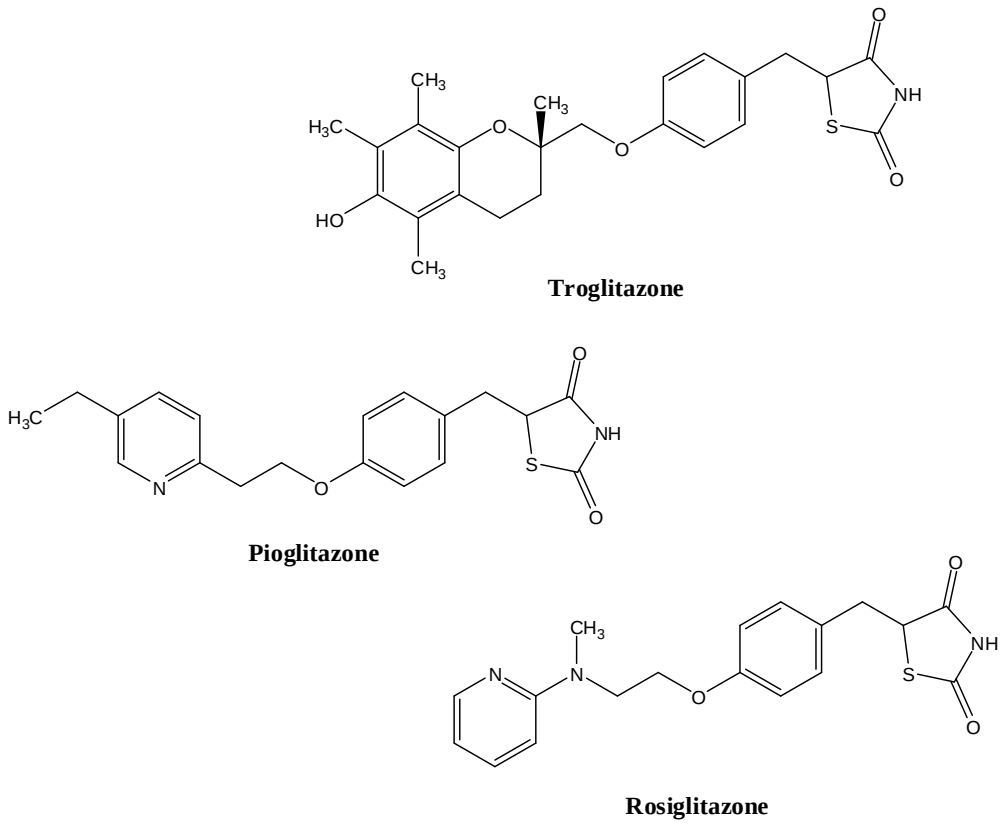

Figure 1.10: Thiazolidenediones as PPAR-γ agonist.

Insulin-secretagogues such as sulfonylureas, meglinides (e.g. repaglinide) both induce hypoglycemia. Metformin is the only anti-diabetic drug which is known to reduce the rate of any diabetes related endpoint. Although these drugs help in reducing hyperglycemia but are unable to maintain long term glycemic control thereby necessitating the use of combination drug therapies. In adverse cases, when all these medications fail, exogenous insulin is administered to control the blood glucose levels.

Various drug classes with their site and mechanism of action and side effects have been listed in Table 1.

Drug Class	Examples	Molecular target	Site of action (Primary tissue target)	Mechanism of Action	Side Effects
Sulfonylureas (SU)	Glypizide, Glymepiride	SU receptor 1/ ATP-K channel	Pancreatic β-cells	Stimulate insulin secretion	Hypoglycemia, weight gain
Biguanide	Metformin	Unknown	Liver, muscle	Inhibition of hepatic glucose output	Gastrointestinal disturbances, lactic acidosis
Meglitinides	Nateglinide, Repaglinide	SU receptor 1 (different binding site from SU)	Pancreatic β-cells	Stimulate insulin secretion	Hypoglycemia, weight gain.
α-glucosidase inhibitor	Acarbose, Miglitol	α-glucosidase	Intestine	Retards carbohydrate absorption in the gut.	Gastrointestinal disturbances
Thiazolidinediones	Pioglitazone, Rosiglitazone	PPAR-γ agonist, PPAR-γ/α dual agonist	Adipose, muscle, liver. Adipose, muscle, liver.	Increase insulin sensitivity, anti-inflamatory. Insulin sensitizing, anti-inflamatory, lipid lowering.	Weight gain, oedema, anemia.
GLP-1 analogues	Exenatide, Liraglutide	GLP-1 receptor	Pancreatic β-cells	Stimulate insulin secretion and β-cell differentiation.	Gastrointestinal disturbances, nausea and weight loss.
Insulin		Insulin receptor	Liver, muscle, adipose	Correct insulin deficiency	Hypoglycemia, weight gain.

Table 1.1: Classification of various insulin secretagogues targets for the treatment of type 2 diabetes mellitus.

Thus the major side effects of all these drug classes are hypoglycemia and weight gain. Hence, newer approaches involving glucose-dependent insulin secretion (GDIS) are needed for regulation of blood glucose to overcome these side effects.

In response to nutrient ingestion, peptide hormones called incretins are released by the gastrointestinal tract, which stimulates insulin secretion. Glucagon-like peptide-1 (GLP-1) and glucose-dependent insulinotropic polypeptide (GIP) are incretin hormones serving as enhancer of glucose dependent secretion of insulin from pancreatic β-cell. Both these hormones play an important role in glucose-dependent insulin secretion (GDIS). However, in patients with type 2 diabetes mellitus the incretin effect is either greatly impaired or completely lost [28].

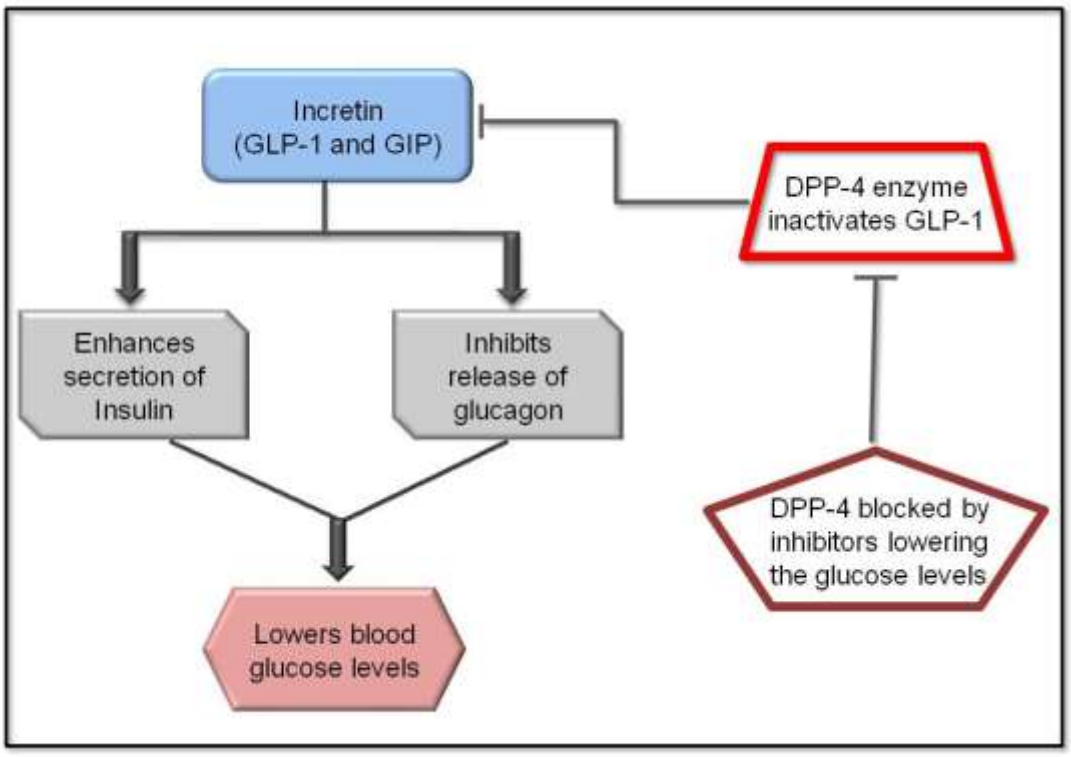

Figure 1.11: The biological role of incretin hormones and DPP-4 along with DPP-4 inhibitors.

GLP-1 is synthesized in the body as a result of tissue-specific processing of proglucagon gene. It is approximately 50% homologous to glucagon. GLP-1 is a 37 amino acid peptide hormone secreted by intestinal L-cells in response to food intake [29-31]. It is the most potent insulinotropic hormone known and has become a promising target for the treatment of type 2 diabetes. The active form of GLP-1 (7-36 residue) amide exhibits several biological effects [32-35] which includes

- glucose-induced stimulation of insulin biosynthesis and secretion
- inhibition of glucagon secretion or release
- slowing of gastric emptying
- reduce appetite by induction of satiety and
- induce pancreatic β-cell proliferation

These biological effects of GLP-1 is beneficial in controlling glucose homeostasis without the induction of hypoglycemia in the patients with type 2 diabetes [36]. The active form of GLP-1(7-36 residues) amide is enzymatically degraded, *in-vivo*, by a serine protease dipeptidyl peptidase IV (DPP-IV) thereby rendering it inactive as GLP-1(9-36 residues) amide [37, 38].

DPP-IV was first identified in 1966 [39]. It is also known as T-cell antigen CD26 (DPP-IV, EC 3.4.14.5). This serine exopeptidase is found in a variety of mammalian tissues and body fluids particularly on the surface of certain T-lymphocyte subsets, either membrane bound or as a soluble enzyme and has several biological roles which include its role as a peptidase responsible for the degradation of incretin hormones namely GLP-1 and GIP [40, 41]. It also contributes to extracellular matrix binding [42-43] and functions as adenosine deaminase (ADA) binding protein [44].

Previous studies have shown that GLP-1 remains strongly insulinotropic even though its secretion levels are reduced in the case of type 2 diabetics as compared to non-diabetic control [45-48]. Although GLP-1 has strong insulinotropic effects, but its poor pharmacokinetic profile leads to the development of GLP-1 agonists being resistant to DPP-IV. Peptides though clinically efficacious, have to be administered either subcutaneously or intravenously. Furthermore, peptides have drawbacks for clinical application due to their low bioavailability, proteolytic ability, rapid biliary excretion and short duration of action. This creates a scope for discovery of synthetic non-peptide derivatives. Consequently, inhibition of DPP-IV has gained importance as new treatment of type 2 diabetes.

If the action of DPP-IV is inhibited, then the half-life of endogenous GLP-1 increases, which has been reported to improve glucose excursion in diabetics. Consequently, inhibition of DPP-IV and prevention of incretin degradation can ultimately produce pharmacological effects especially in diabetes.

The potency and efficacy of GLP-1 can be enhanced upon inhibition of DPP-IV, thereby stimulating insulin secretion. Also, as GLP-1 is secreted on ingestion of food, hypoglycemia and exhaustion of pancreatic β-cells, common side effects of most anti-hyperglycemic drugs, is not observed. Thus small molecule DPP-IV inhibitors, which prolong the beneficial effects of endogenous GLP-1 as well as stabilize GIP, have been pursued as a new drug class.

Vildagliptin (NVP-LAF237), sitagliptin (MK-0431) and alogliptin are some of the most potent DPP-IV inhibitors in the market.

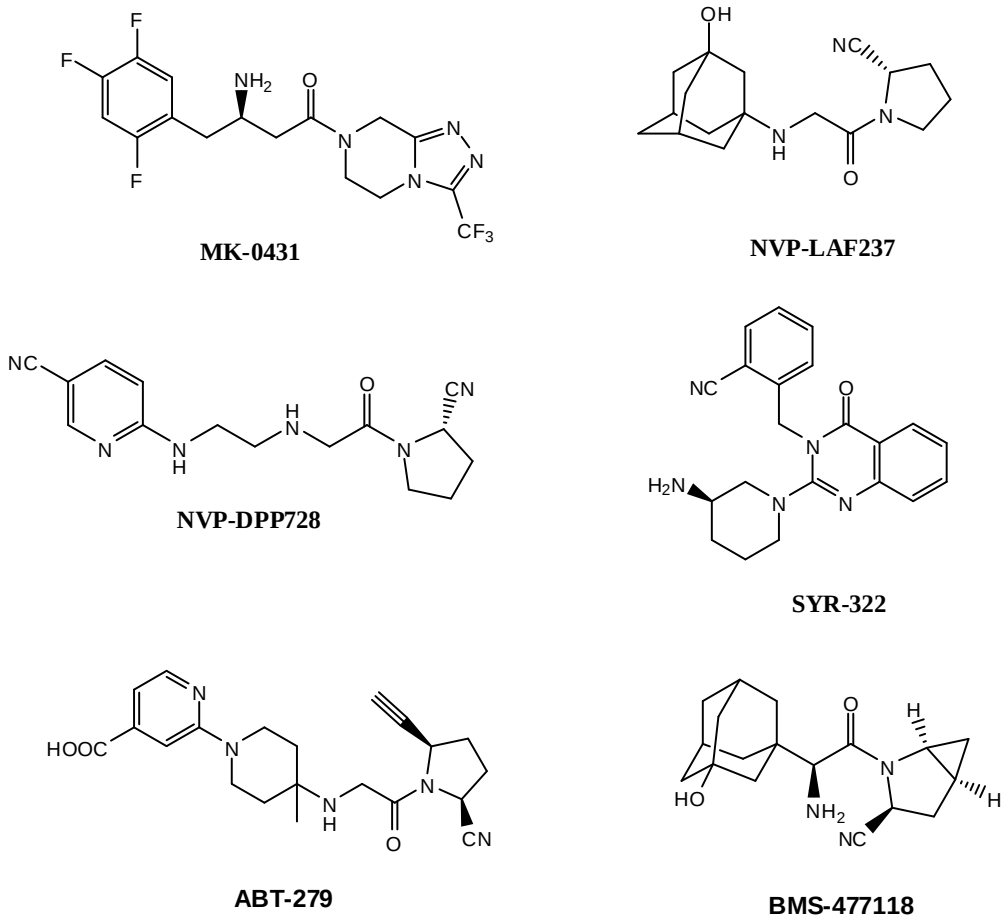

Figure 1.13: Some potent DPP-IV inhibitors.

Crystal structure of Viladagliptin bound to DPP-IV and the interacting residues of DPP-IV bound to Vildagliptin are shown in the Figure.

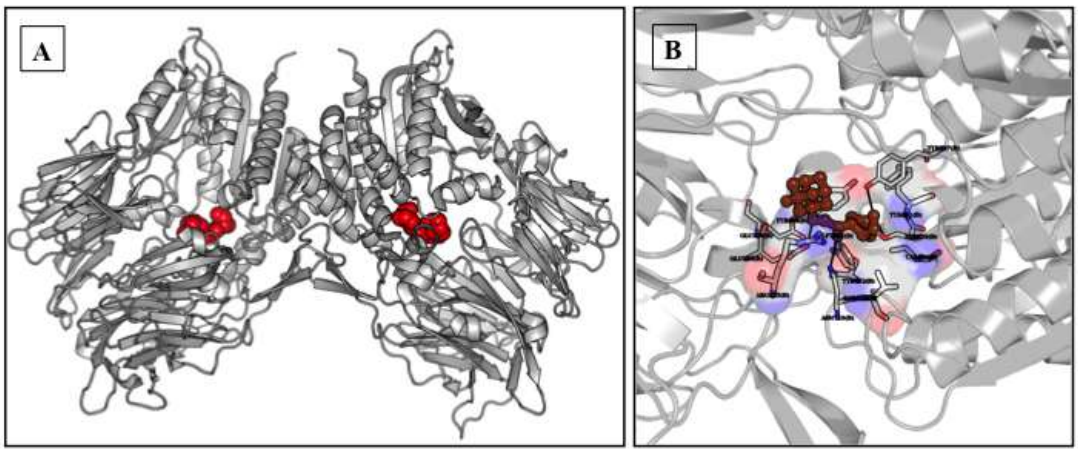

Figure 1.14: A) Crystal structure of DPP-IV with Viladagliptin bound to it and B) binding site and the interacting residues of DPP-IV bound to Vildagliptin.

Source: DOI: 10.2210/pdb3w2t/pdb

Most common feature in the design of all these inhibitors is the glycine moiety contributing the protonable nitrogen at the P2 site. A major part of the work presented in the following chapters is dedicated to design, syntheses and biological evaluation of small molecules containing glycine motif as DPP-IV inhibitors.

Another most dreaded disease with high mortality rate, ranked after the cardiovascular diseases, is Cancer. Uncontrolled cell division and proliferation are hallmark of cancer. Cancerous cells are bestowed with indefinite proliferative capability; this feat is achieved by sustaining growth signals and escaping growth signal suppressors. Cancer cells become immortal by resisting cell death by evading immune surveillance. After indefinite growth cancer cells induce angiogenesis which is followed by invasion and metastasis [49]. Once cancer cells metastasize the disease spreads and proves to be fatal. Thus early detection of cancer is desired for medical intervention. Since cancer cells grow in between normal tissues, synthesis of selective drug for cancer is the biggest challenge, for the drug should cause apoptosis of the cancerous cells and not affecting the surrounding normal tissues.

Various natural and synthetic molecules are reported to exhibit anti-cancer activity [50].

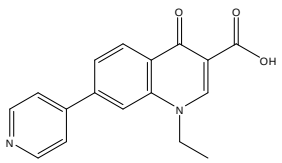

Rosoxacin

Quinolones have promising pharmacological potential due to its drug-like properties and structural similarity to some specific targets and hence have gained importance. Quinolones form the basic framework of many biologically active molecules exhibiting a broad spectrum of bioactivities, primarily, antimicrobial [51, 52], anti-cancer [53-55] and anti-viral [56, 57] activity. Since past five decades, 4(1*H*)-quinolone-3-carboxylic acid derivatives are widely used as antibiotics. Also, 4-(aminomethyl)quinolin-2(1*H*)-one derivatives and various quinolone linked with coumarins via ether linkage have been studied for their anti-microbial and analgesic activities [58, 59]. Various 2-quinolone derivatives have been reported as inducible nitric oxide synthase (iNOS) inhibitors and potent anti-platelet agents [60, 61].

Fluoroquinolones have been approved by WHO as a second line drug for the treatment of tuberculosis. The potential of fluroquinolones as first line drug due to its good pharmacological profile, absorption and penetration into host macrophages is still being investigated. Farnesyl transferase inhibitor, tipifarnib, a 3-aryl-2-quinolone derivative is in its clinical trial stage for the treatment of leukemia and breast cancer [62]. Joseph *et al.,* have reported 3-aryl-2-quinolone derivatives as anti-tumor agents [63].

In the last concluding part, synthesis of 4-aminomethyl-2(1*H*)-quinolone derivatives have been synthesized and their anti-cancer activity against lung cancer A549 cell line has been studied.

References

[1] Gilchrist, T. L. *Heterocyclic Chemistry*, 2nd edn., Longman/Wiley, Harlow/Chichester, **1992**.

[2] Joule, J. A.; Mills, K. *Heterocyclic Chemistry*, 4th edn., Blackwell Science, Oxford, **2000**.

[3] American Diabetes Association. *Diabetes Care*, **2009**, *33*, S62.

[4] King, H., Aubert, R. E.; Herman, W. H. *Diabetes Care*, **1998**, *21*, 1414.

[5] Wild, S.; Roglic, G.; Green, A.; Sicree, R.; King, H. *Diabetes Care*, **2004**, *27*, 1047.

[6] Gavin III, J. R.; Alberti, K.G.M.M.; Davidson, M. B.; DeFronzo, R. A.; Drash, A.; Gabbe, S. G.; Genuth, S.; Harris, M. I.; Kahn, R.; Keen, H.; Knowler, W. C.; Lebovitz, H.; Maclaren, N. K.; Palmer, J. R.; Raskin, P.; Rizza, R. A.; Stern, M. R. *Diabetes Care*, **1997**, *20*, 1183.

[7] World Health Organization. *Definition and diagnosis of diabetes mellitus and intermediate hyperglycemia: report of a WHO/IDF consultation.* Geneva: World Health Organization, **2006**, p. 1-50.

[8] Ahmad, S. and Maraschin, J. *Classification of Diabetes*, in *Diabetes*. **2013**, Springer New York. p. 12-19.

[9] Salomon, J. A.; Wang, H.; Freeman, M. K.; Vos, T.; Flaxman, A. D.; Lopez, A. D.; Murray, C. J. *Lancet*, **2012**, *380*, 2144.

[10] DeFronzo, R. A. *Med Clin North Am* **2004**, *88*, 787.

[11] Leahy, J. L. *Archives of Medical Research* **2005**, *36*, 197.

[12] Bell, G. I.; Pictet, R. L.; Rutter, W. J.; Cordell, B.; Tischer, E.; Goodman, H. M. *Nature*, **1980**, *284*, 26.

[13] Brange, J.; Langkjoer, L. *Pharm Biotechnol*, **1993**, *5*, 315.

[14] Favero-Retto, M.P.; Palmieri, L. C.; Souza, T. A. C. B.; Almeida, F. C. L.; Lima, L. M. T. R. *European Journal of Pharmaceutics and Biopharmaceutics*, **2013**, *85*, 1112.

[15] Ryle, A.P.; Sanger, F. *Biochem J*, **1954**, *58*(330th Meeting), p. v-vi.

[16] Timofeev, V. I.; Chuproy-Netochin, R. N.; Samigina, V. R.; Bezuglov, V. V.; Miroshnikovb K. A.; Kuranova, I. P. *Acta Crystallogr Sect F Struct Biol Cryst Commun*, **2010**, *66*, 259.

[17] Tripathy, D.; Chavez, A. O. *Curr Diab Rep*, **2010**, *10*, 184.

[18] Moller, D. E. *Nature* **2001**, *414*, 821.

[19] Stoffers, D. A.; Ferrer, J.; Clarke, W. L.; Habener, J. F. *Nature Genet* **1997**, *17*, 138.

[20] Philippe, J.; Raccah, D. *Int J Clin Pract* **2009**, *63*, 321.

[21] Krentz, A.J.; Bailey, C. J. *Drugs* **2005**, *653***,** 385.

[22] Tahrani, A. A.; Piya, M. K.; Kennedy, A.; Barnett, A. H. *Pharmacol Ther* **2010**, *125*, 328.

[23] Bailey, C. J.; Turner, R. C. *N Engl J Med* **1996**, *334***,** 574.

[24] Black, C.; Donnelly, P.; McIntyre, L.; Royle, P. L.; Shepherd, J. P.; Thomas, S. *Cochrane Database Syst Rev* **2007, *2*,** p. CD004654.

[25] Kahn, S. E.; Haffner, S. M.; Heise, M. A.; Herman, W. H.; Holman, R. R.; Jones, N. P.; Kravitz, B. G.; Lachin, J. M.; Colleen O'Neill, M.; Zinman, B.; Viberti, G. *N Engl J Med* **2006**, *355*, 2427.

[26] Nissen, S. E.; Wolski, K. *N Engl J Med* **2007**, *356*, 2457.

[27] Yki-Jarvinen, H. *N Engl J Med* **2004**, *351*, 1106.

[28] Holst, J. J.; Gromada, J. *Am J Physiol Endocrinol Metab*, **2004**, *287*, 199.

[29] Drucker, D. J. *Endocrinology* **2001**, *142*, 521.

[30] Holst, J. J.; Orskov, C.; Nielsen, O.V.; Schwartz, T. W. *FEBS Lett.* **1987**, *211*, 169.

[31] Ross, S. A.; Gulve, E. A.; Wang, M. *Chem Rev*, **2004**, *104*, 1255.

[32] Rachman, J.; Barrow, B. A.; Levy, J. C.; Turner, R. C. *Diabetologia* **1997**, *40*, 205.

[33] Nauck, M. A.; Wollschlager, D.; Werner, J.; Holst, J. J.; Orskov, C.; Creutzfeldt, W.; Willms, B. *Diabetologia* **1996**, *39*, 1546.

[34] Drucker, D. J. *Gastroenterology* **2002**, *122*, 531.

[35] Nauck, M. A.; Niedereichholz, U.; Ettler, R.; Holst, J. J.; Orskov, C.; Ritzel, R.; Schmiegel, W. H. *Am. J. Physiol.* **1997**, *273*, E981.

[36] Knudsen, L. B. *J. Med. Chem.* **2004**, *47*, 4128.

[37] Deacon, C. F.; Nauck, M. A.; Toft-Nielson, M.; Pridal, L.; Willms, B.; Holst, J. J. *Diabetes* **1995**, *44*, 1126.

[38] Kieffer, T. J.; McIntosh, C. H. S.; Pederson, T. A. *Endocrinology* **1995**, *136*, 3585.

[39] Hopsu-Havu, V. K.; Glenner, G. G. *Histochemie* **1966**, *7*, 197.

[40] Deacon, C. F.; Johnsen, A. H.; Holst, J. J. *J. Clin. Endocrinol. Metab.* **1995**, *80*, 952.

[41] Mentlein, R.; Gallwitz, B.; Schmidt, W. E. *Eur. J. Biochem.* **1993**, *214*, 829.

[42] Bauvois, B. *Biochem. J.* **1988**, *252*, 723.

[43] Loster, K.; Zeilinger, K.; Schuppan, D.; Reutter, W. *Biochem. Biophys. Res. Commun.* **1995**, *217*, 341.

[44] Kameoka, J.; Tanaka, T.; Nojima, Y.; Schlossman, S. F.; Morimoto, C. *Science* **1993**, *261*, 466.

[45] Nauck, M. A.; Kleine, N.; Orskov, C.; Holst, J. J.;Willms, B.; Creutzfeldt, W. *Diabetologia* **1993**, *36*, 741.
[46] Toft-Nielson, M.; Madsbad, S.; Holst, J. J. *J. Clin. Endocrinol. Metab.* **2001**, *86*, 3853.
[47] Toft-Nielson, M.; Madsbad, S.; Holst, J. J. *Diabetes* **1996**, *45*, 552.
[48] Vilsboll, T.; Krarup, T.; Deacon, C. F.; Madsbad, S.; Holst, J. J. *Diabetes* **2001**, *50*, 609.
[49] Hanahan, D.; Weinberg, R. A. *Cell* **2011**, *144*, 646.
[50] Dobson, R. A.; O'Connor, J. R.; Poulin, S. A.; Kundsin, R. B.; Smith, T. F.; Came, P. E. *Cell* **1980**, *18*, 738.
[51] Letafat, B.; Emami, S.; Mohammadhosseini, N.; Faramarzi, M. A.; Samadi, N.; Shafiee, A.; Foroumadi, A. *Chem. Pharm. Bull.* (Tokyo), **2007**, *55*, 894.
[52] Srivastava, B. K.; Solanki, M.; Mishra, B.; Soni, R.; Jayadev, S.; Valani, D.; Jain, M.; Patel, P. R. *Bioorg. Med. Chem. Lett.* **2007**, *17*, 1924.
[53] A. Ryckebusch, D. Garcin, A. Lansiaux, J. Goossens, B. Baldeyrou, R. Houssin, C. Bailly, J. Hénichart, *J. Med. Chem.* **2008**, *51*, 3617.
[54] Ferlin, M. G.; Chiarelotto, G.; Gasparotto, V.; Dalla Via, L.; Pezzi, V.; Barzon, L.; Palù, G.; Castagliuolo, I. *J. Med. Chem.* **2005**, *48*, 3417.
[55] Gasparotto, V.; Castagliuolo, I.; Chiarelotto, G.; Pezzi, V.; Montanaro, D.; Brun, P.; Palù, G.; Viola, G.; Ferlin, M. G. *J. Med. Chem.* **2006**, *49*, 1910.
[56] Tabarrini, O.; Stevens, M.; Cecchetti, V.; Sabatini, S.; Dell'Uomo, M.; Manfroni, G.; Palumbo, M.; Pannecouque, C.; De Clercq, E.; Fravolini, A. *J. Med. Chem.* **2004**, *47*, 5567.
[57] Cecchetti, V.; Parolin, C.; Moro, S.; Pecere, T.; Filipponi, E.; Calistri, A.; Tabarrini, O.; Gatto, B.; Palumbo, M.; Fravolini, A. *J. Med. Chem.* **2000**, *43*, 3799.
[58] Kalkhambkar, R. G.; Kulkarni, G. M.; Kamanavalli, C. M.; Premkumar, N.; Asdaq, S.M.B.; Sun, C. M. *Eur. J. Med. Chem.* **2008**, *43*, 2178.
[59] Kalkhambkar, R. G.; Aridoss, G.; Kulkarni, G. M.; Bapset, R. M.; Mudaraddi, T. Y.; Premkumar, N.; Jeong, Y. T. *Monatsh Chem.* **2011**, *142*, 305.
[60] Bonnefous, C.; Payne, J. E.; Roppe, J.; Zhuang, H.; Chen, X.; Symons, K. T.; Nguyen, P. M.; Sablad, M.; Rozenkrants, N.; Zhang, Y.; Wang, L.; Severance, D.; Walsh, J. P.; Yazdani, N.; Shiau, A. K.; Noble, S. A.; Rix, P.; Rao, T. S.; Hassig, C. A.; Smith, N. D. *J. Med. Chem.* **2009**, *52*, 3047.
[61] Priya, N.; Gupta, A.; Chand, K.; Singh, P.; Kathuria, A.; Raj, H. G.; Parmar, V. S.; Sharma, K. *Bioorg. Med. Chem.* **2010**, *18*, 4085.
[62] Sparano, J. A.; Moulder, S.; Kazi, A.; Coppola, D.; Negassa, A.; Vahdat, L.; Li, T.; Pellegrino, C.; Fineberg, S.; Munster, P.; Malafa, M.; Lee, D.; Hoschander, S.; Hopkins, U.; Hershman, D.; Wright, J. J.; Kleer, C.; Merajver, S.; Sebti, S. M. *Clin. Cancer Res.* **2009**, *15*, 2942.
[63] Joseph, B.; Darro, F.; Behard, A.; Lesur, B.; Collignon, F.; Decaestecker, C.; Frydman, A.; Guillaumet, G.; Kiss, R. *J. Med. Chem.* **2002**, *45*, 2543.

CHAPTER 2

SYNTHESIS OF SULFONAMIDE DERIVATIVES AS DPP-IV INHIBITORS

2.1 Introduction:

Dipeptidyl peptidase IV (DPP-IV, E.C.3.4.14.5, CD26) is a widely expressed serine protease in many tissues and body fluids of mammals and exists as either a membrane bound or a soluble enzyme. It is primarily found on vascular endothelium, epithelial cells of kidney, liver, intestine, pancreas, lymphoid and myeloid cells and contributes to the extracellular matrix binding [1, 2]. It functions as a protease, cleaving dipeptides comprising of either proline or alanine at the penultimate position from the amino terminus of the peptide or protein [3, 4].

Glucagon like peptide 1 (GLP-1) [5] and glucose dependent insulinotropic polypeptide (GIP) are incretin hormones released from the gut in response to the food intake and are responsible for the glucose dependent stimulation of insulin secretion through pancreatic β-cells [6-10]. Furthermore, GLP-1 slows gastric emptying, stimulates regeneration and differentiation of pancreatic β-cells while inhibiting glucagon secretion [11-14]. But all these therapeutic effects of both these hormones are lost due to their rapid degradation ($t_{½}$ ~ 1 minute) by DPP-IV [5, 14, 15]. Thus inhibition of DPP-IV has emerged as a novel approach for the treatment of type 2 diabetes (T2D) [16-17].

Owing to DPP-IV's substrate specificity, various proline mimetics have been explored as DPP-IV inhibitors as shown in Figure 2.1.

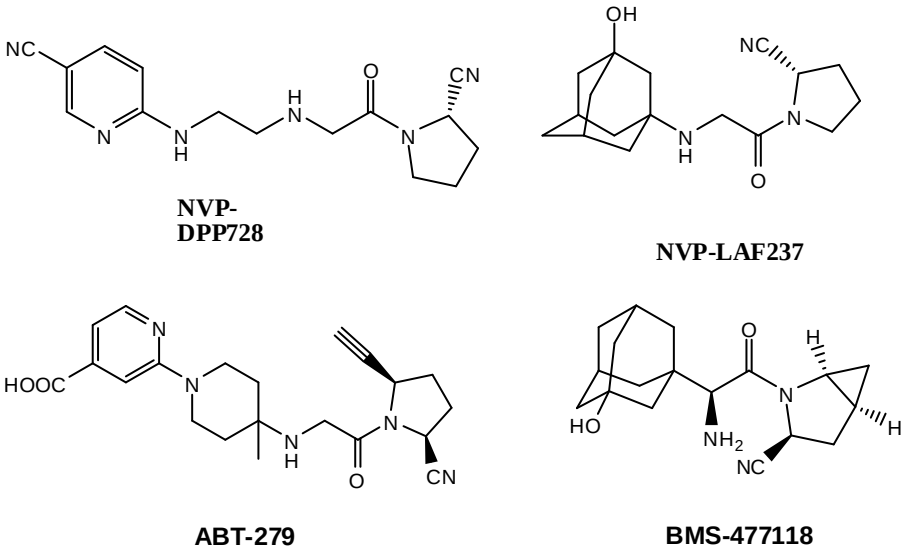

Figure 2.1: Some proline mimetic DPP-IV inhibitors.

Designing of the DPP-IV inhibitors is based on the general structure as shown in Figure 2.2.

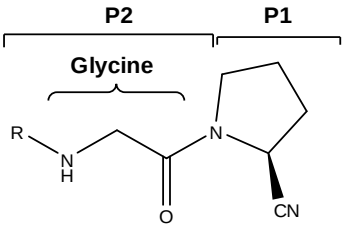

Figure 2.2: General structure of DPP-IV inhibitors.

Most of DPP-IV inhibitors reported till date have been designed taking into account the N-terminal dipeptide residue of enzymatic substrate which comprises of a proline mimic, usually a cyanopyrrolidine at the P1 site, coupled with an additional amino acid or a similar substituted amino acid at the P2 site by formation of an amide bond as shown in Figure 2.2.

Thus, in the design of DPP-IV inhibitor, a common structural motif comprises of an L-amino acid surrogate at the P1 site and a N-substituted glycine with a protonable amine responsible for the enhanced the potency of the inhibitor, at the P2 site [18].

A number of diverse N-substituted glycine when combined with 2S-cyanopyrrolidide at the P1 site have been reported to show better inhibition. Some laboratories have reported potent DPP-IV inhibitors 1(IC_{50} = 6.7 nM) [19] and 2 (K_i = 39 nM) [20] having sulfonamide at the P2 site as shown in Figure 2.3.

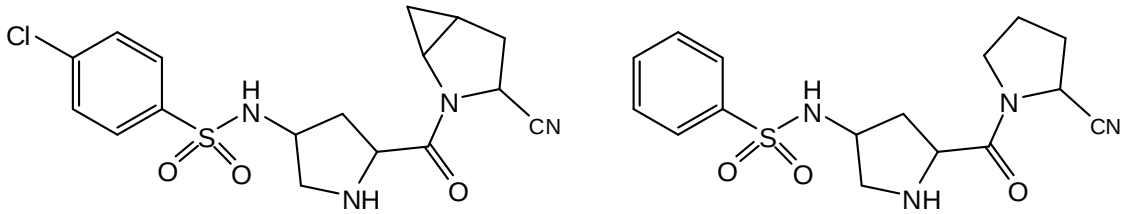

1 **2**

Figure 2.3: Some sulfonamide containing DPP-IV inhibitors.

Thus considering all these structure activity relationship studies, design and synthesis of novel DPP-IV inhibitors with sulfonamide derivatives at the P2 site while keeping the active pharmacophore same has been carried out and reported in this chapter. All the molecules synthesized were screened for *in-vitro* DPP-IV inhibition.

2.2 Results and Discussion

2.2.1 Chemistry

Small molecule DPP-IV inhibitors were synthesized using commercially available amino acids L-proline amide, L-proline and piperidine-3-carboxylic acid.

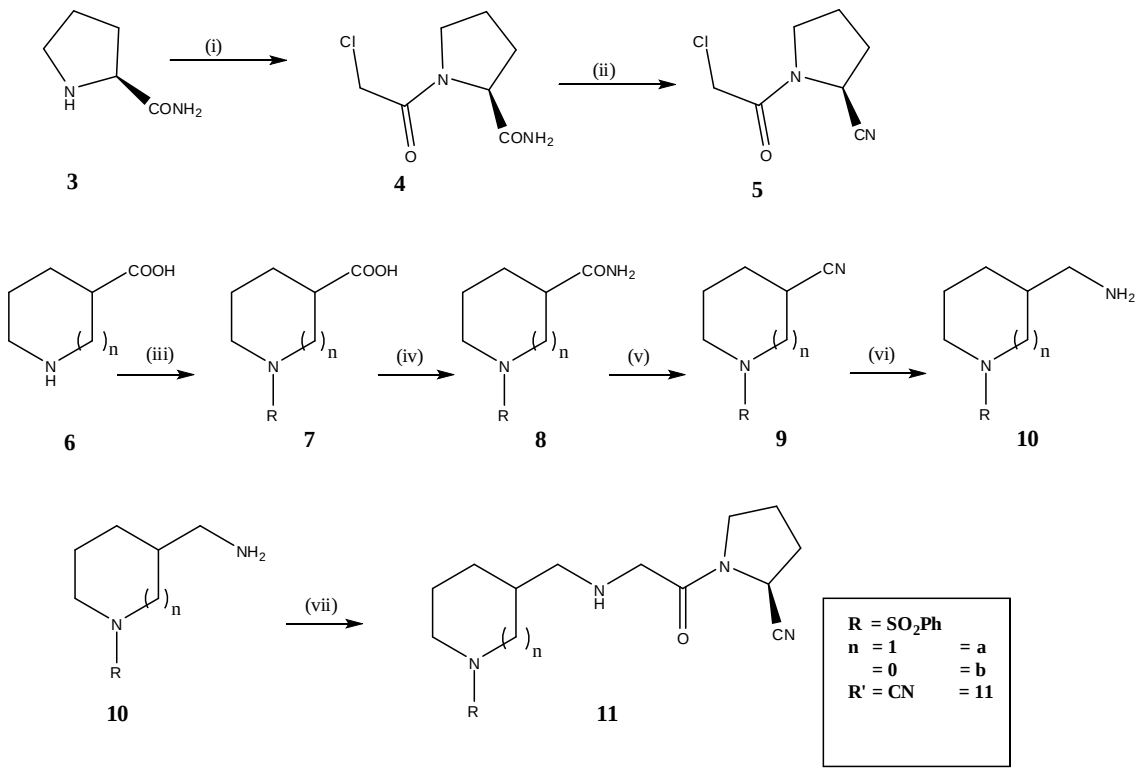

Scheme 2.1: Reagents (i) $ClCH_2COCl$, K_2CO_3, THF; (ii) TFAA, THF, NH_4HCO_3; (iii) (a) $PhSO_2Cl$, Na_2CO_3, DCM : H_2O (1:1); (b) HCl; (iv) EDCI, NH_4HCO_3, DCM; (v) TFAA, THF, NH_4HCO_3; (vi) LAH, THF, 10% NaOH; (vii) K_2CO_3, **5**, CH_3CN.

L-proline amide **3**, on reaction with chloroacetyl chloride gave *(S)*-1-(2-chloroacetyl)pyrrolidine-2-carboxamide **4** (Scheme 2.1), which on dehydration

with trifluoroacetic anhydride (TFAA) gave *(S)*-1-(2-chloroacetyl)pyrrolidine-2-carbonitrile **5**. The IR spectrum of **5** (Figure 2.4.1) showed strong bands at 2241 and 1656 cm^{-1} for the nitrile and amide groups respectively while its ^{1}H NMR spectrum (Figure 2.4.2) showed peak at δ 4.076 for the methylene protons of glycine and multiplet at δ 4.69-4.71 for -CH proton of the cyanopyrrolidide and Figures 2.4.3 and 2.4.4 shows ^{13}C NMR and ESI-MS spectra of **5**, thus confirming its structure.

Piperidine-3-carboxylic acid **6a** or L-proline **6b** on reaction with benzene sulfonyl chloride in (1:1) dichloromethane : water (DCM : H_2O), in the presence of sodium carbonate as base gave corresponding sulfonamide **7a** or **7b** as shown in Scheme 2.1. The structures of **7a** or **7b** were confirmed by their IR spectrum (Figure 2.5.1) and ^{1}H NMR spectrum (Figure 2.5.2) which clearly showed presence of aromatic protons at δ 7.54-7.79 along with aliphatic $–CH_2$ protons of piperidyl or pyrrolidyl ring from δ 1.65-3.83. A broad singlet at δ 8.89 indicated the presence of carboxylic acid proton which disappeared on formation of **8a**. Figures 2.5.3and 2.5.4 shows ^{13}C NMR and ESI-MS spectrum of **7a**. Figures 2.6.1, 2.6.2, 2.6.3 and 2.6.4 show IR, ^{1}H NMR, ^{13}C NMR and ESI-MS spectra of **7b** respectively. The carboxylic acid group of **7a**, **7b** was then coupled with ammonium bicarbonate in the presence of 1-ethyl-3-(3-dimethylaminopropyl) carbodiimide hydrochloride (EDCI), 1-hydroxybenzotriazole (HOBt) in DCM to give corresponding amide **8a, 8b** respectively. The IR spectrum of **8a** (Figure 2.7.1) showed two bands at 3346 and 3173 cm^{-1} for $–NH_2$ group and a band at 1665 cm^{-1} for the carbonyl group of the amide. In the ^{1}H NMR of **8a** (Figure 2.7.2), disappearance of peak at δ 8.89 for –COOH proton and appearance of two new peaks at δ 6.96 and 7.46 for $–NH_2$ protons which disappeared on D_2O exchange thus confirmed the formation of **8a**.

Figures 2.7.3 and 2.7.4 show ^{13}C NMR and ESI-MS spectrum of **8a** respectively. Similarly, Figures 2.8.1, 2.8.2, 2.8.3 and 2.8.4 respectively show IR, ^{1}H NMR, ^{13}C NMR and ESI-MS spectra of **8b**, thus confirms the structure of **8b**. Addition of trifluoroacetic anhydride (TFAA) to a solution of **8a-b** in tetrahydrofuran (THF) leads to dehydration of amide, thereby yielding nitrile **9a-b** which was confirmed by its IR. The IR spectrum of **9a** (Figure 2.9.1) showed strong band at 2239 cm^{-1} for nitrile group. In the ^{1}H NMR of **9a** (Figure 2.9.2), the two peaks at δ 6.08 and 6.94 for the $–NH_2$ protons of **8a** disappeared thus supported the formation of **9a.** Further, structure of **9a** was confirmed by its ^{13}C NMR (Figure 2.9.3) and ESI-MS (Figure 2.9.4) spectra and Figures 2.10.1, 2.10.2, 2.10.3 and 2.10.4 shows IR, ^{1}H NMR, ^{13}C NMR and ESI-MS spectra of **9b** respectively, thus confirms its structure. **9a-b** was reduced to its corresponding amine **10a-b** by lithium aluminium hydride (LAH). The formation of **10a** was confirmed from its ^{1}H NMR (Figure 2.11.1) and ESI-MS spectrum (Figure 2.11.2). Reaction of amines **10a** and **10b** with **5** gave compounds **11a-b** respectively, as shown in Scheme 2.1. Figure 2.12.1, 2.12.2, 2.12.3 and 2.12.4 shows IR, ^{1}H NMR, ^{13}C NMR and ESI-MS spectra of **11a** respectively.

Attempts were made to synthesize molecules with substitution of amines other than those derived from proline at the P1 site while substituting sulphonamide at the P2 site.

For this purpose compound **7** was at first reacted with oxalyl chloride to give a reactive intermediate, acid chloride which on further reaction with methanol gave corresponding methyl ester **12** as shown in Scheme 2.2**.** The structure of **12** was confirmed from its IR spectrum (Figure 2.13.1) which showed a band at 1726 cm^{-1} characteristic of carbonyl of the ester with the disappearance of a broad band at 3100-2500 cm^{-1} for the –OH of

carboxyl group and the ^{1}H NMR spectrum (Figure 2.13.2) wherein a peak at δ 8.98 for the –COOH proton of **7** disappears and a singlet at δ 3.59 for the $–OCH_3$ protons of the ester appears; ^{13}C NMR spectrum (Figure 2.13.3) and also its ESI-MS spectrum (Figure 2.13.4) with a peak at m/z 283.9 for $[M+H]^+$ confirms the formation of methyl ester **12**. The methyl ester **12** on reduction with lithium aluminium hydride (LAH) yielded (1-(phenylsulfonyl)piperidin-3-yl)methanol **13.**

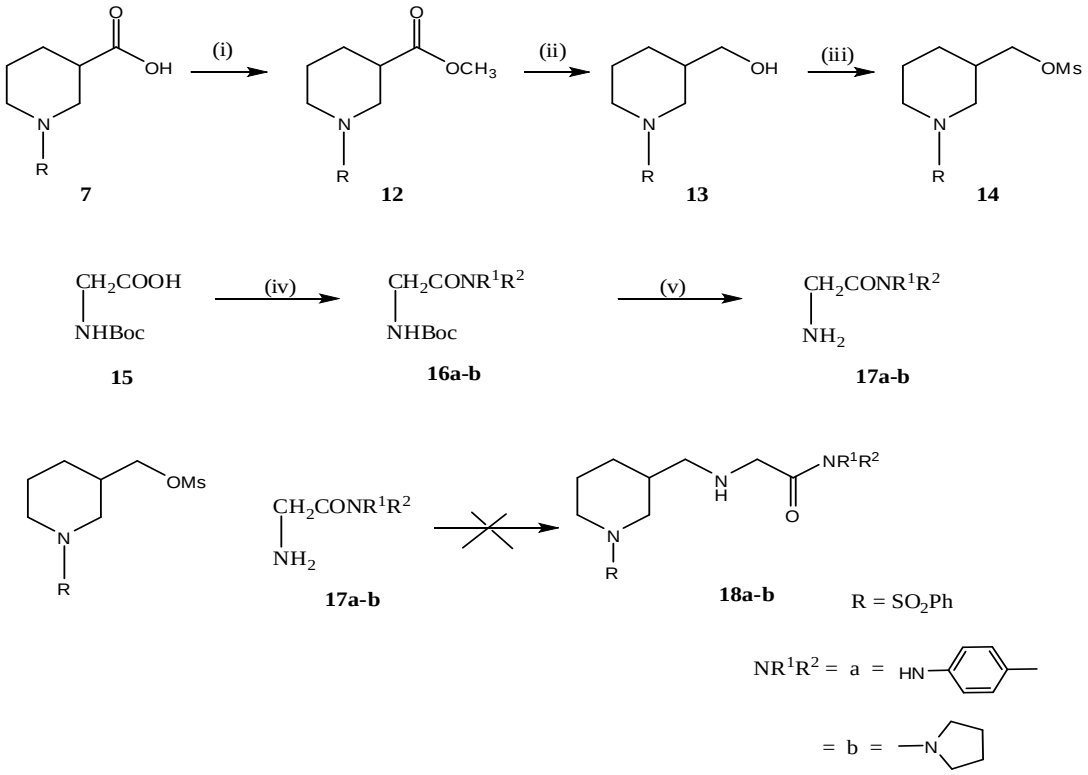

Scheme 2.2: Reagents: (i) (a) $C_2O_2Cl_2$, DCM; (b) CH_3OH; (ii) LAH, THF; (iii) CH_3SO_2Cl, Et_3N, DCM; (iv) EDCI, HOBt, DMAP, various amines, DCM; (v) TFA, DCM.

The IR spectrum of **13** (Figure 2.14.1) showed absence of a band at 1726 cm^{-1} for the carbonyl of ester functionality while a strong band at 3531 cm^{-1} for the –OH group supports the structure of **13** which is also supported by its ^{1}H NMR spectrum (Figure 2.14.2) wherein a multiplet at δ 3.50-3.60 for the two $–CH_2$ protons of methanol group is observed and ESI-MS spectrum (Figure 2.14.3) with a $[M+H]^+$ peak at *m/z* 256.0 confirmed formation of **13**. Reaction of **13** with methane sulfonyl chloride in the presence of base, triethylamine gave **14**. The formation of **14** could be confirmed from its ^{1}H NMR spectrum (Figure 2.15.1) wherein a singlet at δ 3.07 for the $–CH_3$ protons of the mesylate group was observed. The reaction of **14** with boc-de-protected glycylamide **17a-b** failed and products **18a-b** could not be isolated. The structure of **17a** has been proved in by its IR, ^{1}H NMR, ^{13}C NMR and ESI-MS spectra as shown in Figures 5.5.1, 5.5.2, 5.5.3, 5.5.4 **(Chapter 5)** respectively. Also, the IR, ^{1}H NMR, ^{13}C NMR and ESI-MS spectra: Figures 5.8.1, 5.8.2, 5.8.3, 5.8.4 **(Chapter 5)** respectively, prove the structure of **17b** .

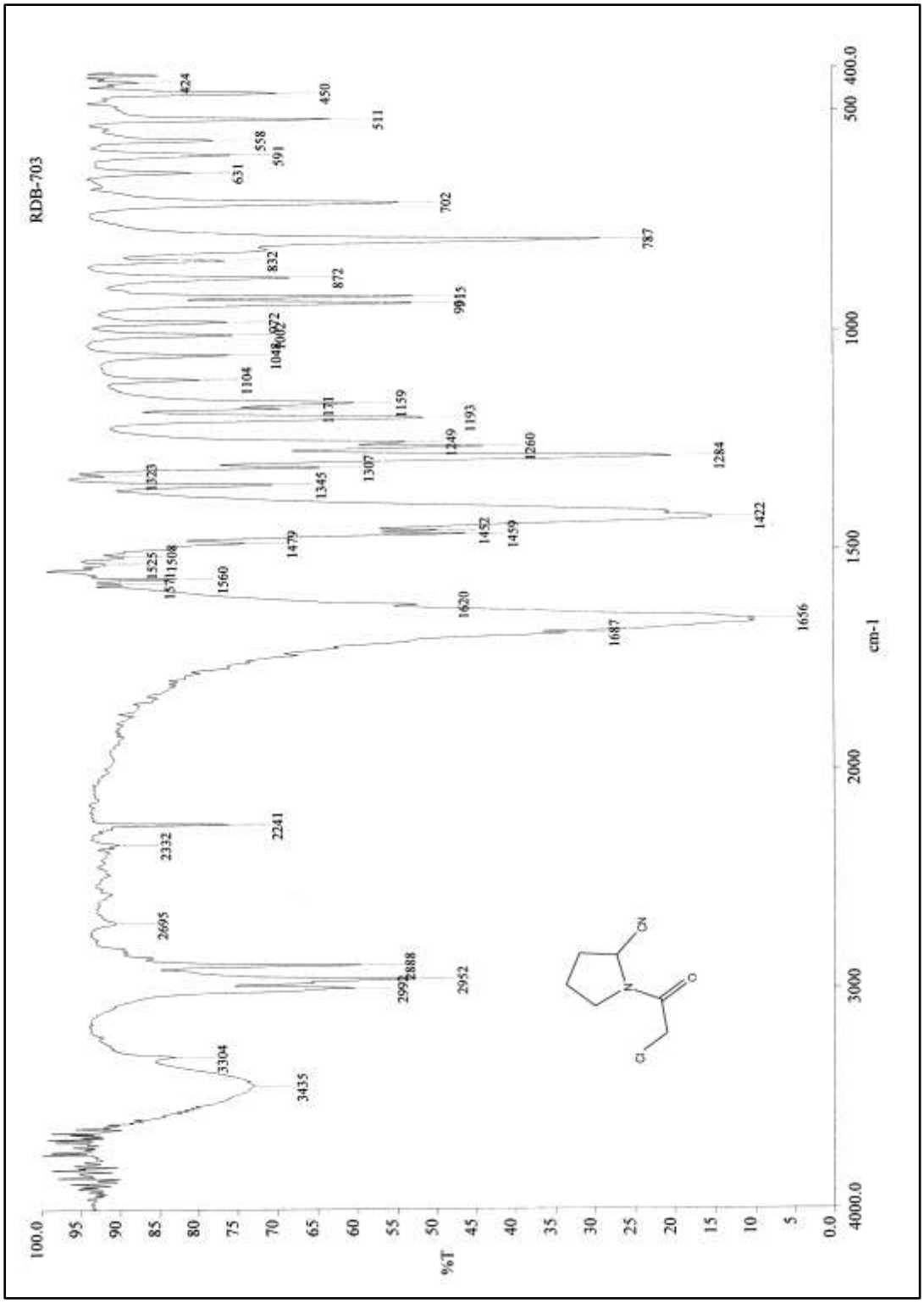

Figure 2.4.1: IR spectrum of *(S)*-1-(2-chloroacetyl)pyrrolidine-2-carbonitrile **5a**

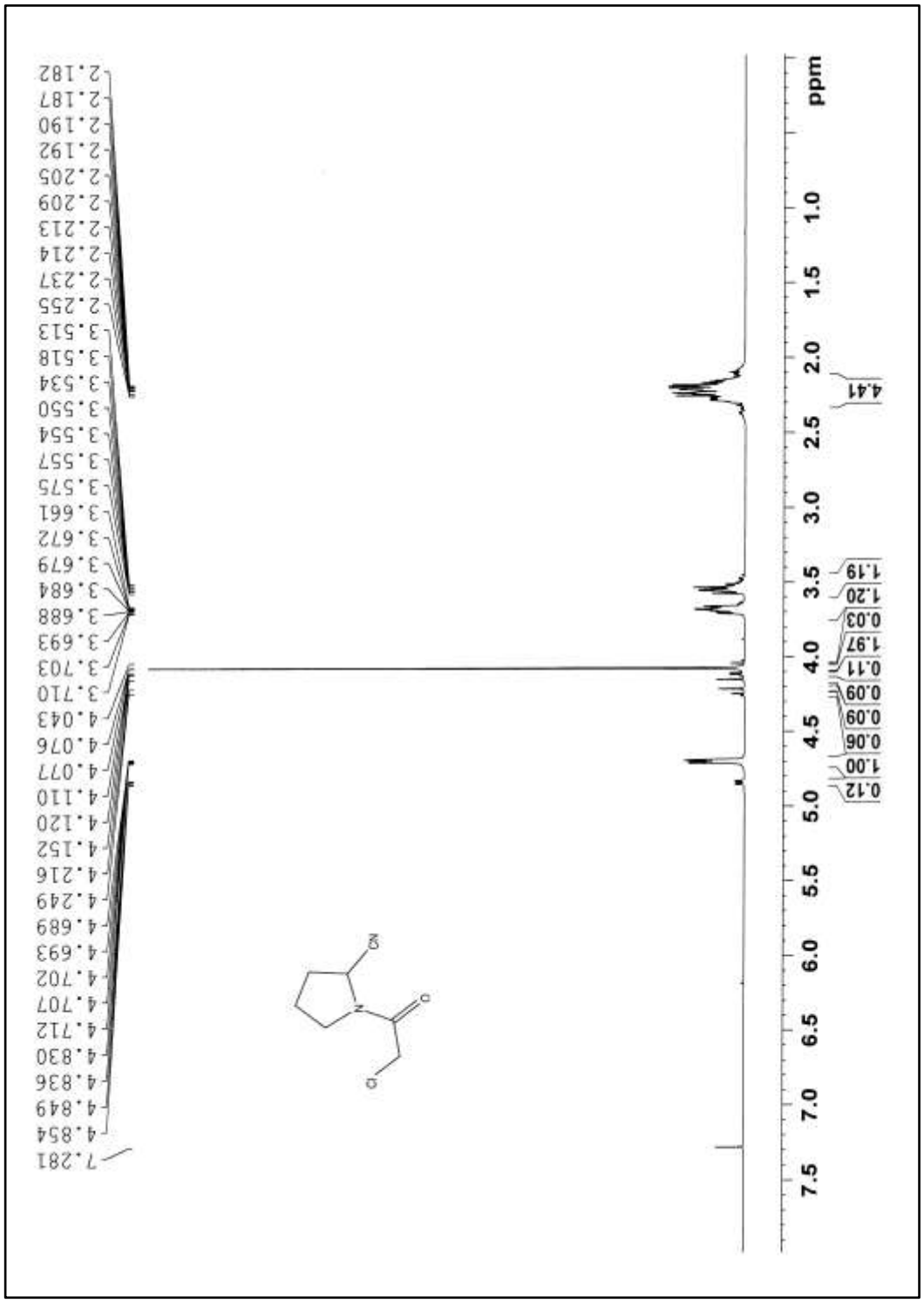

Figure 2.4.2: ^{1}H NMR spectrum of *(S)*-1-(2-chloroacetyl)pyrrolidine-2-carbonitrile **5a**

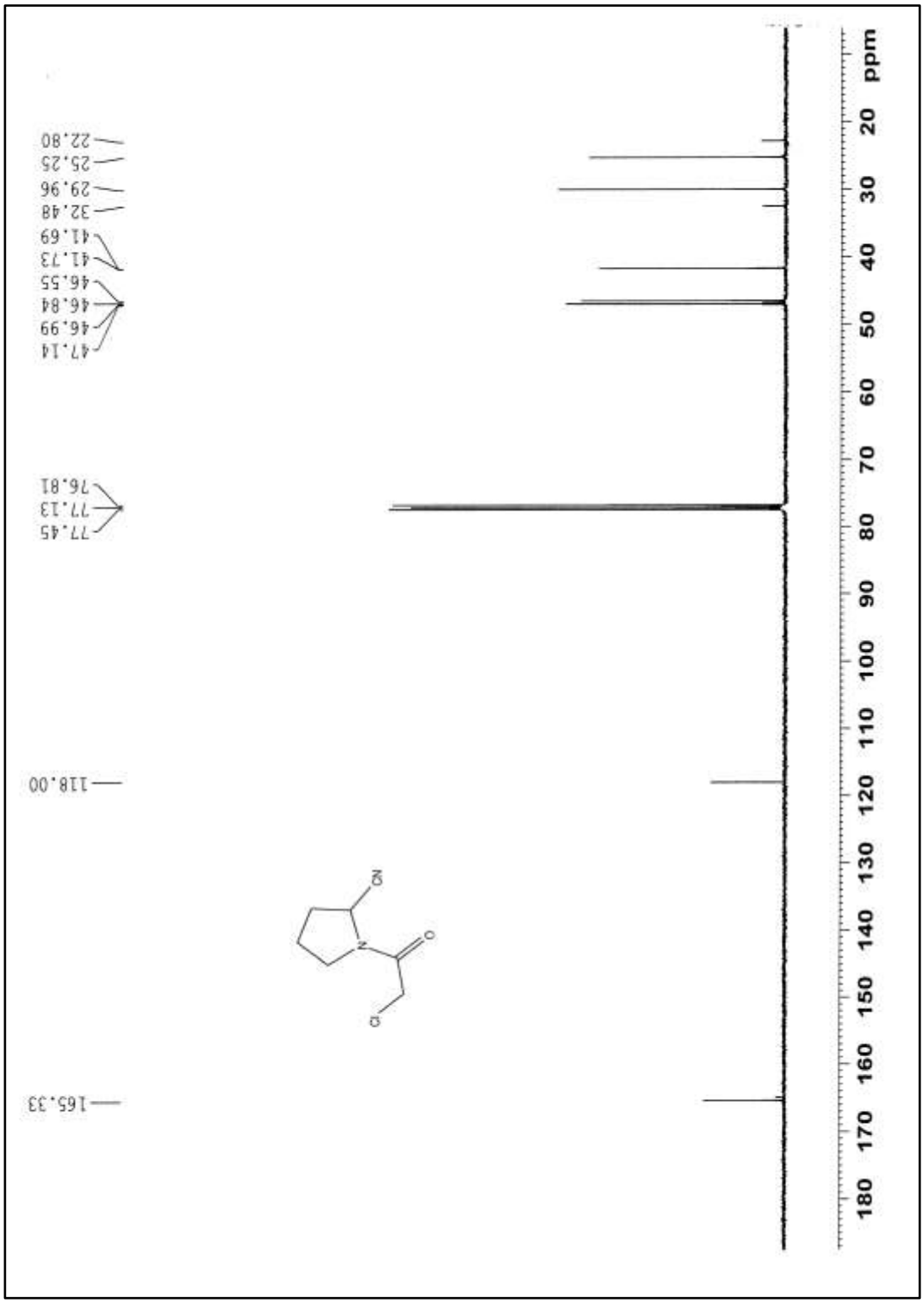

Figure 2.4.3: ^{13}C NMR spectrum of *(S)*-1-(2-chloroacetyl)pyrrolidine-2-carbonitrile **5a**

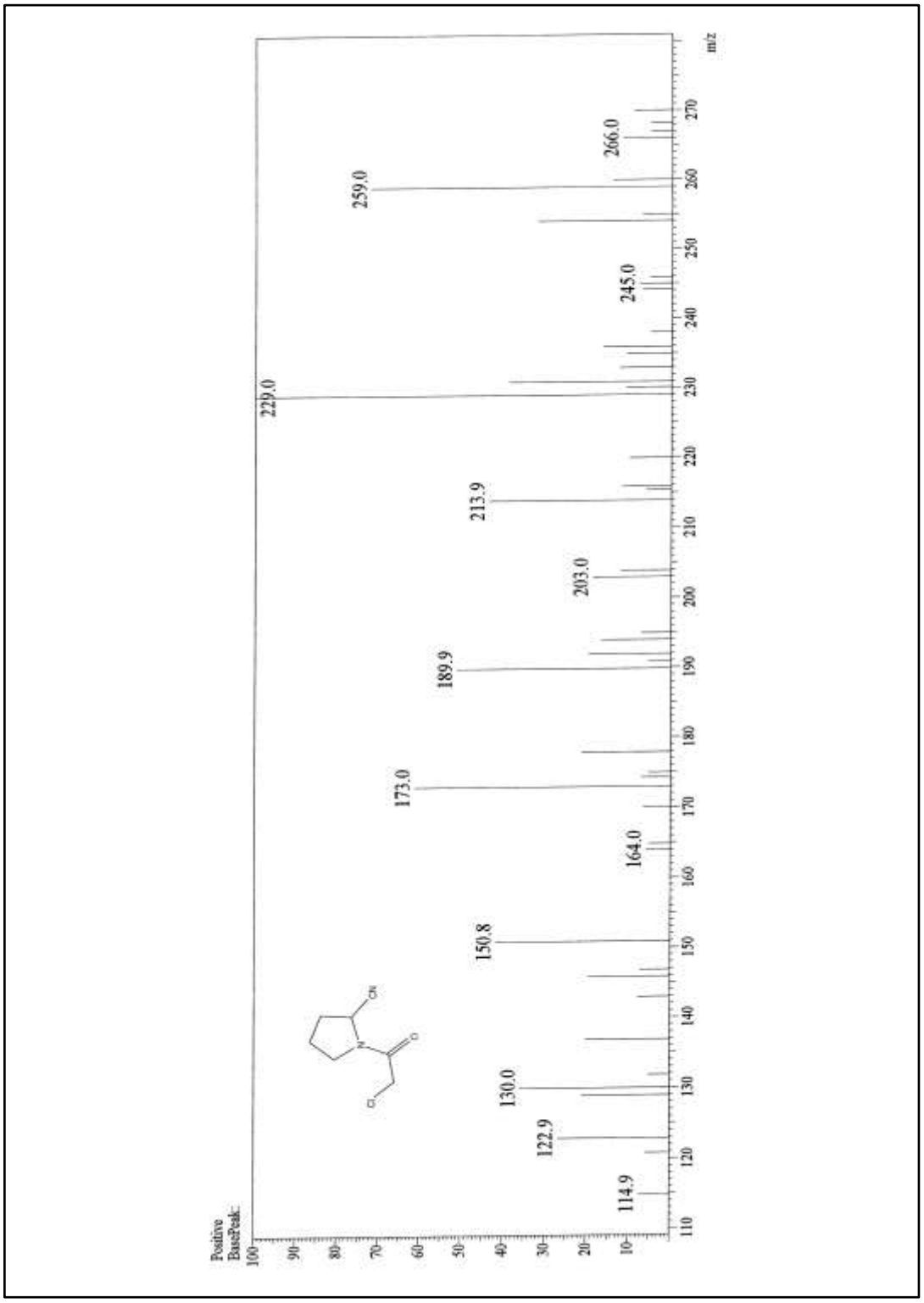

Figure 2.4.4: ESI-MS spectrum of *(S)*-1-(2-chloroacetyl)pyrrolidine-2-carbonitrile **5a**

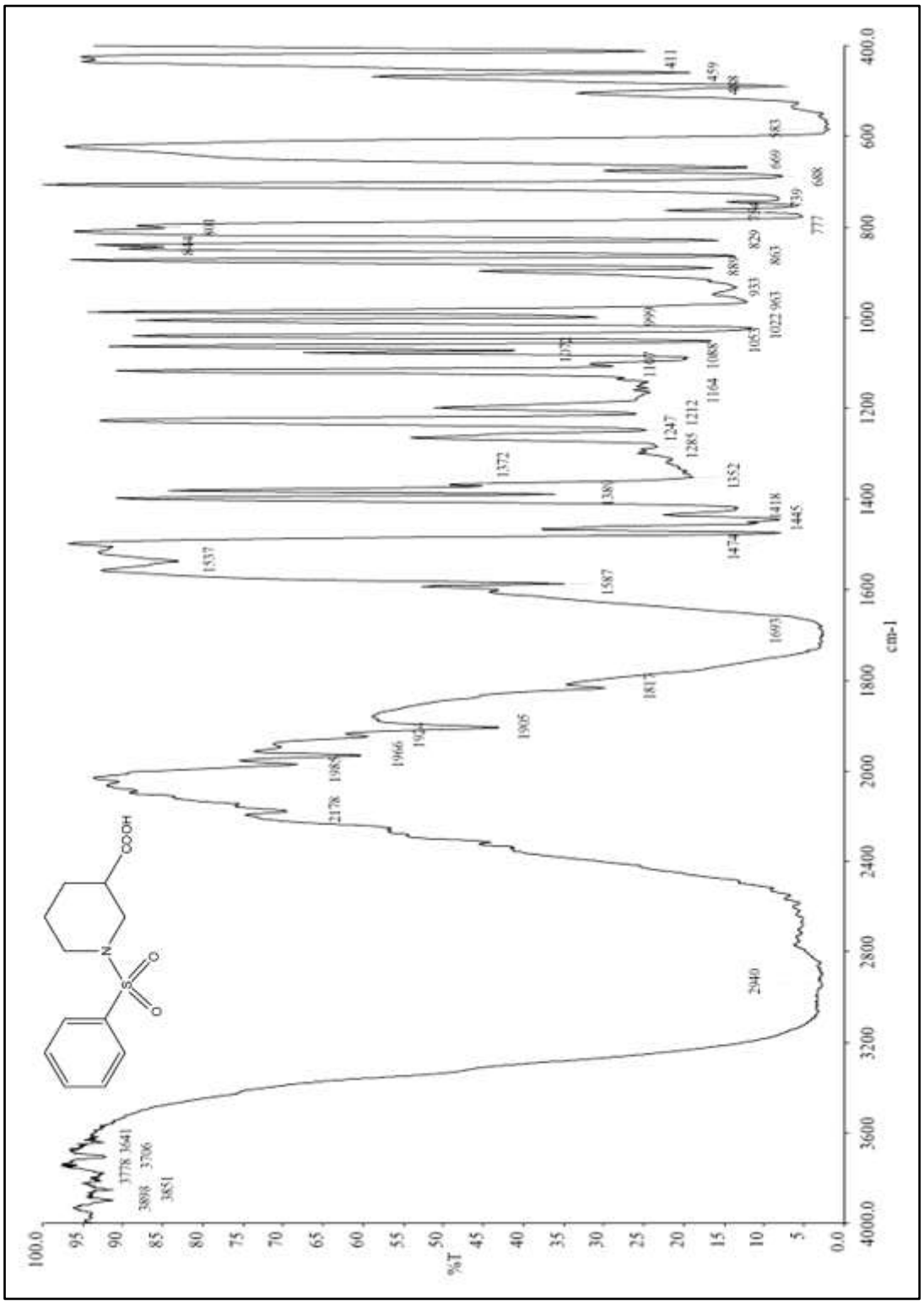

Figure 2.5.1: IR spectrum of 1-(phenylsulfonyl)piperidine-3-carboxylic acid **7a**

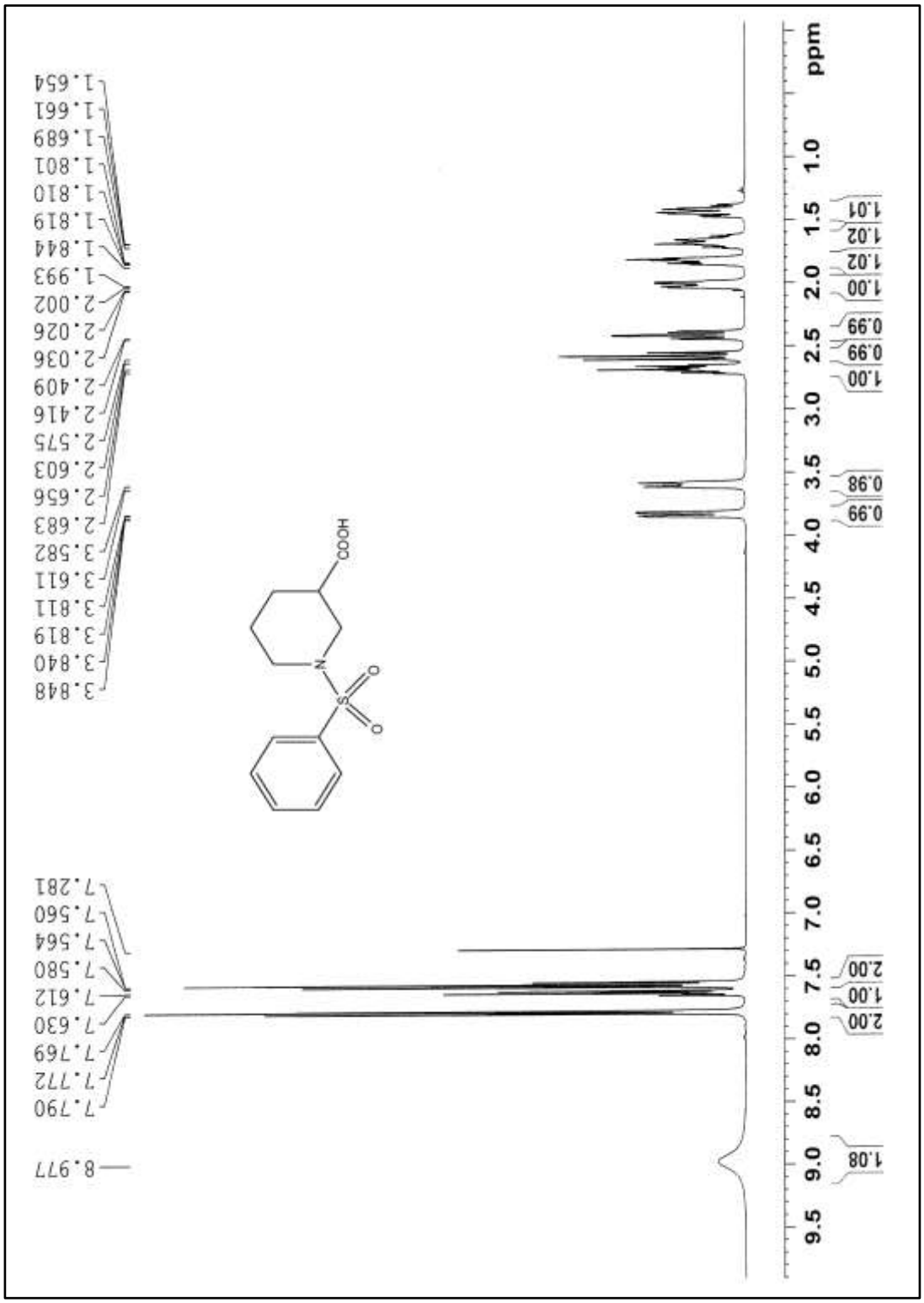

Figure 2.5.2: ^{1}H NMR spectrum of 1-(phenylsulfonyl)piperidine-3-carboxylic acid **7a**

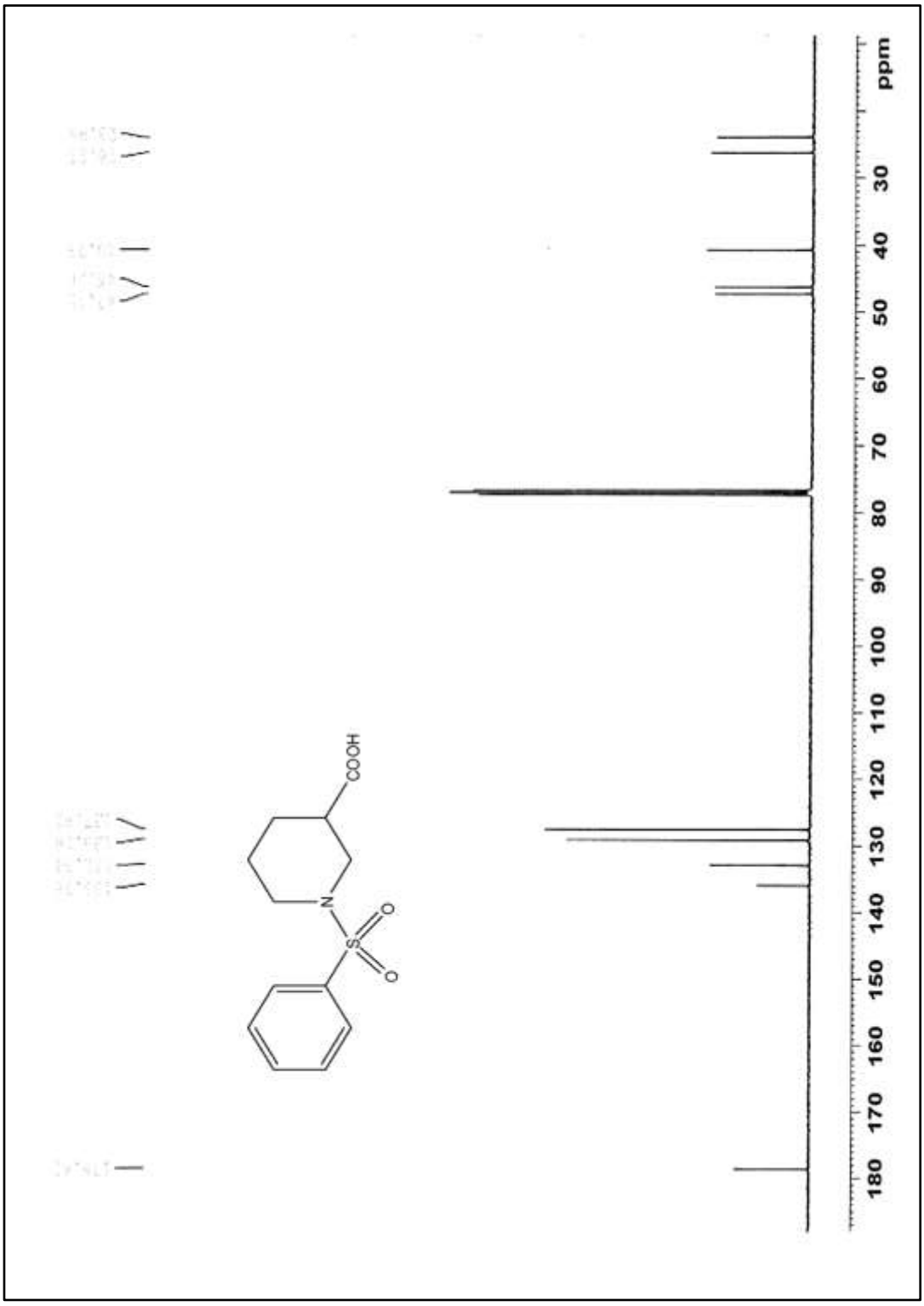

Figure 2.5.3: ^{13}C NMR spectrum of 1-(phenylsulfonyl)piperidine-3-carboxylic acid **7a**

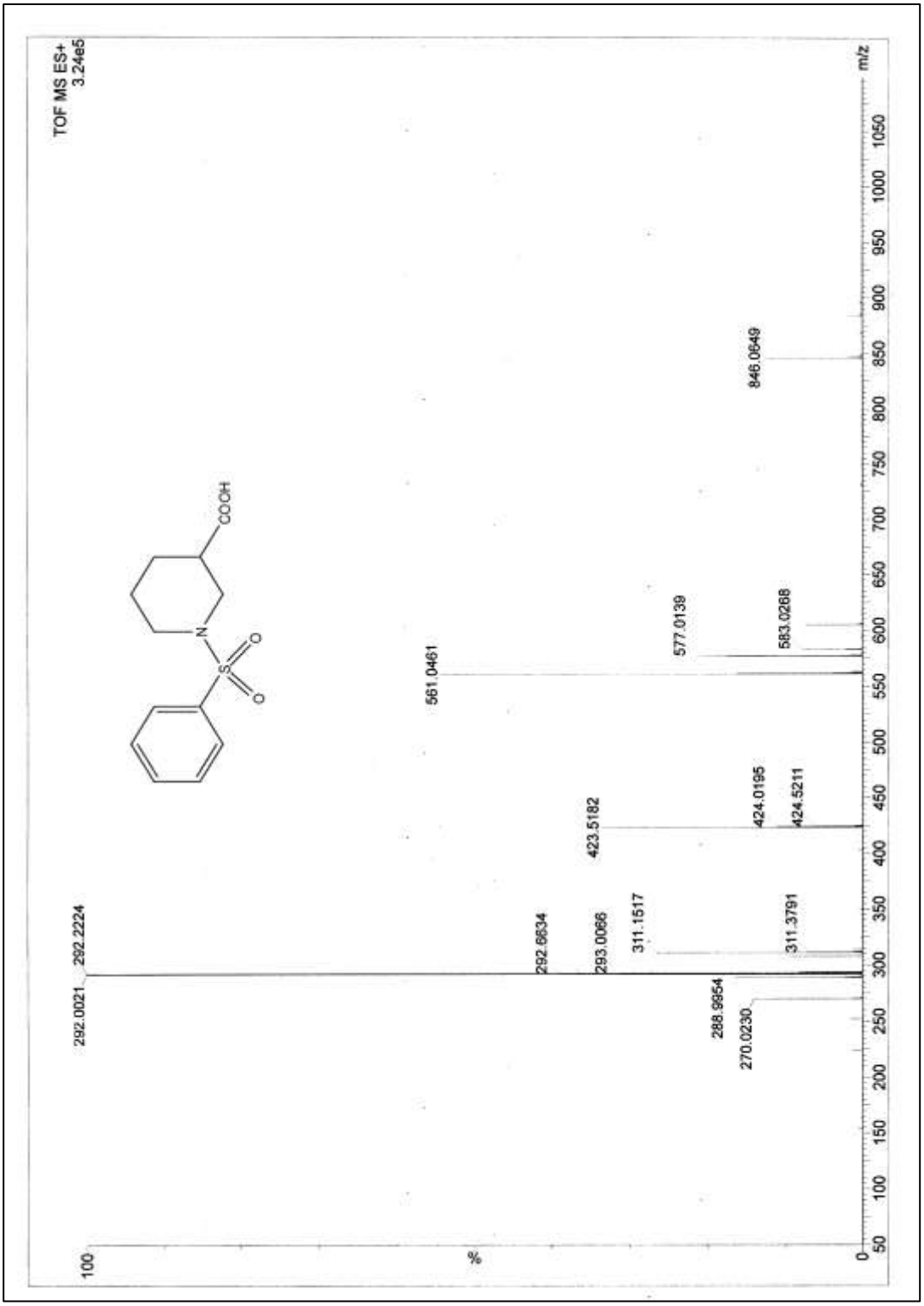

Figure 2.5.4: ESI-MS spectrum of 1-(phenylsulfonyl)piperidine-3-carboxylic acid **7a**

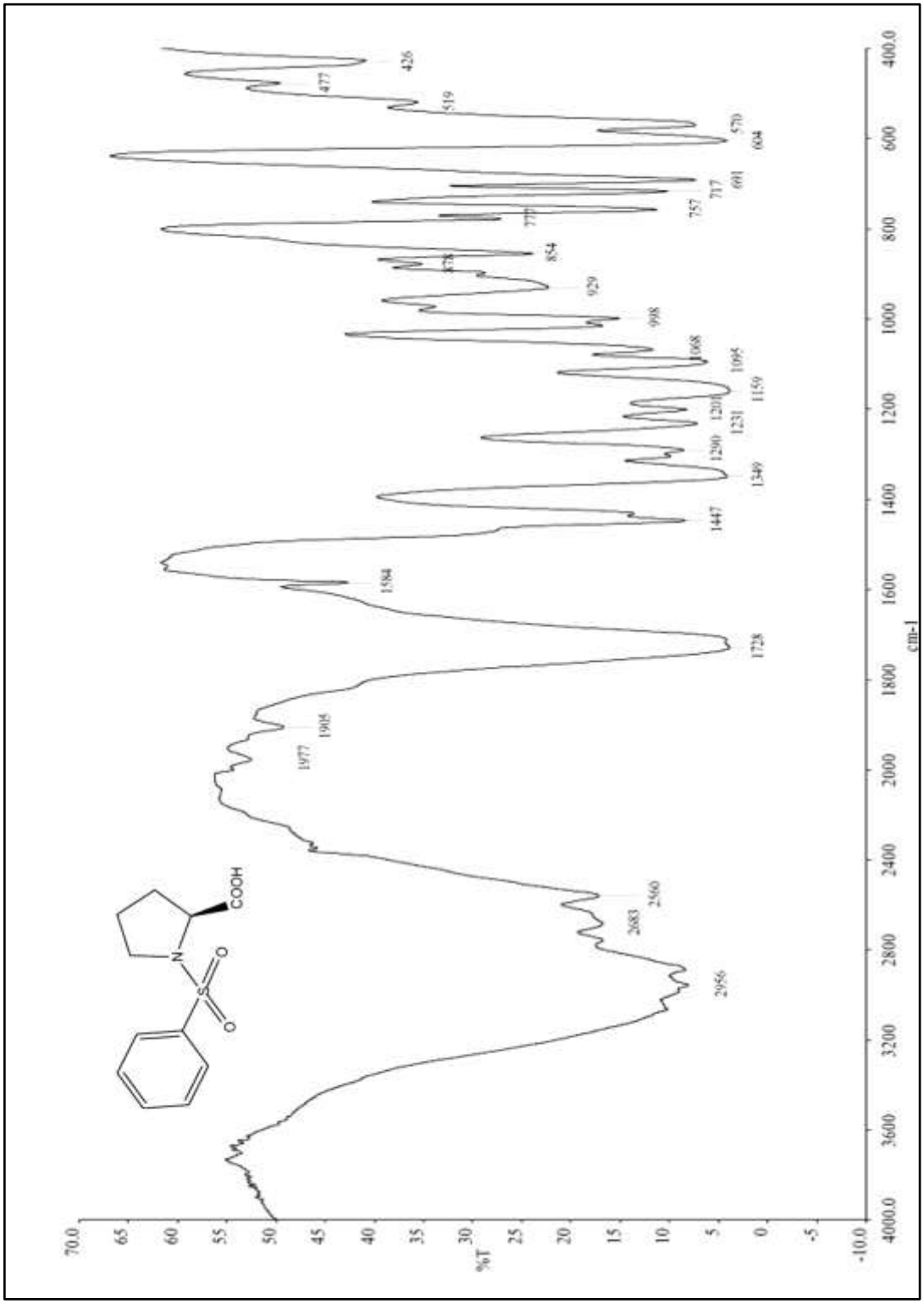

Figure 2.6.1: IR spectrum of *(S)*-1-(phenylsulfonyl)pyrrolidine-2-carboxylic acid **7b**

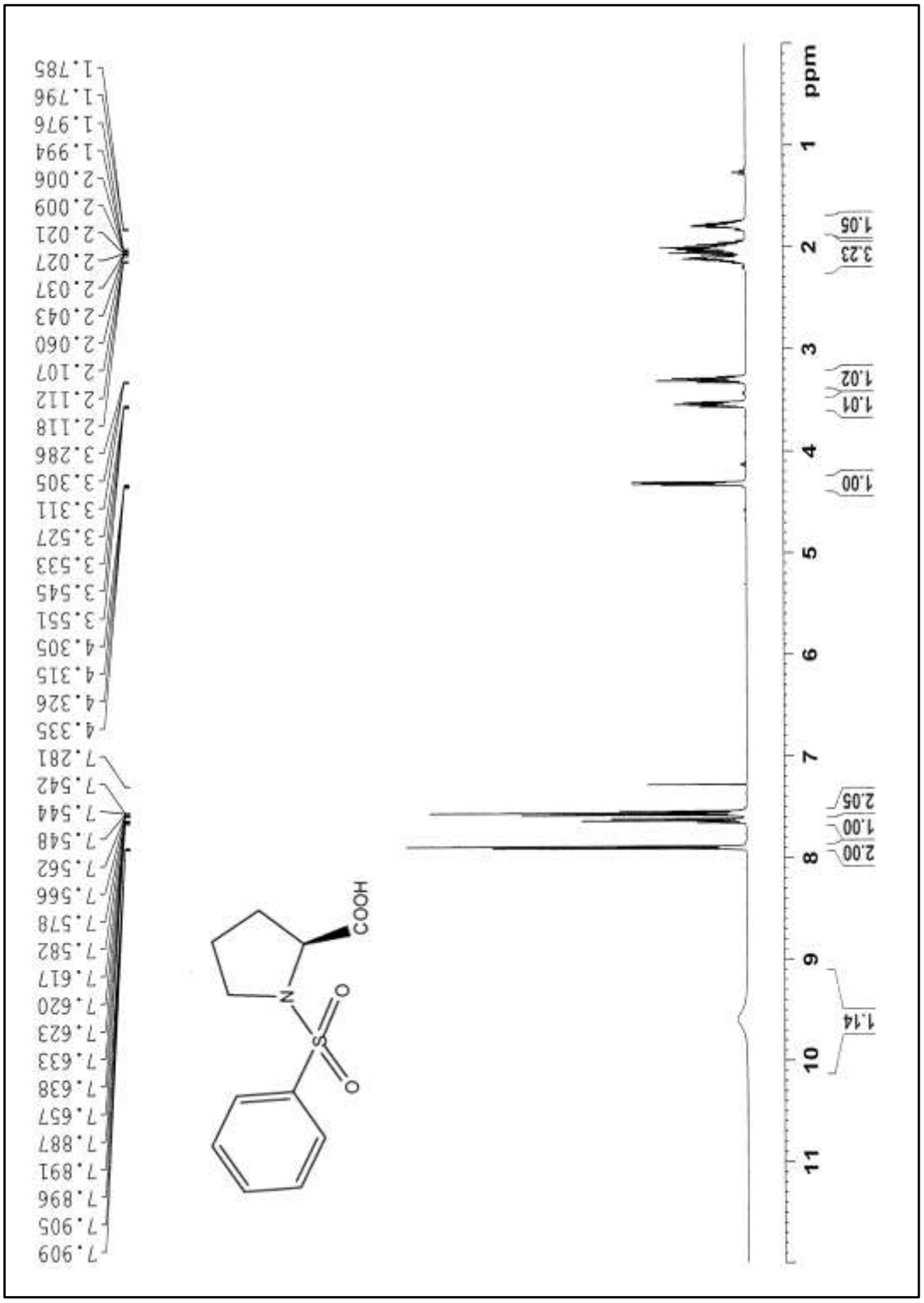

Figure 2.6.2: ^{1}H NMR spectrum of *(S)*-1-(phenylsulfonyl)pyrrolidine-2-carboxylic acid **7b**

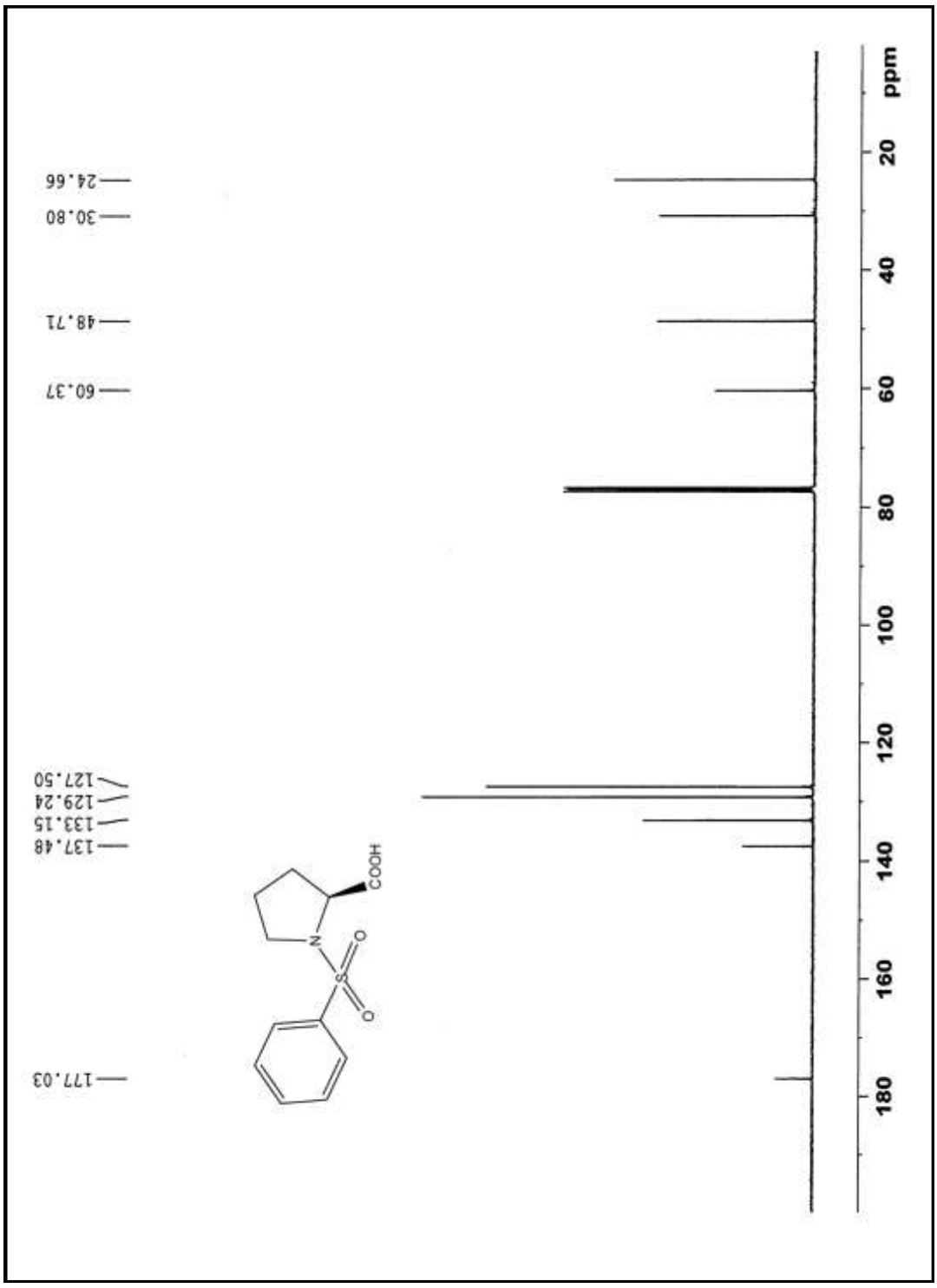

Figure 2.6.3: ^{13}C NMR spectrum of *(S)*-1-(phenylsulfonyl)pyrrolidine-2-carboxylic acid **7b**

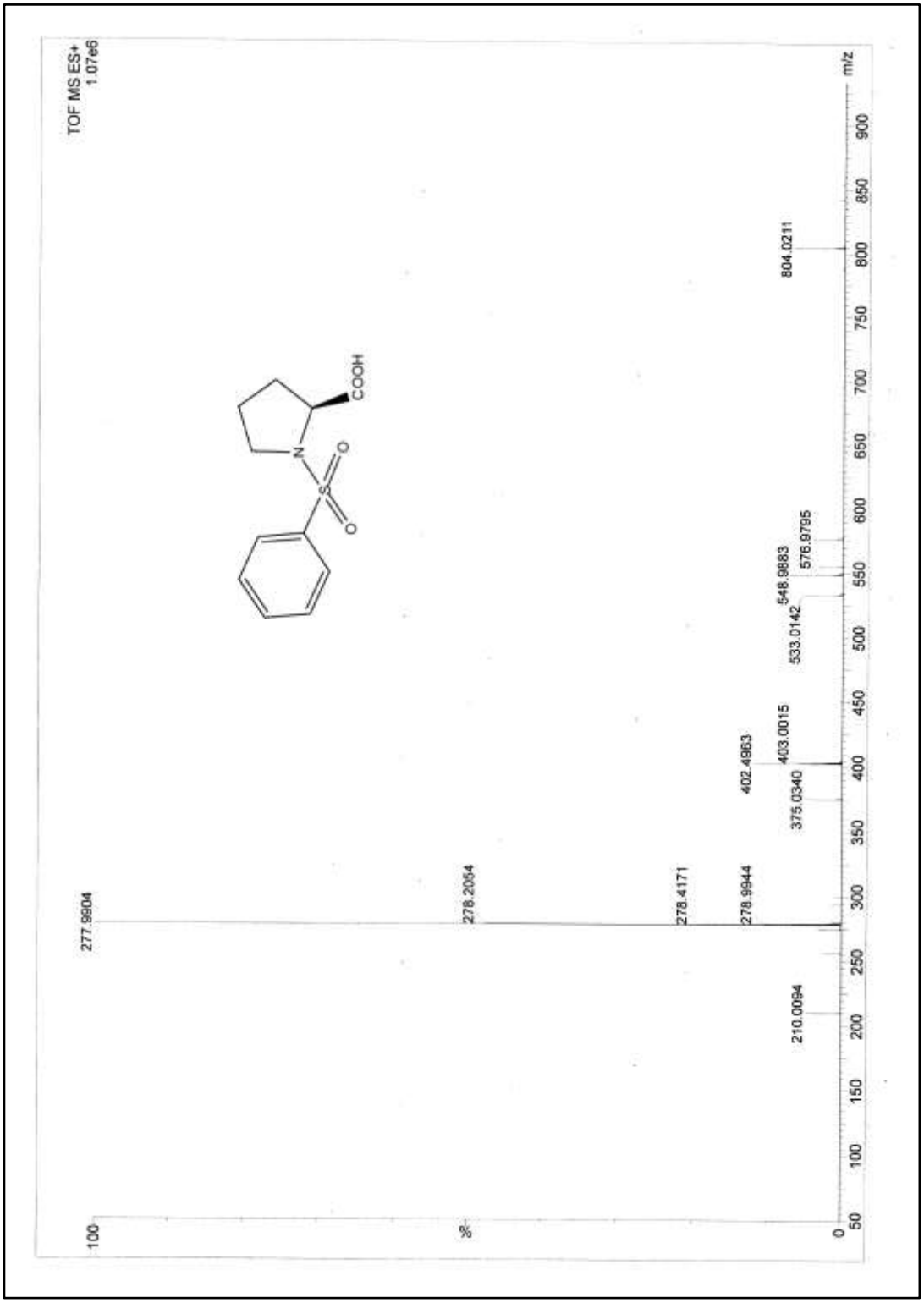

Figure 2.6.4: ESI-MS spectrum of *(S)*-1-(phenylsulfonyl)pyrrolidine-2-carboxylic acid **7b**

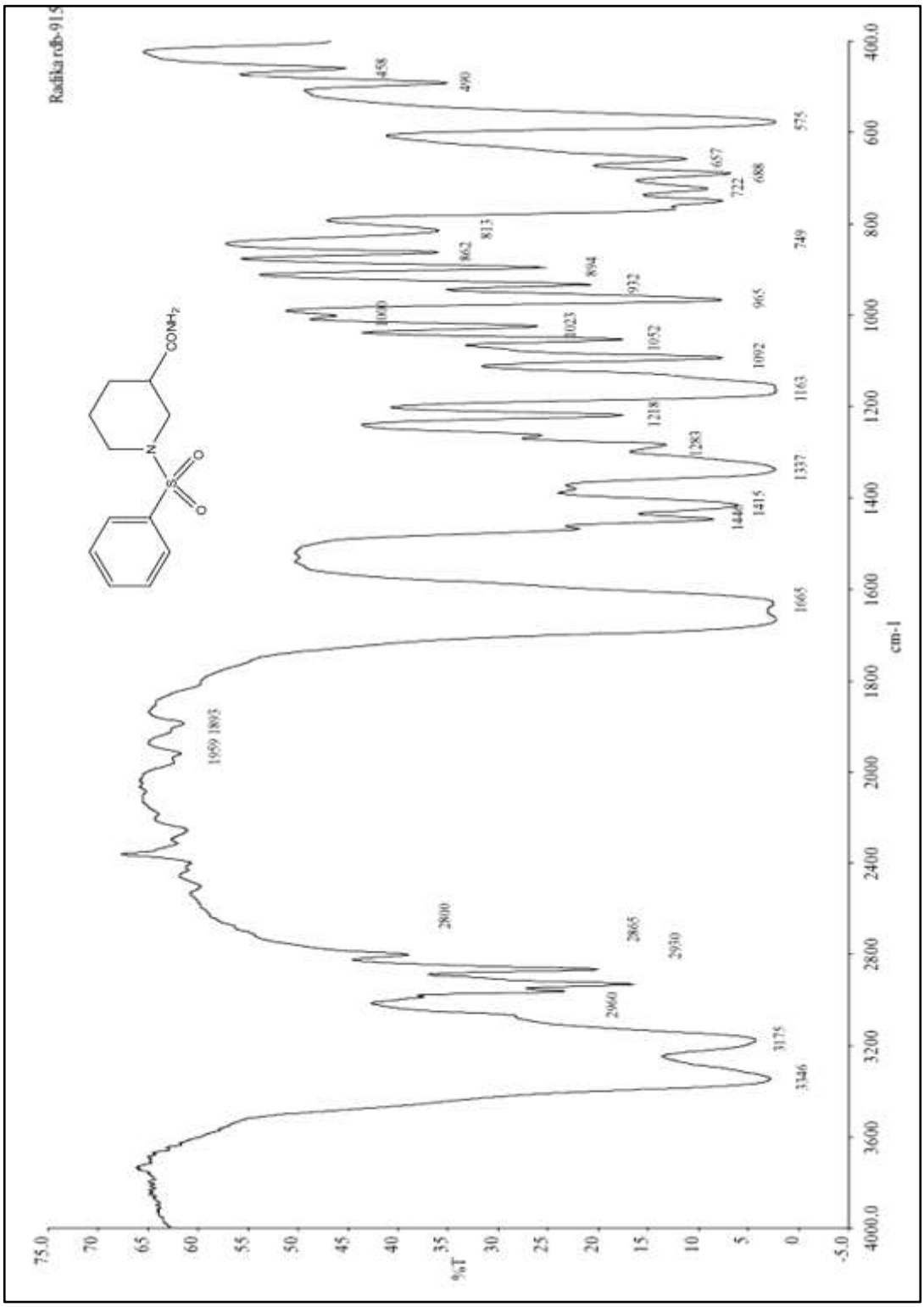

Figure 2.7.1: IR spectrum of 1-(phenylsulfonyl)piperidine-3-carboxamide **8a**

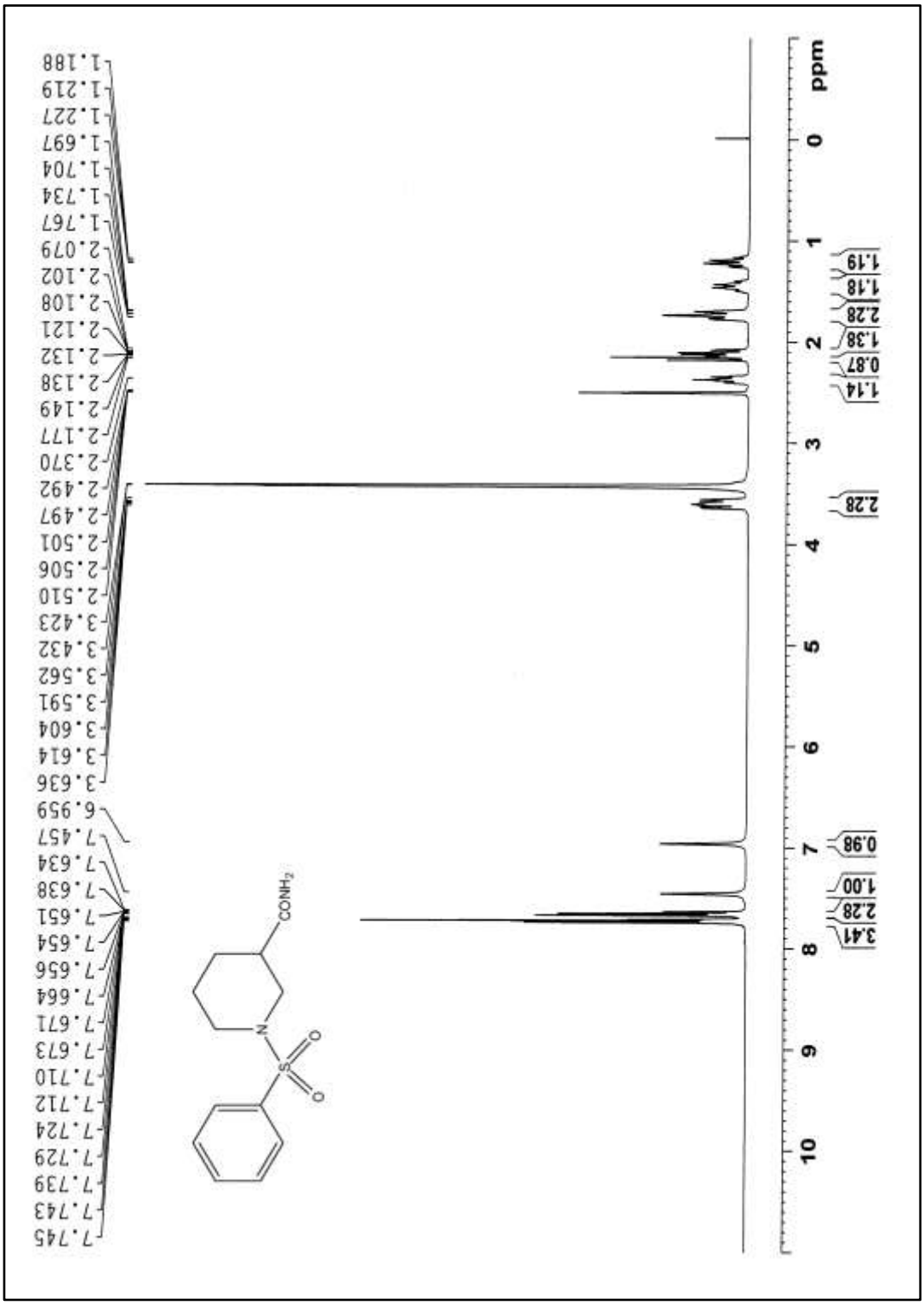

Figure 2.7.2: ^{1}H NMR spectrum of 1-(phenylsulfonyl)piperidine-3-carboxamide **8a**

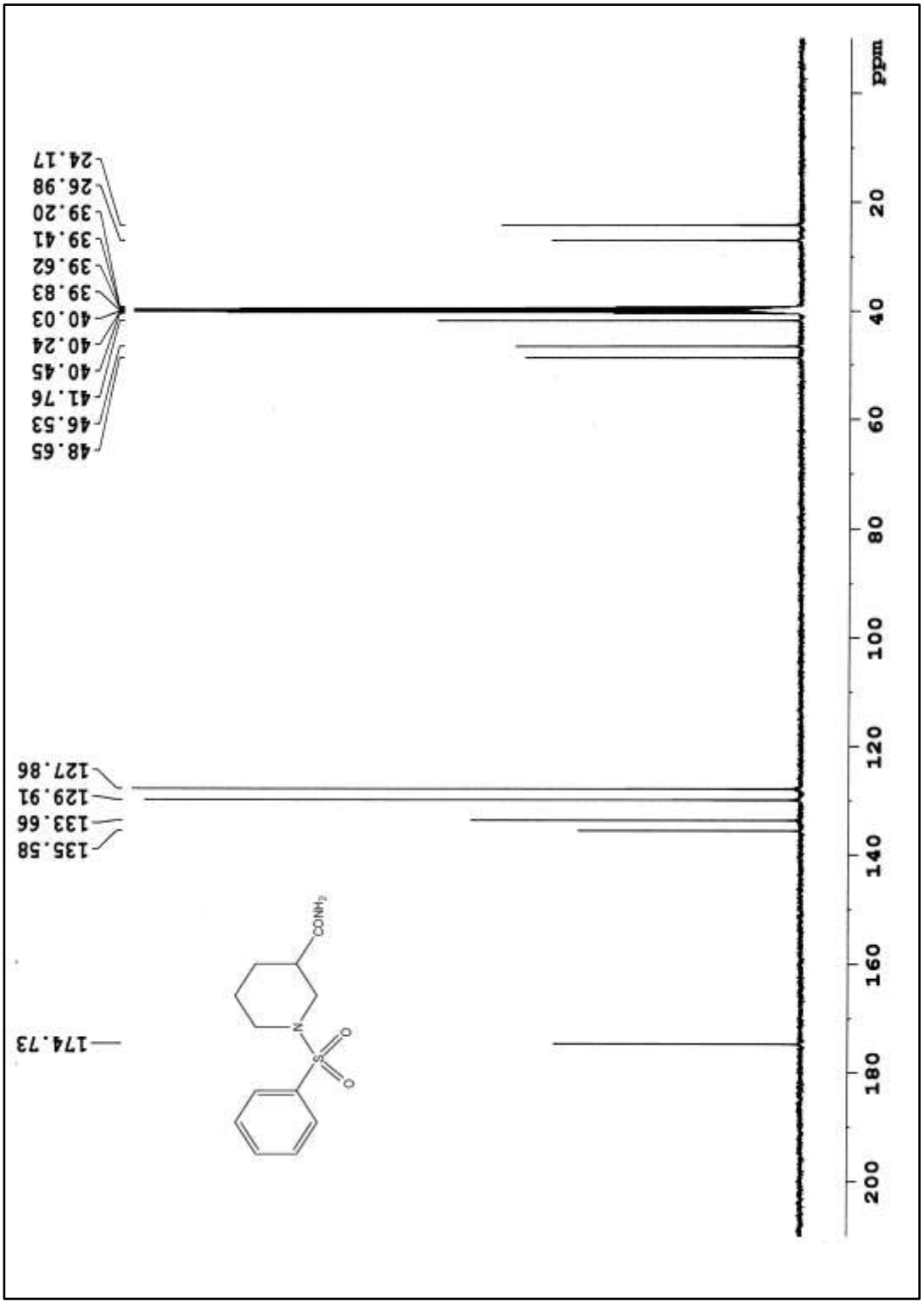

Figure 2.7.3: ^{13}C NMR spectrum of 1-(phenylsulfonyl)piperidine-3-carboxamide **8a**

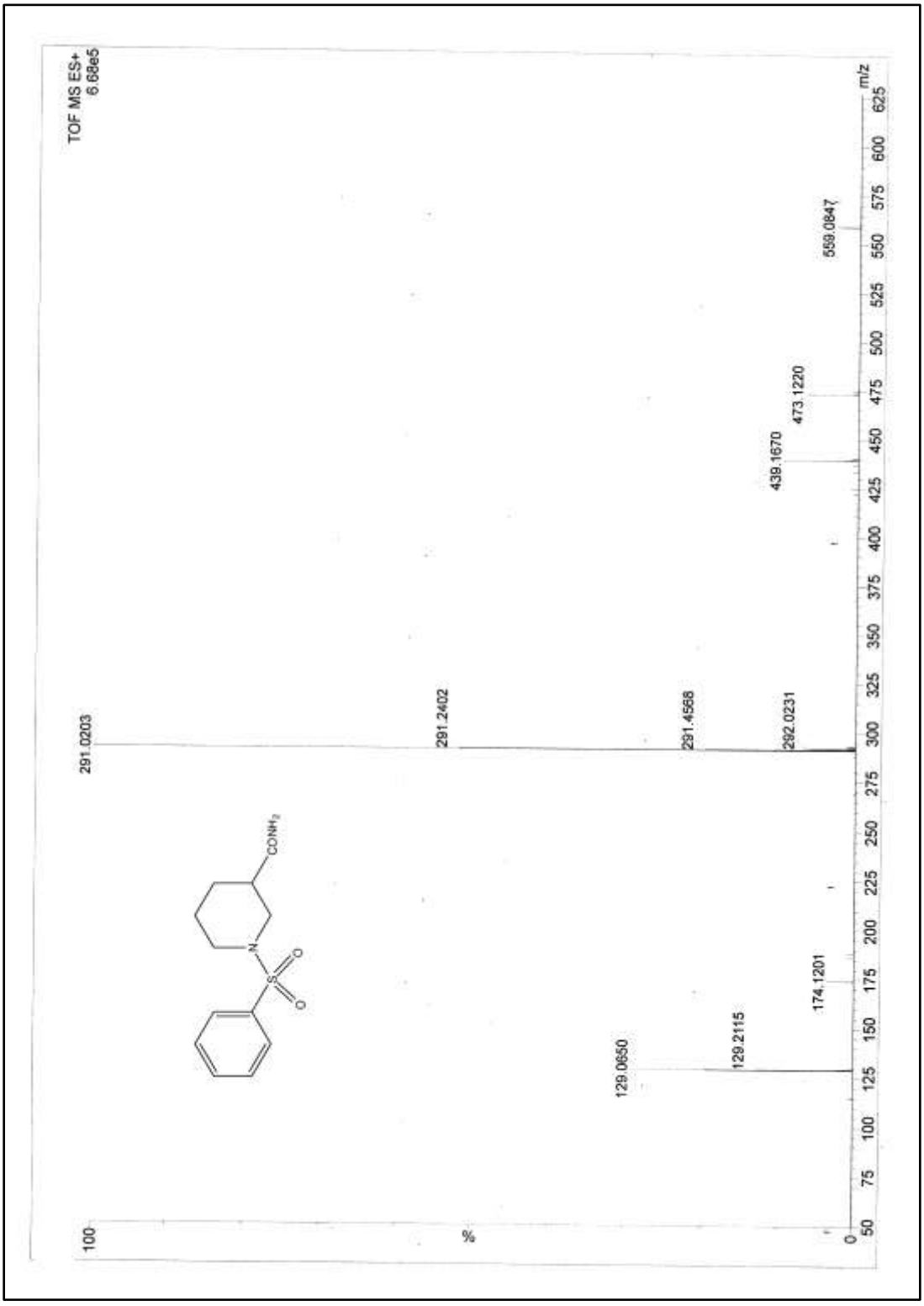

Figure 2.7.4: ESI-MS spectrum of 1-(phenylsulfonyl)piperidine-3-carboxamide **8a**

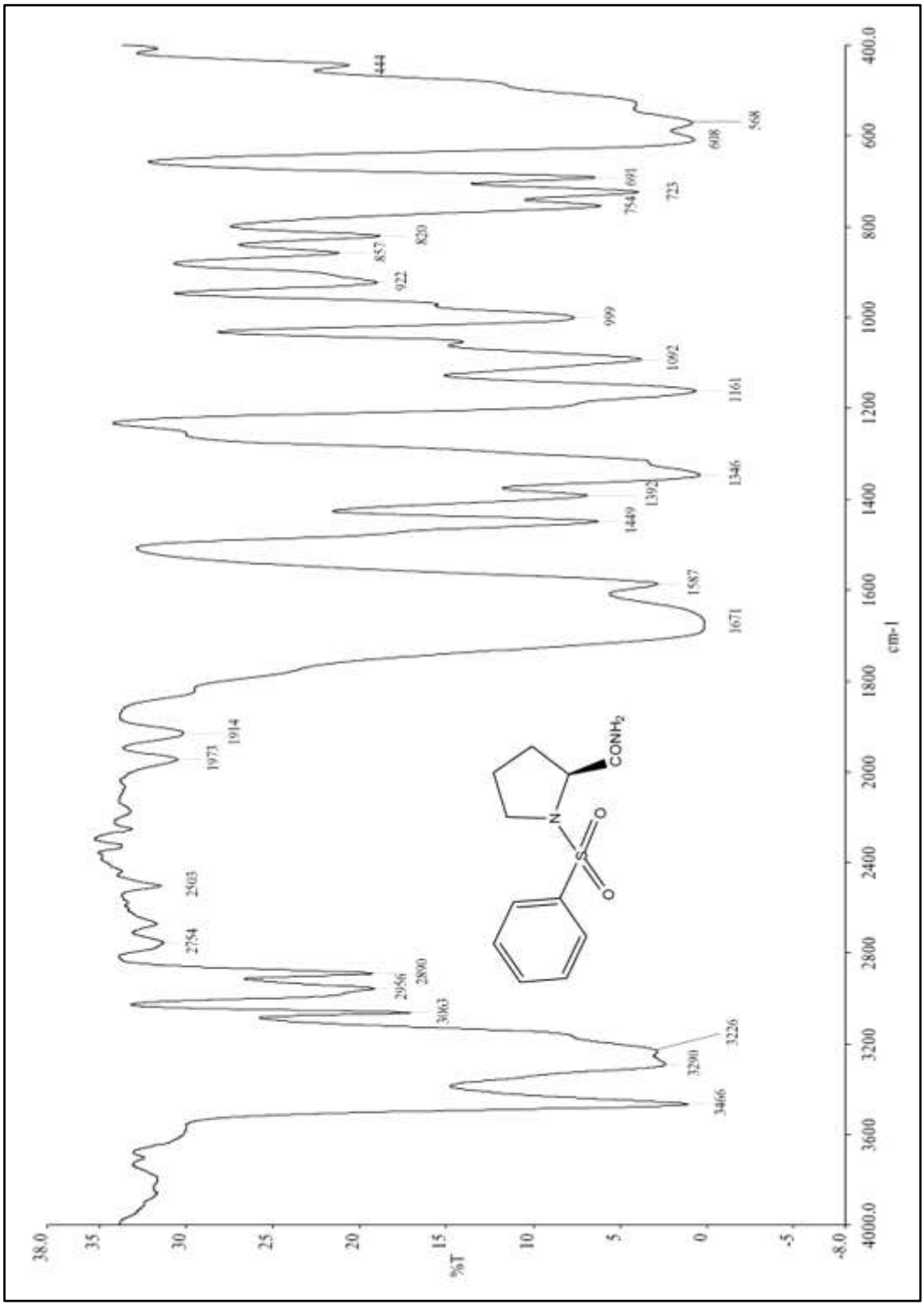

Figure 2.8.1: IR spectrum of *(S)*-1-(phenylsulfonyl)pyrrolidine-2-carboxamide **8b**

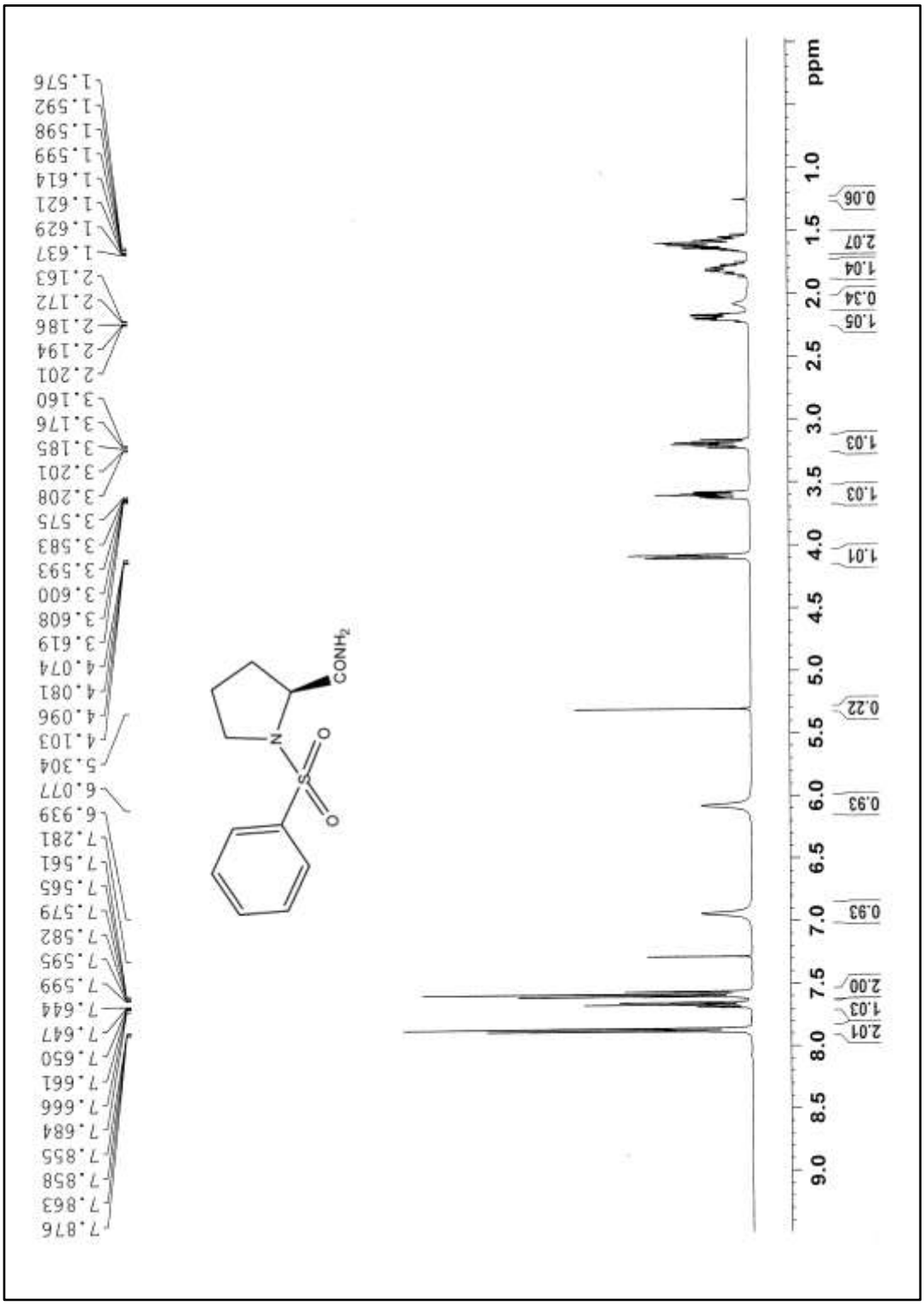

Figure 2.8.2: ^{1}H NMR spectrum of *(S)*-1-(phenylsulfonyl)pyrrolidine-2-carboxamide **8b**

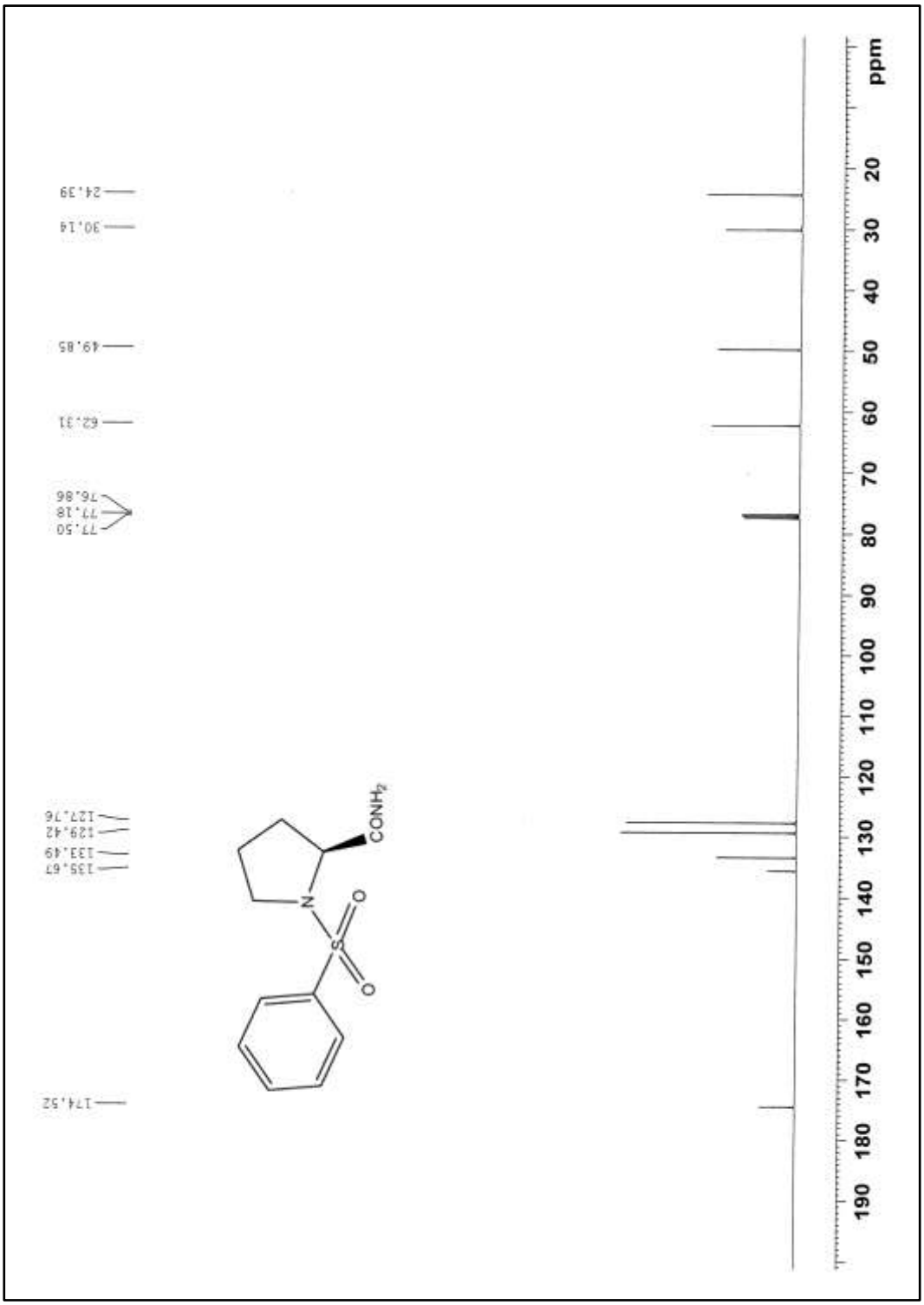

Figure 2.8.3: ^{13}C NMR spectrum of *(S)*-1-(phenylsulfonyl)pyrrolidine-2-carboxamide **8b**

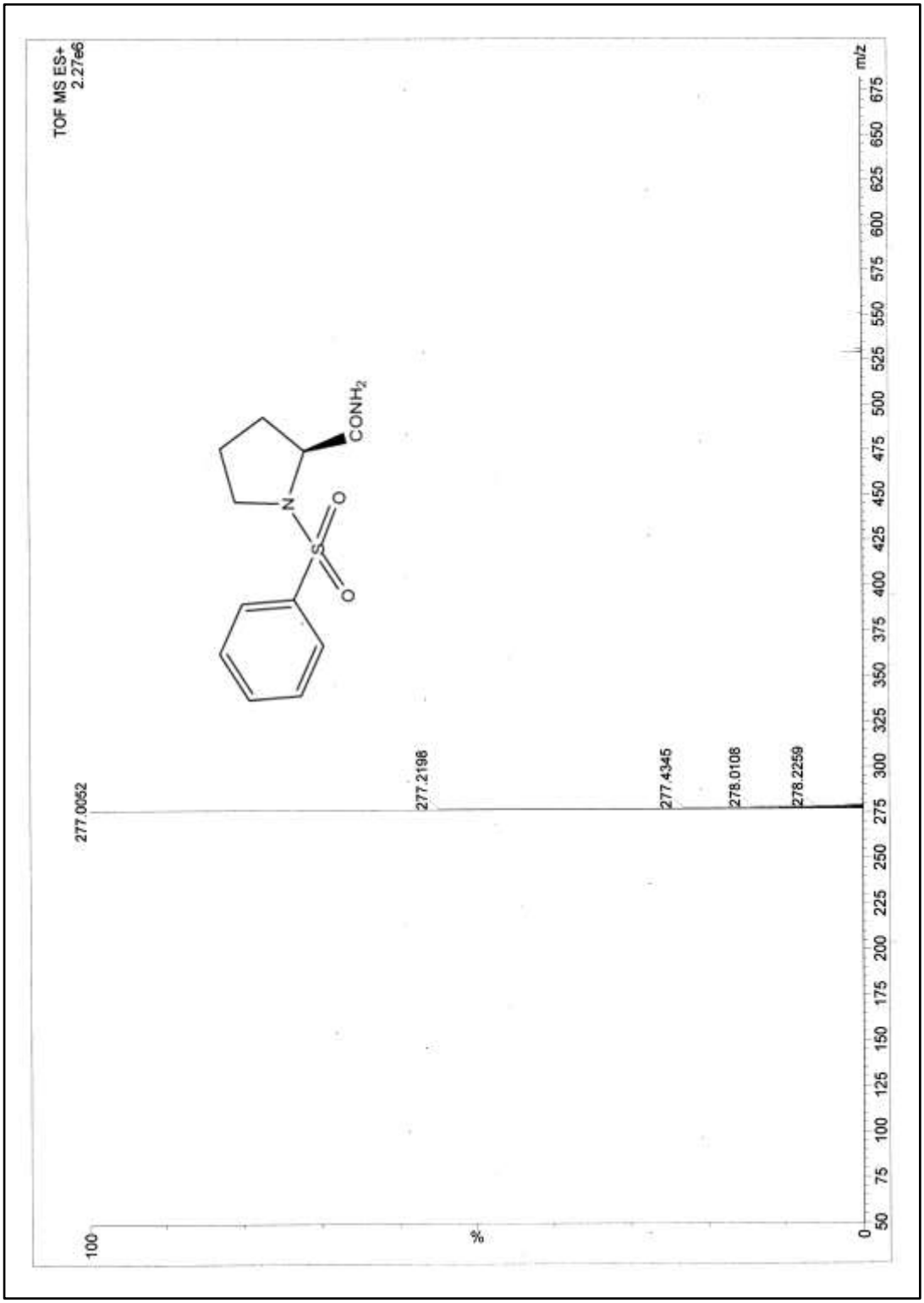

Figure 2.8.4: ESI-MS spectrum of *(S)*-1-(phenylsulfonyl)pyrrolidine-2-carboxamide **8b**

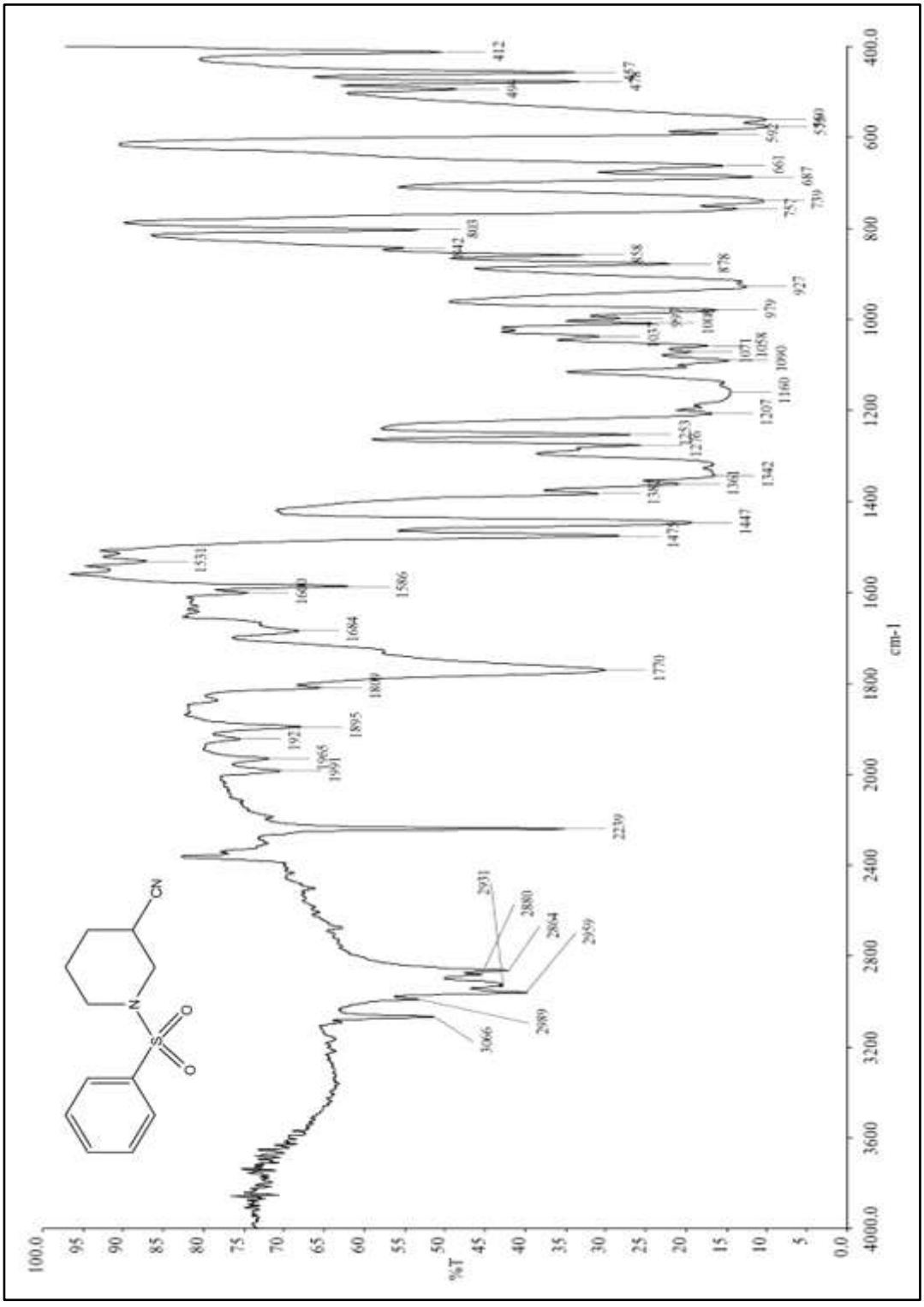

Figure 2.9.1: IR spectrum of 1-(phenylsulfonyl)piperidine-3-carbonitrile **9a**

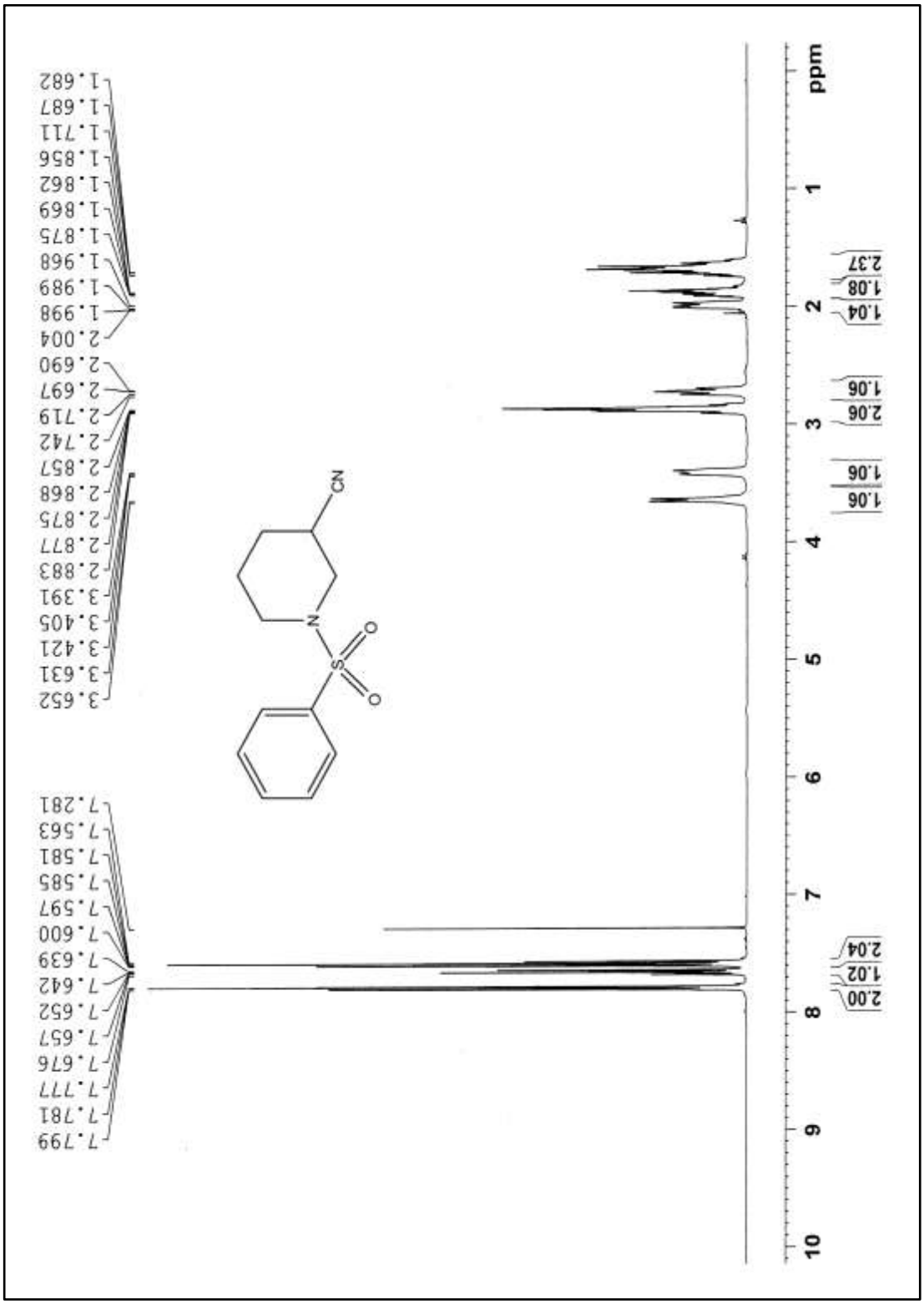

Figure 2.9.2: ^{1}H NMR spectrum of 1-(phenylsulfonyl)piperidine-3-carbonitrile **9a**

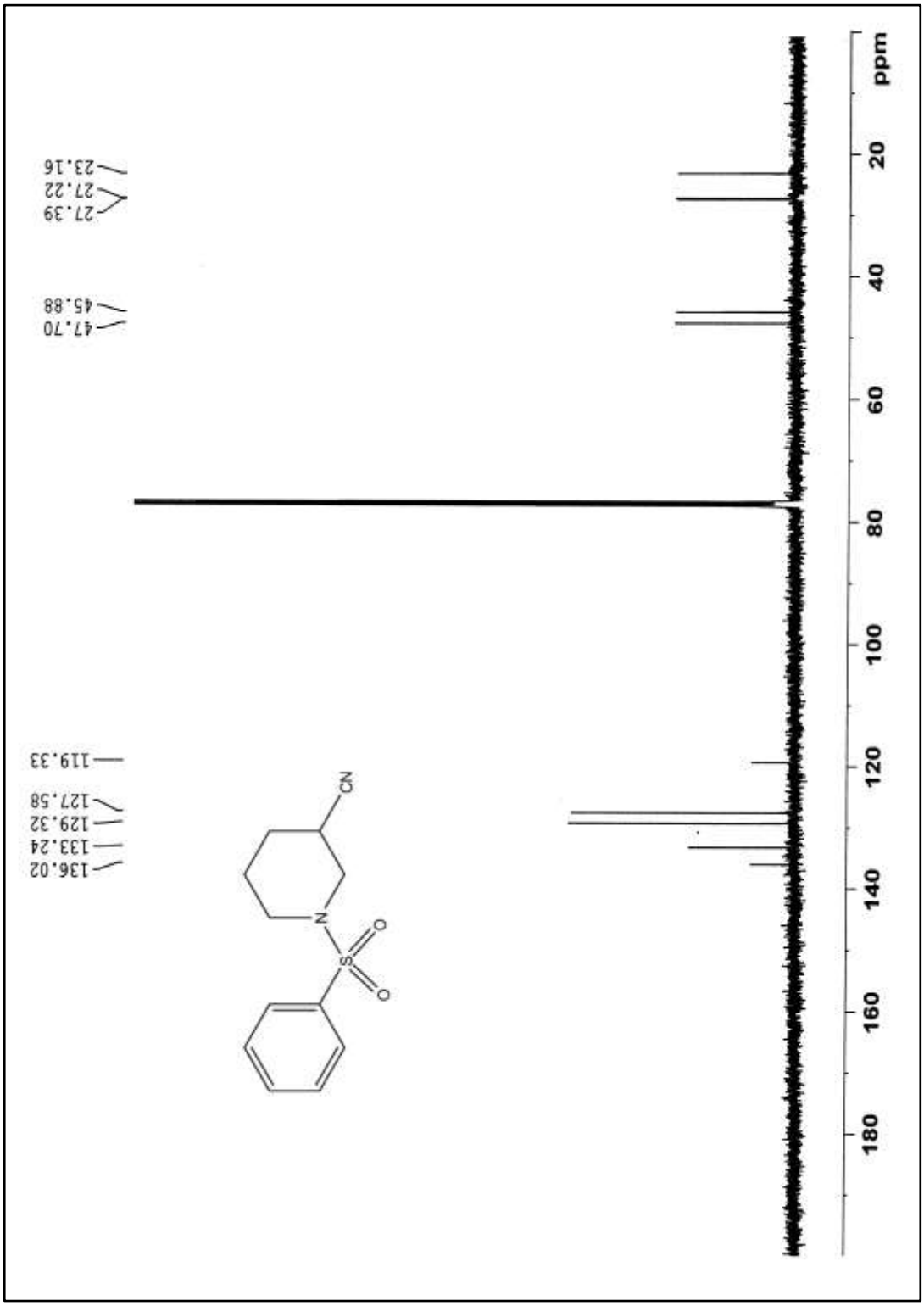

Figure 2.9.3: ^{13}C NMR spectrum of 1-(phenylsulfonyl)piperidine-3-carbonitrile **9a**

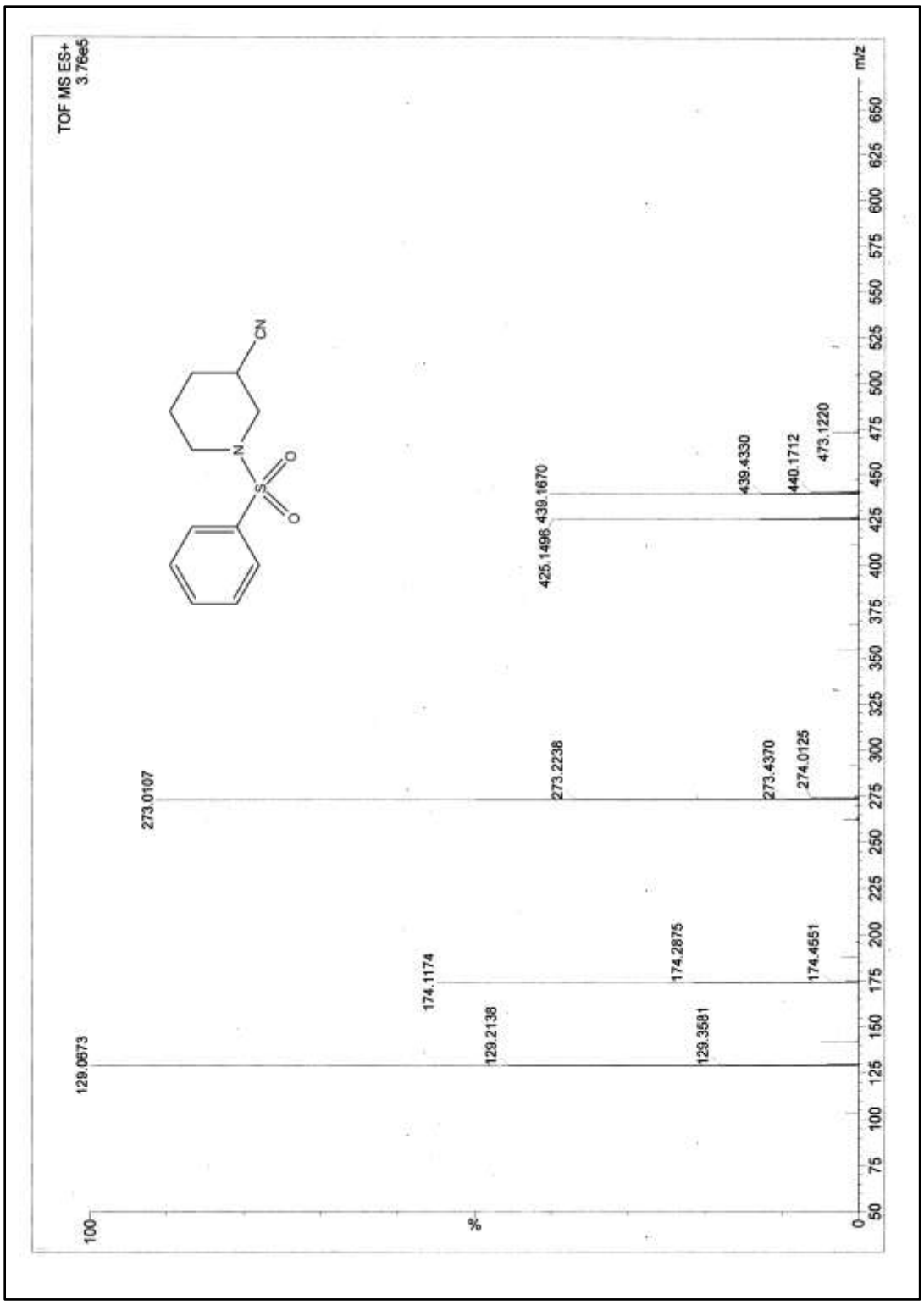

Figure 2.9.4: ESI-MS spectrum of 1-(phenylsulfonyl)piperidine-3-carbonitrile **9a**

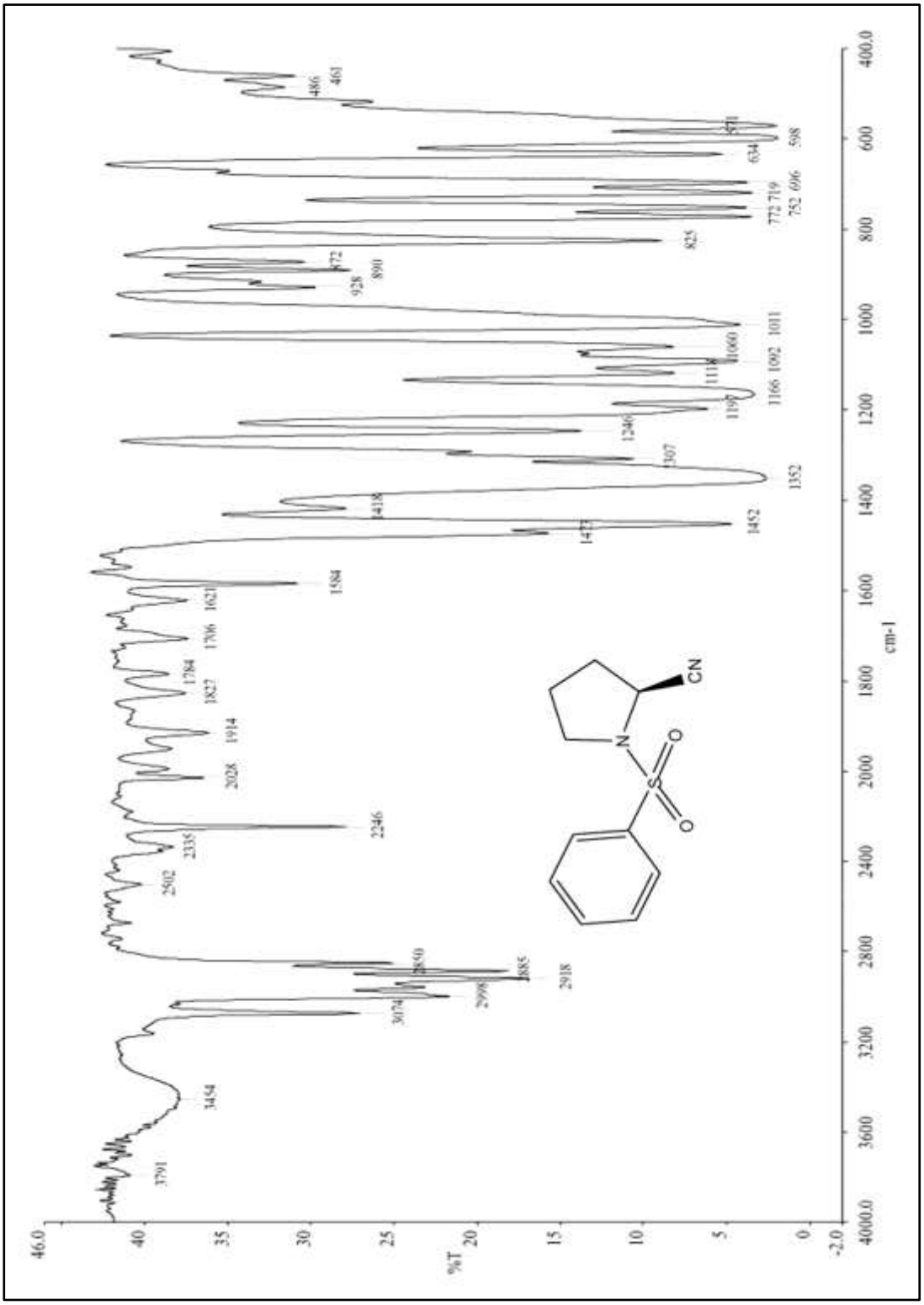

Figure 2.10.1: IR spectrum of *(S)*-1-(phenylsulfonyl)pyrrolidine-2-carbonitrile **9b**

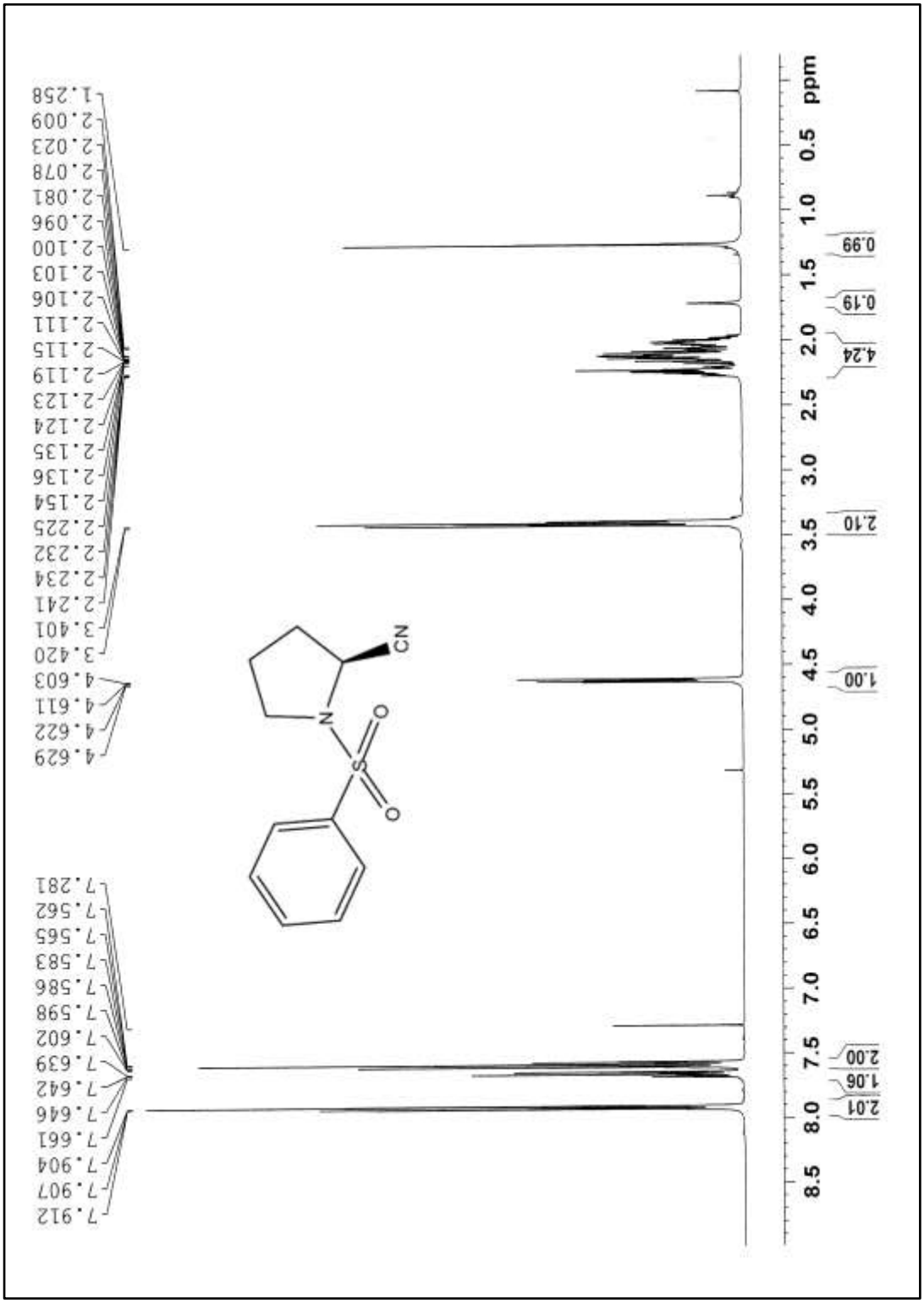

Figure 2.10.2: ^{1}H NMR spectrum of *(S)*-1-(phenylsulfonyl)pyrrolidine-2-carbonitrile **9b**

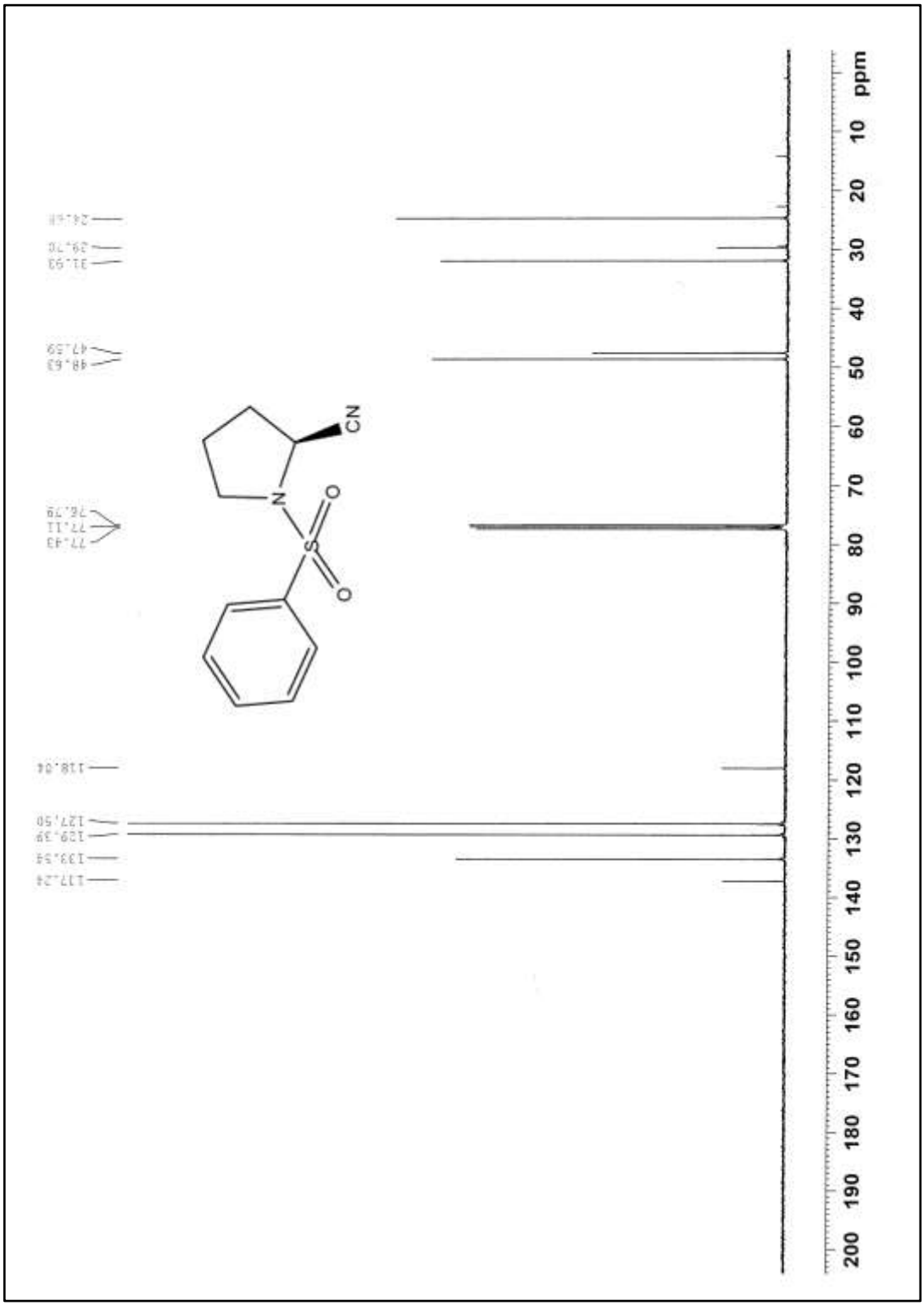

Figure 2.10.3: ^{13}C NMR spectrum of *(S)*-1-(phenylsulfonyl)pyrrolidine-2-carbonitrile **9b**

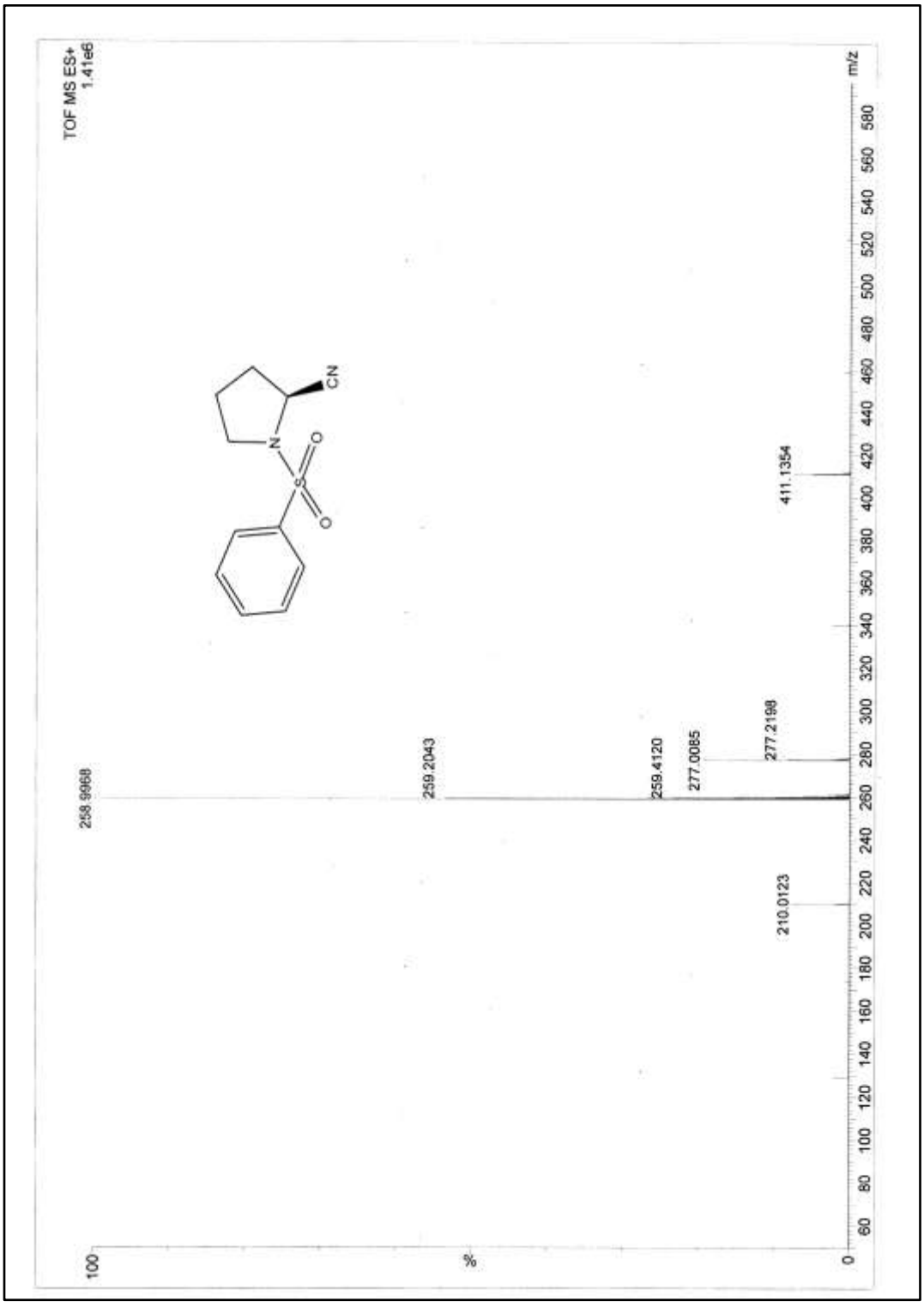

Figure 2.10.4: ESI-MS spectrum of *(S)*-1-(phenylsulfonyl)pyrrolidine-2-carbonitrile **9b**

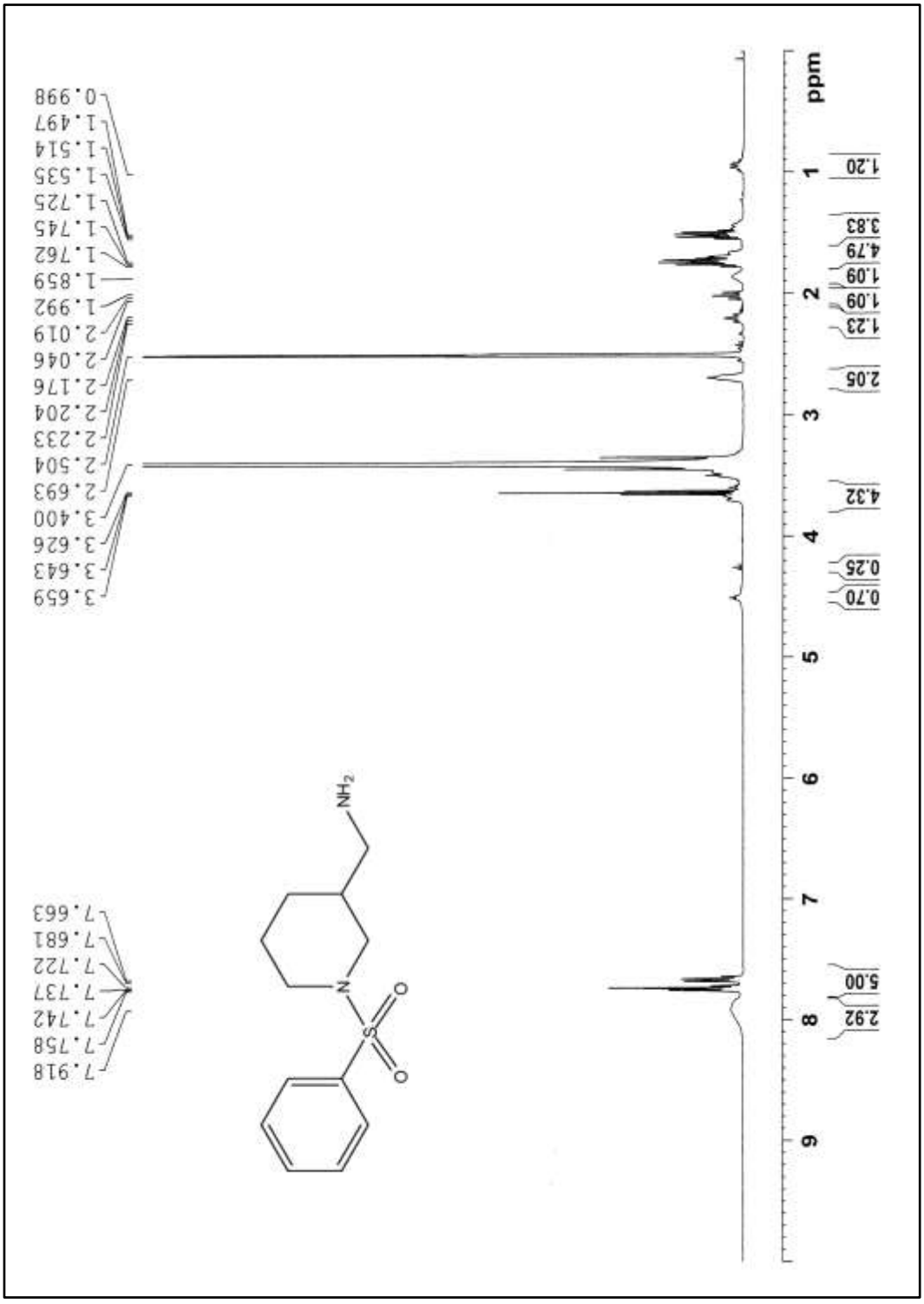

Figure 2.11.1: ^{1}H NMR spectrum of (1-(phenylsulfonyl)piperidin-3-yl)methanamine **10a**

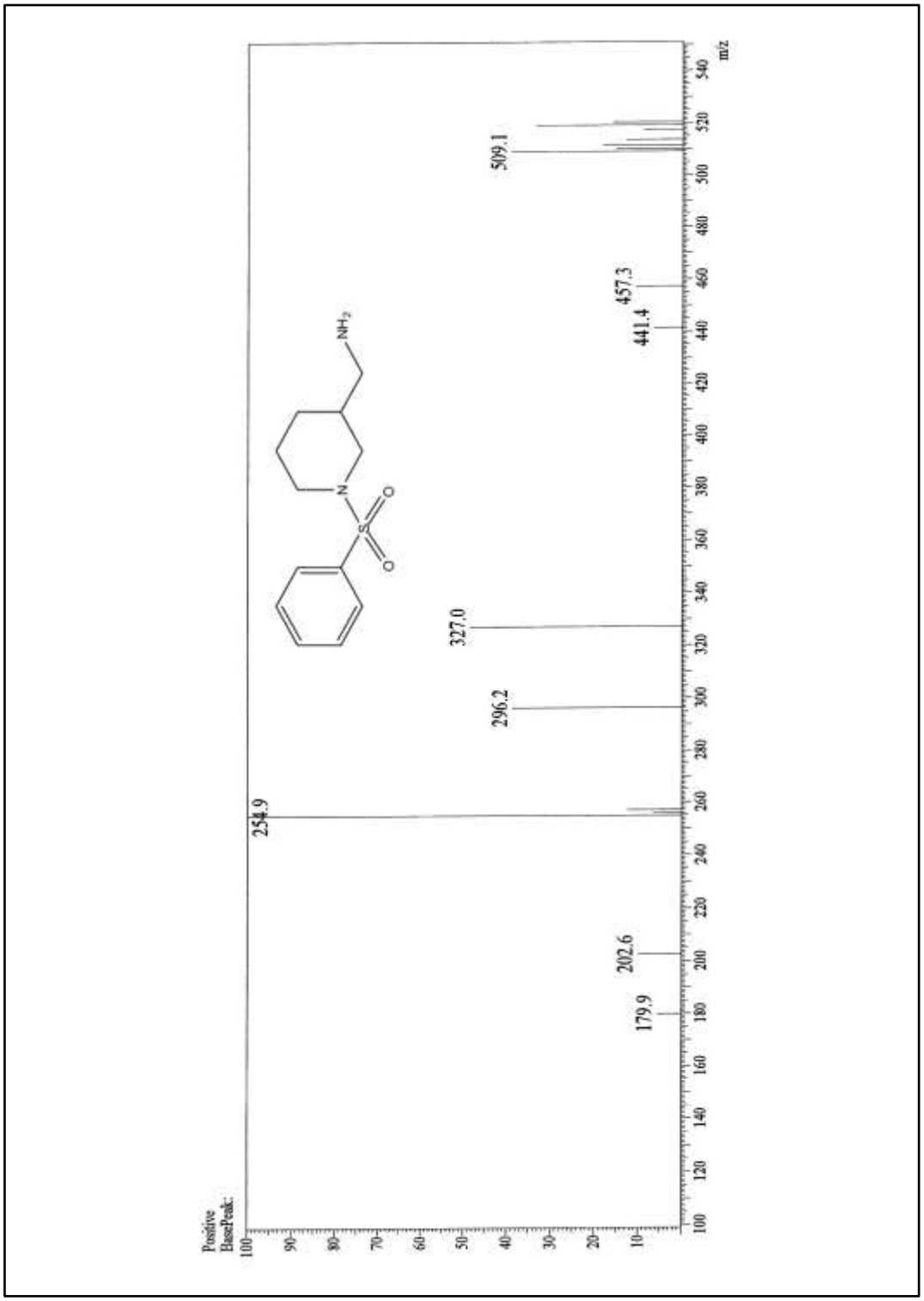

Figure 2.11.2: ESI-MS spectrum of (1-(phenylsulfonyl)piperidin-3-yl)methanamine **10a**

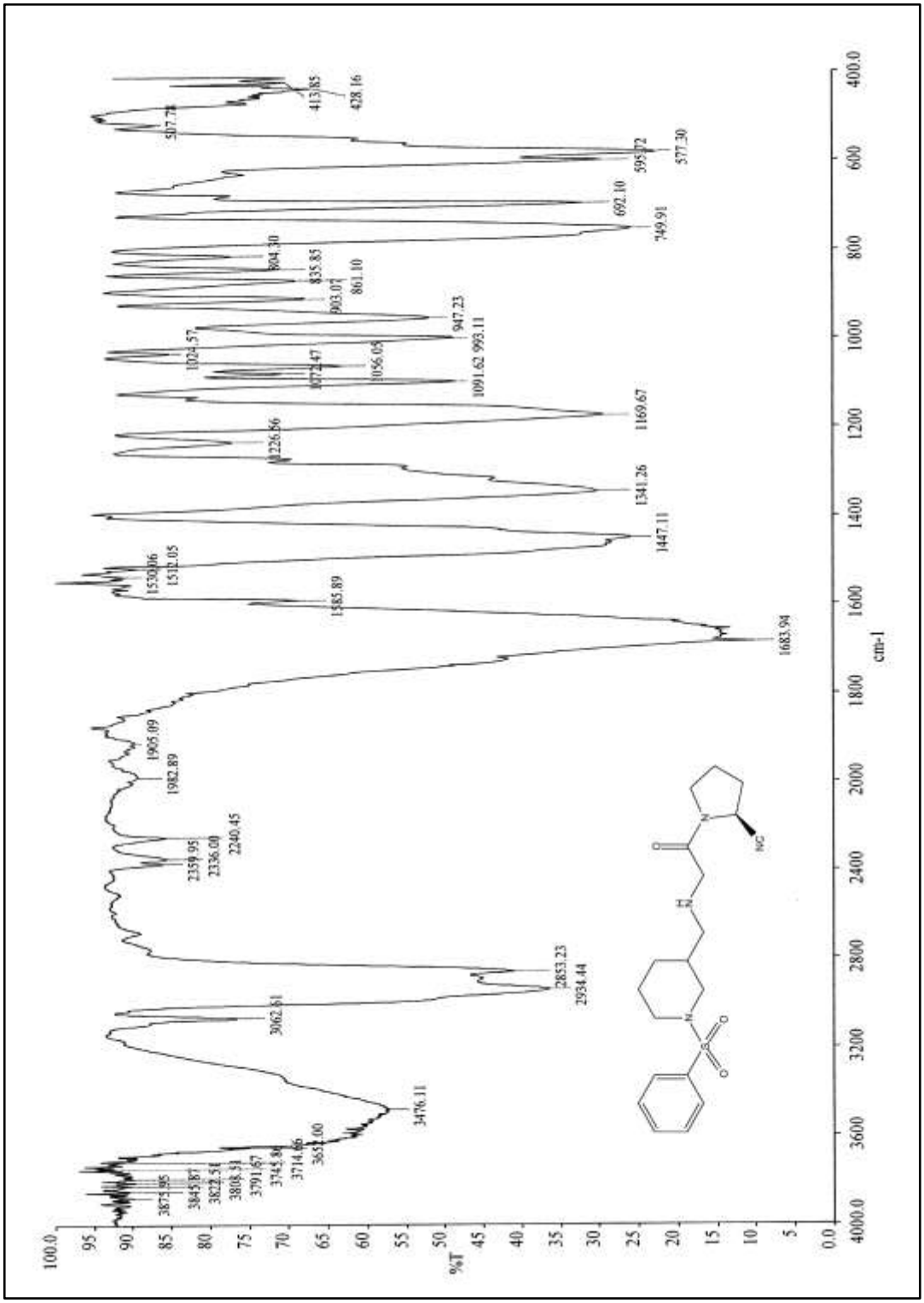

Figure 2.12.1: IR spectrum of (2S)-1-(2-((1-(phenylsulfonyl)piperidin-3-yl) methylamino)acetyl)pyrrolidine-2-carbonitrile **11a**

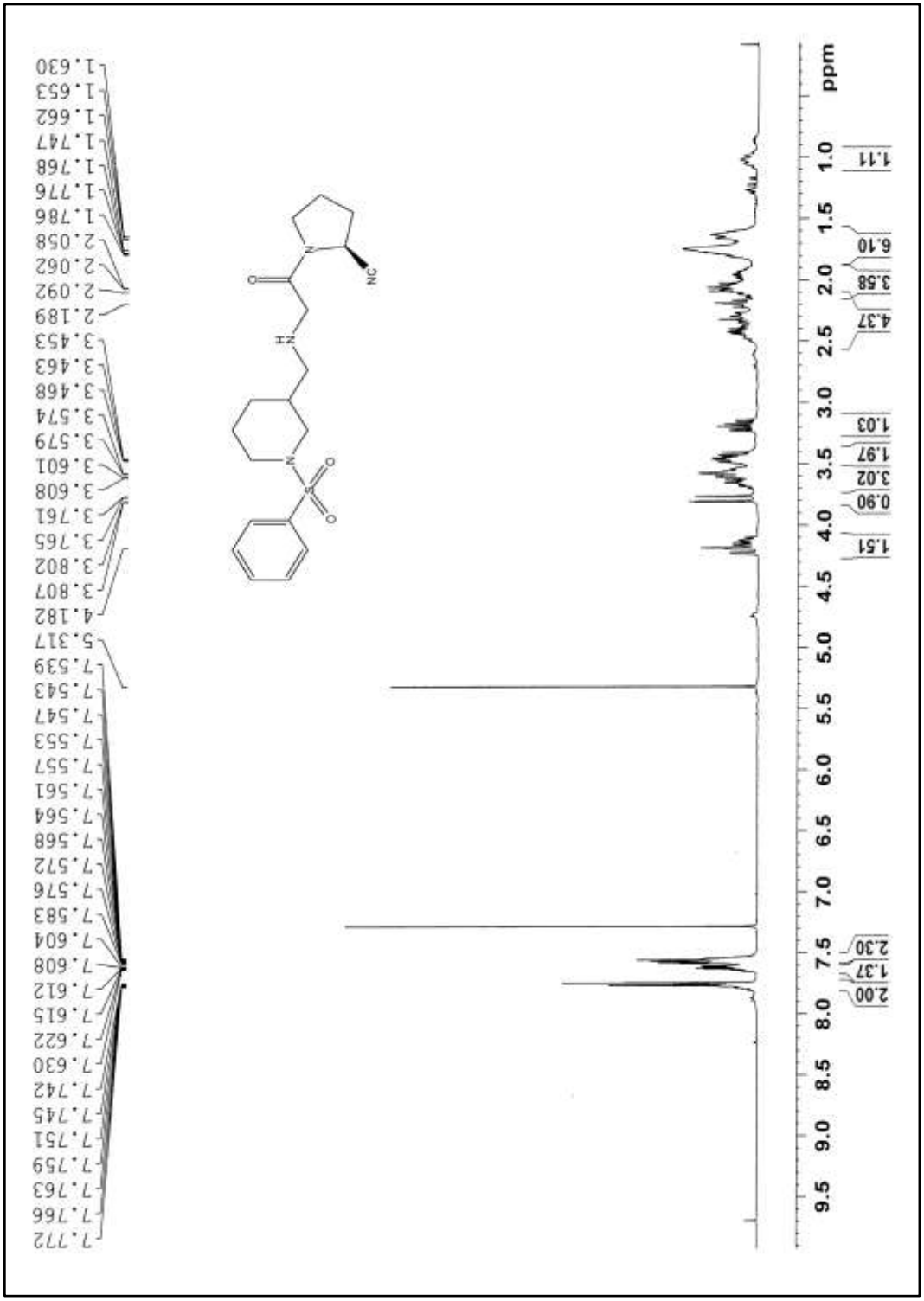

Figure 2.12.2: ^{1}H NMR spectrum of (2S)-1-(2-((1-(phenylsulfonyl)piperidin-3-yl) methylamino)acetyl)pyrrolidine-2-carbonitrile **11a**

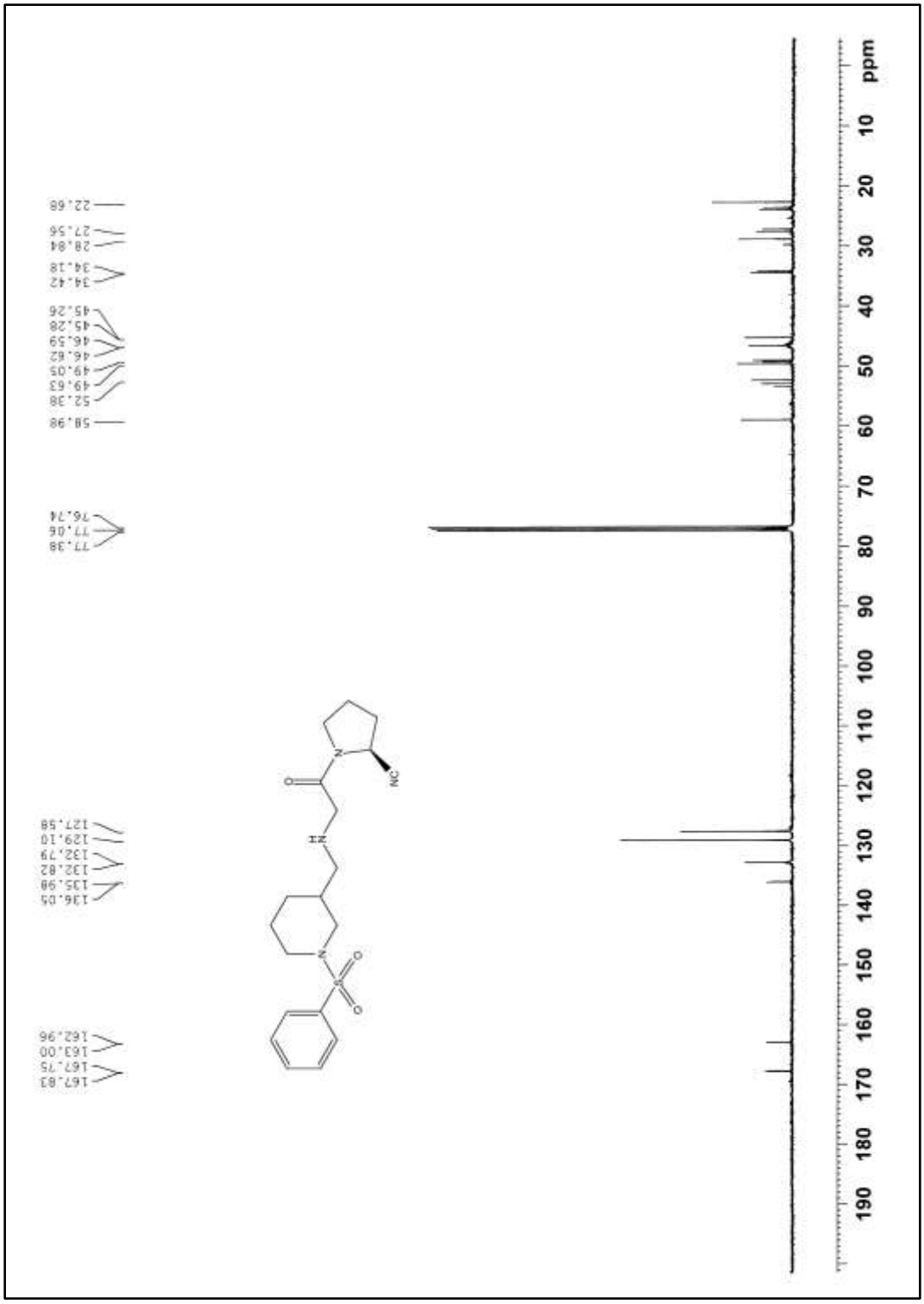

Figure 2.12.3: ^{13}C NMR spectrum of (2S)-1-(2-((1-(phenylsulfonyl)piperidin-3-yl) methylamino)acetyl)pyrrolidine-2-carbonitrile **11a**

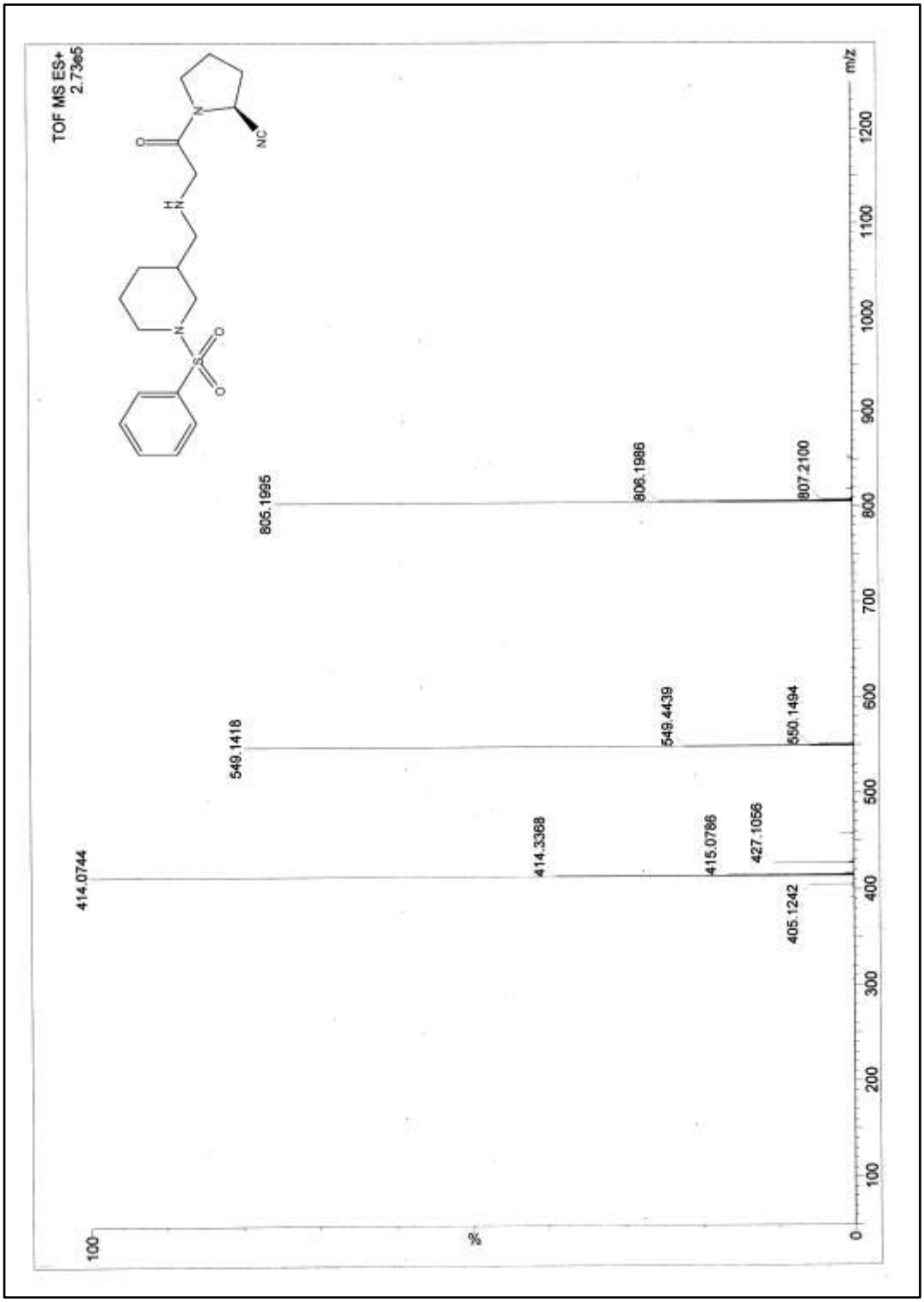

Figure 2.12.4: ESI-MS spectrum of (2S)-1-(2-((1-(phenylsulfonyl)piperidin-3-yl) methylamino)acetyl)pyrrolidine-2-carbonitrile **11a**

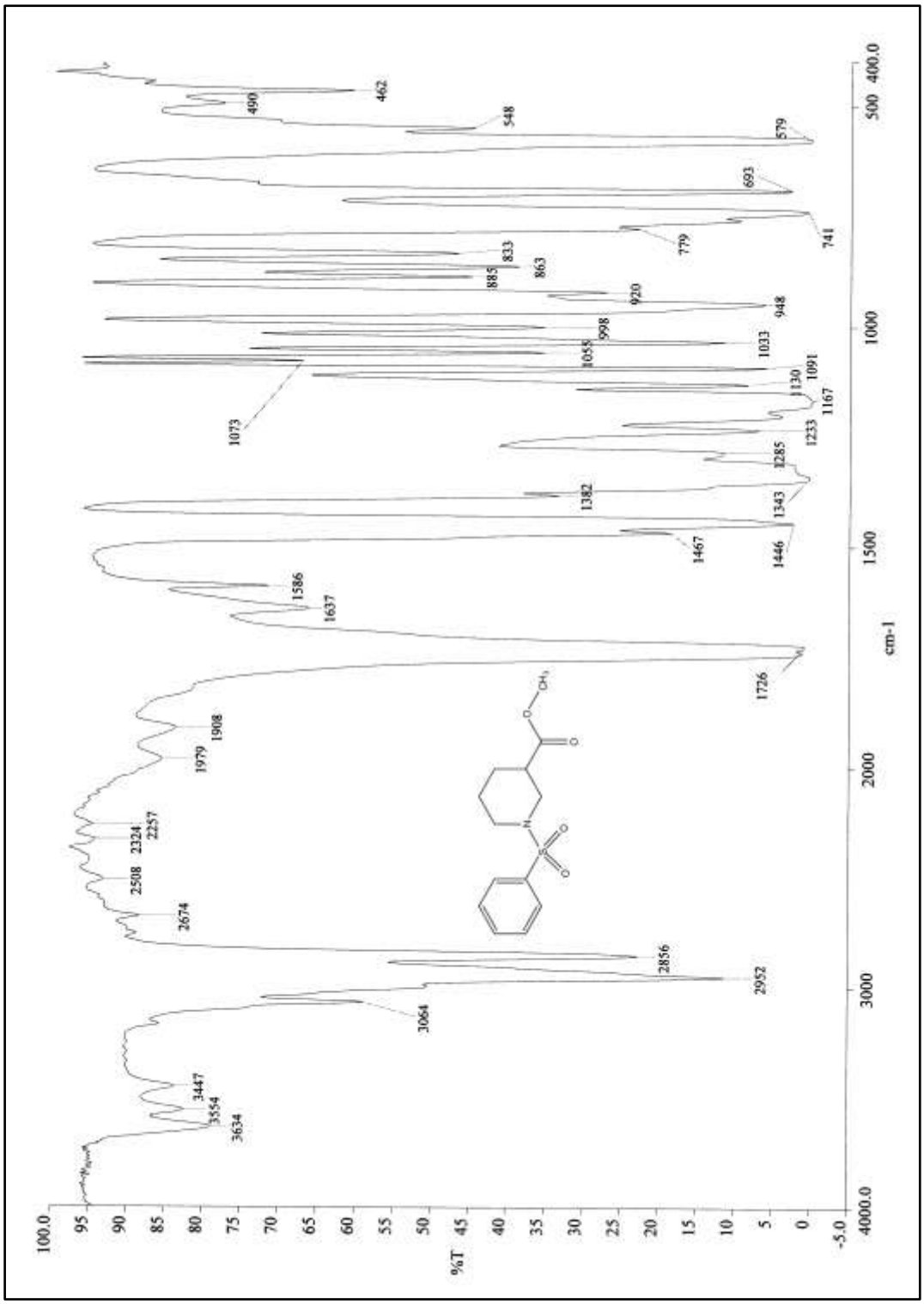

Figure 2.13.1: IR spectrum of 1-(phenylsulfonyl)piperidine-3-carboxylate **12**

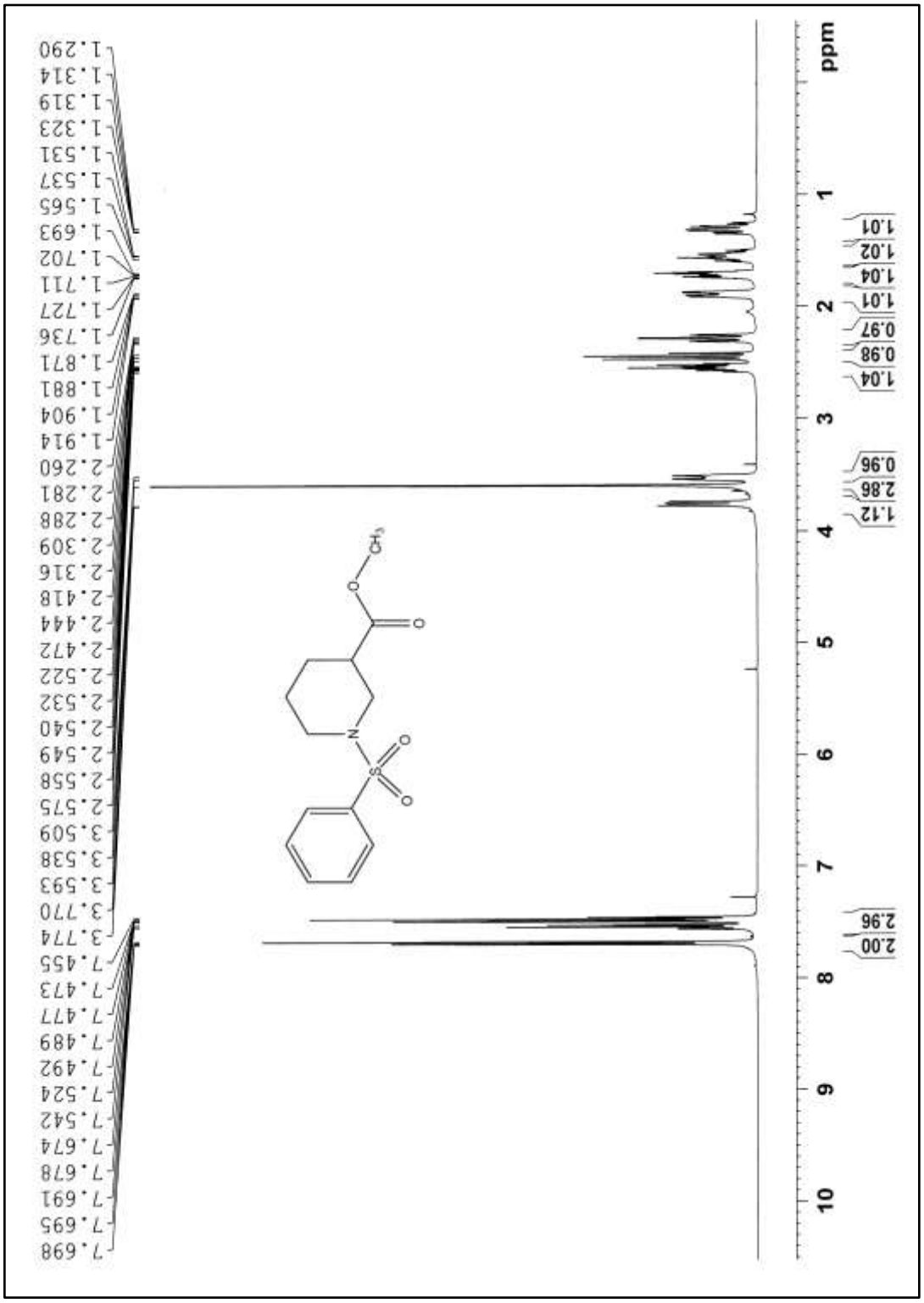

Figure 2.13.1: IR spectrum of 1-(phenylsulfonyl)piperidine-3-carboxylate **12**

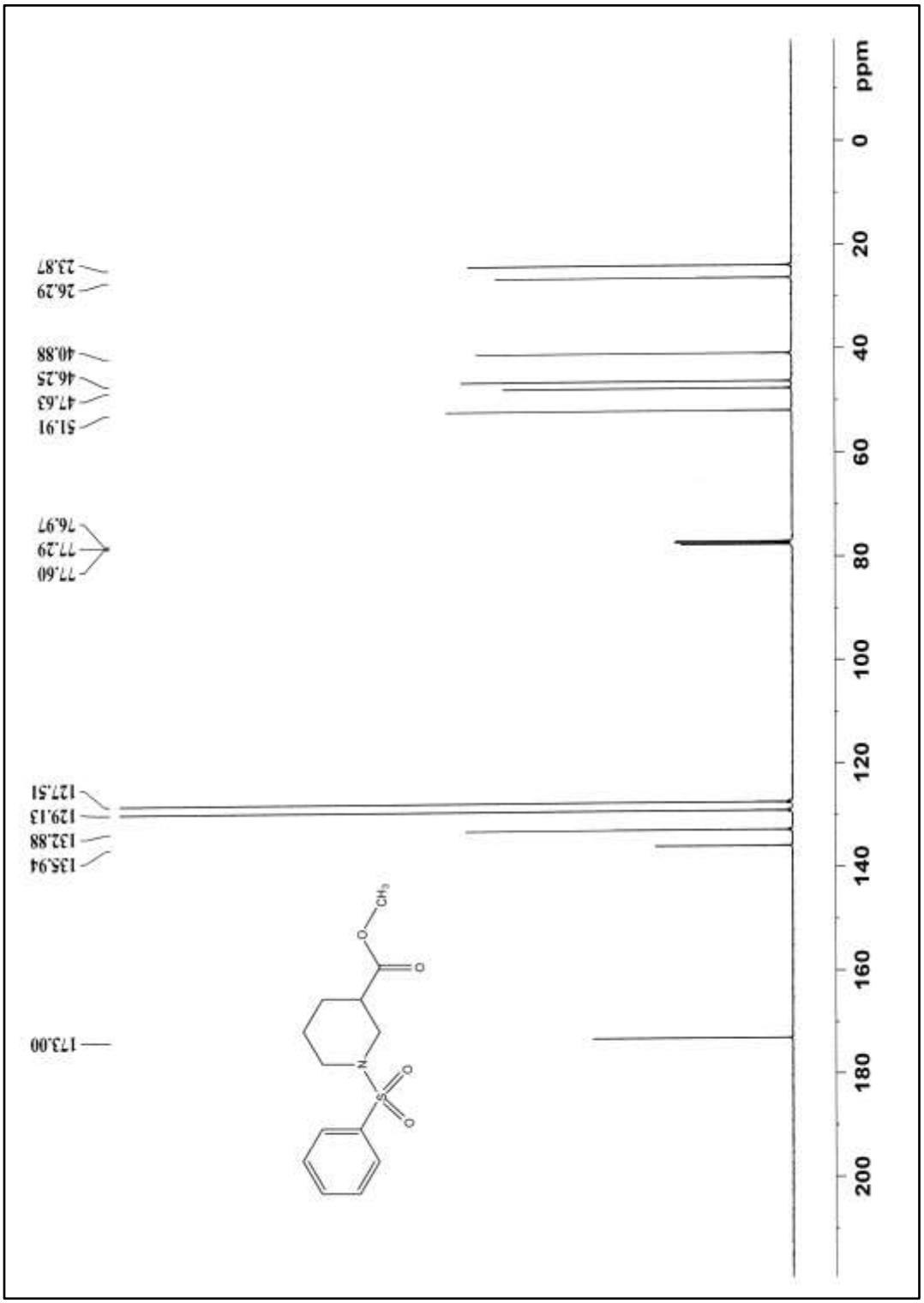

Figure 2.13.3: ^{13}C NMR spectrum of 1-(phenylsulfonyl)piperidine-3-carboxylate **12**

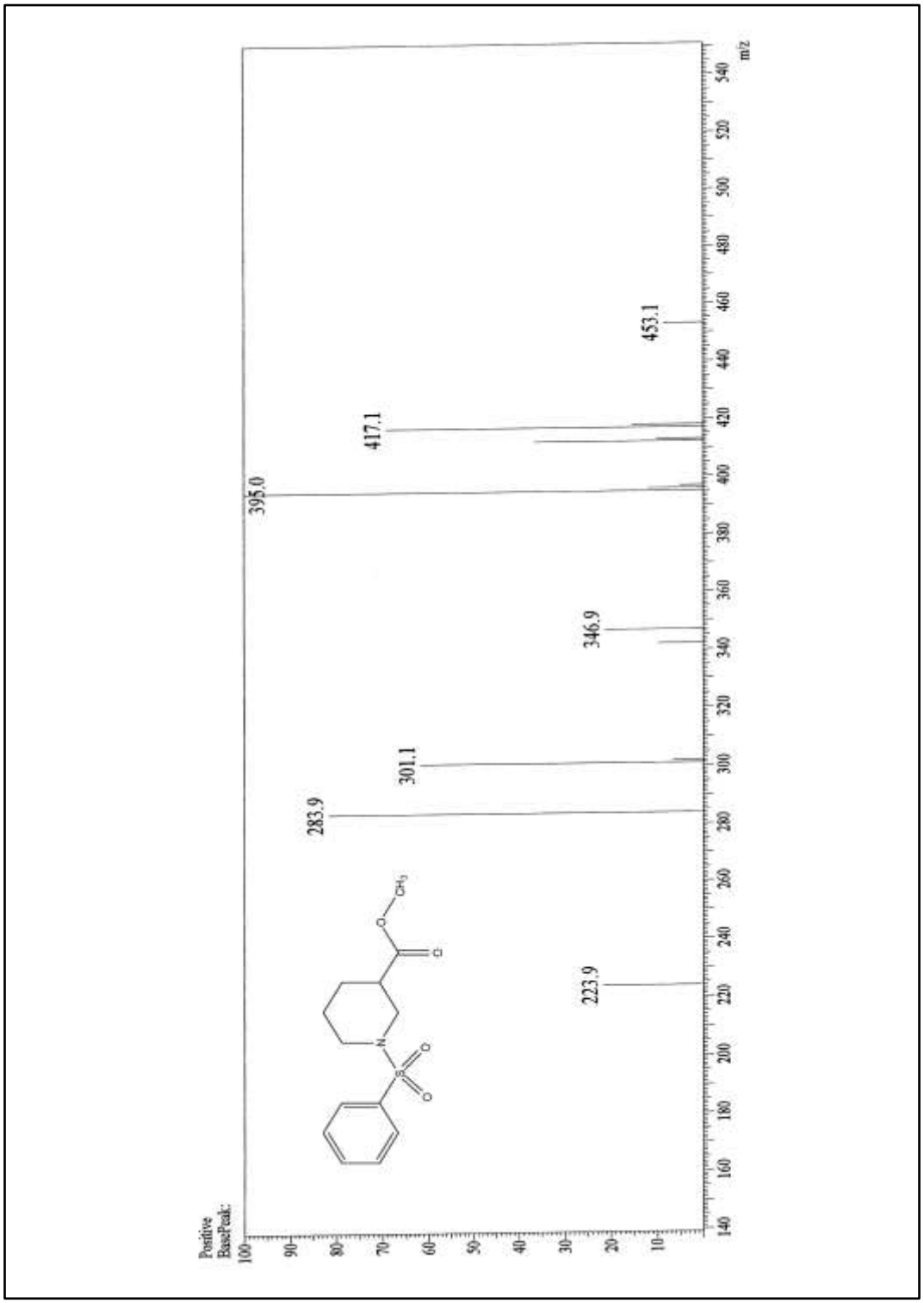

Figure 2.13.4: ESI-MS spectrum of 1-(phenylsulfonyl)piperidine-3-carboxylate **12**

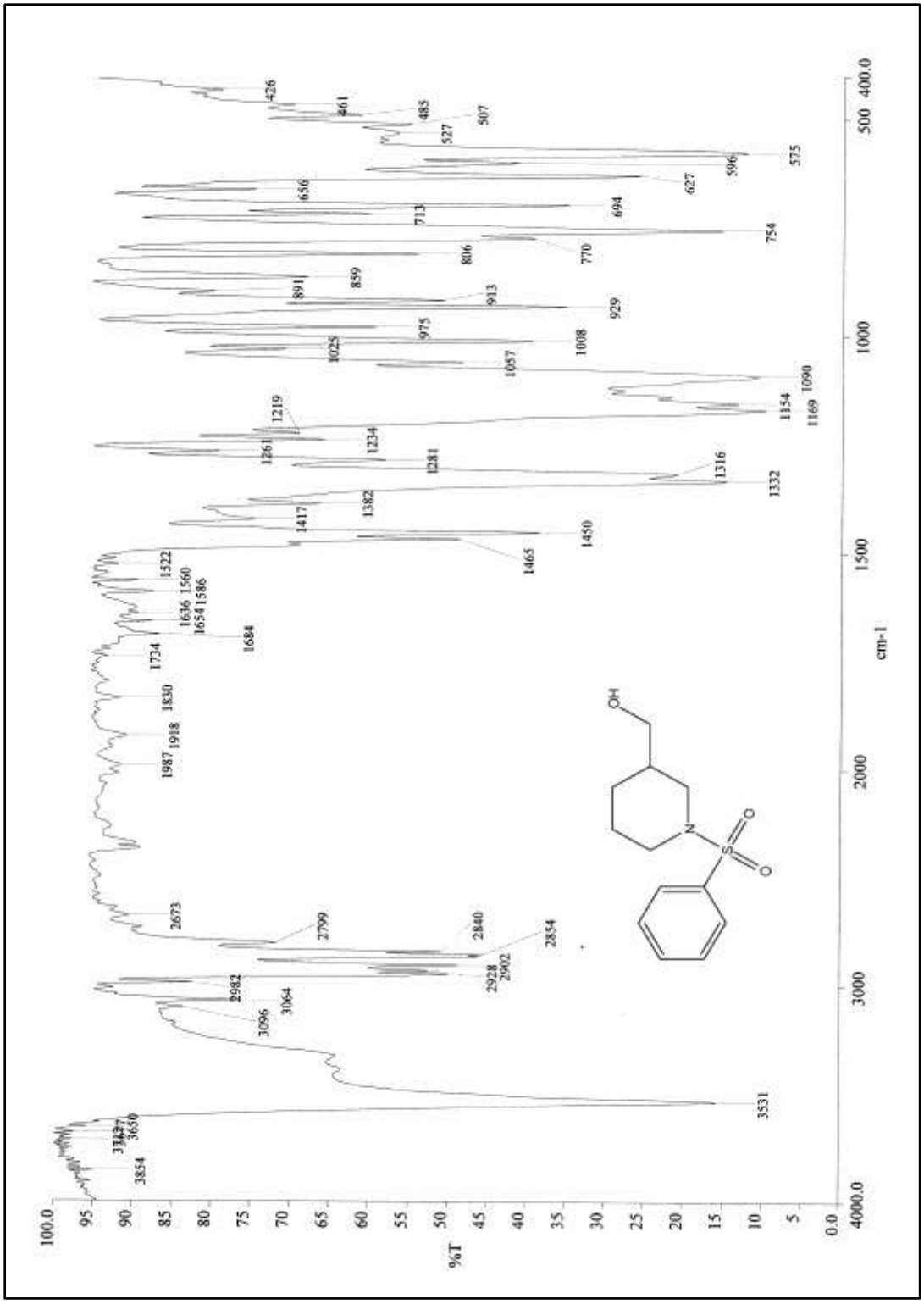

Figure 2.14.1: IR spectrum of (1-(phenylsulfonyl)piperidin-3-yl)methanol **13**

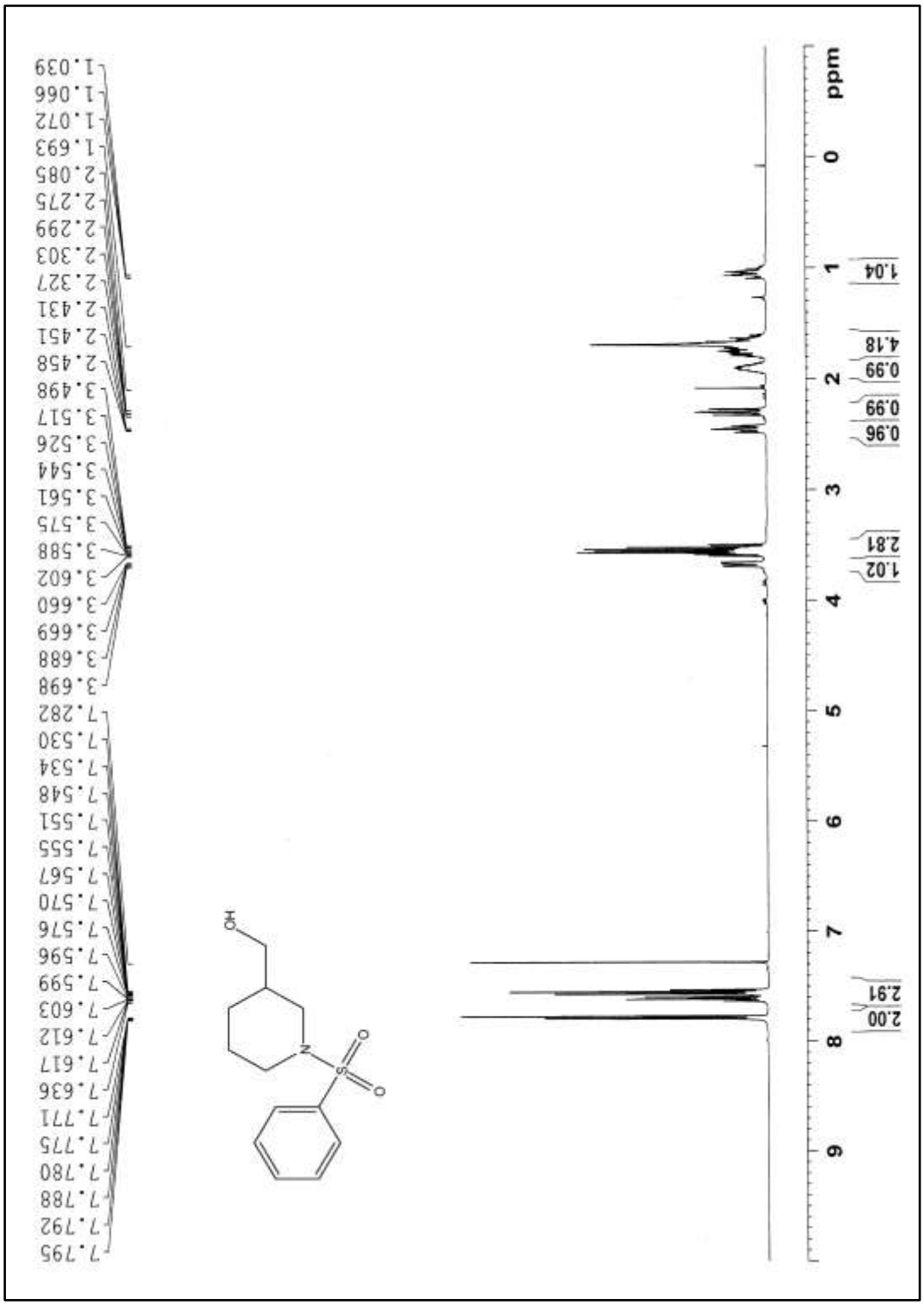

Figure 2.14.2: ^{1}H NMR spectrum of (1-(phenylsulfonyl)piperidin-3-yl)methanol **13**

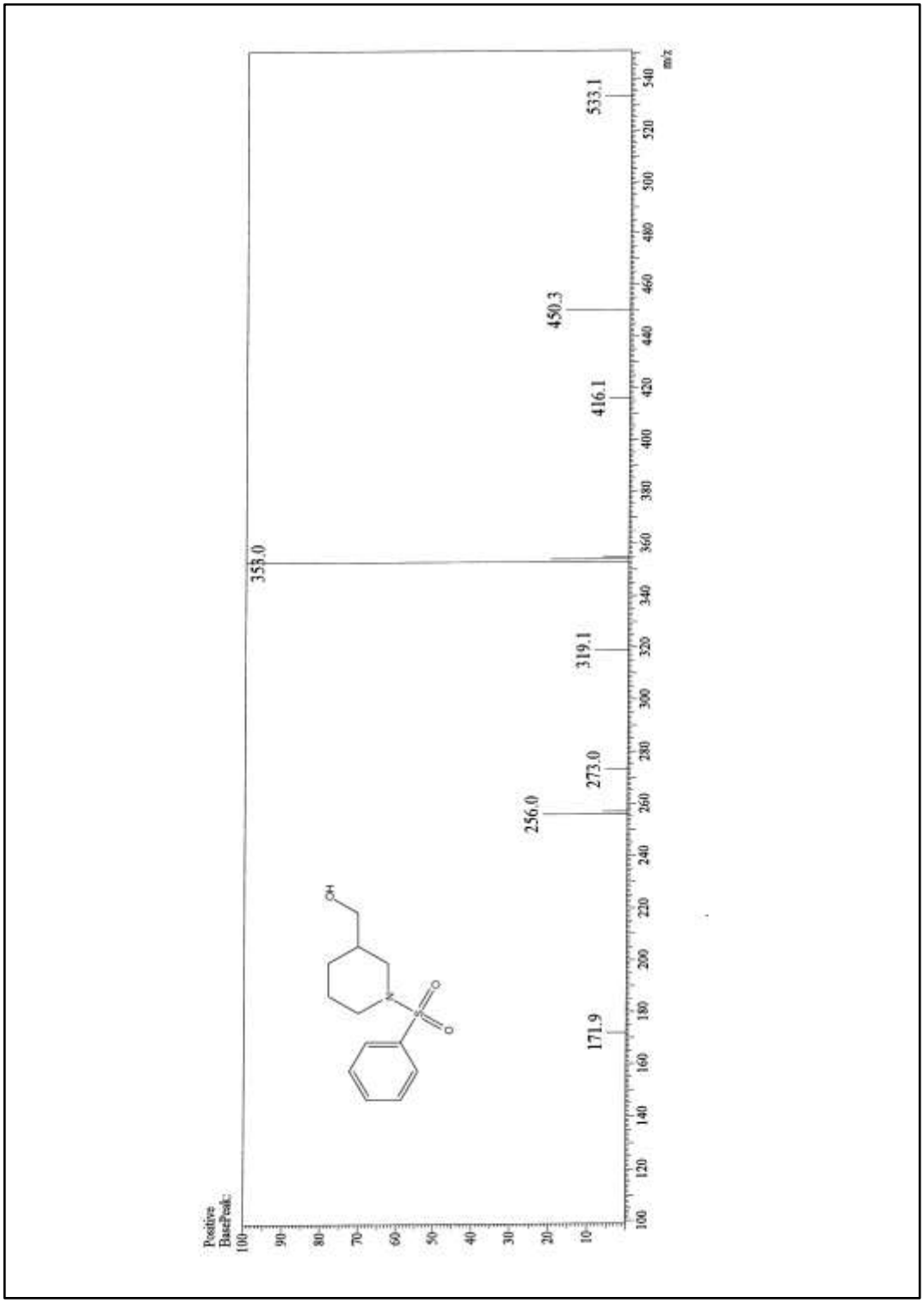

Figure 2.14.3: ESI-MS spectrum of (1-(phenylsulfonyl)piperidin-3-yl)methanol **13**

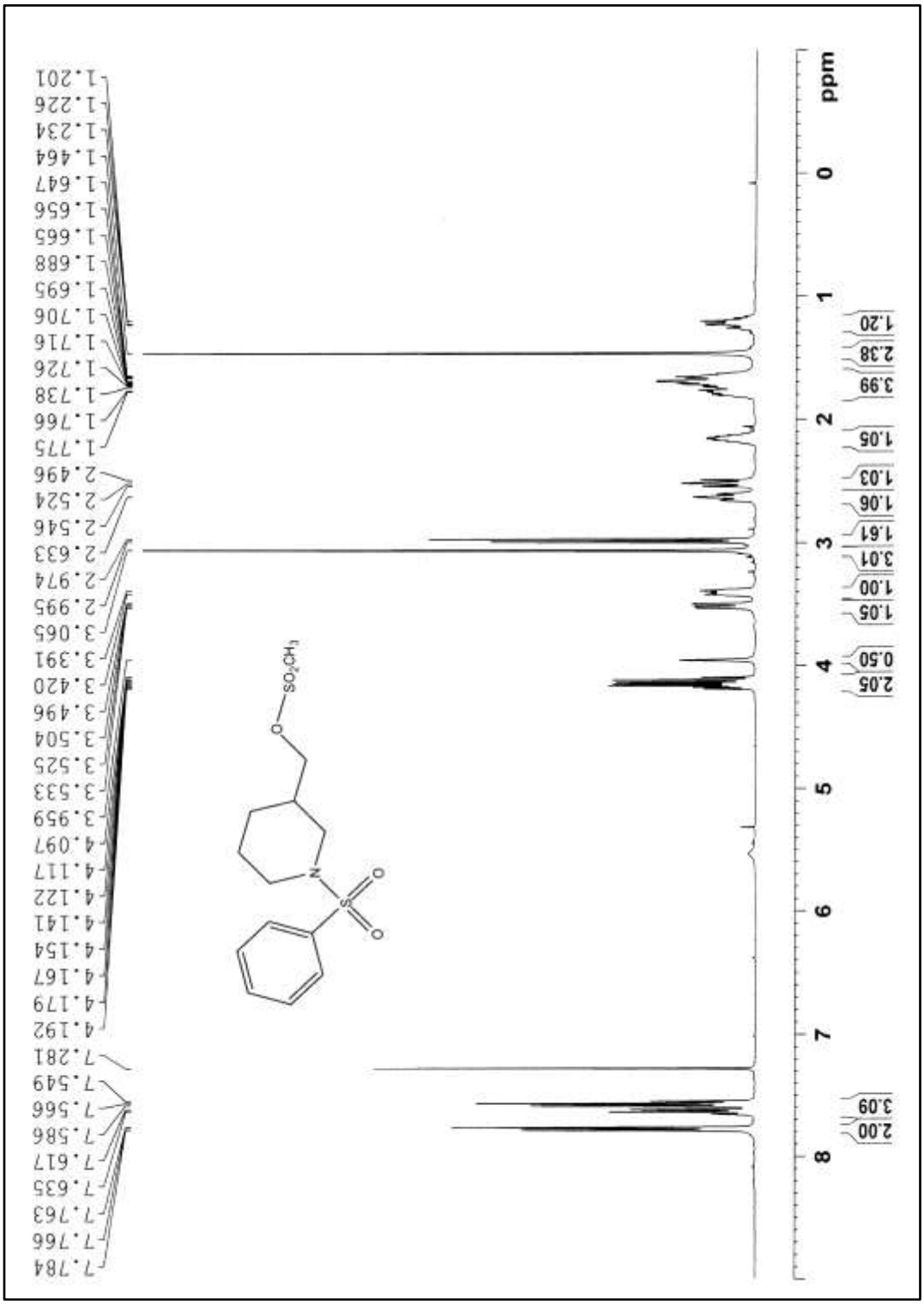

Figure 2.15.1: ^{1}H NMR spectrum of (1-(phenylsulfonyl)piperidin-3-yl)methyl methanesulfonate **14**

2.2.2 Biological Evaluation

DPP-IV inhibition assay uses fluorogenic substrate, Gly-Pro-Aminomethylcoumarin (AMC), to measure DPP-IV activity. Cleavage of the peptide bond by DPP-IV releases the free AMC group, resulting in fluorescence that is analysed using an excitation wavelength of 350-360 nm and emission wavelength of 450-465 nm. Human recombinant DPP-IV enzyme procured from Prospec (**enz-375-b.**), substrate, H-Gly-Pro-AMC procured from Enzo life science (Lot No. : **01221304)** and assay buffer, prepared in-house containing TrisHCl (50 mM), ethylenediamminetetraaceticacid (EDTA) (1mM), sodium chloride (100mM) in deionized water having pH. 7.5 were used in the assay.

DPP-IV activity was measured by mixing reagents in 96-well plate (order of addition of reagents: Assay Buffer, enzyme, solvent/inhibitor and finally substrate). Both the enzyme & 96-well plate was incubated for 30 min and the resulting fluorescence was measured using Spectra Max fluorometer (Molecular Devices, Sunnyvale CA) by exciting at 360 nm and emission at 460 nm. The IC_{50} values were determined for test compounds using Graph Pad prism software.

Calculation:-

(Fluorescence of 100% activity – Fluorescence of test / Fluorescence of 100% activity)*100

Preliminary DPP-IV inhibition assay was performed to screen test compounds **8a-b**, **9a-b**, **11a-b** for their inhibition potential at 2µM concentration as shown in Table 2.1, taking vildagliptin as a standard which exhibited 93.62% enzyme inhibition at the same concentration.

Compound	Structure	% Inhibition of DPP-IV at 2µM
8a	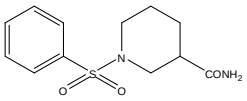	30.20
8b	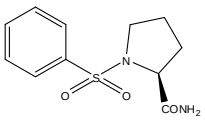	15.00
9a	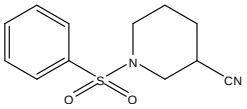	59.17
9b	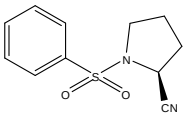	75.13
11a	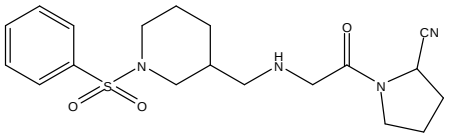	24.68
11b	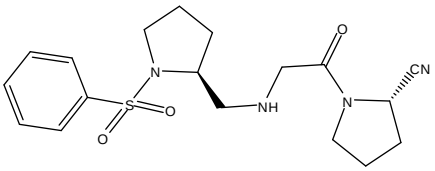	67.91

Table 2.1: *DPP-IV inhibition by test compounds at 2µM concentrations*

IC_{50} (nM) values were determined for **9a-b**, **11a-b** as shown in Table 2.2.

Compound	IC_{50} (nM)
9a	41.17
9b	250.4
11a	2367
11b	274.4

Table 2.2: *Inhibition of DPP-IV (IC_{50} nM) of selected compounds*

From the IC_{50} values of the selected compounds **9a**, **9b**, **12a**, **12b**, it can be inferred that nitrile functionality at the P1 site is responsible for the potency of the DPP-IV inhibitors.

2.3 Docking Studies:

In order to perform the docking studies, binding site residues of the A chain of DPP-4 (PDB ID: 3W2T) [21] at a distance of 4.5 Å from **NVP-LAF237** (Vildagliptin) were selected. AutoDock Vina [22] was used for carrying out docking studies. The affinity for the compound **9a** was -7.4 kcal/mol while that of Vildagliptin was shown to be -6.7 kcal/mol. LigPlot [23] was used to observe the interaction of the ligand with the binding site residues as seen in Figure 2.16.

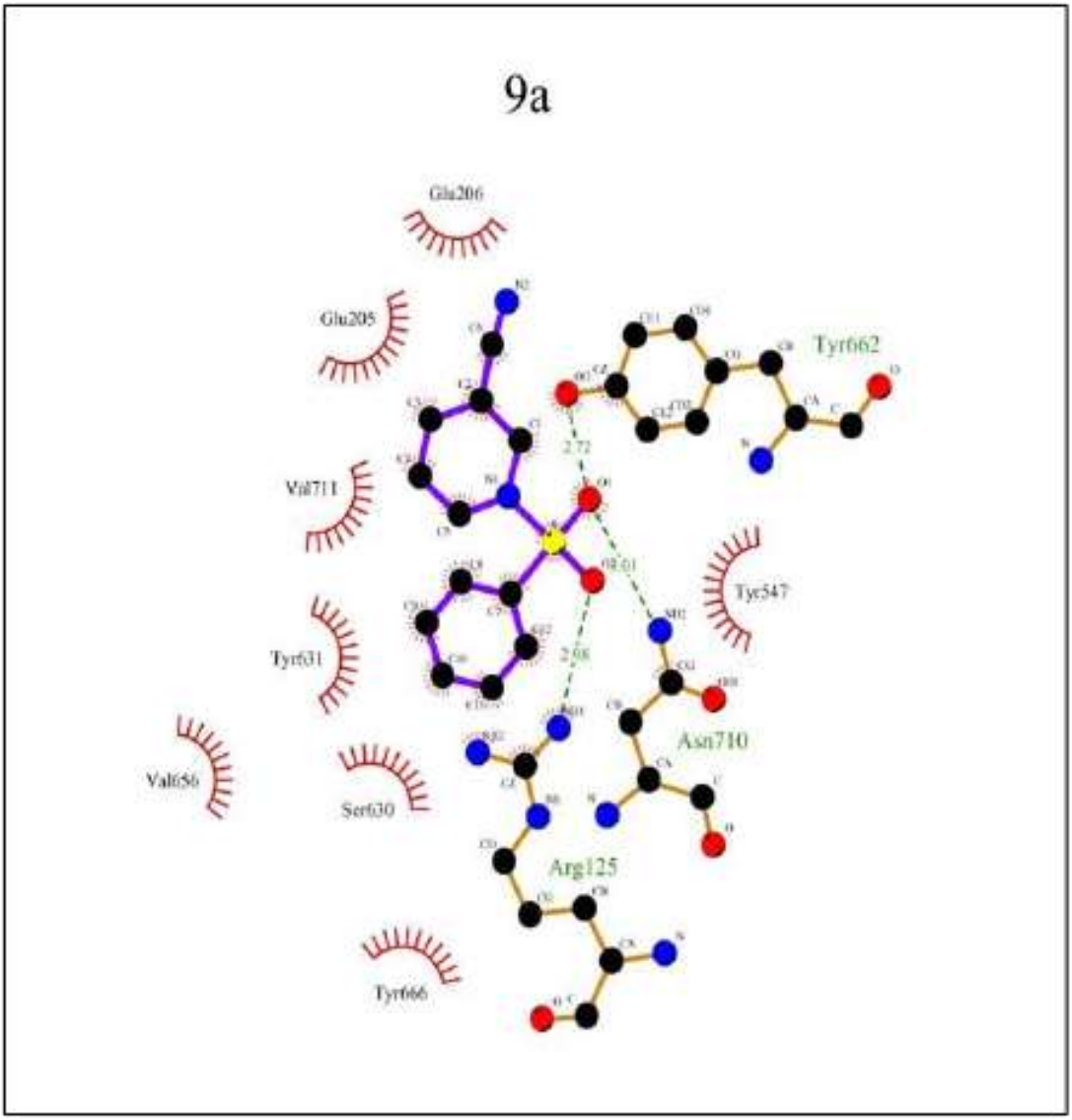

Figure 2.16.1: *LigPlot of compound 1-(phenylsulfonyl)piperidine-3-carbonitrile* ***9a***

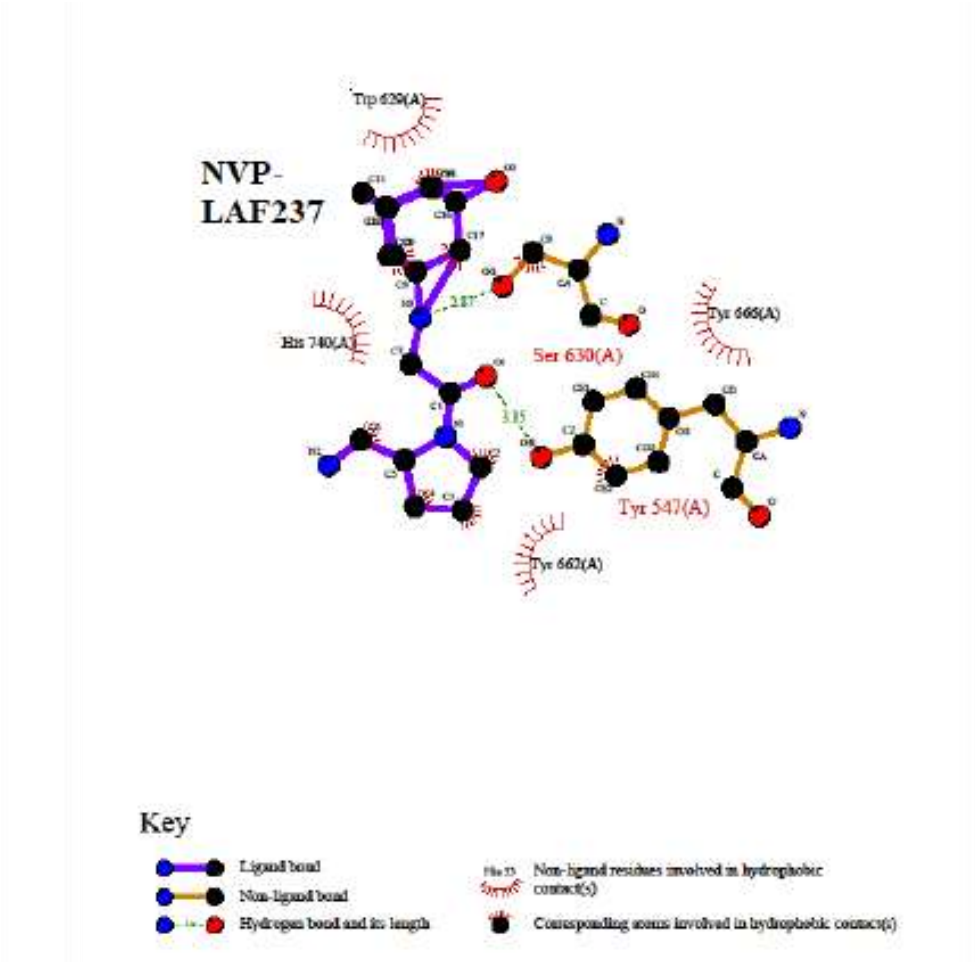

Figure 2.16.2: *LigPlot of compound* ***NVP-LAF237*** *(Vildagliptin)*

Pymol [24] was used to visualize the protein and the docked compound **9a** as seen in Figure 2.17.

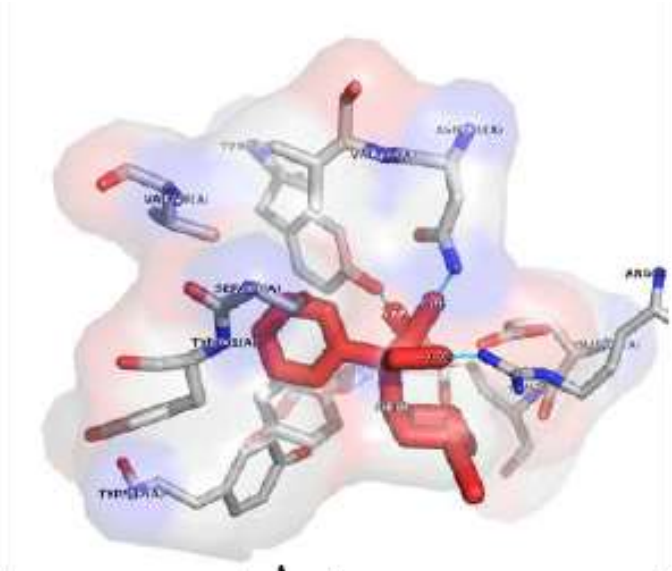

A

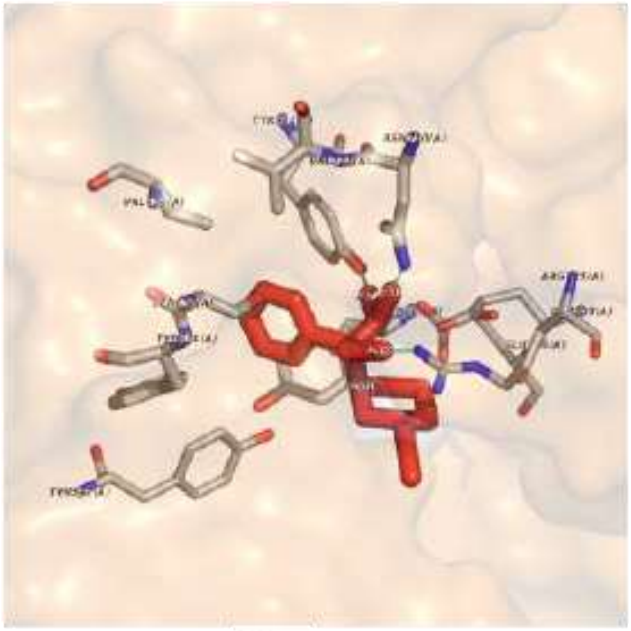

B

Figure 2.17: *Binding of 1-(phenylsulfonyl)piperidine-3-carbonitrile* ***9a*** *at the active site of DPP-IV*

2.3 Conclusion

Thus from the structure activity relationship study of the compounds **8a-b**, **9a-b**, **11a-b**, it can be concluded that the presence of nitrile group at the P1 site is inevitable for the DPP-IV inhibition. Small molecules, sulphonamide derivatives of piperidine-3-carbonitrile and pyrrolidine-2-carbonitrile **9a**, **9b** showed better inhibition with IC_{50} of 41.17 and 250.4 nM respectively, of which the most potent DPP-IV inhibitor of all the molecules synthesized in the series is **9a**.

According to the reported literature, proline mimic is essential for DPP-IV enzyme inhibition but an interesting observation is **9a** (derived from piperidine-3-carboxylic acid) showed five-fold greater potency than **9b** (derived from L-proline). Also amide functionality is not desirable at the P1 site as it lead to very low inhibition of the enzyme as is observed from the % inhibition of compounds **8a-b**.

N-substituted glycine with 2-cyanopyrrolidide at the P1 site and sulfonamide derivatives at the P2 site showed good DPP-IV inhibition but are still not as potent as the vildagliptin since their high IC_{50} values indicates the low potency of these compounds.

2.4 Experimental:

Reagent grade chemicals and solvents were purchased from commercial supplier and used after purification. TLC was performed on silica gel F254 plates (Merck). Acme's silica gel (60-120 mesh) was used for column chromatographic purification. Melting points are uncorrected and were measured in open capillary tubes, using a Rolex melting point apparatus. IR spectra were recorded as KBr pellets on Perkin Elmer RX 1 spectrometer. ^{1}H NMR and ^{13}C NMR spectral data were recorded on Advance Bruker 400 spectrometer (400 MHz) with $CDCl_3$ or DMSO-d_6 as solvent and TMS as internal standard. *J* values are in Hz. Mass spectra were determined by ESI-MS, using a Shimadzu LCMS 2020 apparatus. All the reactions were carried out under nitrogen atmosphere.

Procedure for the synthesis of (S)-1-(2-chloroacetyl)pyrrolidine-2-carboxamide 4:

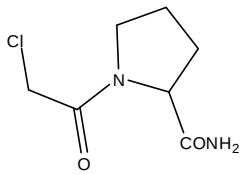

To a solution of L-proline amide **3** in chloroacetyl chloride (1.2 mmol) in tetrahydrofuran (THF) (5 mL) and triethylamine (catalytic), a solution of L-proline amide (1.0 mmol) in THF (10 mL), was added drop-wise, at room temperature for 10 minutes and the resulting solution was refluxed for an hour. On completion of reaction, as monitored by TLC, the reaction mixture was concentrated, washed with saturated sodium bicarbonate solution (1X10 mL), dried over anhydrous sodium sulfate and recrystallized from isopropyl alcohol to give the product **4** as white solid.

Yield: 50%; white solid; $[\alpha]_D$ = -64.33; m.p.: 138-140 ^oC; IR (KBr): 3360, 3158, 2982, 1682, 1657, 1408, 1275, 787 cm^{-1}; ^1H NMR (400 MHz, $CDCl_3$): δ 1.99-2.07 (m, 2H), 2.11-2.16 (m, 1H), 2.25-2.29 (m, 1H), 3.52-3.58 (m, 1H), 3.69-3.74 (m, 1H), 4.14 (s, 2H), 4.54 (dd, 1H, J_1 = 2.8 Hz, J_2 = 8.0 Hz), 5.95 (s, 1H), 7.07 (s, 1H); ^{13}C NMR (400 MHz, $CDCl_3$): δ 8.64, 24.93, 28.29, 42.25, 45.81, 47.44, 60.26, 166.21, 173.48; $C_7H_{11}ClN_2O_2$; ESI-MS: *m/z* 213 $[M+Na]^+$.

Procedure for the synthesis of (S)-1-(2-chloroacetyl)pyrrolidine-2-carbonitrile 5:

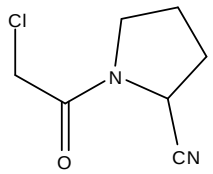

To a suspension of *(S)*-1-(2-chloroacetyl)pyrrolidine-2-carboxamide **4** (1.0 mmol) in THF (10 mL) trifluoroacetic anhydride (2.0 mmol) added at 0–5 °C and the reaction mixture was then stirred at room temperature for 4 h. The reaction was monitored by TLC. On completion of the reaction, to this mixture ammonium bicarbonate (7.0 mmol) added portion wise (over 15 min) while maintaining the temperature of the mixture at 5–10 °C. The mixture again stirred at room temperature for an hour and then concentrated under vacuum at 40 °C to give the product **5**.

Yield: 64%; white solid; $[\alpha]_D$ = -155.21; m.p.: 53-55 ^oC; IR (KBr): 3435, 2992, 2952, 2888, 2241, 1687, 1656, 1422, 1284, 915, 787 cm^{-1}; ^1H NMR (400 MHz, CDCl3): δ 2.18-2.25 (m, 4H), 3.51-3.57 (m, 1H), 3.66-3.71 (m, 1H), 4.08 (s, 2H), 4.69-4.71 (m, 1H); ^{13}C NMR (400 MHz, $CDCl_3$): δ 22.80, 25.25, 29.96, 32.48, 41.69, 41.73, 46.55, 46.84, 46.99, 47.14, 118.00, 165.33; ESI-MS: *m/z* 173.0 $[M+H]^+$.

General procedure for the preparation of compound 7a, 7b:

To a mixture amino acid, piperidine-3-carboxylic acid **6a** or L-proline **6b** (1.0 mmol) and sodium carbonate (3.0 mmol) in DCM:water (1:1) benzene sulphonyl chloride (1.1 mmol) added and the reaction mixture stirred at room temperature for 16 hours or till the completion of reaction as monitored by TLC. On completion of reaction, the reaction mixture washed with petroleum ether (20 mL) and then acidified till pH 2 using conc.HCl. The white solid thus separated was filtered, washed with water several times and then dried to yield the desired products **7a-b** as white solid.

***1-(phenylsulfonyl)piperidine-3-carboxylic acid* 7a:**

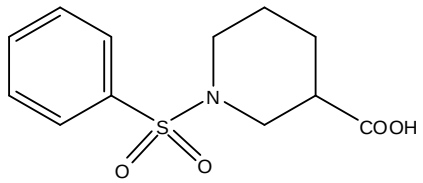

Yield: 91%; white solid; m.p.: 115-117 ^{o}C; IR (KBr): 3100-2500 (b), 2940, 1812, 1693, 1352 cm^{-1}; ^{1}H NMR (400 MHz, $CDCl_3$): δ 1.41-1.50 (m, 1H), 1.65-1.73 (m, 1H), 1.80-1.85 (m, 1H), 1.99-2.04 (m, 1H), 2.41 (dt, 1H, J_1 = 2.8 Hz, J_2 = 11.2 Hz), 2.57 (t, 1H, J = 10.8 Hz), 2.65-2.71 (m, 1H), 3.59 (br d, 1H, J = 11.6 Hz), 3.83 (dd, 1H, J_1 = 3.2 Hz, J_2 = 7.2 Hz), 7.54-7.58 (m, 2H), 7.61-7.63 (m, 1H), 7.77-7.79 (m, 2H), 8.98 (br s, 1H); ^{13}C NMR (400 MHz, $CDCl_3$): δ 23.88, 26.21, 40.73, 46.26, 47.35, 127.62, 129.18, 132.94, 135.96, 178.63; $C_{12}H_{15}NO_4S$; ESI-MS**:** *m/z* 292.0 $[M+Na]^+$

(S)-1-(phenylsulfonyl)pyrrolidine-2-carboxylic acid 7b:

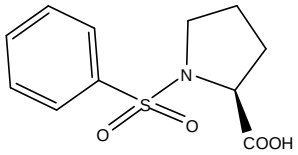

Yield: 90%; white solid; $[\alpha]_D$ = -101.38; m.p.: 86 - 88 ^oC; IR (KBr): 3180-2560 (b), 2956, 2683, 1728, 1584, 1447, 1349, 1290, 1159, 1095 cm^{-1}; ^1H NMR (400 MHz, $CDCl_3$): δ 1.76-1.80 (m, 1H), 1.97-2.14 (m, 3H), 3.26-3.32 (m, 1H), 3.52-3.57 (m, 1H), 4.30-4.33 (m, 1H), 7.54-7.58 (m, 2H), 7.61-7.66 (m, 1H), 7.88-7.91 (m, 2H), 8.65 (br s, 1H); ^{13}C NMR (400 MHz, $CDCl_3$): δ 24.66, 30.80, 48.71, 60.37, 127.50, 129.24, 133.15, 137.48, 177.03; $C_{11}H_{13}NO_4S$; ESI-MS: *m/z* 277.9 $[M+Na]^+$.

General procedure for the preparation of compound 8a, 8b:

To a solution of compound **7** (1 mmol) in dichloromethane (10 mL), slowly a solution of 1-ethyl-3-(3-dimethylaminopropyl)carbodiimide hydrochloride (EDCI) (1.5 mmol) and 1-hydroxybenzotriazole (HOBt) (1.0 mmol) in dichloromethane added at 10–15 °C (duration 5.0 min) and the mixture stirred at room temperature for 5 h. To this ammonium bicarbonate (5.0 mmol) was added and the mixture stirred for 1 h. The reaction was monitored by TLC (5% MeOH-$CHCl_3$, anisaldehyde & I_2). After completion of the reaction, the mixture filtered and the residue washed with DCM. The filtrates were collected and combined, washed with water (2X10 mL), dried over anhydrous sodium sulphate and the solvent evaporated under reduced pressure to give the crude product which was then purified by column chromatography using silica gel employing ethylacetate as eluent to yield desired products **8a-b** as white solid.

***1-(phenylsulfonyl)piperidine-3-carboxamide 8a**:*

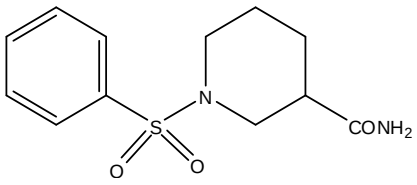

Yield: 65 %; white solid; m.p.: 162-164 ^{o}C; IR (KBr): 3346, 3173, 2961, 2931, 2865, 1665, 1629, 1446, 1341, 1164, 1151 cm^{-1}; ^{1}H NMR (400 MHz, DMSO-d_6): δ 1.42-1.46 (m, 1H), 1.69-1.77 (m, 2H), 2.08-2.18 (m, 2H), 2.34-2.49 (m, 1H), 2.50 (m, 1H), 3.56-3.64 (m, 2H), 6.96 (s, 1H), 7.46 (s, 1H), 7.63-7.67 (m, 2H), 7.71-7.74 (m, 3H),; ^{13}C NMR (400 MHz, $CDCl_3$): δ 23.75, 26.95, 41.91, 46.42, 48.12, 127.60, 129.24, 133.05, 135.57, 175.16; $C_{12}H_{16}N_2O_3S$; ESI-MS: *m/z* 291.0 $[M+Na]^+$.

(S)-1-(phenylsulfonyl)pyrrolidine-2-carboxamide 8b:

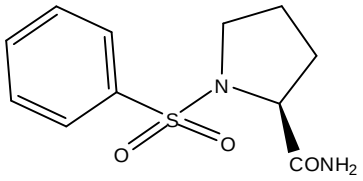

Yield: 55%; white solid; $[\alpha]_D$ = -163.72; m.p.: 78-80 ^{o}C; IR (KBr): 3466, 3290, 3226, 2956, 2890, 1671, 1587, 1499, 1346, 1161, 1092 cm^{-1}; ^{1}H NMR (400 MHz, $CDCl_3$): δ 1.54-1.65 (m, 2H), 1.79-1.82 (m, 1H), 2.16-2.21 (m, 1H), 3.16-3.22 (m, 1H), 3.57-3.63 (m, 1H), 4.09 (dd, 1H, J_1 = 2.8 Hz, J_2 = 8.8 Hz), 6.08 (br s, 1H), 6.94 (br s, 1H), 7.56-7.60 (m, 2H), 7.64-7.68 (m, 1H), 7.85-7.88 (m, 2H); ^{13}C NMR (400 MHz, $CDCl_3$): δ 24.39, 30.14, 49.85, 62.31, 127.76, 129.42, 133.49, 135.67, 174.52; $C_{11}H_{14}N_2O_3S$; ESI-MS: *m/z* 277.0 $[M+Na]^+$.

General procedure for the preparation of compound 9a, 9b:

To a suspension of amide **8** (1.0 mmol) in THF (10 mL) trifluoroacetic anhydride (2.0 mmol) added at 0–5 °C and the reaction mixture stirred at room temperature for 4 h. The reaction was monitored by TLC. On completion of the reaction, to this mixture ammonium bicarbonate (7 mmol) added portion wise (over 15 min), maintaining the temperature of the mixture at 5–10 °C and the mixture stirred at room temperature for an hour and then concentrated under vacuum at 40 °C to give the crude product which was then purified by column chromatography using silica gel and employing DCM : methanol (95:5) as eluent to yield desired product **9a-b** as white solid.

1-(phenylsulfonyl)piperidine-3-carbonitrile 9a:

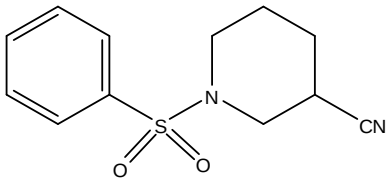

Yield: 75 %; white solid; m.p.: 122-124 ^{o}C; IR (KBr): 3066, 2959, 2880, 2864, 2239, 1770, 1586, 1475, 1447, 1342, 1207 cm^{-1}; ^{1}H NMR (400 MHz, $CDCl_3$): δ 1.62-1.72 (m, 2H), 1.86-1.91 (m, 1H), 1.97-2.00 (m, 1H), 2.69-2.74 (m, 1H), 2.86-2.90 (m, 2H), 3.39-3.42 (m, 1H), 3.64 (d, 1H, *J* = 8.4 Hz), 7.56-7.60 (m, 2H), 7.64-7.68 (m, 1H), 7.78-7.80 (m, 2H); ^{13}C NMR (400 MHz, $CDCl_3$): δ 23.06, 27.37, 29.50, 45.91, 47.69, 119.40, 127.54, 129.33, 133.25, 136.02; $C_{12}H_{14}N_2O_2S$; ESI-MS: *m/z* 273.0 $[M+Na]^+$.

(S)-1-(phenylsulfonyl)pyrrolidine-2-carbonitrile 9b:

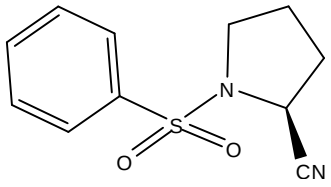

Yield: 70 %; white solid; $[\alpha]_D$ = -116.60; m.p.: 118-120 ^oC; IR (KBr): 3454, 3074, 2998, 2918, 2885, 2850, 2246, 1584, 1452, 1352, 1246, 1197, 1166, 1092, 1011 cm^{-1}; ^1H NMR (400 MHz, $CDCl_3$): δ 2.01-2.24 (m, 4H), 3.40-3.42 (m, 2H), 4.60-4.63 (m, 1H), 7.56-7.60 (m, 2H), 7.64-7.66 (m, 1H), 7.90-7.91 (m, 2H); ^{13}C NMR (400 MHz, $CDCl_3$): δ 24.68, 29.70, 31.93, 47.59, 48.63, 118.04, 127.50, 129.39, 133.54, 137.24; $C_{11}H_{12}N_2O_2S$; ESI-MS**:** *m/z* 258.9 $[M+Na]^+$

General procedure for the preparation of compound 10a, 10b:

To a solution of compound 9a or 9b (1.0 mmol) in THF (25 mL) at -18 ^oC, lithium aluminium hydride (LAH) (4.0 mmol) was added portion-wise over a period of 30 minutes and the reaction mixture stirred at room temperature for 4 hours or till the completion of reaction as monitored by TLC. On completion of reaction, 10% aq. NaOH solution, at 5-10 ^oC, added drop wise to the reaction mixture till effervescence ceases, filtered through hy-flow and extracted with ethylacetate several times. The filtrates were collected and concentrated to give crude product **10a-b**, as viscous liquid which was used directly for the next reaction.

General procedure for the preparation of compound 11a, 11b:

A mixture of anhydrous K_2CO_3 (3.0 mmol), amine **10a** or **10b** (1.7 mmol) and compound **5** (1.5 mmol) was refluxed for 2 hours or till the completion of reaction as detected on the TLC. It was then cooled to room temperature, filtered and the residue was washed with ethylacetate. The filtrate was collected, solvent evaporated under reduced pressure to give the crude product which was purified by column chromatography using neutral alumina as stationary phase and 7:3 ethylacetate : pet.ether as mobile phase to yield product **11a-b** as thick viscous liquids.

(2S)-1-(2-((1-(phenylsulfonyl)piperidin-3-yl)methylamino)acetyl)pyrrolidine-2-carbonitrile 11a:

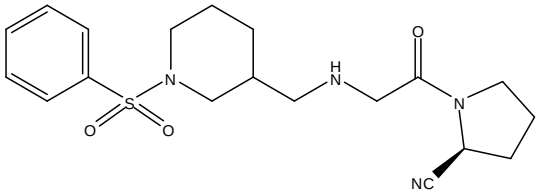

Yield: 45%; viscous liquid; $[\alpha]_D$ = -517.04; IR (Neat): 3476, 3063, 2934, 2853, 1684, 1585, 1447, 1341, 1227, 1170, 1092, 993, 947, 750, 692, 596, 577 cm^{-1}; ^1H NMR (400 MHz, $CDCl_3$): δ 1.63-1.79 (m, 6H), 1.95-2.45 (m, 7H), 3.15-3.25 (m, 1H), 3.45-3.47 (m, 2H), 3.57-3.61 (m, 3H), 3.76-3.81 (m, 1H), 4.08-4.18 (m, 1H), 7.54-7.63 (m, 3H), 7.74-7.77 (m, 2H); ^{13}C NMR (400 MHz, $CDCl_3$): δ 22.68, 27.56, 28.84, 34.18, 34.42, 45.26, 45.28, 46.59, 46.62, 49.05, 49.63, 52.38, 58.98, 127.58, 129.10, 132.79, 132.82, 135.98, 136.05, 162.96, 163.00, 167.75, 167.83; $C_{19}H_{26}N_4O_3S$; ESI-MS: *m/z* 414.07 $[M+Na]^+$

(2S)-1-(2-((1-(phenylsulfonyl)pyrrolidin-2-yl)methylamino)acetyl)pyrrolidine-2-carbonitrile 11b:

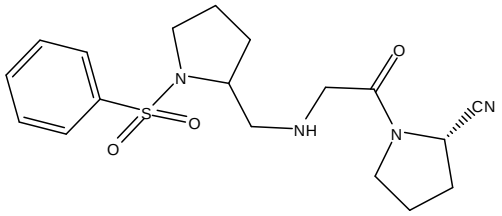

Yield: 20%; viscous liquid; $[\alpha]_D$ = -116.60; IR (Neat): 3480, 2954, 2879, 1661, 1652, 1645, 1446, 1336, 1162, 1091, 1072, 758, 573 cm^{-1}; ^1H NMR (400 MHz, $CDCl_3$): δ 1.26-2.30 (m, 8H), 2.92-3.1 (m, 2H), 3.50-3.73 (m, 8H), 4.74-4.76 (m, 1H), 7.55-7.61 (m, 3H), 7.81-7.84 (m, 2H); ^{13}C NMR (400 MHz, $CDCl_3$): δ 22.73, 23.93, 24.08, 25.36, 29.71, 29.80, 29.88, 32.25, 45.92, 46.09, 46.30, 46.44, 46.53, 46.79, 48.69, 48.77, 56.27, 57.27, 58.88, 59.29, 59.46, 60.19, 60.50, 62.82, 118.50, 119.13, 127.40, 127.48, 127.81, 129.19, 129.27, 132.79, 132.90, 137.07, 137.57, 168.86, 169.28, 169.62; $C_{18}H_{24}N_4O_3S$; ESI-MS: *m/z* 376.8 $[M+H]^+$

Procedure for the preparation of methyl 1-(phenylsulfonyl)piperidine-3-carboxylate 12:

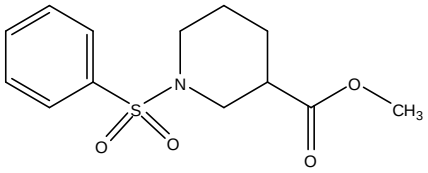

To a solution of compound **7** (1.0 mmol) in DCM, oxalyl chloride (1.5 mmol) was added at 0-5 ^oC and stirred at room temperature for an hour and then methanol (1.1 mmol) added and the reaction mixture stirred for another hour or till the completion of reaction as monitored by TLC to yield product **12** as a viscous liquid.

Yield: 90%; viscous liquid; IR (Neat): 3064, 2952, 2856, 1726, 1637, 1586, 1467, 1446, 1343, 1233, 1167, 1130, 1091, 1033, 948, 741, 693, 579 cm^{-1}; ^1H NMR (400 MHz, $CDCl_3$): δ 1.25-1.35 (m, 1H), 1.53-1.59 (m, 1H), 1.69-1.75 (m, 1H), 1.87-1.91 (m, 1H), 2.28 (dt, 1H, J_1 = 2.8 Hz, J_2 = 11.2 Hz), 2.45 (t, 1H, J = 11.2 Hz), 2.51-2.58 (m, 1H), 3.52 (d, 1H, J = 11.6 Hz), 3.59 (s, 3H), 3.77 (d, 1H, J = 11.6 Hz), 7.46-7.54 (m, 3H), 7.67-7.70 (m, 2H); ^{13}C NMR (400 MHz, $CDCl_3$): δ 23.87, 26.29, 40.88, 46.25, 47.63, 51.91, 127.51, 129.13, 132.88, 135.94, 173.00; $C_{13}H_{17}NO_4S$; ESI-MS: *m/z* 283.9 $[M+H]^+$

Procedure for the preparation of (1-(phenylsulfonyl) piperidin-3-yl)methanol 13:

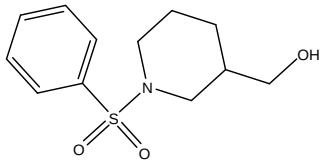

To a solution of 1-(phenylsulfonyl)piperidine-3-carboxylate **12** (1.0 mmol) in THF (25 mL), LAH (2.5 mmol) added portionwise at -18 ^oC over a period of 15 minutes and the reaction mixture was stirred at room temperature for 4 hours or till the completion of reaction as monitored by TLC. On completion of reaction, 10% aq. NaOH solution, at 5-10 ^oC, added drop wise to the reaction mixture till effervescence ceases, filtered through hy-flow and extracted with ethylacetate several times. The filtrates were collected and concentrated to give crude product **13**, as viscous liquid.

Yield: 80%; viscous liquid; IR (Neat): 3531, 2928, 2902, 2854, 2840, 1465, 1450, 1332, 1316, 1169, 1154, 1090, 1008, 929, 754, 694, 627, 575 cm^{-1}; ^1H NMR (400 MHz, $CDCl_3$): δ 1.01-1.10 (m, 1H), 1.61-1.80 (m, 4H), 1.87-1.94 (m, 1H), 2.30 (t, 1H, J = 10.4 Hz), 2.45 (dt, 1H, J_1 = 2.8 Hz, J_2 = 10.8 Hz), 3.50-3.60 (m, 3H), 3.68 (dd, 1H, J_1 = 4.0

Hz, J_2 = 11.2 Hz), 7.53-7.64 (m, 3H), 7.77-7.80 (m, 2H); $C_{12}H_{17}NO_3S$; ESI-MS: *m/z* 256.0 $[M+H]^+$

Procedure for the preparation of (1-(phenylsulfonyl)piperidin-3-yl)methyl methanesulfonate 14:

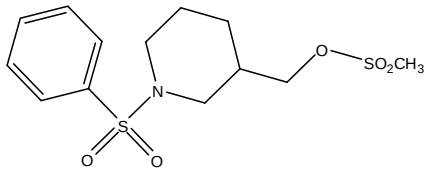

(1-(phenylsulfonyl)piperidin-3-yl)methanol **13** (1.0 mmol) mixed with triethyl amine (1.2 mmol) and methane sulfonyl chloride (1.2 mmol) in THF (25 mL) and stirred at room temperature for 2 hours. Then reaction mixture washed with water (1X10 mL), sat. sodium bicarbonate solution (1X25 mL) and solvent evaporated under reduced pressure to give product **14** as viscous liquid.

Yield: 65%; viscous liquid; ^{1}H NMR (400 MHz, $CDCl_3$): δ 1.20-1.26 (m, 1H), 1.46 (s, 1H), 1.65-1.78 (m, 4H), 2.13-2.18 (m, 1H), 2.50-2.55 (m, 1H), 2.61-2.66 (m, 1H), 2.98 (d, 1H, *J* = 8.4Hz), 3.07 (s, 3H), 3.39-3.42 (m, 1H), 3.50-3.53 (m, 1H), 4.10-4.19 (m, 2H), 7.55-7.65 (m, 3H), 7.76-7.78 (m, 2H).

2.5 References

[1] Bauvois, B. *Biochem. J.* **1988,** *252*, 723.

[2] Piazza, G. A.; Callanan, H. M.; Mowrey, J.; Hixson, D. C. *Biochem. J.* **1989**, *262*, 327.

[3] Mentlein, R. *Regulatory Peptides* **1999**, *85*, 9.

[4] Deacon, C.F.; Nauck, M. A.; Toft-Nielsen, M.; Pridal, L.; Willms, B.; Holst, J. J. *Diabetes* **1995**, *44*, 1126.

[5] Drucker, D. J. *Diabetes* **1998**, *47*, 159.

[6] Vilsboll, T.; Krarup, T.; Madsbad, S.; Holst, J. J. *Regulatory Peptides* **2003**, *114*, 115.

[7] Deacon, C. F.; Hughes, T. E.; Holst, J. J. *Diabetes* **1998**, *47*, 764.

[8] Pederson, R.A.; White, H. A.; Schlenzig, D.; Pauly, R. P.; Mclntosh, C. H. S.; Demuth, H-U. *Diabetes* **1998**, *47*, 1253.

[9] Pospisilik, J. A.; Stafford, S. G.; Demuth, H-U.; Brownsey, R.; Parkhouse, W.; Finegood, D. T.; McIntosh, C. H. S.; Pederson, R. A. *Diabetes* **2002**, *51*, 943.

[10] Be´atrice Sudre, B.; Broqua, P.; White, R. B; Ashworth, D.; Evans, D. M.; Haigh, R.; Junien, J-L.; Aubert, M. L. *Diabetes* **2002**, *51*, 1461.

[11] Drucker, D. J.; Philippe, J.; Mojsov, S.; Chick, W. L.; Habener, J. F. *Proc. Natl. Acad. Sci.* **1987**, *84*, 3434.

[12] Mentlein, R.; Gallwitz, B.; Schmidt, W. E. *Eur. J. Biochem.* **1993**, *214*, 829.

[13] Drucker, D. J. *Gastroenterology* **2002**, *122*, 531.

[14] Li, Y.; Hansotia, T.; Yusta, B.; Ris, F.; Halban, P. A.; Drucker, D. J. *J. Biol. Chem.* **2003**, *278*, 471.

[15] Pospisilik, J. A.; Stafford, S. G.; Demuth, H-U.; McIntosh, C. H. S.; Pederson, R. A. *Diabetes* **2002**, *51*, 2267.

[16] Zander, M.; Madsbad, S.; Madsen, J. L.; Holst, J. J. *Lancet*, **2002**, *359*, 824.

[17] Drucker, D. J. *Diabetes Care* **2007**, *30*, 1335.

[18] Villhauer, E. B.; Brinkman, J. A.; Naderi, G. B.; Burkey, B. F.; Dunning, B. E.; Prasad, K.; Mangold, B. L.; Russell, M. E.; Hughes, T. E. *J. Med. Chem.* **2003,** *46*, 2774.

[19] Sakashita, H.; Kitajima, H.; Nakamura, M.; Akahoshia, F.; Hayashi, Y. *Bioorg. Med. Chem. Lett.* **2005**, *15*, 2441.

[20] Zhao, G.; Taunk, P. C.; Magnin, D. R.; Simpkins, L. M.; Robl, J. A.; Wang, A.; Robertson, J. G.; Marcinkeviciene, J.; Sitkoff, D. F.; Parker, R. A.; Kirby, M. S.; Hamann, L. G. *Bioorg. Med. Chem. Lett.* **2005**, *15*, 3992.

[21] Berman, H. M.; Westbrook, J.; Feng, Z.; Gilliland, G.; Bhat, T. N.; Weissig, H.; Shindyalov, I. N.; Bourne, P. E. *The Protein Data Bank Nucleic Acids Research* **2002**, *28*, 235 and PubMed: 23501107

[22] Trott, O.; Olson, A. J. *Journal of Computational Chemistry* **2010**, *31*, 455.

[23] Wallace, A. C.; Laskowski, R. A.; Thornton, J. M. *Protein Eng.* **1995**, *8*, 127.

[24] http://www.pymol.org

CHAPTER 3

SYNTHESIS OF 3-AMINOCOUMARIN DERIVATIVES AS ANTI-HYPERGLYCEMIC AGENTS

3.1 Introduction

Diabetes is a serious metabolic disorder affecting more than 347 million people worldwide [1] with more than 90% suffering from type 2 diabetes (T2D).

Management of T2D can be achieved by controlling hyperglycemia through various targets but the major drawback in all these therapies is induction of hypoglycemia and weight gain. Hence newer approaches involve glucose-dependent insulin secretion (GDIS) for regulation of blood glucose levels to overcome these side-effects.

Glucagon-like peptide-1 (GLP-1), is the most potent insulinotropic hormone secreted by the intestinal L-cells in response to the food intake [2, 3]. It exhibits several biological effects including stimulation of insulin secretion and biosynthesis while inhibiting glucagon secretion and induces pancreatic β-cell proliferation each of which benefits in the control of glucose homeostasis without inducing hypoglycemia in patients with T2D [4, 5]. Thus GLP-1 has become a promising target for the treatment and management of T2D. This highly potent GLP-1 is rapidly degraded ($t_{½}$ ~ 1 min) by a serine protease dipeptidyl peptidase-IV (DPP-IV), *in vivo*, thereby rendering it pharmacologically inactive [6]. Even the synthetic GLP-1 agonists, although clinically efficacious have low bioavailability and most of them need to be dosed either subcutaneously or intravenously. Hence from medicinal chemistry point of view, inhibition of DPP-IV has gained importance as a new target for treatment of T2D which in turn will lead to increased half-life of GLP-1 and thereby enhancing the efficacy and potency of the incretin hormone. Also, GLP-1 is secreted in a glucose-dependent manner, hence hypoglycemia and pancreatic β-cell exhaustion, as in the case of other anti-hyperglycemic drugs, is not observed.

Some of the most potent DPP-IV inhibitors are as shown in the Figure 3.1.

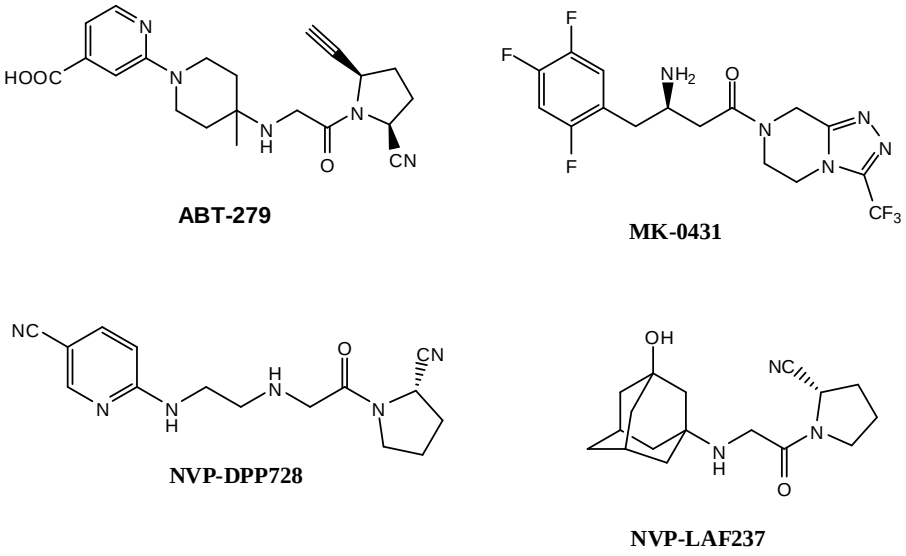

Figure 3.1: Some DPP-IV inhibitors

Amongst the first reported DPP-IV inhibitors is NVP-DPP728 [7], in a buffered aqueous medium (pH 7.4) gets converted to cyclic amidine, with $t_{½}$ ~ 48 h to > 70 days but has been reported to exist as a stable solid for months to year, as shown in Figure 3.2.

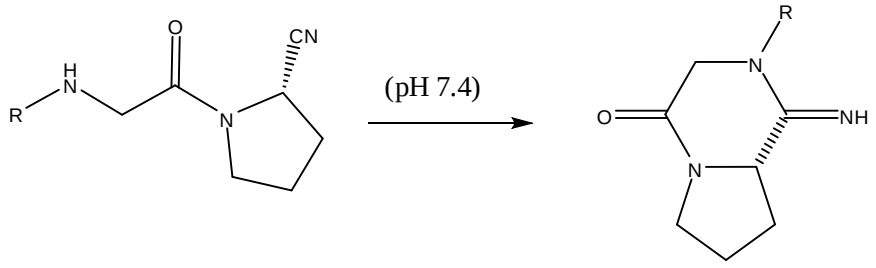

Figure 3.2: Intramolecular cyclization in a solution (pH 7.4)

But when adamantyl analogues were substituted at the P2 site, imidine formation was restricted due to stearic hindrance thereby rendering the molecule more potent (e.g. NVP-LAF237). Thus substitution of bulky groups at the P2 site is the key to increase the potency of the enzyme inhibitor.

In the previous chapter it was observed that substitution of sulphonamide derivatives at the P2 site acted as potent DPP-IV inhibitors. Hence, bulky heterocyclic molecules, like coumarin can be substituted at the P2 site, as shown in Figure 3.3, and its efficacy as DPP-IV enzyme inhibitor can be studied.

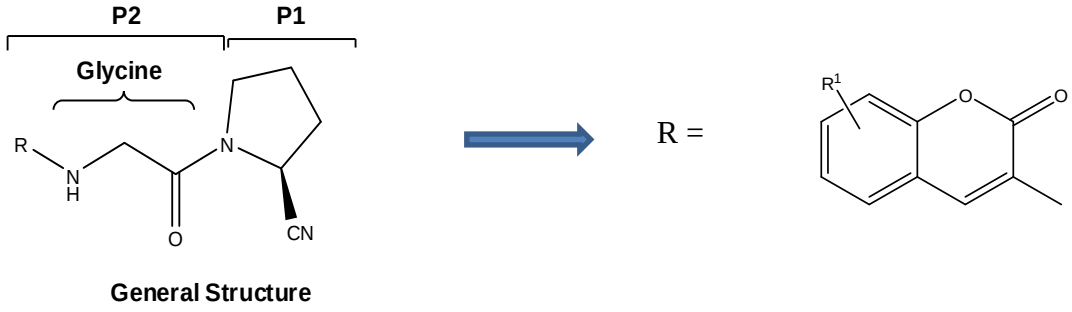

Figure 3.3: Designing of substituted 3-aminocoumarin derivatives as DPP-IV inhibitors.

Coumarin derivatives exhibit a wide spectrum of bioactivity. Both synthetic and naturally occurring coumarin derivatives have been widely studied for their various pharmacological activities. 3-amino coumarin derivatives have been reported for their antimicrobial and antioxidant activity [7] as well as anti-inflamatory properties [8]. They are also selective inhibitors MAO-B and acetylcholinesterase (AChE) for the treatment of Alzheimer's disease [9-11]. Recently, 3-aminocoumarin derivatives have been reported to show anti hyperglycemic activity [12, 13].

Synthesis and biological evaluation of 3-amino coumarin derivatives as DPP-IV inhibitors has been discussed in this chapter.

3.2 Results and Discussion

3.2.1 Chemistry

Classically, coumarin is synthesized by reaction of substituted salicyladehyde with N-acetyl glycine in acetic anhydride, better known as Perkin reaction to yield substituted 3-acetamidocoumarin which on hydrolysis by methanolic HCl gives the desired substituted 3-aminocoumarin. Thus heating α-naphthaldehyde **1a**, N-acetlyglycine and sodium acetate in acetic anhydride for seven hours at 100 ^{o}C yielded N-(2-oxo-2H-benzo[h]chromen-3-yl)acetamide **2a**, Scheme 3.1, confirmed from its IR spectrum (Figure 3.5.1) which shows bands at 3341, 1709, 1676 cm^{-1} for the –NH of amide, lactone carbonyl and amide carbonyl groups respectively while the ^{1}H NMR spectrum (Figure 3.5.2) shows two singlet's at δ 2.32 and 9.53 for the acetamido methyl group and amide -NH protons respectively. Figure 3.5.3 and Figure 3.5.4 shows ^{13}C NMR and ESI-MS spectrum of **2a**. Figures 3.6.1, 3.6.2, 3.6.3 and 3.6.4 show IR, ^{1}H NMR, ^{13}C NMR and ESI-MS spectra of compound **2b** respectively. Similarly, Figure nos. 3.7.1, 3.7.2, 3.7.3 and 3.7.4 shows the IR, ^{1}H NMR, ^{13}C NMR and ESI-MS spectra of **2d**. Further hydrolysis of **2a** by methanolic HCl gave free amine **3a** as confirmed from its IR spectrum (Figure 3.8.1) with bands at 3448 and 3366 cm^{-1} for the amino group and a strong band at 1713 cm^{-1} for the lactone carbonyl group and ^{1}H NMR spectrum (Figure 3.8.2) wherein a singlet at δ 4.44 for the two amino protons ($-NH_2$) and absence of signal for the $–CH_3$ of acetamide in the aliphatic region confirms the structure of **3a**. Figure 3.8.3 shows ^{13}C NMR spectrum and Figure 3.8.4 shows ESI-MS spectrum further confirm the structure of **3a**. Figures 3.9.1, 3.9.2, 3.9.3 and 3.9.4 show IR, ^{1}H NMR, ^{13}C

NMR and ESI-MS spectra of **3b** respectively while Figure 3.10.1, 3.10.2, 3.10.3 and 3.10.4 shows IR, ^{1}H NMR, ^{13}C NMR and ESI-MS spectra of **3d** thereby confirming their structures.

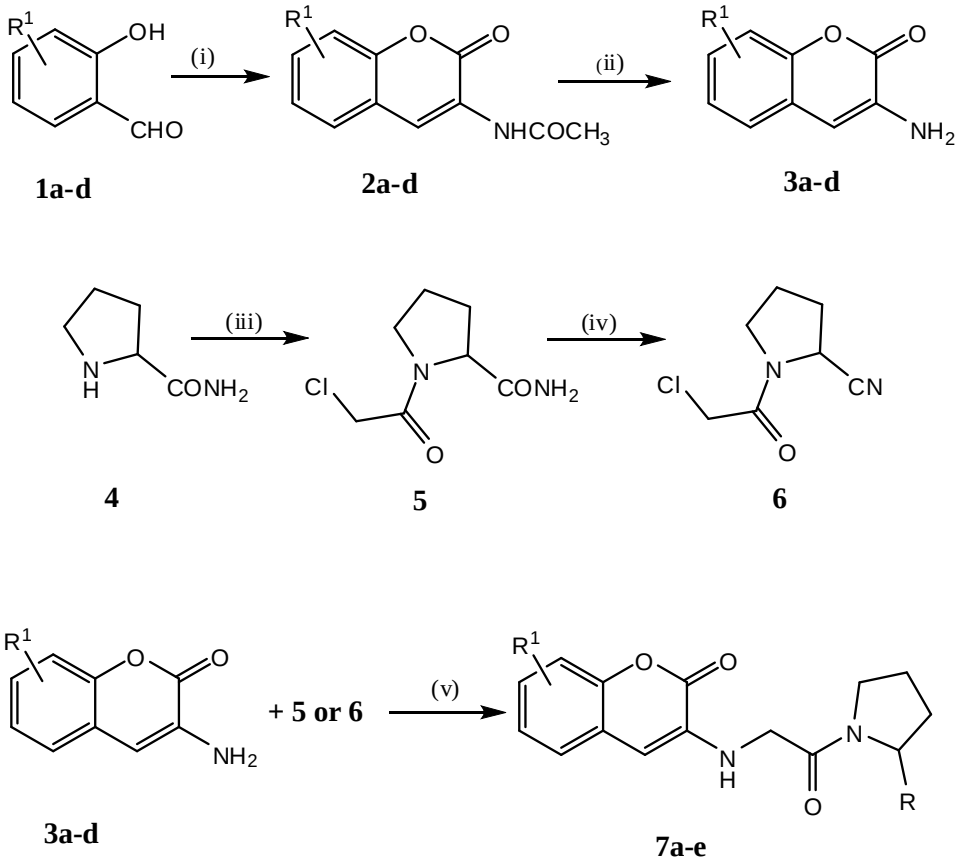

R = CN, R^1 = 7,8-Ph = a
= H = b
= 7-OH = c
= 8-OCH_3 = d
R = $CONH_2$, R^1 = H = e

Scheme 3.1: Reagents: (i) N-acetylglycine, $(CH_3CO)_2O$, CH_3COONa; (ii) CH_3OH-HCl; (iii) $ClCH_2COCl$, K_2CO_3, THF; (iv) TFAA, THF, NH_4HCO_3; (v) K_2CO_3, dry DMF.

On the other hand when chloroacetyl chloride was added to a solution of L-proline amide **4** in THF, *(S)*-1-(2-chloroacetyl)pyrrolidine-2-carboxamide **5** is obtained, the structure of which was confirmed by IR spectrum which shows two bands at 1686, 1709 cm^{-1} for amides carbonyls, one of which disappears when **5** is dehydrated with trifluoroacetic anhydride (TFAA) to yield *(S)*-1-(2-chloroacetyl)pyrrolidine-2-carbonitrile **6**. The IR spectrum (**Figure 2.4.1**, **Chapter 2**) of **6** shows two strong bands at 2241 and 1656 cm^{-1} for the nitrile and amide carbonyl groups respectively while its ^{1}H NMR spectrum (**Figure 2.4.2**, **Chapter 2**) showed a singlet at δ 4.076 for the methylene protons and multiplet at δ 4.69-4.71 for -CH proton of the cyanopyrrolidide thus confirming its structure. Reaction of **3a-d** with **5** or **6** in DMF in presence of potassium carbonate as a base gave the compounds **7a-e (**Scheme 3.1**).** The IR spectrum of **7a** (Figure 3.11.1) showed two strong bands at 1709 and 1653 cm^{-1} for the lactone and amide groups respectively. ^{1}H NMR spectrum (Figure 3.11.2) showed multiplets from δ 2.28-2.41 for the four $–CH_2$ protons, a multiplet from 3.63 to 3.79 for two $–CH_2$ protons and another multiplet from δ 4.89-4.91 for the –CH proton of the cyanopyrrolidide; a doublet at δ 4.01 indicated the glycyl $–CH_2$ protons and multiplets from δ 6.99-8.18 indicated aromatic protons thereby confirming the formation of **7a.** Figures 3.11.3 and 3.11.4 shows ^{13}C NMR and ESI-MS spectra of **7a** which further supported its structure. The specific optical rotation of **7a** was found to be -272.11 due to the chirality of the cyanopyrrolidide system. Figures 3.12.1, 3.12.2, 3.12.3 and 3.12.4 shows IR, ^{1}H NMR, ^{13}C NMR and ESI-MS spectra of **7b** respectively thus confirming its structure. Figures 3.13.1, 3.13.2, 3.13.3 and 3.13.4 shows IR, ^{1}H NMR, ^{13}C NMR and ESI-MS spectra of **7c**

respectively and Figures 3.14.1, 3.14.2, 3.14.3 and 3.14.4 shows IR, ^{1}H NMR, ^{13}C NMR and ESI-MS spectra of **7d** respectively thus confirming their respective structures

3-amino-2H-chromen-2-one **3b** on reaction with *(S)*-1-(2-chloroacetyl)pyrrolidine-2-carboxamide **5** gave *(S)*-1-(2-(2-oxo-2H-chromen-3-ylamino)acetyl)pyrrolidine-2-carboxamide **7e.** Its structure was also proved by its IR spectrum (Figure 3.15.1), ^{1}H NMR spectrum (Figure 3.15.2), ^{13}C NMR spectrum (Figure 3.15.3) and ESI-MS spectrum (Figure 3.15.4). Another compound **7g** was synthesized by reaction of 3-amino-7-hydroxy-2*H*-chromen-2-one **3c** with 2-chloro-1-morpholinoethanone, obtained by the reaction of morpholine with chloroacetyl chloride. The structures of all these compounds were characterized by IR, ^{1}H NMR, ^{13}C NMR spectra and ESI-MS analyses.

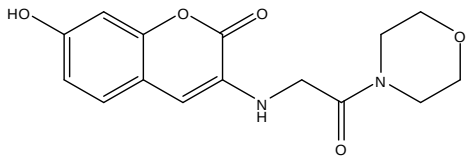

Figure 3.4: *Structure of 7-hydroxy-3-(2-morpholino-2-oxoethylamino)-2H-chromen-2-one **7g***

Figure 3.16.1 and 3.16.2 show IR and ^{1}H NMR of **7g** thus confirming the formation of **7g**.

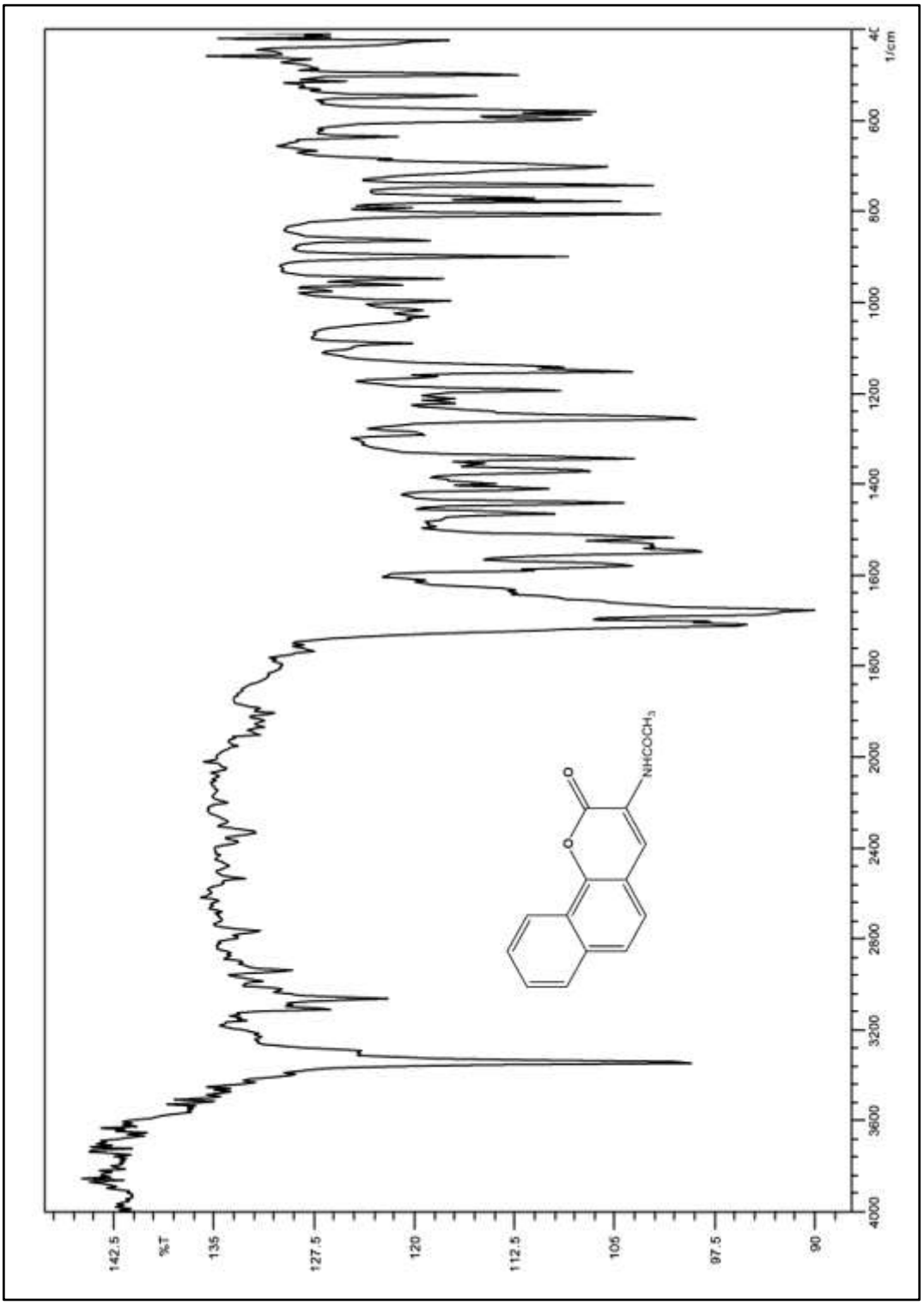

Figure 3.5.1: IR spectrum of N-(2-oxo-2H-benzo[h]chromen-3-yl)acetamide-acetyl-2H-benzo[h]chromen-2-one **2a**

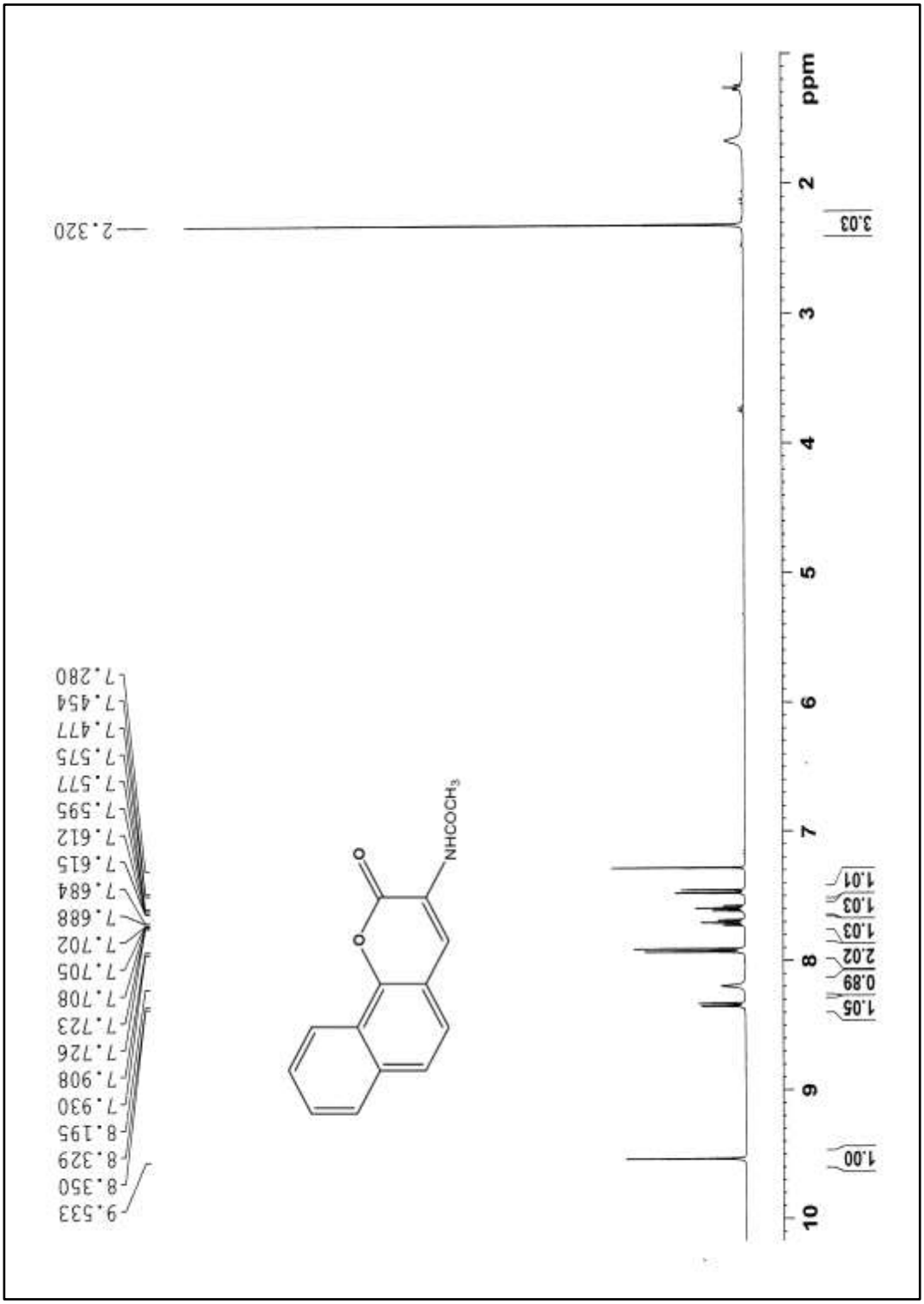

Figure 3.5.2: ^{1}H NMR spectrum of N-(2-oxo-2H-benzo[h]chromen-3-yl)acetamide-acetyl-2H-benzo[h]chromen-2-one **2a**

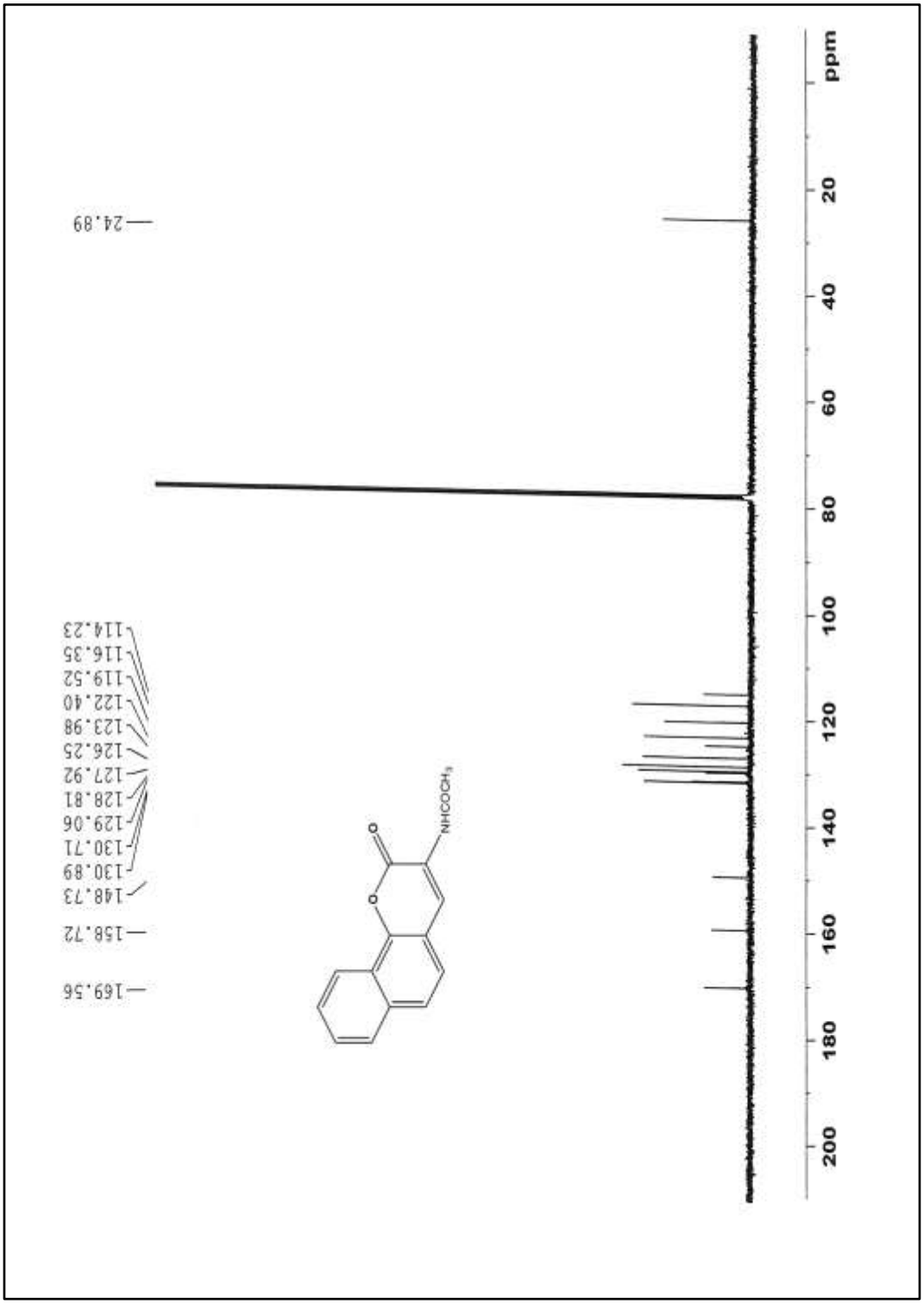

Figure 3.5.3: ^{13}C NMR spectrum of N-(2-oxo-2H-benzo[h]chromen-3-yl)acetamide-acetyl-2H-benzo[h]chromen-2-one **2a**

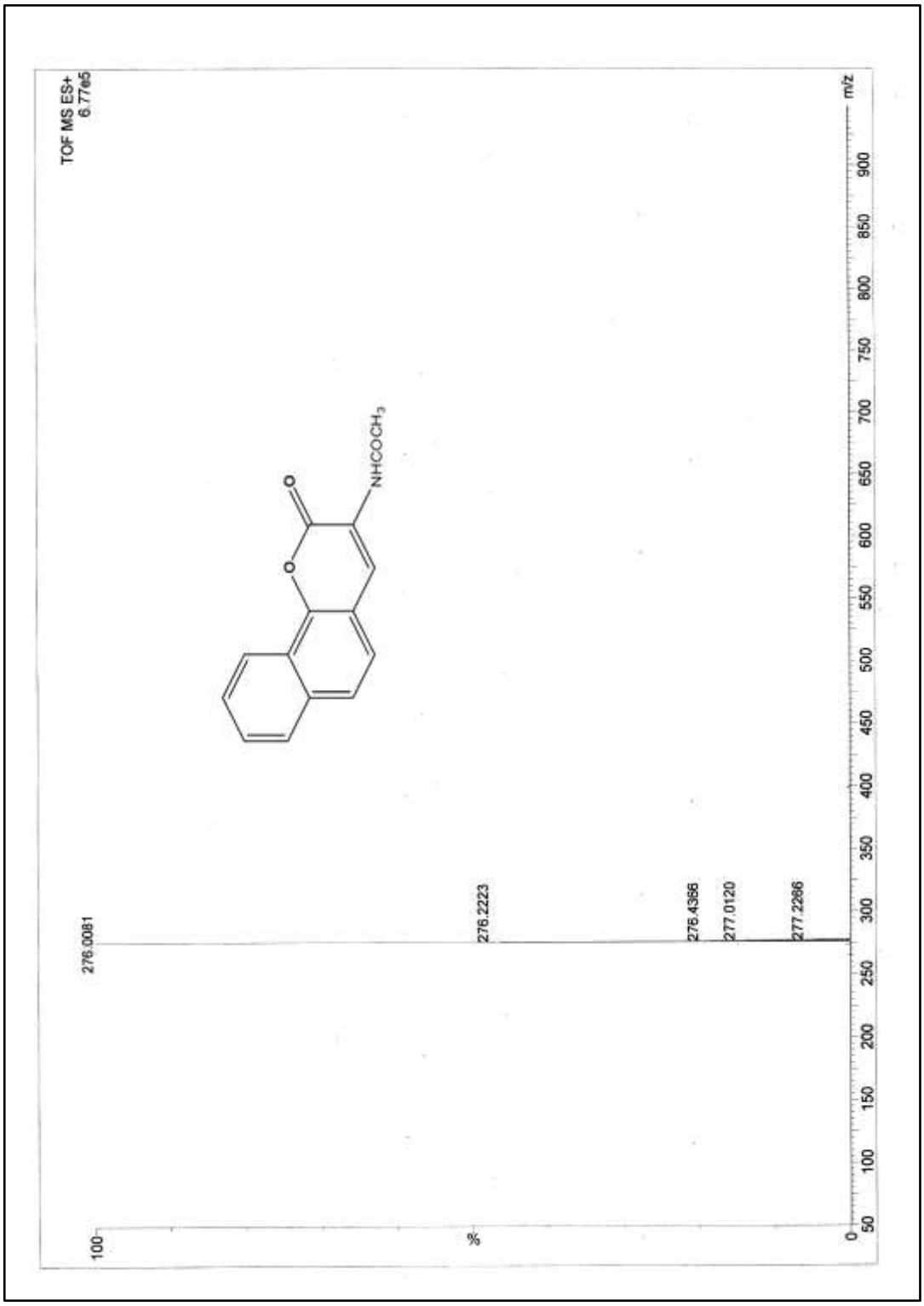

Figure 3.5.4: ESI-MS spectrum of N-(2-oxo-2H-benzo[h]chromen-3-yl)acetamide-acetyl-2H-benzo[h]chromen-2-one **2a**

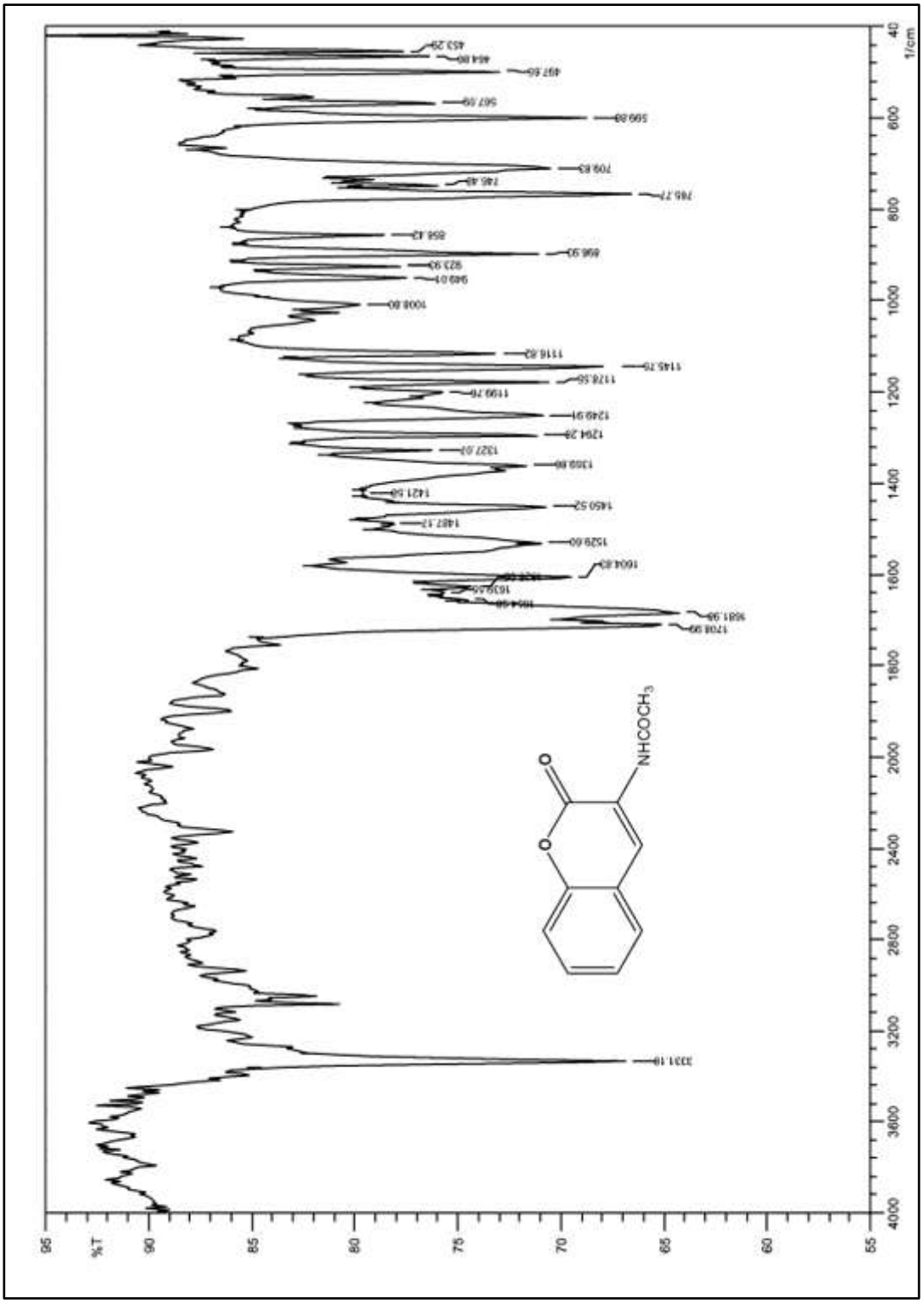

Figure 3.6.1: IR spectrum of N-(2-oxo-2H-chromen-3-yl)acetamide **2b**

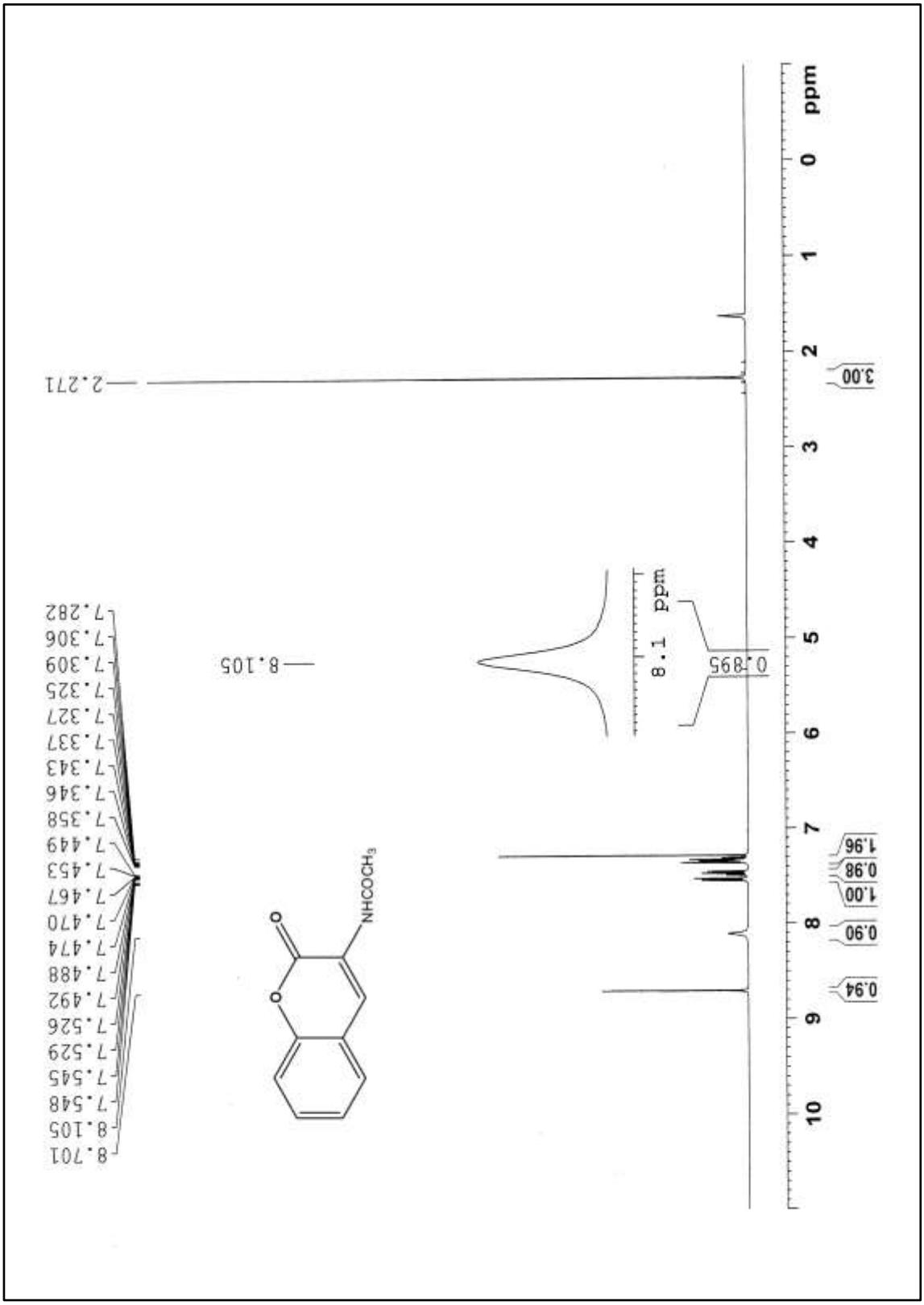

Figure 3.6.2: ^{1}H NMR spectrum of N-(2-oxo-2H-chromen-3-yl)acetamide **2b**

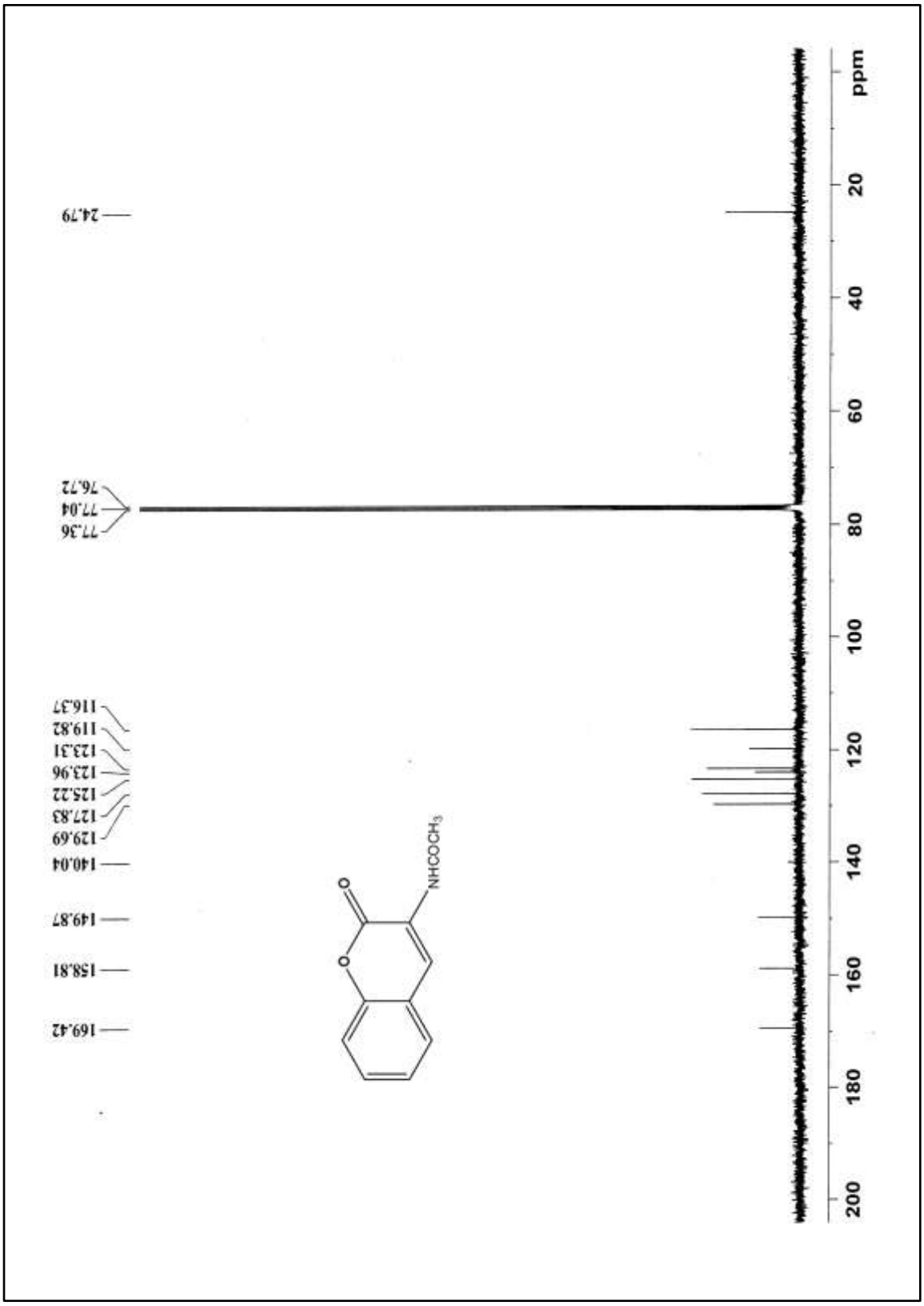

Figure 3.6.3: ^{13}C NMR spectrum of N-(2-oxo-2H-chromen-3-yl)acetamide **2b**

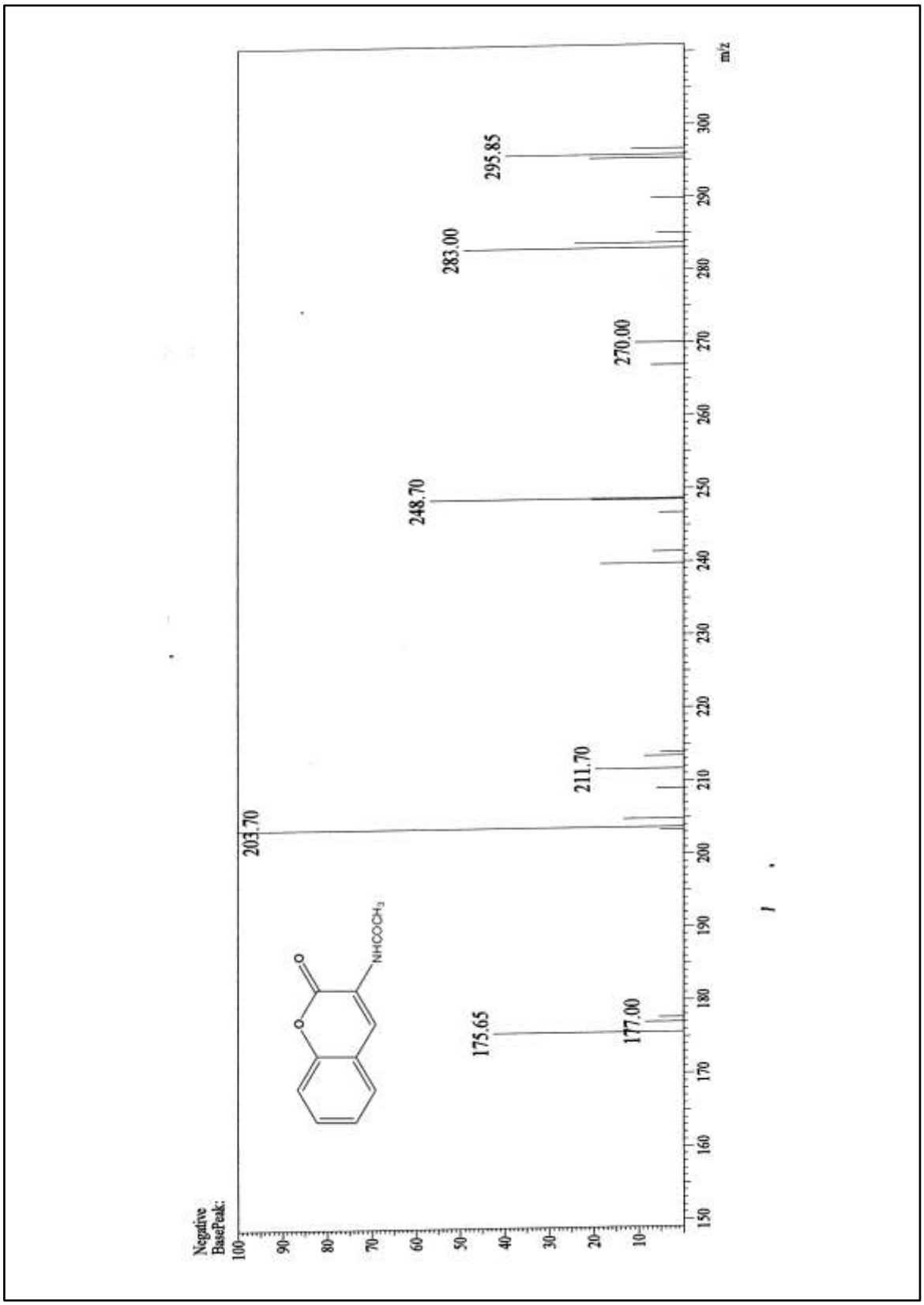

Figure 3.6.4: ESI-MS spectrum of N-(2-oxo-2H-chromen-3-yl)acetamide **2b**

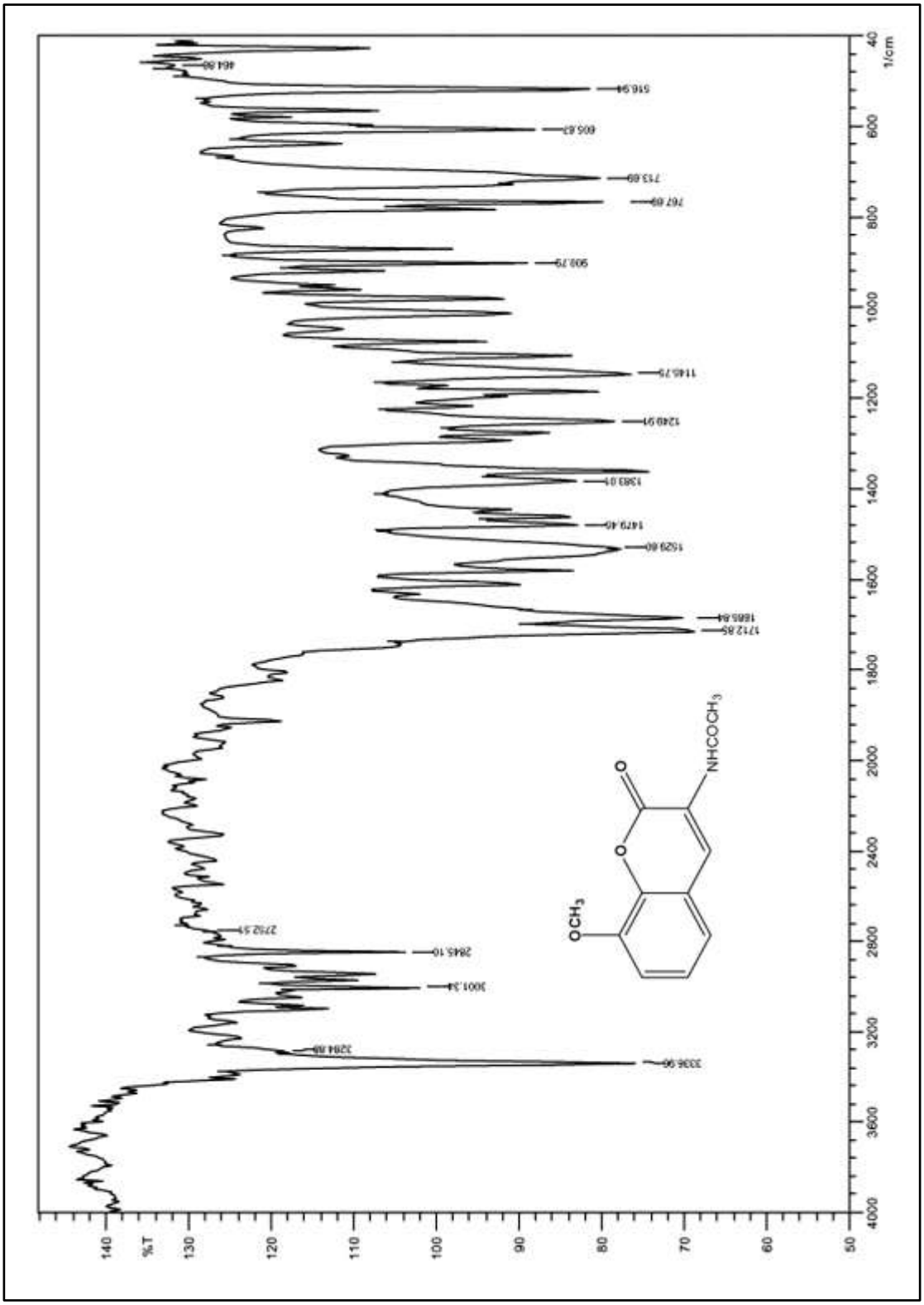

Figure 3.7.1: IR spectrum of N-(8-methoxy-2-oxo-2H-chromen-3-yl)acetamide **2d**

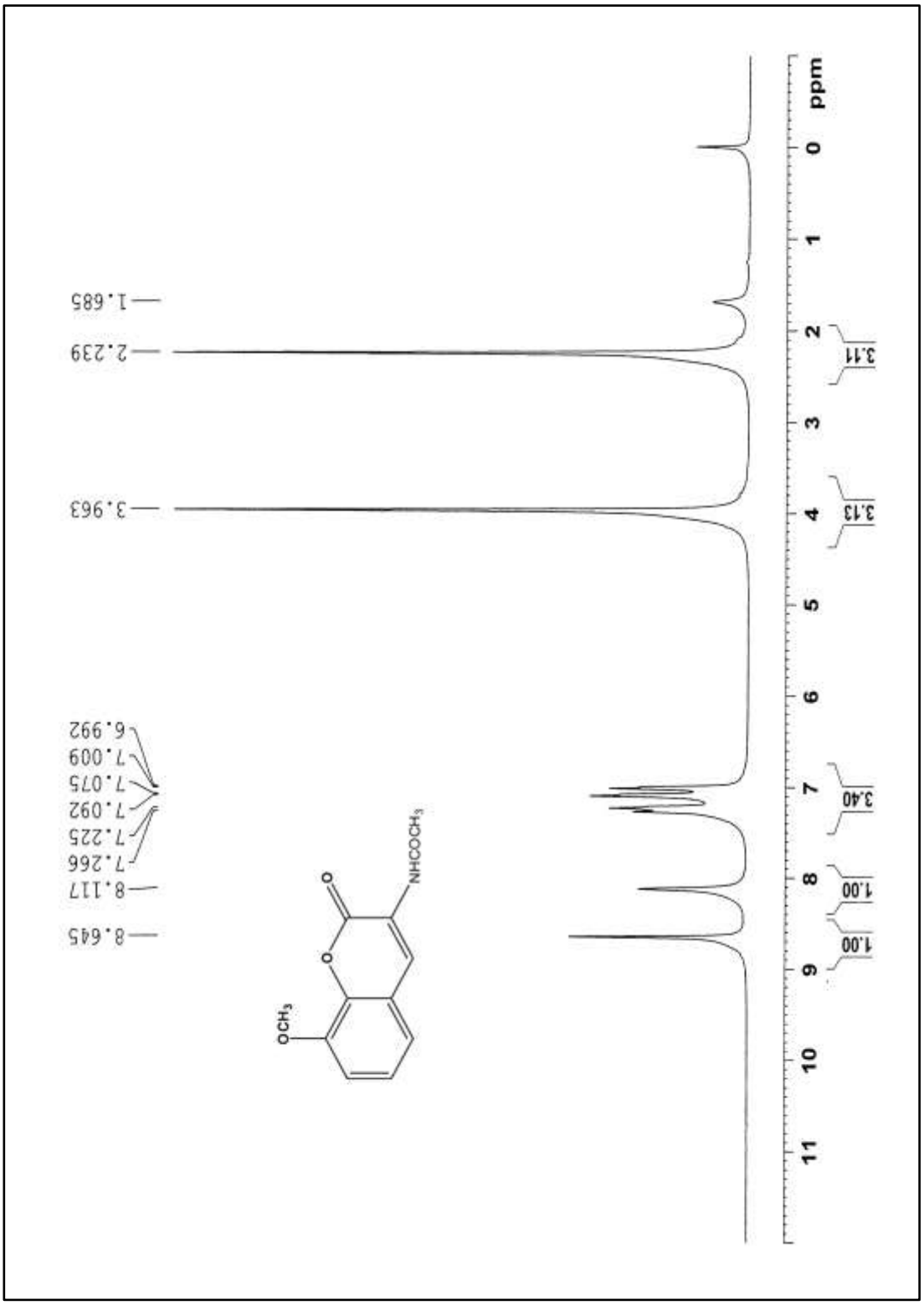

Figure 3.7.2: ^{1}H NMR spectrum of N-(8-methoxy-2-oxo-2H-chromen-3-yl)acetamide **2d**

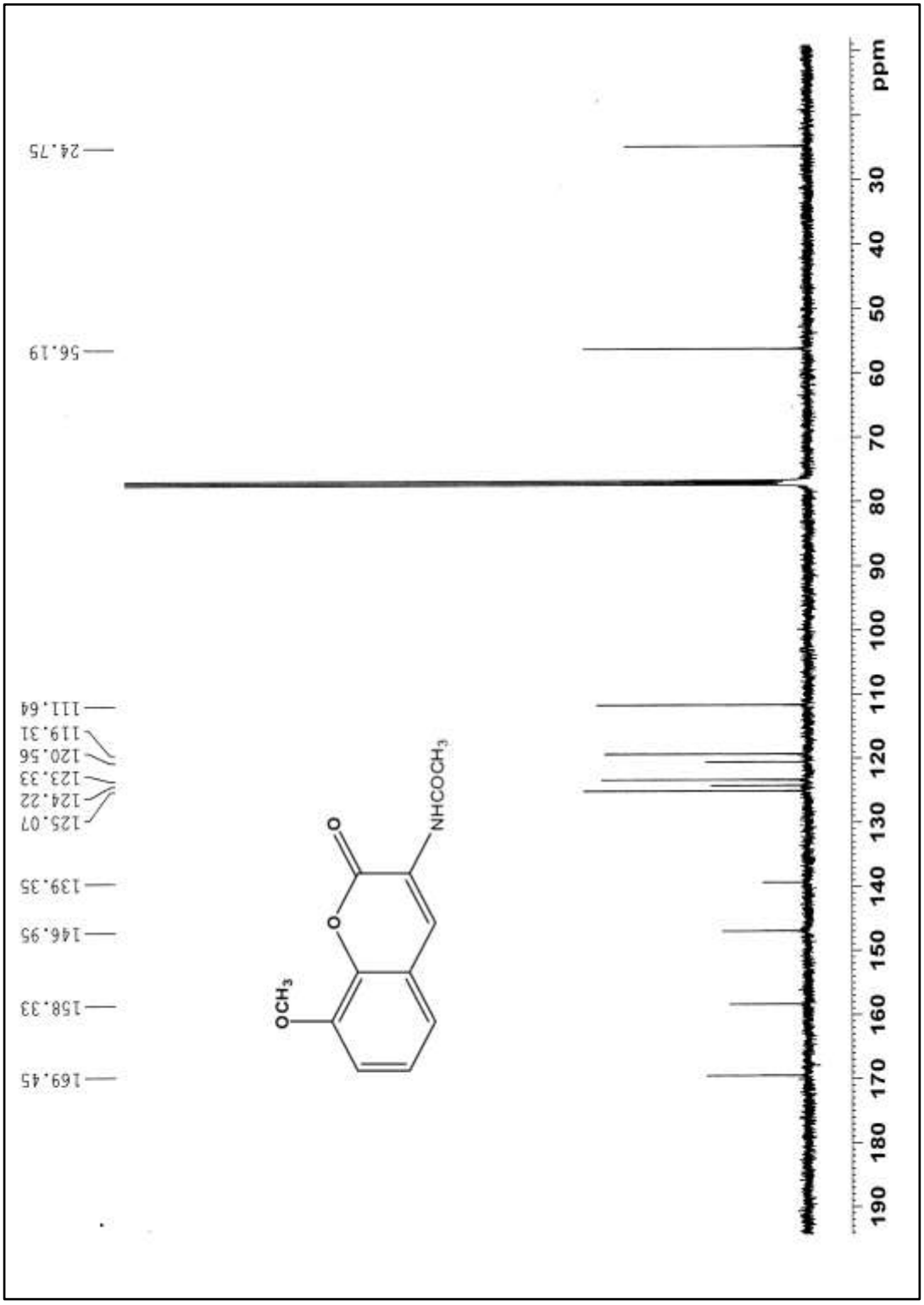

Figure 3.7.3: ^{13}C NMR spectrum of N-(8-methoxy-2-oxo-2H-chromen-3-yl)acetamide **2d**

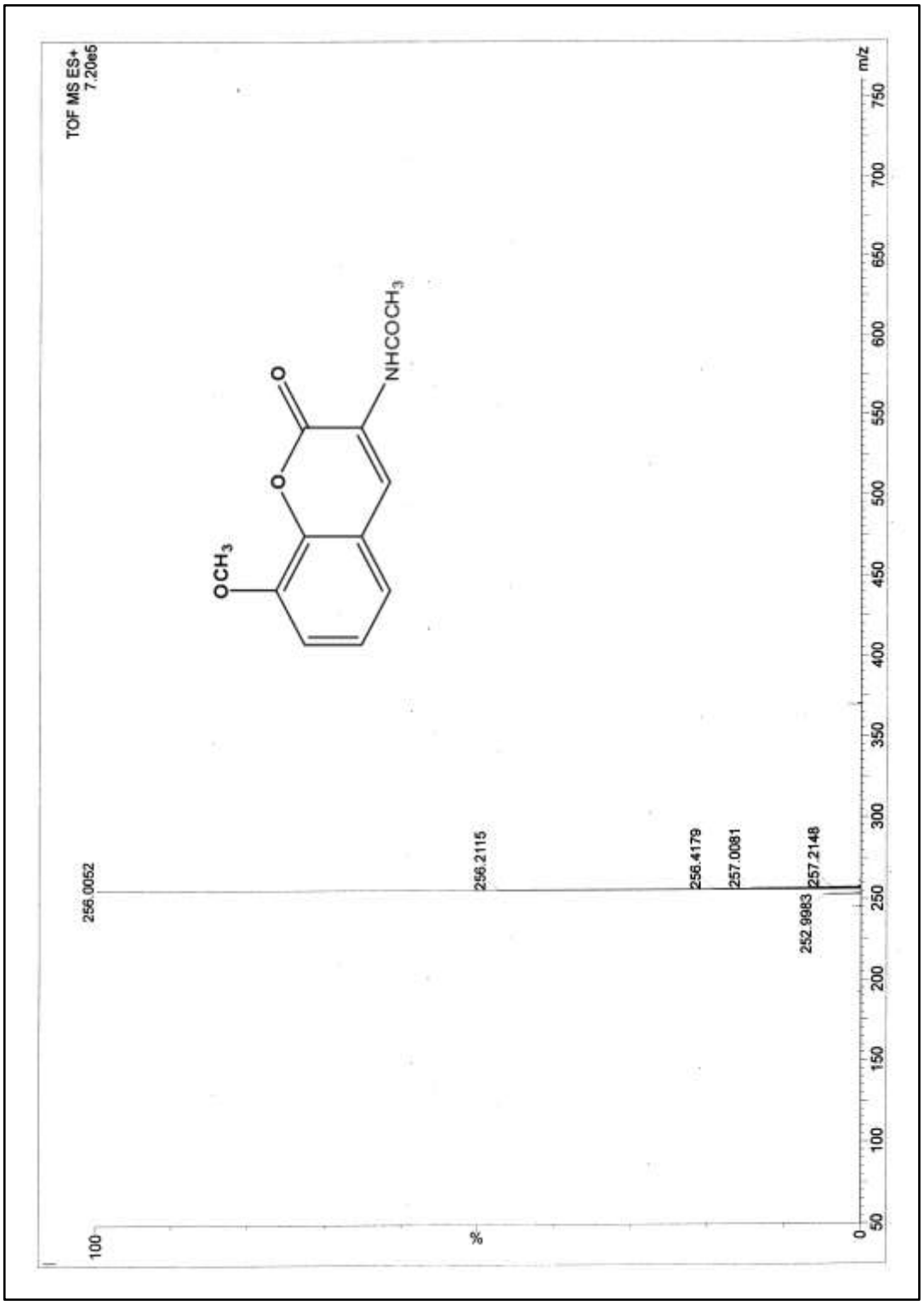

Figure 3.7.4: ESI-MS spectrum of N-(8-methoxy-2-oxo-2H-chromen-3-yl)acetamide **2d**

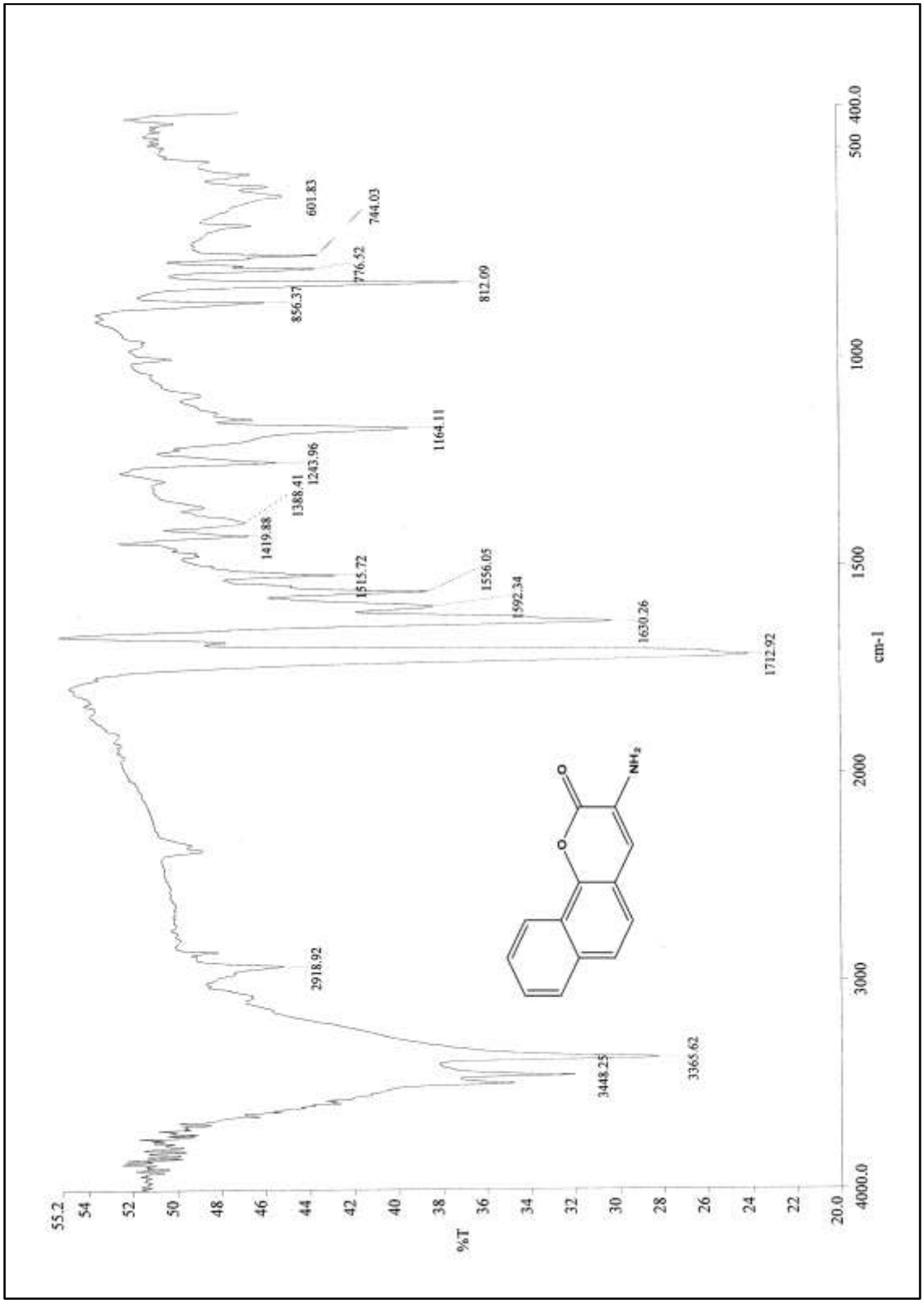

Figure 3.8.1: IR spectrum of 3-amino-2H-benzo[h]chromen-2-one **3a**

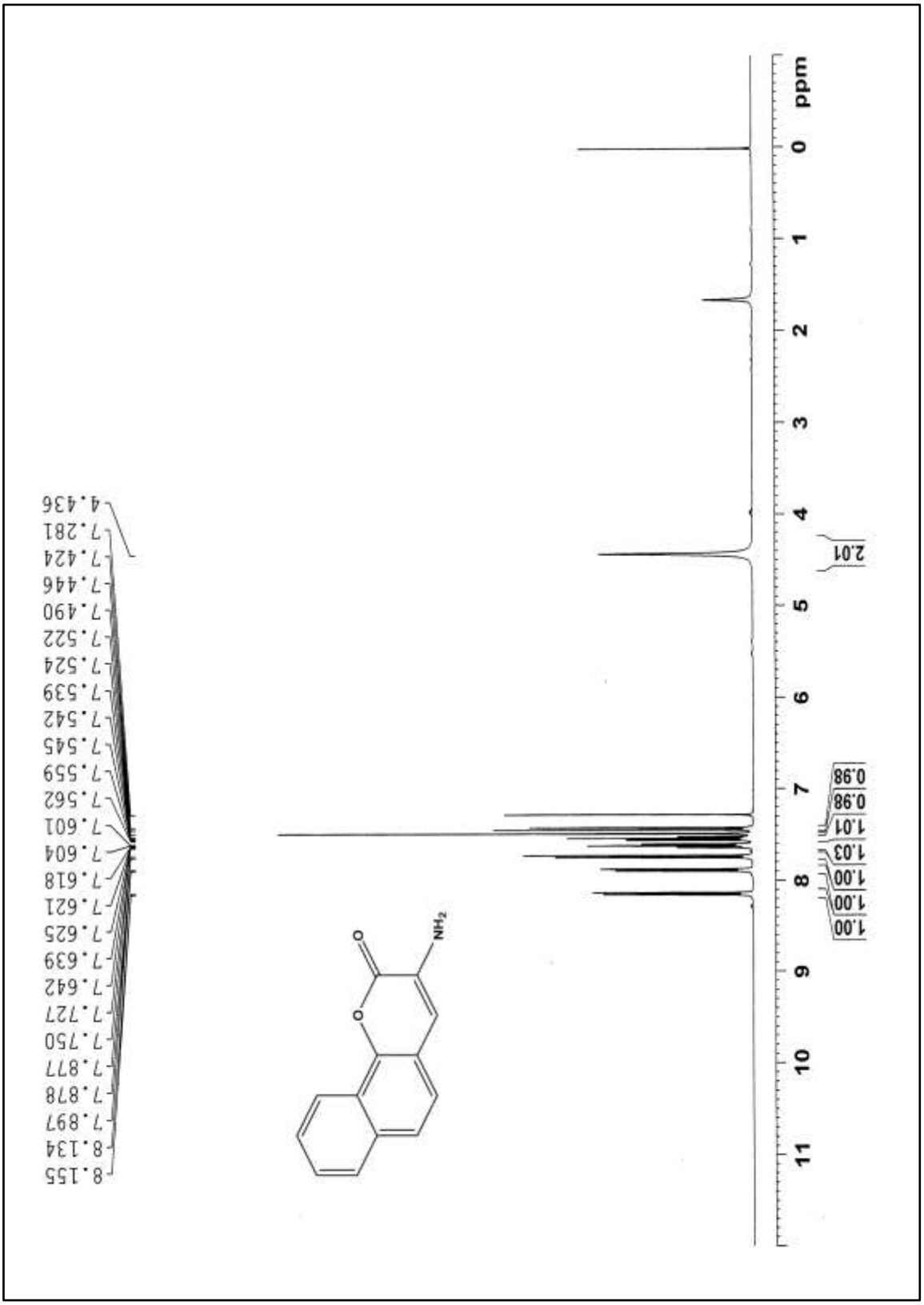

Figure 3.8.2: ^{1}H NMR spectrum of 3-amino-2H-benzo[h]chromen-2-one **3a**

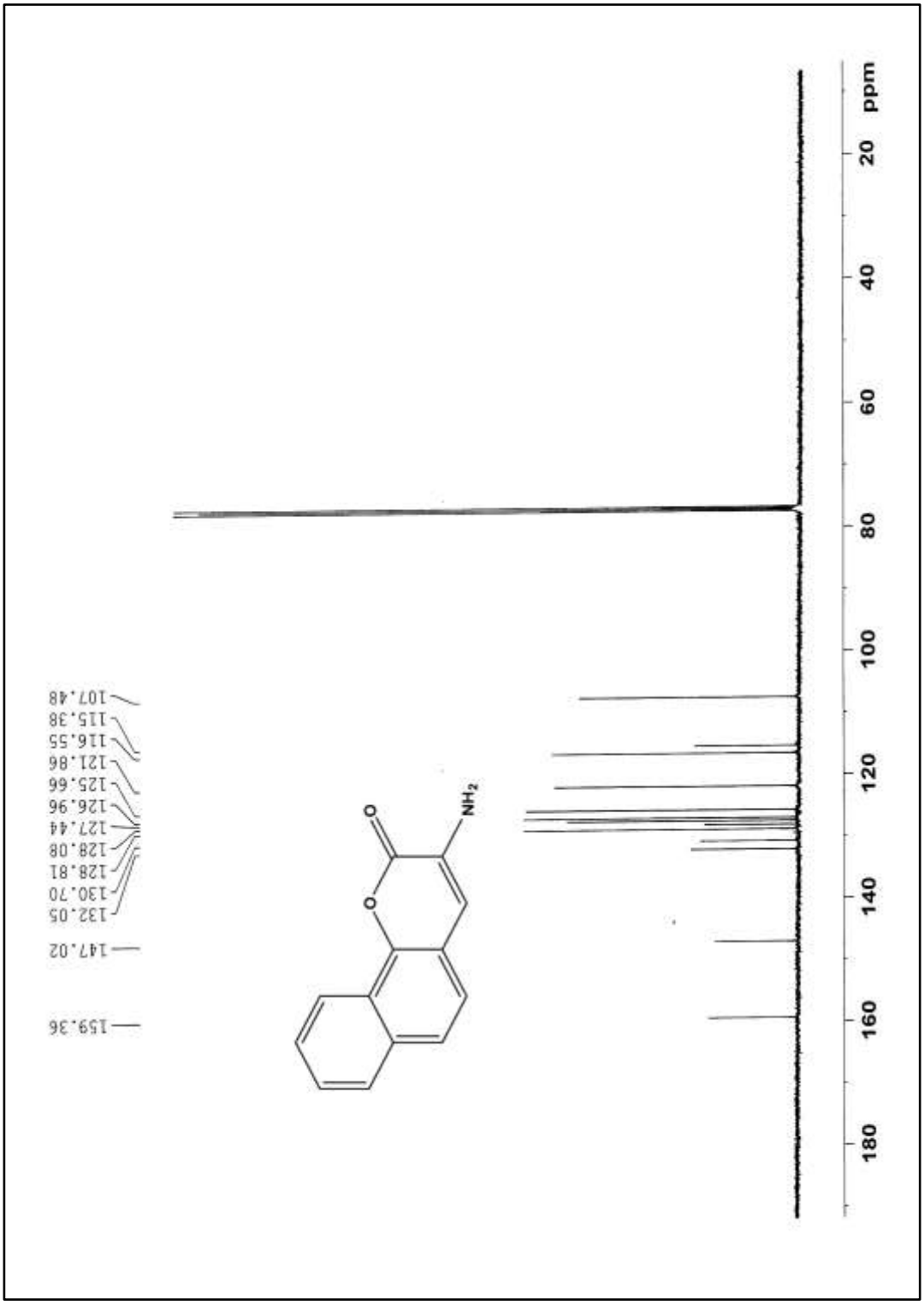

Figure 3.8.3: ^{13}C NMR spectrum of 3-amino-2H-benzo[h]chromen-2-one **3a**

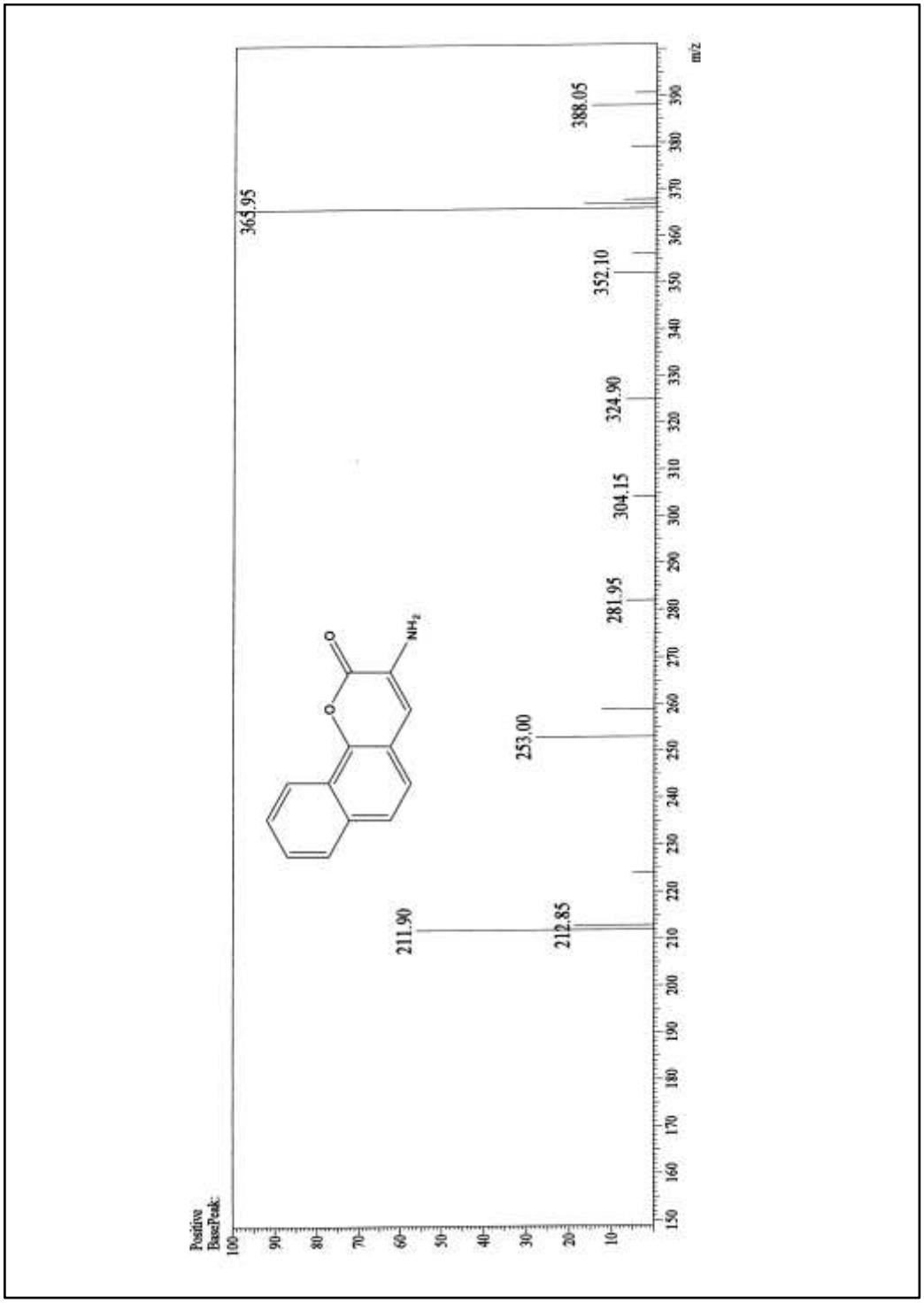

Figure 3.8.4: ESI-MS spectrum of 3-amino-2H-benzo[h]chromen-2-one **3a**

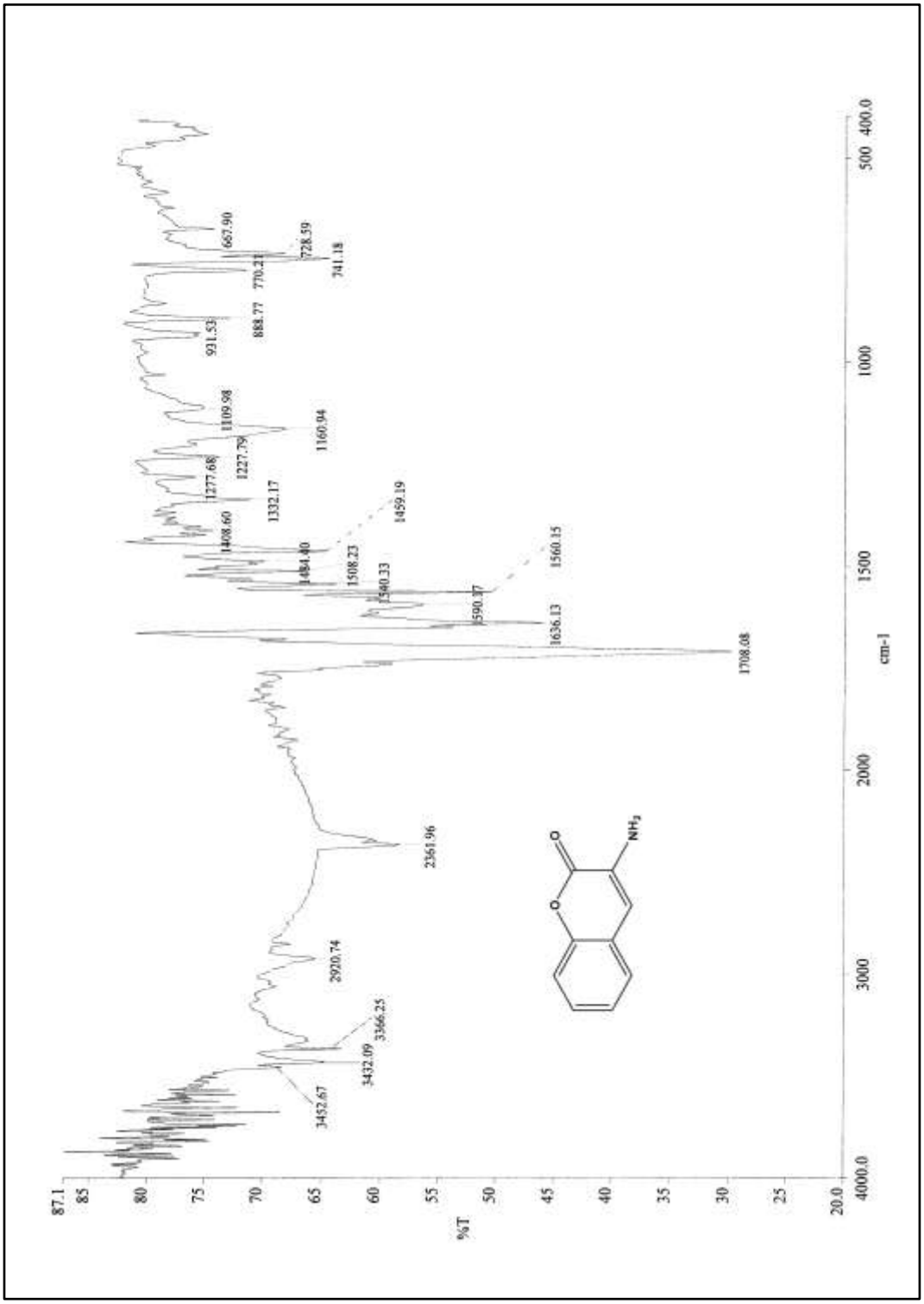

Figure 3.9.1: IR spectrum of 3-amino-2H-chromen-2-one **3b**

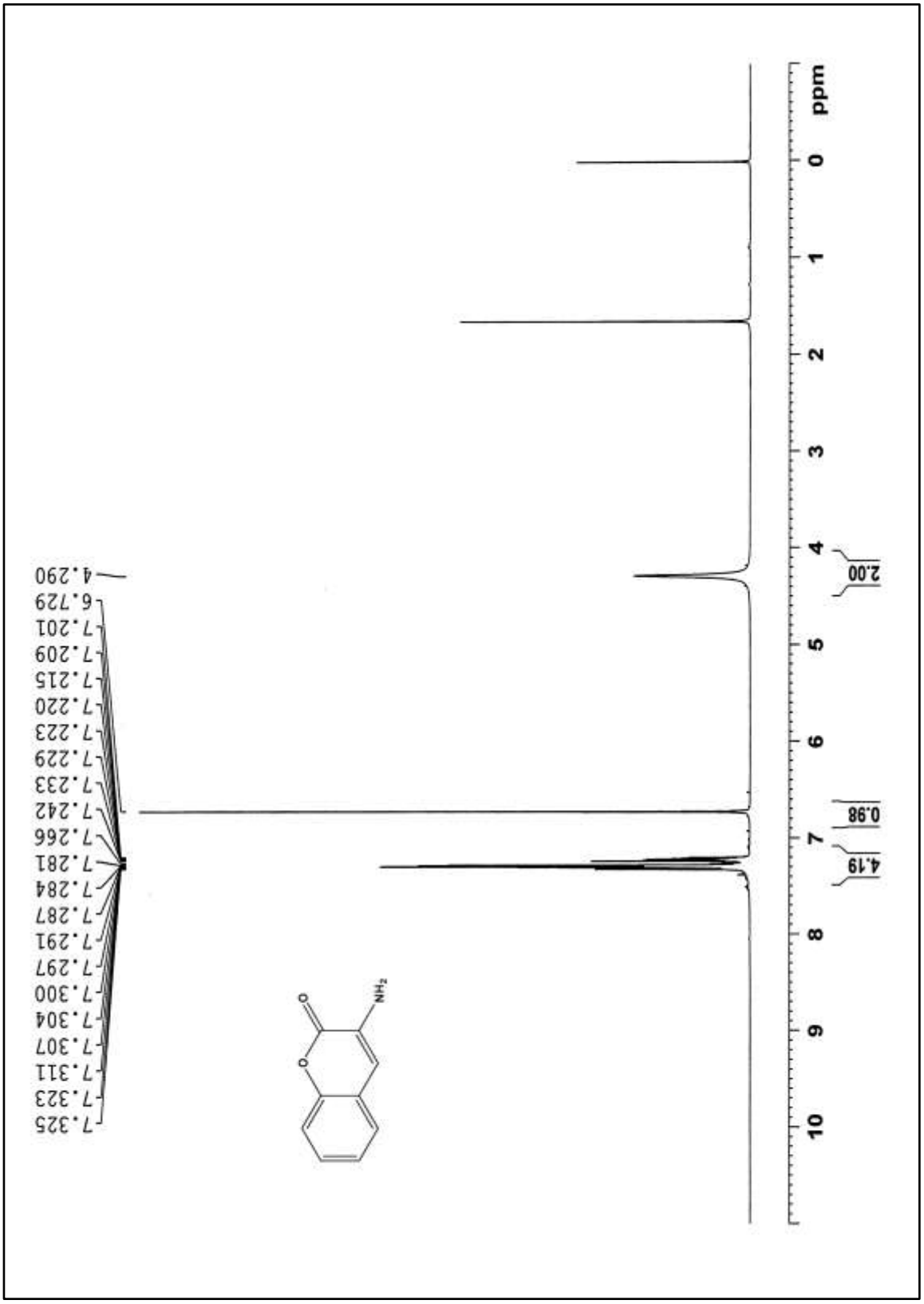

Figure 3.9.2: ^{1}H NMR spectrum of 3-amino-2H-chromen-2-one **3b**

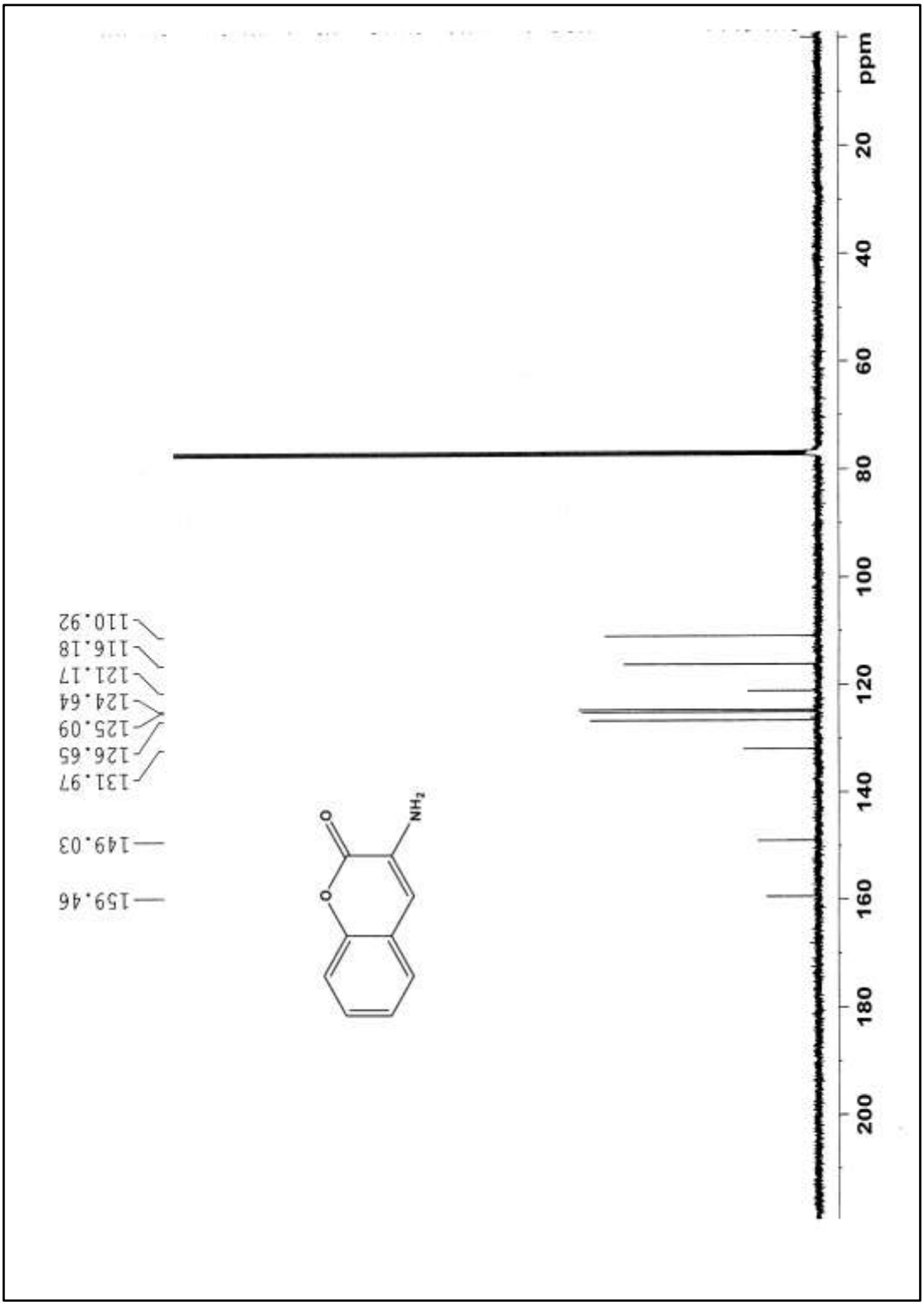

Figure 3.9.3: ^{13}C NMR spectrum of 3-amino-2H-chromen-2-one **3b**

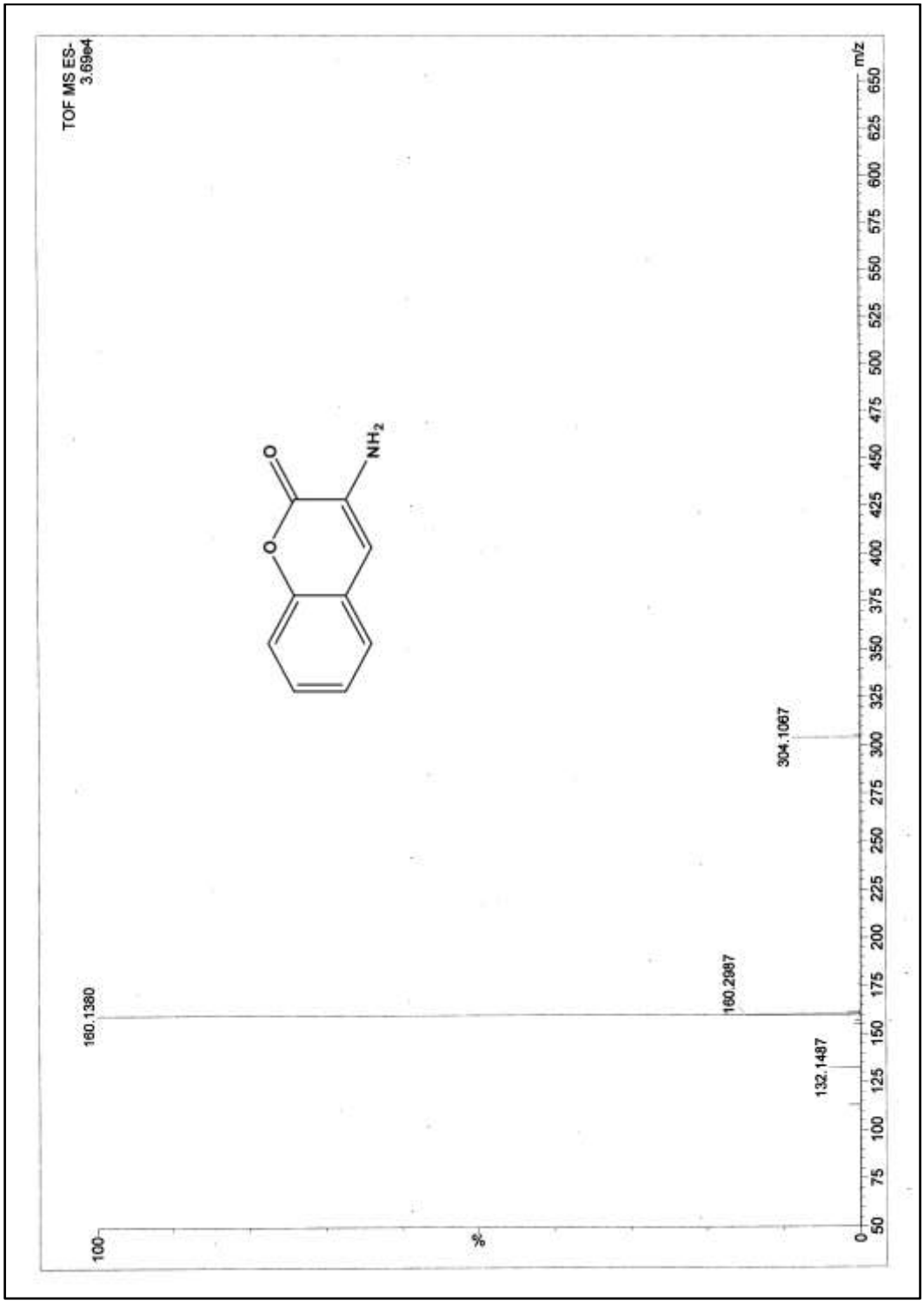

Figure 3.9.4: ESI-MS spectrum of 3-amino-2H-chromen-2-one **3b**

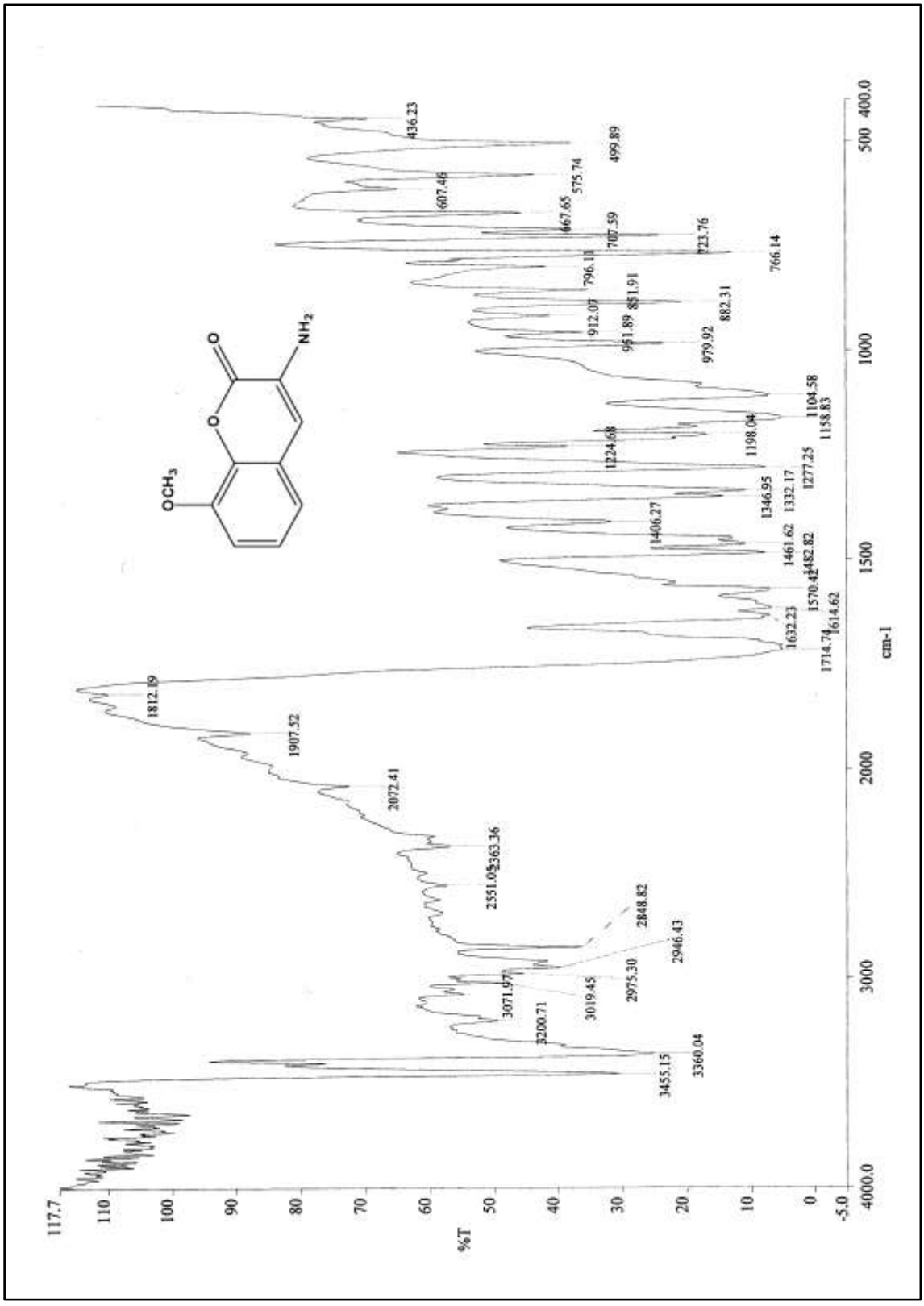

Figure 3.10.1: IR spectrum of 3-amino-8-methoxy-2H-chromen-2-one **3d**

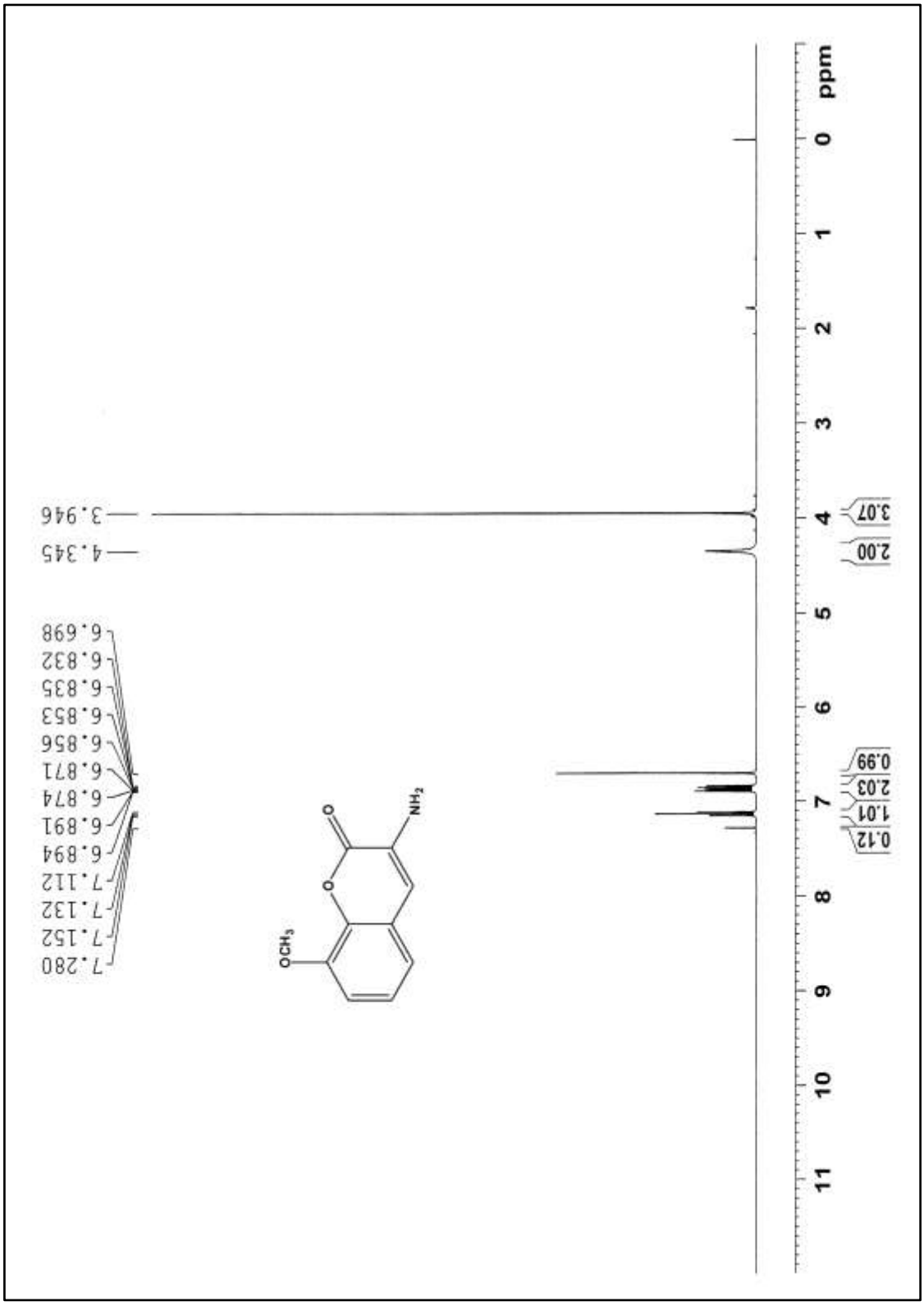

Figure 3.10.2: ^{1}H NMR spectrum of 3-amino-8-methoxy-2H-chromen-2-one **3d**

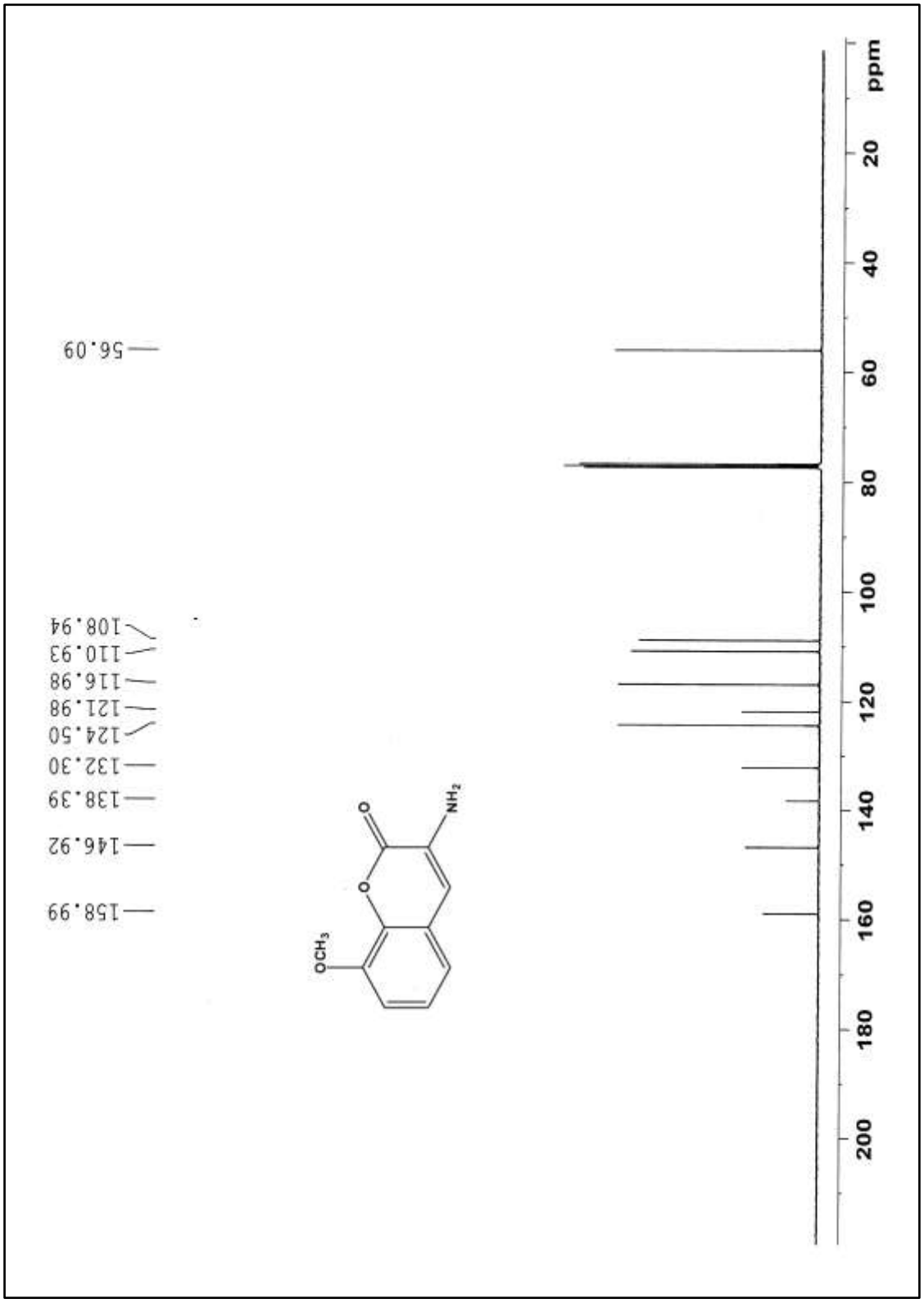

Figure 3.10.3: ^{13}C NMR spectrum of 3-amino-8-methoxy-2H-chromen-2-one **3d**

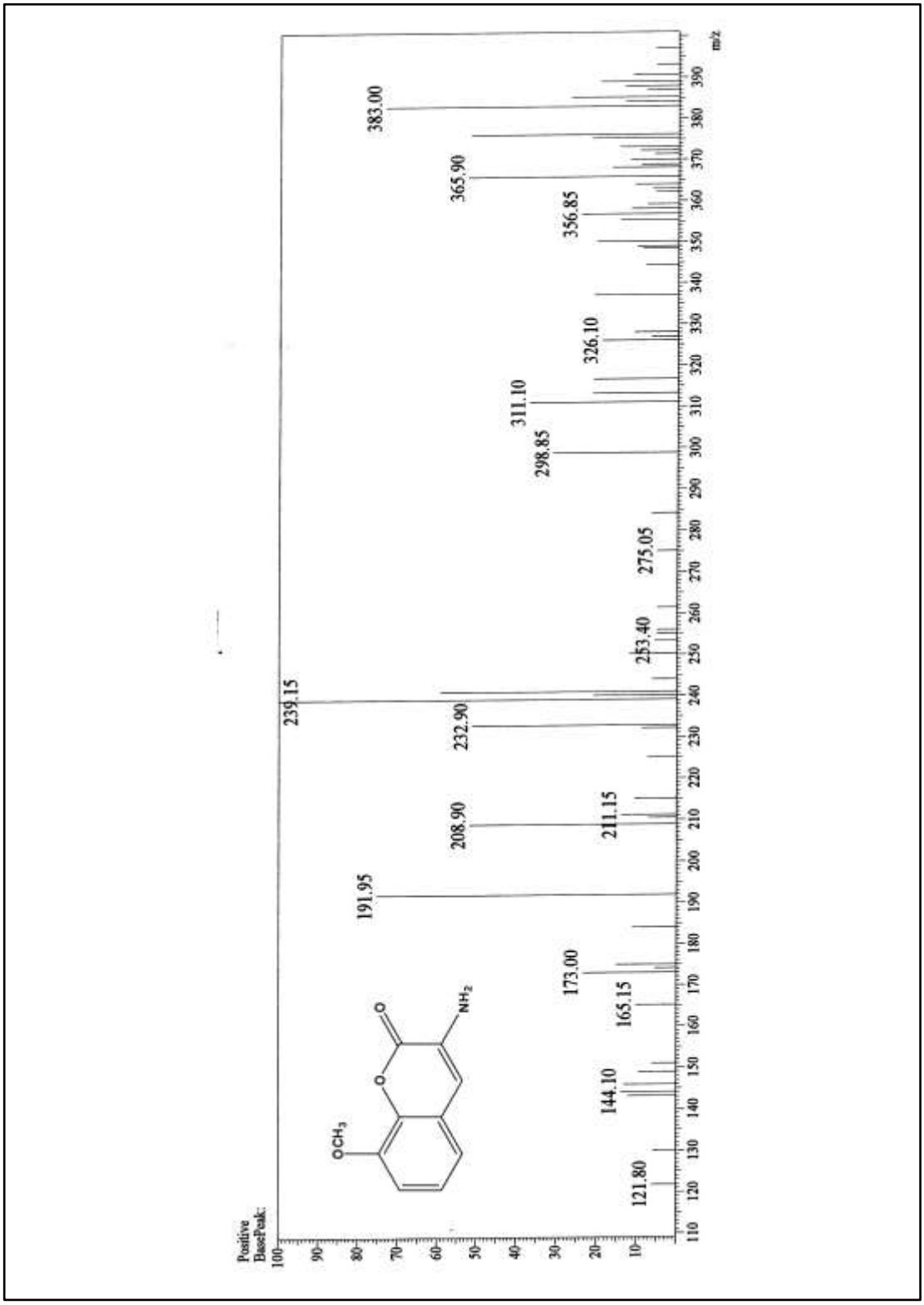

Figure 3.10.4: ESI-MS spectrum of 3-amino-8-methoxy-2H-chromen-2-one **3d**

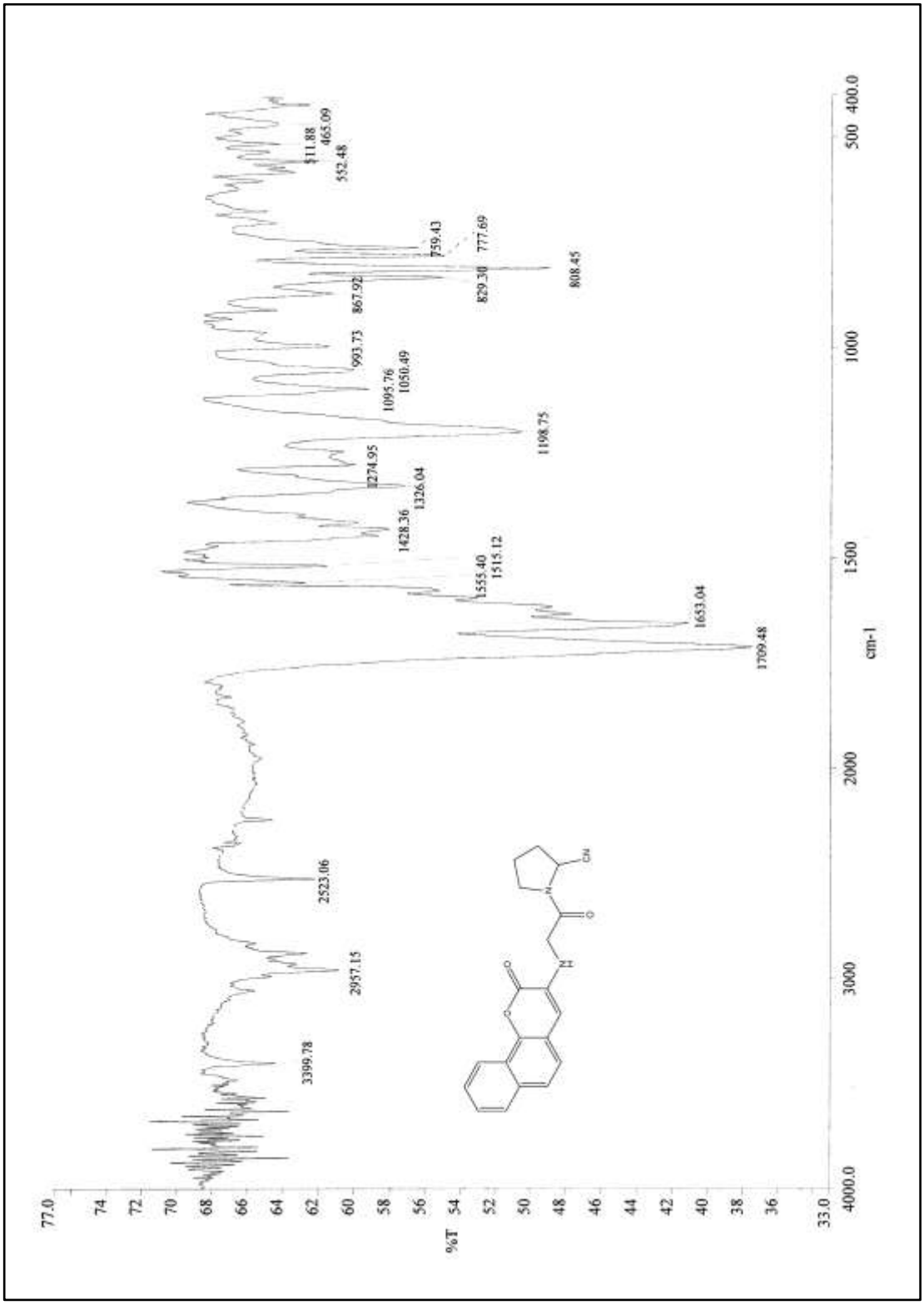

Figure 3.11.1: IR spectrum of *(S)*-1-(2-(2-oxo-2H-benzo[h]chromen-3-ylamino)acetyl)pyrrolidine-2-carbonitrile **7a**

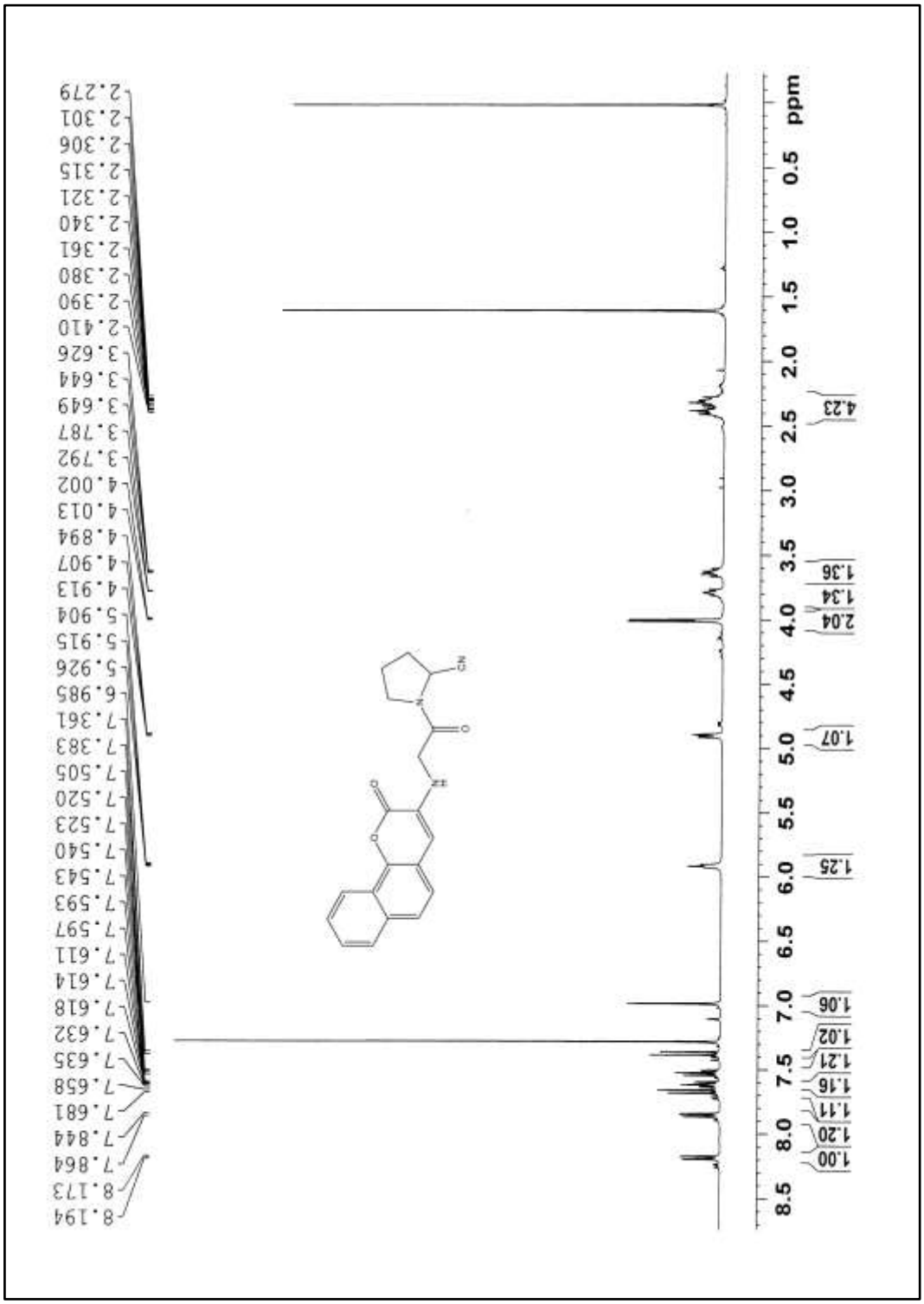

Figure 3.11.2: ^{1}H NMR spectrum of *(S)*-1-(2-(2-oxo-2H-benzo[h]chromen-3-ylamino)acetyl)pyrrolidine-2-carbonitrile **7a**

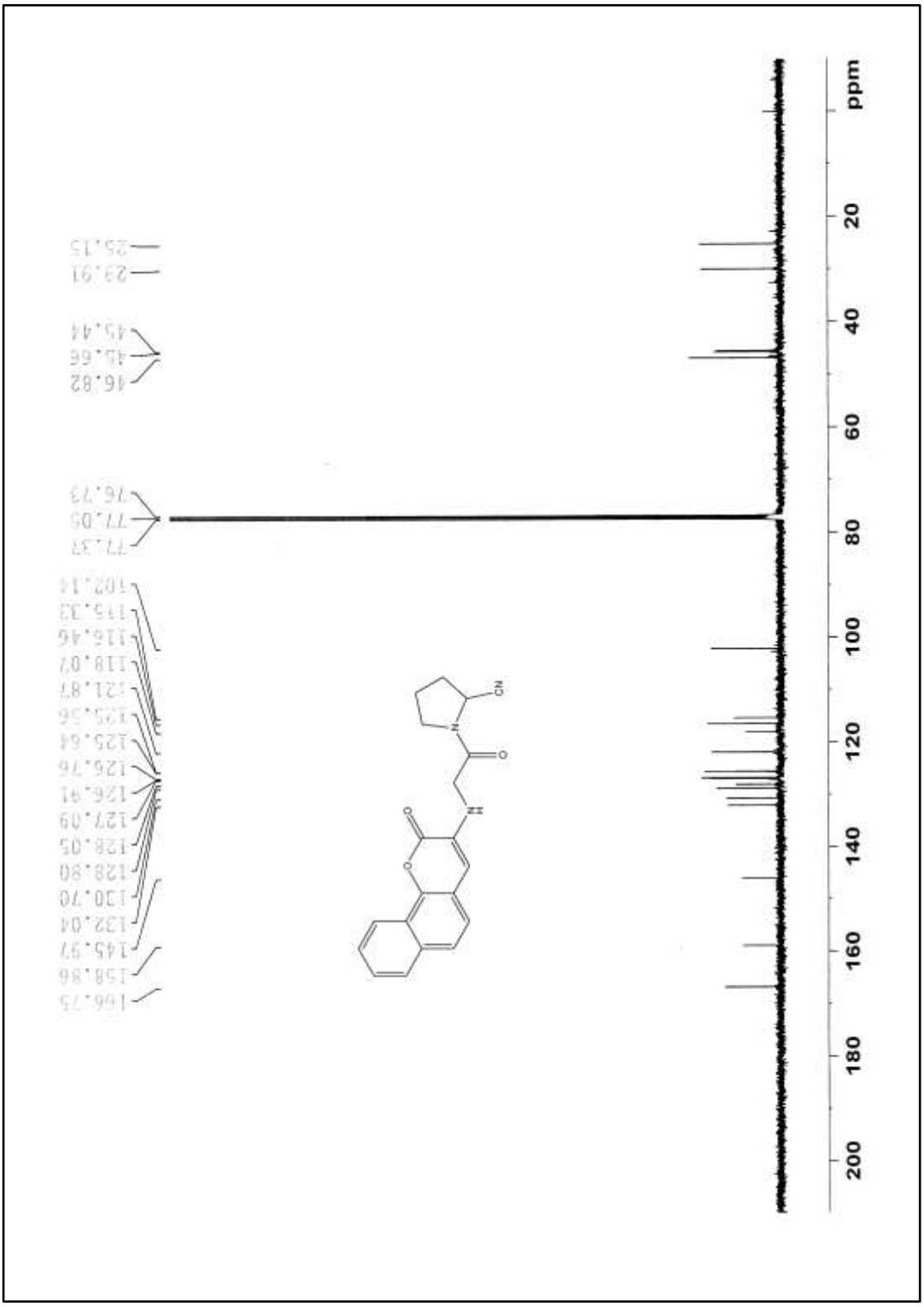

Figure 3.11.3: ^{13}C NMR spectrum of *(S)*-1-(2-(2-oxo-2H-benzo[h]chromen-3-ylamino)acetyl)pyrrolidine-2-carbonitrile **7a**

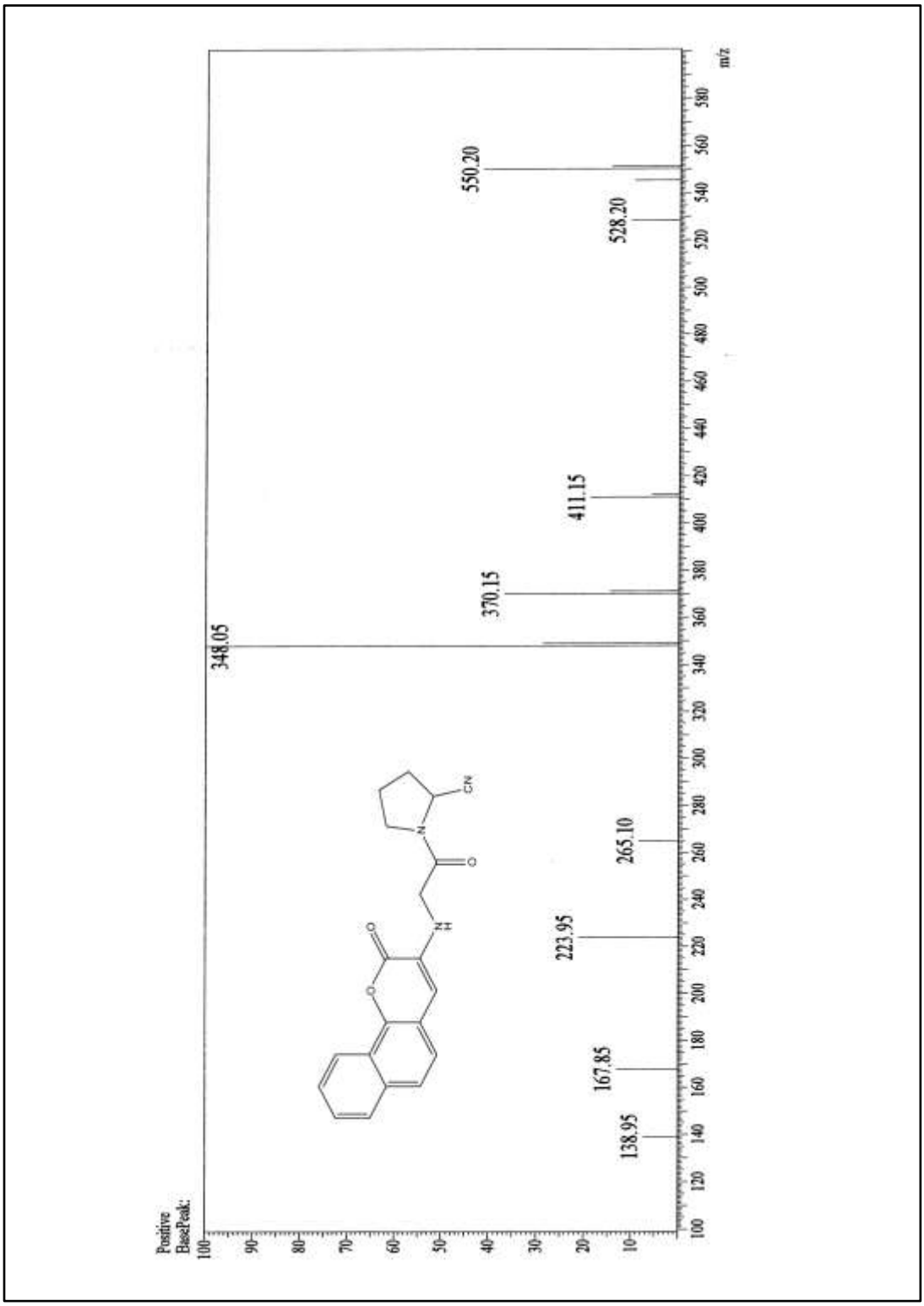

Figure 3.11.4: ESI-MS spectrum of (*S*)-1-(2-(2-oxo-2H-benzo[h]chromen-3-ylamino)acetyl)pyrrolidine-2-carbonitrile **7a**

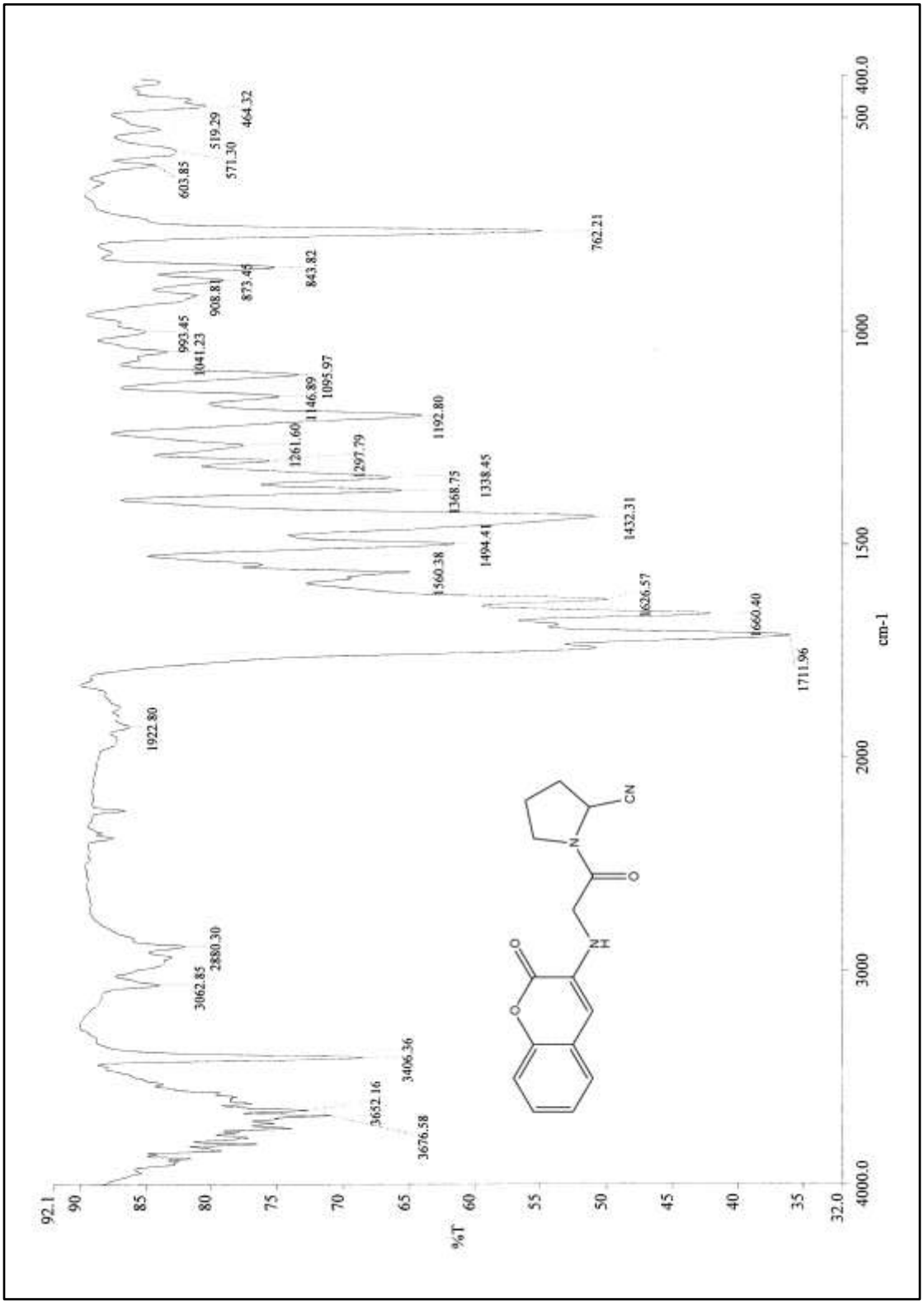

Figure 3.12.1: IR spectrum of (*S*)-1-(2-(2-oxo-2H-chromen-3-ylamino)acetyl)pyrrolidine-2-carbonitrile **7b**

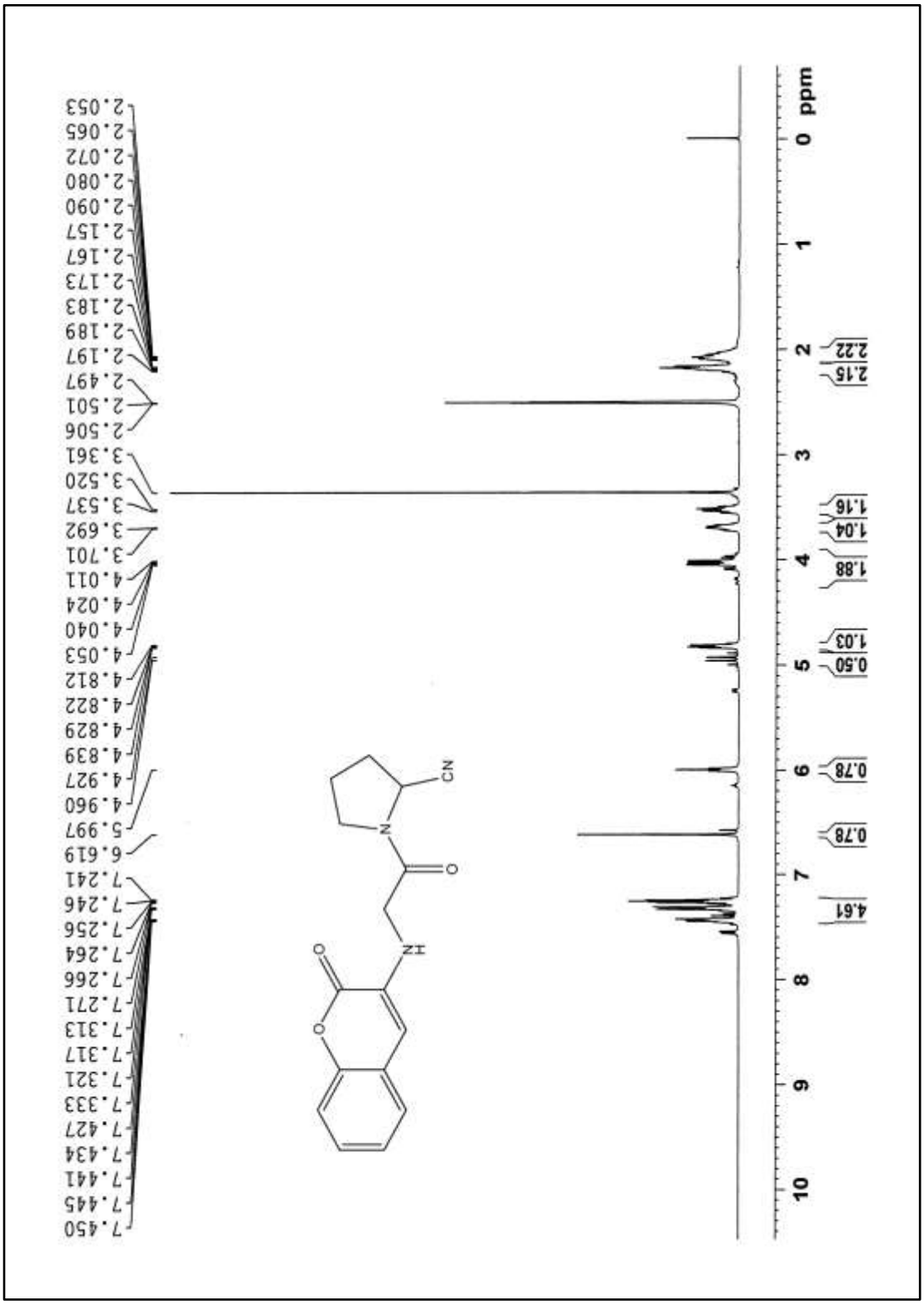

Figure 3.12.2: ^{1}H NMR spectrum of (*S*)-1-(2-(2-oxo-2H-chromen-3-ylamino)acetyl)pyrrolidine-2-carbonitrile **7b**

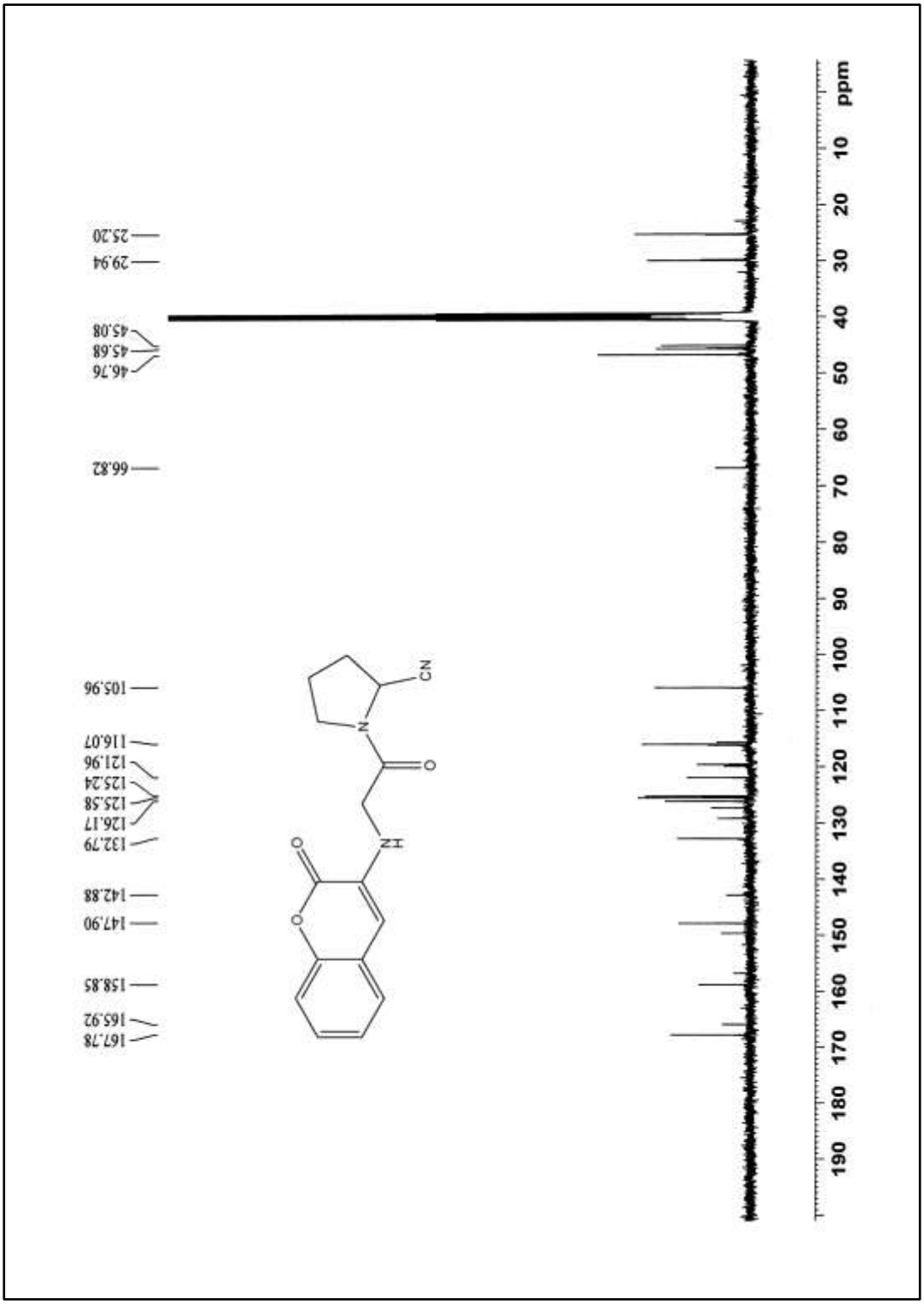

Figure 3.12.3: ^{13}C NMR spectrum of (*S*)-1-(2-(2-oxo-2H-chromen-3-ylamino)acetyl)pyrrolidine-2-carbonitrile **7b**

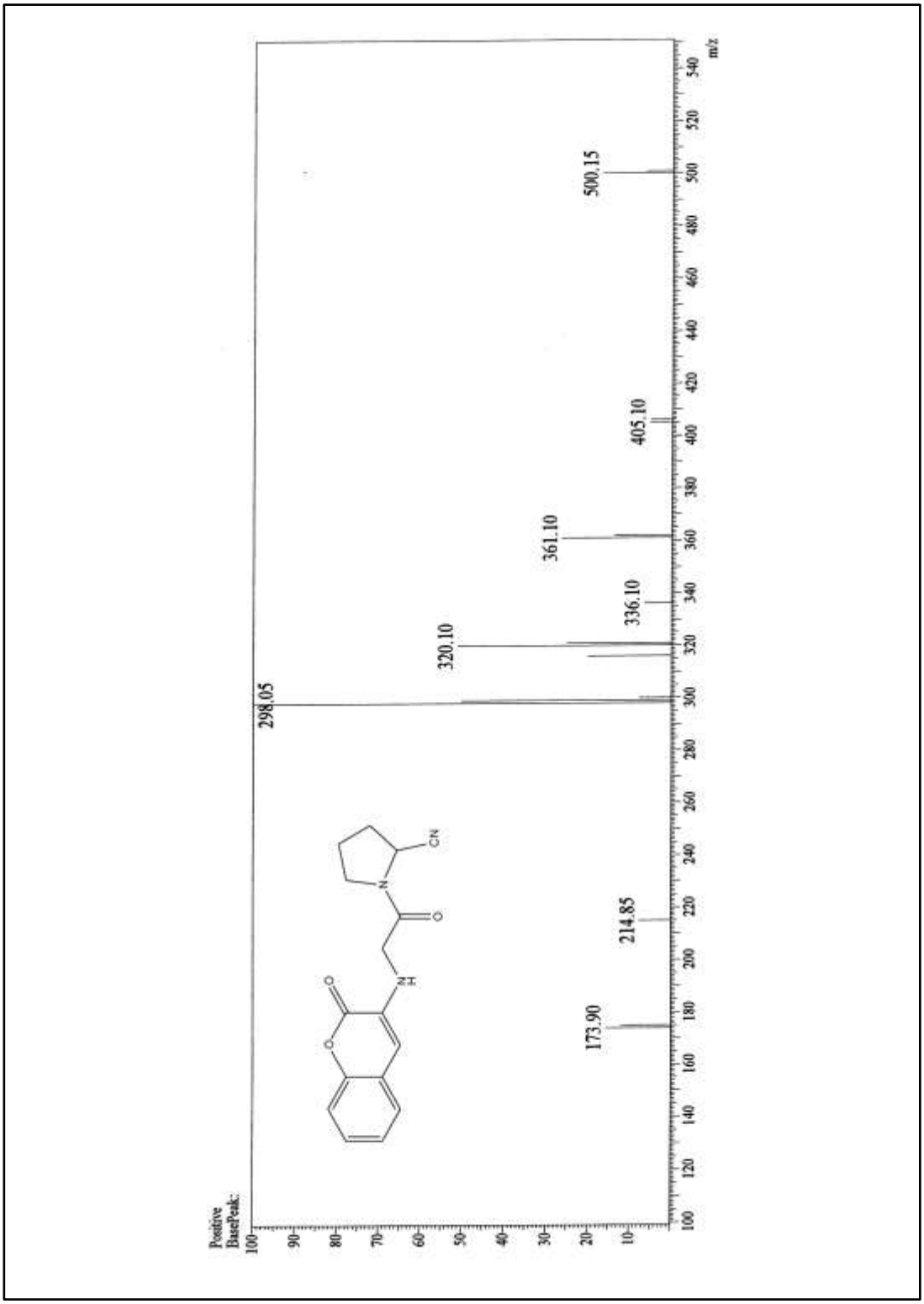

Figure 3.12.4: ESI-MS spectrum of (*S*)-1-(2-(2-oxo-2H-chromen-3-ylamino)acetyl)pyrrolidine-2-carbonitrile **7b**

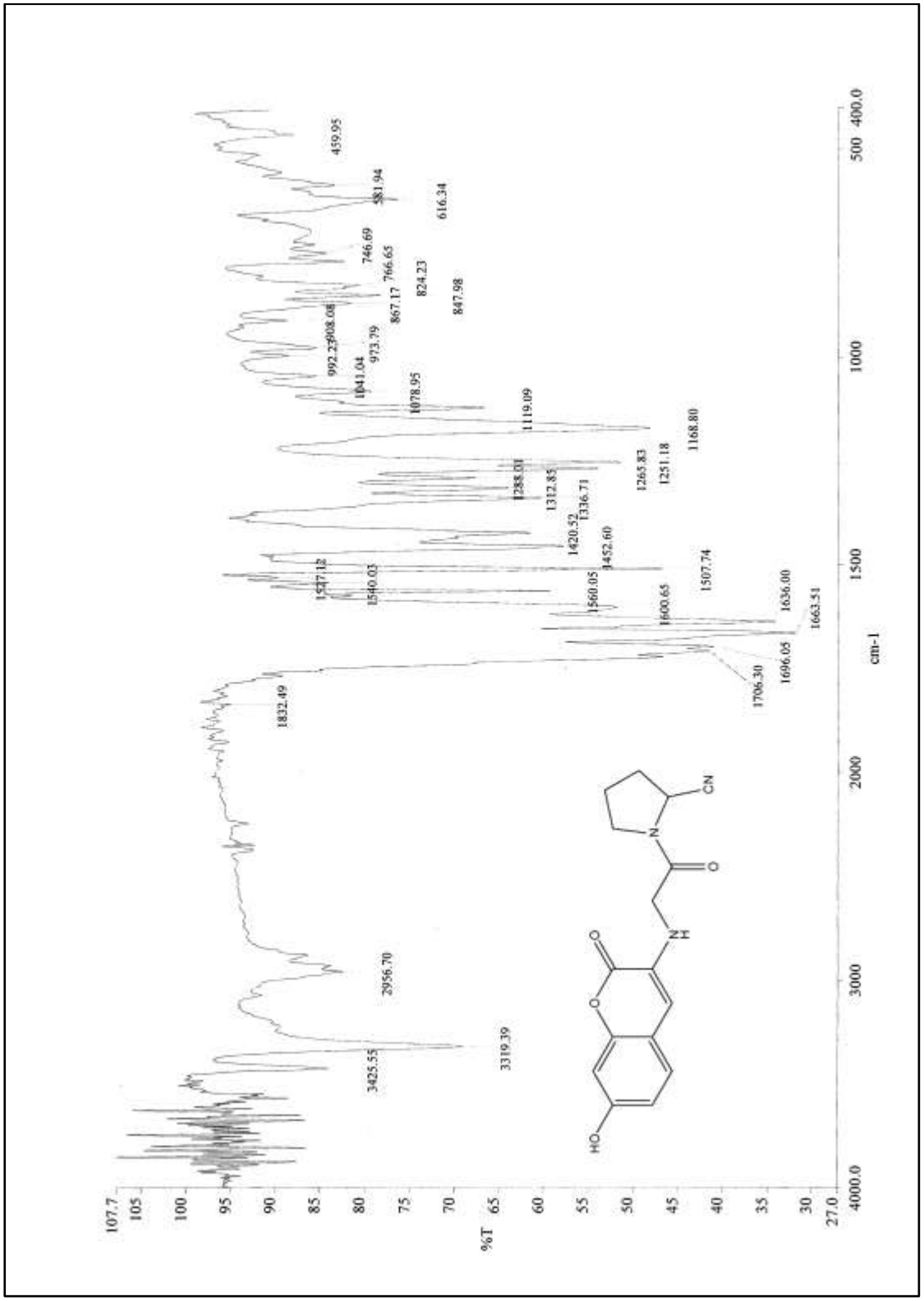

Figure 3.13.1: IR spectrum of (*S*)-1-(2-(7-hydroxy-2-oxo-2H-chromen-3-ylamino)acetyl)pyrrolidine-2-carbonitrile **7c**

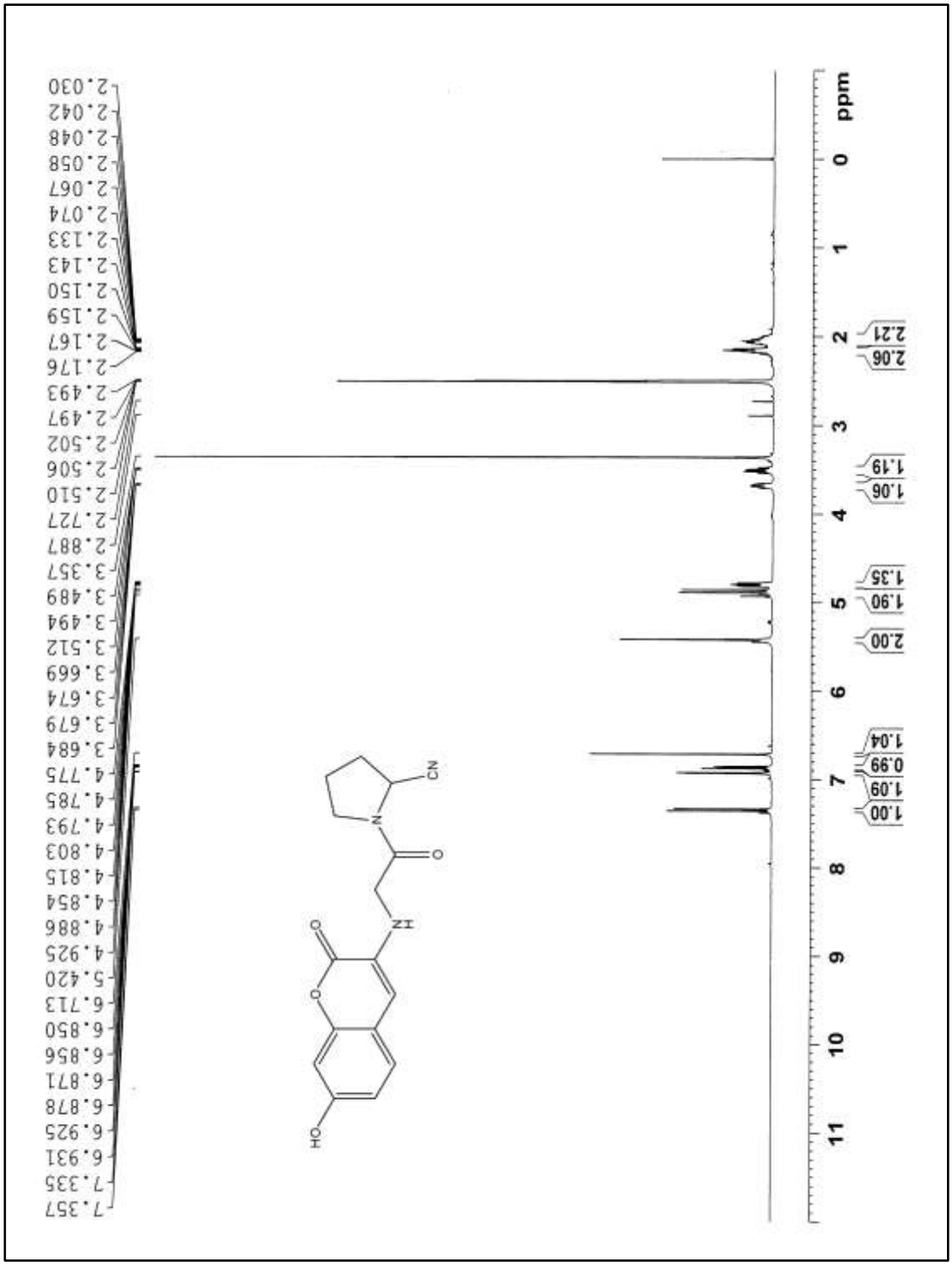

Figure 3.13.2: ^{1}H NMR spectrum of (*S*)-1-(2-(7-hydroxy-2-oxo-2H-chromen-3-ylamino)acetyl)pyrrolidine-2-carbonitrile **7c**

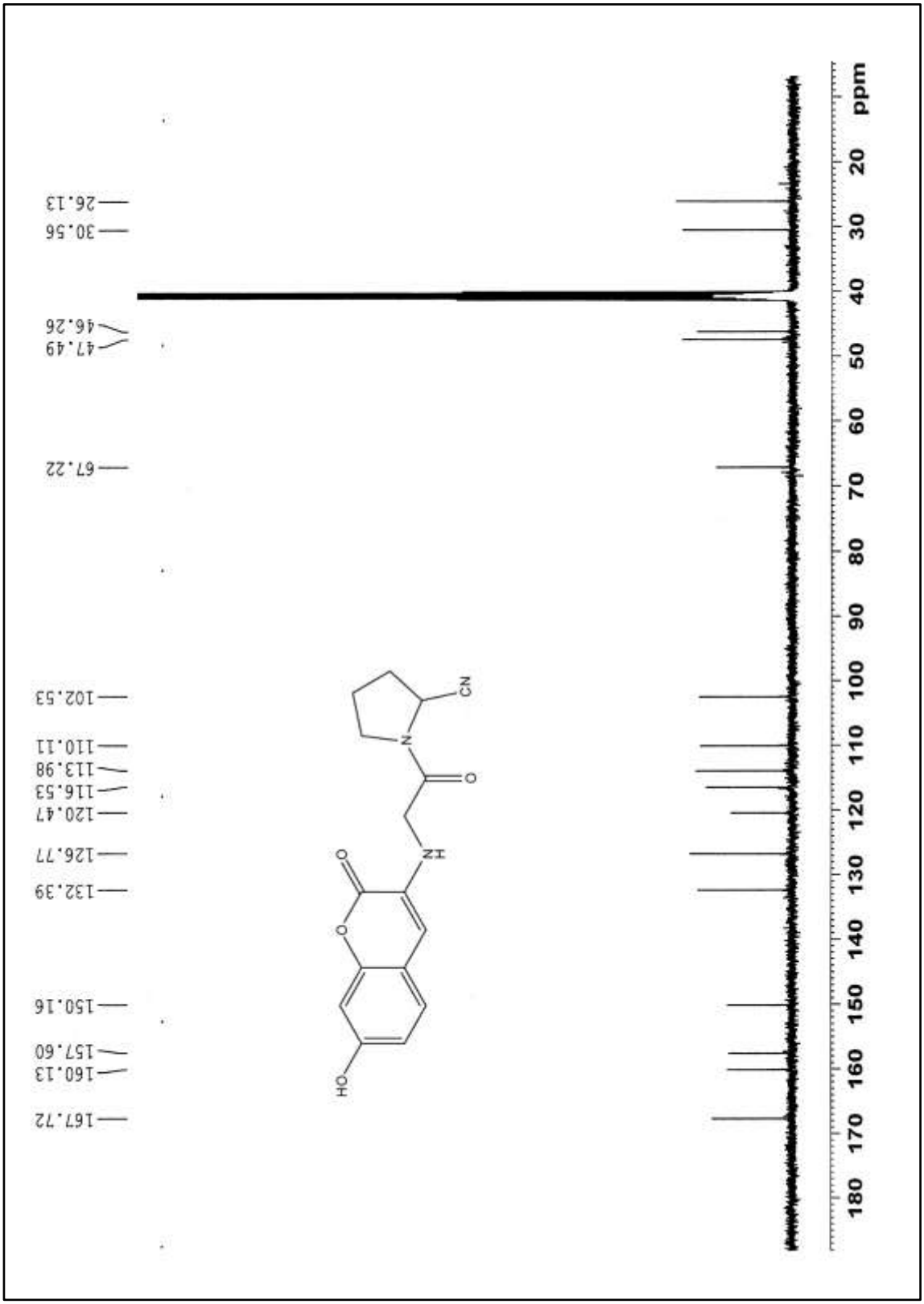

Figure 3.13.3: ^{13}C NMR spectrum of (*S*)-1-(2-(7-hydroxy-2-oxo-2H-chromen-3-ylamino)acetyl)pyrrolidine-2-carbonitrile **7c**

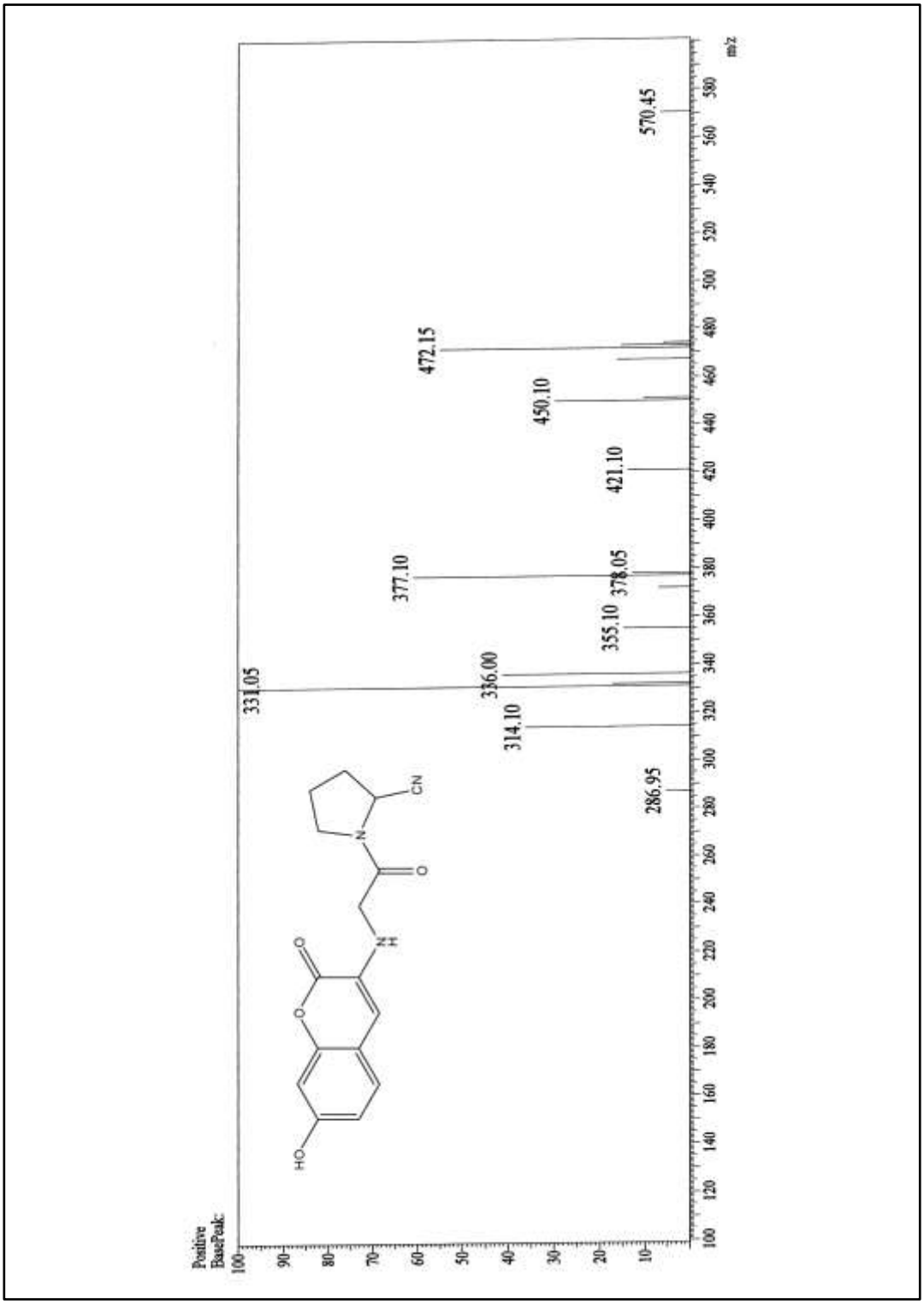

Figure 3.13.4: ESI-MS spectrum of (*S*)-1-(2-(7-hydroxy-2-oxo-2H-chromen-3-ylamino)acetyl)pyrrolidine-2-carbonitrile **7c**

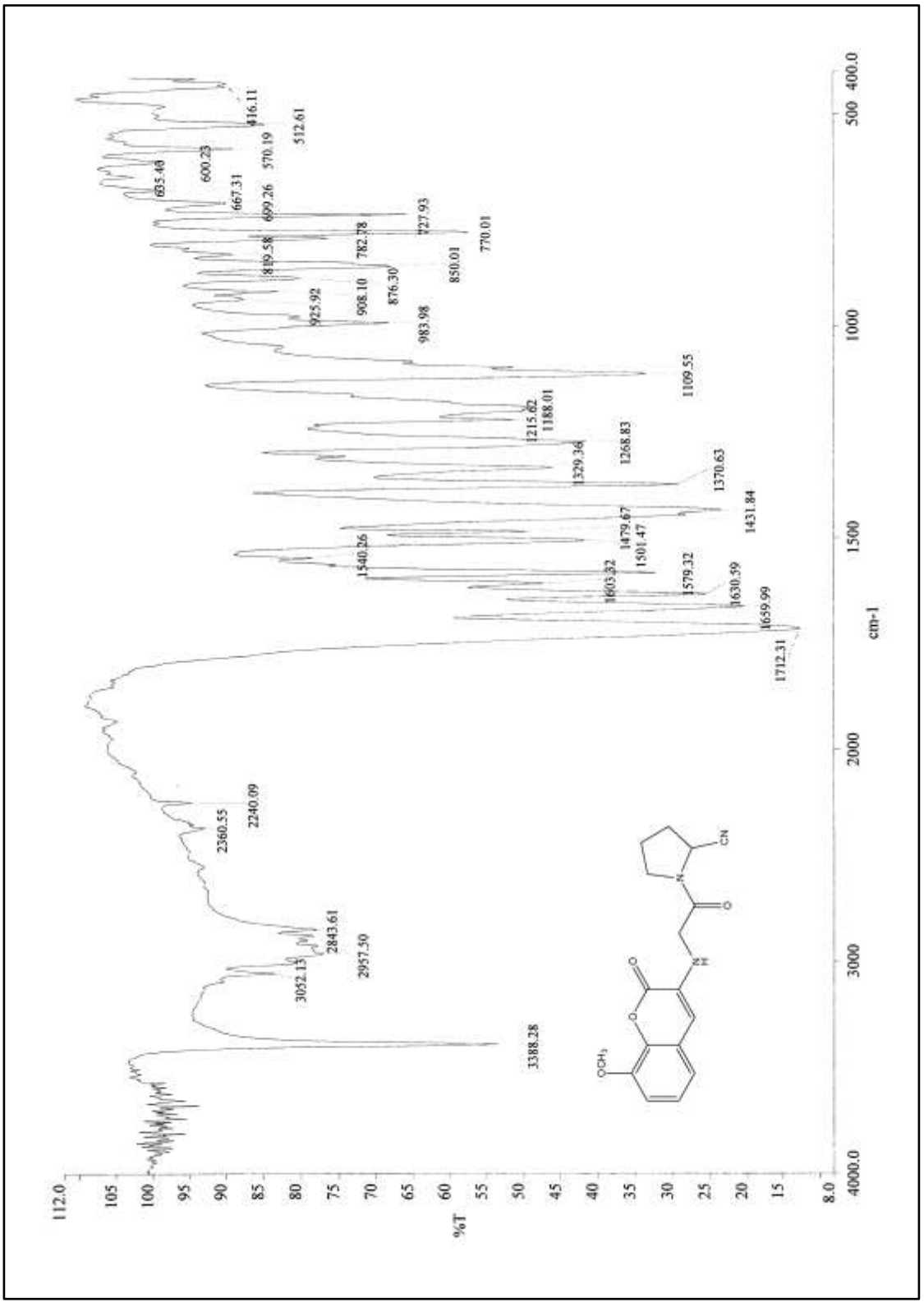

Figure 3.14.1: IR spectrum of (*S*)-1-(2-(8-methoxy-2-oxo-2H-chromen-3-ylamino)acetyl)pyrrolidine-2-carbonitrile **7d**

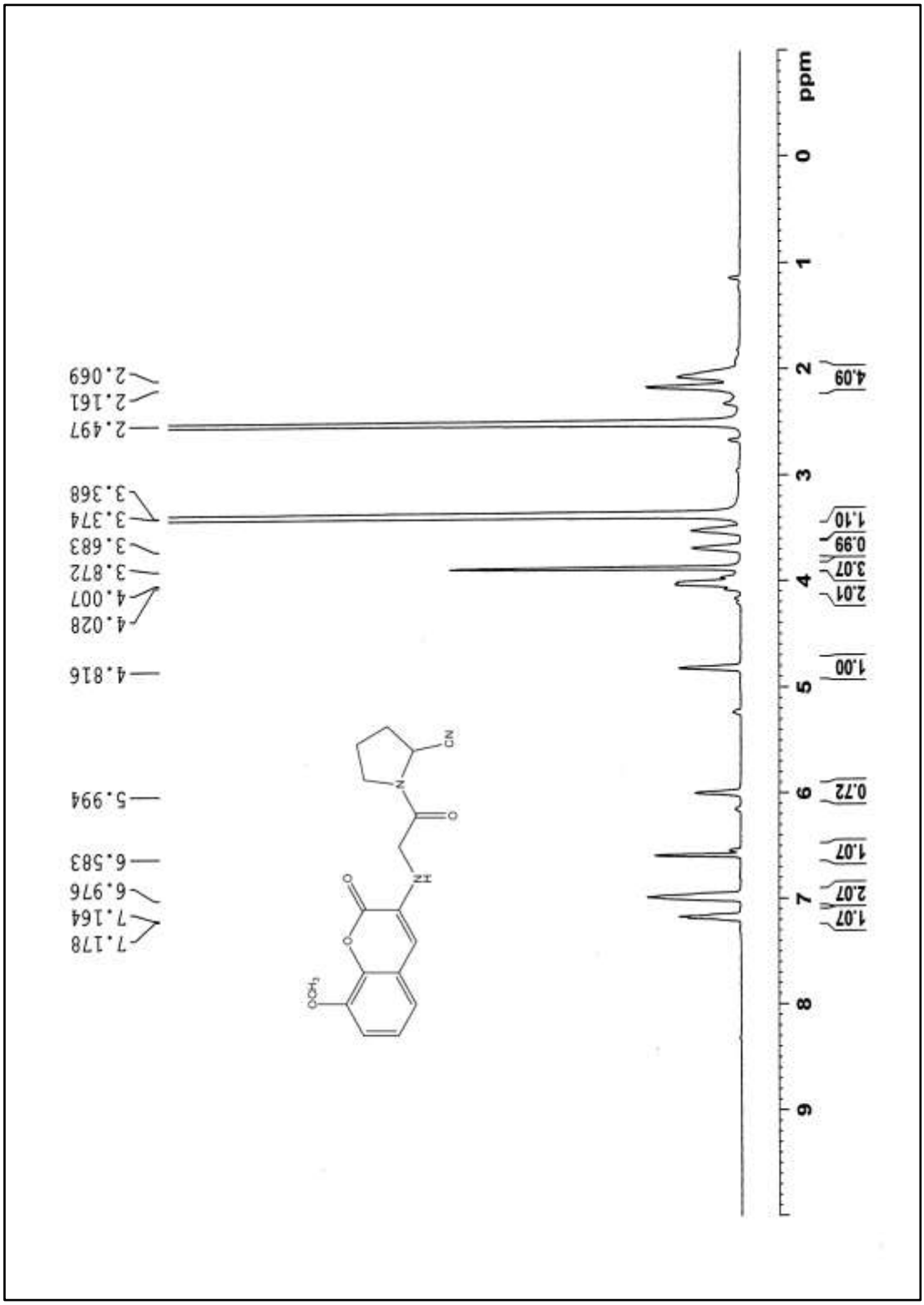

Figure 3.14.2: ^{1}H NMR spectrum of (*S*)-1-(2-(8-methoxy-2-oxo-2H-chromen-3-ylamino)acetyl)pyrrolidine-2-carbonitrile **7d**

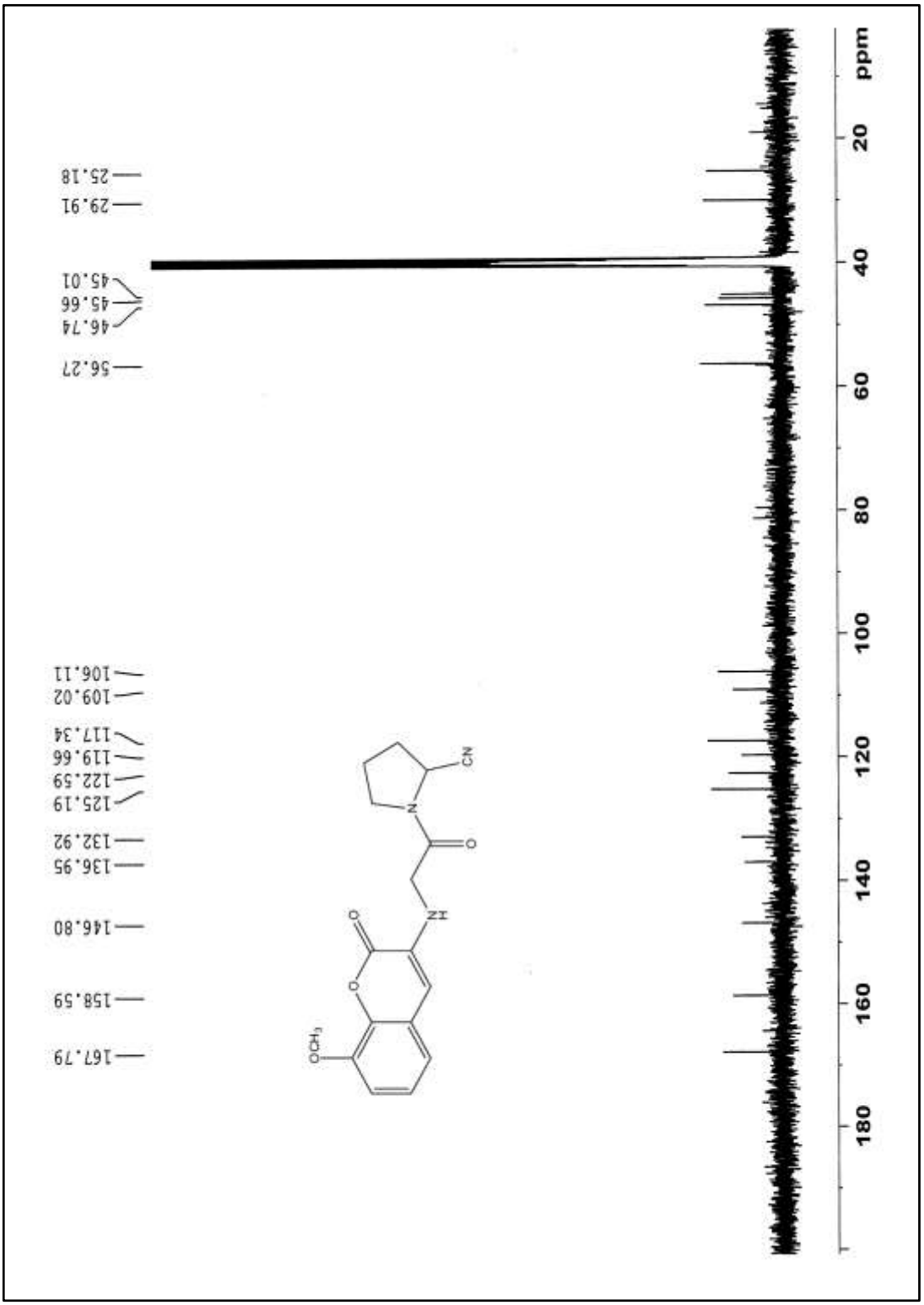

Figure 3.14.3: ^{13}C NMR spectrum of (*S*)-1-(2-(8-methoxy-2-oxo-2H-chromen-3-ylamino)acetyl)pyrrolidine-2-carbonitrile **7d**

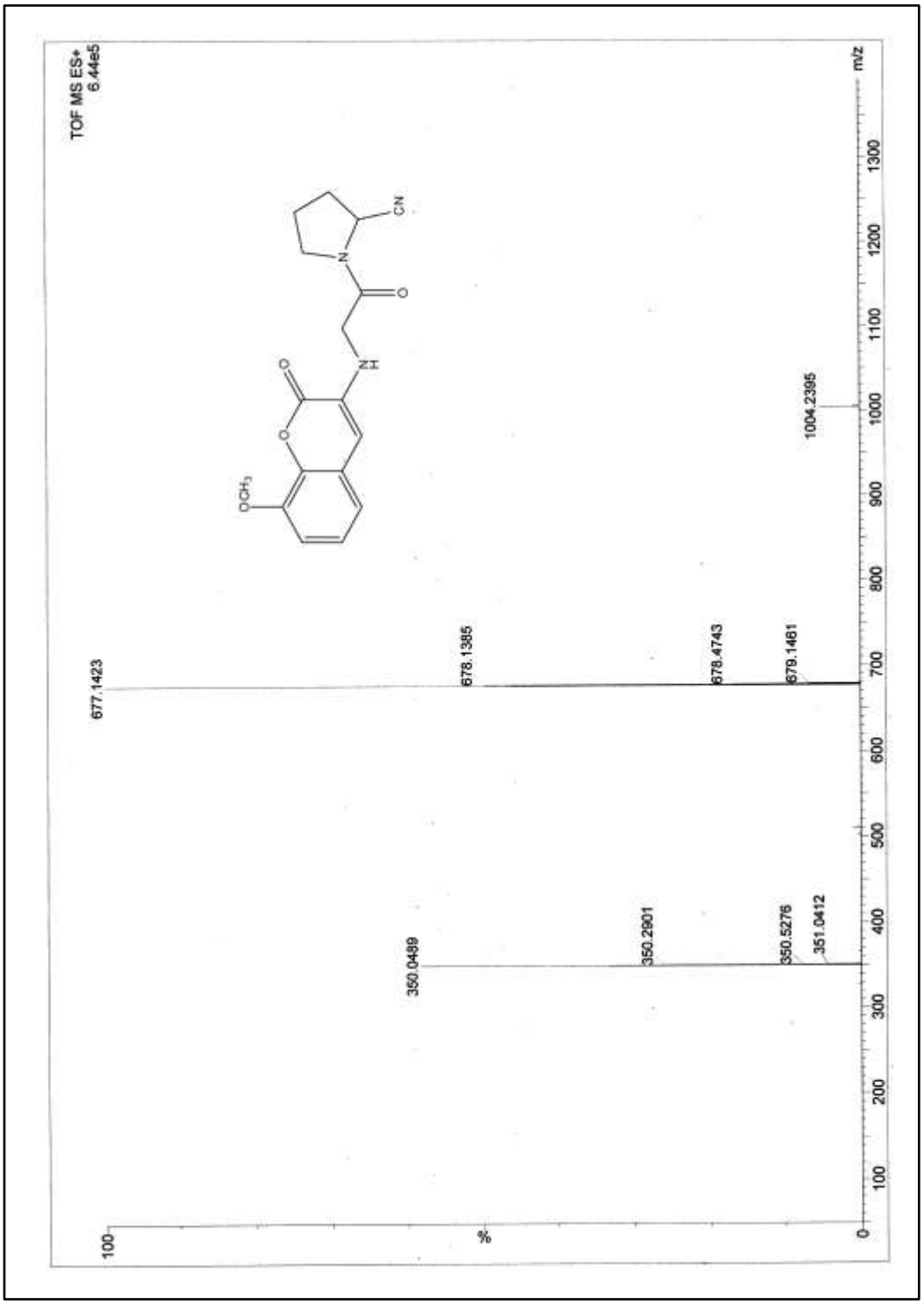

Figure 3.14.4: ESI-MS spectrum of (*S*)-1-(2-(8-methoxy-2-oxo-2H-chromen-3-ylamino)acetyl)pyrrolidine-2-carbonitrile **7d**

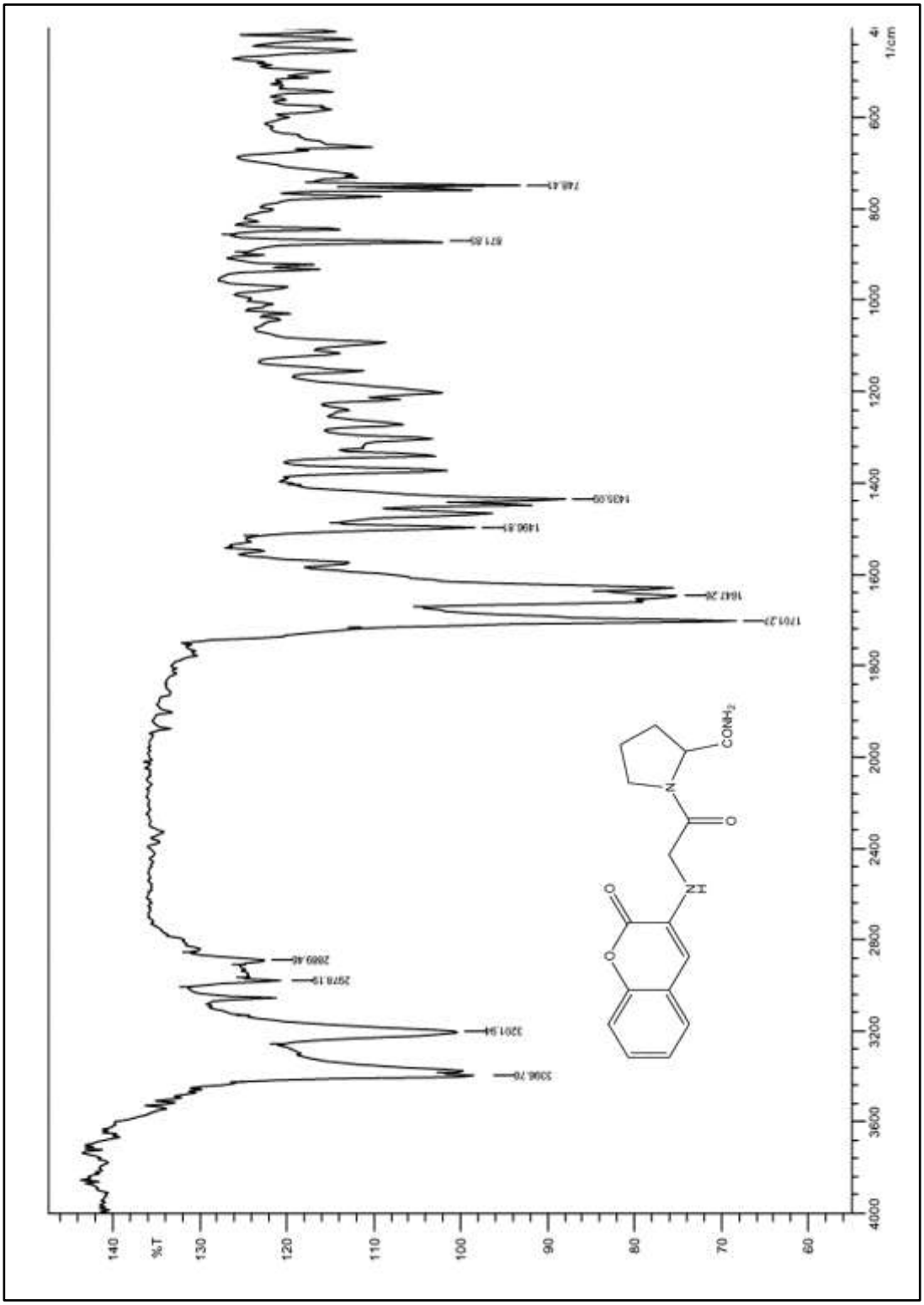

Figure 3.15.1: IR spectrum of (*S*)-1-(2-(2-oxo-2H-chromen-3-ylamino)acetyl)pyrrolidine-2-carboxamide **7e**

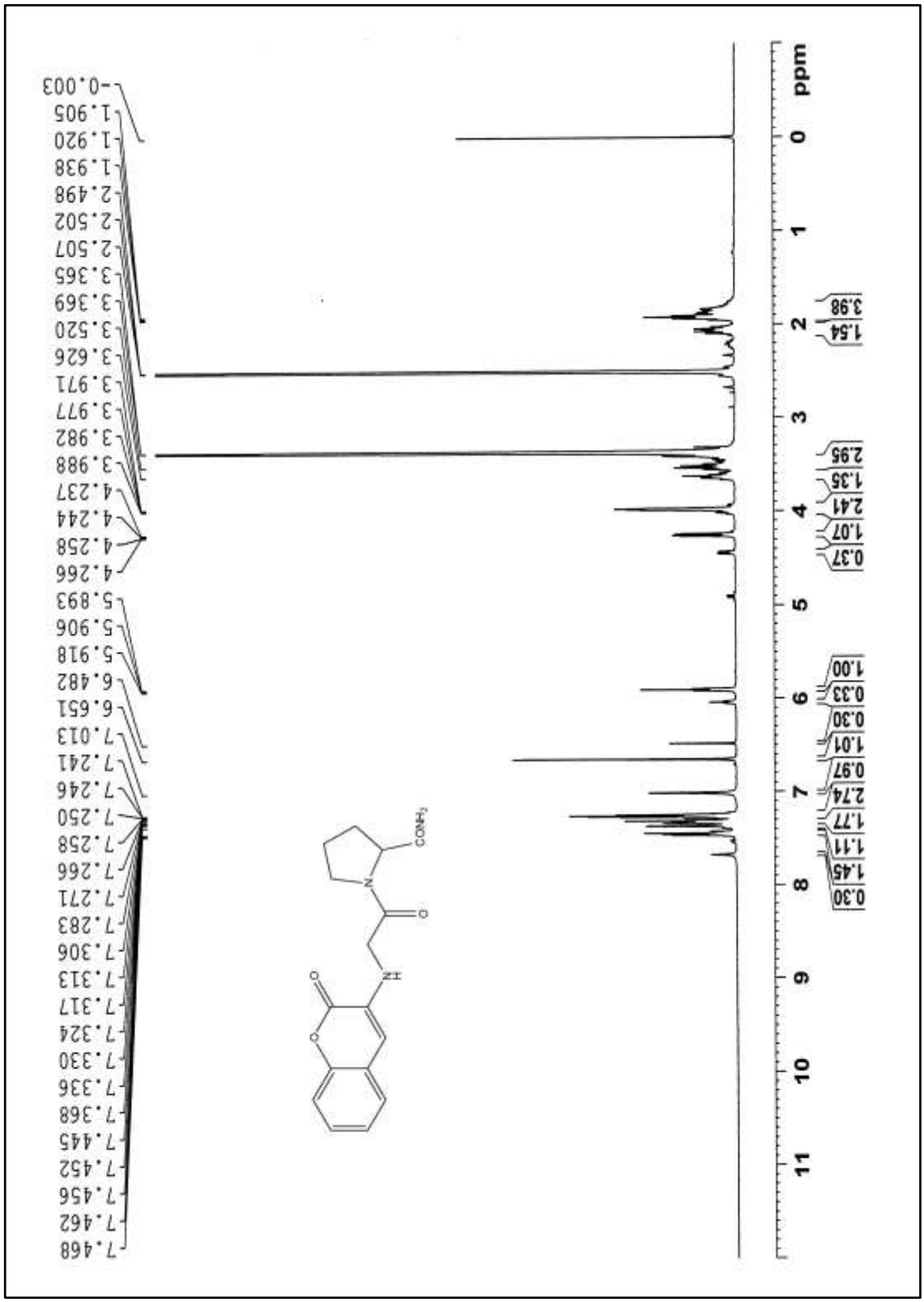

Figure 3.15.2: ^{1}H NMR spectrum of (*S*)-1-(2-(2-oxo-2H-chromen-3-ylamino)acetyl)pyrrolidine-2-carboxamide **7e**

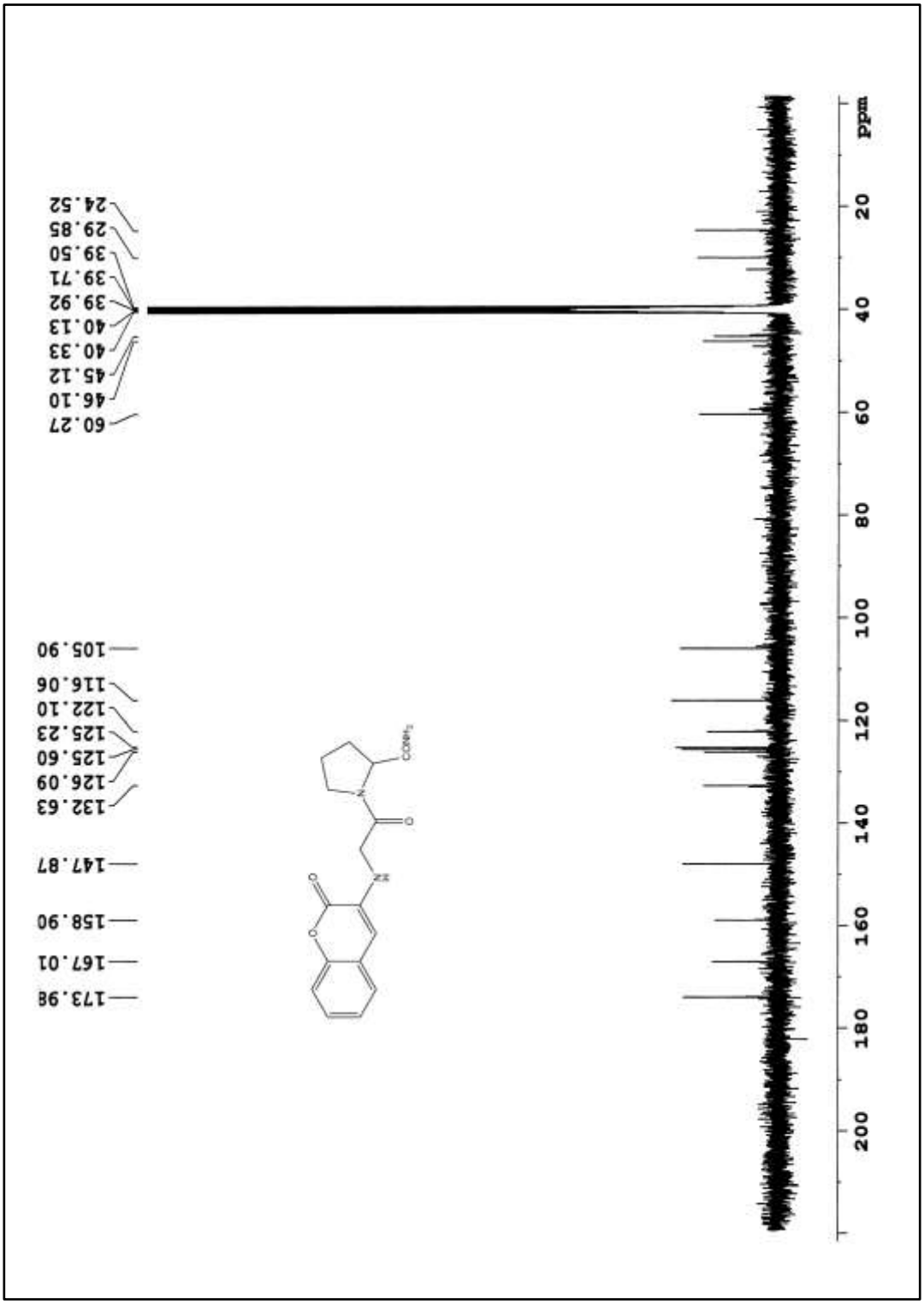

Figure 3.15.3: ^{13}C NMR spectrum of (*S*)-1-(2-(2-oxo-2H-chromen-3-ylamino)acetyl)pyrrolidine-2-carboxamide **7e**

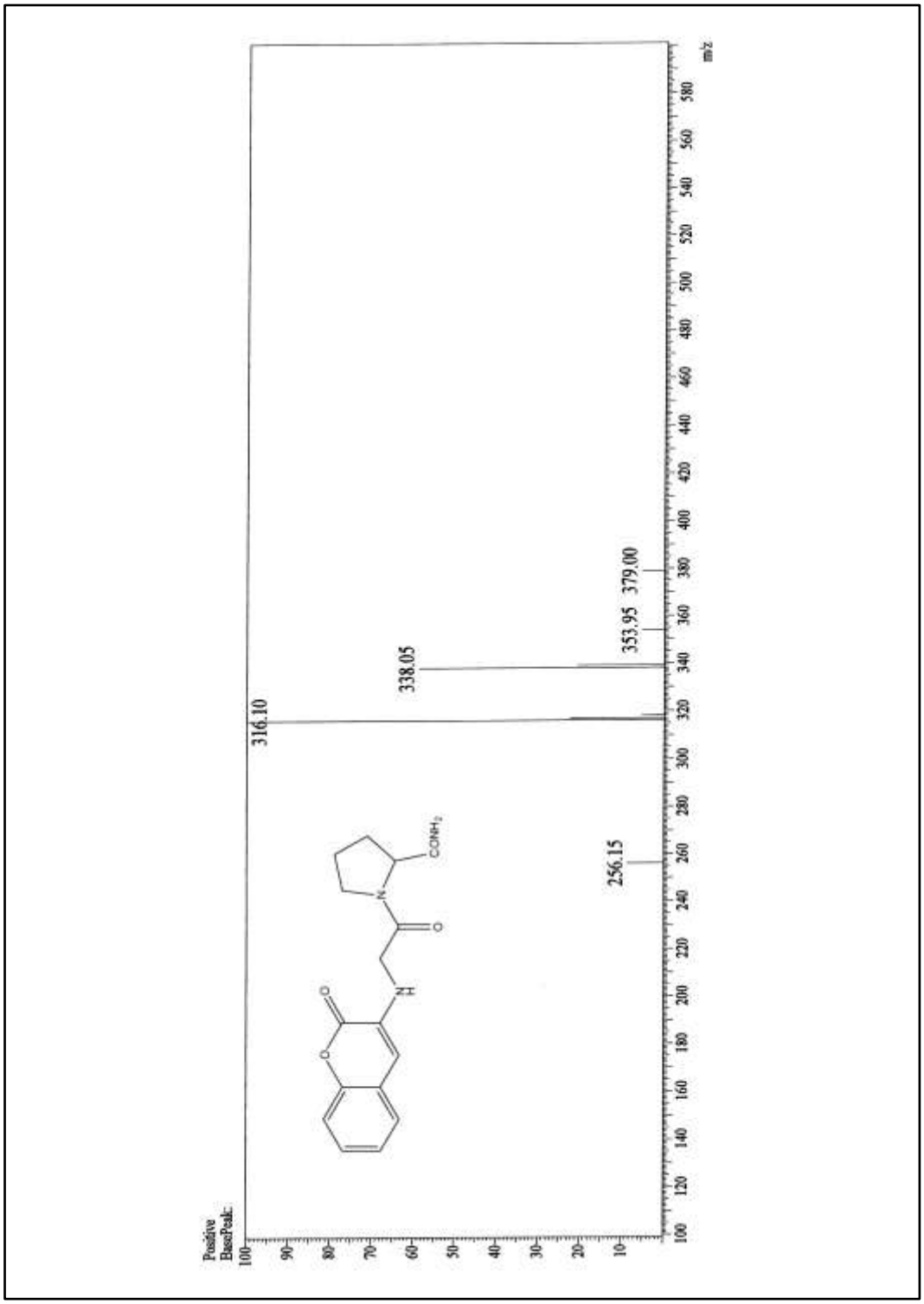

Figure 3.15.4: ESI-MS spectrum of (*S*)-1-(2-(2-oxo-2H-chromen-3-ylamino)acetyl)pyrrolidine-2-carboxamide **7e**

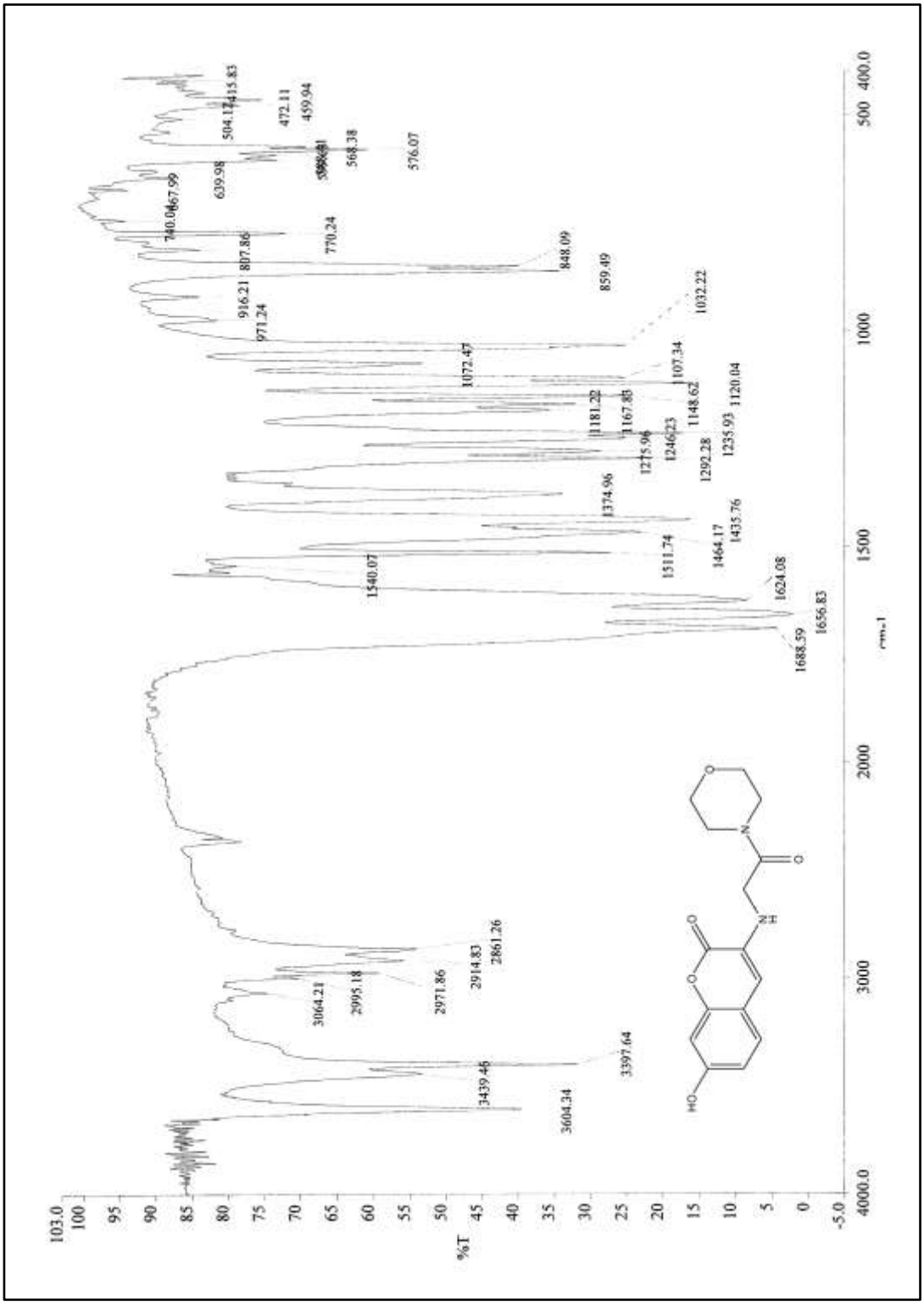

Figure 3.16.1: IR spectrum of 7-hydroxy-3-(2-morpholino-2-oxoethylamino)-2H-chromen-2-one **7g**

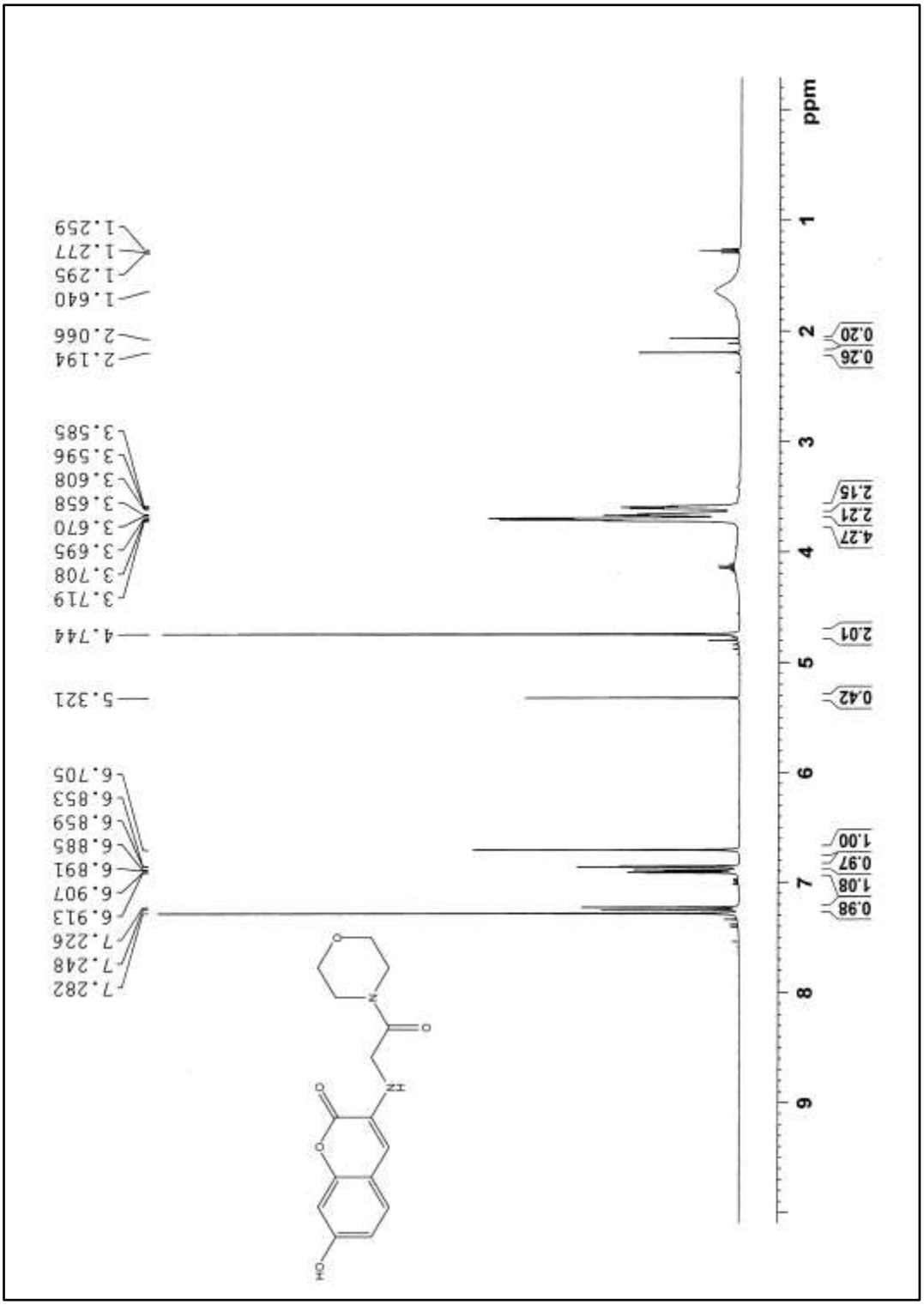

Figure 3.16.2: ^{1}H NMR spectrum of 7-hydroxy-3-(2-morpholino-2-oxoethylamino)-2H-chromen-2-one **7g**

3.2.2 Biological evaluation:

Compounds **7a-g** were then tested for their in-vitro DPP-IV inhibition using human recombinant DPP-IV enzyme procured form Prospec (enz-375-b), substrate : H-Gly-Pro-AMC procured from Enzo life science (Lot No. : 01221304**)** and assay buffer was prepared in-house consisting TrisHCl (50 mM), EDTA (1mM), sodium chloride (100mM) in deionized water having pH 7.5. DPP-IV inhibition assay uses fluorogenic substrate, Gly-Pro-Aminomethylcoumarin (AMC), to measure DPP-IV activity. DPP-IV activity was measured by mixing reagents in 96-well plate (order of addition of reagents: assay buffer, enzyme, solvent/test sample and finally substrate). Both the enzyme and 96 well-plate were incubated for 30 minutes. Cleavage of the peptide bond by DPP-IV releases the free AMC group, resulting in fluorescence that was analyzed using an excitation wavelength of 360 nm and emission wavelength of 450 nm and % inhibition of the test compounds was calculated as shown in Table 3.1.

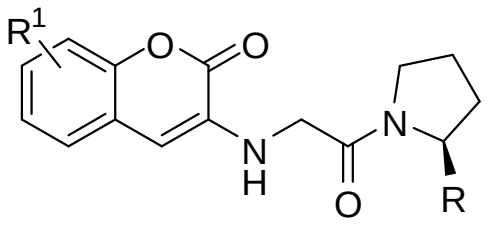

Compound	R^1	R	% Inhibition of DPP-IV at 10µM
7a	7,8-Ph	CN	84.43
7b	H	CN	36.36
7c	7-OH	CN	34.23
7d	8-OCH_3	CN	17.01
7e	H	$CONH_2$	18.01
7g	7-OH	Instead of proline, morpholine ring substituted	36.36

Table 3.1: DPP-IV inhibition by compounds **7a-g** at 10 µM concentration

Vildagliptin (NVP-LAF237), was used as a standard for the assay with an IC_{50} of 2.9 nM. Amongst all the test samples, compound **7a** was found to be the most potent with an IC_{50} of 3.16 µM. For compounds **7b-g** as the % inhibition of DPP-IV were less than 50% at 10 µM concentration, their IC_{50} values were not determined.

3.2.3 Docking studies:

AutoDock Vina [15] was used for the docking studies. To perform the docking studies, binding site residues of the A chain of DPP-IV (PDB ID: 3W2T) [16] at a distance of 4.5 Å from vildagliptin were selected. The affinity for the compound **7a** was -8.4 kcal/mol while that of vildagliptin was shown to be -6.7 kcal/mol. LigPlot [17] was used to observe the interaction of the ligand with the binding site residues (Figure 3.18).

Pymol [18] was used to visualize the protein and the docked compounds **7a** and **NVP-LAF237** as seen in Figure 3.17.

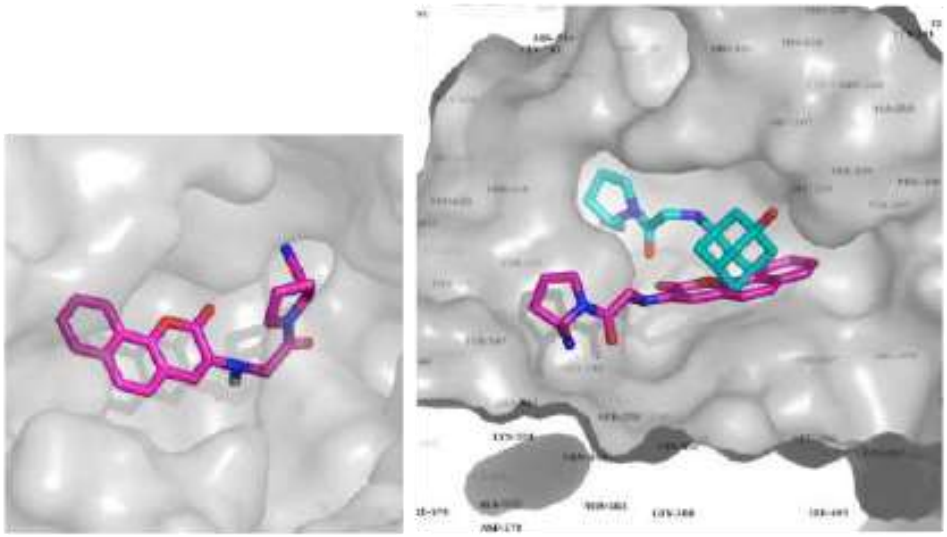

Figure 3.17: (**A**) Interaction of **7a** at the active site of DPP-IV; (**B**) Comparison of binding of **7a** and **NVP-LAF237** at the active site of DPP-IV.

Figure 3.18.1 shows Ligplot of vildagliptin (**NVP-LAF237**) while 3.18.2 shows the Ligplot of **7a**.

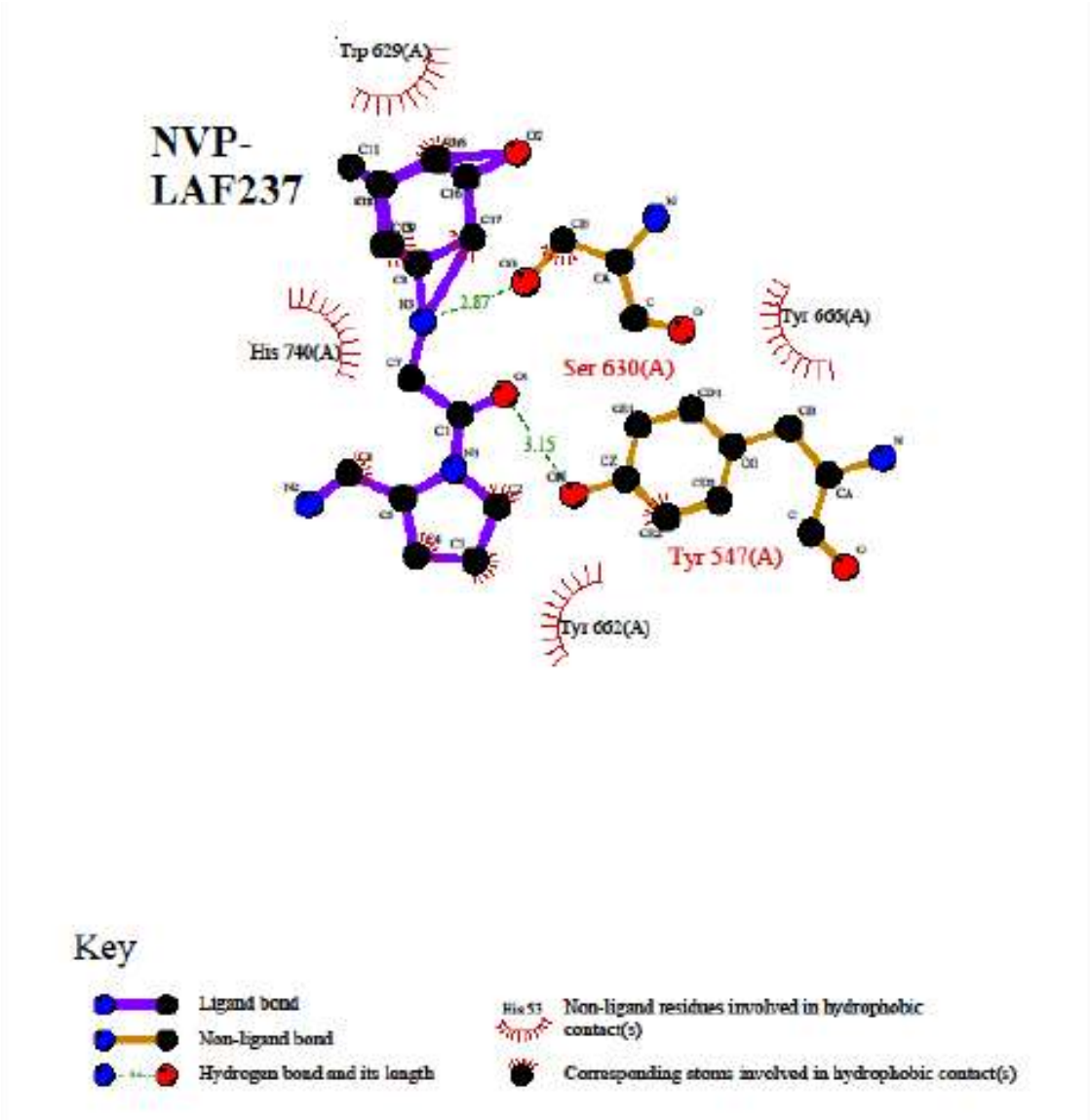

Figure 3.18.1: Ligplot of **NVP-LAF237 (**vildagliptin**)**.

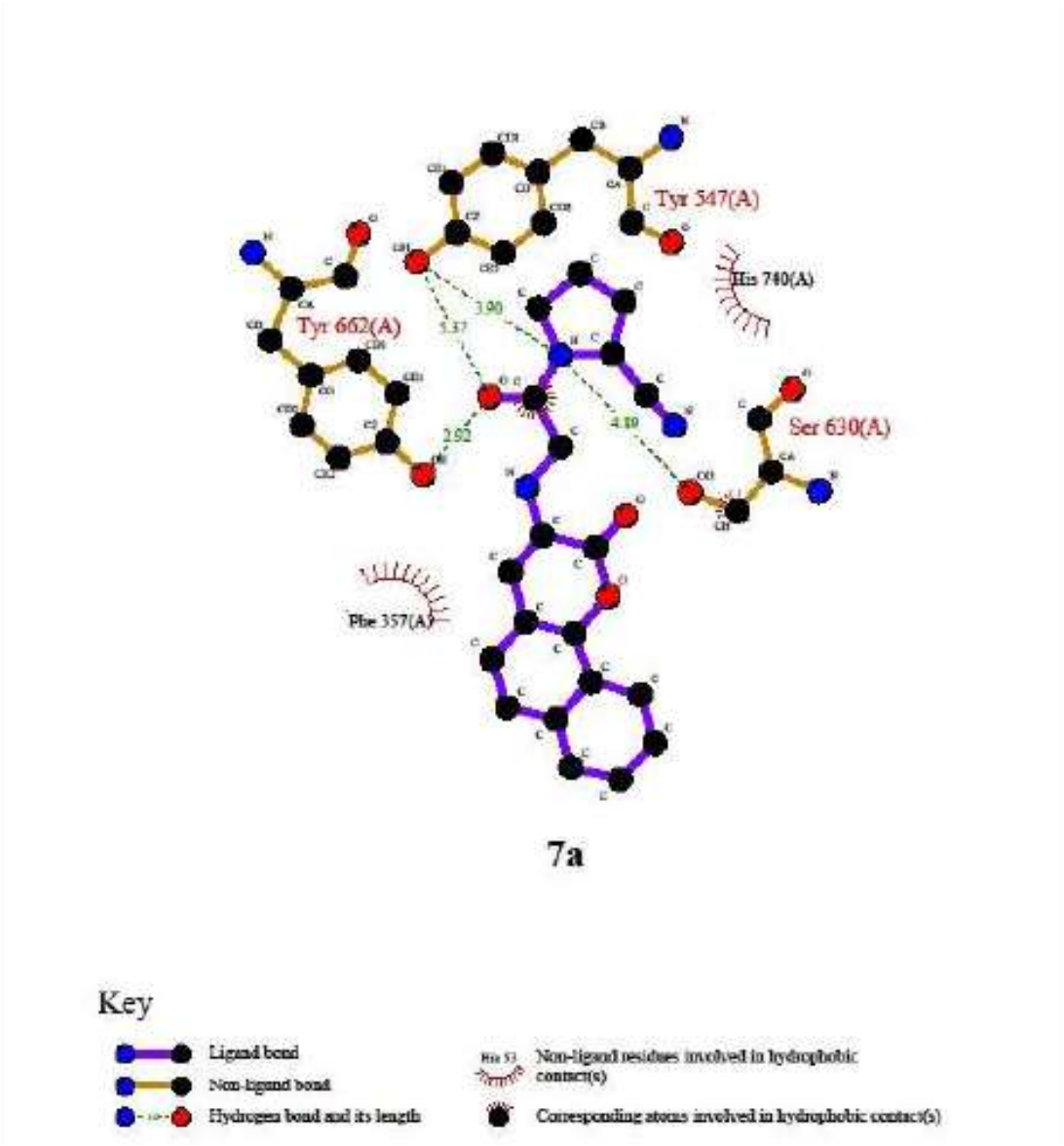

Figure 3.18.2: Ligplot of 1-(2-(2-oxo-2H-benzo[h]chromen-3-ylamino)acetyl)pyrrolidine-2-carbonitrile **7a**.

3.3 Conclusion

While pharmacophore (cyanopyrrolidine) remained constant, it was expected that 3-amino-7-hydroxy-2*H*-chromen-2-one derivative **7c,** mimicking hydroxyl adamantyl group would be most potent molecule in the series but to our surprise it was observed that substituted 3-aminocoumarin derivatives **7c**, **7d** were less potent than the non-substituted derivative **7b** as seen in table 3.1. Yet the most sterically rigid, 3-aminocoumarin derivative **7a** was found to be the most potent of all the molecules synthesised in the series with an IC_{50} of 3.16 μM.

Replacement of hydroxyl adamantyl amine group in vildagliptin by various substituted 3-aminocoumarins does not lead to greater enzyme inhibition which can be attributed to different interaction at the binding site of DPP-IV, as can be seen in Figure 3.17 wherein binding interactions of **7a** and **NVP-LAF237** can be seen.

Hence, it can be concluded that more sterically rigid substituent at the P2 site does lead to better DPP-IV inhibition.

3.4 Experimental

Reagent grade chemicals and solvents were purchased from commercial supplier and used after purification. TLC was performed on silica gel F254 plates (Merck). Acme's silica gel (60-120 mesh) was used for column chromatographic purification. Melting points are uncorrected and were measured in open capillary tubes, using a Rolex melting point apparatus. IR spectra were recorded as KBr pellets on Perkin Elmer RX 1 spectrometer. ^{1}H NMR and ^{13}C NMR spectral data were recorded on Advance Bruker 400 spectrometer (400 MHz) with $CDCl_3$ or DMSO-d_6 as solvent and TMS as internal standard. *J* values are in Hz. Mass spectra were determined by ESI-MS, using a Shimadzu LCMS 2020 apparatus. Methanol was used as a solvent for determining SOR using A.Kruss Optronic polarimeter. All reactions were carried out under nitrogen atmosphere.

General method for the synthesis of compounds 2a-d:

To a stirring solution of substituted salicyladehyde **1a-d** (1.0 mmol) in acetic anhydride (5.0 mmol) N-acetylglycine (1.0 mmol) and sodium acetate (4.0 mmol) were added and the resulting mixture was heated at 100-110 ^{o}C for 7 hours or till the completion of reaction as monitored by TLC. On completion of reaction it was cooled to room temperature, water (20 mL) was added and the resulting solid was filtered, dried and then recrystallized from absolute ethanol to give the product as crystalline solid.

***N-(2-oxo-2H-benzo[h]chromen-3-yl)acetamide-acetyl-2H-benzo[h]chromen-2-one* 2a:**

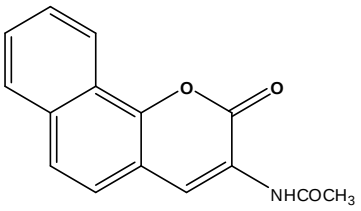

Yield: 35 %; pale pink solid; m.p.: 238-240 ^{o}C; IR (KBr): 3340, 3105, 3059, 1709, 1676, 1578, 1547, 1254, 1142, 804 cm^{-1}; ^{1}H NMR (400 MHz, $CDCl_3$): δ 2.32 (s, 3H), 7.47 (d, 1H, *J* = 9.2 Hz), 7.58-7.62 (m, 1H), 7.68-7.73 (m, 1H), 7.92 (d, 2H, *J* = 8.8 Hz), 8.20 (s, 1H), 8.34 (d, 1H, *J* = 8.4 Hz), 9.53 (s, 1H); ^{13}C NMR (400 MHz, $CDCl_3$): δ 24.89, 114.23, 116.35, 119.52, 122.40, 123.98, 126.25, 127.92, 128.81, 129.06, 130.71, 130.89, 148.73, 158.72, 169.56; $C_{15}H_{11}NO_3$; ESI-MS: *m/z* 276.0 $[M+Na]^+$.

***N-(2-oxo-2H-chromen-3-yl)acetamide* 2b:**

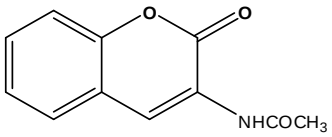

Yield: 32%; white solid; m.p.: 198-200 ^{o}C (Lit.[19] 201.5 °C, Lit.[20] 206 °C); IR (KBr): 3331, 3080, 3044, 2934, 2322, 1709, 1682, 1605, 1530, 1450, 1360, 1294, 1250, 1179, 1146, 897, 766, 708, 600 cm^{-1}; ^{1}H NMR (400 MHz, $CDCl_3$): δ 2.27 (s, 3H), 7.30-7.36 (m, 2H), 7.45-7.49 (m, 1H), 7.54 (dd, 1H, J_1 = 7.6 Hz, J_2 = 1.2 Hz), 8.11 (s, 1H), 8.70 (s, 1H); ^{13}C NMR (400 MHz, $CDCl_3$): δ 24.79, 116.37, 119.82, 123.31, 123.96, 125.22, 127.83, 129.69, 140.04, 149.87, 158.81, 169.42; $C_{11}H_9NO_3$; ESI-MS: *m/z* 203.7 $[M+H]^+$.

***N-(8-methoxy-2-oxo-2H-chromen-3-yl)acetamide* 2d:**

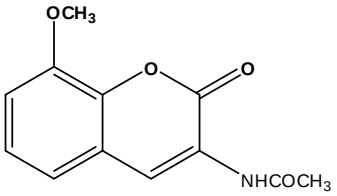

Yield: 41%; yellow solid; m.p.: 240-242 ^{o}C (Lit.[21] 237-239 °C); IR (KBr): 3337, 3098, 3001, 2969, 2943, 2845, 1713, 1684, 1609, 1580, 1535, 1479, 1460, 1383, 1360, 1250, 1184, 1146, 1105, 1074, 1015, 980, 781, 714, 517 cm^{-1}; ^{1}H NMR (400 MHz, $CDCl_3$): δ 2.24 (s, 3H), 3.96 (s, 3H), 6.99-7.27 (m, 3H), 8.12 (s, 1H), 8.65 (s, 1H); ^{13}C NMR (400 MHz, $CDCl_3$): δ 24.75, 56.19, 111.64, 119.31, 120.56, 123.33, 124.22, 125.07, 139.35, 146.95, 158.33, 169.45; $C_{12}H_{11}NO_4$; ESI-MS: *m/z* 256.01 $[M+Na]^+$.

General method for the synthesis of compounds 3a-d:

To a solution of compound **5a-d** (1.0 mmol) in methanol (10 mL), conc. HCl (0.5 mL) was added and the resulting solution was refluxed for an hour. On completion of reaction it was cooled to room temperature, concentrated to a small volume and then neutralized with saturated sodium bicarbonate solution to yield crude compound which on purification by column chromatography using silica gel as stationary phase and ethylacetate : petroleum ether (15:85) as the eluent gave pure crystalline product.

***3-amino-2H-benzo[h]chromen-2-one* 3a:**

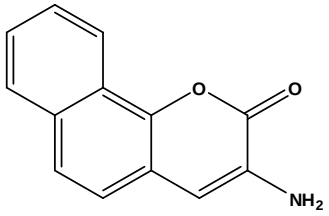

Yield: 50%; yellow solid; m.p.: 150-152 ^{o}C; IR (KBr): 3448, 3366, 2919, 1713, 1630, 1592, 1556, 1515, 1244, 1164, 856, 812 cm^{-1}; ^{1}H NMR (400 MHz, $CDCl_3$): δ 4.44 (s, 2H), 7.44 (d, 1H, *J* = 8.8 Hz), 7.49 (s, 1H), 7.52-7.56 (m, 1H), 7.60-7.64 (m, 1H), 7.74 (d, 1H, *J* = 9.2 Hz), 7.88-7.90 (m, 1H), 8.14 (d, 1H, *J* = 8.4 Hz); ^{13}C NMR (400 MHz, $CDCl_3$): δ 107.48, 115.38, 116.55, 121.86, 125.66, 126.96, 127.44, 128.08, 128.81, 130.70, 132.05, 147.02, 159.36; $C_{13}H_9NO_2$; ESI-MS: *m/z* 211.9 $[M+H]^+$.

***3-amino-2H-chromen-2-one* 3b:**

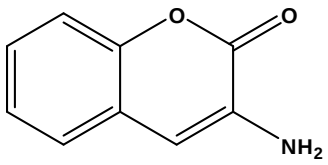

Yield: 45%; pale yellow solid; m.p.: 128-130 ^{o}C (Lit.[20] 132-135 °C); IR (KBr): 3432, 3366, 2921, 2362, 1708, 1636, 1590, 1560, 1459, 1161, 889, 770, 741 cm^{-1}; ^{1}H NMR (400 MHz, $CDCl_3$): δ 4.29 (s, 2H), 6.73 (s, 1H), 7.20-7.33 (m, 4H); ^{13}C NMR (400 MHz, $CDCl_3$): δ 110.92, 116.18, 121.17, 124.64, 125.09, 126.65, 131.97, 149.03, 159.46; $C_9H_7NO_2$; ESI-MS: *m/z* 184.0 $[M+Na]^+$.

***3-amino-8-methoxy-2H-chromen-2-one* 3d:**

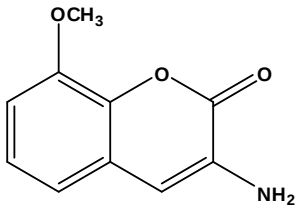

Yield: 52%; yellow solid; m.p.: 116-118 ^{o}C (Lit.[22] 124-126 °C); IR (KBr): 3455, 3360, 2946, 2849, 1715, 1623, 1615, 1570, 1483, 1332, 1277, 1159, 1105, 979, 882, 766 cm^{-1}; ^{1}H NMR (400 MHz, $CDCl_3$): δ 3.93 (s, 3H), 4.34 (s, 2H), 6.70 (s, 1H), 6.83-6.89 (m, 2H), 7.13 (t, 1H, *J* = 8.0 Hz); ^{13}C NMR (400 MHz, $CDCl_3$): δ 56.09, 108.94, 110.93, 116.98, 121.98, 124.50, 132.30, 138.39, 146.92, 158.99; $C_{10}H_9NO_3$; ESI-MS: *m/z* 191.95 $[M+H]^+$.

General method for the synthesis of compounds 7a-g:

A mixture of compound **3a-d** (1.0 mmol), compound **5** or **6** (1.1 mmol) and anhydrous potassium carbonate (5.0 mmol) in dimethyl formamide (DMF) (5.0 mL) was heated at 80-85 ^{o}C for about four hours. On completion of reaction, as monitored on TLC the reaction mixture was poured onto ice cold water and stirred. The resulting solid that separated out was then filtered and dried to yield crude product which was purified by column chromatography using silica gel as stationary phase and ethylacetate : petroleum ether (70:30) as the eluent to give pure product.

(*S*)-*1-(2-(2-oxo-2H-benzo[h]chromen-3-ylamino)acetyl)pyrrolidine-2-carbonitrile* 7a:

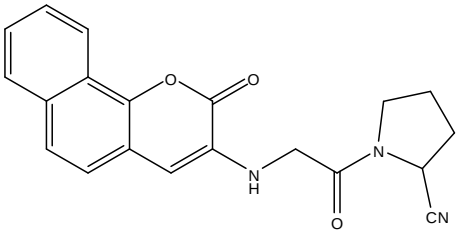

Yield: 10%; pale brown solid; $[\alpha]_D$ = -272.11; m.p.: 115-117 ^oC; IR (KBr): 3400, 2957, 2523, 1709, 1653, 1555, 1515, 1199, 808, 778 cm^{-1}; ^1H NMR (400 MHz, $CDCl_3$): δ 2.28-2.41 (m, 4H), 3.63-3.65 (m, 1H), 3.78-3.79 (m, 1H), 4.01 (d, 2H, *J* = 4.4 Hz), 4.89-4.91 (m, 1H), 5.90-5.93 (m, 1H), 6.99 (s, 1H), 7.36-7.38 (m, 1H), 7.52-7.68 (m, 3H), 7.85 (d, 1H, *J* = 8.0 Hz), 8.18 (d, 1H, *J* = 8.4 Hz); ^{13}C NMR (400 MHz, $CDCl_3$): δ 25.15, 29.91, 45.44, 45.66, 46.82, 102.14, 115.33, 116.46, 118.07, 121.87, 125.56, 125.64, 126.76, 126.91, 127.09, 128.05, 128.80, 130.70, 132.04, 145.97, 158.86, 166.75; $C_{20}H_{17}N_3O_3$; ESI-MS: *m/z* 348.05 $[M+H]^+$.

(*S*)-*1-(2-(2-oxo-2H-chromen-3-ylamino)acetyl)pyrrolidine-2-carbonitrile* 7b:

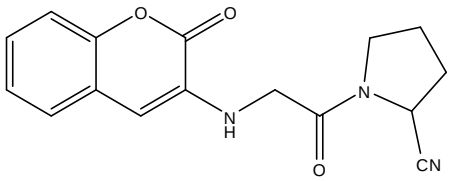

Yield: 20%; pale yellow solid; $[\alpha]_D$ = -92.93; m.p.: 236-238 ^oC; IR (KBr): 3406, 3063, 2880, 1712, 1660, 1627, 1432, 1193, 844, 762 cm^{-1}; ^1H NMR (400 MHz, DMSO-d_6): δ 2.05-2.20 (m, 4H), 3.50-3.56 (m, 1H), 3.67-3.73 (m, 1H), 3.97-4.01 (m, 2H), 4.80-4.84 (m, 1H), 6.00 (t, 1H, *J* = 5.2 Hz), 6.62 (s, 1H), 7.22-7.46 (m, 4H); ^{13}C NMR (400 MHz,

DMSO-d_6): δ 25.20, 29.94, 45.08, 45.68, 46.76, 66.82, 105.96, 116.07, 121.96, 125.24, 125.58, 126.17, 132.79, 142.88, 147.90, 158.85, 165.92, 167.78; $C_{16}H_{15}N_3O_3$; ESI-MS: *m/z* 298.05 $[M+H]^+$.

(*S*)-*1-(2-(7-hydroxy-2-oxo-2H-chromen-3-ylamino)acetyl)pyrrolidine-2-carbonitrile* 7c:

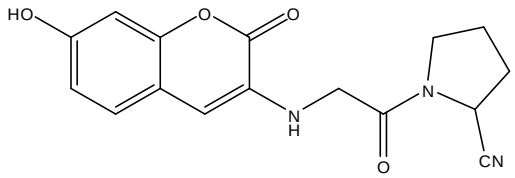

Yield: 25%; yellow solid; $[\alpha]_D$ = -147.53; m.p.: 158-160 ^oC; IR (KBr): 3426, 3319, 2957, 1706, 1696, 1664, 1636, 1508, 1251, 1169, 1119, 848, 824, 616 cm^{-1}; ^1H NMR (400 MHz, DMSO-d_6): δ 2.00-2.08 (m, 2H), 2.13-2.18 (m, 2H), 3.47-3.53 (m, 1H), 3.65-3.70 (m, 1H), 4.78-4.82 (m, 1H), 4.85-4.93 (m, 2H), 5.42 (s, 2H), 6.71 (s, 1H), 6.86 (dd, 1H, J_1 = 2.4 Hz, J_2 = 8.8 Hz), 6.93 (d, 1H, J = 2.4 Hz), 7.35 (d, 1H, J = 8.8 Hz); ^{13}C NMR (400 MHz, DMSO-d_6): δ 26.13, 30.56, 46.26, 47.49, 67.22, 102.53, 110.11, 113.98, 116.53, 120.47, 126.77, 132.39, 150.16, 157.60, 160.13, 167.72; $C_{16}H_{15}N_3O_4$; ESI-MS: *m/z* 331.05 $[M+NH_4]^+$.

(*S*)-*1-(2-(8-methoxy-2-oxo-2H-chromen-3-ylamino)acetyl)pyrrolidine-2-carbonitrile*

7d:

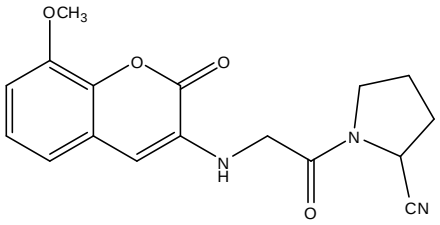

Yield: 25%; pale yellow solid; $[\alpha]_D$ = -98.80; m.p.: 205-207 ^oC; IR (KBr): 3388, 3052, 2958, 2844, 1712, 1660, 1631, 1579, 1432, 1371, 1329, 1269, 1110, 984, 850, 770, 728 cm^{-1}; ^1H NMR (400 MHz, DMSO-d_6): δ 2.07-2.16 (m, 4H), 3.50 (s, 1H), 3.68 (s, 1H), 3.87 (s, 3H), 4.01-4.03 (m, 2H), 4.82 (m, 1H), 5.99 (s, 1H), 6.58 (s, 1H), 6.98-7.18 (m, 3H); ^{13}C NMR (400 MHz, DMSO-d_6): δ 25.18, 29.91, 45.01, 45.66, 46.74, 56.27, 106.11, 109.02, 117.34, 119.66, 122.59, 125.19, 132.92, 136.95, 146.80, 158.59, 167.79; $C_{17}H_{17}N_3O_4$; ESI-MS: *m/z* 350.05 $[M+Na]^+$.

(S)-1-(2-(2-oxo-2H-chromen-3-ylamino)acetyl)pyrrolidine-2-carboxamide 7e (exists as a mixture of rotamers (3:1):

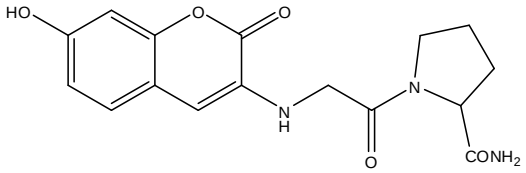

Yield: 28%; white solid; m.p.: 262-264 ^oC; IR (KBr): 3397, 3395, 3202, 3053, 2978, 2889, 1701, 1647, 1628, 1466, 1447, 1435, 1373, 1339, 1302, 1269, 1202, 872, 758, 748 cm^{-1}; ^1H NMR (400 MHz, DMSO-d_6): δ 1.84-2.10 (m, 4H), 3.47-3.56 (m, 1H), 3.59-3.67 (m, 1H), 3.97-3.99 (m, 2H), 4.24-4.27 (m, 0.74H), 4.40-4.45 (m, 0.26H), 5.91 (t, 0.75H, *J* = 5.2 Hz), 6.04 (t, 0.25H, *J* = 5.2 Hz), 6.48 (s, 0.23H), 6.65 (s, 0.77H), 7.01 (s, 1H), 7.23-

7.47 (m, 4H); ^{13}C NMR (400 MHz, DMSO-d_6): δ 24.52, 29.85, 45.12, 46.10, 60.27, 105.90, 116.06, 122.10, 125.23, 125.60, 126.09, 132.63, 147.87, 158.90, 167.01, 173.98; $C_{16}H_{17}N_3O_4$; ESI-MS: *m/z* 316.10 $[M+H]^+$.

***7-hydroxy-3-(2-morpholino-2-oxoethylamino)-2H-chromen-2-one* 7g:**

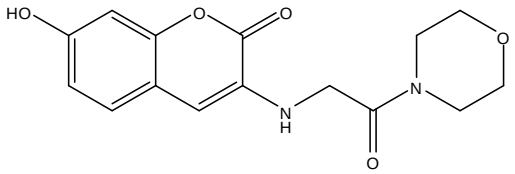

Yield: 20%; yellow solid; m.p.: 164-166 ^{o}C; IR (KBr): 3604, 3398, 2972, 2915, 2861, 1689, 1657, 1624, 1512, 1464, 1436, 1375, 1292, 1236, 1236, 1149, 1120, 1032, 859, 848, 770, 576 cm^{-1}; ^{1}H NMR (400 MHz, $CDCl_3$): δ 3.59-3.61 (m, 2H), 3.66-3.67 (m, 2H), 3.70-3.72 (m, 4H), 4.74 (s, 2H), 6.71 (s, 1H), 6.85-6.86 (m, 1H), 6.89-6.91 (m, 1H), 7.23-7.25 (m, 1H); ^{13}C NMR (400 MHz, $CDCl_3$): δ 18.91, 42.02, 45.06, 56.52, 66.31, 66.41, 66.48, 101.67, 106.93, 109.55, 113.20, 115.58, 125.98, 131.45, 149.34, 156.90, 159.37, 166.27, 167.22; $C_{15}H_{16}N_2O_5$; ESI-MS: *m/z* 327.03 $[M+Na]^+$.

3.5 References

[1] Danaei, G.; Finucane, M. M.; Lu, Y.; Singh, G. M.; Cowan, M. J.; Paciorek, C. J.; Lin, J. K.; Farzadfar, F.; Khang, Y.; Stevens, G.A.; Rao, M., Ali, M. K.; Riley, L. M.; Robinson, C. A.; Ezzati, M. *Lancet*, **2011**, *378*, 31.

[2] Drucker, D. J. *Endocrinology* **2001**, *142*, 521.

[3] Ross, E. A.; Wang, M. *Chem Rev.* **2004**, *104*, 1255.

[4] Nauck, M. A.; Wollschlager, D.; Werner, J.; Holst, J. J.; Orskov, C.; Creutzfeldt, W.; Willms, B. *Diabetologia* **1996**, *39*, 1546.

[5] Drucker, D. J. *Gastroenterology* **2002**, *122*, 531.

[6] Kieffer, T. J.; McIntosh, C. H. S.; Pederson, T. A. *Endocrinology* **1995**, *136*, 3585.

[7] Villhauer, E. B.; Brinkman, J. A.; Naderi, G. B.; Burkey, B. F.; Dunning, B. E.; Prasad, K.; Mangold, B. L.; Russell, M. E.; Hughes, T. E. *J. Med. Chem.* **2003**, *46*, 2774.

[8] Kadhum, A. A. H.; Mohamad, A. B.; Al -Amiery, A. A.; Takriff, M. S. *Molecules*, **2011**, *16*, 6969.

[9] Maddi, V.; Mamledesai, N.; Satyanarayana, D.; Swamy, S. *Indian J. Pharm. Sci.*, **2007**, *69*, 847.

[10] Matos, M.J.; Vilar, S.; Gonzalez-Franco, R. M.; Uriarte, E.; Santana, L.; Friedman, C.; Tatonetti, N. P.; Vina, D.; Fontenla, J. A. *Eur. J. Med. Chem.*, **2013**, *63*, 151.

[11] Vina, D.; Matos, M. J.; Yanez, M.; Santana, L.; Uriarte, E. *Med. Chem. Commun.*, **2012**, *3*, 213.

[12] Catto, M.; Pisani, L.; Leonetti, F.; Nicolotti, O.; Pesce, P.; Stefanachi, A.; Cellamare, S.; Carotti, A. *Bioorg. Med. Chem.*, **2013**, *21*, 146.

[13] Lee, S. O.; Choi, S. Z.; Lee, J. H.; Chung, S. H.; Park, S. H.; Kang, H. C.; Yang, E. Y.; Cho, H. J.; Lee, K. R. *Arch Pharm Res*, **2004**, *27*, 1207.

[14] Kini, D.; Ghate, M. *E-Journal of Chemistry*, **2011**, *8*, 386.

[15] Trott, O.; Olson, A. J. *Journal of Computational Chemistry*, **2011**, *31*, 455.

[16] Berman, H. M.; Westbrook, J.; Feng, Z.; Gilliland, G.; Bhat, T. N.; Weissig, H.; Shindyalov, I. N.; Bourne, P. E. *The Protein Data Bank Nucleic Acids Research*, **2000,** *28*, 235 and *PubMed:* 23501107

[17] Wallace, A. C.; Laskowski, R. A.; Thornton, J. M. *Protein Eng.* **1995**, *8*, 127.

[18] http://www.pymol.org

[19] Dakin, J. *Biol. Chem.* **1929**, 82, 439.

[20] Linch, F. W. *J. Chem. Soc.* **1912**, *101*, 1755.

[21] Connor, D. T. *US Patent* **1981**, *126*, 287.

[22] Khoo, L. E. *Synth. Comm.* **1999**, *29*, 2533.

CHAPTER 4

SYNTHESIS OF DIAMIDES DERIVATIVES OF GLYCINE AS DIPEPTIDYL PEPTIDASE-IV INHIBITORS

4.1 Introduction

In recent years, diabetes has become a severe and increasingly prevalent disease due to urbanization and lifestyle changes [1]. The symptoms of this chronic disease being less marked often leads to late diagnosis until the microvascular or macrovascular complications set to show [2-6]. Treatment includes various therapies, acting through different pathways, including the dipeptidy peptidase IV (DPP-IV) inhibition.

Dipeptidyl peptidase IV (EC 3.4.14.5) is a highly specific, cell surface, serine protease which is responsible for rendering the incretin hormones like the GLP-1 and GIP inactive, *in-vivo*, by cleaving the N-terminal dipeptides with L-proline or L-alanine at the penultimate position [7-9].

Glucagon-like peptide-1 (GLP-1), secreted by the L-cells of intestine in response to the food intake, acts as a stimulator of endogenous insulin release while inhibiting the glucagon secretion in a glucose dependent manner, thereby reducing the risk of hypoglycemia [10-13]. Continuous infusion of GLP-1 has been reported to significantly reduce the blood glucose level in patients with T2D [14]. This active form of GLP-1[7-36]amide is rapidly degraded by DPP-IV in about a minute, to its inactive form GLP-1[9-36]amide which has no therapeutic effect [15-16]. Thus inhibition of DPP-IV will help to increase the half-life of GLP-1 *in-vivo*, thereby increasing its bio-activity.

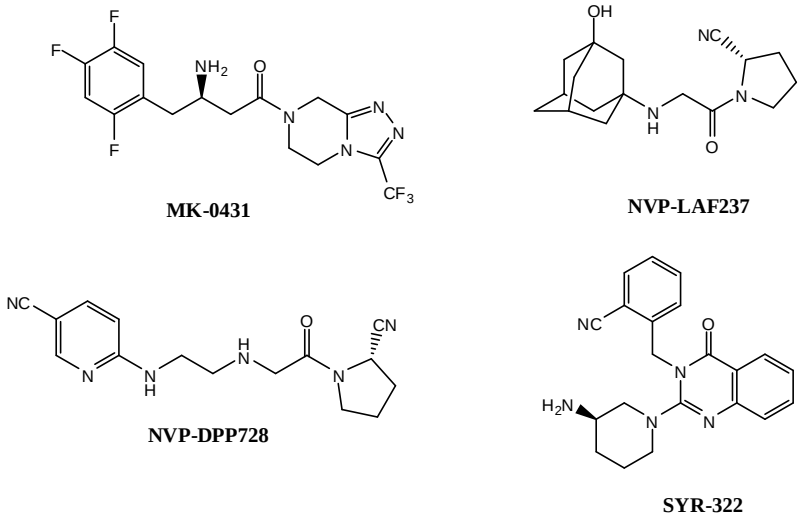

Figure 4.1: DPP-IV inhibitors

Various classes of DPP-IV inhibitors (Figure 4.1) have been reported from many laboratories, and most of them are derived from α- and β-amino acids aping the N-terminal dipeptide residues of the incretin hormones. Amongst them sitagliptin (MK-0431) and alogliptin (SYR-322) are exceptions [17-18]. Some of the potent DPP-IV inhibitors reported so far, have sulfonamide at the P-2 position.

So far, effect of substitution of sulphonamide (Chapter 2) and coumarin derivatives (Chapter 3) at the P-1 site on DPP-IV inhibition have been studied.

From both these studies it can be concluded that substitution of sulphonamide at the P2 site resulted in better enzyme inhibition. Taking into account all these structure activity relationship studies, diamide derivatives of glycine with 1-(phenylsulfonyl)piperidine-3-carboxylic acid condensed at the N-terminus of glycine while condensing various 1^o or 2^o amines at the C-terminus have been designed (Figure 4.2), synthesized and studied for their anti-diabetic activity. All these synthesized molecules were then screened for *in-vitro* DPP-IV inhibition.

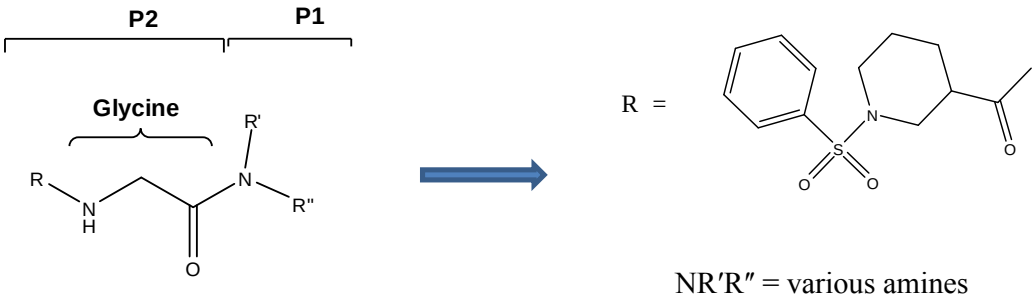

Figure 4.2: Design of diamides derivatives of glycine as DPP-IV inhibitors.

4.2 Results and Discussion

4.2.1 Chemistry

In order to synthesize diamide derivatives of glycine, commercially available boc-protected glycine **1** was at first reacted with various amines in the presence of 1-ethyl-3-(3-dimethylaminopropyl)carbodiimide hydrochloride (EDCI), 1-hydroxybenzotriazole (HOBt), 4-dimethylaminopyridine (DMAP), to yield corresponding C-substituted amide derivatives of glycine **2a-k** as shown in Scheme 4.1. The structures of few intermediates from **2a-k** have been proved in Chapter 5 **(**compounds **5a-f)**. Figure 5.3.1 to 5.8.4 shows IR, ^{1}H NMR, ^{13}C NMR and ESI-MS spectra of few boc-glycylamides **2a-k**. On the other hand, reaction of piperidine-3-carboxylic acid **4** with benzenesulfonyl chloride, in the presence of sodium carbonate as a base, in a mixture of dichloromethane : water (1:1) gave 1-(phenylsulfonyl)piperidine-3-carboxylic acid **5** on acidification. IR spectrum of **5** (**Figure 2.5.1**, **Chapter 2**) showed bands at 1693 and 1349 cm^{-1} for the carbonyl group of carboxylic acid and sulfonamide group respectively while the ^{1}H NMR (**Figure 2.5.2**, **Chapter 2**) showed multiplet from δ 7.56-7.79 for the five aromatic protons and a broad singlet at δ 8.98 indicating the proton of the carboxylic acid group thereby confirming the formation of **5.** Free bases **3a-k** were obtained on stirring boc-protected glycine derivatives **2a-k** in 10% TFA in DCM, which on further reaction with 1-(phenylsulfonyl)piperidine-3-carboxylic acid **5** in the presence of peptide coupling agents EDCI, HOBt, DMAP gave the desired diamide derivatives of glycine **6a-k** as shown in Scheme 4.1.

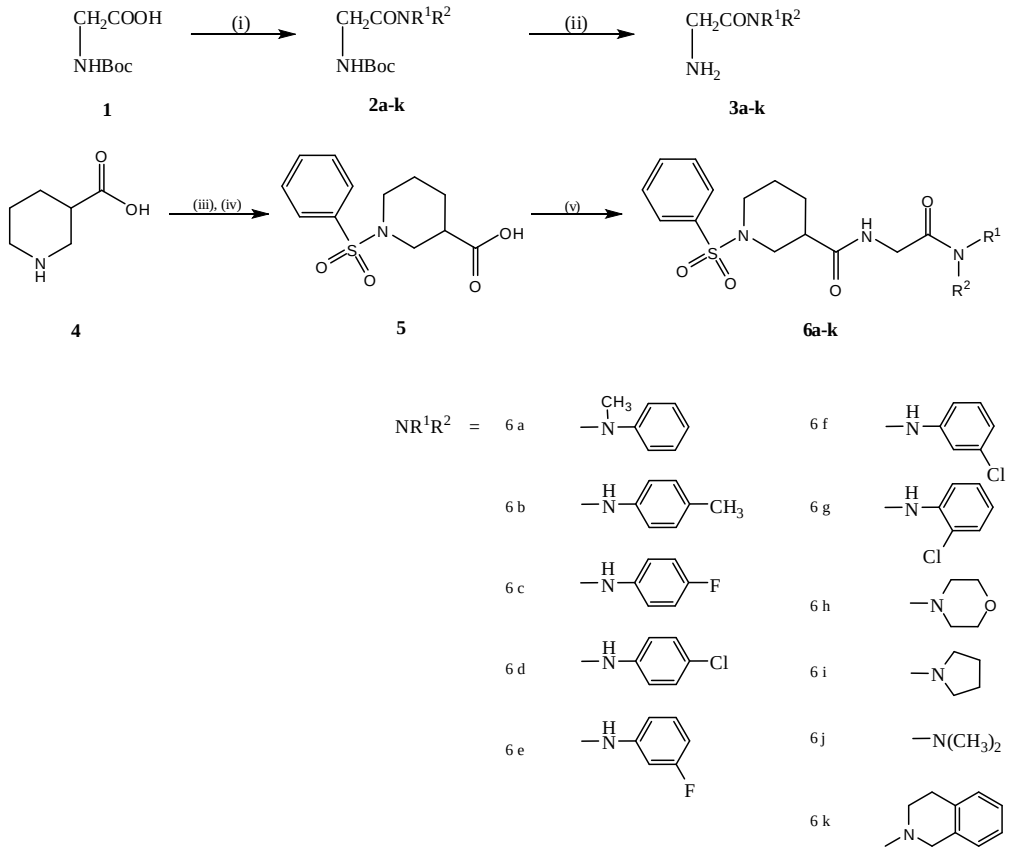

Scheme 4.1 : Reagents: (i) EDCI, DMAP, DCM, primary or secondary amine; (ii) TFA, DCM; (iii) $PhSO_2Cl$, Na_2CO_3, DCM, H_2O; (iv) HCl; (v) EDCI, HOBt, DMAP, DCM, **3a-k**.

The structures of **6a-k** were confirmed by their IR, ^{1}H NMR, ^{13}C NMR and ESI-MS analysis. The IR spectrum of compounds **6d** (Figure 4.6.1) exhibited two strong band at 3329, 3303 cm^{-1} for the two amide –NH protons, another two strong bands 1679 and 1644 cm^{-1} for amide carbonyl groups and a strong band at 1355 cm^{-1} for sulfonamide group. In the ^{1}H NMR spectrum of **6d** (Figure 4.6.2), the methylene group of glycine showed a multiplet at δ 3.84-3.86 due to the interactions with the neighbouring amide groups and multiplet form δ 7.36-7.74 represented the aromatic protons while in the ^{13}C NMR spectrum (Figure 4.6.3), two peaks at 168.26 and 173.16 for the carbonyl

carbons of the amide groups, six peaks from 24.14 to 48.63 for the piperidyl and glycyl carbons and eight peaks ranging from 121.10-138.25 for the aromatic carbons thereby confirming the formation of **6d** which is also supported by its ESI-MS spectrum (Figure 4.6.4) with a peak at *m/z* 435.9 for $[M+H]^+$.

Figures from 4.3.1 onwards, upto 4.13.4 show IR, ^{1}H NMR, ^{13}C NMR and ESI-MS spectra of compounds **6a-k** thus confirming the structure of all the synthesised compounds.

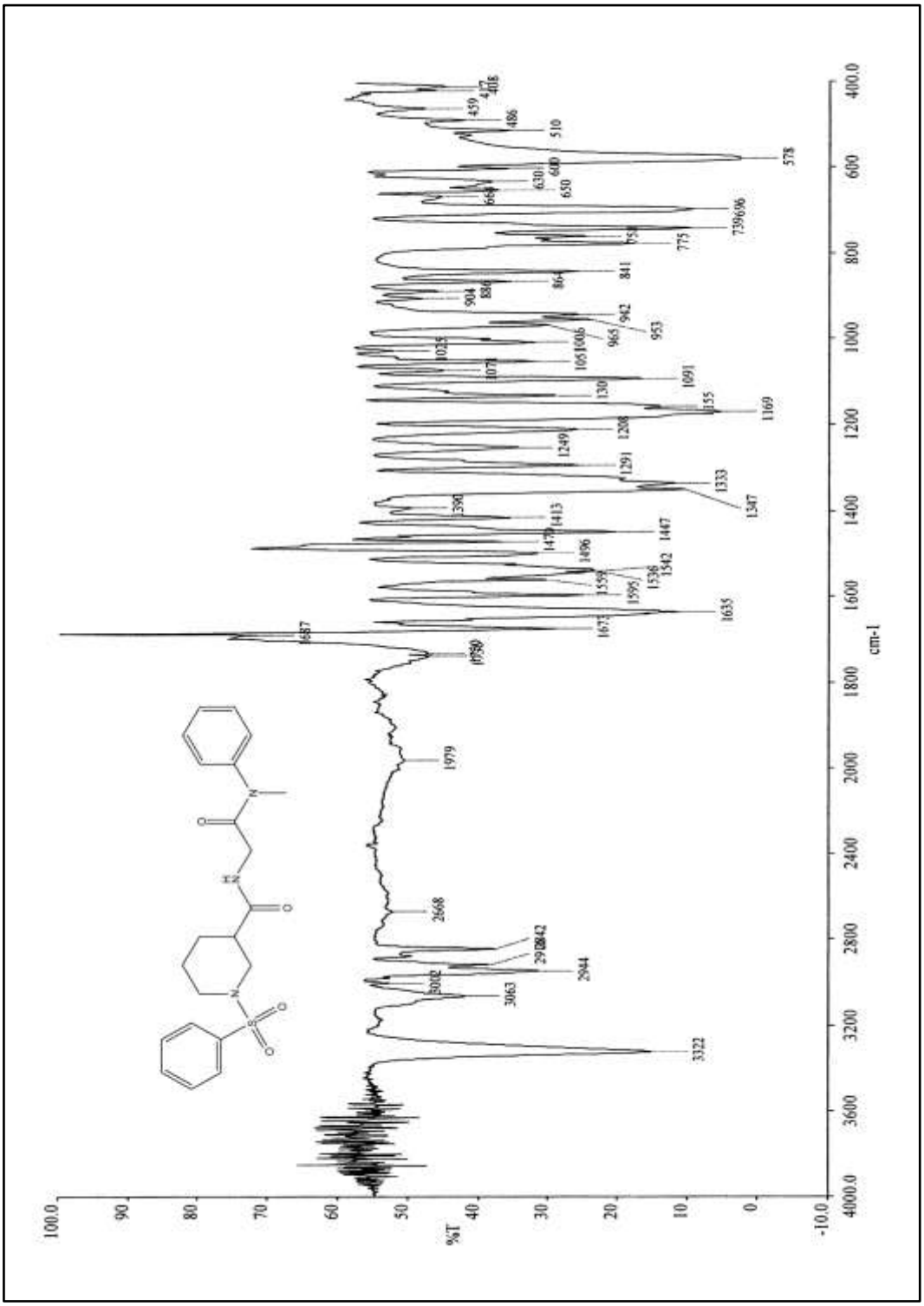

Figure 4.3.1: IR spectrum of N-(2-(methyl(phenyl)amino)-2-oxoethyl)-1-(phenylsulfonyl)piperidine-3-carboxamide **6a**

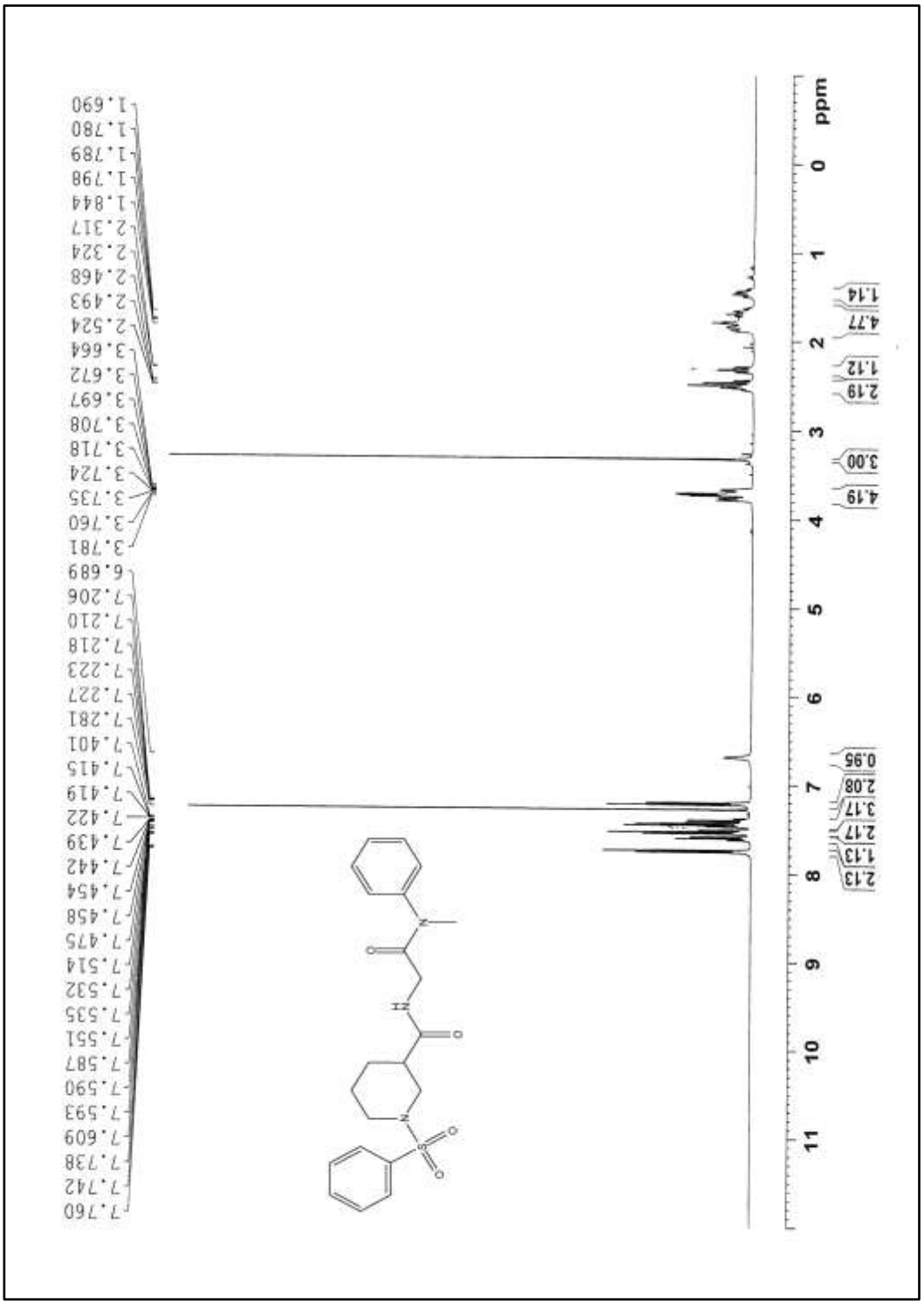

Figure 4.3.2: ^{1}H NMR spectrum of N-(2-(methyl(phenyl)amino)-2-oxoethyl)-1-(phenylsulfonyl)piperidine-3-carboxamide **6a**

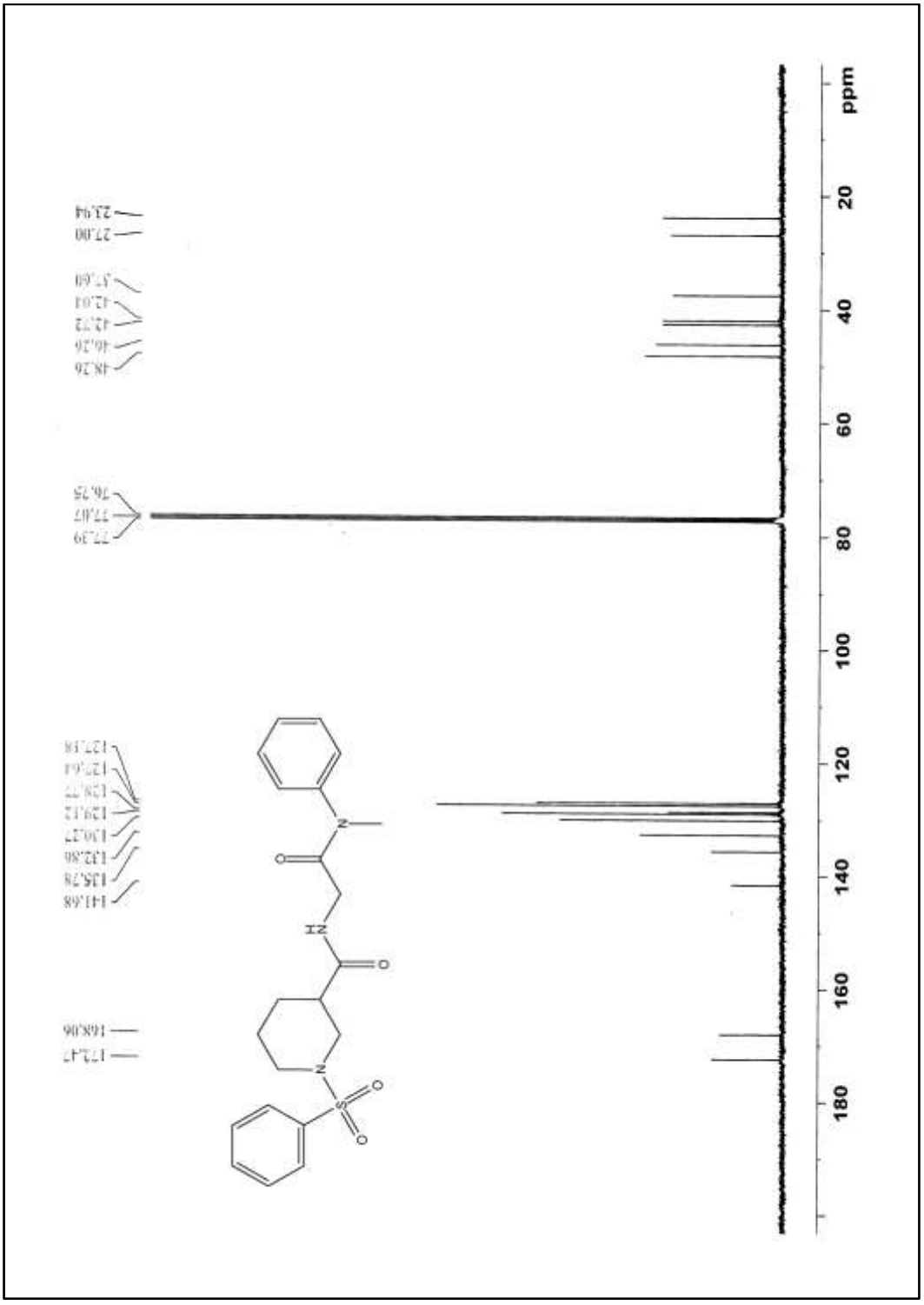

Figure 4.3.3: ^{13}C NMR spectrum of N-(2-(methyl(phenyl)amino)-2-oxoethyl)-1-(phenylsulfonyl)piperidine-3-carboxamide **6a**

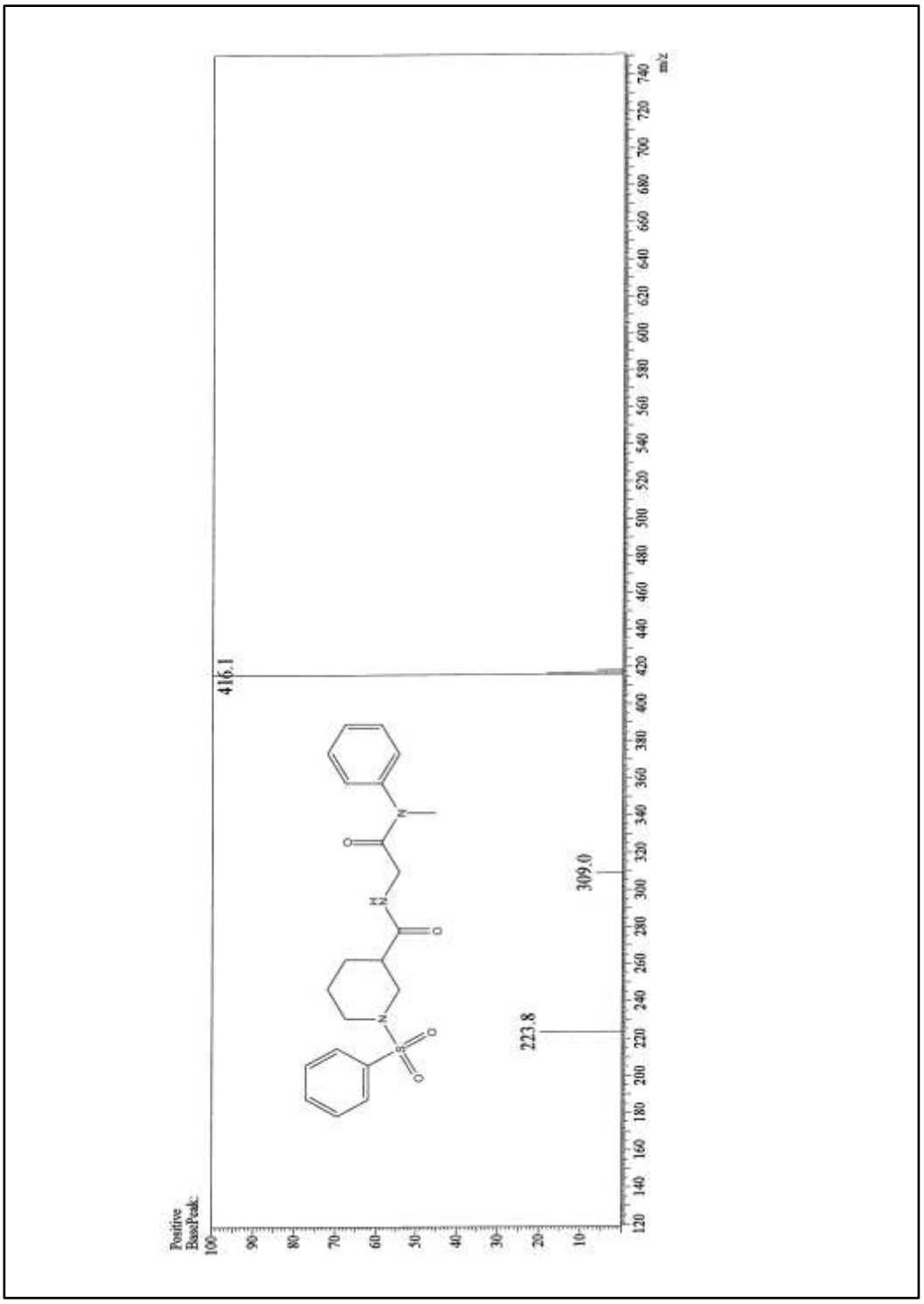

Figure 4.3.4: ESI-MS spectrum of N-(2-(methyl(phenyl)amino)-2-oxoethyl)-1-(phenylsulfonyl)piperidine-3-carboxamide **6a**

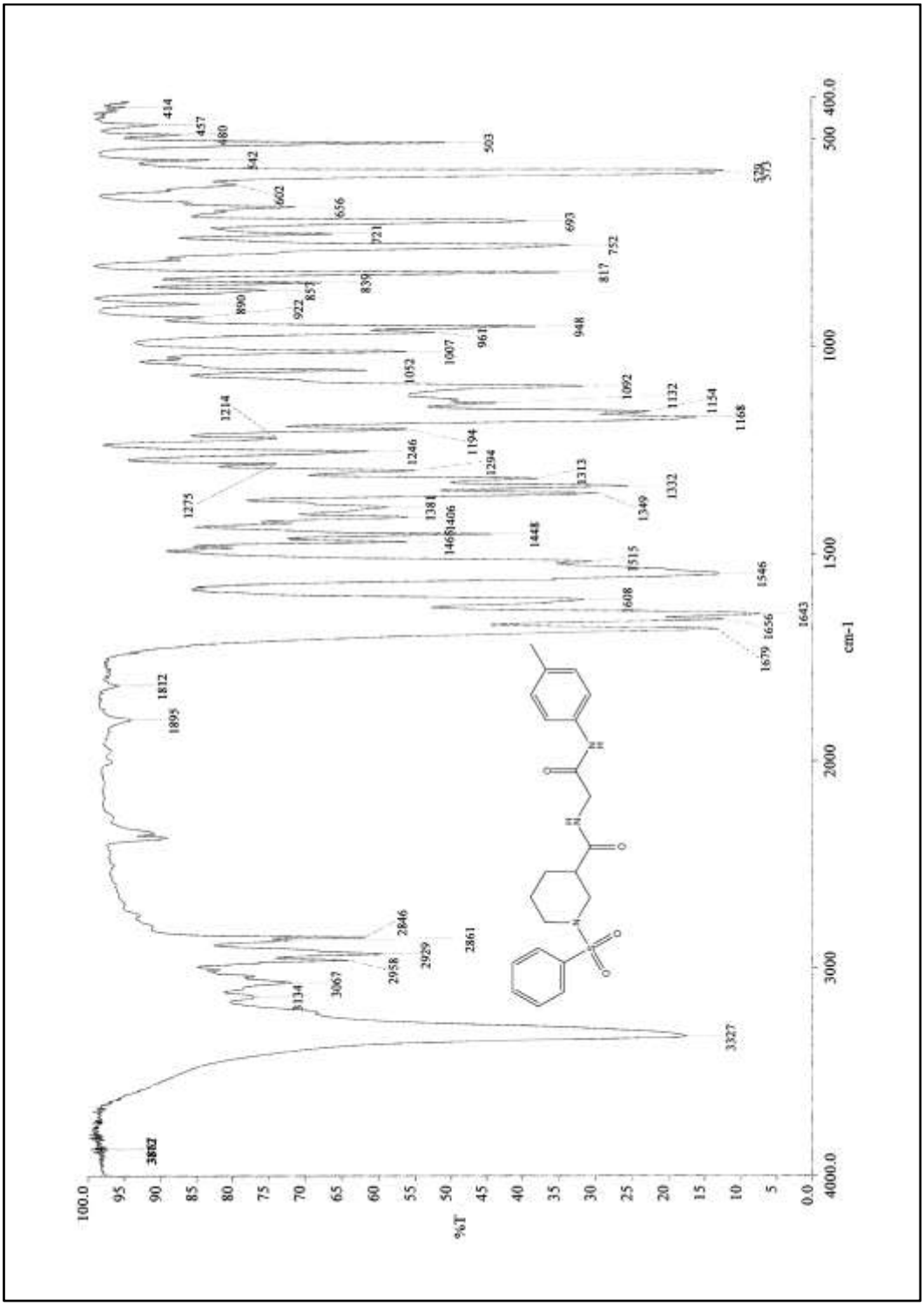

Figure 4.4.1: IR spectrum of N-(2-oxo-2-(p-tolylamino)ethyl)-1-(phenylsulfonyl)piperidine-3-carboxamide **6b**

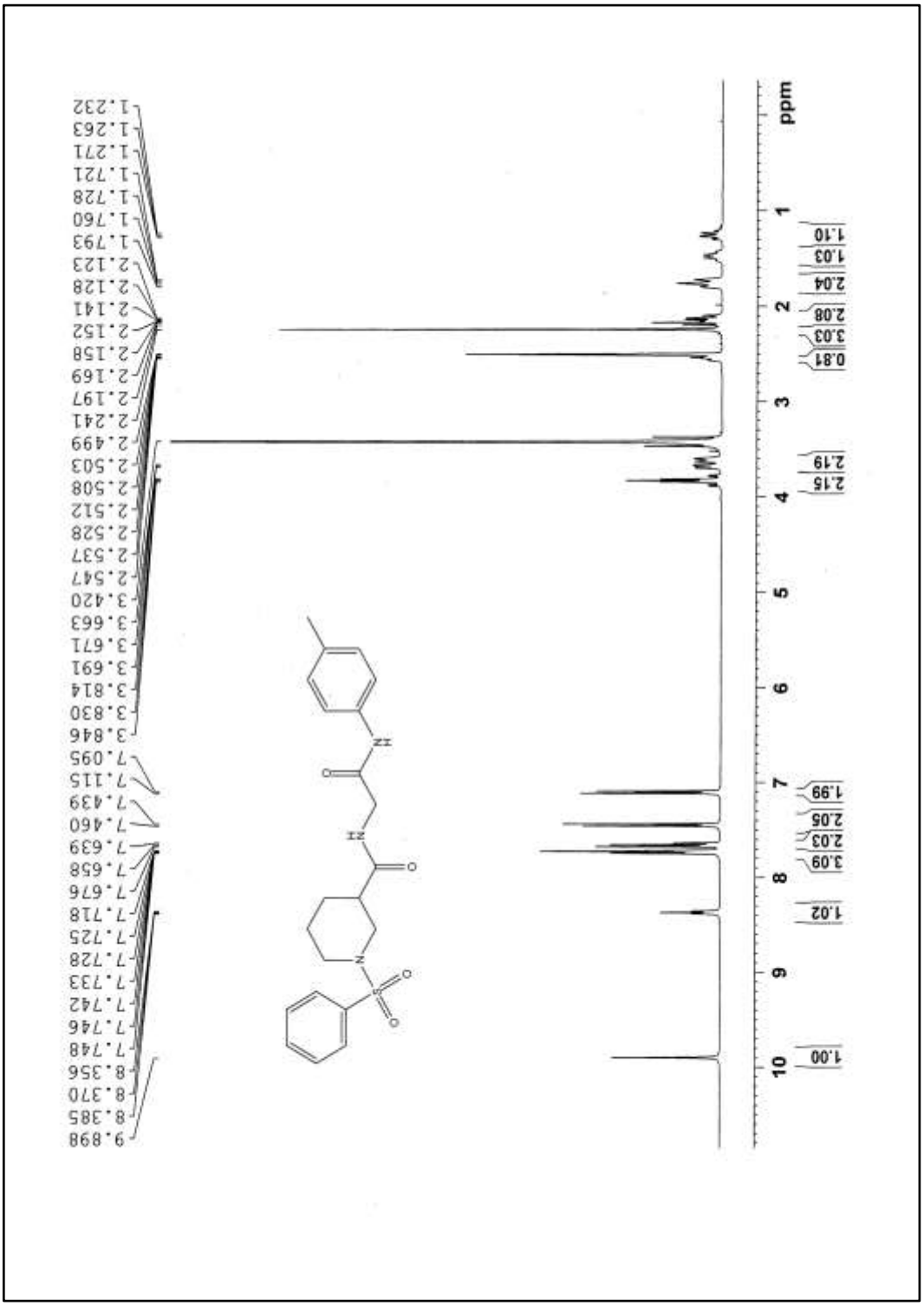

Figure 4.4.2: ^{1}H NMR spectrum of N-(2-oxo-2-(p-tolylamino)ethyl)-1-(phenylsulfonyl)piperidine-3-carboxamide **6b**

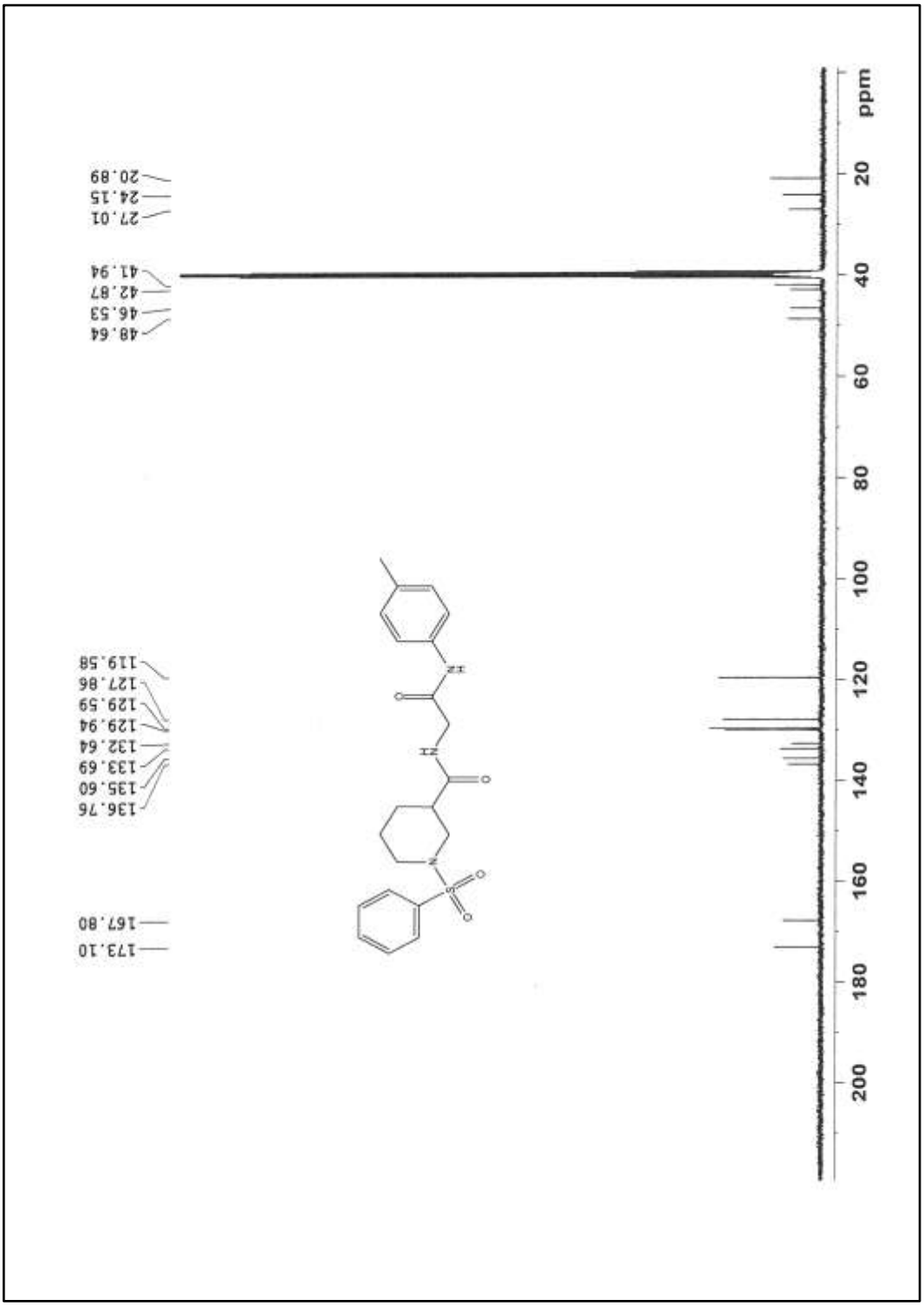

Figure 4.4.3: ^{13}C NMR spectrum of N-(2-oxo-2-(p-tolylamino)ethyl)-1-(phenylsulfonyl)piperidine-3-carboxamide **6b**

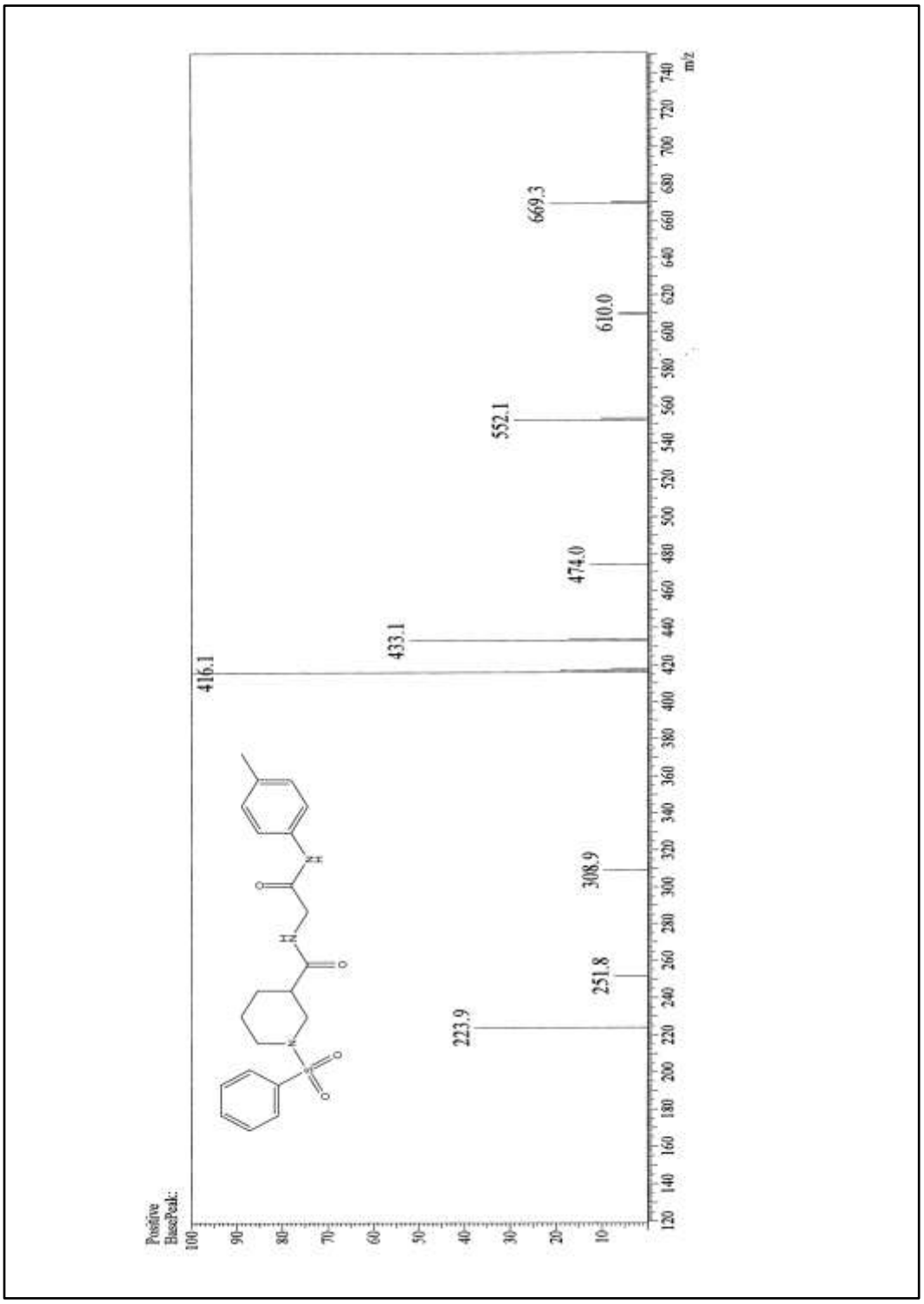

Figure 4.4.4: ESI-MS spectrum of N-(2-oxo-2-(p-tolylamino)ethyl)-1-(phenylsulfonyl)piperidine-3-carboxamide **6b**

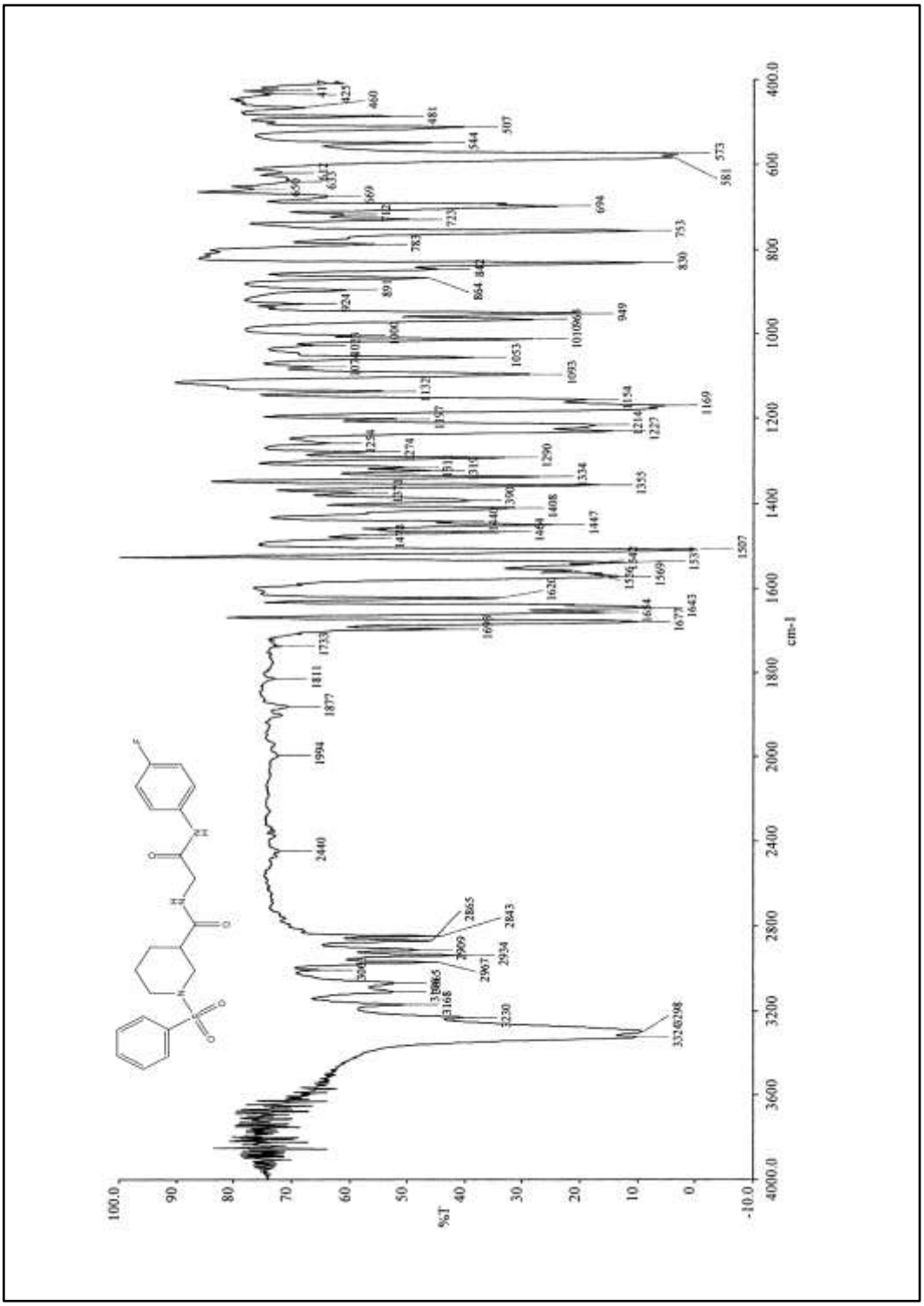

Figure 4.5.1: IR spectrum of N-(2-(4-fluorophenylamino)-2-oxoethyl)-1-(phenylsulfonyl)piperidine-3-carboxamide **6c**

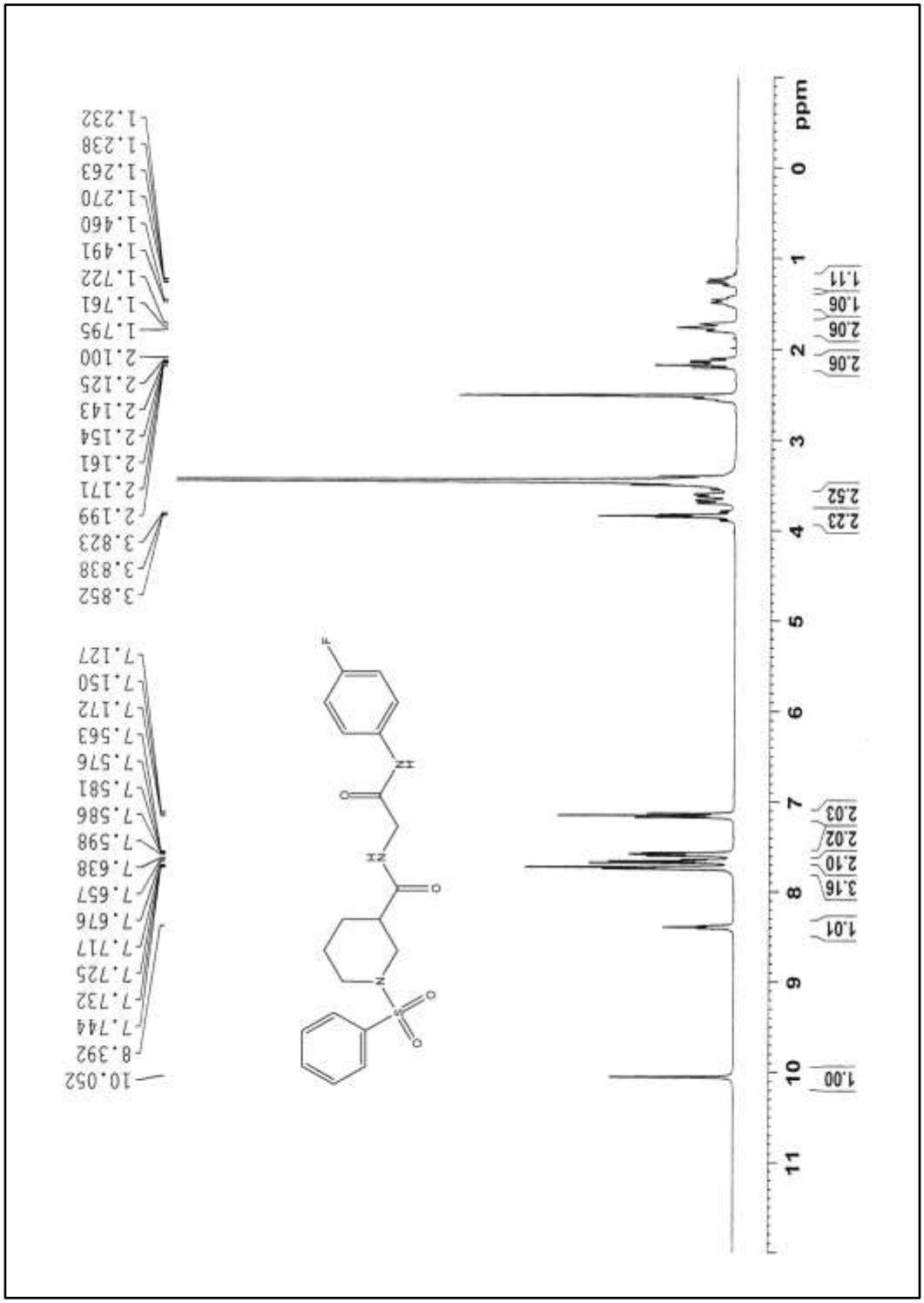

Figure 4.5.2: ^{1}H NMR spectrum of N-(2-(4-fluorophenylamino)-2-oxoethyl)-1-(phenylsulfonyl)piperidine-3-carboxamide **6c**

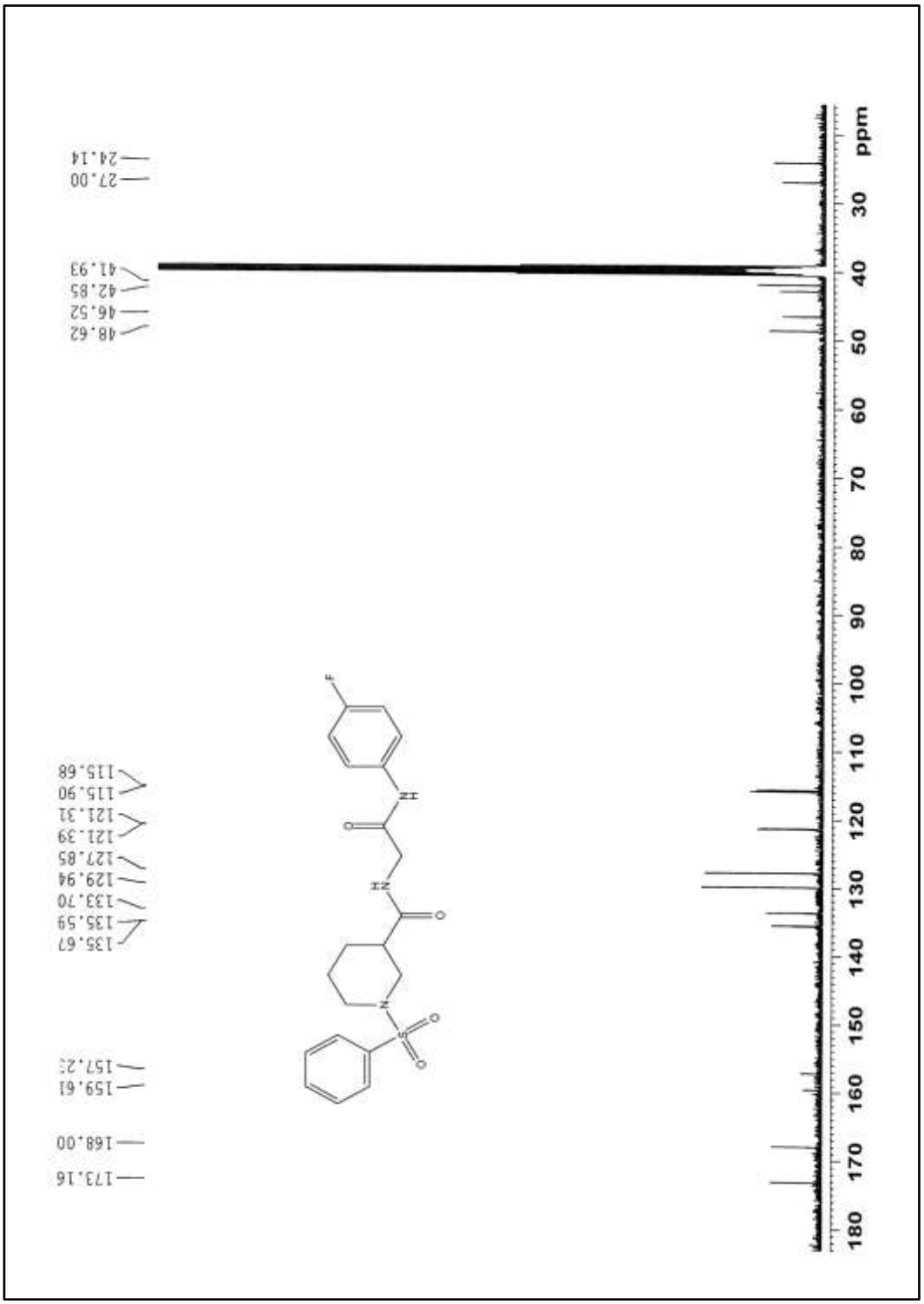

Figure 4.5.3: ^{13}C NMR spectrum of N-(2-(4-fluorophenylamino)-2-oxoethyl)-1-(phenylsulfonyl)piperidine-3-carboxamide **6c**

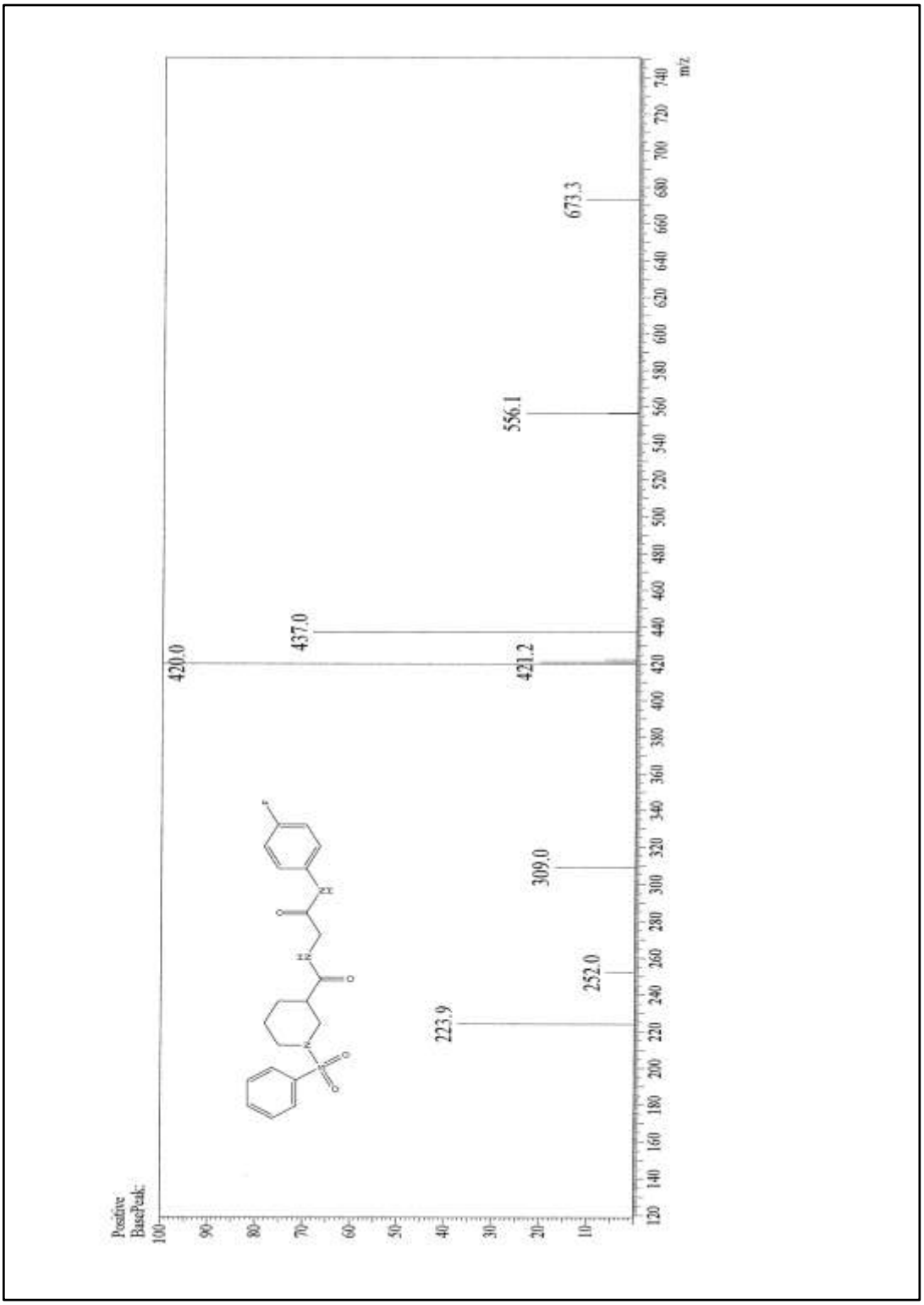

Figure 4.5.4: ESI-MS spectrum of N-(2-(4-fluorophenylamino)-2-oxoethyl)-1-(phenylsulfonyl)piperidine-3-carboxamide **6c**

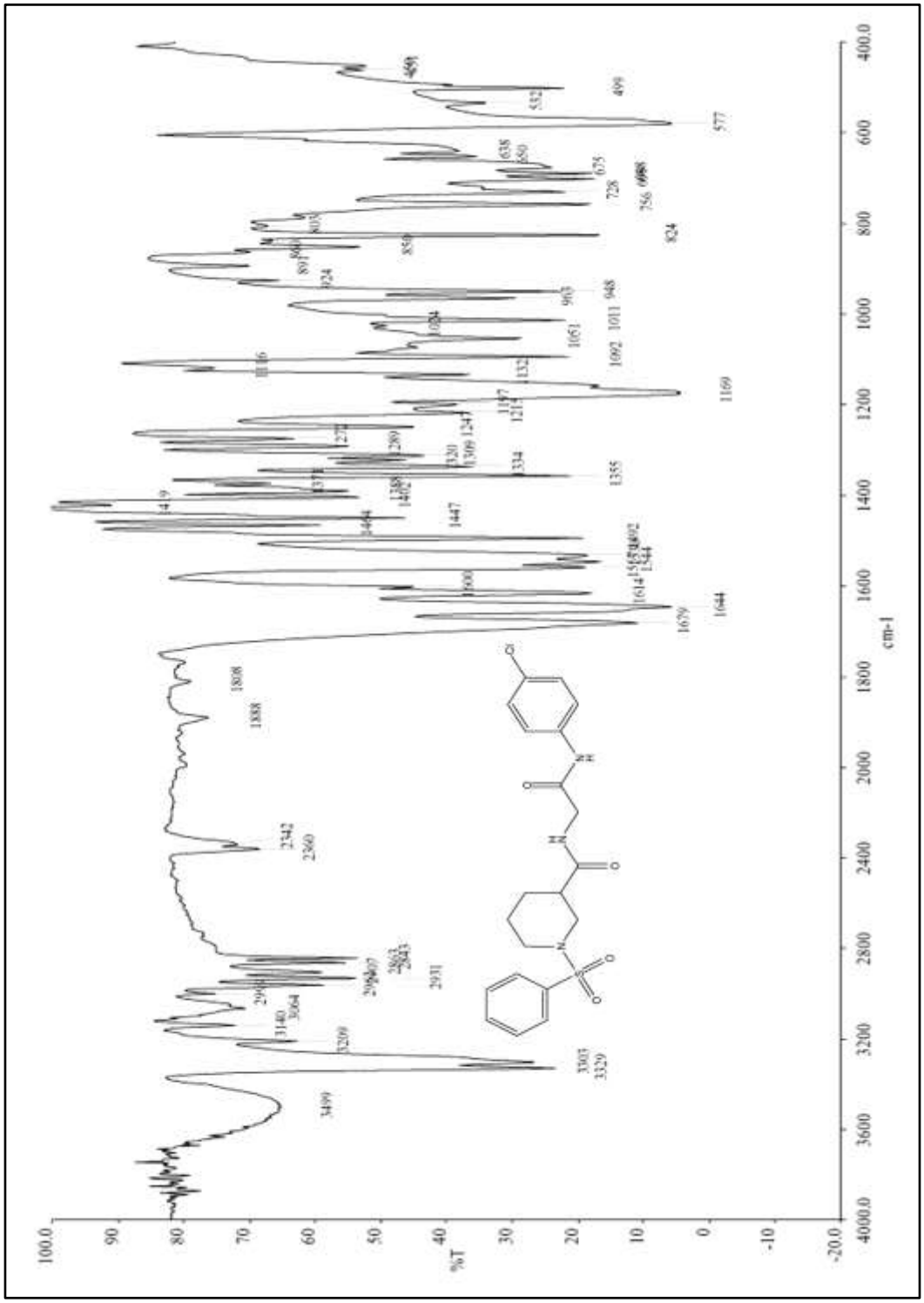

Figure 4.6.1: IR spectrum of N-(2-(4-chlorophenylamino)-2-oxoethyl)-1-(phenylsulfonyl)piperidine-3-carboxamide **6d**

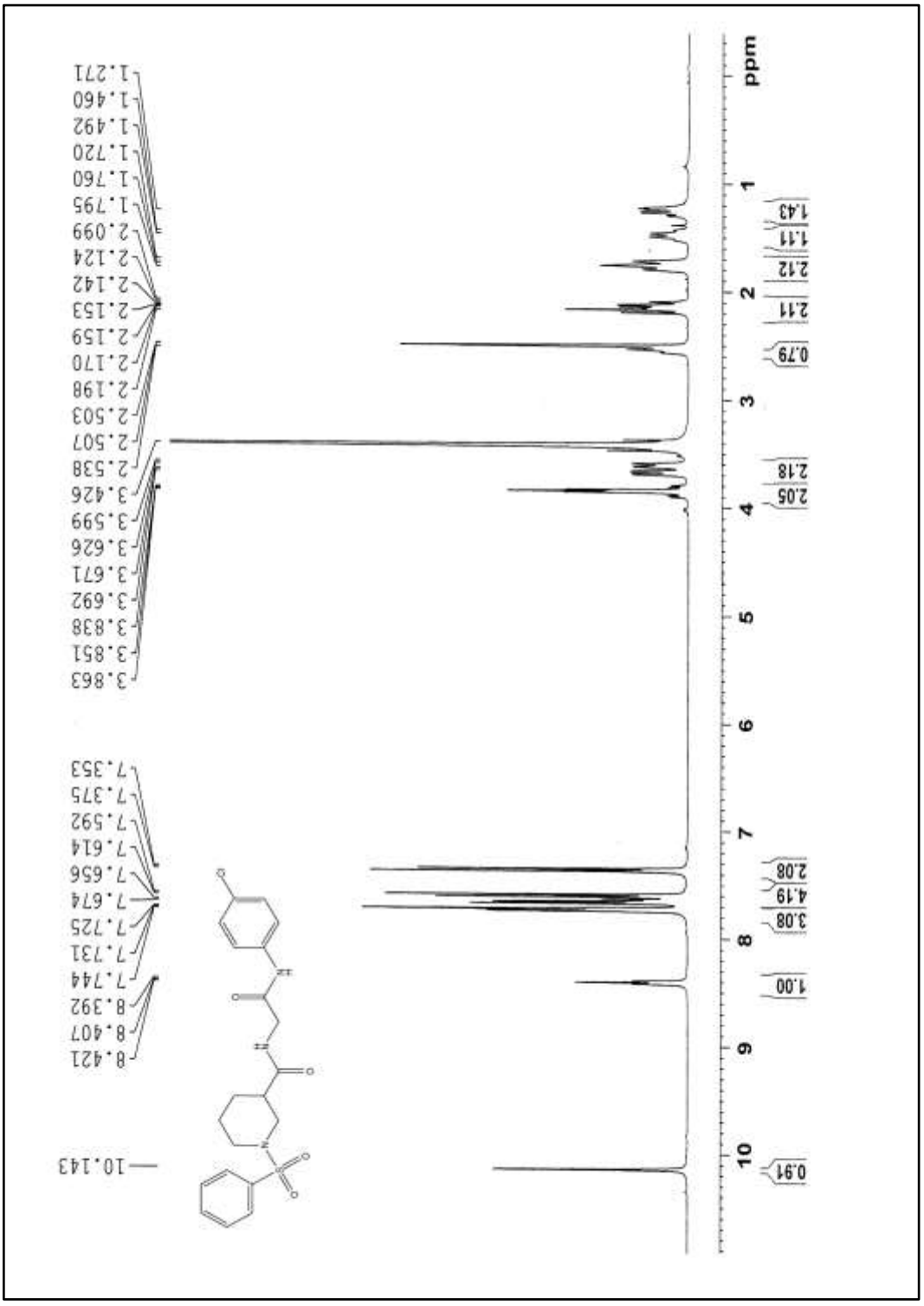

Figure 4.6.2: ^{1}H NMR spectrum of N-(2-(4-chlorophenylamino)-2-oxoethyl)-1-(phenylsulfonyl)piperidine-3-carboxamide **6d**

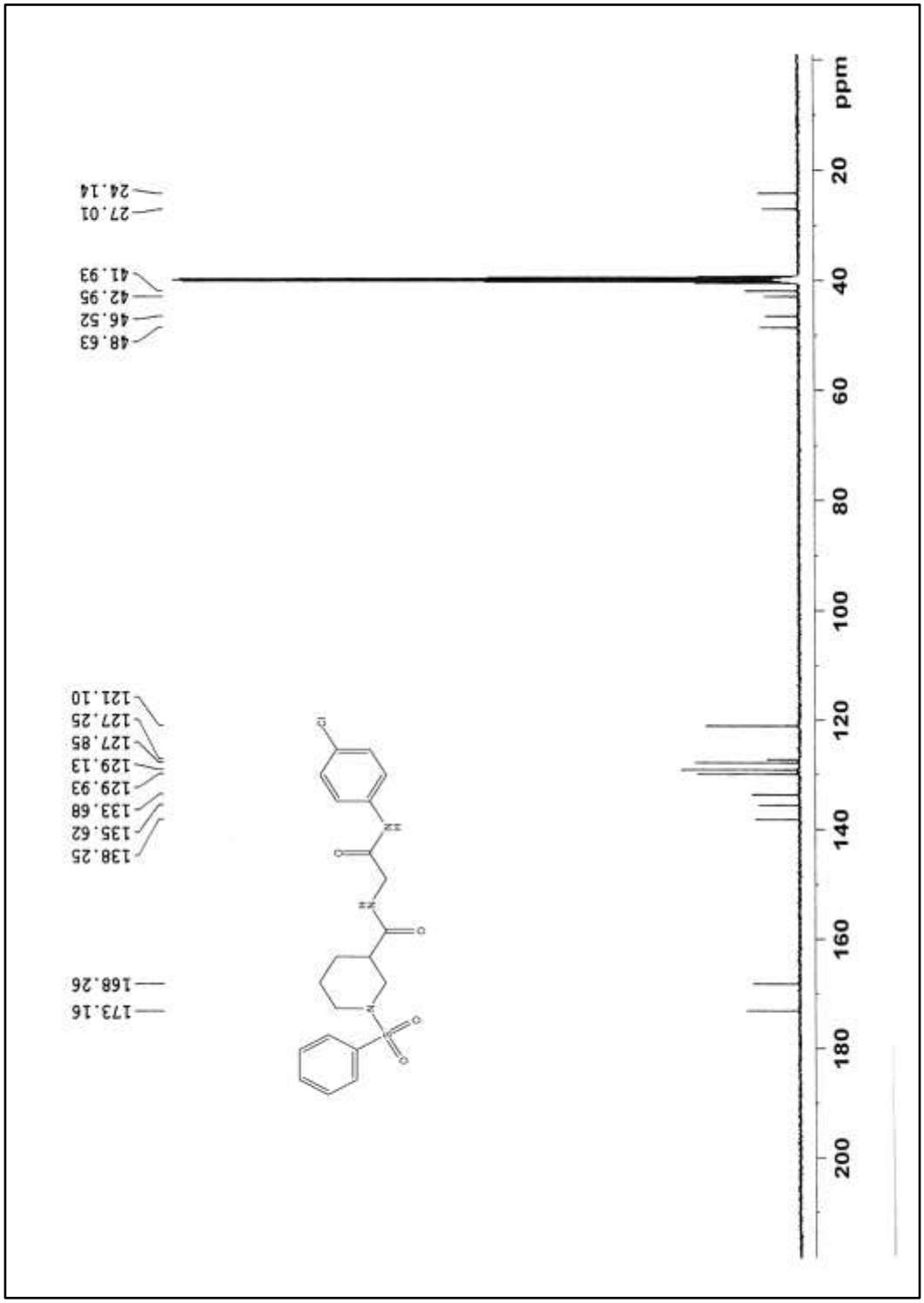

Figure 4.6.3: ^{13}C NMR spectrum of N-(2-(4-chlorophenylamino)-2-oxoethyl)-1-(phenylsulfonyl)piperidine-3-carboxamide **6d**

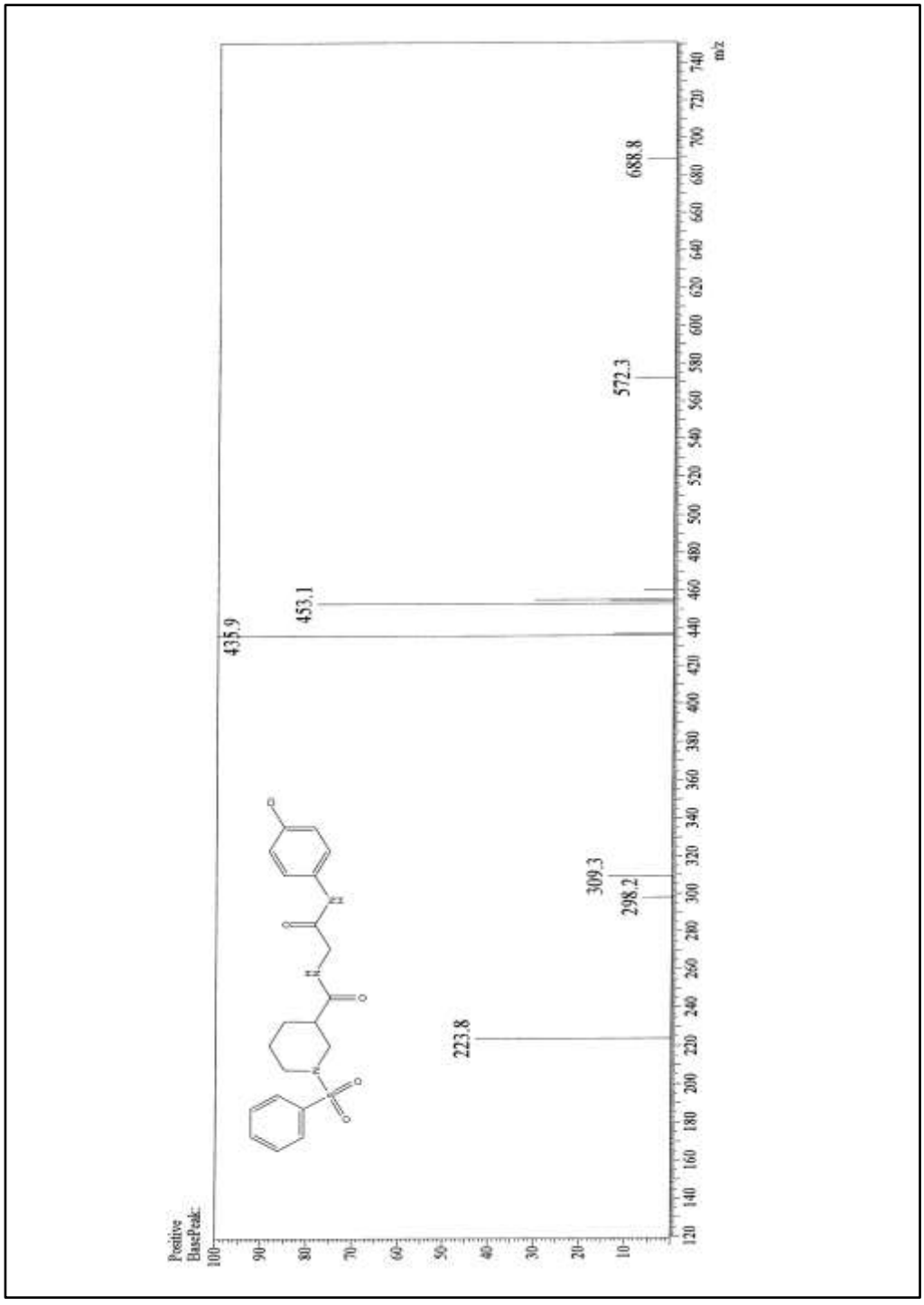

Figure 4.6.4: ESI-MS spectrum of N-(2-(4-chlorophenylamino)-2-oxoethyl)-1-(phenylsulfonyl)piperidine-3-carboxamide **6d**

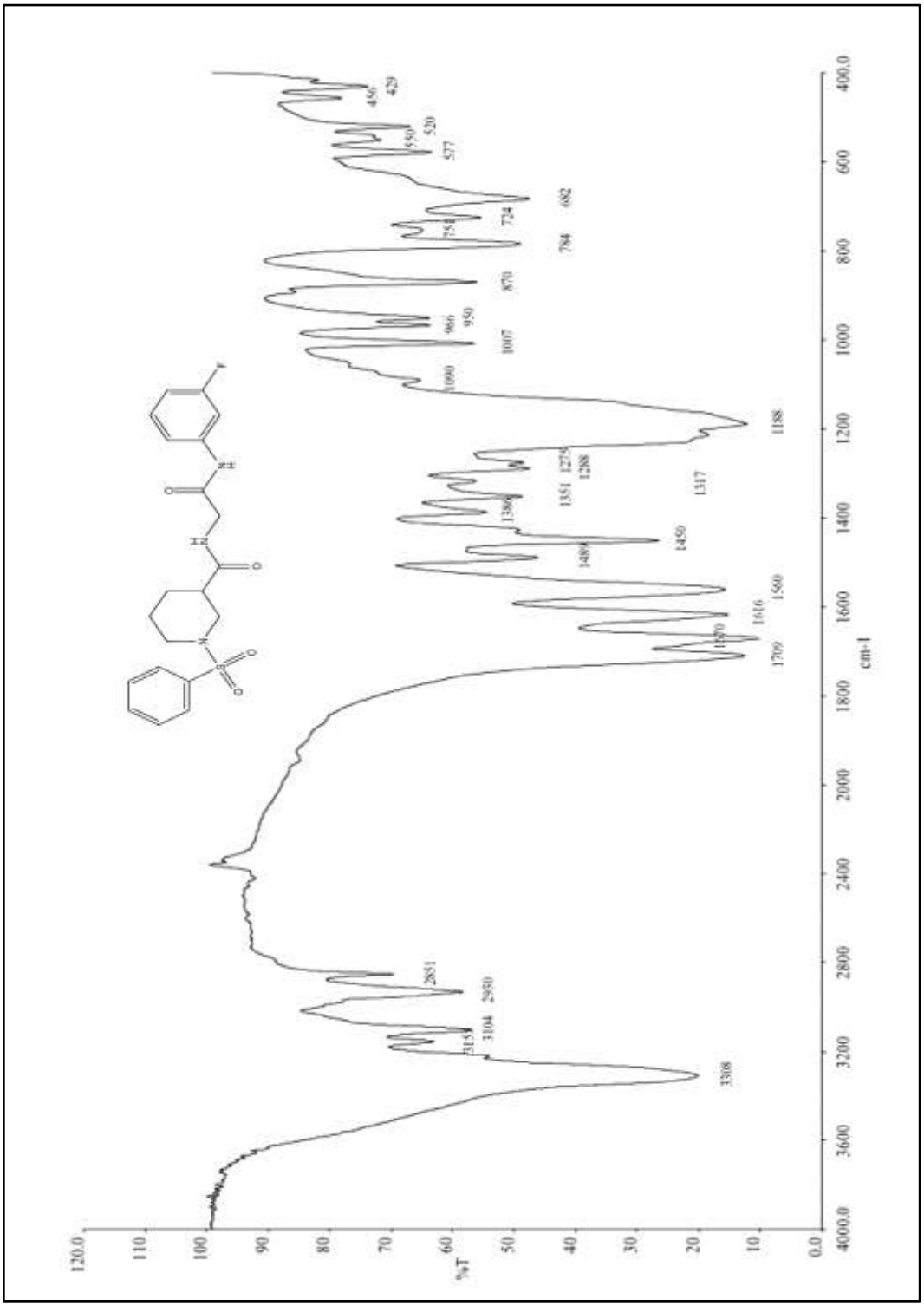

Figure 4.7.1: IR spectrum of N-(2-(3-fluorophenylamino)-2-oxoethyl)-1-(phenylsulfonyl)piperidine-3-carboxamide **6e**

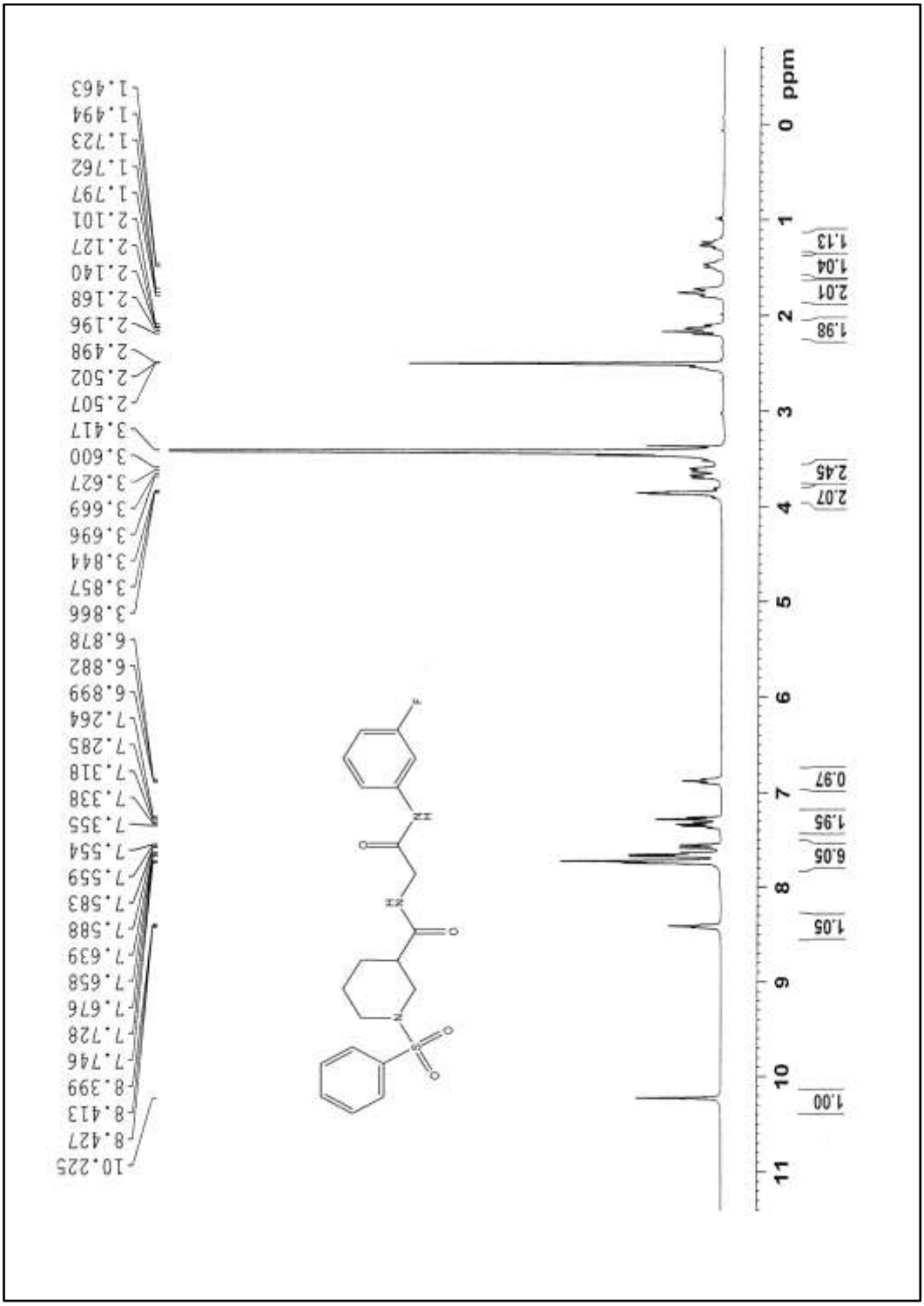

Figure 4.7.2: ^{1}H NMR spectrum of N-(2-(3-fluorophenylamino)-2-oxoethyl)-1-(phenylsulfonyl)piperidine-3-carboxamide **6e**

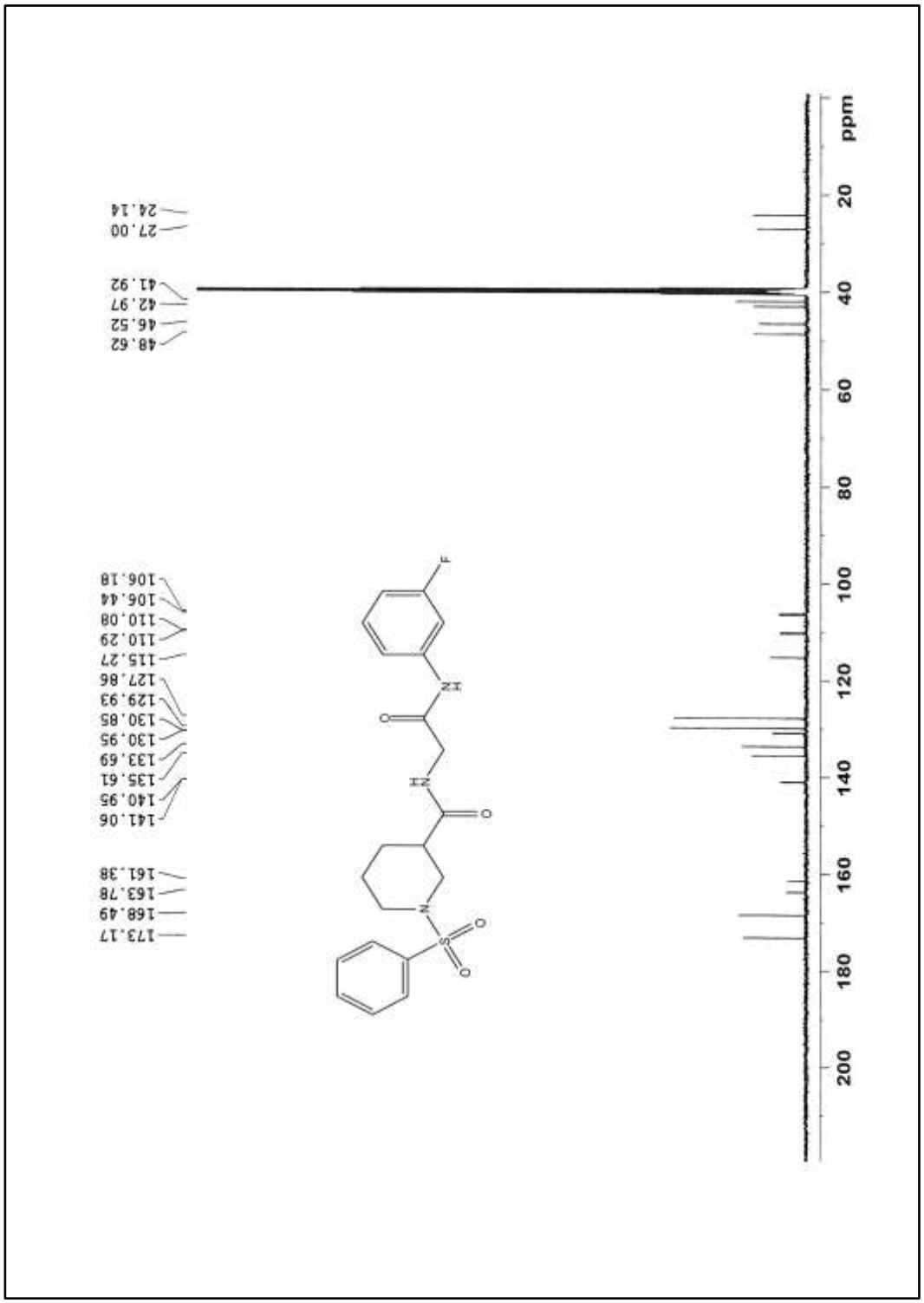

Figure 4.7.3: ^{13}C NMR spectrum of N-(2-(3-fluorophenylamino)-2-oxoethyl)-1-(phenylsulfonyl)piperidine-3-carboxamide **6e**

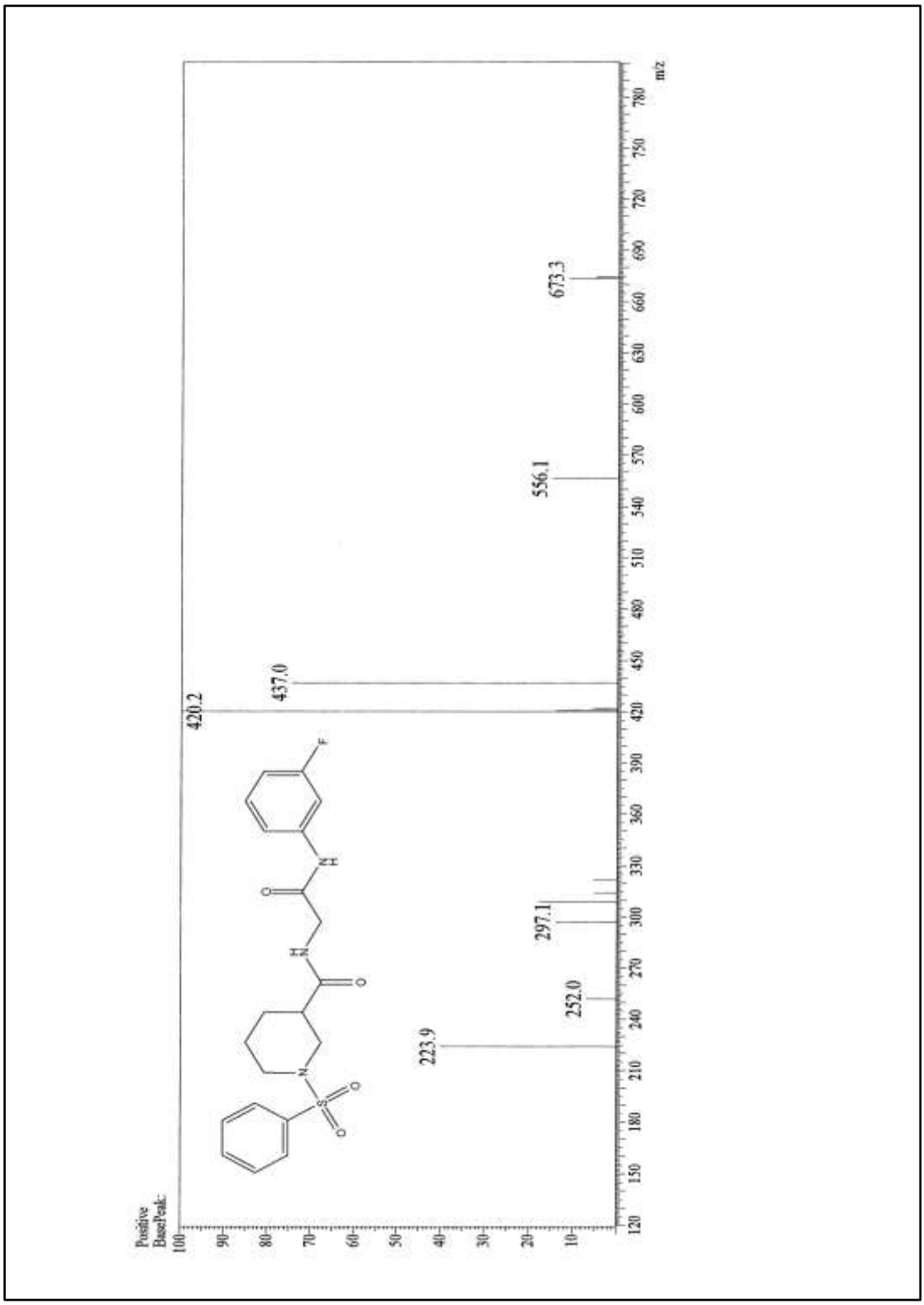

Figure 4.7.4: ESI-MS spectrum of N-(2-(3-fluorophenylamino)-2-oxoethyl)-1-(phenylsulfonyl)piperidine-3-carboxamide **6e**

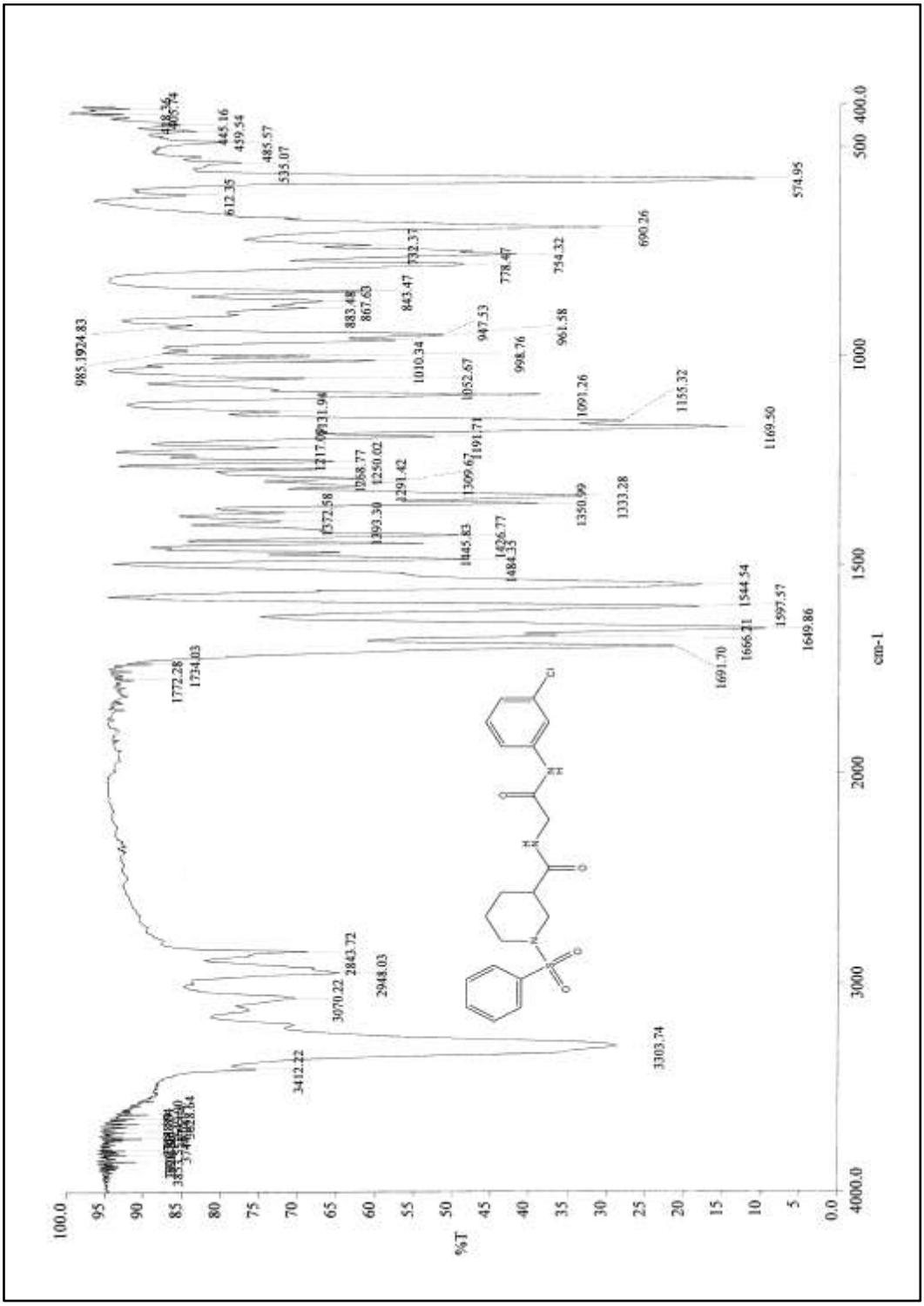

Figure 4.8.1: IR spectrum of N-(2-(3-chlorophenylamino)-2-oxoethyl)-1-(phenylsulfonyl)piperidine-3-carboxamide **6f**

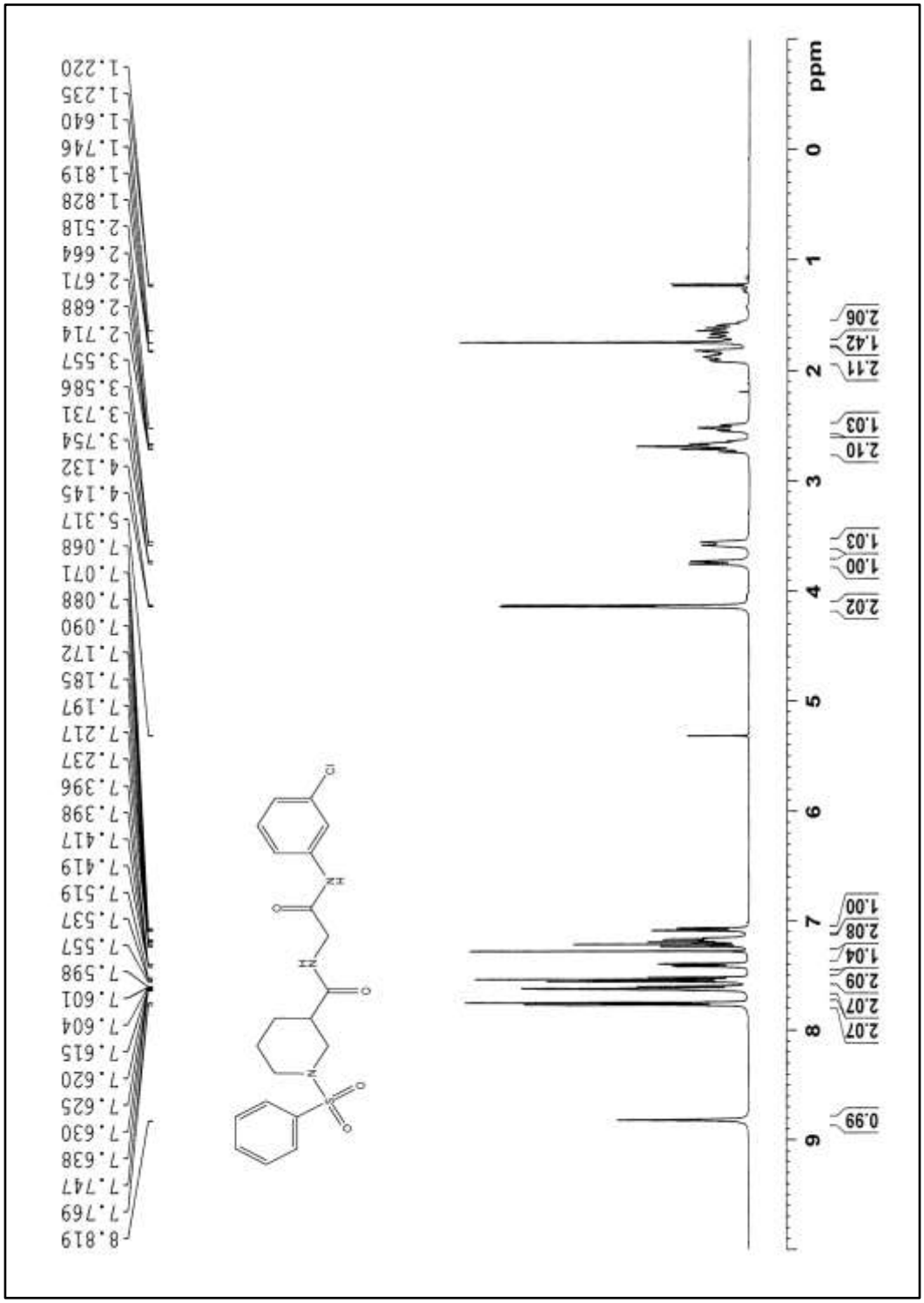

Figure 4.8.2: ^{1}H NMR spectrum of N-(2-(3-chlorophenylamino)-2-oxoethyl)-1-(phenylsulfonyl)piperidine-3-carboxamide **6f**

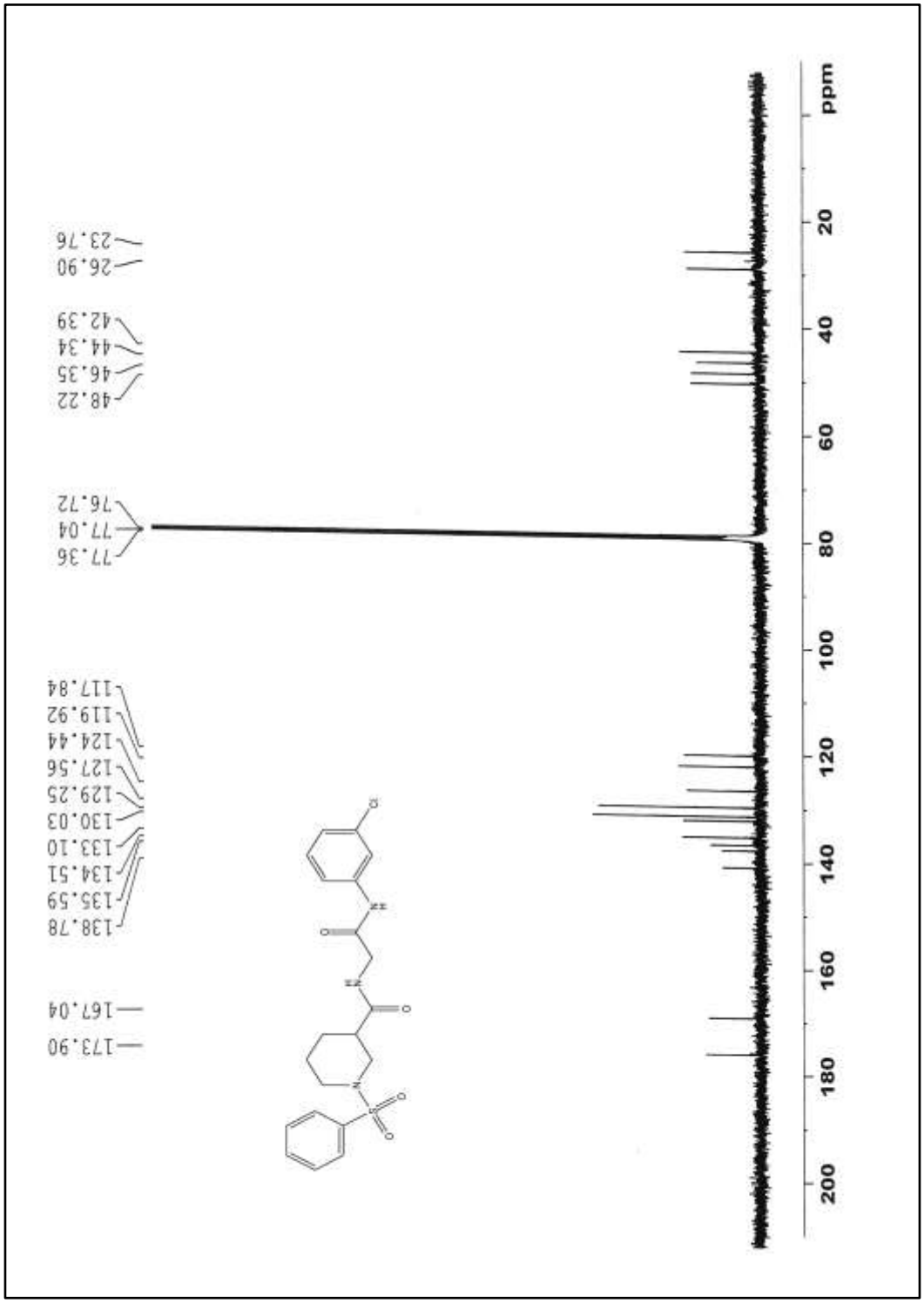

Figure 4.8.3: ^{13}C NMR spectrum of N-(2-(3-chlorophenylamino)-2-oxoethyl)-1-(phenylsulfonyl)piperidine-3-carboxamide **6f**

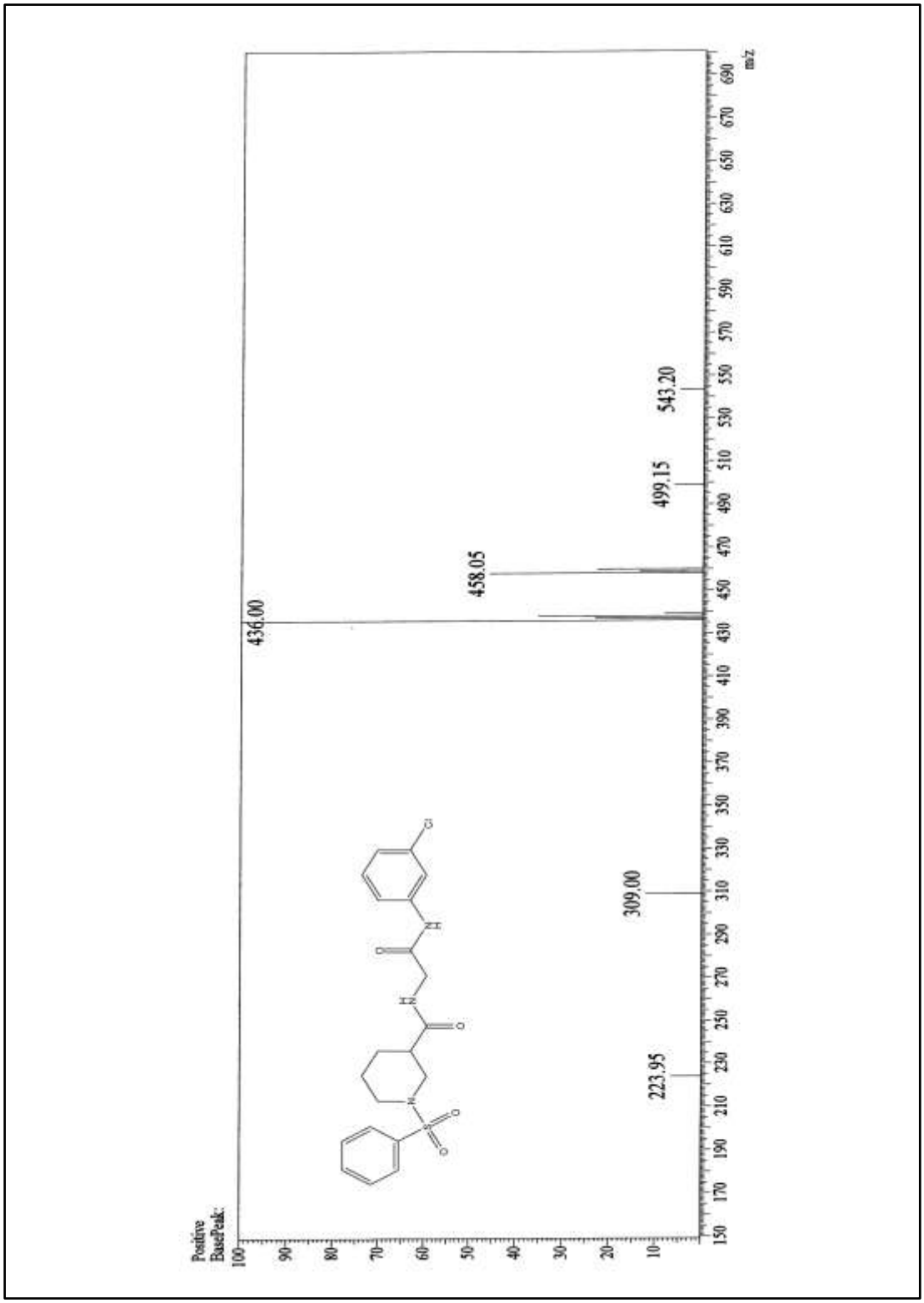

Figure 4.8.4: ESI-MS spectrum of N-(2-(3-chlorophenylamino)-2-oxoethyl)-1-(phenylsulfonyl)piperidine-3-carboxamide **6f**

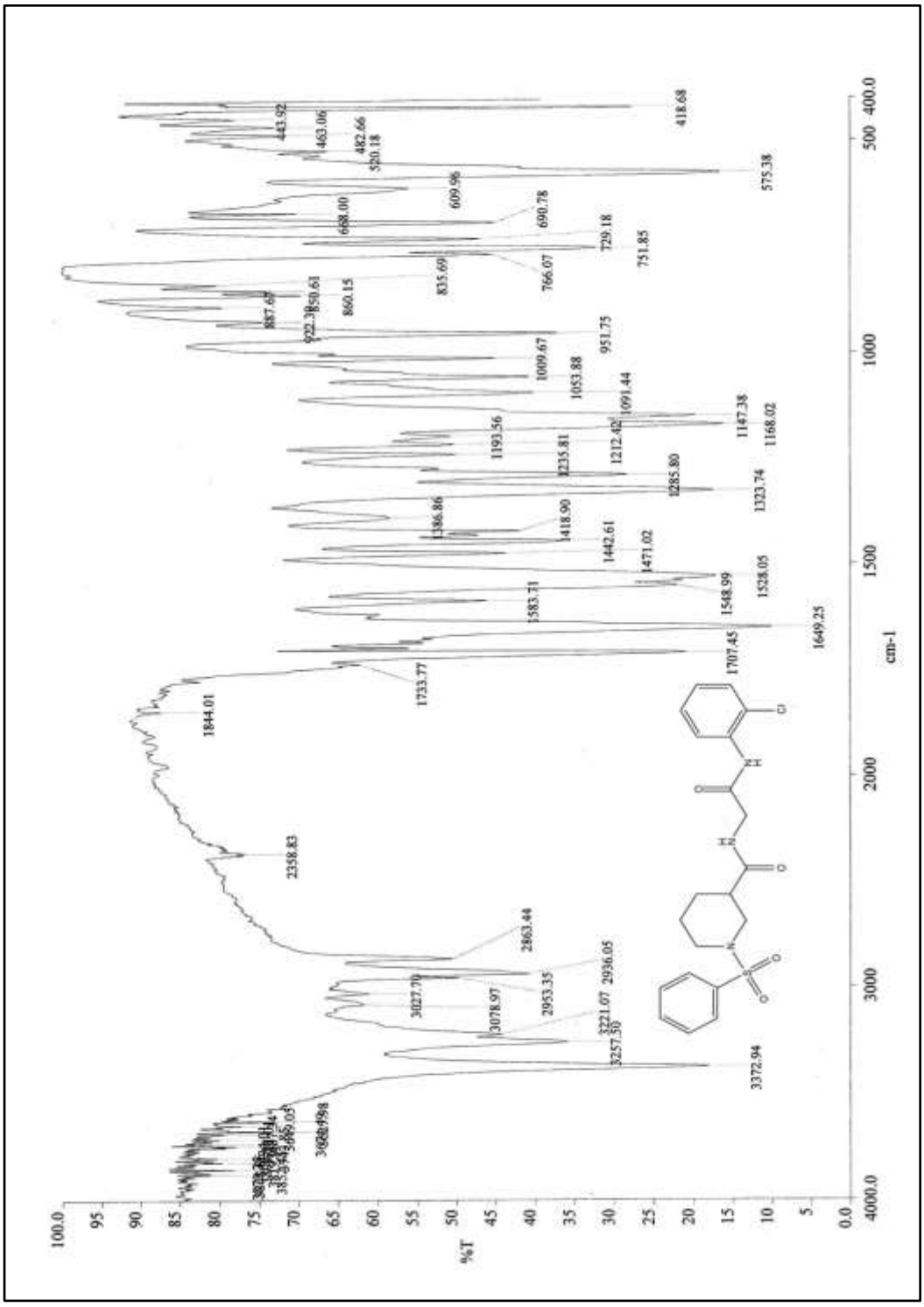

Figure 4.9.1: IR spectrum of N-(2-(2-chlorophenylamino)-2-oxoethyl)-1-(phenylsulfonyl)piperidine-3-carboxamide **6g**

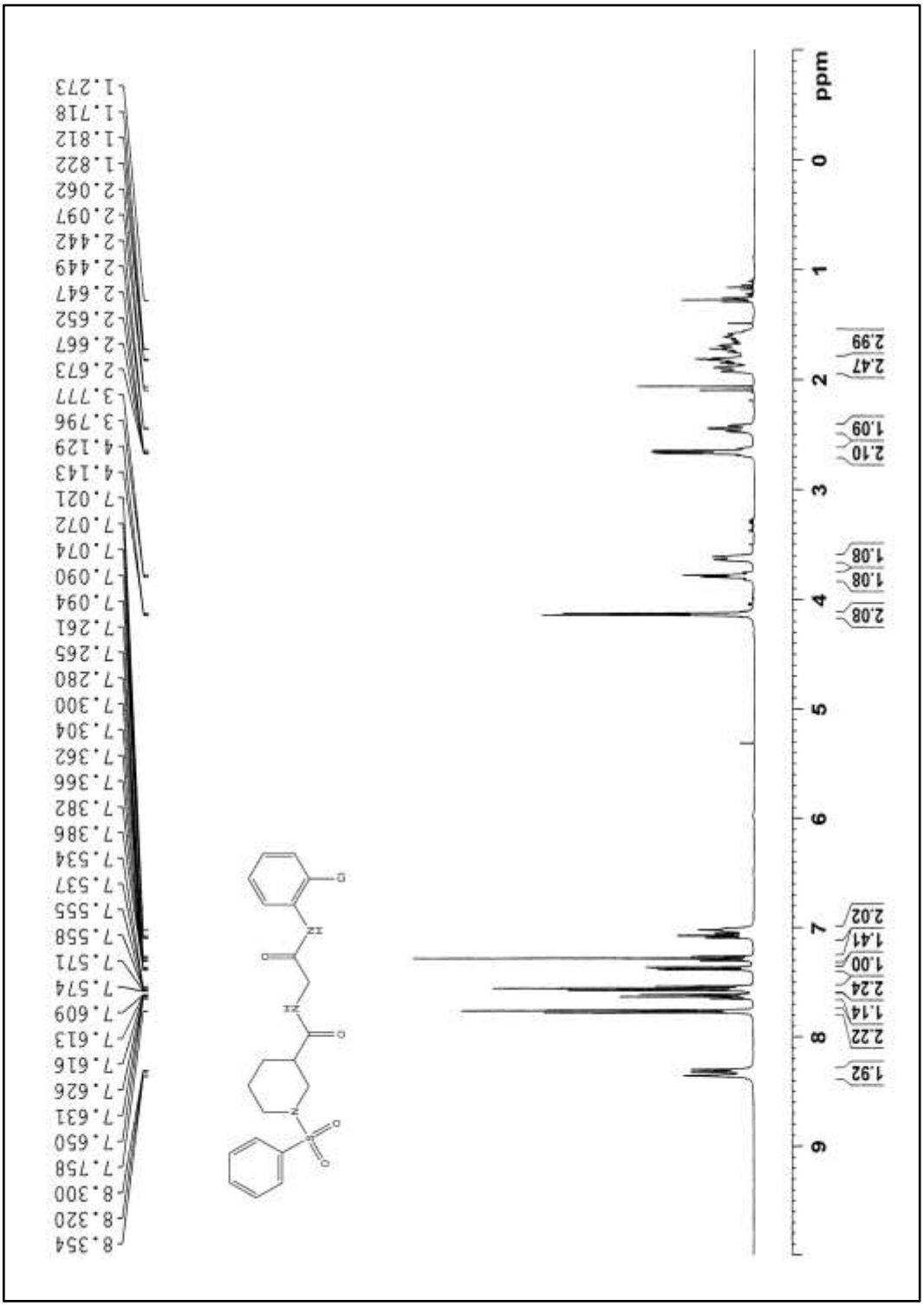

Figure 4.9.2: ^{1}H NMR spectrum of N-(2-(2-chlorophenylamino)-2-oxoethyl)-1-(phenylsulfonyl)piperidine-3-carboxamide **6g**

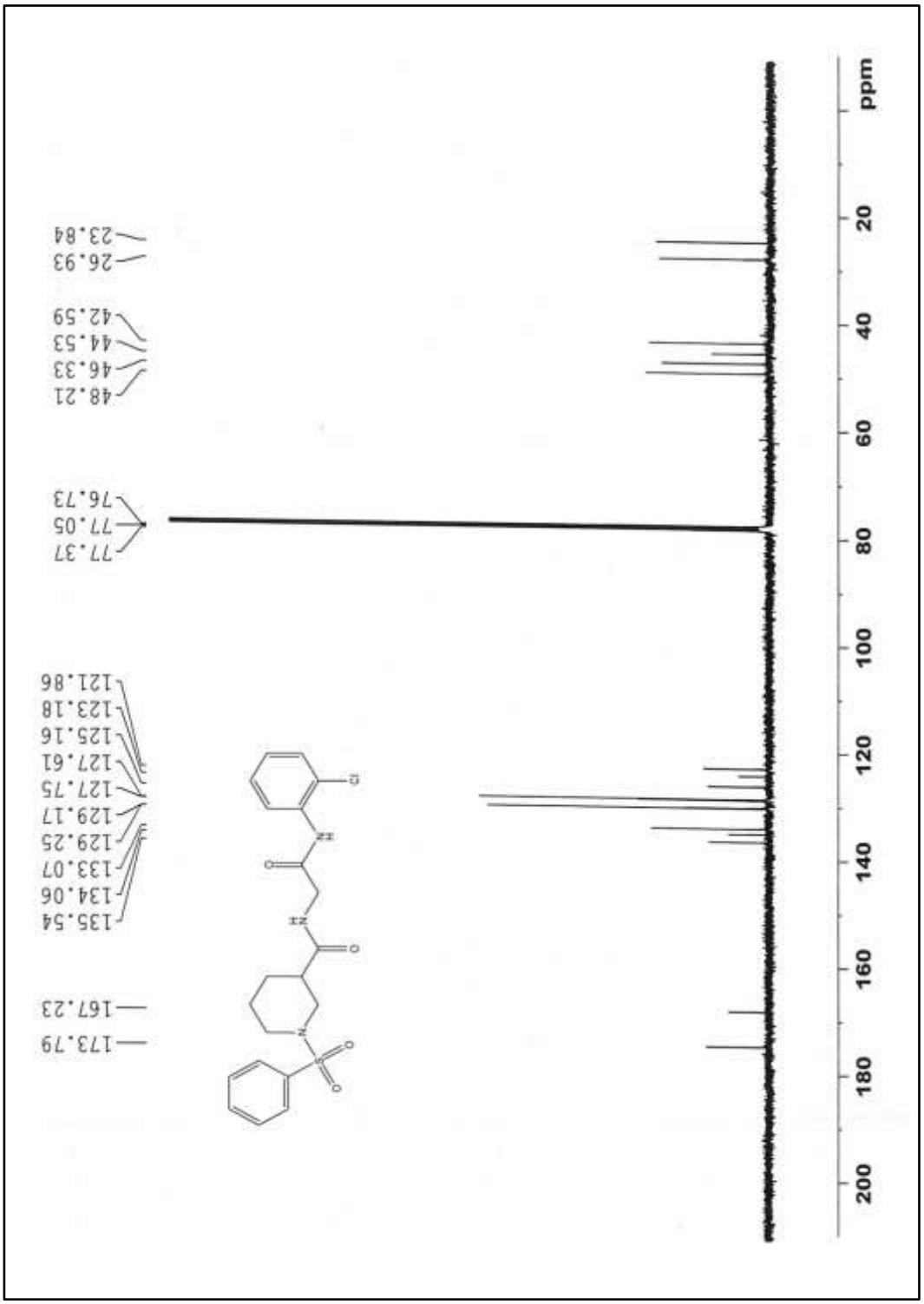

Figure 4.9.3: ^{13}C NMR spectrum of N-(2-(2-chlorophenylamino)-2-oxoethyl)-1-(phenylsulfonyl)piperidine-3-carboxamide **6g**

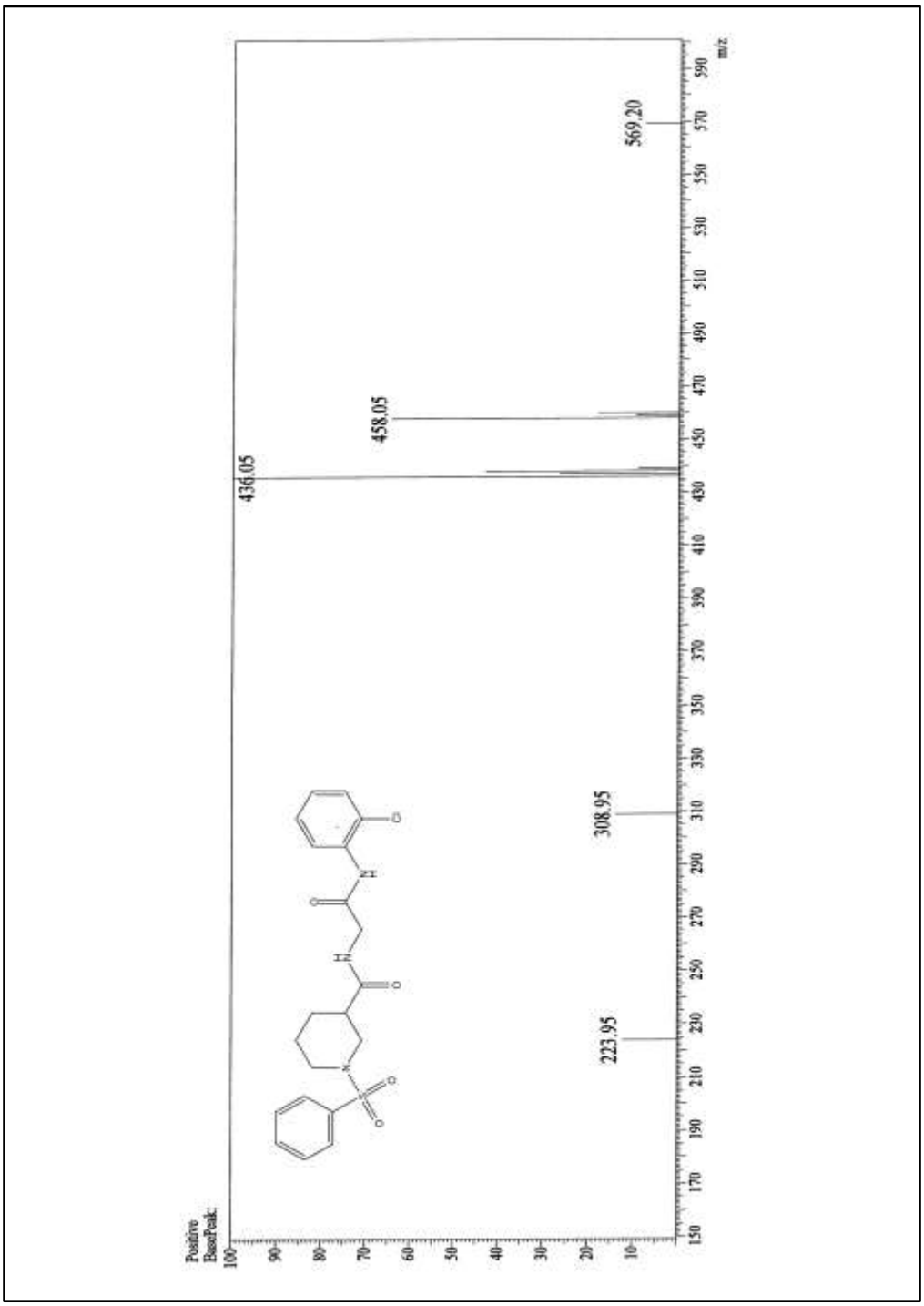

Figure 4.9.4: ESI-MS spectrum of N-(2-(2-chlorophenylamino)-2-oxoethyl)-1-(phenylsulfonyl)piperidine-3-carboxamide **6g**

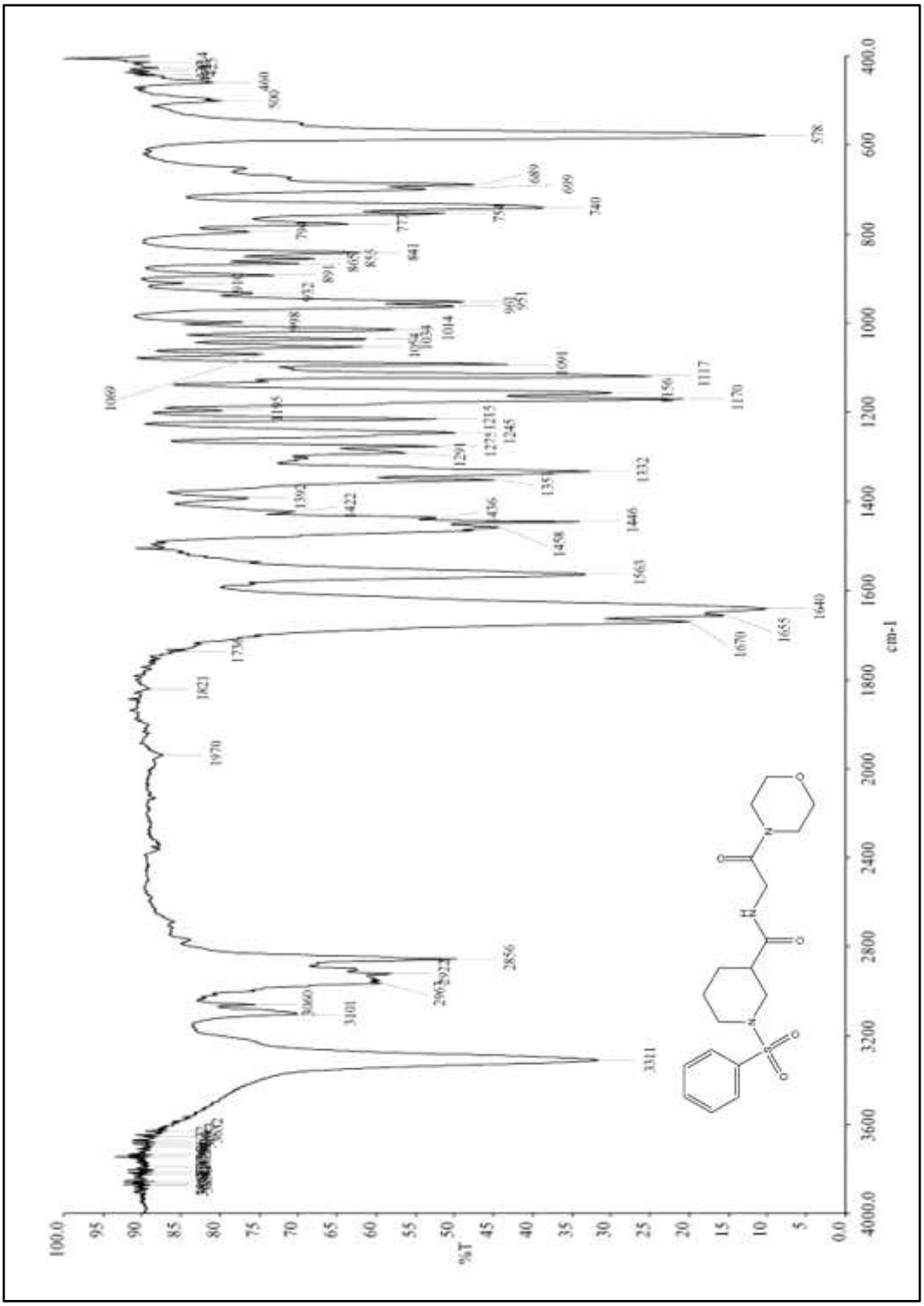

Figure 4.10.1: IR spectrum of N-(2-morpholino-2-oxoethyl)-1-(phenylsulfonyl)piperidine-3-carboxamide **6h**

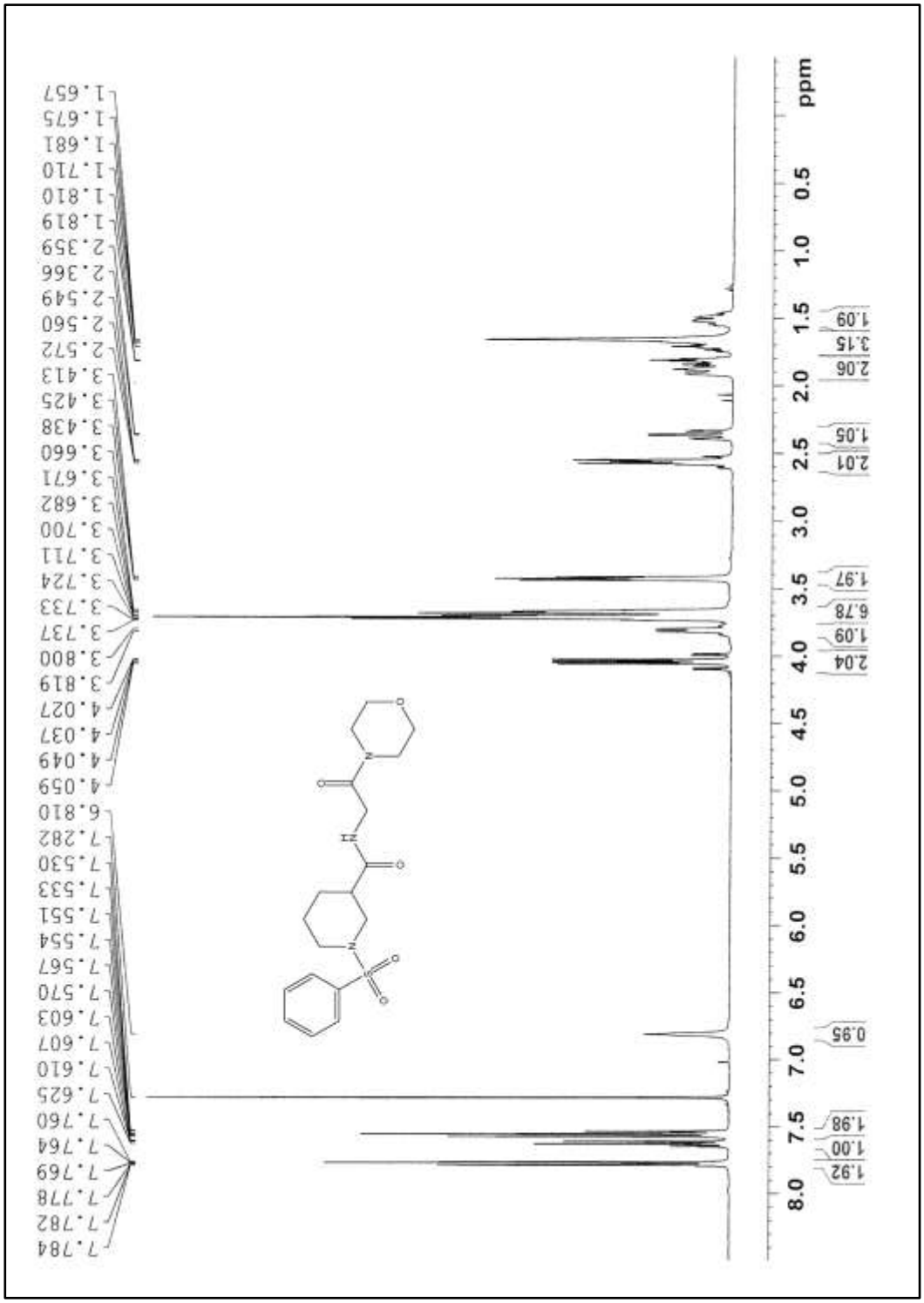

Figure 4.10.2: ^{1}H NMR spectrum of N-(2-morpholino-2-oxoethyl)-1-(phenylsulfonyl)piperidine-3-carboxamide **6h**

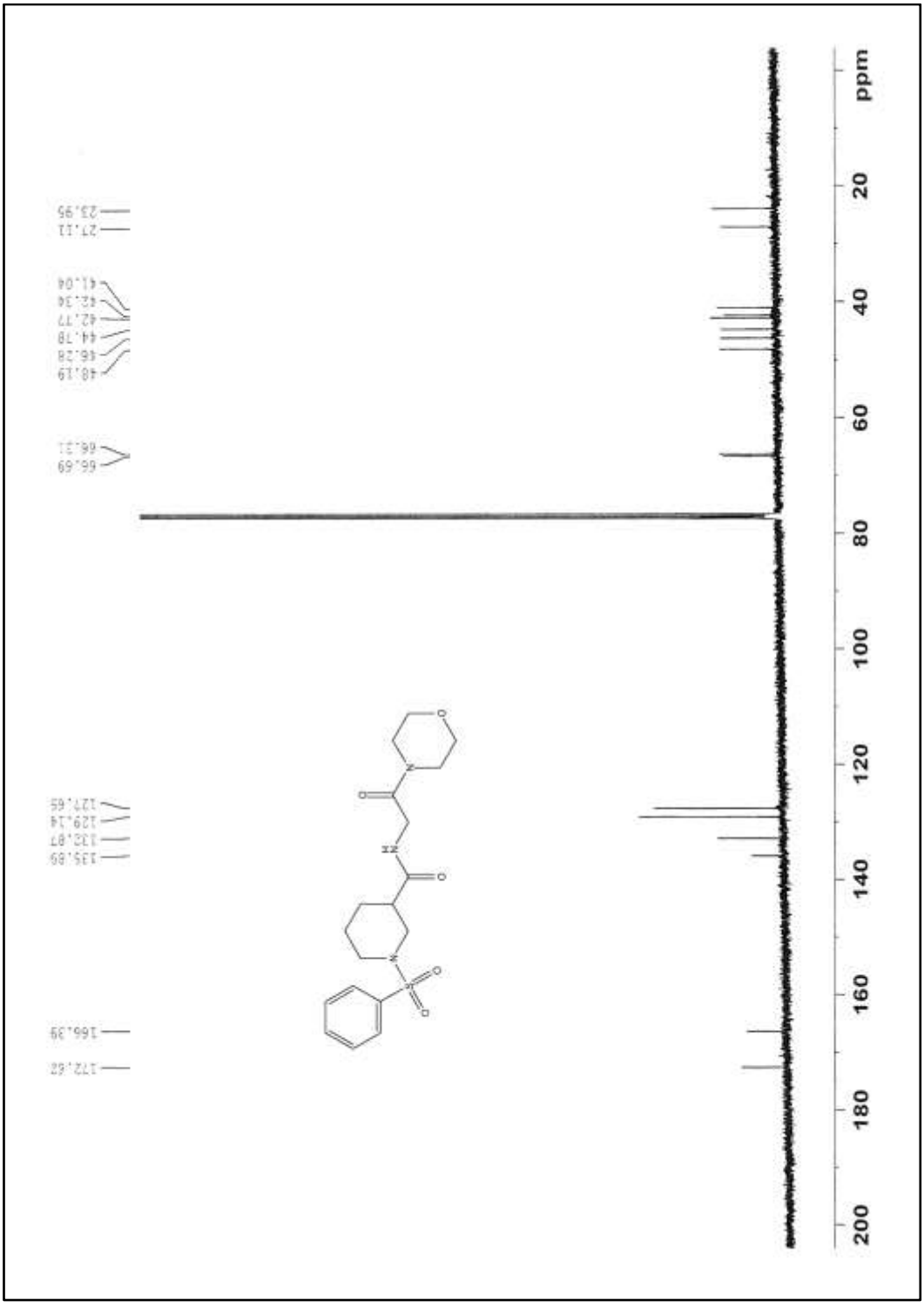

Figure 4.10.3: ^{13}C NMR spectrum of N-(2-morpholino-2-oxoethyl)-1-(phenylsulfonyl)piperidine-3-carboxamide **6h**

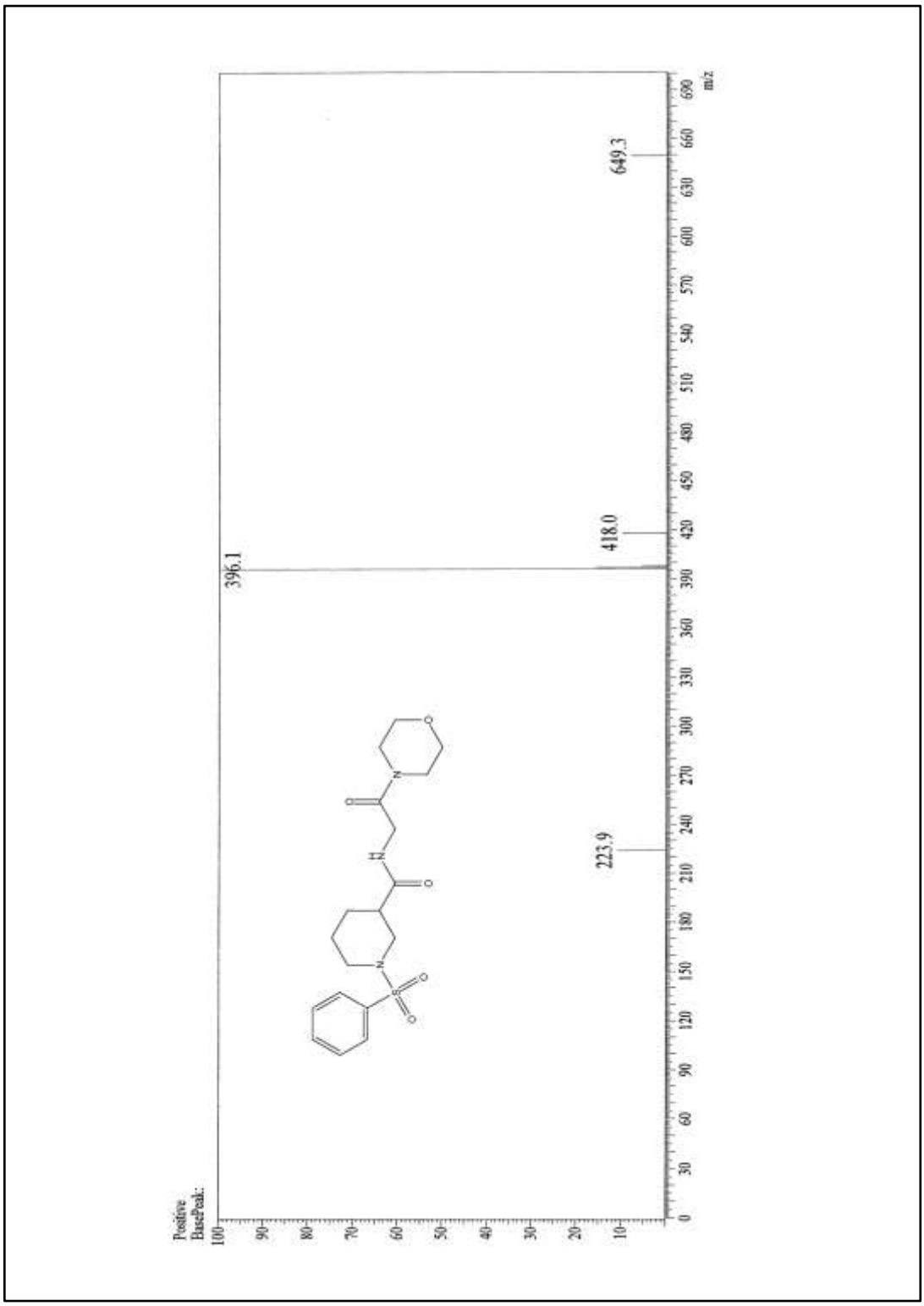

Figure 4.10.4: ESI-MS spectrum of N-(2-morpholino-2-oxoethyl)-1-(phenylsulfonyl)piperidine-3-carboxamide **6h**

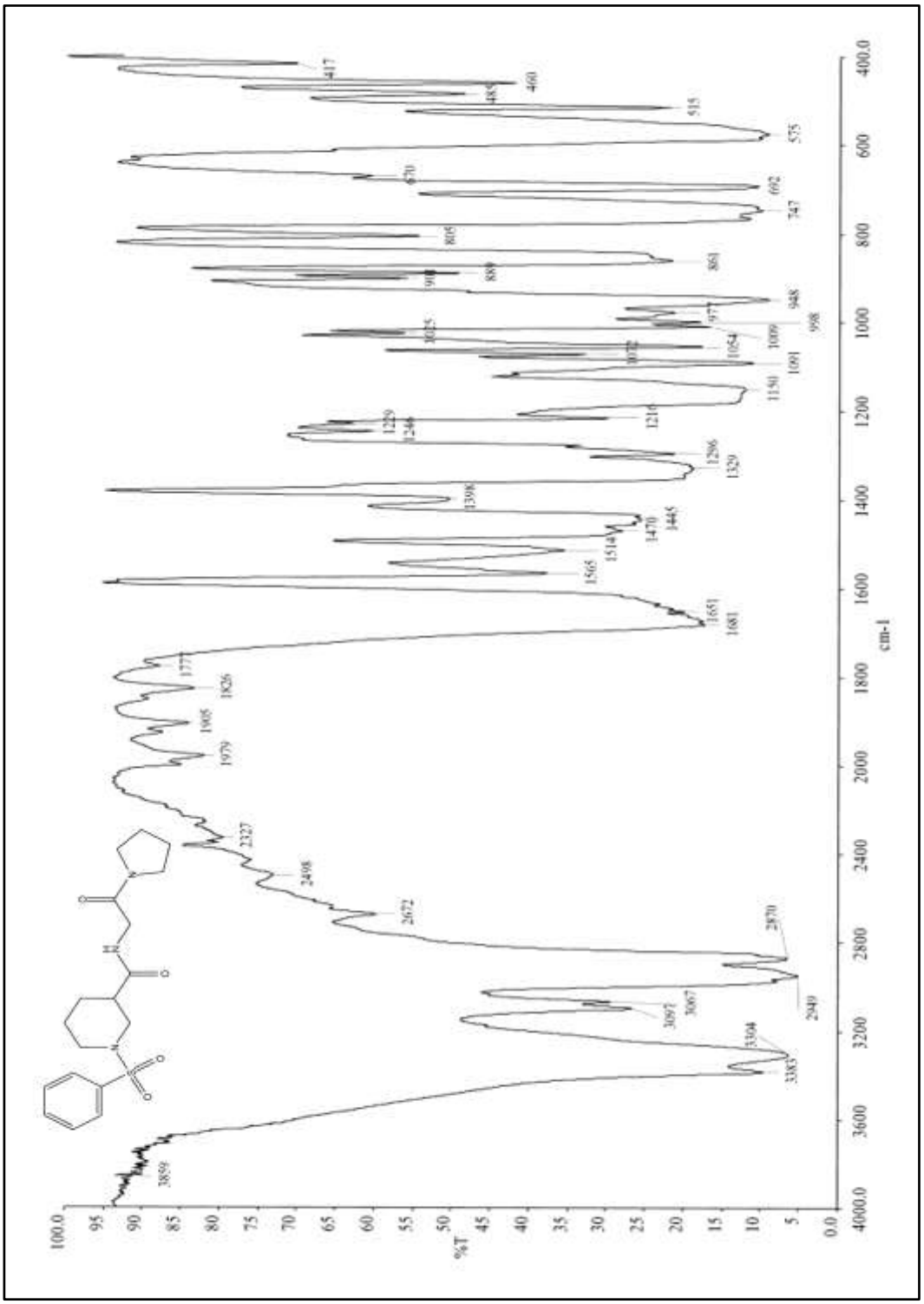

Figure 4.11.1: IR spectrum of N-(2-oxo-2-(pyrrolidin-1-yl)ethyl)-1-(phenylsulfonyl)piperidine-3-carboxamide **6i**

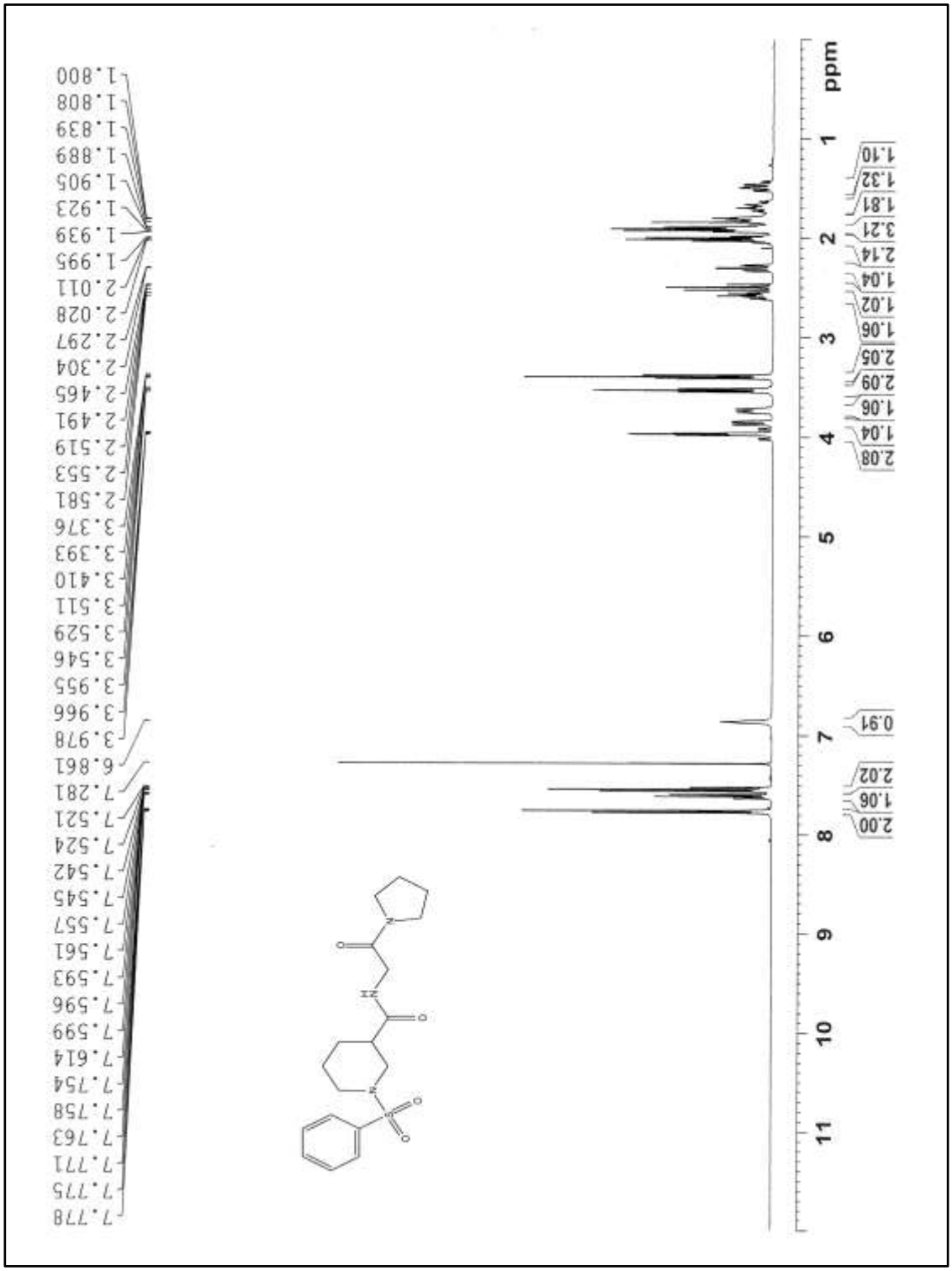

Figure 4.11.2: ^{1}H NMR spectrum of N-(2-oxo-2-(pyrrolidin-1-yl)ethyl)-1-(phenylsulfonyl)piperidine-3-carboxamide **6i**

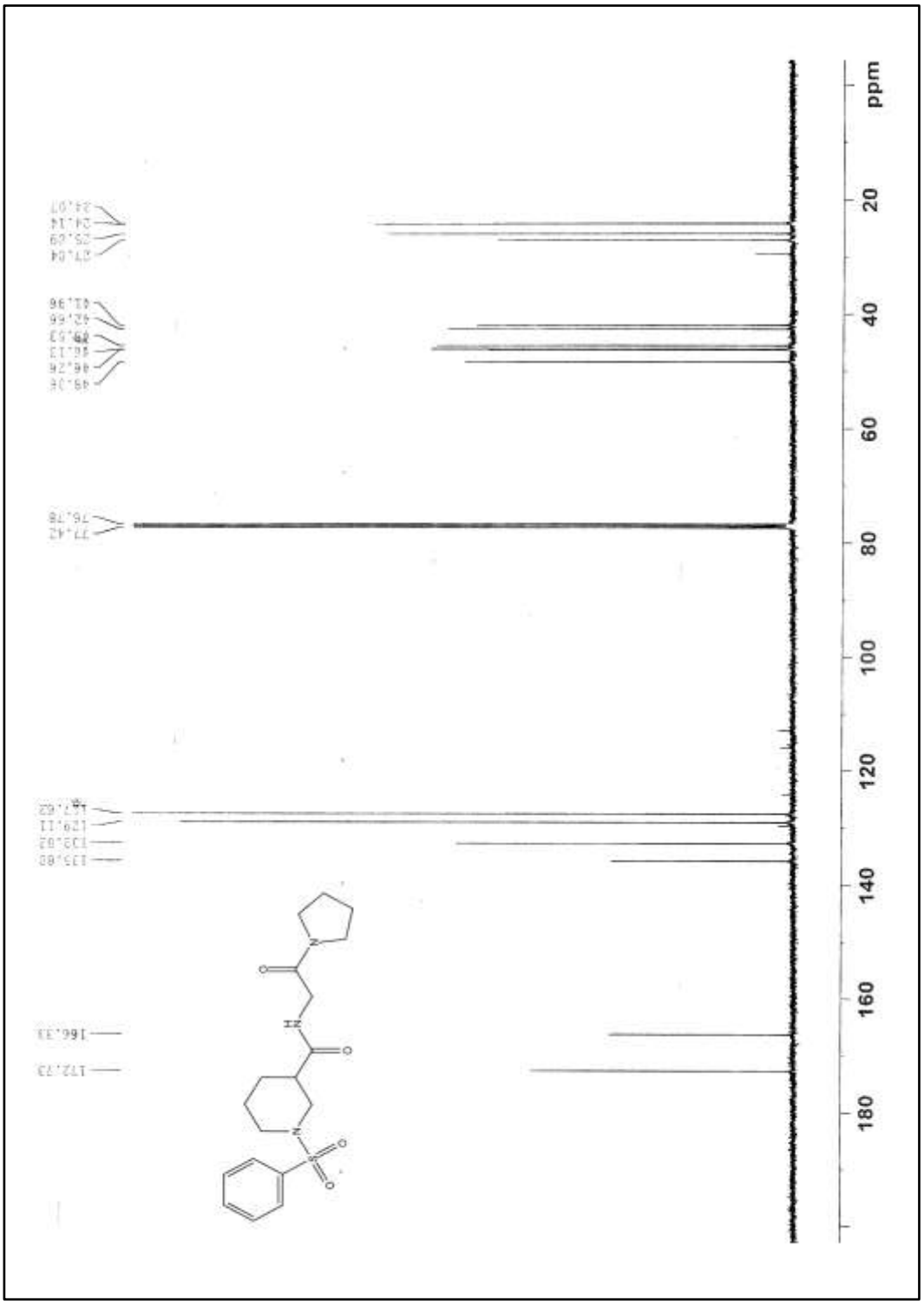

Figure 4.11.3: ^{13}C NMR spectrum of N-(2-oxo-2-(pyrrolidin-1-yl)ethyl)-1-(phenylsulfonyl)piperidine-3-carboxamide **6i**

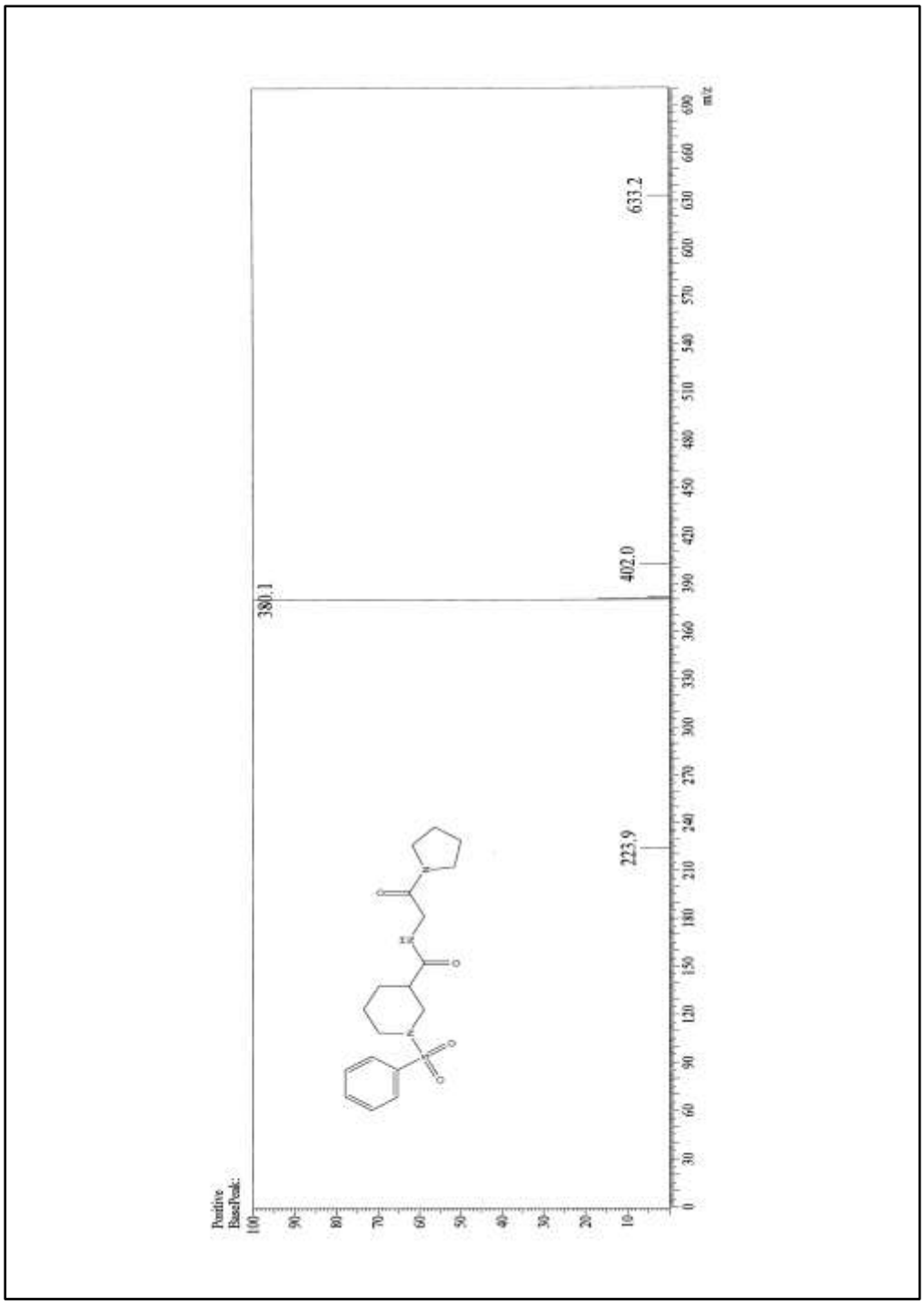

Figure 4.11.4: ESI-MS spectrum of N-(2-oxo-2-(pyrrolidin-1-yl)ethyl)-1-(phenylsulfonyl)piperidine-3-carboxamide **6i**

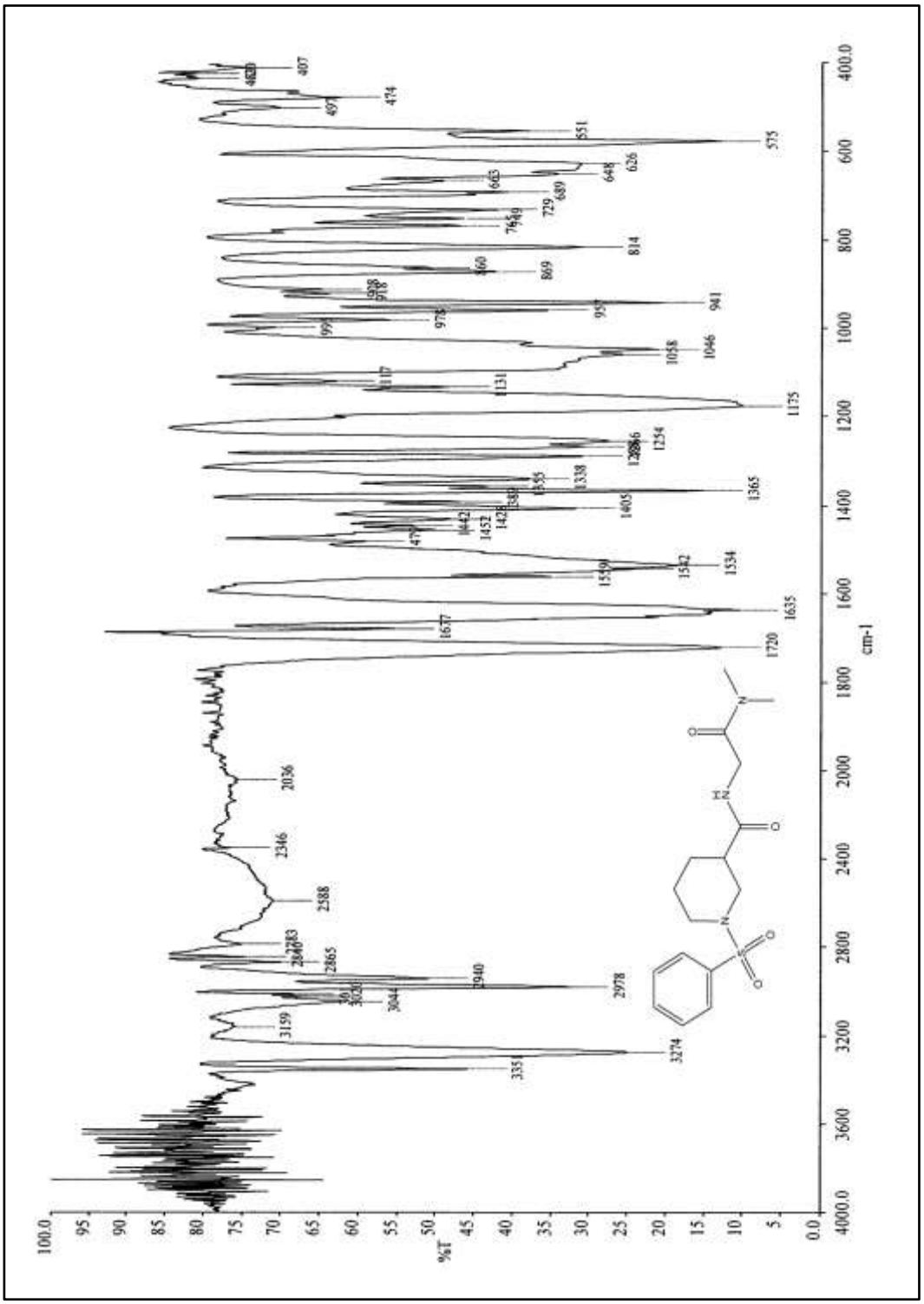

Figure 4.12.1: IR spectrum of N-(2-(dimethylamino)-2-oxoethyl)-1-(phenylsulfonyl)piperidine-3-carboxamide **6j**

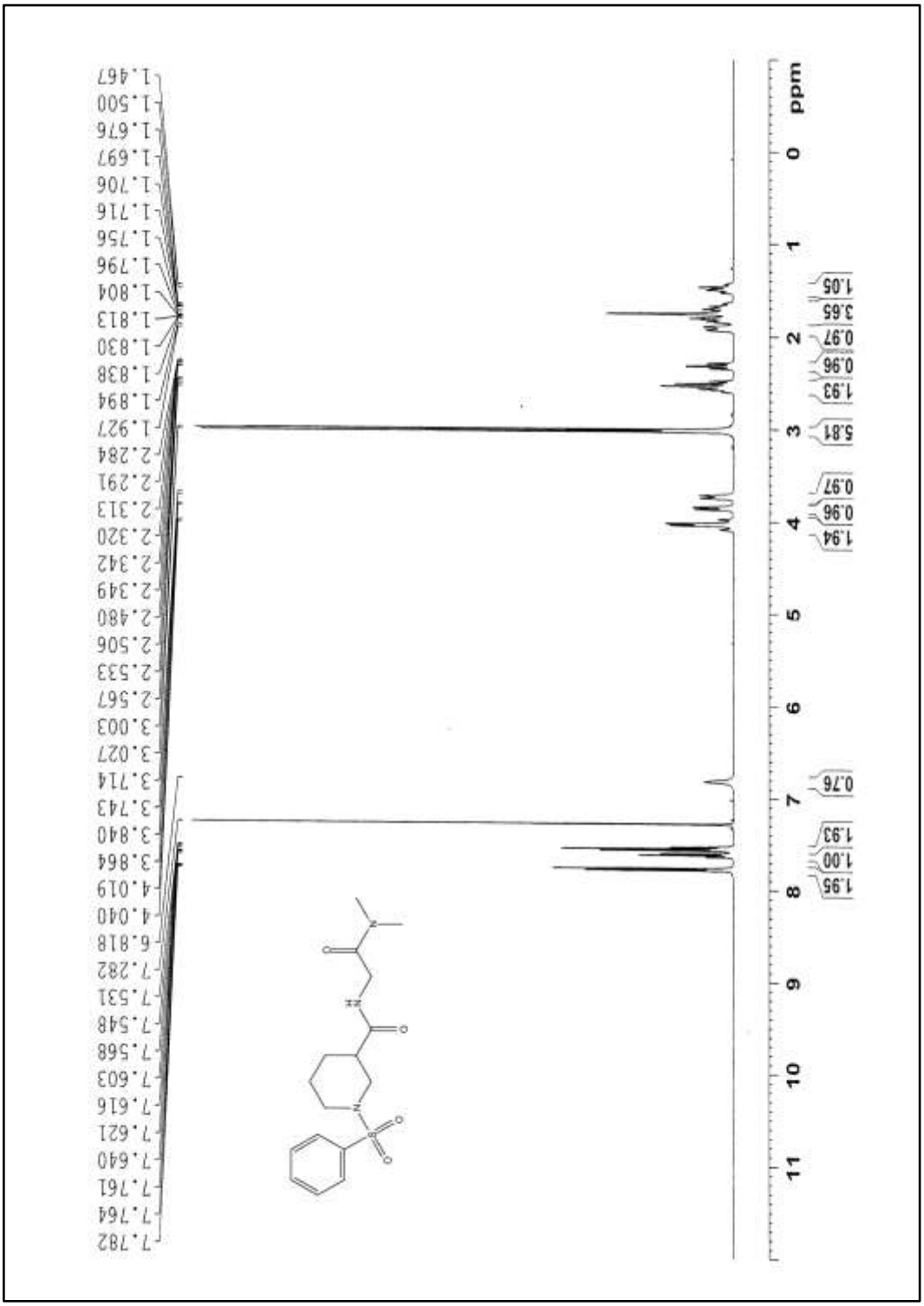

Figure 4.12.2: ^{1}H NMR spectrum of N-(2-(dimethylamino)-2-oxoethyl)-1-(phenylsulfonyl)piperidine-3-carboxamide **6j**

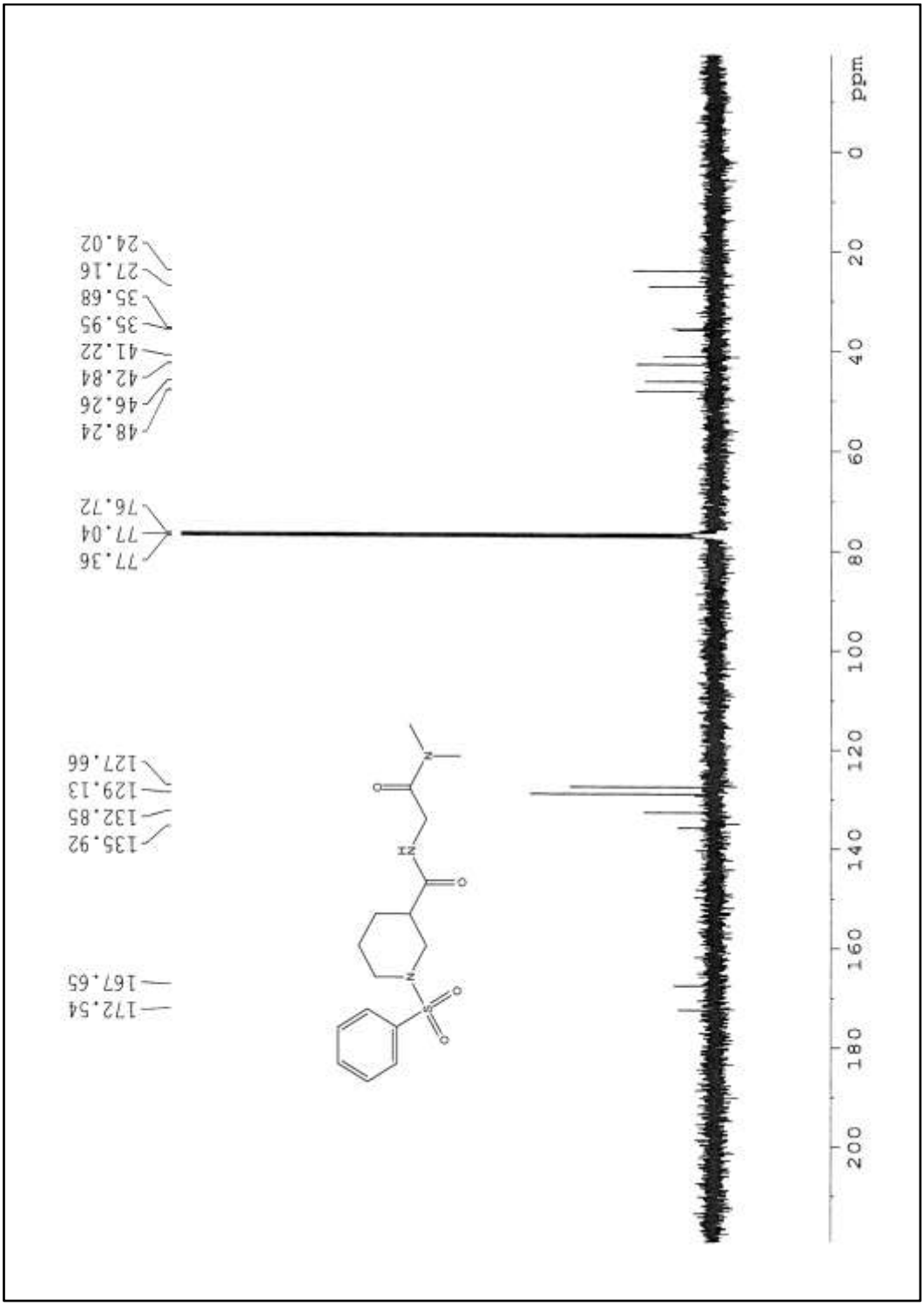

Figure 4.12.3: ^{13}C NMR spectrum of N-(2-(dimethylamino)-2-oxoethyl)-1-(phenylsulfonyl)piperidine-3-carboxamide **6j**

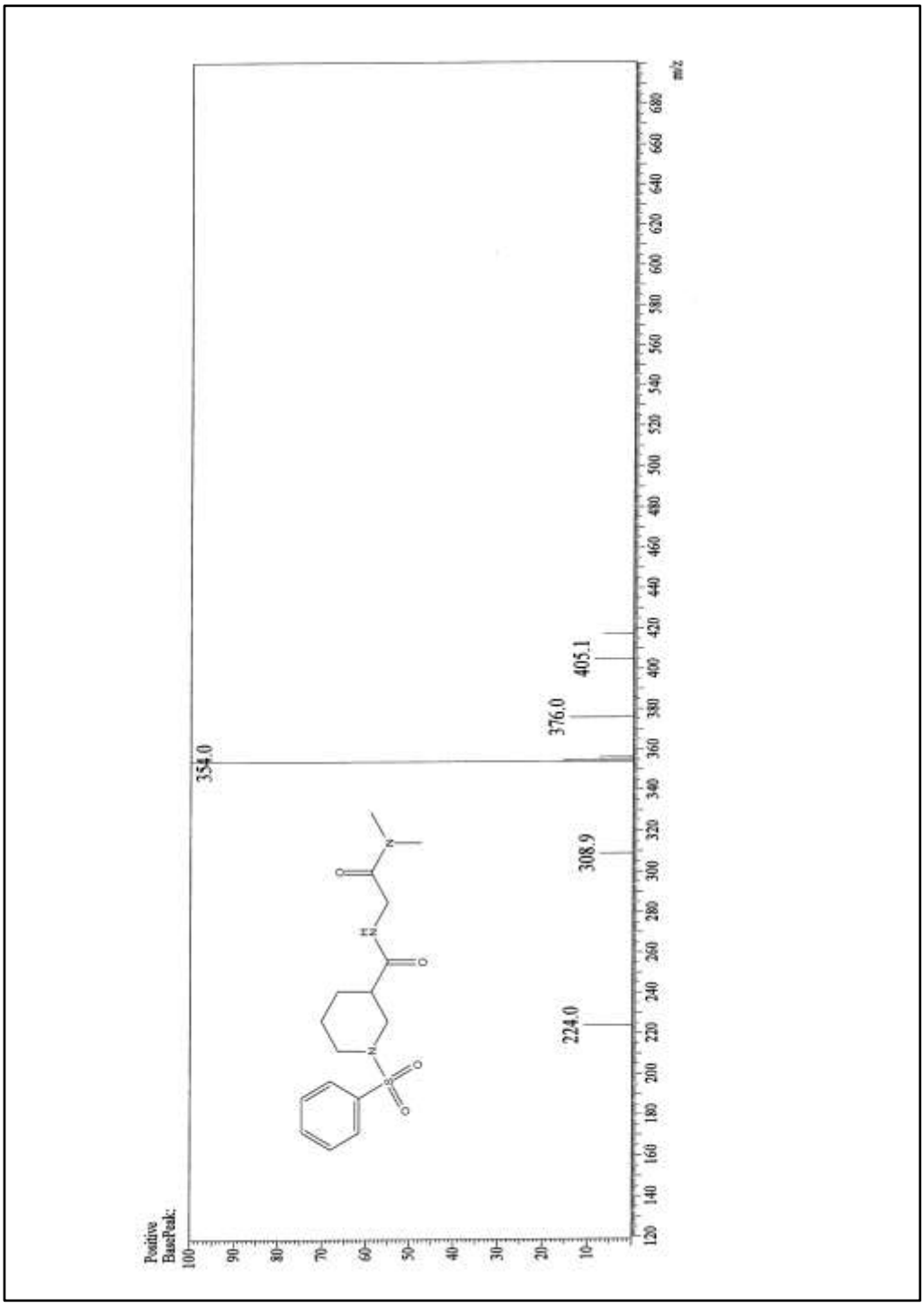

Figure 4.12.4: ESI-MS spectrum of N-(2-(dimethylamino)-2-oxoethyl)-1-(phenylsulfonyl)piperidine-3-carboxamide **6j**

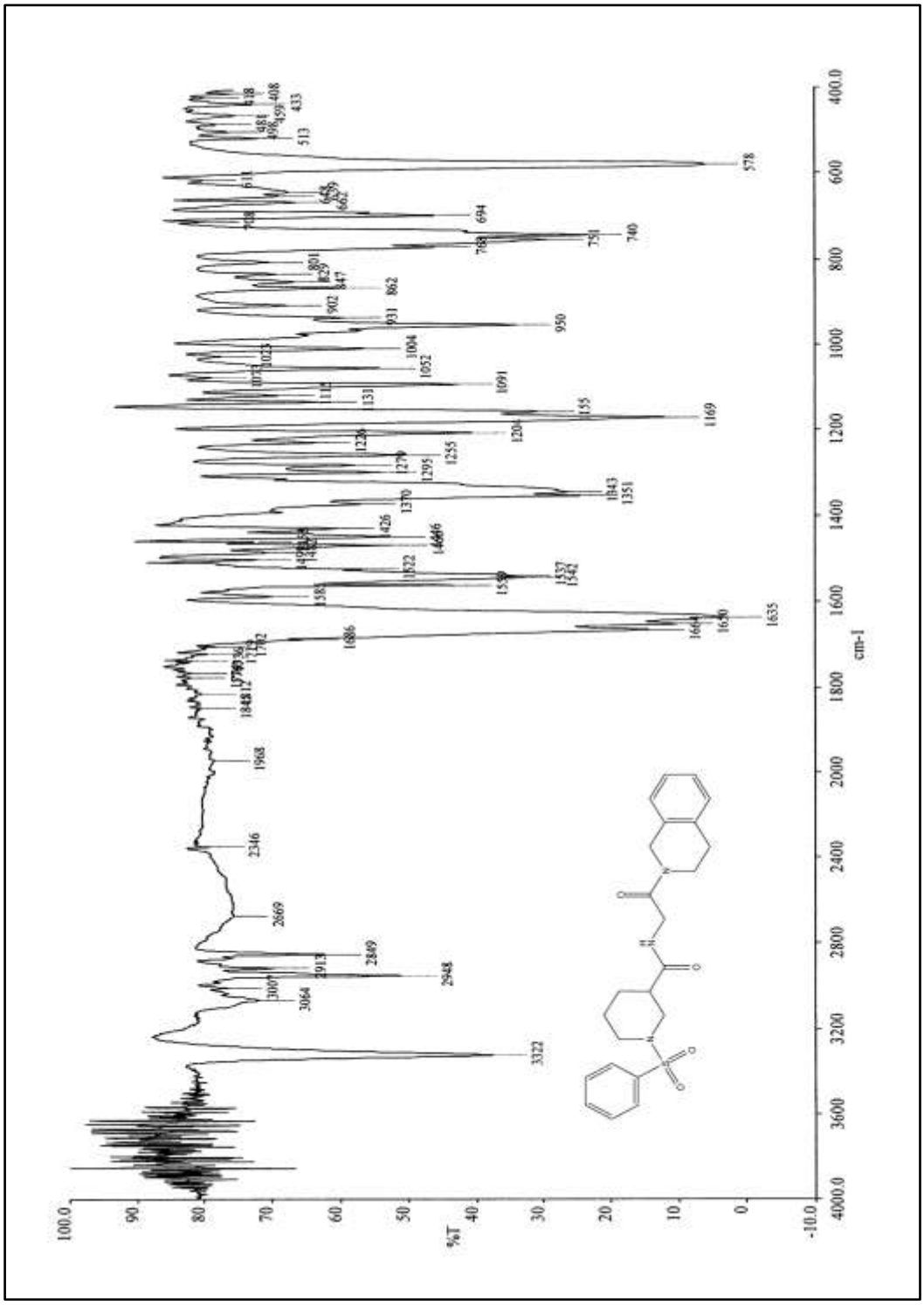

Figure 4.13.1: IR spectrum of N-(2-(3,4-dihydroisoquinolin-2(1H)-yl)-2-oxoethyl)-1-(phenylsulfonyl)piperidine-3-carboxamide **6k**

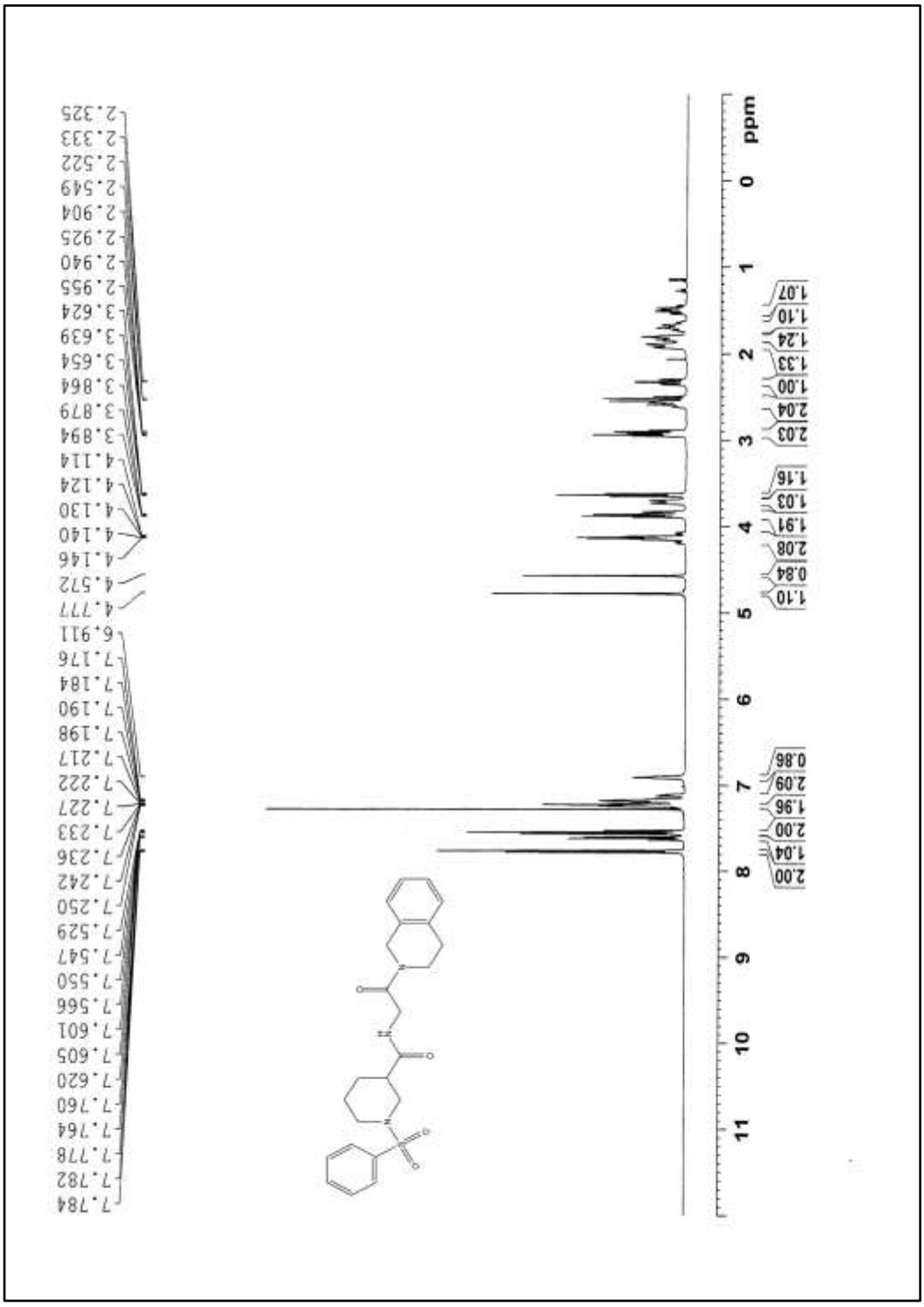

Figure 4.13.2: ^{1}H NMR spectrum of N-(2-(3,4-dihydroisoquinolin-2(1H)-yl)-2-oxoethyl)-1-(phenylsulfonyl)piperidine-3-carboxamide **6k**

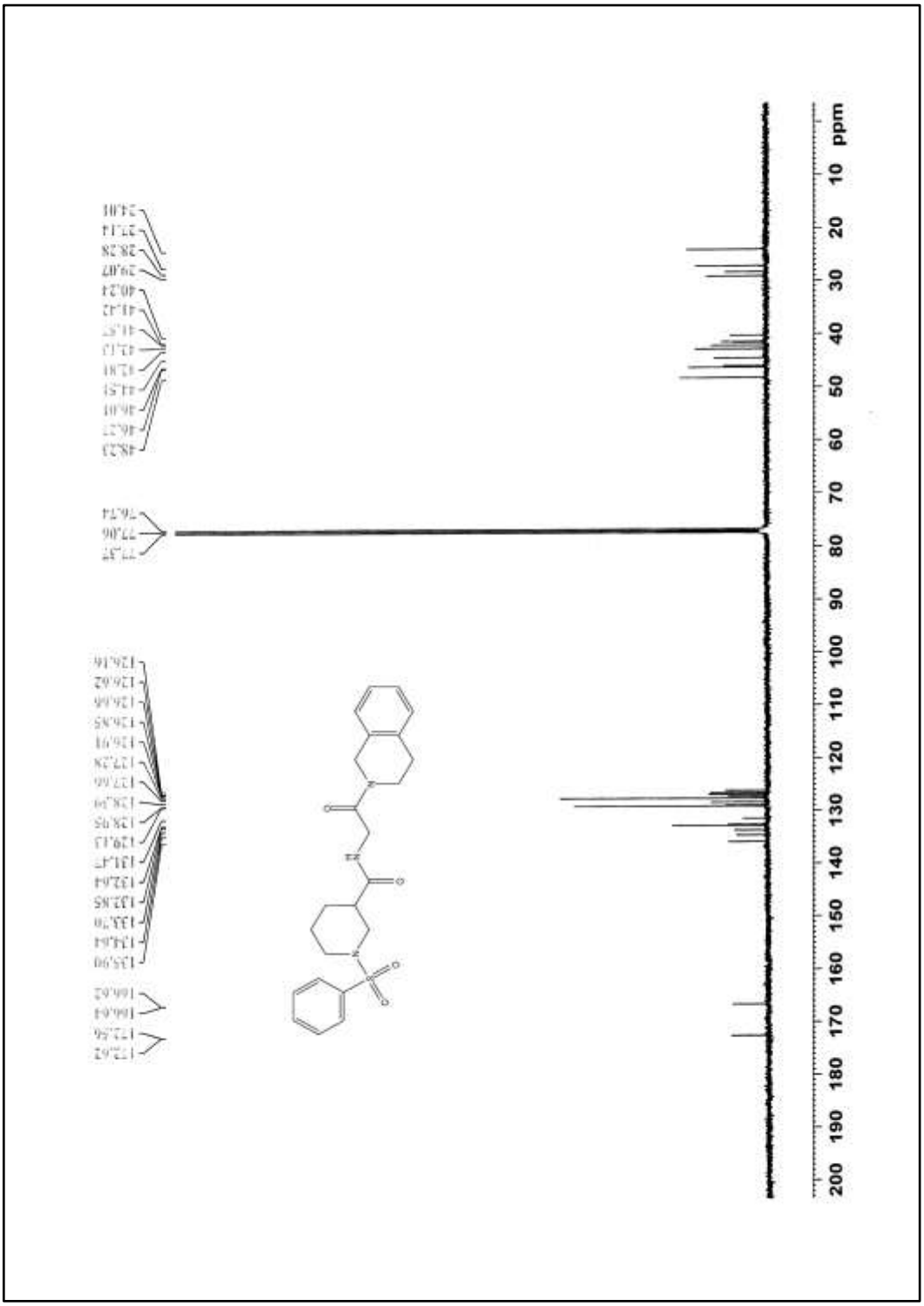

Figure 4.13.3: ^{13}C NMR spectrum of N-(2-(3,4-dihydroisoquinolin-2(1H)-yl)-2-oxoethyl)-1-(phenylsulfonyl)piperidine-3-carboxamide **6k**

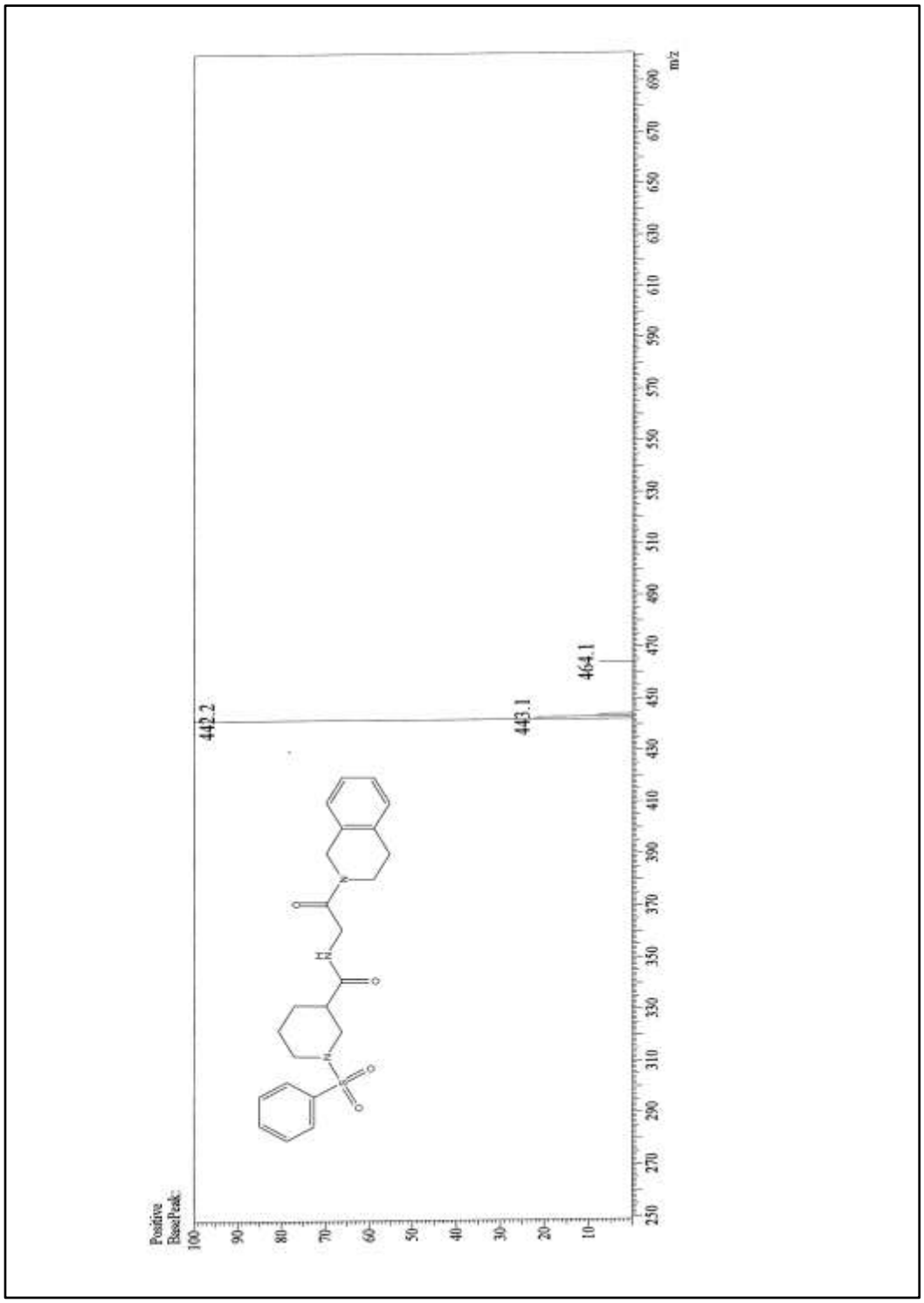

Figure 4.13.4: ESI-MS spectrum of N-(2-(3,4-dihydroisoquinolin-2(1H)-yl)-2-oxoethyl)-1-(phenylsulfonyl)piperidine-3-carboxamide **6k**

4.2.2 Biological evaluation

DPP-IV inhibition assay uses fluorogenic substrate, Gly-Pro-Aminomethylcoumarin (AMC), to measure DPP-IV activity. Cleavage of the peptide bond by DPP-IV releases the free AMC group, resulting in fluorescence that is analyzed using an excitation wavelength of 350-360 nm and emission wavelength of 450-465 nm. Human recombinant DPP-IV enzyme procured from Enzo life science (batch no BML-SE434-9091), substrate, H-Gly-Pro-AMC procured from Enzo life science (batch no BML-P189-9091) and assay buffer, prepared in-house containing HEPES (25 mM), NaCl(140 mM), $MgCl_2$ (80 mM) and BSA (1 % v/v) in deionized water having pH. 7.8 were used in the assay.

DPP-IV activity was measured by mixing reagents in 96-well plate (order of addition of reagents: assay buffer, enzyme, solvent/inhibitor and finally substrate). Both the enzyme and 96-well plate were incubated for 30 min and the resulting fluorescence was measured using Spectra Max fluorometer (Molecular Devices, Sunnyvale CA) by exciting at 360 nm and emission at 460 nm with the excitation filter at 360 nm and emission filter at 460 nm at sensitivity of 45.

The IC_{50} values were determined for test compounds using Graph Pad prism software.

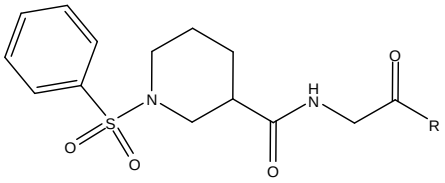

Compound	R	% Inhibition of DPP-IV at 3µM
6 a	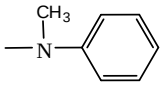	50.5
6 b	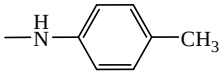	14.4
6 c	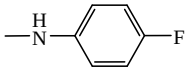	55.0
6 d	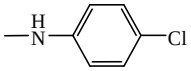	69.5
6 e	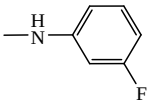	58.5
6 f	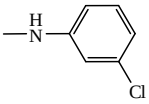	14.1
6 g	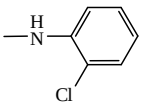	14.4
6 h	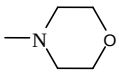	10.1
6 i	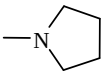	12.4
6 j	$-N(CH_3)_2$	51.3
6 k	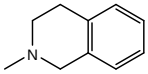	51.6

Table 4.1: *DPP-IV inhibition by compounds* ***6a-k*** *at 3µM concentrations.*

Preliminary DPP-IV inhibition assay was performed to test compounds **6a-k** for their inhibition potential at 3µM concentration and sitagliptin phosphate was used as a standard exhibiting 91.7% inhibition at the same concentration. Compounds showing greater than 50% inhibition at 3µM, qualified for IC_{50} determination.

Compound	**IC_{50} (nM)**
6 a	592.56
6 c	573.74
6 d	94.82
6 e	205.40
6 j	188.97
6 k	448.60

Table 4.2: *Inhibition of DPP-IV (IC_{50} nM) of selected compounds.*

4.2.3 Structure activity relationship

From the *in-vitro* assay it was observed that substitution of secondary amines at the C-terminus of glycine did not show good inhibition. Substitution of cyclic aliphatic secondary amines like morpholine **6h** and pyrrolidine **6i** did not show good inhibition while substitution of N-methyl aniline **6a** and cyclic aliphatic aromatic amine 1,2,3,4-tetrahydroisoquinoline **6k** and dimethyl amine **6j** showed better DPP-IV inhibition, latter exhibited the best enzyme inhibition with an IC_{50} of 188.97 nM. Further, effect of substitution of halogens and methyl on the aniline at the P1 site was studies and it was found that *para*- substituted aniline showed better inhibition than the *meta*- or

ortho-substituted anilines. As seen in table 4.2, it was observed that *m*-fluoro aniline **6e** is twice more potent than *p*-fluoro aniline derivative **6c** but similar trend was not observed on substitution of chlorine instead of fluorine. Compound **6d** with *p*-chloro aniline substituted at the C-terminus amide of glycine was found to be the most potent of all the compounds synthesized in the series with an IC_{50} of 94.82 nM.

4.2.4 Molecular Docking Study

For docking studies, binding site residues of the A chain of DPP-4 (PDB ID: 3W2T) [19] at a distance of 4.5 A from vildagliptin were selected. AutoDock Vina [20] was used for carrying out docking studies. Initial docking studies showed higher affinity of diamides as compared to the standard and so these molecules were synthesised. The affinity for the compound **6d** was -8.5 kcal/mol while that of NVP-LAF237 (vildagliptin) was shown to be -6.7 kcal/mol. LigPlot [21] was used to observe the interaction of the ligand with the binding site residues as seen in Figure 4.14. Pymol [22] was used to visualize the protein and the docked compound **6d** as seen in Figure 4.15.

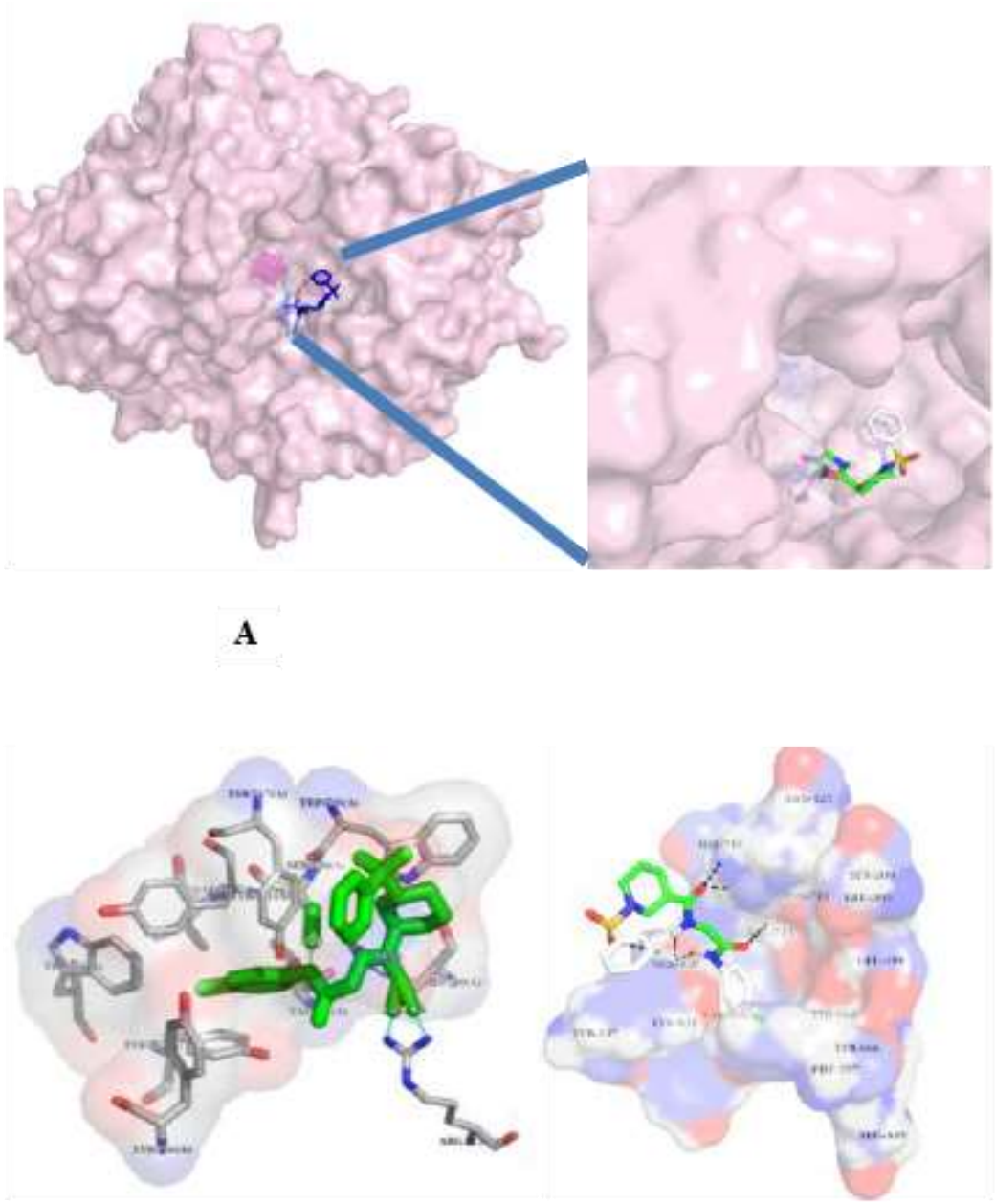

Figure 4.14: Binding of **6d** at the active site of DPP-IV

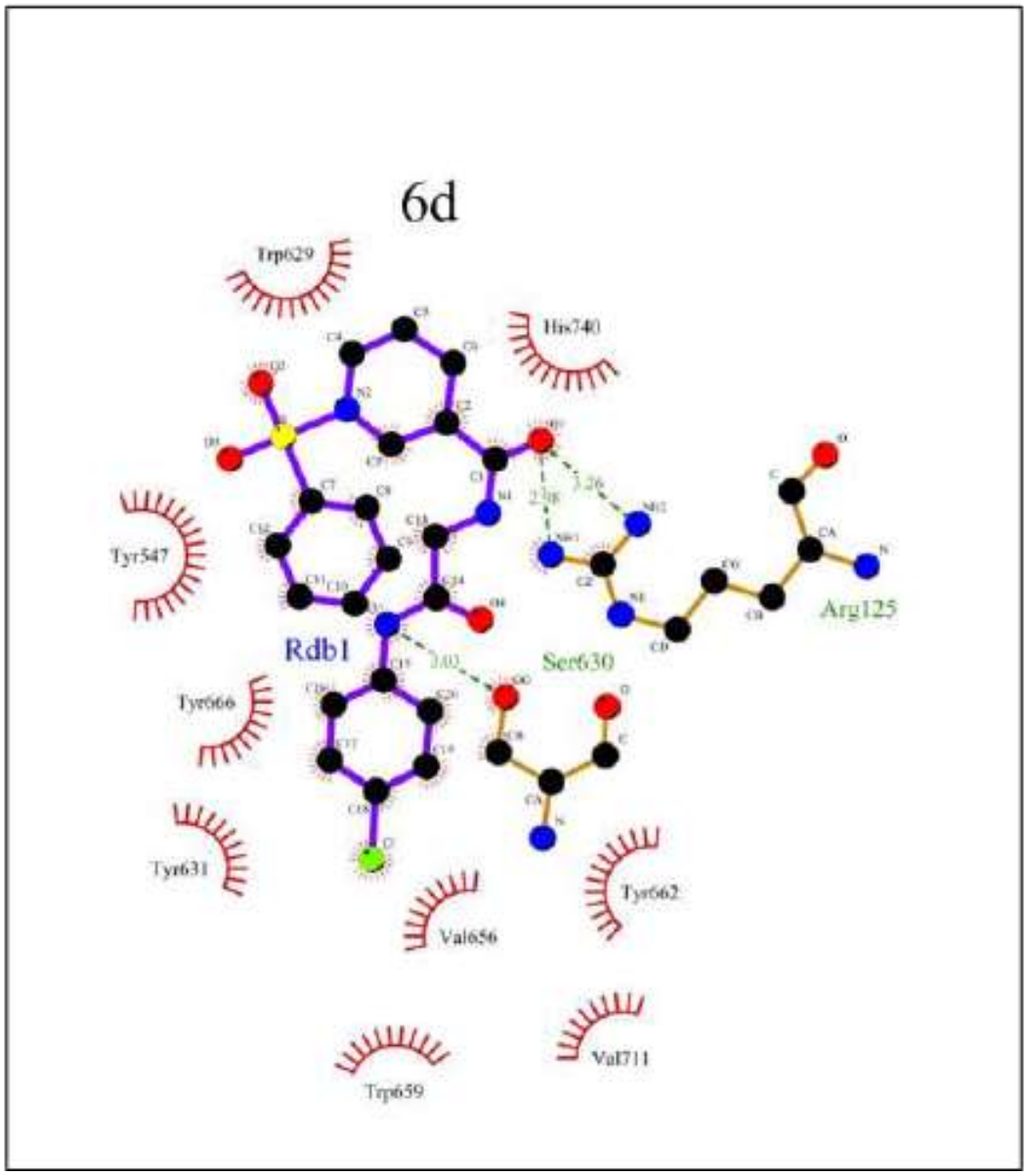

Figure 4.15: Interaction of **6d** with the binding site residues of DPP-IV

4.3 Conclusion

Thus it has been observed that cyclic secondary amines like pyrrolidine and morpholine are not good substituents for the DPP-IV inhibition. It was also observed that aliphatic amine, dimethyl amine, when substituted at the P1 site shows good enzyme inhibition. Substitution of chlorine at the *para* position of aniline, at the P1 site renders the compound more potent than any other substitution. This study was further supported by molecular modelling of **6d** at the active site of DPP-IV which suggested H-bonding interactions with SER630, ARG125 and TYR547 as seen in Figure 4.15.

4.4 Experimental

4.4.1 Chemistry

Reagent grade chemicals and solvents were purchased from commercial supplier and used after purification. TLC was performed on silica gel F254 plates (Merck). Acme's silica gel (60-120 mesh) was used for column chromatographic purification. All reactions were carried out in nitrogen atmosphere. Melting points are uncorrected and were measured in open capillary tubes, using a Rolex melting point apparatus. IR spectra were recorded as KBr pellets on Perkin Elmer RX 1 spectrometer. ^{1}H NMR and ^{13}C NMR spectral data were recorded on Advance Bruker 400 spectrometer (400 MHz) with $CDCl_3$ or DMSO-d_6 as solvent and TMS as internal standard. *J* values are in Hz. Mass spectra were determined by ESI-MS, using a Shimadzu LCMS 2020 apparatus. Elemental analyses were recorded on Thermosinnigan Flash 11-12 series EA. All the reactions were carried out under nitrogen atmosphere.

General procedure for the preparation of compounds 2a-k

A mixture of boc-glycine **1** (1.11 mmol), 1-ethyl-3-(3-dimethylaminopropyl)carbodiimide hydrochloride (1.67 mmol) (EDCI), 1-hydroxybenzotriazole (1.11 mmol) (HOBt), 4-dimethylaminopyridine (1.34mmol) (DMAP) and amine (1^0 and 2^0) (1.22 mmol) in dichloromethane (50 mL) (DCM) was stirred at room temperature for 16 hours. The reaction was monitored using TLC. On completion of the reaction, it was washed with water (2X20 mL), brine (1X10 mL), dried over anhydrous sodium sulphate and the solvent evaporated under reduced pressure to give the crude product which was then purified by column chromatography using silica

gel as stationary phase and methanol:dichloromethane (5:95) as eluent to yield desired N-boc glycine amide **3a-k**, as white solid.

1-(phenylsulfonyl)piperidine-3-carboxylic acid 5:

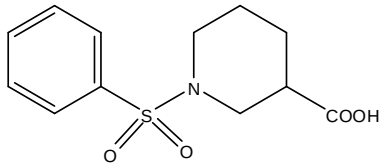

To a mixture piperidine-3-carboxylic acid **4** (1.0 mmol) and sodium carbonate (3.0 mmol) in 25 mL DCM:water (1:1) benzene sulphonyl chloride (1.1 mmol) was added and the reaction mixture stirred at room temperature for 16 hours or till the completion of reaction, as monitored by TLC. On completion of reaction, the reaction mixture was washed with petroleum ether (20 mL) and then acidified with conc. HCl, till pH 2. The white solid thus separated was filtered, washed with water several times and then dried to yield the desired product as white solid.

Yield : 91%; white solid; m.p. : 115-117 ^{o}C; IR (KBr) : 3100-2500 (b), 2940, 1812, 1693, 1352 cm^{-1}; ^{1}H NMR (400 MHz, $CDCl_3$) : δ 1.41-1.50 (m, 1H), 1.65-1.73 (m, 1H), 1.80-1.85 (m, 1H), 1.99-2.04 (m, 1H), 2.41 (dt, 1H, J_1 = 2.8 Hz, J_2 = 11.2 Hz), 2.57 (t, 1H, J = 10.8 Hz), 2.65-2.71 (m, 1H), 3.59 (br d, 1H, J = 11.6 Hz), 3.83 (dd, 1H, J_1 = 3.2 Hz, J_2 = 7.2 Hz), 7.54-7.58 (m, 2H), 7.61-7.63 (m, 1H), 7.77-7.79 (m, 2H), 8.98 (br s, 1H); ^{13}C NMR (400 MHz, $CDCl_3$) : δ 23.88, 26.21, 40.73, 46.26, 47.35, 127.62, 129.18, 132.94, 135.96, 178.63; $C_{12}H_{15}NO_4S$; ESI-MS**:** *m/z* 292.0 $[M+Na]^+$

General procedure for the preparation of compounds 6a-k

Compounds **3a-k** were de-protected by stirring it in 10% trifluoroacetic acid (TFA) in DCM. On completion of the reaction after an hour or as monitored by TLC, the solvent was evaporated under reduced pressure and once again the product was dissolved in DCM to give solution of compounds **3a-k**. To a solution of compound **5** (1.0 mmol), in DCM (20 mL), EDCI (1.5 mmol), HOBt (1.0 mmol) and DMAP (1.0 mmol) were added at 0-5 ^{o}C, followed by the solution of compound **3a-k** (1.1 mmol) in DCM (5 mL) and the reaction mixture was then stirred at room temperature for 10 hours or till the completion of the reaction as detected by TLC. After completion of the reaction, it was washed with water (2X20 mL), brine (1X10 mL), dried over anhydrous sodium sulphate and the solvent evaporated under reduced pressure to give the crude product which was then purified by column chromatography using silica gel, employing ethylacetate : petroleum ether (70:30) as eluent to give pure product **6a-k** as white solid.

N-(2-(methyl(phenyl)amino)-2-oxoethyl)-1-(phenylsulfonyl)piperidine-3-carboxamide 6a:

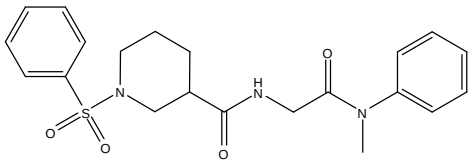

Yield: 65%; white solid; m.p.: 156-158 ^{o}C; IR (KBr): 3322, 2944, 1673, 1635, 1347, 1333cm^{-1}; ^{1}H NMR (400 MHz, $CDCl_3$): δ 1.44-1.50 (m, 1H), 1.66-1.89 (m, 3H), 2.29-2.35 (m, 1H), 2.44-2.56 (m, 2H), 3.31 (s, 3H), 3.66-3.78 (m, 4H), 6.69 (br s, 1H), 7.21-7.23 (m, 2H), 7.38-7.48 (m, 3H), 7.51-7.55 (m, 2H), 7.59-7.63 (m, 1H), 7.73-7.76 (m, 2H); ^{13}C NMR (400 MHz, $CDCl_3$): δ 23.94, 27.00, 37.60, 42.04, 42.72, 46.26, 48.26,

127.18, 127.64, 128.77, 129.12, 130.27, 132.86, 135.78, 141.68, 168.06, 172.47; Anal. Calc. for $C_{21}H_{25}N_3O_4S$: C, 60.70; H, 6.06; N, 10.11; found: C, 60.71; H, 5.85; N, 10.12%; ESI-MS: *m/z* 416.1 $[M+H]^+$.

N-(2-oxo-2-(p-tolylamino)ethyl)-1-(phenylsulfonyl)piperidine-3-carboxamide 6b:

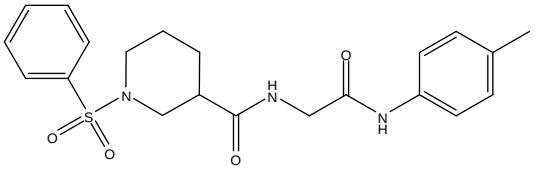

Yield: 85%; white solid; m.p.: 194-196 ^oC; IR (KBr): 3331, 3327, 2956, 2929, 2846, 1678, 1657, 1644, 1358, 1332 cm^{-1}; ^1H NMR (400 MHz, DMSO-d_6): δ 1.23-1.27 (m, 1H), 1.46-1.49 (m, 1H), 1.72-1.79 (m, 2H), 2.10-2.20 (m, 2H), 2.24 (s, 3H), 2.50-2.56 (m, 1H), 3.66-3.69 (m, 2H), 3.77-3.85 (m, 2H), 7.10 (d, 2H, *J* = 8.0 Hz), 7.45 (d, 2H, *J* = 8.0 Hz), 7.64-7.68 (m, 2H), 7.72-7.75 (m, 3H), 8.36 (m, 1H,), 9.90 (s, 1H); ^{13}C NMR (400 MHz, DMSO-d_6) : δ 20.89, 24.15, 27.01, 41.94, 42.87, 46.53, 48.64, 119.58, 127.86, 129.59, 129.94, 132.64, 133.69, 135.60, 136.76, 167.80, 173.10; Anal. Calc. for $C_{21}H_{25}N_3O_4S$: C, 60.70; H, 6.06; N, 10.11; found: C, 60.78; H, 6.18; N, 9.90%; ESI-MS: *m/z* 416.1 $[M+H]^+$.

N-(2-(4-fluorophenylamino)-2-oxoethyl)-1-(phenylsulfonyl)piperidine-3-carboxamide 6c:

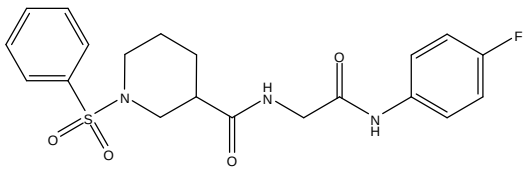

Yield: 70%; white solid; m.p.: 196-198 ^oC; IR (KBr): 3324, 3298, 2967, 2934, 2843, 2865, 1677, 1654, 1643, 1355 cm^{-1}; ^1H NMR (400 MHz, DMSO-d_6): δ 1.23-1.27

(m, 1H), 1.46-1.49 (m, 1H), 1.72-1.79 (m, 2H), 2.10-2.20 (m, 2H), 2.50-2.51 (m, 1H), 3.58-3.63 (m, 1H), 3.66-3.72 (m, 1H), 3.82-3.85 (m, 2H), 7.15 (t, 2H, *J* = 8.8 Hz), 7.56-7.60 (m, 2H), 7.66 (t, 2H, *J* = 8.4 Hz), 7.72-7.74 (m, 3H), 8.39 (br s, 1H), 10.05 (s, 1H); ^{13}C NMR (400 MHz, DMSO-d_6): δ 24.14, 27.00, 41.93, 42.85, 46.52, 48.62, 115.68, 115.90, 121.31, 121.39, 127.85, 129.94, 133.70, 135.59, 135.67, 157.23, 159.61, 168.00, 173.16; Anal. Calc. for $C_{20}H_{22}FN_3O_4S$: C, 57.27; H, 5.29; N, 10.02; found: C, 57.42; H, 4.90; N, 9.97%; ESI-MS: *m/z* 420.0 $[M+H]^+$.

N-(2-(4-chlorophenylamino)-2-oxoethyl)-1-(phenylsulfonyl)piperidine-3-carboxamide 6d:

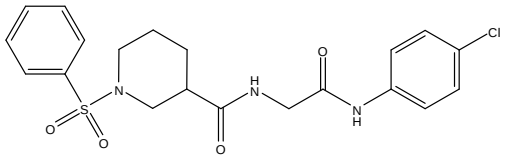

Yield: 55%; white solid; m.p.: 178-180 ^{o}C; IR (KBr): 3329, 3303, 2931, 2863, 2843, 1679, 1644, 1614, 1355, 1334 cm^{-1}; ^{1}H NMR (400 MHz, DMSO-d_6): δ 1.22-1.27 (m, 1H), 1.46-1.49 (m, 1H), 1.75 (t, 2H, *J* = 15 Hz), 2.10-2.20 (m, 2H), 2.50-2.54 (m, 1H), 3.60-3.69 (m, 2H), 3.84-3.86 (m, 2H), 7.36 (d, 2H, *J* = 8.8 Hz), 7.59-7.67 (m, 4H), 7.72-7.74 (m, 3H), 8.41 (t, 1H, *J* = 8.0 Hz), 10.14 (s, 1H); ^{13}C NMR (400 MHz, DMSO-d_6): δ 24.14, 27.01, 41.93, 42.95, 46.52, 48.63, 121.10, 127.25, 127.85, 129.13, 129.93, 133.68, 135.62, 138.25, 168.26, 173.16; $C_{20}H_{22}ClN_3O_4S$ ESI-MS: *m/z* 435.9 $[M+H]^+$.

N-(2-(3-fluorophenylamino)-2-oxoethyl)-1-(phenylsulfonyl)piperidine-3-carboxamide 6e:

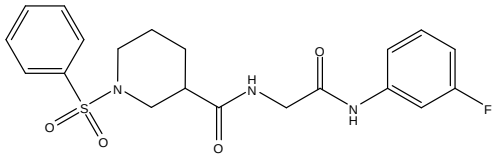

Yield: 62%; white solid; m.p.: 186-188 ^{o}C; IR (KBr) : 3308, 3104, 2930, 2851, 1709, 1670, 1616, 1351, 1317 cm^{-1}; ^{1}H NMR (400 MHz, DMSO-d$_6$): δ 1.23-1.27 (m, 1H), 1.46-1.49 (m, 1H), 1.72-1.79 (m, 2H), 2.10-2.20 (m, 2H), 2.50-2.51 (m, 1H), 3.61 (d, 1H, *J* = 10.8 Hz), 3.68 (d, 1H, *J* = 10.8 Hz), 3.84-3.87 (m, 2H), 6.88-6.90 (m, 1H), 7.26-7.36 (m, 2H), 7.55-7.75 (m, 6H), 8.41 (br s, 1H), 10.22 (s, 1H); ^{13}C NMR (400 MHz, DMSO-d$_6$) : δ 24.14, 27.00, 41.92, 42.97, 46.52, 48.62, 106.18, 106.44, 110.08, 110.29, 115.27, 127.86, 129.93, 130.85, 130.95, 133.69, 135.61, 140.95, 141.06, 161.38, 163.78, 168.49, 173.17; Anal. Calc. for $C_{20}H_{22}FN_3O_4S$: C, 57.27; H, 5.29; N, 10.02; found: C, 57.42; H, 4.90; N, 9.97%. ESI-MS: *m/z* 420.2 $[M+H]^+$.

N-(2-(3-chlorophenylamino)-2-oxoethyl)-1-(phenylsulfonyl)piperidine-3-carboxamide 6f:

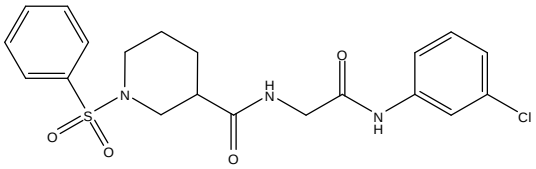

Yield: 59%; white solid; m.p.: 140-142 ^{o}C; IR (KBr): 3412, 3303, 2948, 2843, 1692, 1666, 1650, 1350, 1333 cm^{-1}; ^{1}H NMR (400 MHz, $CDCl_3$): δ 1.67-1.71 (m, 1H), 1.75 (s, 1H), 1.82-1.91 (m, 2H), 2.45-2.55 (m, 1H), 2.64-2.74 (m, 2H), 3.57 (d, 1H, *J* = 11.6 Hz),3.74 (d, 1H, *J* = 9.2 Hz), 4.14 (d, 2H, *J* = 5.2 Hz), 7.01-7.10 (m, 1H), 7.16-7.24 (m, 2H), 7.40-7.42 (m, 1H), 7.52-7.56 (m, 2H), 7.60-7.64 (m, 2H), 7.75-7.77 (m, 2H),

8.82 (s, 1H); ^{13}C NMR (400 MHz, $CDCl_3$): δ 23.76, 26.90, 42.39, 44.34, 46.35, 48.22, 117.84, 119.92, 124.44, 127.56, 129.25, 130.03, 133.10, 134.51, 135.59, 138.78, 167.04, 173.90; $C_{20}H_{22}ClN_3O_4S$; ESI-MS: *m/z* 436.00 $[M+H]^+$

N-(2-(2-chlorophenylamino)-2-oxoethyl)-1-(phenylsulfonyl)piperidine-3-carboxamide 6g:

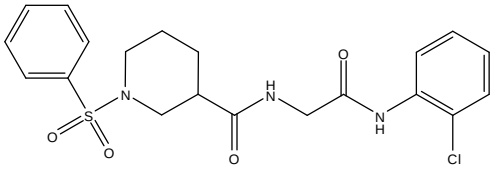

Yield: 48%; white solid; m.p.: 162-164 ^oC; IR (KBr): 3373, 3257, 2953, 2936, 2863, 1707, 1649, 1583, 1386, 1323 cm^{-1}; ^{1}H NMR (400 MHz, $CDCl_3$): δ 1.58-1.76 (m, 2H), 1.80-1.93 (m, 2H), 2.41-2.48 (m, 1H), 2.63-2.70 (m, 2H), 3.61-3.64 (m, 1H), 3.75-3.82 (m, 1H), 4.13-4.14 (m, 2H), 7.01-7.10 (m, 2H), 7.26-7.30 (m, 1H), 7.36-7.39 (m, 1H), 7.53-7.57 (m, 2H), 7.61-7.65 (m, 1H), 7.76-7.78 (m, 2H), 8.30-8.35 (m, 2H); ^{13}C NMR (400 MHz, $CDCl_3$): δ 23.84, 26.93, 42.59, 44.53, 46.33, 48.21, 121.86, 123.18, 125.16, 127.61, 127.75, 129.17, 129.25, 133.07, 134.06, 135.54, 167.23, 173.79; $C_{20}H_{22}ClN_3O_4S$; ESI-MS: *m/z* 436.05 $[M+H]^+$.

N-(2-morpholino-2-oxoethyl)-1-(phenylsulfonyl)piperidine-3-carboxamide 6h:

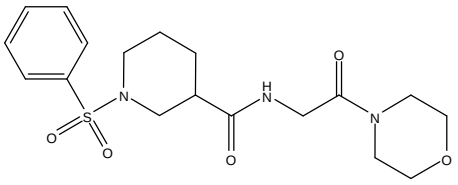

Yield: 79%; white solid; m.p.: 178-180 ^oC; IR (KBr): 3311, 2963, 2922, 2856, 1670, 1655, 1640, 1351, 1332 cm^{-1}; ^{1}H NMR (400 MHz, $CDCl_3$): δ 1.49-1.56 (m, 1H),

1.66-1.74 (m, 1H), 1.80-1.91 (m, 2H), 2.33-2.39 (m, 1H), 2.52-2.58 (m, 2H), 3.41-3.44 (m, 2H), 3.66-3.74 (m, 7H), 3.81 (d, 1H, *J* = 8.0 Hz), 4.03-4.10 (m, 2H), 6.81 (br s, 1H), 7.53-7.57 (m, 2H), 7.60-7.64 (m, 1H), 7.76-7.78 (m, 2H); ^{13}C NMR (400 MHz, $CDCl_3$): δ 23.95, 27.11, 41.04, 42.34, 42.77, 44.78, 46.28, 48.19, 66.31, 66.69, 127.65, 129.14, 132.87, 135.89, 166.39, 172.62; Anal. Calc. for $C_{18}H_{25}N_3O_5S$: C, 54.67; H, 6.37; N, 10.63; found: C, 54.75; H, 5.86; N, 10.32%. ESI-MS: *m/z* 396.1 $[M+H]^+$.

N-(2-oxo-2-(pyrrolidin-1-yl)ethyl)-1-(phenylsulfonyl)piperidine-3-carboxamide 6i:

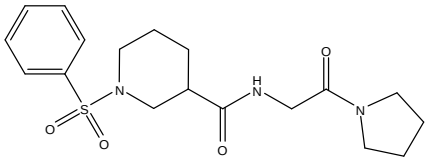

Yield: 66%; white solid; m.p.: 138-140 ^{o}C; IR (KBr): 3383, 3304, 2949, 2870, 1681, 1651, 1398 cm^{-1}; ^{1}H NMR (400 MHz, $CDCl_3$): δ 1.43-1.53 (m, 1H), 1.66-1.73 (m, 1H), 1.79-1.84 (m, 2H), 1.90-1.94 (m, 2H), 1.98-2.03 (m, 2H), 2.27-2.33 (m, 1H), 2.49 (t, 1H, *J* = 10.4 Hz) 2.55-2.60 (m, 1H), 3.39 (t, 2H, *J* = 6.8 Hz), 3.53 (t, 2H, *J* = 6.8 Hz), 3.84-3.85 (m, 1H), 3.86-3.87 (m, 1H), 3.95-3.99 (m, 2H), 6.86 (br s, 1H), 7.52-7.56 (m, 2H), 7.59-7.63 (m, 1H), 7.75-7.78 (m, 2H); ^{13}C NMR (400 MHz, $CDCl_3$): δ 24.07, 24.14, 25.89, 27.04, 41.96, 42.66, 45.53, 46.13, 46.26, 48.36, 127.62, 129.11, 132.82, 135.88, 166.33, 172.73. Anal. Calc. for $C_{18}H_{25}N_3O_4S$: C, 56.97; H, 6.64; N, 11.07; found: C, 57.00; H, 6.82; N, 11.30%. ESI-MS: *m/z* 380.1 $[M+H]^+$.

N-(2-(dimethylamino)-2-oxoethyl)-1-(phenylsulfonyl)piperidine-3-carboxamide 6j:

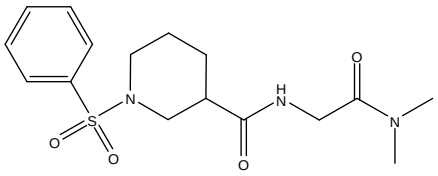

Yield: 80%; white solid; m.p.: 128-130 ^{o}C; IR (KBr): 3351, 3274, 2978, 2940, 1720, 1677, 1635, 1365, 1338 cm^{-1}; ^{1}H NMR (400 MHz, $CDCl_3$): δ 1.46-1.50 (m, 1H), 1.65-1.85 (m, 2H), 1.89-1.93 (m, 1H), 2.28-2.35 (m, 1H), 2.48-2.60 (m, 2H), 3.02 (d, 6H, *J* = 9.6 Hz), 3.73 (d, 1H, *J* = 11.6 Hz), 3.85 (d, 1H, *J* = 9.6 Hz), 4.03 (d, 2H, *J* = 8.4 Hz), 6.82 (br s, 1H), 7.53-7.57 (m, 2H), 7.60-7.64 (m, 1H), 7.77 (d, 2H, *J* = 7.2 Hz); ^{13}C NMR (400 MHz, $CDCl_3$) : δ 24.02, 27.16, 35.68, 35.95, 41.22, 42.84, 46.26, 48.24, 127.66, 129.13, 132.85, 135.92, 167.65, 172.54; $C_{16}H_{23}N_3O_4S$; ESI-MS**:** *m/z* 354.0 $[M+H]^+$.

N-(2-(3,4-dihydroisoquinolin-2(1H)-yl)-2-oxoethyl)-1-(phenylsulfonyl)piperidine-3-carboxamide 6k:

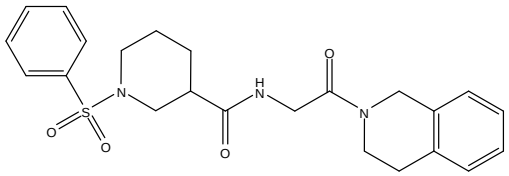

Yield: 62%; white solid; m.p.: 142-144 ^{o}C; IR (KBr): 3322, 2948, 2913, 2849, 1664, 1650, 1635, 1351, 1343 cm^{-1}; ^{1}H NMR (400 MHz, $CDCl_3$): δ 1.48-1.51 (m, 1H), 1.67-1.70 (m, 1H), 1.80-1.85 (m, 1H), 1.90-1.93 (m, 1H), 2.30-2.36 (m, 1H), 2.50-2.60 (m, 2H), 2.90-2.96 (m, 2H), 3.64 (t, 1H, *J* = 6.0 Hz), 3.72 (d, 1H, *J* = 11.2 Hz), 3.83-3.89 (m, 2H), 4.11-4.16 (m, 2H), 4.57 (s, 1H), 4.78 (s, 1H), 7.11-7.13 (m, 1H), 7.16-7.20

(m, 2H), 7.22-7.25 (m, 2H), 7.53-7.57 (m, 2H), 7.60-7.64 (m, 1H), 7.76-7.78 (m, 2H); ^{13}C NMR (400 MHz, $CDCl_3$): δ 24.01, 27.14, 28.28, 29.07, 40.24, 41.42, 41.57, 42.13, 42.81, 44.51, 46.01, 46.27, 48.23, 126.16, 126.62, 126.66, 126.85, 126.91, 127.28, 127.66, 128.39, 128.95, 129.13, 131.47, 132.64, 132.85, 133.70, 134.64, 135.90, 166.62, 166.64, 172.56, 172.62. Anal. Calc. for $C_{23}H_{27}N_3O_4S$: C, 62.56; H, 6.16; N, 9.52; found: C, 62.46; H, 6.07; N, 9.49%; ESI-MS: *m/z* 442.2 $[M+H]^+$.

4.5 References

[1] Zimmet, P. Z. *Diabetes Care* **1995**, *18***,** 1050.

[2] Bearse, M. A. Jr.; Han, Y.; Schneck, M. E.; Barez, S.; Jacobsen, C.; Adams, A. J. *Invest Ophthal Vis Sci* **2004**, *45*, 3259.

[3] Hove, M. N.; Kristensen, J. K.; Lauritzen, T.; Bek, T. *Acta Ophthalmol Scand* **2004**, *82*, 443.

[4] Seki, M.; Tanaka, T.; Nawa, H.; Usui, T.; Fukuchi, T.; Ikeda, K.; Abe, Haruki.; Takei, N. *Diabetes* **2004,** *53*, 2412.

[5] Moran, A.; Palmas, W.; Field, L.; Bhattaraj, J.; Schwartz, J.E.; Weinstock, R. S.; Shea, S. *Diabetes care* **2004**, *27*, 972.

[6] Huang, C.; Kim, Y.; Caramori, M. L.; Fish, A. J.; Rich, S. S.; Miller, M. E.; Russell, G. B.; Mauer, M. *Diabetes* **2002**, *51*, 3577.

[7] Yaron, A.; Naider, F. *Crit. Rev. Biochem. Mol. Biol.* **1993**, *28*, 31.

[8] Mentlein, R.; Gallwitz, B.; Schmidt, W. E. *Eur. J. Biochem.* **1993**, *214*, 829.

[9] Deacon, C. F.; Johnsen, A. H.; Holst, J. J. *J. Clin. Endocrinol. Metab.* **1995**, *80*, 952.

[10] Drucker, D. J. *Endocrinology* **2001**, *142*, 521.

[11] Holst, J. J.; Orskov, C.; Nielsen, O.V.; Schwartz, T. W. *FEBS Lett.* **1987**, *211*, 169.

[12] Ahren, B.; Larsson, H.; Holst, J. J. *J. Clin. Endocrinol. Metab*. **1997**, *82*, 473.

[13] Drucker, D. J. *Gastroenterology* **2002**, *122*, 531.

[14] Nauck, M. A.; Wollschlager, D.; Werner, J.; Holst, J. J.; Orskov, C.; Creutzfeldt, W.; Willms, B. *Diabetologia* **1996**, *39*, 1546.

[15] Kieffer, T. J.; McIntosh, C. H. S.; Pederson, T. A. *Endocrinology* **1995**, *136*, 3585.

[16] Deacon, C. F.; Nauck, M. A.; Toft-Nielson, M.; Pridal, L.; Willms, B.; Holst, J. J. *Diabetes* **1995**, *44*, 1126.

[17] Kim, D.; Wang, L.; Beconi, M.; Eiermann, G. J.; Fisher, M. H.; He, H.; Hickey, G. J.; Kowalchick, J. E.; Leiting, B.; Lyons, K.; Marsilio, F.; McCann, M. E.; Patel, R. A.; Petrov, A.; Scapin, G.; Patel, S. B.; Roy, R. S.; Wu, J. K.; Wyvratt, M. J.; Zhang, B. B.; Zhu, L.; Thornberry, N. A.; Weber, A. E. *J. Med. Chem.* **2005**, *48*, 141.

[18] Feng, J.; Zhang, J.; Wallace, M. B.; Stafford, J. A.; Kaldor, S. W.; Kassel, D.B.; Navre, M.; Shi, L.; Skene, R. J.; Asakawa, T.; Takeuchi, K.; Xu, R.; Webb, D. R.; Gwaltney, S. L. *J. Med. Chem.* **2007**, *50*, 2297.

[19] Berman, H. M.; Westbrook, J.; Feng, Z.; Gilliland, G.; Bhat, T. N.; Weissig, H.; Shindyalov, I. N.; Bourne, P. E. *The Protein Data Bank Nucleic Acids Research*, **2000**, *28*, 235 and PubMed: 23501107

[20] Trott, O.; Olson, A. J. *Journal of Computational Chemistry* **2010**, *31* 455.

[21] Wallace, A. C.; Laskowski, R. A.; Thornton, J. M. *Protein Eng.* **1995**, *8*, 127.

[22] http://www.pymol.org

CHAPTER 5

SYNTHESIS OF

4-(AMINOMETHYL)QUINOLIN-2(1*H*)-ONE

DERIVATIVES AS ANTI-CANCER AGENTS

5.1 Introduction

Over the past few decades with the advances in medicine, life expectancy of individuals has increased many folds, yet cancer is still most dreaded disease with highest mortality rate, ranked after the cardiovascular diseases. The biggest challenge faced by the health industry lies in the treatment of cancer. Cancer is curable if detected at an early stage or else it proves to be fatal. Uncontrolled cell differentiation and growth in any part of the body leads to cancer. From the medicinal chemistry point of view, the drug administered to patients suffering from cancer should cause selective induction of apoptosis in cancerous cells while leaving normal cells unaffected. Thus safe yet selective drug for the treatment of cancer is the need of the hour.

Various natural and synthetic molecules are reported to exhibit anti-cancer activity. Quinolones have promising pharmacological potential due to its drug-like properties and structural similarity to some specific targets and hence have gained importance. 2-Quinolone (carbostyril, 1-azacoumarin) are lactams whose derivatives are widely studied for their applications in the field of chemistry and biology. Joseph *et al* reported 3-aryl-2-quinolone derivatives as anti-tumor agents [1].

7-amino-4-methyl-2[1H]-quinolinone derivatives have been reported to act as antenna molecules which transfers the energy absorbed from the light to the lanthanide ions on the complex thereby rendering the complex fluorescent [2].

Substituted 4-aminomethyl-2[1H]-quinolone derivatives and various quinolone linked with coumarins via ether linkage have been studied for their anti-microbial and analgesic activities [3, 4].

Various 2-quinolone derivatives have been reported as inducible nitric oxide synthase (iNOS) inhibitors and potent anti-platelet agents [5, 6].

Recently, 7-amino-4-methyl-2[1H]-quinolinone derivatives have been reported to show anti-cancer activity [6, 7]. Present work has been designed for the synthesis of substituted 4-aminomethyl-2[1H]-quinolinone derivatives with application in the treatment of cancer. The molecules thus synthesized have been subjected to *in-vitro* anti-cancer activity of against A549 cell line

5.2 Results and Discussion

5.2.1 Chemistry

Bromination of acetoacetanilide **1** using bromine in glacial acetic acid gave bromoacetoacetanilide **2** which cyclizes on reaction with concentrated sulphuric acid (conc. H_2SO_4) to give 4-(bromomethyl)quinolin-2[1H]-one **3**. The structure of compound **3** was confirmed from its IR spectrum (Figure 5.2.1) which shows a strong band at 1653 cm^{-1} for the lactam carbonyl and its ^1H NMR spectrum (Figure 5.2.2) shows two singlets, one at δ 4.90 for the methylene protons at C-4 and another at δ 11.86 for the –NH lactam proton. Figure 5.2.3 and Figure 5.2.4 shows the ^{13}C NMR and ESI-MS spectra of **3** respectively. Presence of M^+ and $[M+2]^+$ peak if equal intensity confirms the presence of bromine in the structure of **3.**

Commercially available boc-protected glycine **4** was reacted with various amines in the presence of 1-ethyl-3-(3-dimethylaminopropyl)carbodiimide hydrochloride (EDCI), 1-hydroxybenzotriazole (HOBt), 4-dimethylaminopyridine (DMAP) to yield corresponding C-substituted amide derivatives of glycine **5a-e** as shown in Scheme 5.1.

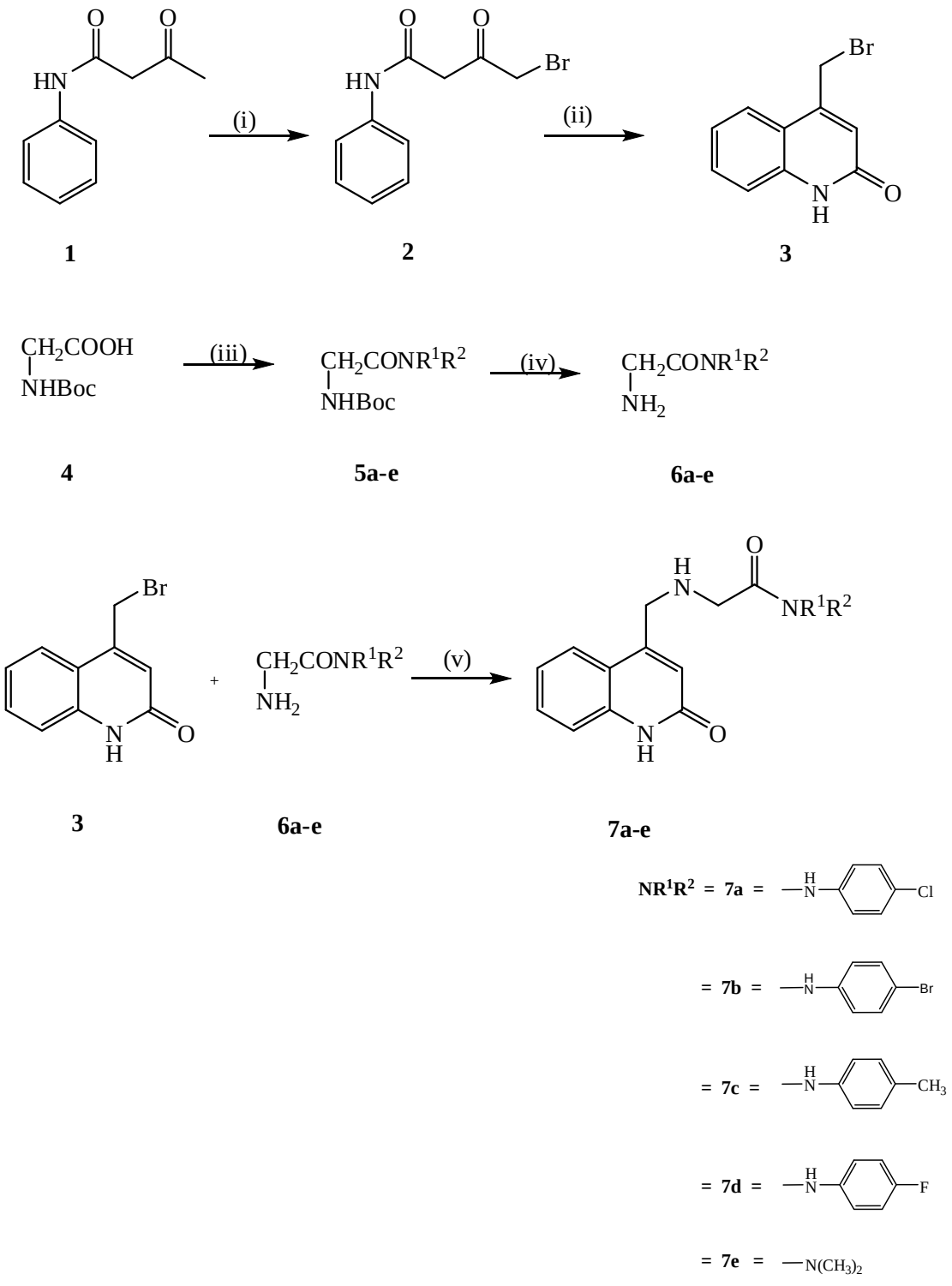

Scheme 5.1: Reagents: (i) Br_2, CH_3COOH, I_2; (ii) conc.H_2SO_4; (iii) EDCI, HOBt, DMAP, various amines, DCM; (iv) 10% TFA in DCM; (v) $LiOH.H_2O$, DMF.

The IR spectrum of **5a** (Figure 5.3.1) shows two bands at 1681 and 1673 cm^{-1} for the amide carbonyl while in the ^{1}H NMR spectrum (Figure 5.3.2) a peak at δ 3.71 for the methylene protons of glycine and two doublets at δ 7.36 and 7.61 for the aromatic protons and molecular ion peak at *m/z* 307.0 $[M+Na]^{+}$ in the ESI-MS spectrum (Figure 5.3.4) confirms the formation of **5a** Figures 5.4.1 to 5.8.4 shows the IR, ^{1}H NMR, ^{13}C NMR and ESI-MS spectra of compounds **5b-f**. Deprotection of boc-protected glycine amides **5a-e** by trifluoroacetic acid (TFA) gave corresponding free bases **6a-e** which were not isolated and used for subsequent reaction after concentration. Further reaction of **3** with various free bases **6a-e** was carried out using various bases. Initially, organic bases like triethyl amine (TEA) and diisopropyl ethylamine (DIPEA) and later inorganic bases like potassium carbonate (K_2CO_3) were used from 3 to 10 equivalents and later effect on the progress of reaction by change of solvent, temperature were also experimented but all the reactions failed. Later, the reaction succeeded by use of a very strong inorganic base lithium hydroxide monohydrate and that too at room temperature. Thus by the use of strong base, gave the desired substituted 4-aminomethyl-2[1H]-quinolinone derivatives **7a-e** as shown in Scheme 5.1. The IR spectrum (Figure 5.9.1) of **7a** shows two strong bands at 3336 and 3260 cm^{-1} for –NH stretching vibrations of amide group and a strong band at 1660 cm^{-1} for the amide carbonyl group. The ^{1}H NMR spectrum (Figure 5.9.2) of **7a** shows two singlets at δ 2.9 and 3.9 for the $–CH_2$ groups, three singlets at δ 6.58, 9.90 and 11.60 indicates three –NH protons and the remaining aromatic protons were observed from δ 7.18-7.82 confirmed the structure of **7a**. Figures 5.9.3 and 5.9.4 shows the ^{13}C NMR and ESI-MS spectra of **7a**, thus confirms its formation.

An interesting observation under similar reaction conditions was disubstitution of the glycyl amino $–NH_2$ group by **3** thereby leading to formation of **7f** (Figure 5.1) which due to its poor solubility was not evaluated for its anti-cancer activity. The structure of **7f** was confirmed by its IR, spectrum (Figure 5.10.1) which shows bands at 3414 cm^{-1} for –NH of amide group and a strong band at 1659 cm^{-1} indicating lactam carbonyl group. The ^1H NMR spectrum (Figure 5.10.2) shows multiplet from δ 1.70-1.74 for four protons (C2-C3) and other multiplets at δ 3.15-3.50 for the remaining four protons (C1, C4) of the pyrrolidide group; a singlet δ 4.04 indicates the two sets of $–CH_2$ protons attached to the quinolinone system. And multiplets from δ 6.53 to 7.87 for the ten aromatic protons thus confirmed the formation of disubstituted product **7f**. Further, ESI-MS spectrum (Figure 5.10.4) of **7f** shows a peak at *m/z* 465 for $[M+Na]^+$ also supports the formation of **7f**.

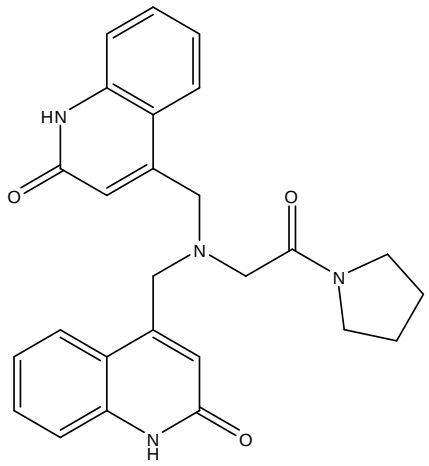

Figure 5.1: Structure of 4,4'-(2-oxo-2-(pyrrolidin-1-yl)ethylazanediyl)bis(methylene) diquinolin-2(1H)-one **7f**

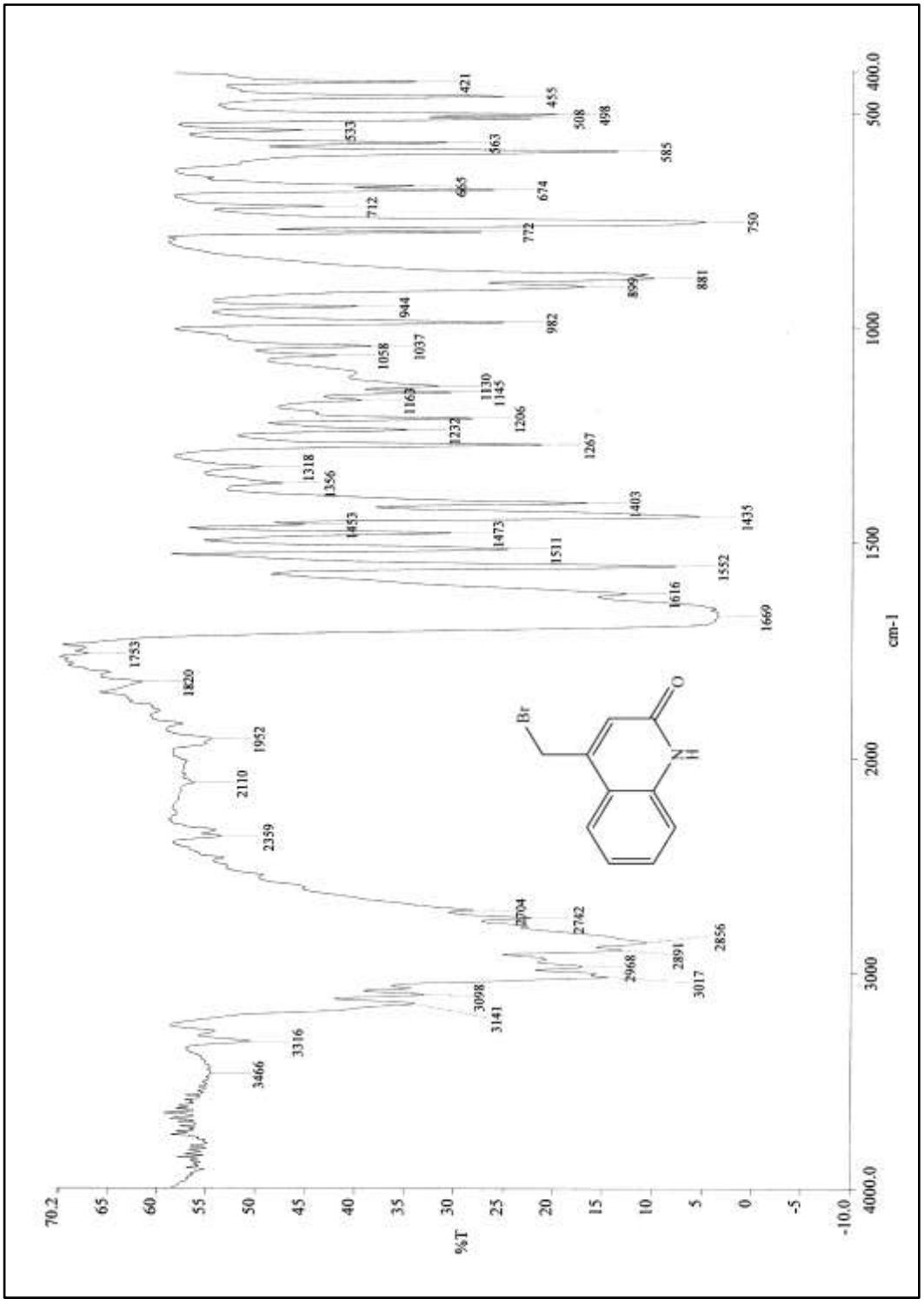

Figure 5.2.1: IR spectrum of 4-(bromomethyl)quinolin-2(1H)-one **3**

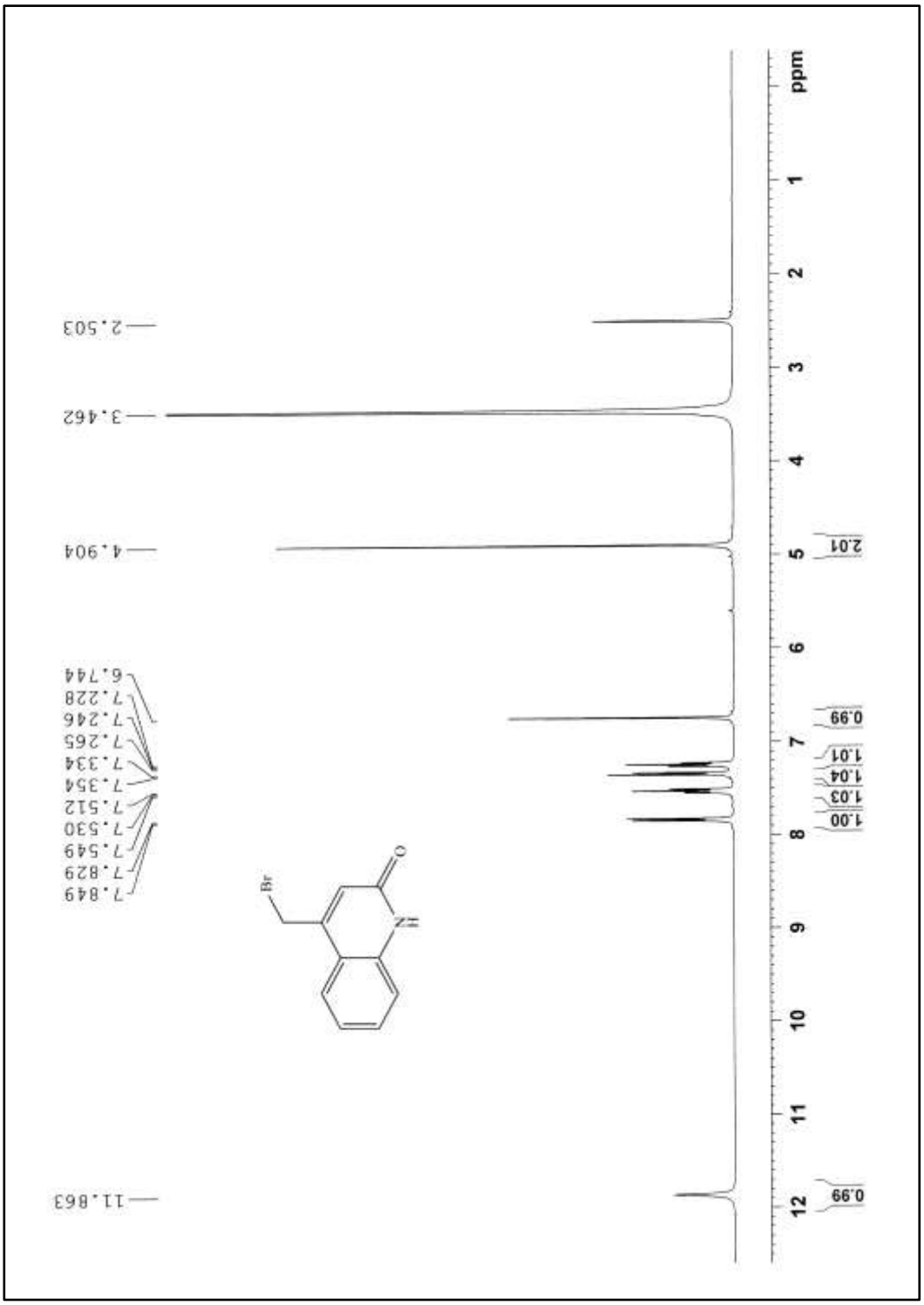

Figure 5.2.2: ^{1}H NMR spectrum of 4-(bromomethyl)quinolin-2(1H)-one **3**

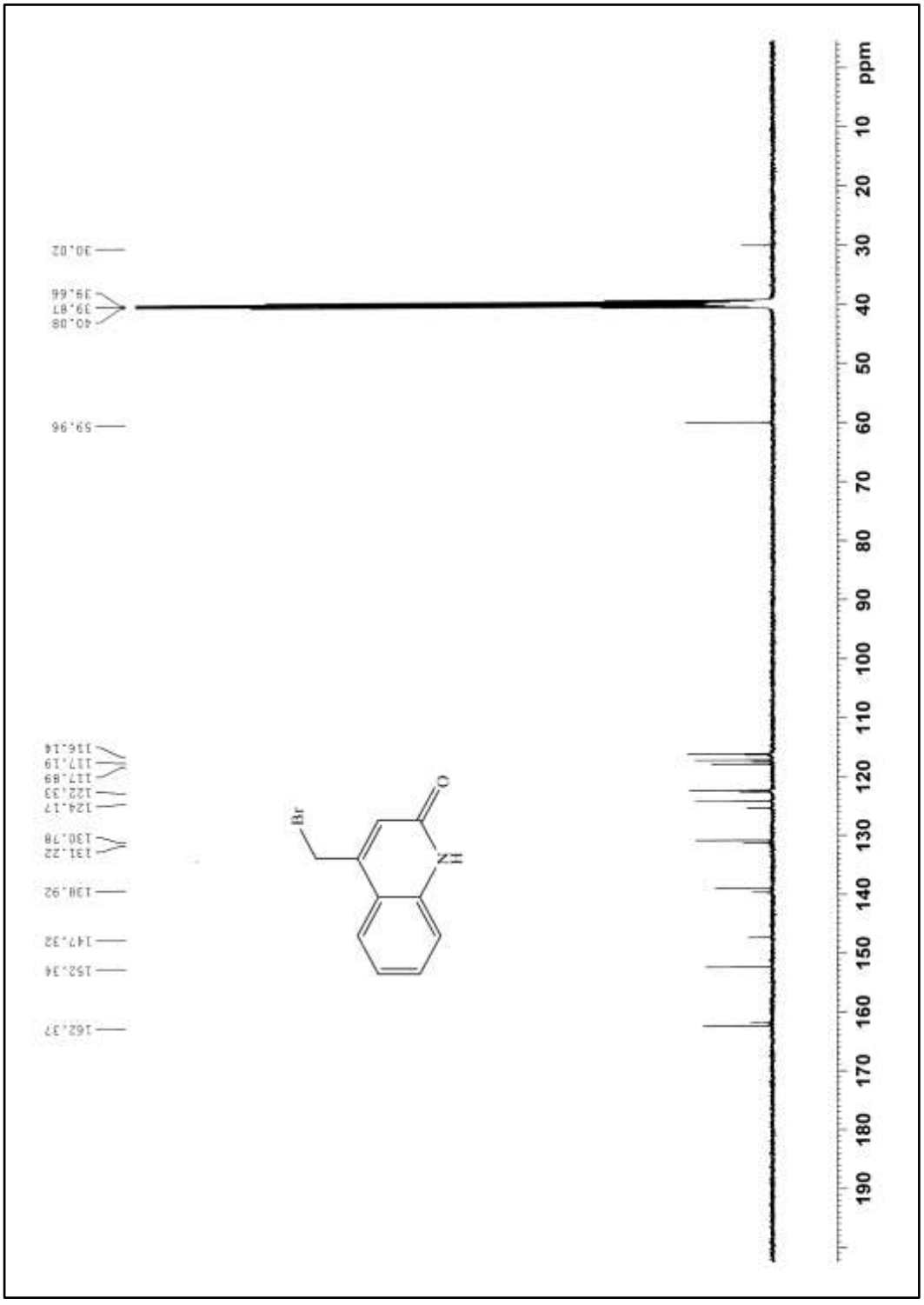

Figure 5.2.3: ^{13}C NMR spectrum of 4-(bromomethyl)quinolin-2(1H)-one **3**

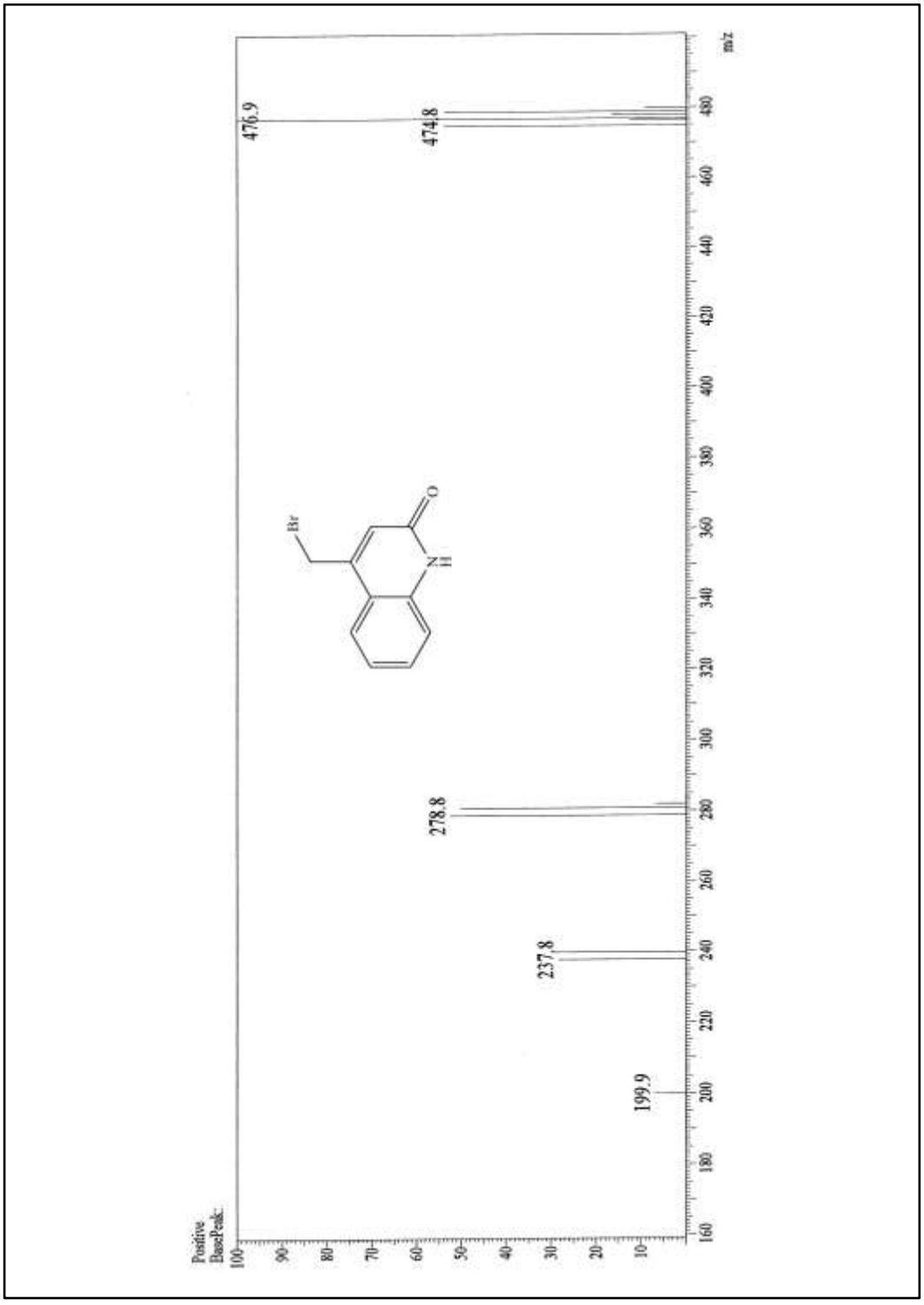

Figure 5.2.4: ESI-MS spectrum of 4-(bromomethyl)quinolin-2(1H)-one **3**

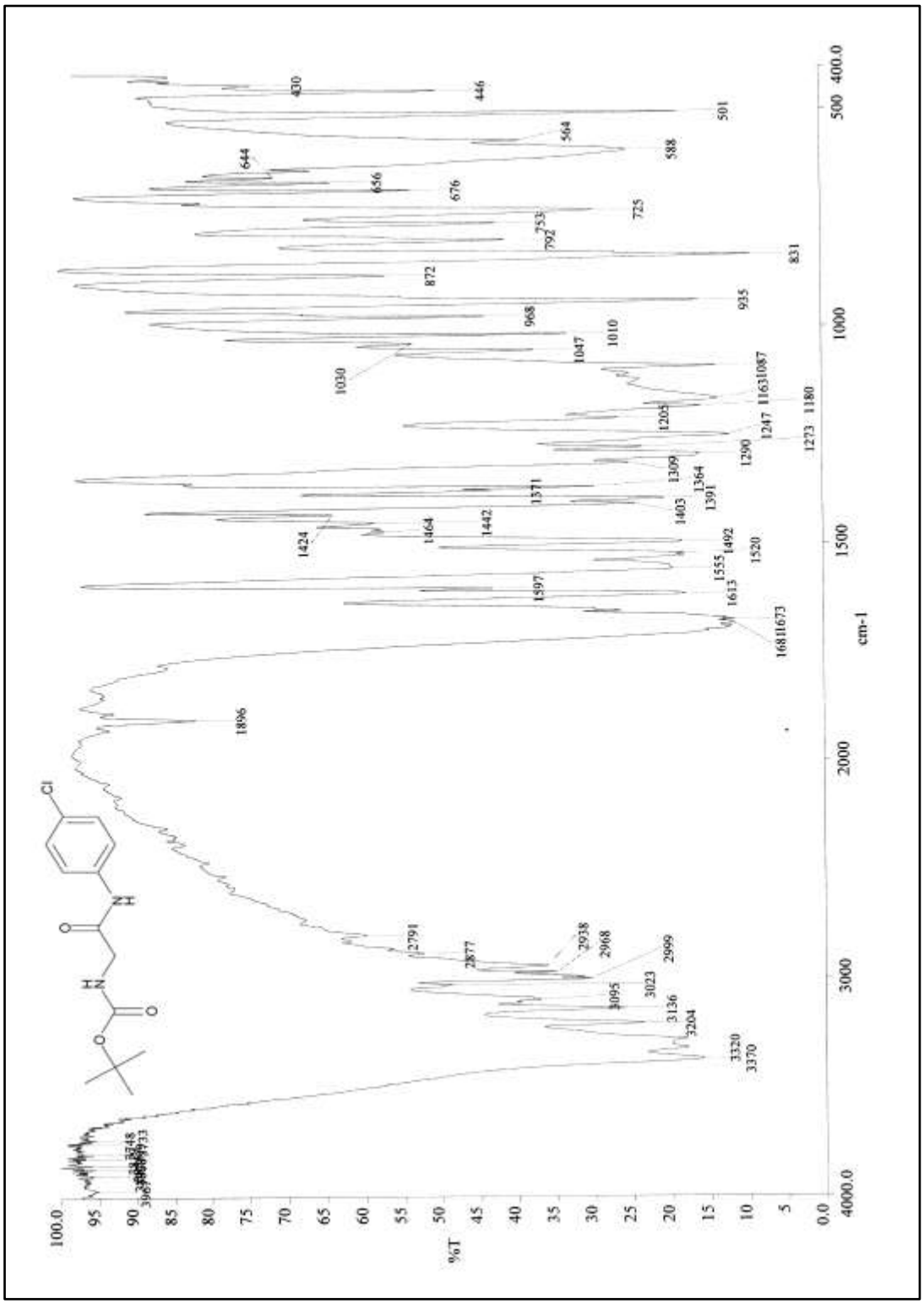

Figure 5.3.1: IR spectrum of *tert*-butyl 2-(4-chlorophenylamino)-2-oxoethylcarbamate **5a**

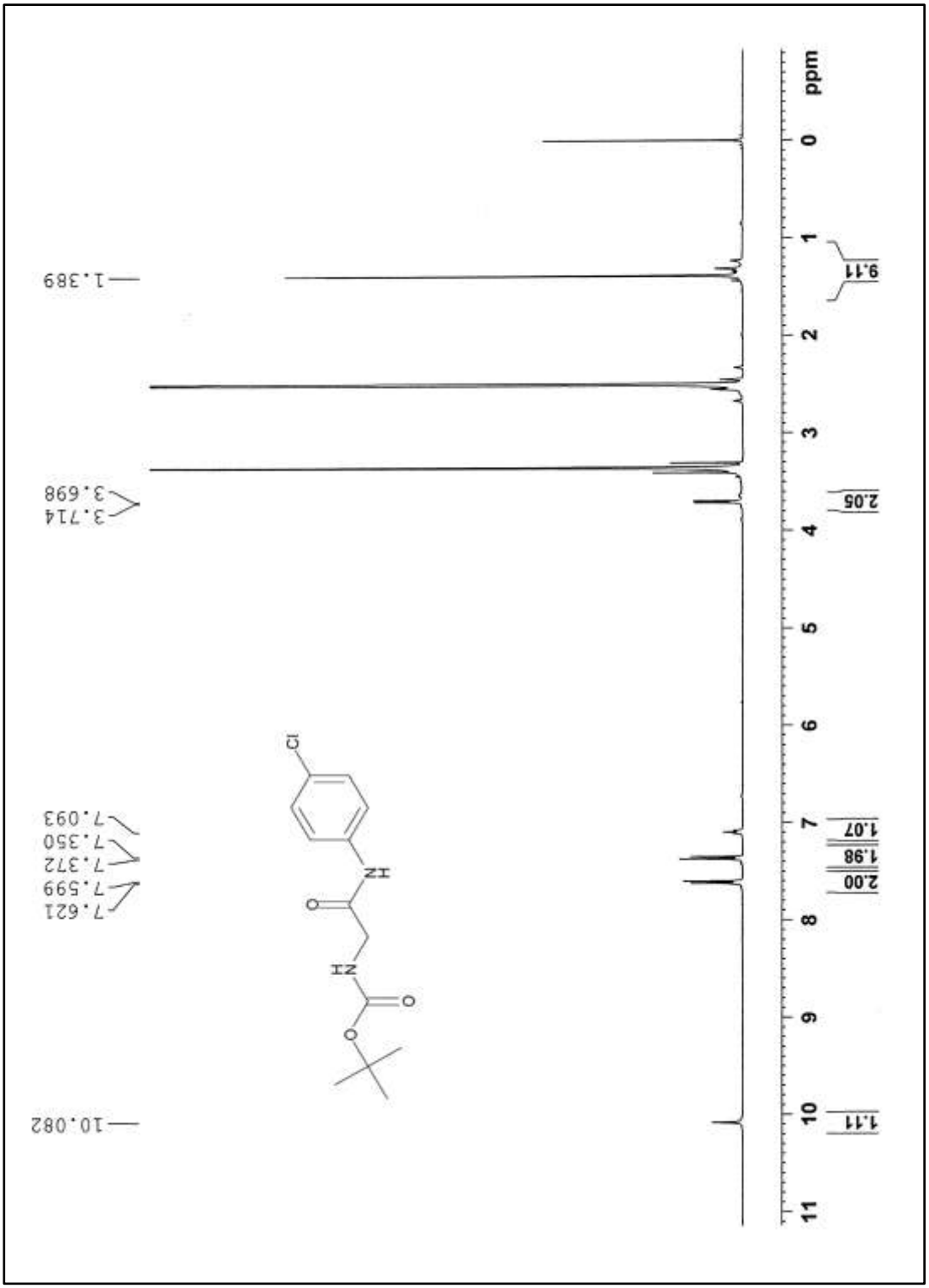

Figure 5.3.2: ^{1}H NMR spectrum of *tert*-butyl 2-(4-chlorophenylamino)-2-oxoethylcarbamate **5a**

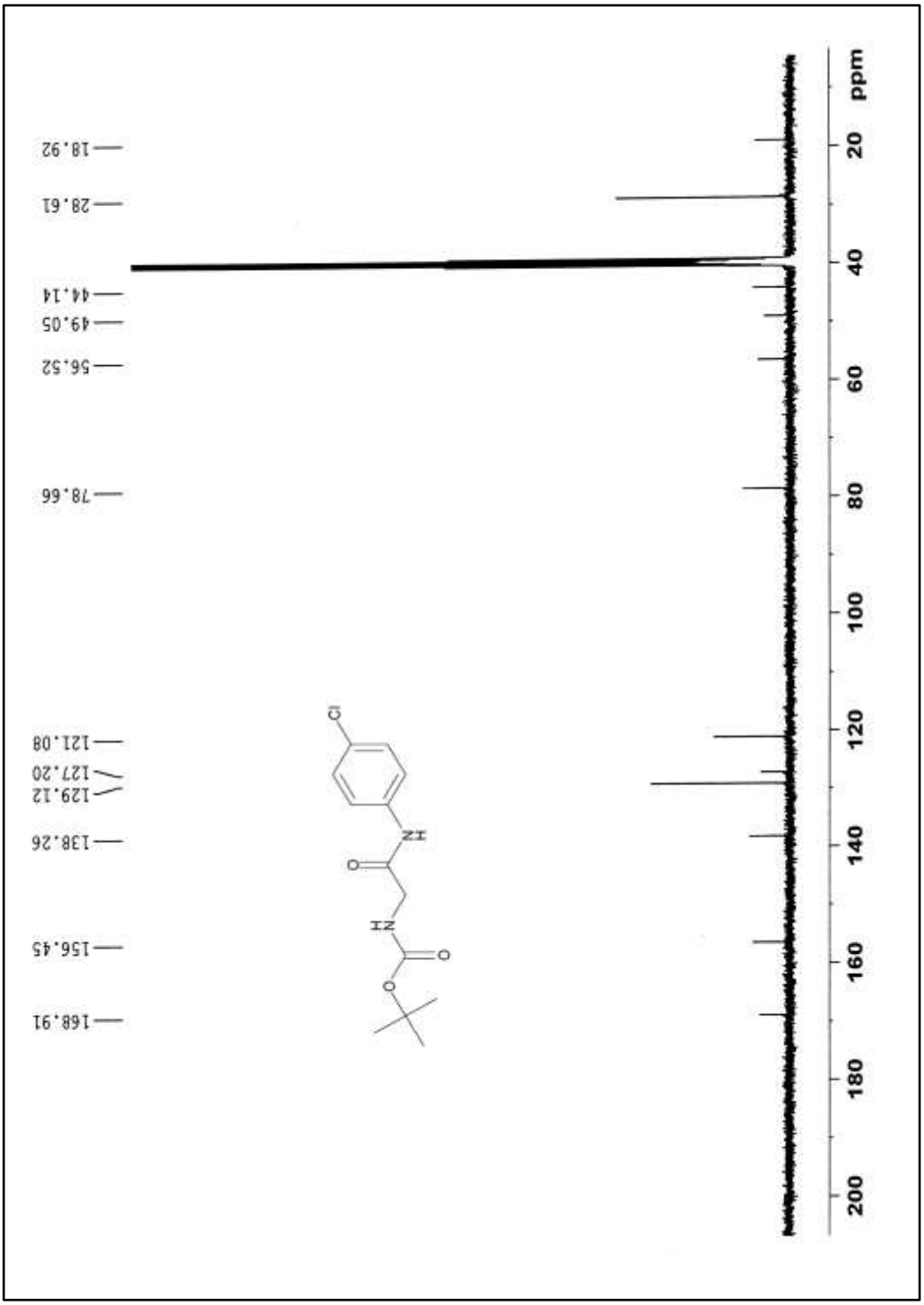

Figure 5.3.3: ^{13}C NMR spectrum of *tert*-butyl 2-(4-chlorophenylamino)-2-oxoethylcarbamate **5a**

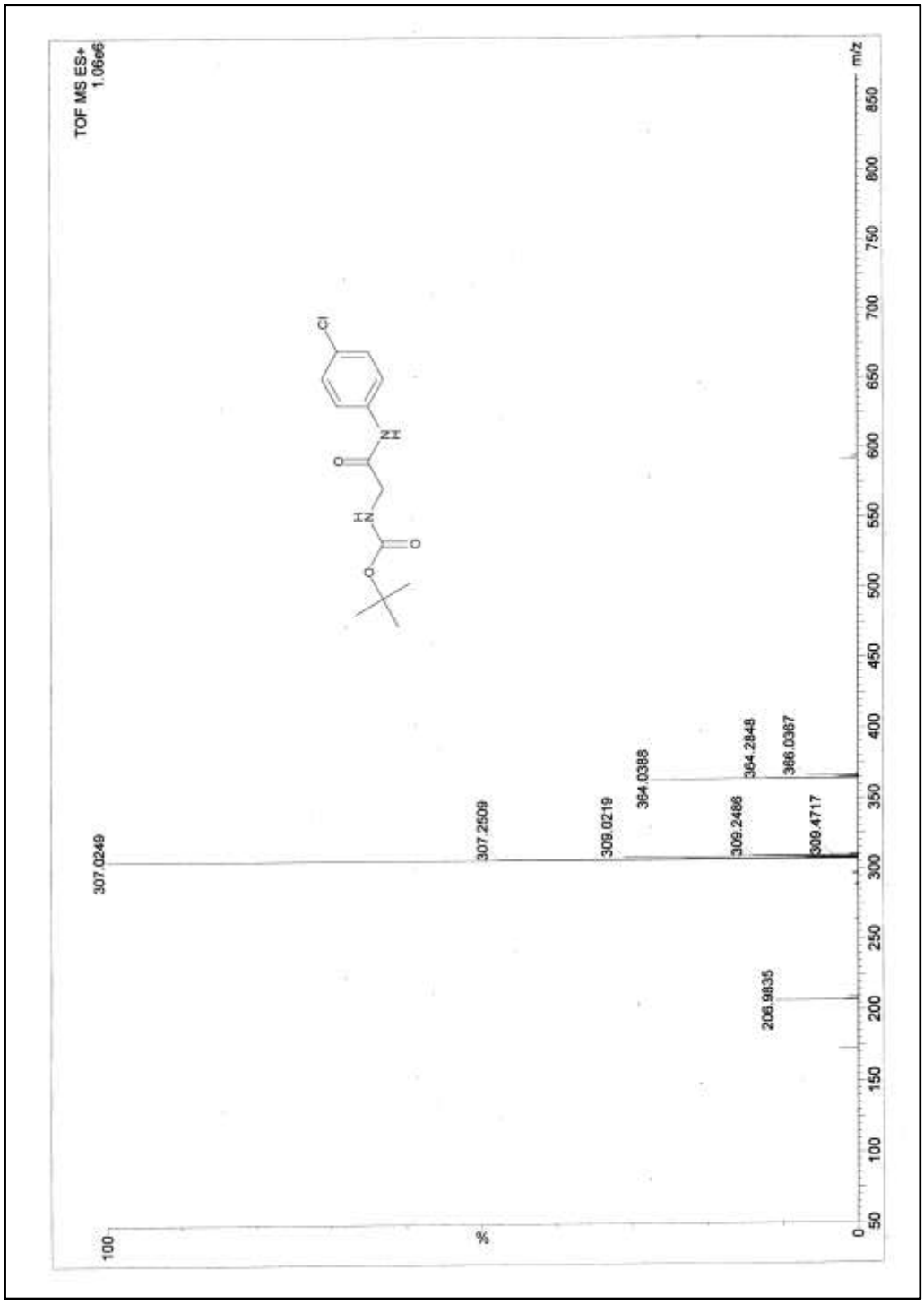

Figure 5.3.4: ESI-MS spectrum of *tert*-butyl 2-(4-chlorophenylamino)-2-oxoethylcarbamate **5a**

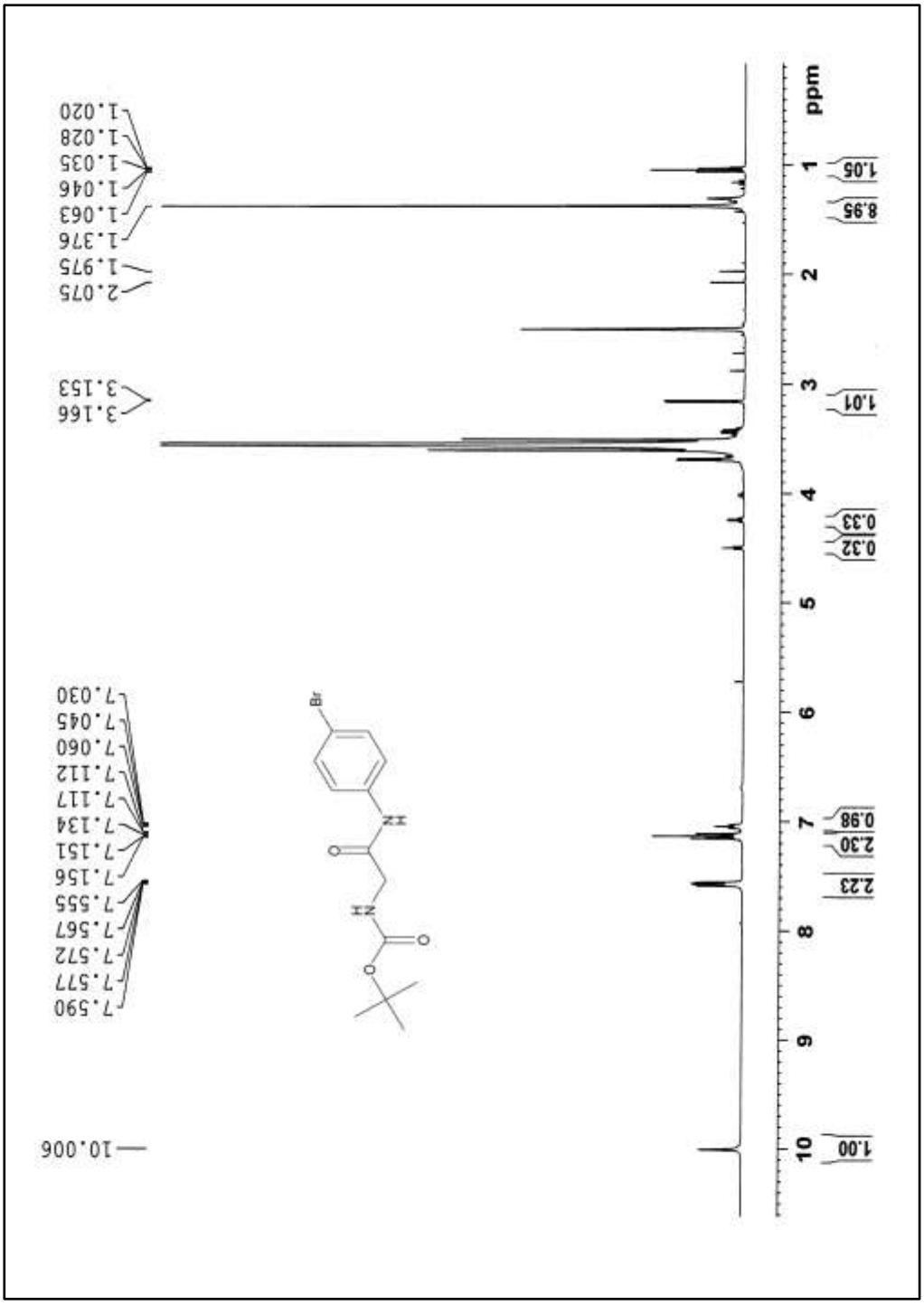

Figure 5.4.2: ^{1}H NMR spectrum of *tert*-butyl 2-(4-bromophenylamino)-2-oxoethylcarbamate **5b**

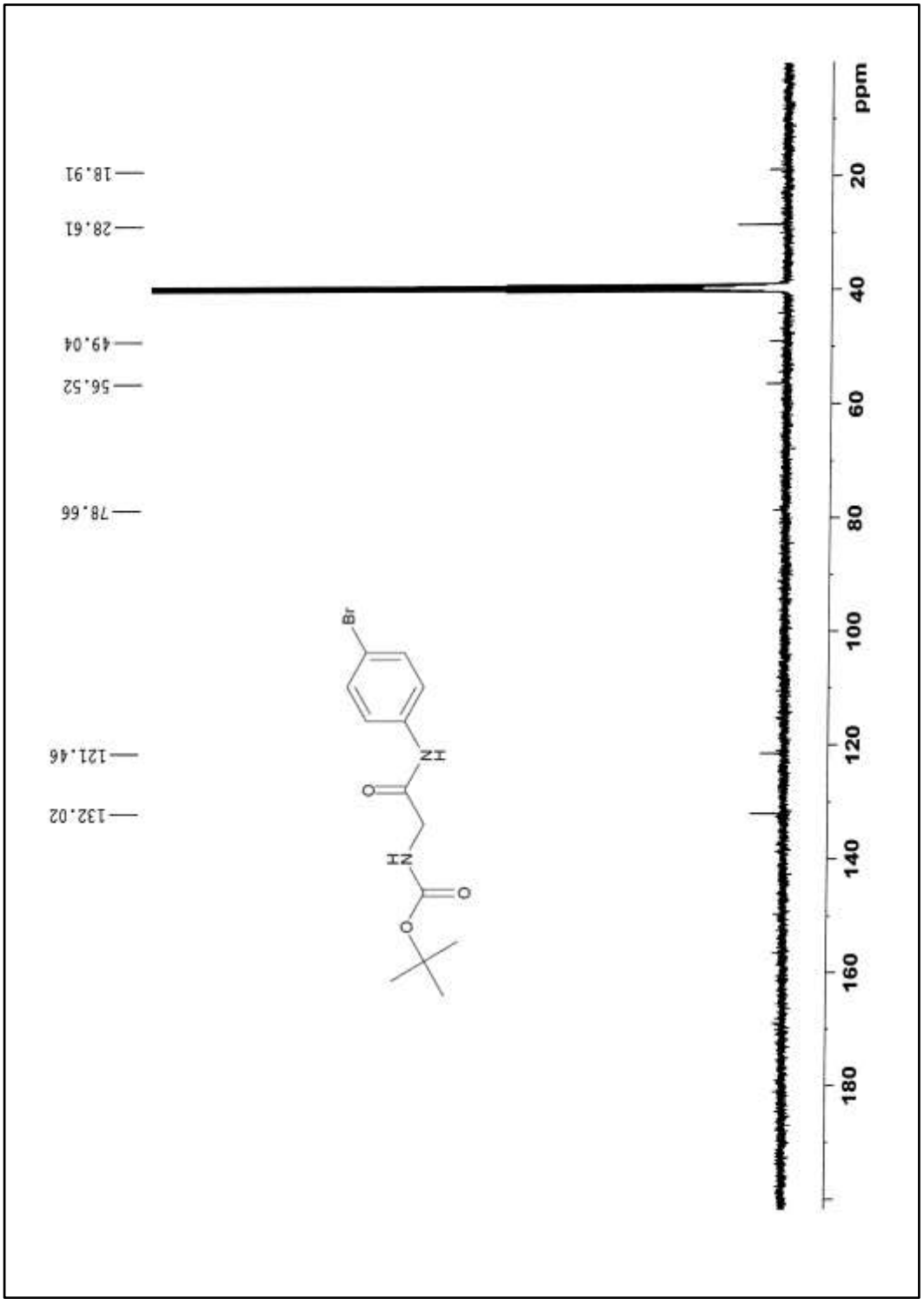

Figure 5.4.3: ^{13}C NMR spectrum of *tert*-butyl 2-(4-bromophenylamino)-2-oxoethylcarbamate **5b**

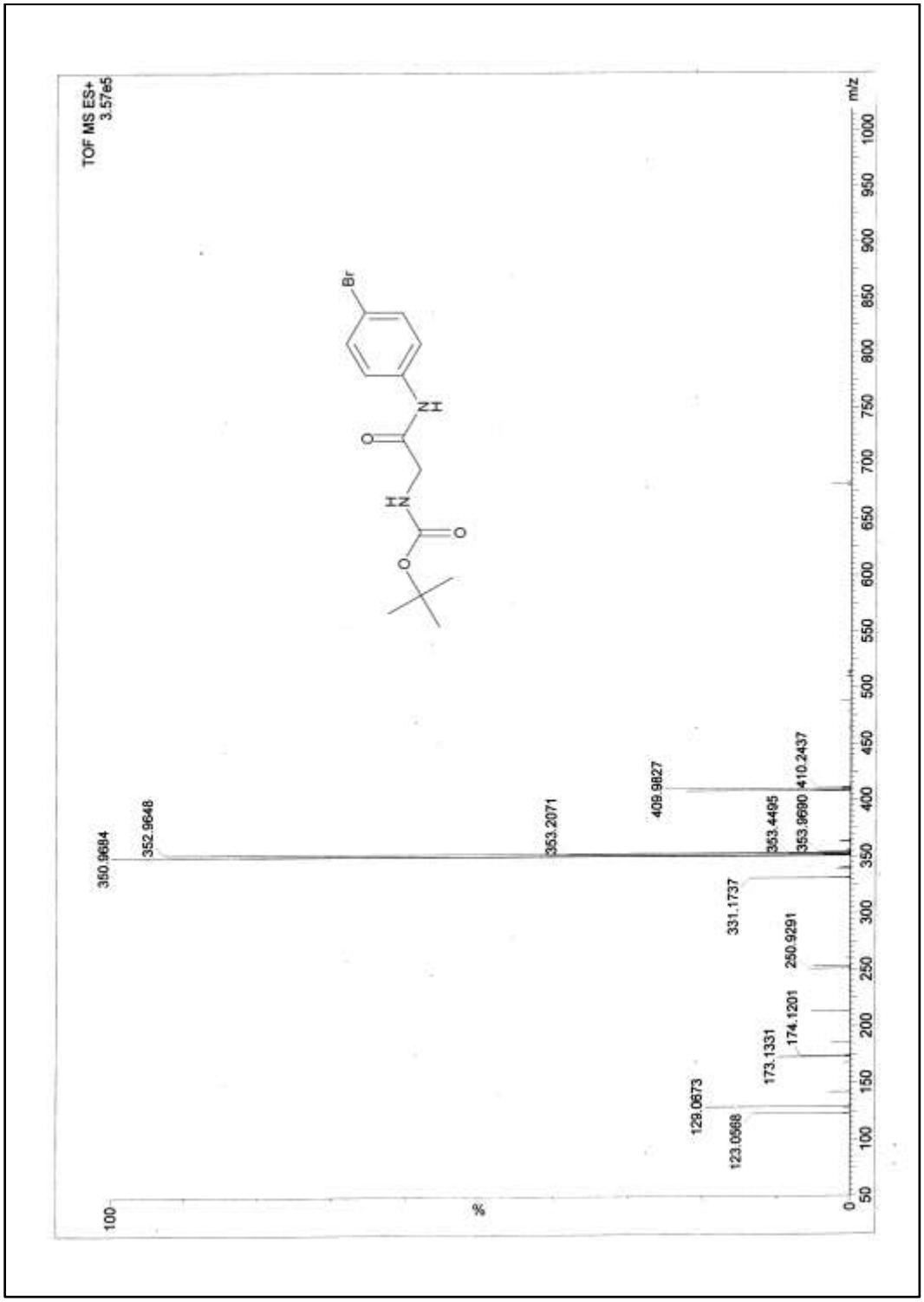

Figure 5.4.4: ESI-MS spectrum of *tert*-butyl 2-(4-bromophenylamino)-2-oxoethylcarbamate **5b**

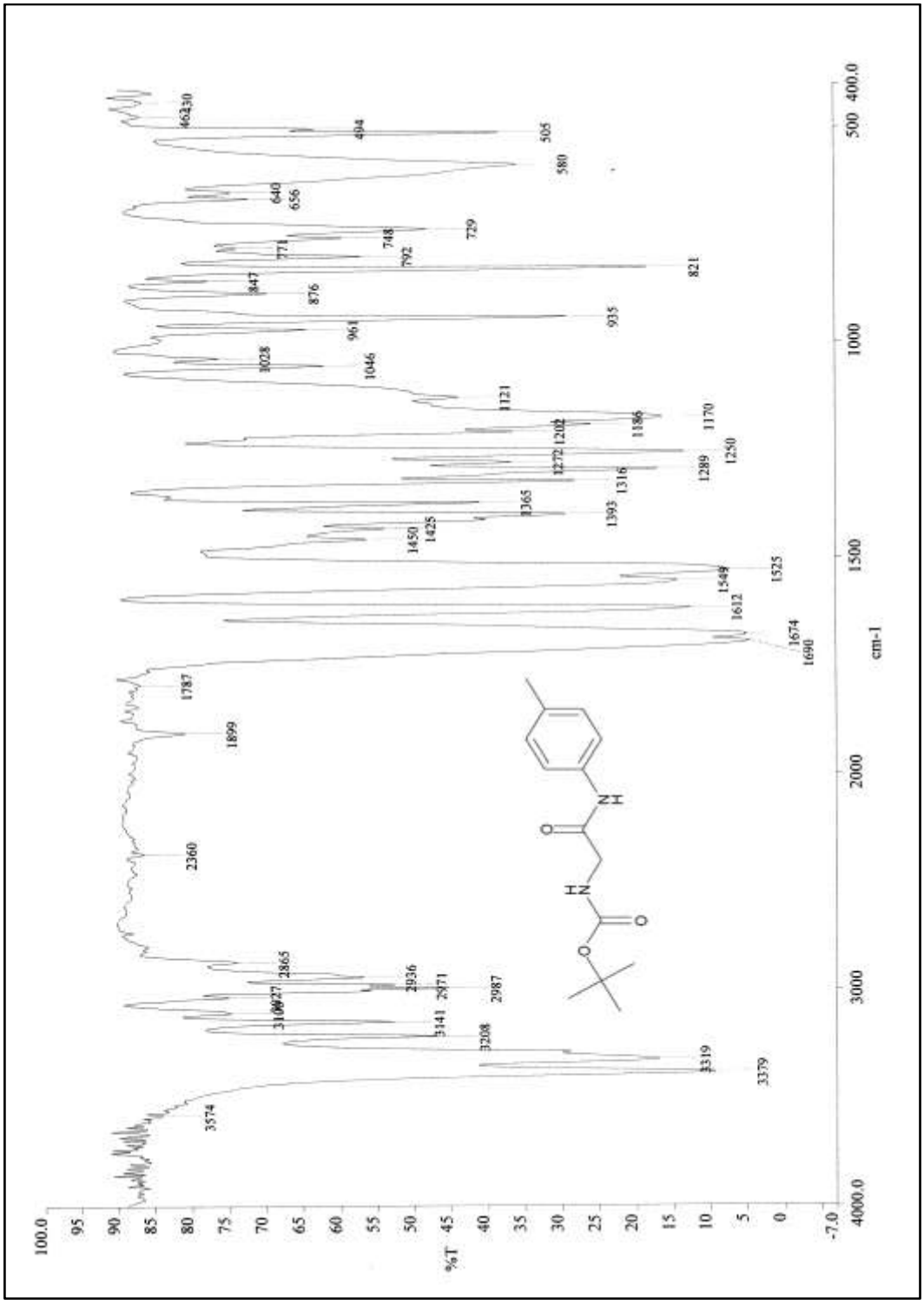

Figure 5.5.1: IR spectrum of *tert*-butyl 2-oxo-2-(p-tolylamino)ethylcarbamate **5c**

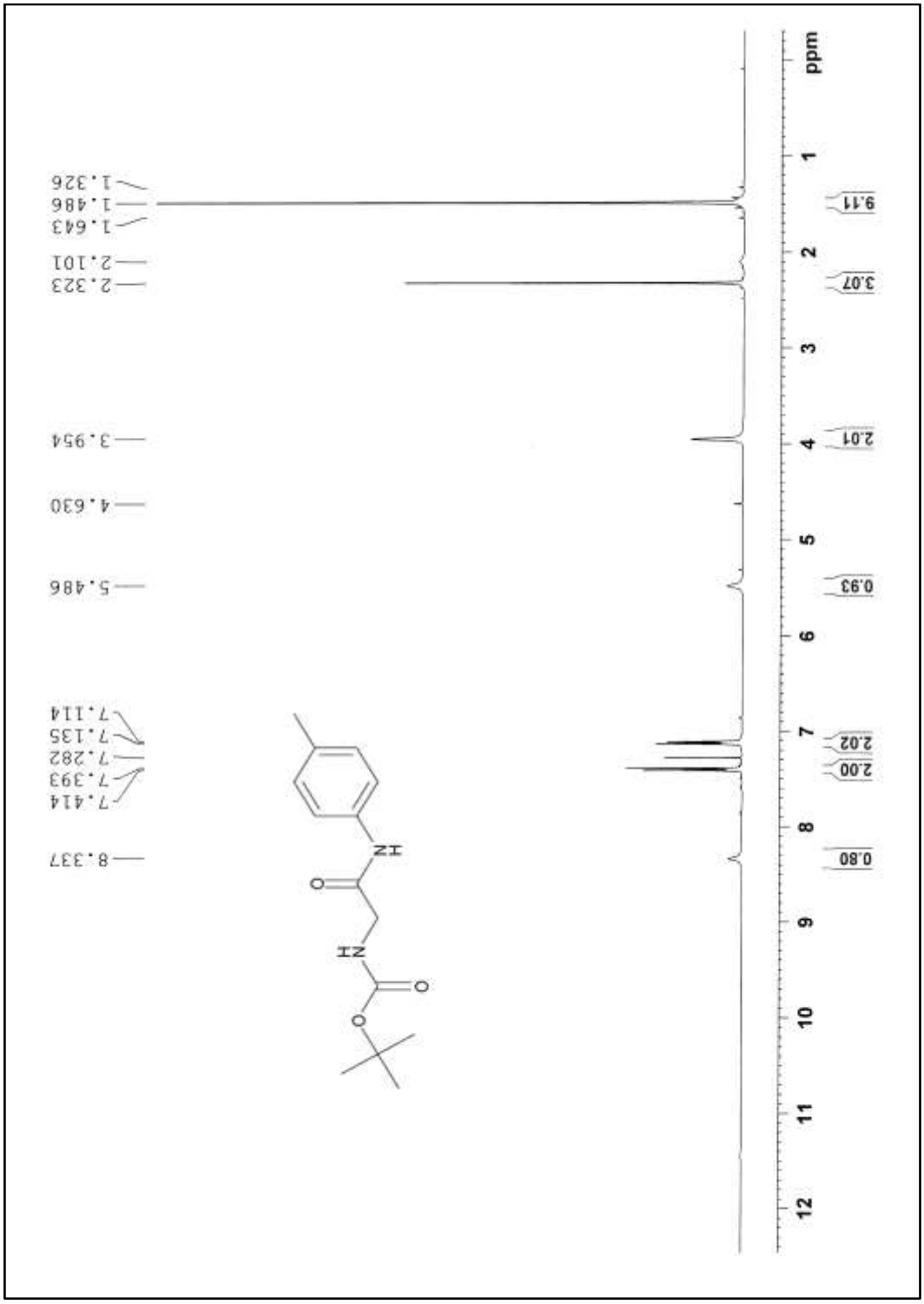

Figure 5.5.2: ^{1}H NMR spectrum of *tert*-butyl 2-oxo-2-(p-tolylamino)ethylcarbamate **5c**

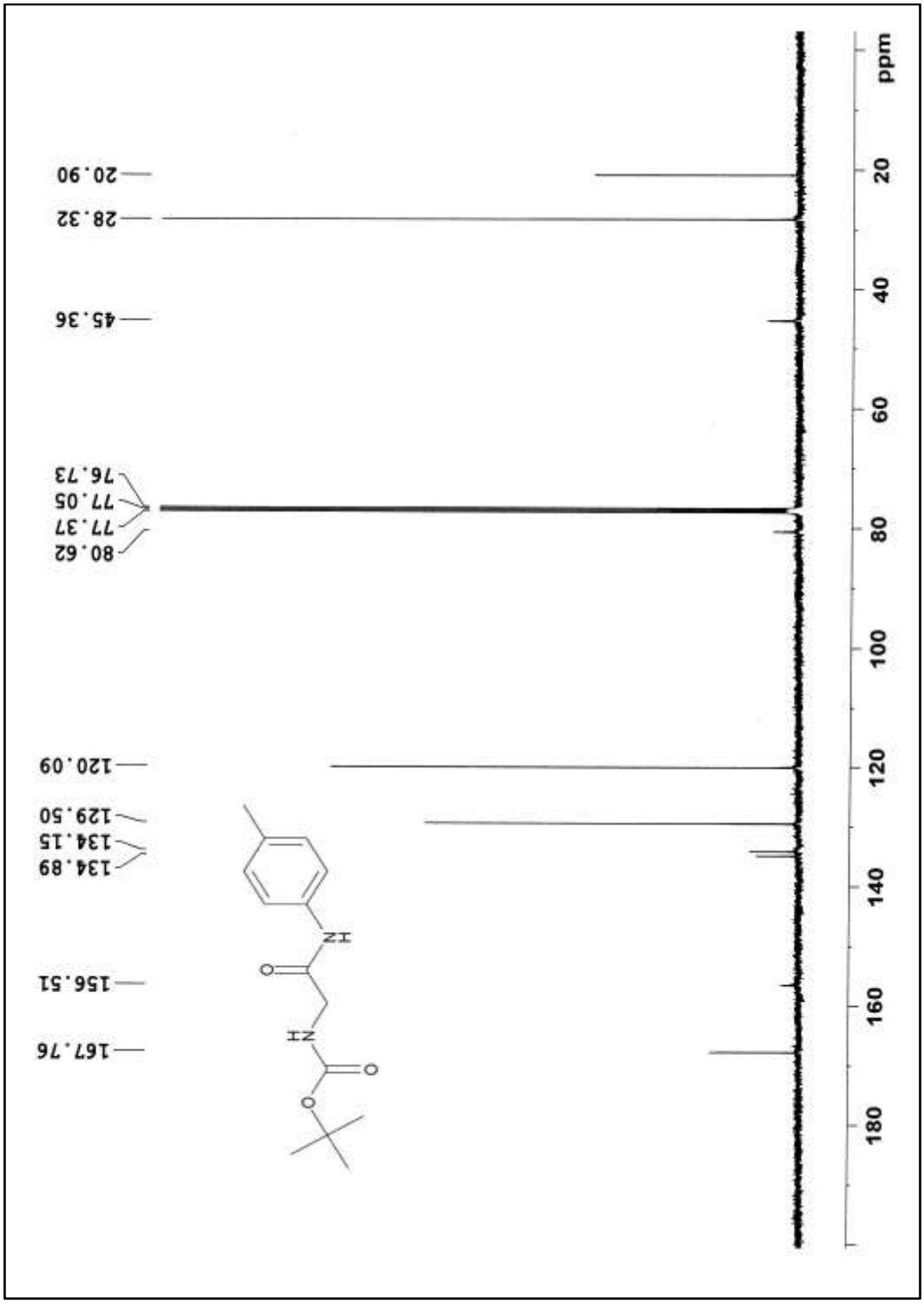

Figure 5.5.3: ^{13}C NMR spectrum of *tert*-butyl 2-oxo-2-(p-tolylamino)ethylcarbamate **5c**

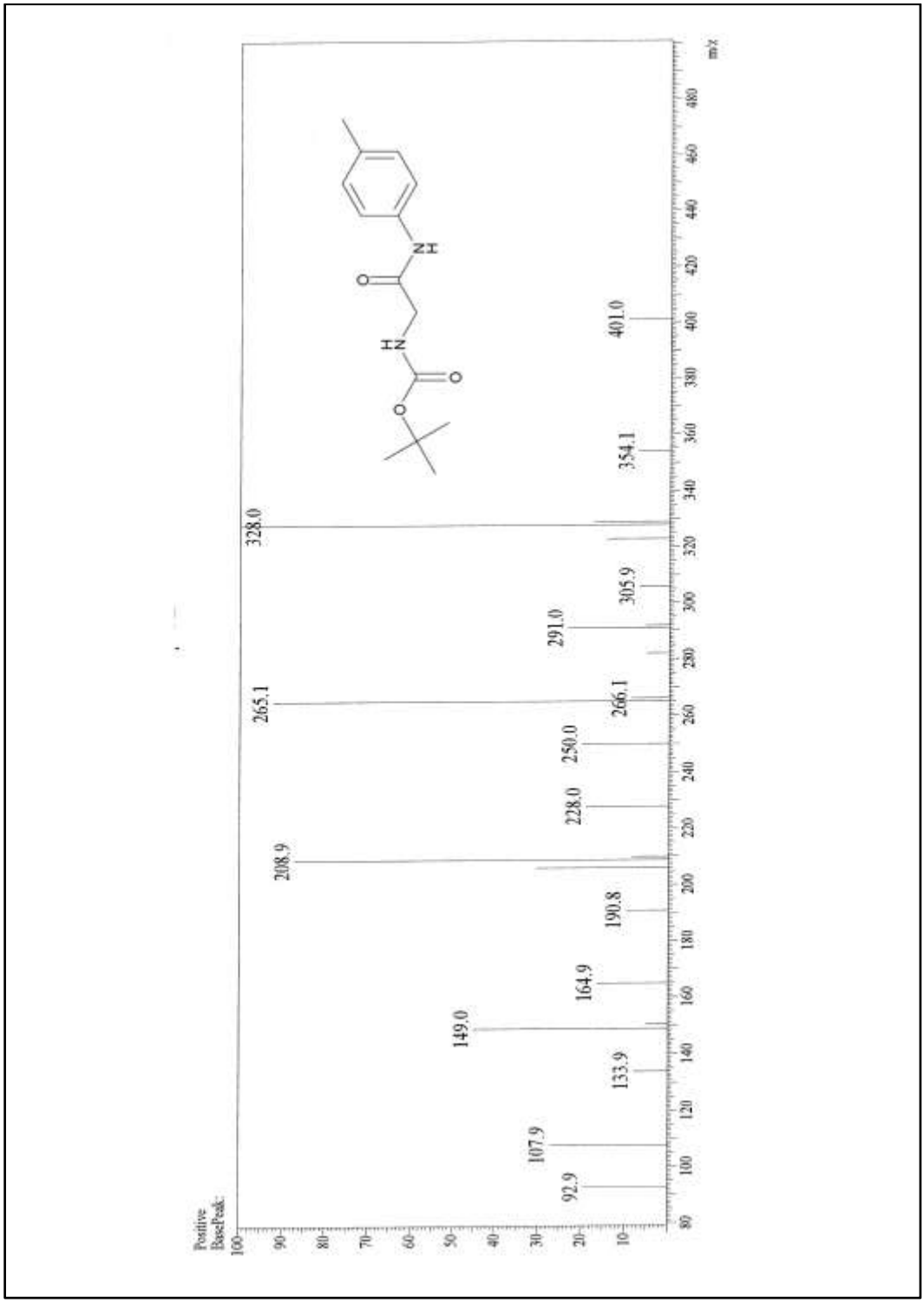

Figure 5.5.4: ESI-MS spectrum of *tert*-butyl 2-oxo-2-(p-tolylamino)ethylcarbamate **5c**

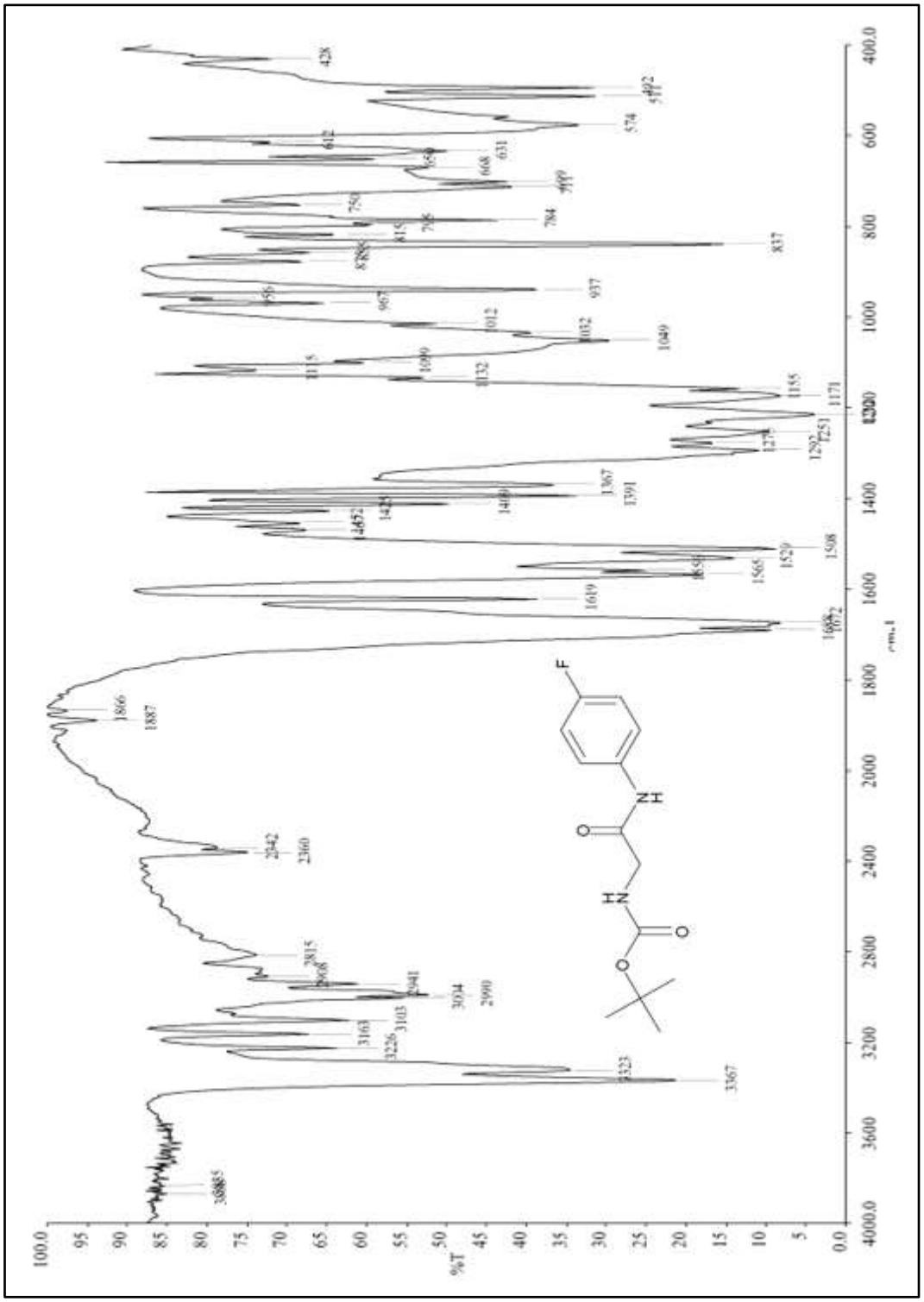

Figure 5.6.1: IR spectrum of *tert*-butyl 2-(4-fluorophenylamino)-2-oxoethylcarbamate **5d**

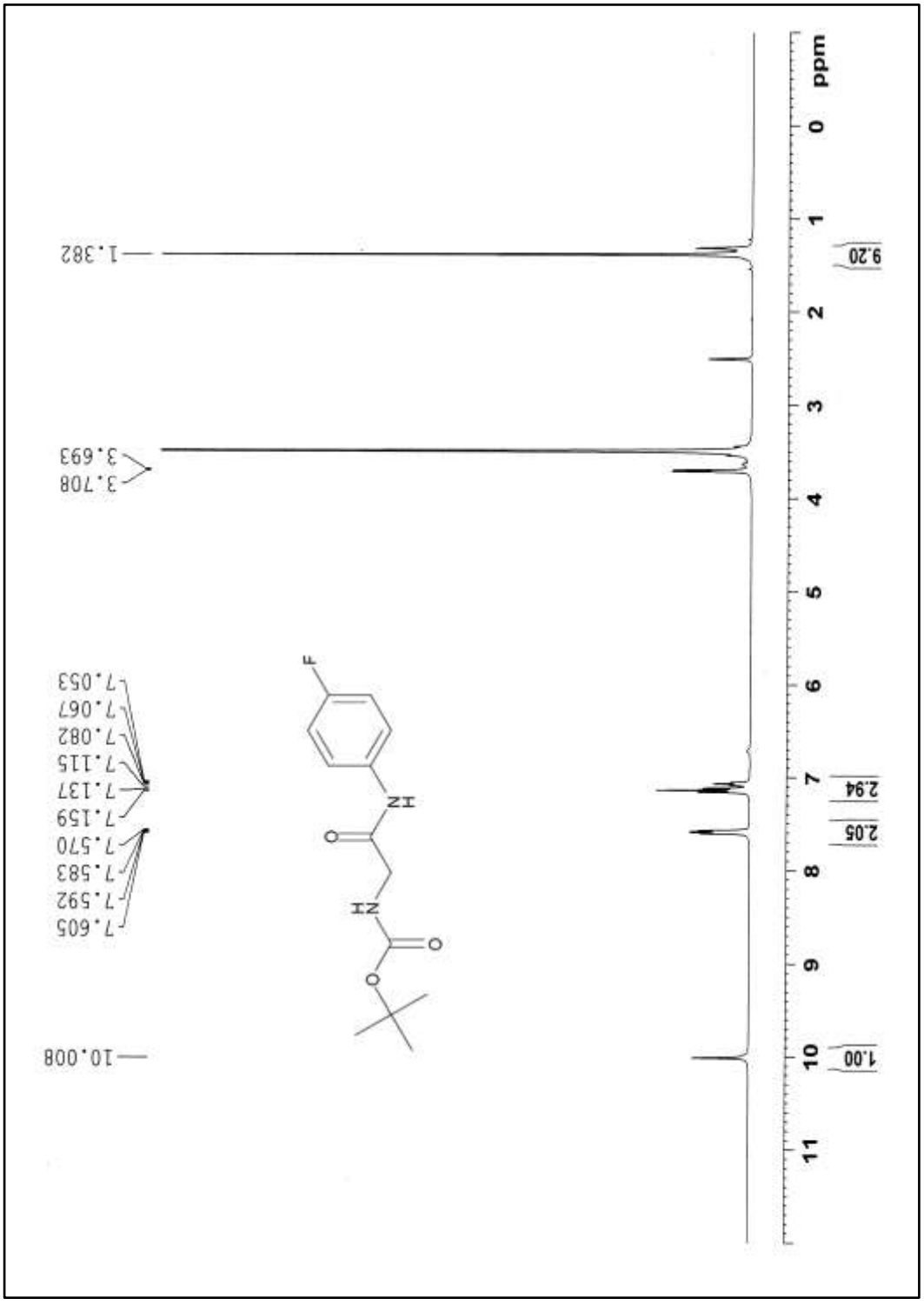

Figure 5.6.2: ^{1}H NMR spectrum of *tert*-butyl 2-(4-fluorophenylamino)-2-oxoethylcarbamate **5d**

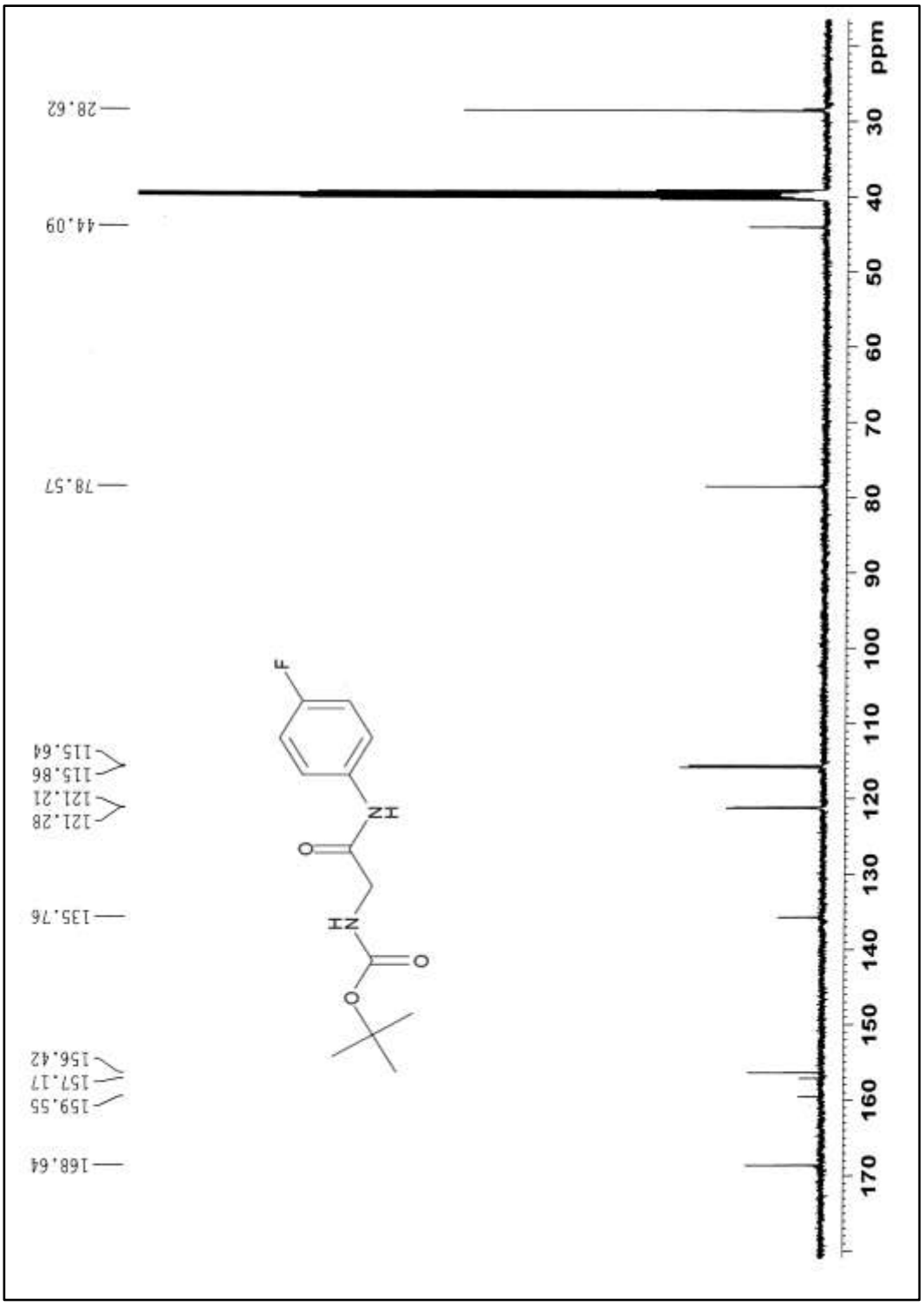

Figure 5.6.3: ^{13}C NMR spectrum of *tert*-butyl 2-(4-fluorophenylamino)-2-oxoethylcarbamate **5d**

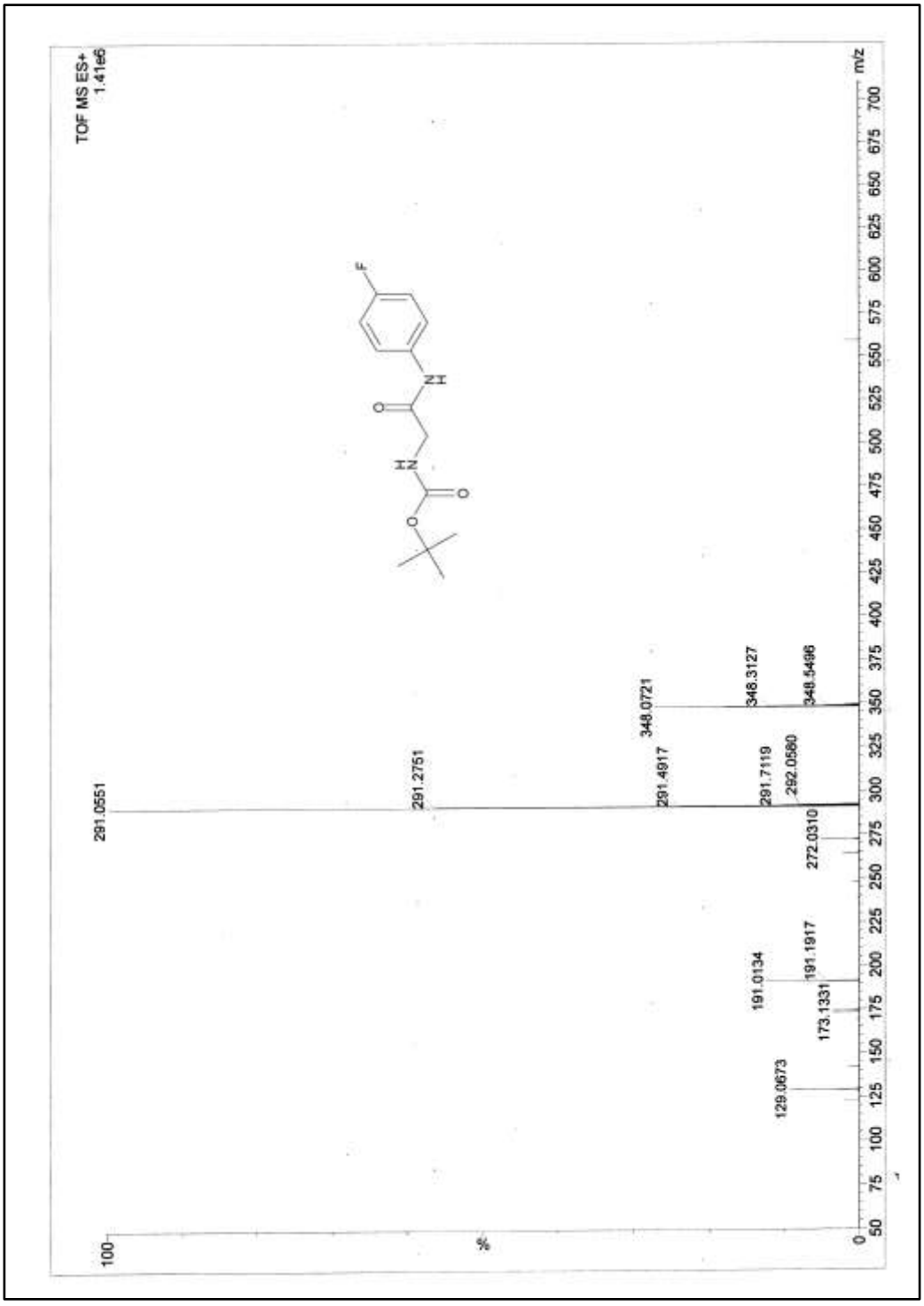

Figure 5.6.4: ESI-MS spectrum of *tert*-butyl 2-(4-fluorophenylamino)-2-oxoethylcarbamate **5d**

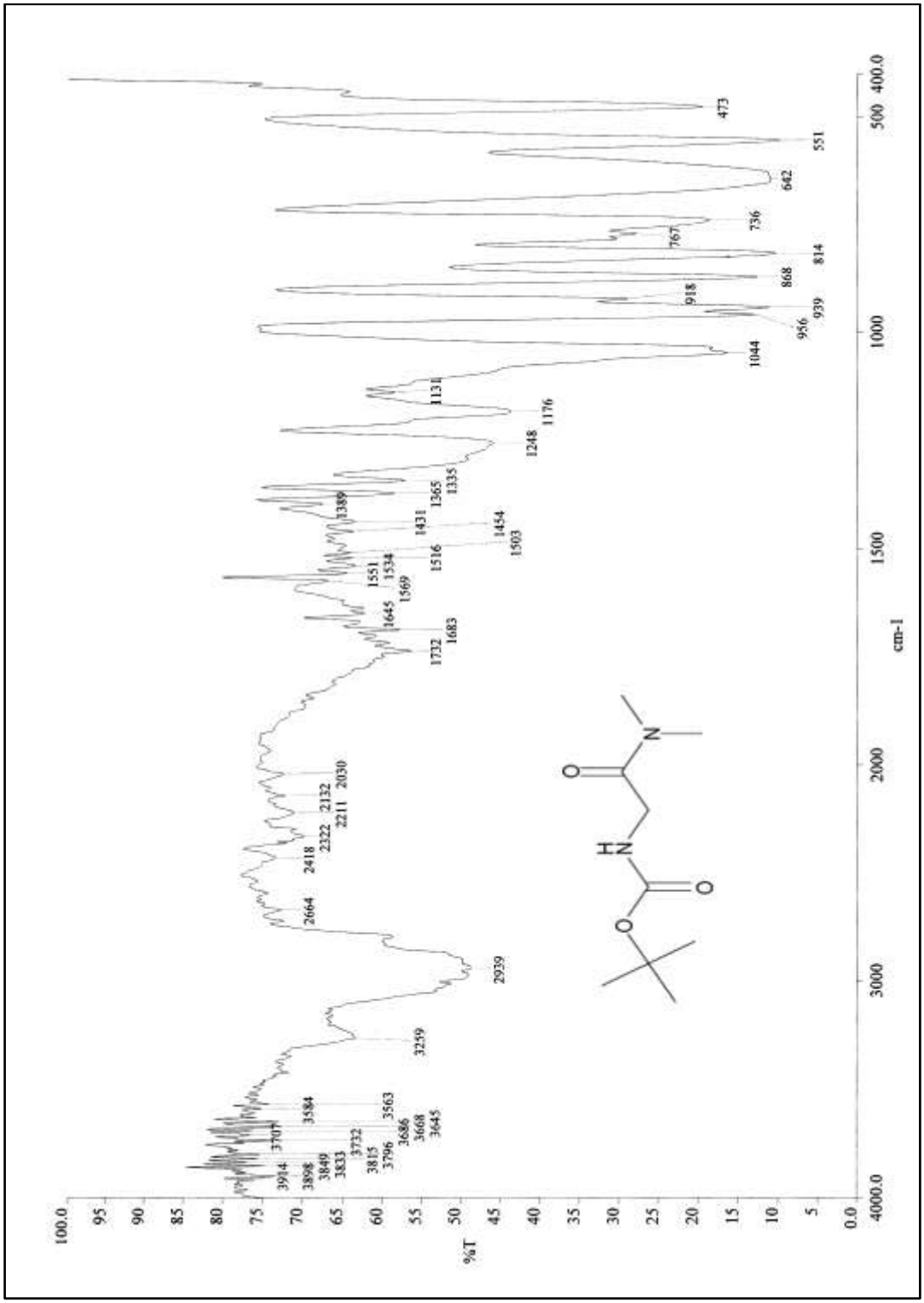

Figure 5.7.1: IR spectrum of *tert*-butyl 2-(dimethylamino)-2-oxoethylcarbamate **5e**

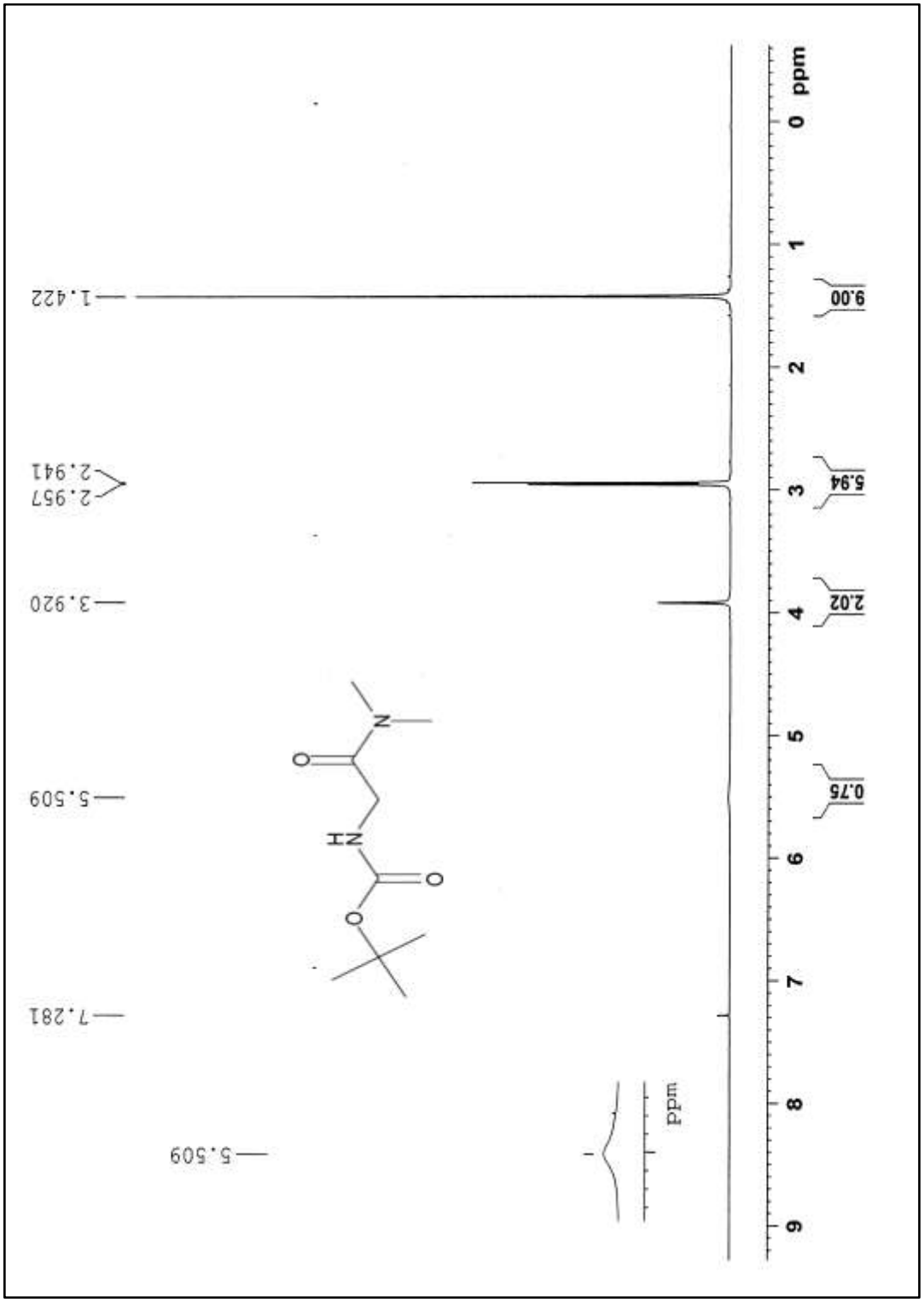

Figure 5.7.2: ^{1}H NMR spectrum of *tert*-butyl 2-(dimethylamino)-2-oxoethylcarbamate **5e**

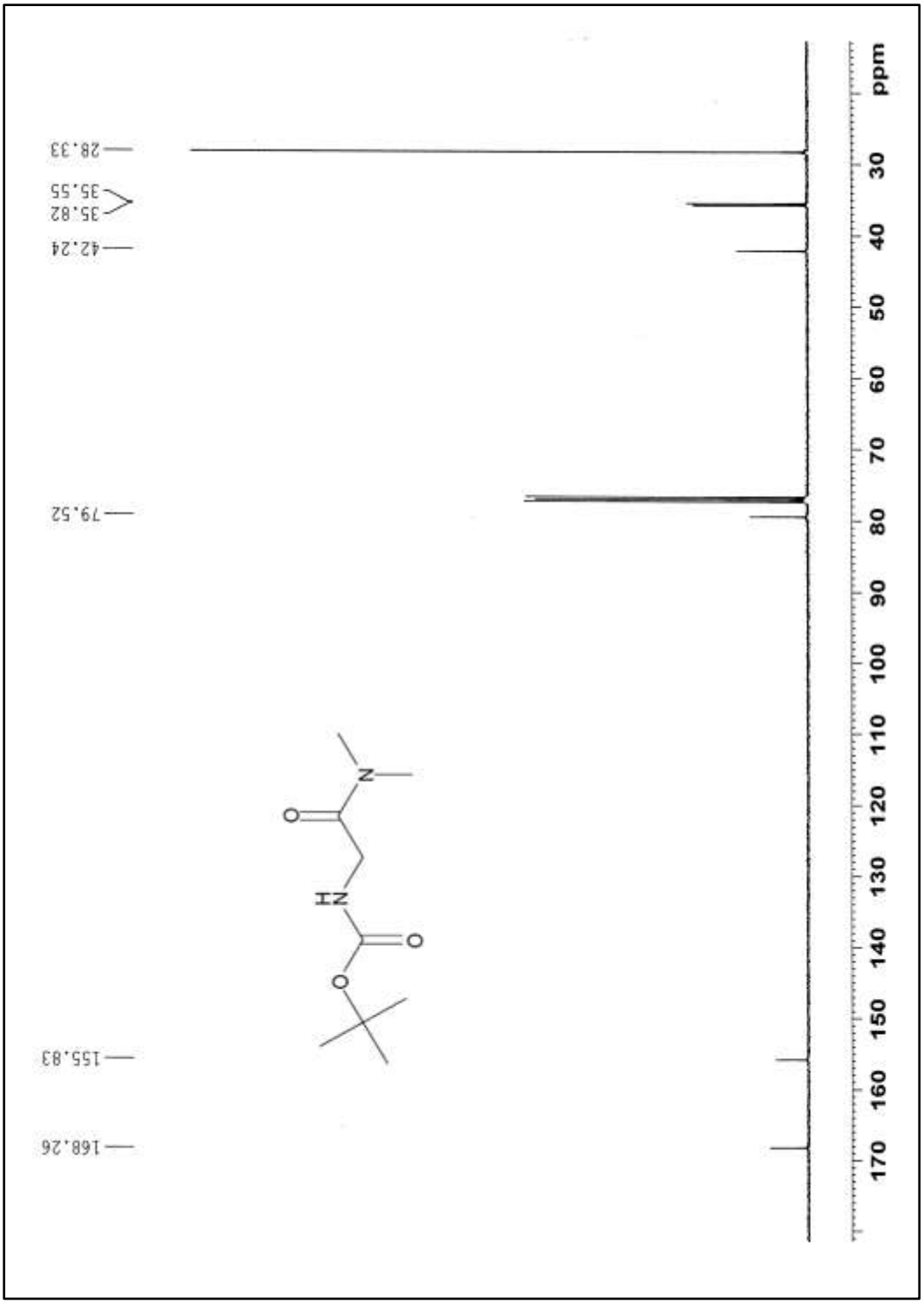

Figure 5.7.3: ^{13}C NMR spectrum of *tert*-butyl 2-(dimethylamino)-2-oxoethylcarbamate **5e**

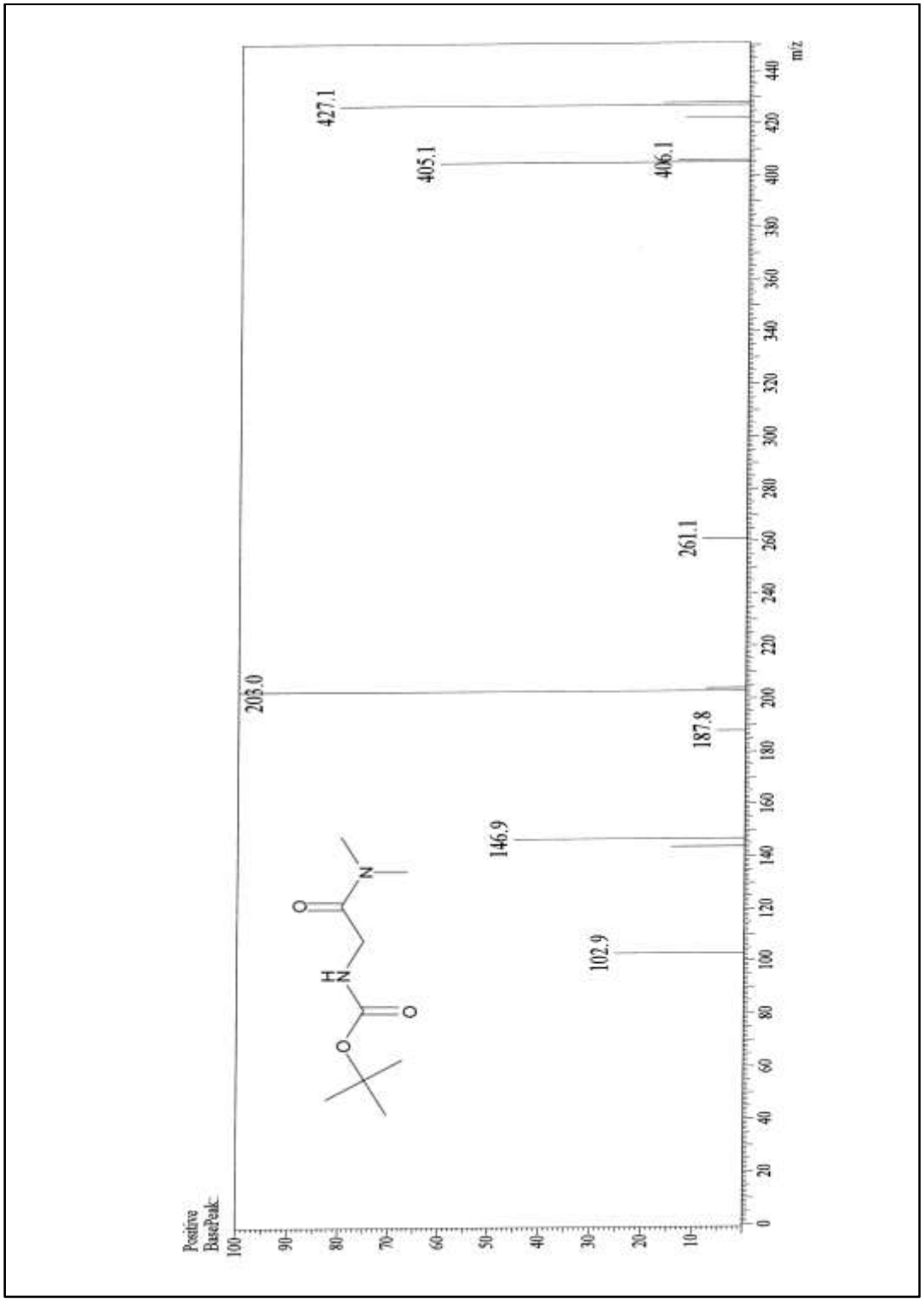

Figure 5.7.4: ESI-MS spectrum of *tert*-butyl 2-(dimethylamino)-2-oxoethylcarbamate **5e**

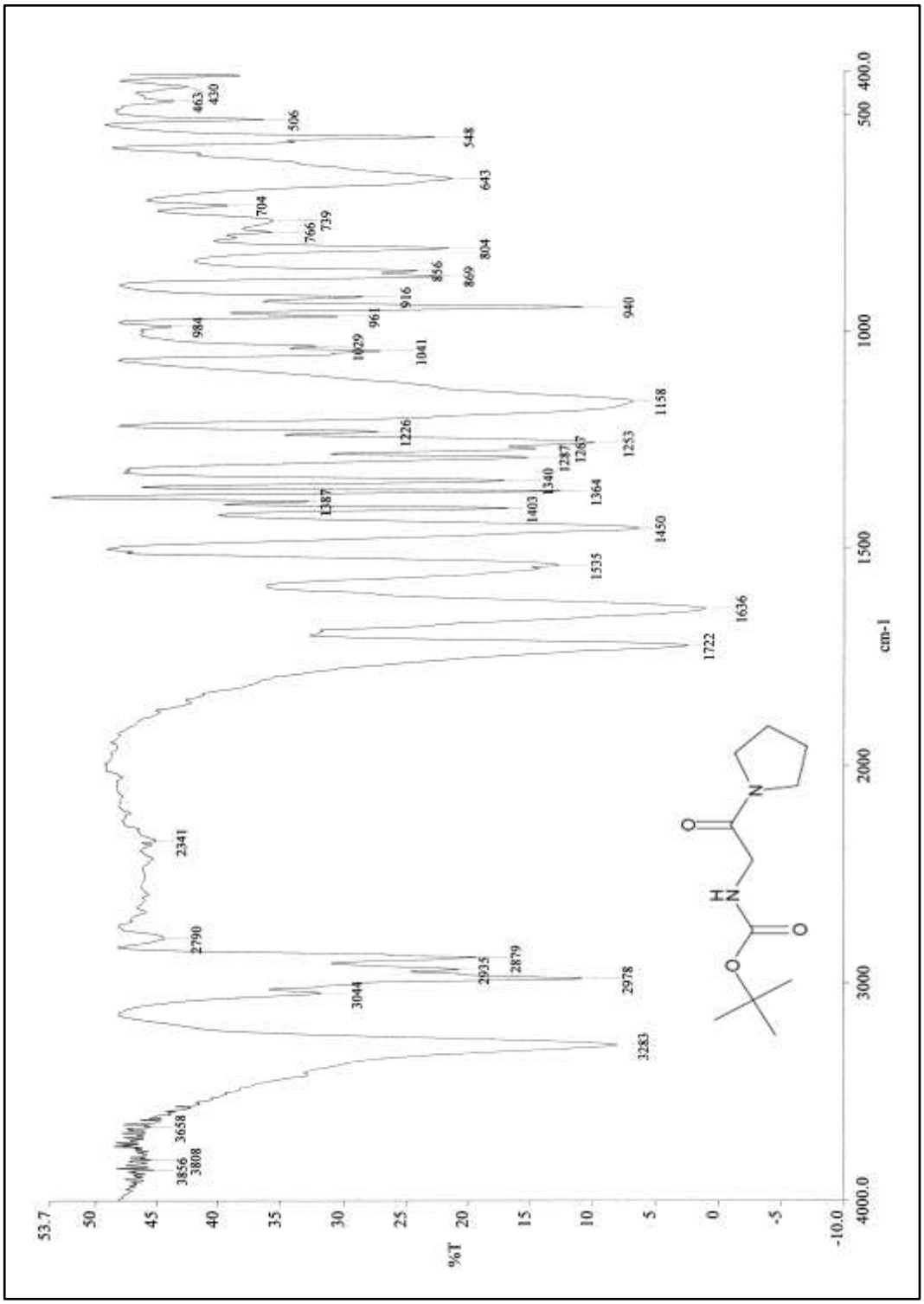

Figure 5.8.1: IR spectrum of *tert*-butyl 2-oxo-2-(pyrrolidin-1-yl)ethylcarbamate **5f**

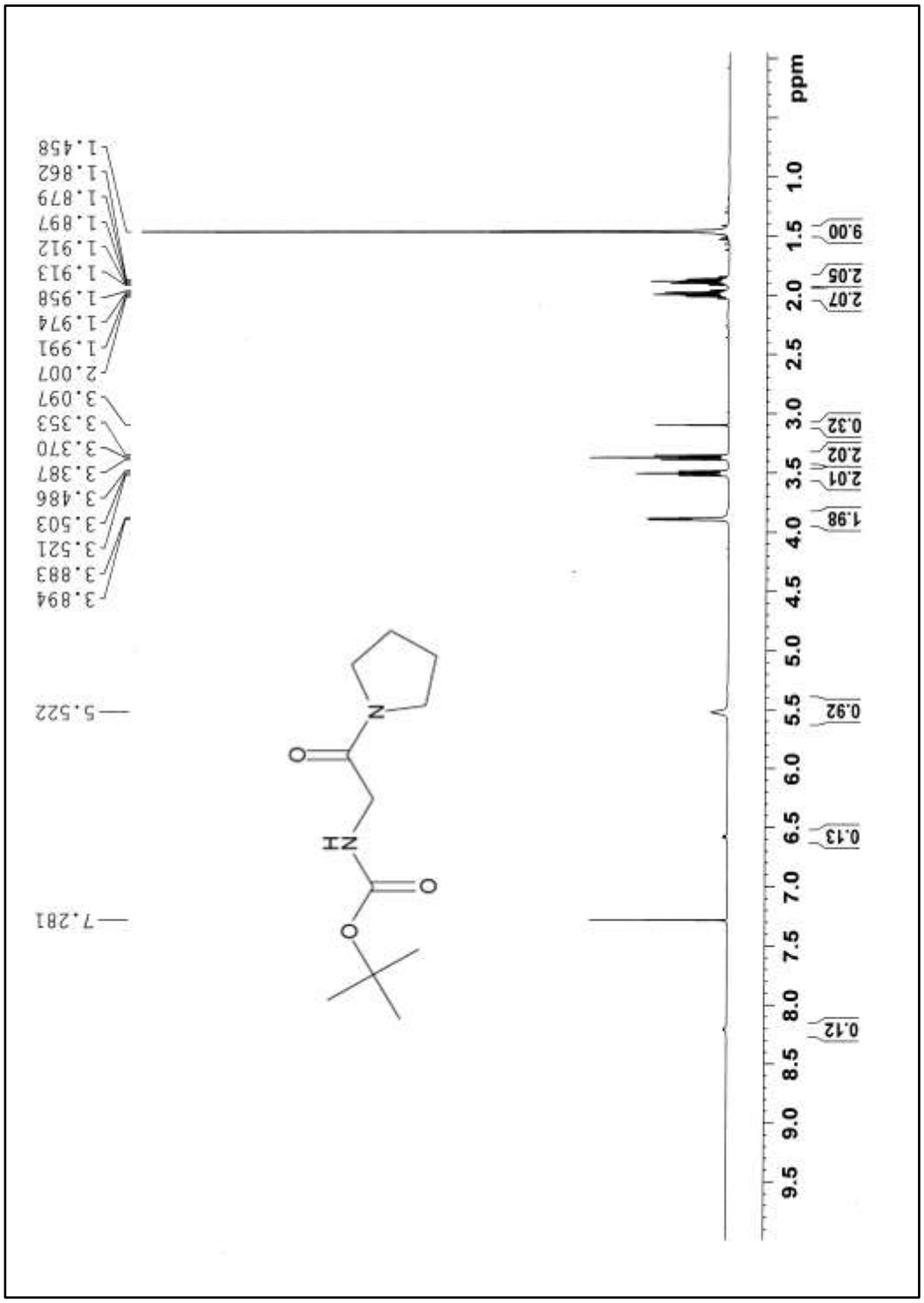

Figure 5.8.2: ^{1}H NMR spectrum of *tert*-butyl 2-oxo-2-(pyrrolidin-1-yl)ethylcarbamate **5f**

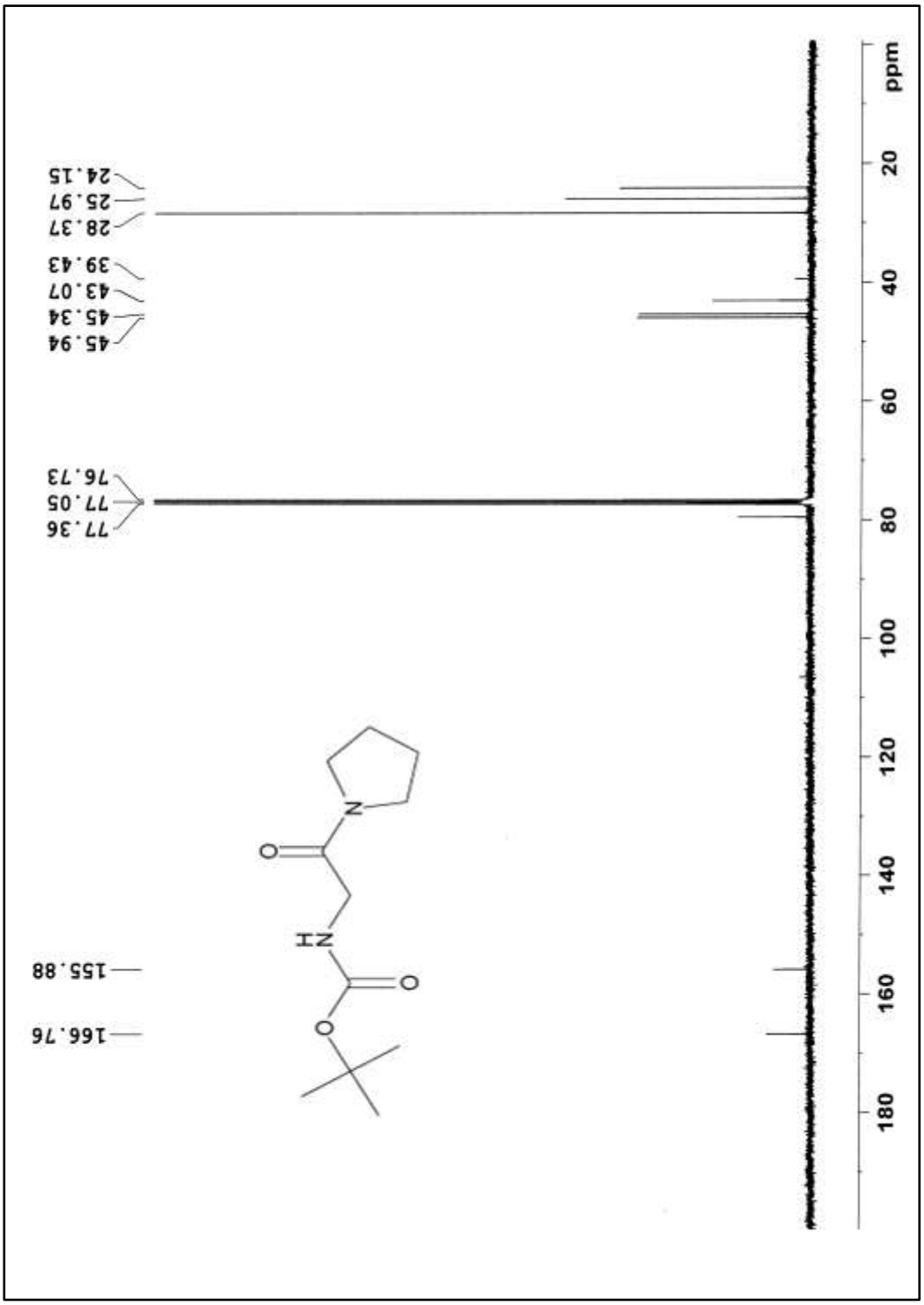

Figure 5.8.3: ^{13}C NMR spectrum of *tert*-butyl 2-oxo-2-(pyrrolidin-1-yl)ethylcarbamate **5f**

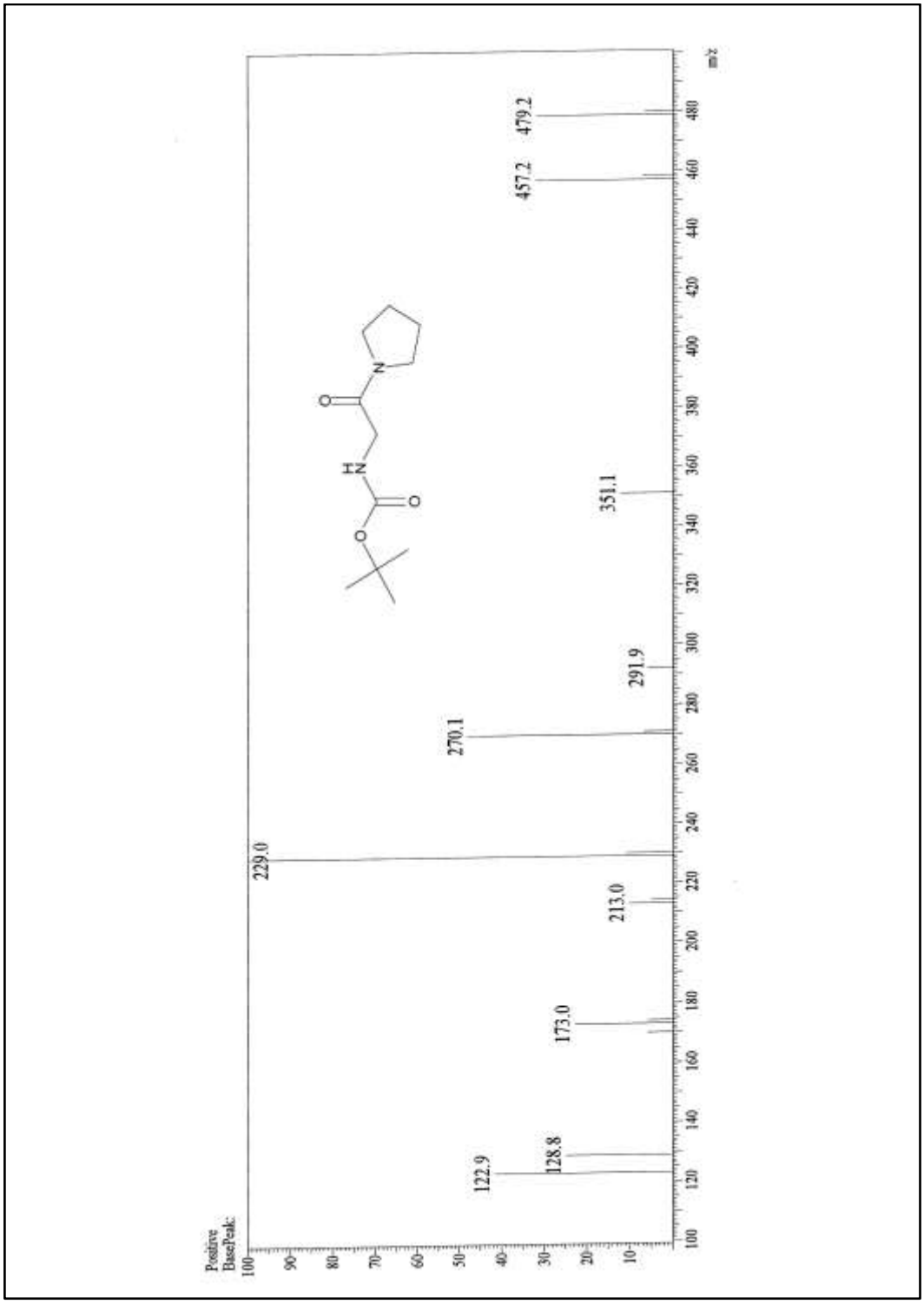

Figure 5.8.4: ESI-MS spectrum of *tert*-butyl 2-oxo-2-(pyrrolidin-1-yl)ethylcarbamate **5f**

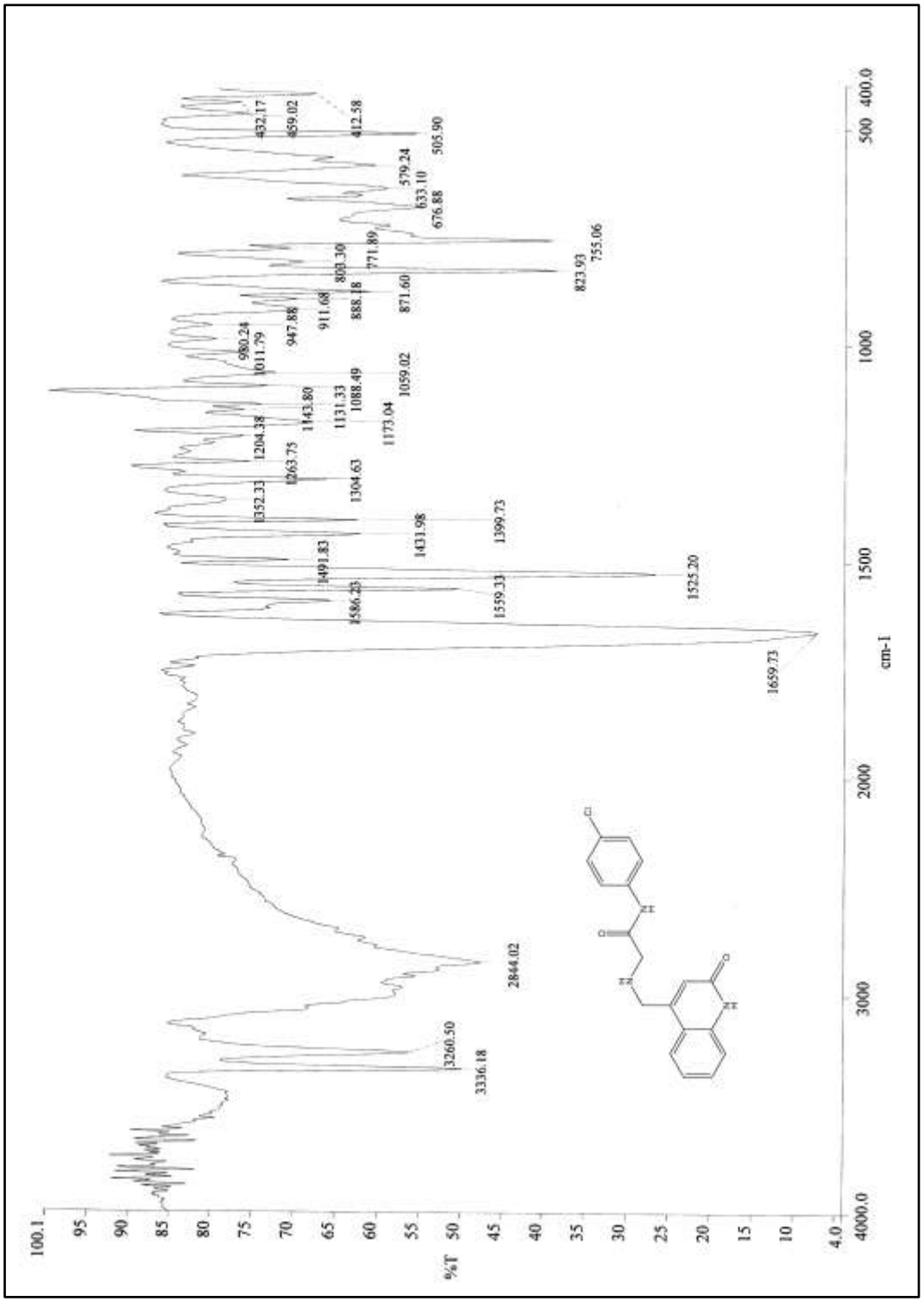

Figure 5.9.1: IR spectrum of N-(4-chlorophenyl)-2-((2-oxo-1,2-dihydroquinolin-4-yl)methylamino)acetamide **7a**

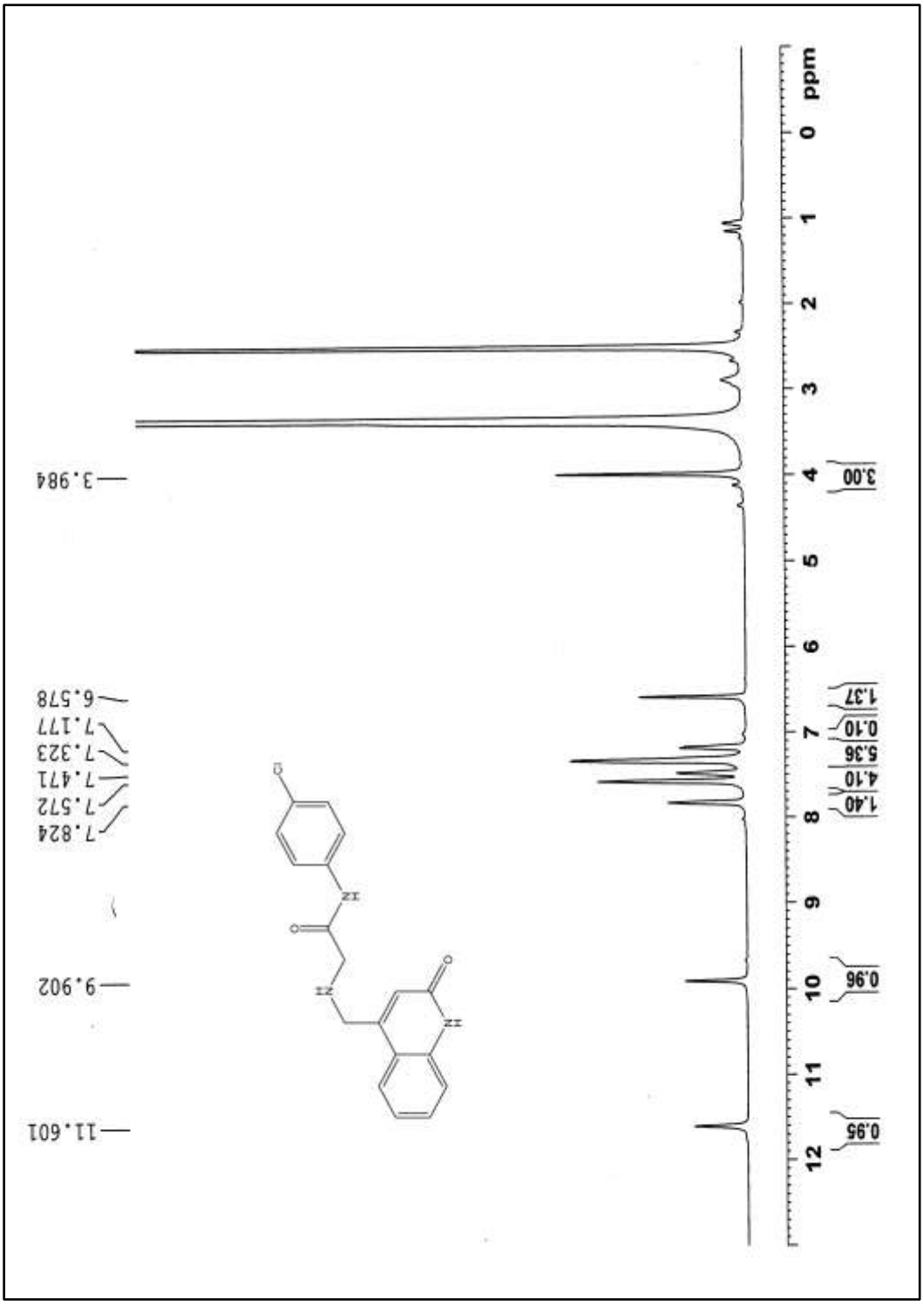

Figure 5.9.2: ^{1}H NMR spectrum of N-(4-chlorophenyl)-2-((2-oxo-1,2-dihydroquinolin-4-yl)methylamino)acetamide **7a**

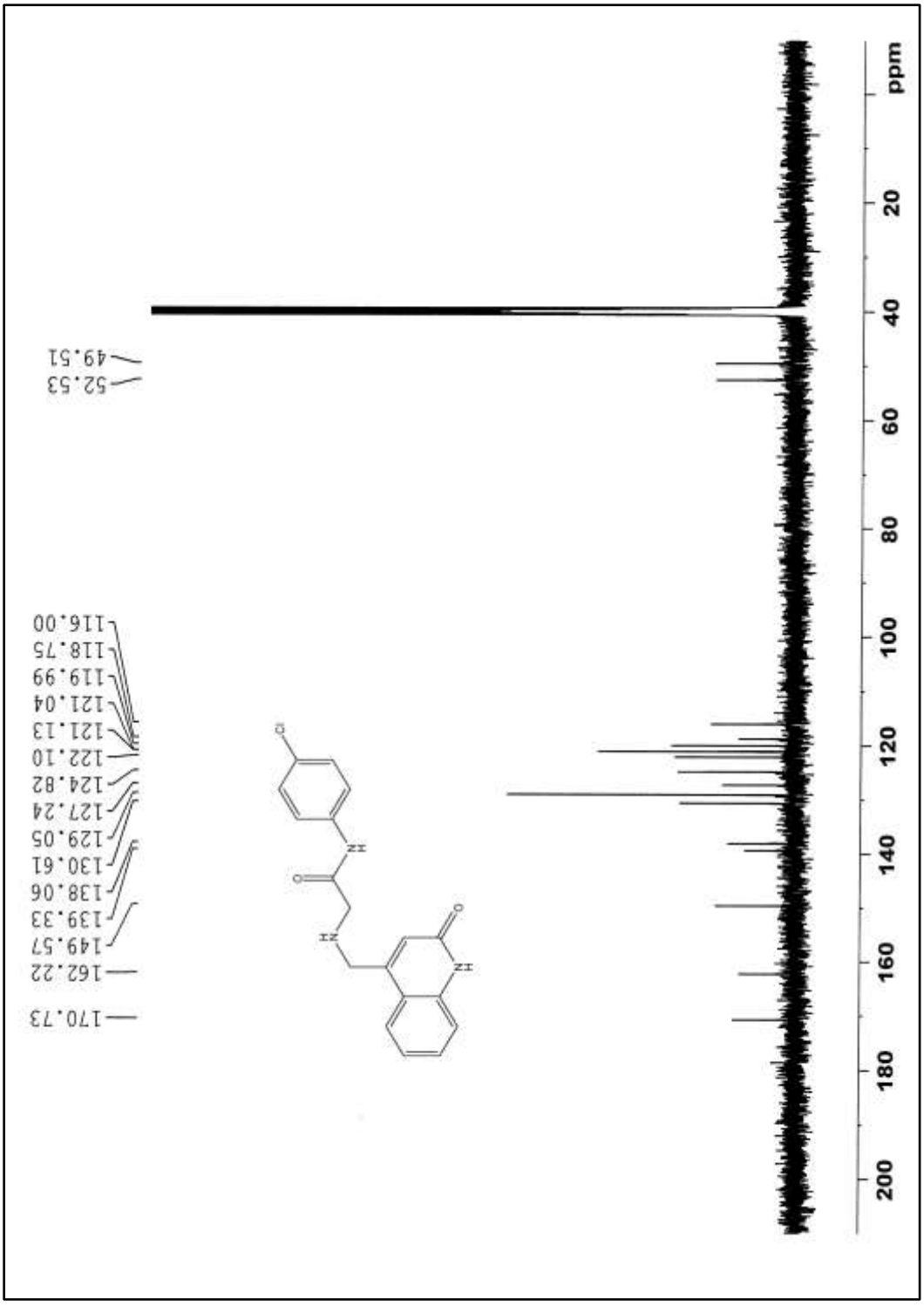

Figure 5.9.3: ^{13}C NMR spectrum of N-(4-chlorophenyl)-2-((2-oxo-1,2-dihydroquinolin-4-yl)methylamino)acetamide **7a**

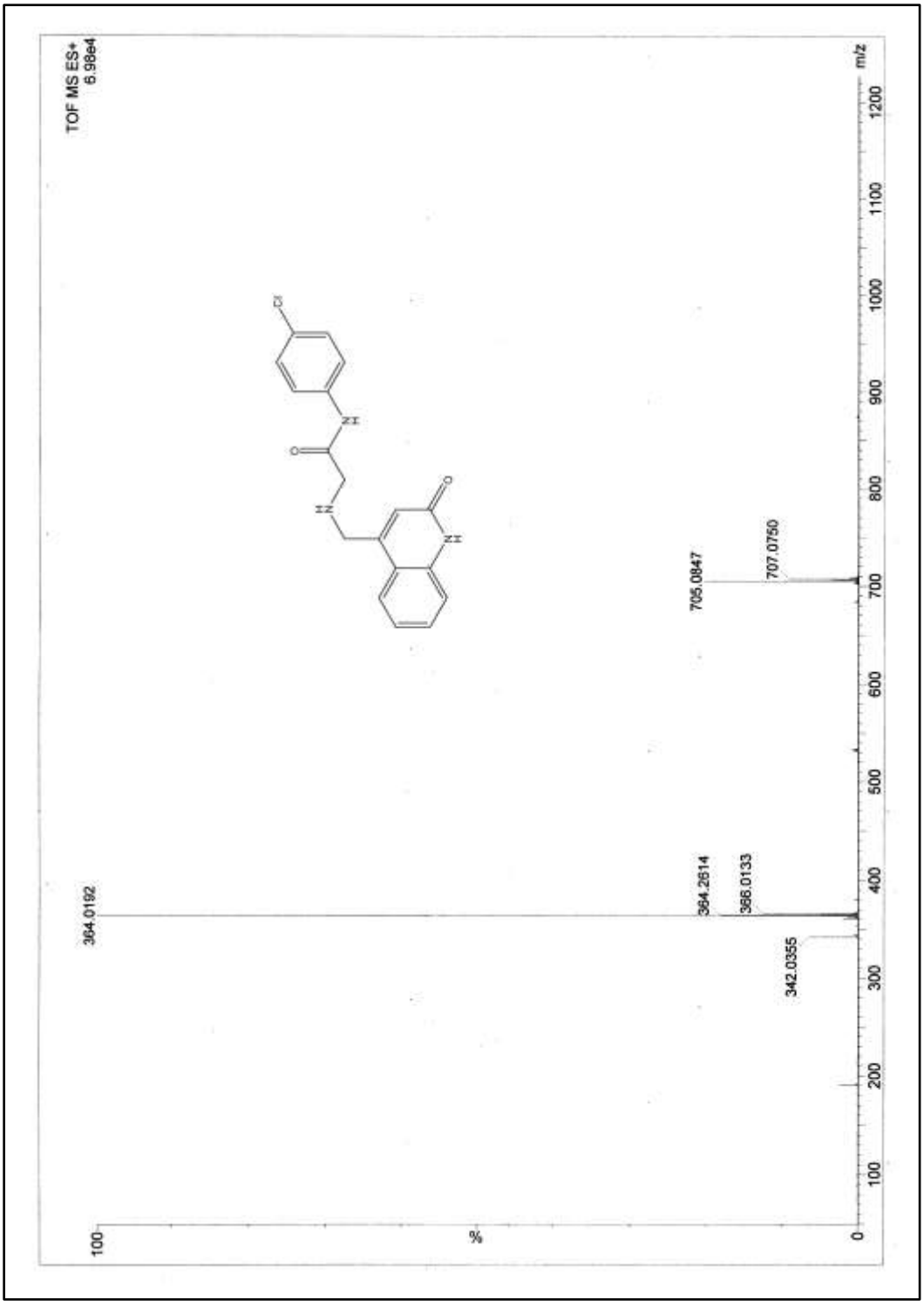

Figure 5.9.4: ESI-MS spectrum of N-(4-chlorophenyl)-2-((2-oxo-1,2-dihydroquinolin-4-yl)methylamino)acetamide **7a**

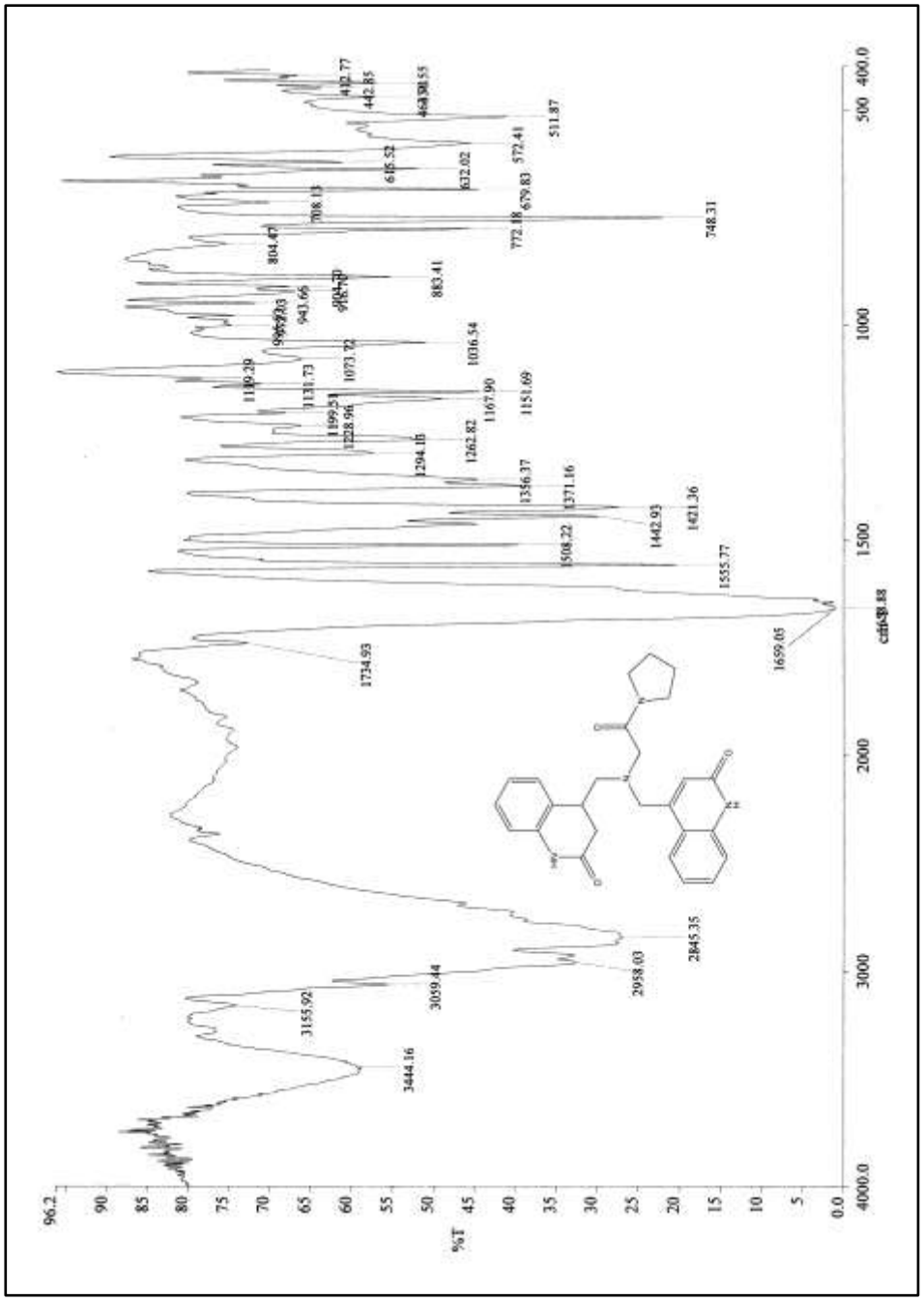

Figure 5.10.1: IR spectrum of 4,4'-(2-oxo-2-(pyrrolidin-1-yl)ethylazanediyl)bis(methylene)diquinolin-2(1H)-one **7f**

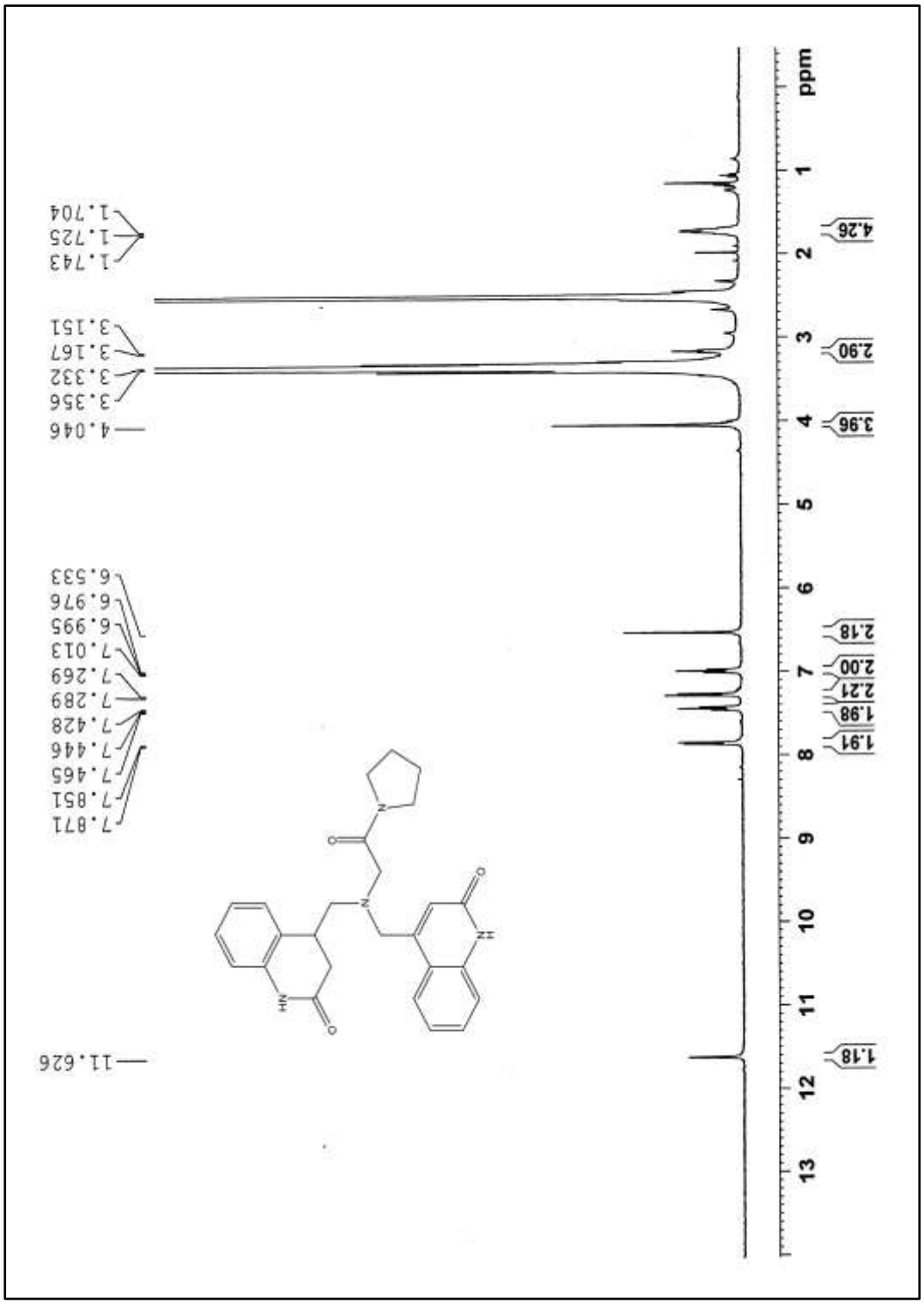

Figure 5.10.2: ^{1}H NMR spectrum of 4,4'-(2-oxo-2-(pyrrolidin-1-yl)ethylazanediyl)bis(methylene)diquinolin-2(1H)-one **7f**

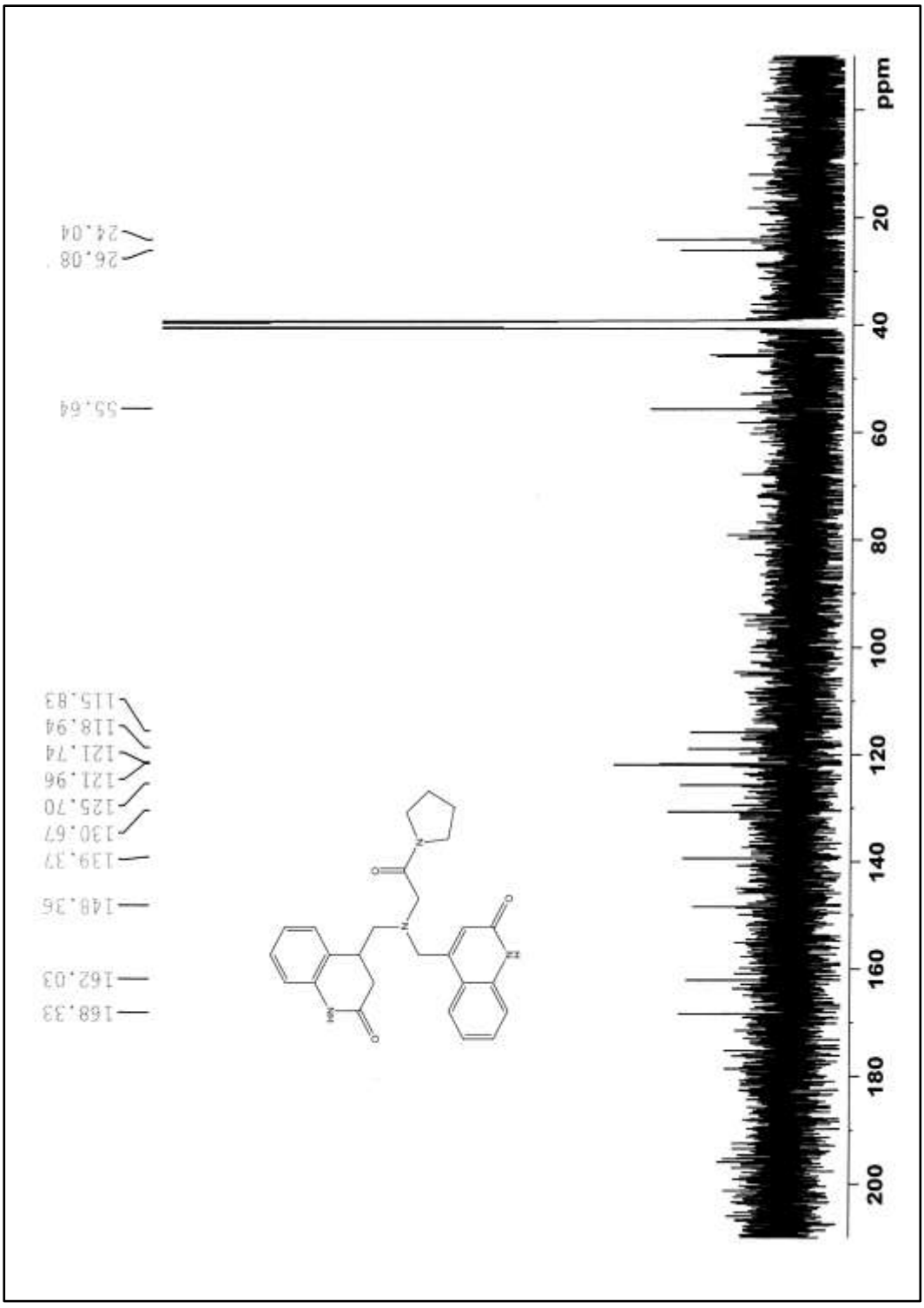

Figure 5.10.3: ^{13}C NMR spectrum of 4,4'-(2-oxo-2-(pyrrolidin-1-yl)ethylazanediyl)bis(methylene)diquinolin-2(1H)-one **7f**

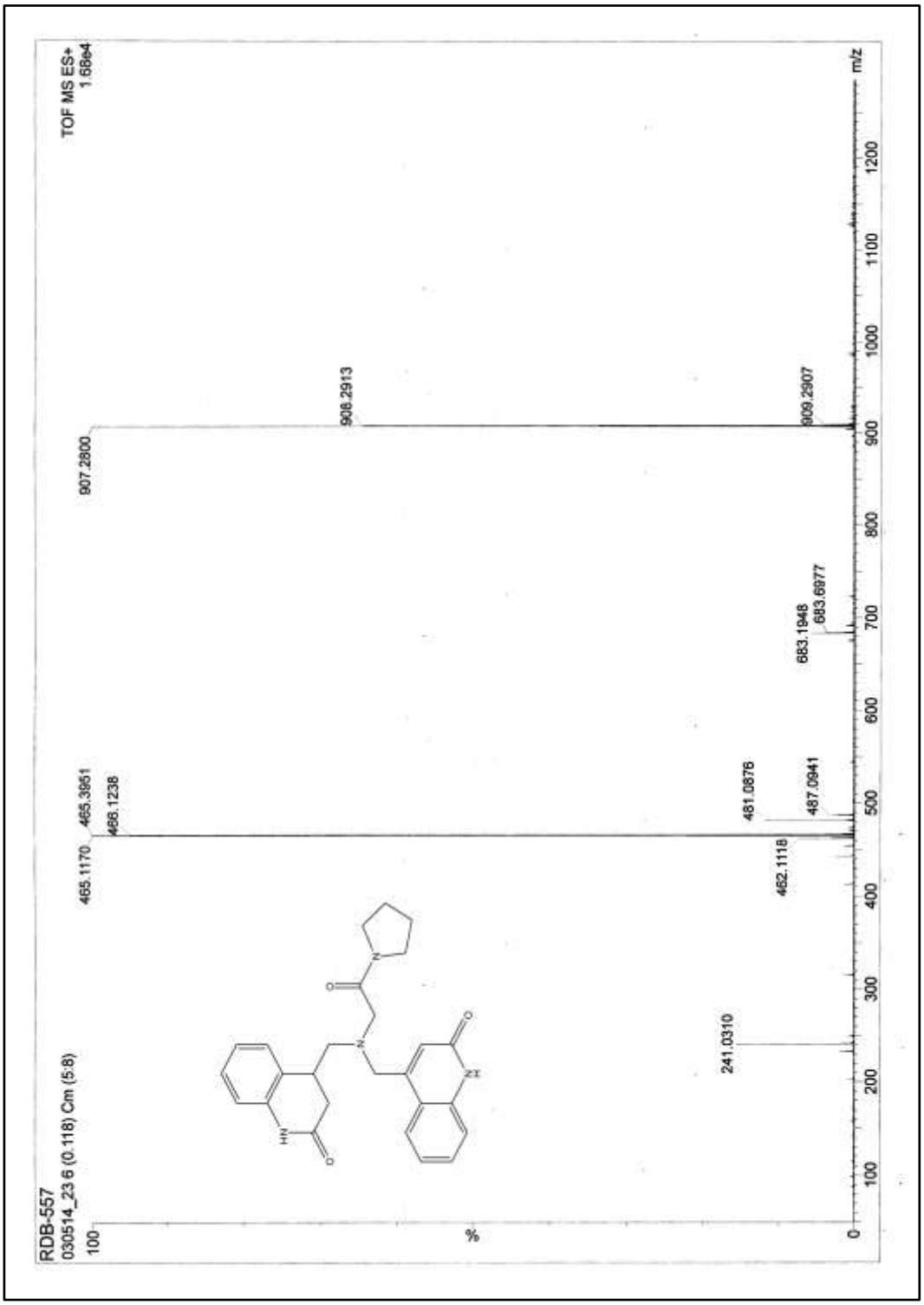

Figure 5.10.4: ESI-MS spectrum of 4,4'-(2-oxo-2-(pyrrolidin-1-yl)ethylazanediyl)bis(methylene)diquinolin-2(1H)-one **7f**

5.2.2 Biological activity

Cytotoxicity assay

For testing cytotoxicity potential of test compounds 7a-e, MTT assay was performed. In a 96 well plate A549 cells were plated (104 cells ⁄ well in 100 µL of medium) in their exponential growth phase , the cells were incubated for 24 hr. Test compounds were prepared in 1% DMSO at 2 fold concentration (12.5, 25.0, 50.0 and 100.0 µg/mL) and cells were exposed to different concentration of test compounds. Post incubation media was removed and cell were incubated with 100 µL MTT reagent (1 mg ⁄ mL) at 37 ^{o}C for 160 min. DMSO (100 µL) was used to solubilize formazan, produced by only viable cells. Plate was placed on micro-vibrator for 5 min to assist solublization; absorbance at 540nm was read by microplate reader. Percentage cytotoxicity was calculated against control (media with DMSO only) for test compounds **7a-e.** The results are shown in Figure 5.10.

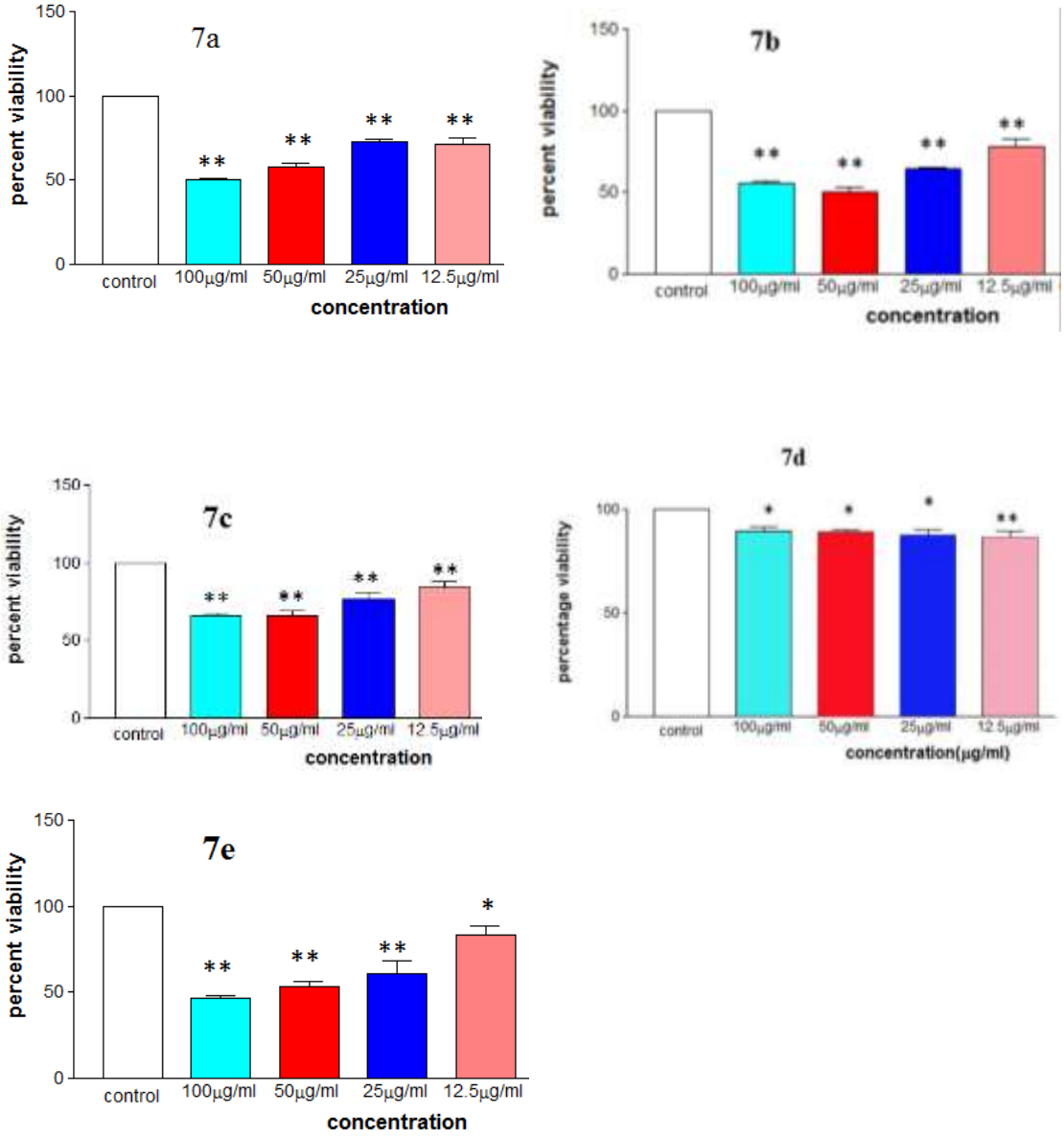

Data expressed as mean ± S.E.M. for n=3.
***P<0.05, **P<0.01, ***P<0.001 and ns = not significant compared to DMSO (control)**

Figure 5.10: MTT assay of compounds **7a-e**.

5.3 Conclusion

From the MTT assay it can be concluded that amongst the test compounds **7a-e**, *para*-substituted aniline derivatives showed good cytotoxicity of which *p*-bromo aniline derivative **7b** is the most toxic while the aliphatic dimethyl amine derivative **7e** is the most potent anti-cancer agent in the series.

5.4 Experimental

Reagent grade chemicals and solvents were purchased from commercial supplier and used after purification. TLC was performed on silica gel F254 plates (Merck). Acme's silica gel (60-120 mesh) was used for column chromatographic purification. Melting points are uncorrected and were measured in open capillary tubes, using a Rolex melting point apparatus. IR spectra were recorded as KBr pellets on Perkin Elmer RX 1 spectrometer. ^{1}H NMR and ^{13}C NMR spectral data were recorded on Advance Bruker 400 spectrometer (400 MHz) with $CDCl_3$ or DMSO-d_6 as solvent and TMS as internal standard. *J* values are in Hz. Mass of the compounds were determined by ESI-MS, using a Shimadzu LCMS 2020 apparatus. All reactions were carried out under nitrogen condition.

General method for the preparation of 4-(bromomethyl)quinolin-2(1H)-one 3:

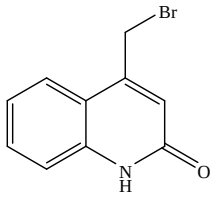

To a solution of acetoacetanilide **1** (0.056 mmol) in glacial acetic acid (10 mL) containing catalytic amount of iodine, bromine (0.056 mmol) in glacial acetic acid (30 mL) was added at 0-5 ^{o}C, over a period of 30 minutes and then the reaction mixture was stirred at room temperature till the completion of reaction as monitored on TLC. On completion of reaction, it was poured onto crushed ice and the solid thus separated was filtered and washed with cold water several times and dried to yield 3-oxo-3-(phenylamino)propanoyl bromide **2**. A solution of compound **2** (1 g) in conc. H_2SO_4 (2 mL) on heating at 90-100 ^{o}C for 2 hours, poured into crushed ice, gave

crude product which on recrystallization from absolute ethanol gave, off-white fluffy mass of 4-(bromomethyl)quinolin-2(1H)-one **3**.

Yield: 65%; off-white solid; m.p.: 258-260 ^{o}C [Lit. 258-260 ^{o}C]; IR (KBr): 3316, 3141,3098, 3017, 2968, 2891, 2856, 2742, 1669, 1616, 1552, 1511, 1473, 1435, 1403, 1267, 1206, 1145, 1130, 982, 899, 881, 750, 585 cm $^{-1}$; ^{1}H NMR (400 MHz, DMSO-d_6): δ 4.90 (s, 2H), 6.74 (s, 1H), 7.24 (t, 1H, *J* = 7.6 Hz), 7.34 (d, 1H, *J* = 8.0 Hz), 7.53 (t, 1H, *J* = 7.2 Hz), 7.84 (d, 1H, *J* = 8.0 Hz), 11.86 (s, 1H); ^{13}C NMR (400 MHz, DMSO-d_6): δ 59.96, 116.14, 117.19, 117.89, 122.33, 124.17, 130.78, 131.22, 138.92, 147.32, 152.34, 162.37; $C_{10}H_8BrNO$; ESI-MS: *m/z* 237.8 $[M]^+$ and 239.8 $[M+2]^+$.

General procedure for the preparation of compounds 5a-f:

A mixture of boc-glycine **4** (1.11 mmol), 1-ethyl-3-(3-dimethylaminopropyl)carbodiimide hydrochloride (1.67 mmol) (EDCI), 1-hydroxybenzotriazole (1.11 mmol) (HOBt), 4-dimethylaminopyridine (1.34mmol) (DMAP) and amine (1^0 and 2^0) (1.22 mmol) in dichloromethane (50 mL) (DCM) was stirred at room temperature for 16 hours. The reaction was monitored using TLC. On completion of the reaction, it was washed with water (2X20 mL), brine (1X10 mL), dried over anhydrous sodium sulphate and the solvent was evaporated under reduced pressure to give the crude product which was then purified by column chromatography using silica gel, employing methanol in dichloromethane (5:95) as eluent to yield desired product as white solid **5a-f**.

tert-butyl 2-(4-chlorophenylamino)-2-oxoethylcarbamate 5a:

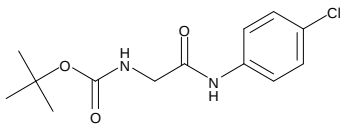

Yield: 70%; white solid; m.p.: 182-184 ^{o}C; IR (KBr): 3370, 3320, 3204, 3136, 2999, 2968, 2938, 1681, 1673, 1613, 1555, 1520, 1492, 1403, 1391, 1290, 1247, 1180, 1163, 1087, 935, 831, 725 cm $^{-1}$; ^{1}H NMR (400 MHz, DMSO-d_6): δ 1.39 (s, 9H), 3.71 (d, 2H, *J* = 6.4 Hz), 7.09 (br s, 1H), 7.36 (d, 2H, *J* = 8.8 Hz), 7.61 (d, 2H, *J* = 8.8 Hz), 10.08 (s, 1H); ^{13}C NMR (400 MHz, DMSO-d_6): δ 18.92, 28.61, 44.14, 49.05, 56.52, 78.66, 121.08, 127.20, 129.12, 138.26, 156.45, 168.91; $C_{13}H_{17}ClN_2O_3$; ESI-MS: *m/z* 307.0 $[M+Na]^+$.

tert-butyl 2-(4-bromophenylamino)-2-oxoethylcarbamate 5b:

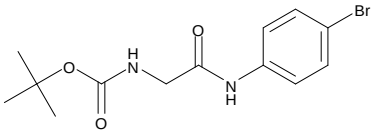

Yield : 75%; white solid; m.p.: 172-174 ^{o}C; IR (KBr) : 3372, 3320, 3281, 3204, 3134, 2996, 1678, 1611, 1545, 1523, 1491, 1391, 1290, 1246, 1180, 827 cm $^{-1}$; ^{1}H NMR (400 MHz, DMSO-d_6): δ 3.71 (m, 2H), 7.03-7.06 (m, 1H), 7.11-7.16 (m, 2H), 7.56-7.59 (m, 2H), 10.01 (s, 1H); ^{13}C NMR (400 MHz, DMSO-d_6): δ 18.92, 28.62, 44.07, 49.05, 56.52, 78.64, 115.65, 115.87, 121.25, 121.33, 135.70, 156.44, 168.65; $C_{13}H_{17}BrN_2O_3$; ESI-MS : *m/z* 350.9 $[M+Na]^+$.

tert-butyl 2-oxo-2-(p-tolylamino)ethylcarbamate 5c:

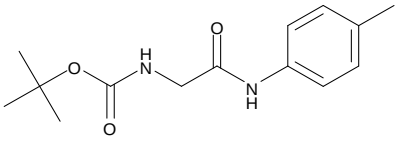

Yield: 55%; white solid; m.p.: 156-158 ^{o}C; IR (KBr): 3379, 3319, 3208, 3141, 2987, 2971, 2936, 1690, 1674, 1612, 1549, 1525, 1393, 1316, 1289, 1250, 1170, 935, 821, 729, 580, 505 cm $^{-1}$; ^{1}H NMR (400 MHz, $CDCl_3$): δ 1.49 (s, 9H), 2.22 (s, 3H), 3.95 (br s, 2H), 5.49 (br s, 1h), 7.12 (d, 2H, *J* = 8.4 Hz), 7.40 (d, 2H, *J* = 8.4 Hz), 8.34 (br s, 1H); ^{13}C NMR (400 MHz, $CDCl_3$): δ 20.90, 28.32, 45.36, 80.62, 120.09, 129.50, 134.15, 134.89, 156.51, 167.76; $C_{14}H_{20}N_2O_3$; ESI-MS: *m/z* 265.1 $[M+H]^+$.

tert-butyl 2-(4-fluorophenylamino)-2-oxoethylcarbamate 5d:

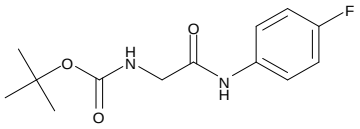

Yield: 69%; white solid; m.p.: 166-164 ^{o}C; IR (KBr): 3367, 3323, 3226, 3163, 3103, 3004, 2990, 2941, 1688, 1672, 1619, 1565, 1529, 1508, 1391, 1367, 1292, 1251, 1171, 1155, 1049, 837 cm $^{-1}$; ^{1}H NMR (400 MHz, DMSO-d_6): δ 1.38 (s, 9H), 3.70 (d, 2H, *J* = 6.0 Hz), 7.05-7.08 (m, 1H), 7.12-7.16 (m, 2H), 7.57-7.61 (m, 2H), 10.01 (s, 1H); ^{13}C NMR (400 MHz, DMSO-d_6): δ 28.62, 44.09, 78.57, 115.64, 115.86, 121.21, 121.28, 135.76, 156.42, 157.17, 159.55, 168.64; $C_{13}H_{17}FN_2O_3$; ESI-MS: *m/z* 291 $[M+Na]^+$.

tert-butyl 2-(dimethylamino)-2-oxoethylcarbamate 5e:

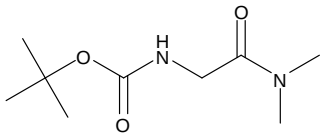

Yield: 50%; white solid; m.p.: 66-68 ^{o}C; IR (KBr): 3563, 3259, 2939, 1569, 1732, 1683, 1645, 1569, 1551, 1534, 1503, 1454, 1431, 1365, 1335, 1248, 1176, 1044, 956, 939, 868, 814, 736, 642, 551 cm $^{-1}$; ^{1}H NMR (400 MHz, $CDCl_3$): δ 1.42 (s, 9H), 2.94 (s, 3H), 2.96 (s, 3H), , 3.92 (s, 2H), 5.51 (s, 1H); ^{13}C NMR (400 MHz, $CDCl_3$): δ 28.33, 35.55, 35.82, 42.24, 79.52, 155.83, 168.26; $C_9H_{18}N_2O_3$; ESI-MS: *m/z* 203.0 $[M+H]^+$.

tert-butyl 2-oxo-2-(pyrrolidin-1-yl)ethylcarbamate 5f:

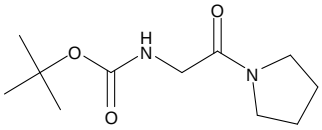

Yield: 45%; viscous liquid; IR (KBr): 3283, 3044, 2978, 2935, 2879, 1722, 1636, 1535, 1450, 1403, 1364, 1340, 1287, 1267, 1253, 1226, 1158, 1041, 940, 869, 856, 804, 766, 643, 548 cm $^{-1}$; ^{1}H NMR (400 MHz, $CDCl_3$): δ 1.46 (s, 9H), 1.86-1.91 (m, 2H), 1.96-2.01 (m, 2H), 3.37 (t, 2H, *J* = 6.8 Hz), 3.50 (t, 2H, *J* = 6.8 Hz), 3.89 (d, 2H, *J* = 4.4 Hz), 5.52 (br s, 1H); ^{13}C NMR (400 MHz, $CDCl_3$): δ 24.15, 25.97, 28.37, 39.43, 43.07, 45.34, 45.94, 155.88, 166.76; $C_{11}H_{20}N_2O_3$; ESI-MS: *m/z* 229.0 $[M+H]^+$.

General procedure for preparation of compounds 7a-e:

Compounds **5a-e** were deprotected by stirring it in a solution of 10% trifluoroacetic acid (TFA) in dichloromethane (DCM). On deprotection of amine, the solvent was evaporated under reduced pressure to give corresponding free base **6a-e** (1.1 mmol), to which a solution of compound **3** (1.0 mmol) in dimethyl formamide (DMF) was added followed by lithium hydroxide mono hydrate (2.0 mmol) and the resulting mixture was stirred at room temperature till completion of reaction, as monitored on TLC. On completion of reaction, it was poured onto crushed ice and the solid filtered, dried and recrystallized from absolute ethanol to yield product **7a-e**.

N-(4-chlorophenyl)-2-((2-oxo-1,2-dihydroquinolin-4-yl)methylamino)acetamide 7a:

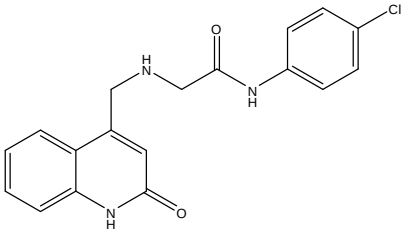

Yield: 25%; white solid; m.p.: 246-248 ^{o}C; IR (KBr): 3336, 3260, 2844, 1660, 1559, 1525, 1432, 1400, 1305, 1173, 1059, 871, 824, 755, 676, 506 cm $^{-1}$; ^{1}H NMR (400 MHz, DMSO-d_6): δ 2.8-3.0 (m, 2H), 3.98 (s, 2H), 6.58 (s, 1H), 7.18-7.82 (m, 10H), 9.90 (s, 1H), 11.60 (s, 1H); ^{13}C NMR (400 MHz, DMSO-d_6): δ 49.51, 52.53, 1116.00, 118.75, 119.99, 121.04, 121.13, 122.10, 124.82, 127.24, 129.05, 130.61, 138.06, 139.33, 149.57, 162.22, 170.73; $C_{18}H_{16}ClN_3O_2$; ESI-MS: *m/z* 364 $[M+Na]^+$.

N-(4-bromophenyl)-2-((2-oxo-1,2-dihydroquinolin-4-yl)methylamino)acetamide 7b:

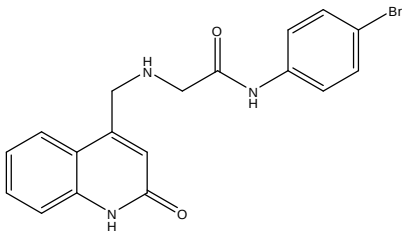

Yield: 15%; white solid; m.p.: 260 ^{o}C (decomposes); IR (KBr): 3338, 3250, 2854, 1666, 1531, 1435, 1314, 1072, 892, 818, 751cm $^{-1}$; ^{1}H NMR (400 MHz, DMSO-d_6): δ; ^{13}C NMR (400 MHz, DMSO-d_6): δ 2.8-3.0 (m, 2H), 3.98 (s, 2H), 6.58 (s, 1H), 7.07-7.93 (m, 8H), 9.72 (s, 1H), 11.67 (s, 1H); ^{13}C NMR (400 MHz, DMSO-d_6): δ 49.54, 52.57, 116.01, 118.76, 120.00, 121.15, 122.11, 124.82, 127.25, 129.05, 130.61, 138.07, 139.34, 149.57, 162.23, 170.74; $C_{18}H_{16}BrN_3O_2$; ESI-MS: *m/z* 407.9 $[M+Na]^+$.

2-((2-oxo-1,2-dihydroquinolin-4-yl)methylamino)-N-p-tolylacetamide 7c:

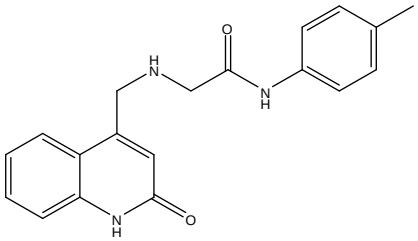

Yield: 25%; white solid; m.p.: 240-242 ^{o}C; IR (KBr): 3337, 3248, 3000, 2852, 1668, 1661, 1559, 1532, 1436, 1408, 1355, 1316, 1206, 1133, 914, 892, 817, 752, 674 cm $^{-1}$; ^{1}H NMR (400 MHz, DMSO-d_6): δ 2.08 (s, 2H), 3.99 (s, 2H), 6.58 (s, 1H), 7.07-7.91 (m, 9H), 9.71 (s, 1H), 11.67 (s, 1H); $C_{19}H_{19}N_3O_2$; ESI-MS: *m/z* 344 $[M+Na]^+$.

N-(4-fluorophenyl)-2-((2-oxo-1,2-dihydroquinolin-4-yl)methylamino)acetamide 7d:

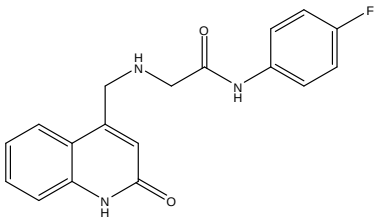

Yield: 35%; white solid; m.p.: 220 ^{o}C (decomposes); IR (KBr): 3265, 1671, 1614, 1559, 1509, 1468, 1407, 1295, 1216, 1155, 958, 836, 754, 689 cm $^{-1}$; ^{1}H NMR (400 MHz, DMSO-d_6): δ 2.5 (s, 2H), 3.97 (s, 2H), 6.58 (s, 1H), 7.06-7.84 (m, 10H), 9.92 (s, 1H), 11.75 (br s, 1H); ^{13}C NMR (400 MHz, DMSO-d_6): δ 26.04, 49.50, 115.55, 115.77, 116.06, 118.76, 119.93, 121.34, 121.42, 122.12, 124.79, 130.60, 135.59, 139.32, 149.62, 157.21, 162.29, 170.53, 174.95; $C_{18}H_{16}FN_3O_2$; ESI-MS: *m/z* 364 $[M+K]^+$.

N,N-dimethyl-2-((2-oxo-1,2-dihydroquinolin-4-yl)methylamino)acetamide 7e:

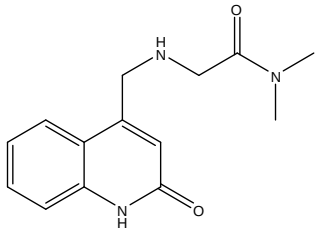

Yield : 25%; yellow solid; m.p. : 200 ^{o}C (decomposes); IR (KBr) : 3260, 2849, 1655, 1557, 1408, 748 cm $^{-1}$; ^{1}H NMR (400 MHz, DMSO-d_6): δ 4.01 (s, 6H), 4.24 (br s, 2H), 4.49 (br s, 2H), 6.53 (s, 1H), 7.00-7.82 (m, 4H), 11.67 (s, 1H); $C_{14}H_{17}N_3O_2$; ESI-MS : *m/z* 282 $[M+Na]^+$.

4,4'-(2-oxo-2-(pyrrolidin-1-yl)ethylazanediyl)bis(methylene)diquinolin-2(1H)-one 7f

Yield : 28%; off-white solid; m.p. : 230 ^{o}C (decomposes); IR (KBr) : 3444, 2958, 2845, 1735, 1659, 1556, 1501, 1443, 1421, 1356, 1294, 1262, 1168, 1151, 1036, 941, 883, 772, 679, 632, 572 cm $^{-1}$; ^{1}H NMR (400 MHz, DMSO-d_6): δ 1.70-1.74 (m, 4H), 3.15-3.50 (m, 4H), 4.04 (s, 4H), 6.53 (s, 1H), 6.98-7.87 (m, 8H), 11.62 (s, 1H); ^{13}C NMR (400 MHz, DMSO-d_6): 24.04, 26.08, 45.34, 45.94, 55.64, 115.83, 118.94, 121.74, 121.96, 125.70, 130.67, 139.37, 148.36, 162.03, 168.33; $C_{26}H_{26}N_4O_3$; ESI-MS : *m/z* 465.11 $[M+Na]^+$.

5.5 References

[1] Joseph, B.; Darro, F.; Behard, A.; Lesur, B.; Collignon, F.; Decaestecker, C.; Frydman, A.; Guillaumet, G.; Kiss, R. *J. Med. Chem.* **2002,** *45***,** 2543.

[2] Pinghua, G.; Paul, S. R. *Bioconjugate Chem.* **2004**, *15*, 1088.

[3] Kalkhambkar, R. G.; Kulkarni, G. M.; Kamanavalli, C. M.; Premkumar, N.; Asdaq, S.M.B.; Sun, C. M. *Eur. J. Med. Chem.* **2008**, *43*, 2178.

[4] Kalkhambkar, R. G.; Aridoss, G.; Kulkarni, G. M.; Bapset, R. M.; Mudaraddi, T. Y.; Premkumar, N.; Jeong, Y. T. *Monatsh Chem* **2011**, *142*, 305.

[5] Bonnefous, C.; Payne, J. E.; Roppe, J.; Zhuang, H.; Chen, X.; Symons, K. T.; Nguyen, P. M.; Sablad, M.; Rozenkrants, N.; Zhang, Y.; Wang, L.; Severance, D.; Walsh, J. P.; Yazdani, N.; Shiau, A. K.; Noble, S. A.; Rix, P.; Rao, T. S.; Hassig, C. A.; Smith, N. D. *J. Med. Chem.* **2009**, *52*, 3047.

[6] Priya, N.; Gupta, A. ; Chand, K.; Singh, P.; Kathuria, A.; Raj, H. G.; Parmar, V. S.; Sharma, S. K. *Bioorg. Med. Chem.* **2010**, *18*, 4085.

[7] Kumar, N.; Raj, V. P.; Jayshree, B. S.; Kar, S. S.; Anandam, A.; Thomas, S.; Jain, P.; Rai, A.; Rao, C. M. *Chem Biol Drug Des* **2012**, *80*, 291.

[8] Kumar, N. ; Dhamija, I.; Raj, P. V.; Jayashree, B. S.; Parihar, V.; Manjula, S. N.; Thomas, S.; Kutty, N. G.; Rao, C. M. *Arabian Journal of Chemistry* **2013**.